Exploring alternative cellular targets amenable to combination therapy in myelofibrosis

This thesis is submitted for the degree of Doctor of Philosophy
by

Dr Simone Claudiani

Centre for Haematology
Department of Immunology and Inflammation
Faculty of Medicine
Hammersmith Campus
Imperial College London
London
United Kingdom

30th June 2021

Alla mia famiglia

Declaration of Originality

I declare that this thesis and the research to which it refers are original and the product my own work and that any work performed by anyone other than myself has been appropriately acknowledged and referenced.

Copyright Declaration

The copyright of this thesis rests with the author. Unless otherwise indicated, its contents are licensed under a Creative Commons Attribution-Non Commercial-No Derivatives 4.0 International Licence (CC BY-NC-ND).

Under this licence, you may copy and redistribute the material in any medium or format on the condition that: you credit the author, do not use it for commercial purposes and do not distribute modified versions of the work.

When reusing or sharing this work, ensure you make the licence terms clear to others by naming the licence and linking to the licence text.

Please seek permission from the copyright holder for uses of this work that are not included in this licence or permitted under UK Copyright Law.

"Up from Earth's Centre through the Seventh Gate
I rose, and on the Throne of Saturn sate,
And many a knot unravelled by the Road,
But not the Master-knot of Human Fate."

Avicenna (A.D. 980-1037)

From the English translation by Edward FitzGerald of the original anthology
Majmaʿu'l-Fusahà
(Bibliography: *Arabian Medicine*, Edward G. Brown,
Cambridge at the University Press, 1921)

Acknowledgments

My first acknowledgement goes to Professor Jane Apperley. She gave me the opportunity to start my PhD and, at the same time, to develop my clinical skills in chronic myeloproliferative neoplasms, conferring to this research experience an ideal translational character.

She wisely guided me throughout a long process of personal, professional and scientific growth, always demonstrating her high dedication in helping me in the critical and objective analysis of problems. I am also very thankful to her for having done all of this with great humanity and generosity.

Dr Jamshid Khorashad has been more than a PhD Supervisor for me, as he spent efforts in designing the project, teaching me the important aspect of scientific research and assisting me with enthusiasm and commitment. He offered me his laboratory research knowledge and passion, helping with the experiments and instructing me on the interpretation of the results and the careful planning of project steps. I am very thankful to him for having been always available and highly supportive during these years.

Big thanks are for our research collaborators Professor Clinton Mason (from Department of Pediatrics, Division of Pediatric Hematology and Oncology, University of Utah, Salt Lake City, UT, USA), who took care of the bioinformatic analysis of the pooled-shRNA library screen, and Dr Andrea Bianchi, Professor Antinisca De Marco (from Department of Information Engineering, University of L'Aquila, Abruzzo, Italy) and Dr. Cristina Pellegrini (from Department of Biotechnological and Applied Clinical Science, University of L'Aquila, Abruzzo, Italy), who performed the bioinformatic analysis of the gene expression data.

My gratitude extends also to Dr Letizia Foroni, for her support, kindness and genuineness, as she demonstrated for example when she prepared the lab bench for me the first time I entered the lab. She also involved me with enthusiasm in the teaching of medical students.

I thank Carme Ripoll Fiol for helping with the lentivirus production and flow cytometry experiments and Dr Georgios Nteliopoulos for assisting me in the lab during the first phase of my project.

I am also grateful to Dr Katya Mokretar and the Hammersmith Hospital Molecular Pathology Lab for their support.

For the flow cytometry analyses I thank Professor Anastasios Karadimitris's Lab (Centre for Haematology), in particular Dr Kanagaraju Ponnusamy; Dr Lucas Black, (from Department of Infectious Disease); Jordie Roberts, Thomas Adejumo and Dr James Elliot (from the MRC-BRC Flow Cytometry Facility, Imperial College London).

I also acknowledge the support from Dr Niklas Feldhahn Lab (Centre for Haematology) and Dr Mark Robinson for preliminary bioinformatic analyses.
I am particularly grateful to my colleagues of the CML/MPN clinical team Professor Dragana Milojkovic, Dr George Nesr, Dr Andrew Innes, Irene Caballes and all the Department of Haematology at Hammersmith Hospital for creating a stimulating and friendly working environment and for accompanying and supporting me during these intense years.
Last but not least acknowledgement is for my family members, who have remained always very close to me, conveying their love across the many miles!

Abstract

Myelofibrosis (MF) is the most aggressive subtype of the classical Philadelphia (Ph)-negative chronic myeloproliferative neoplasms (MPN), characterised by bone marrow fibrosis, splenomegaly, anaemia, debilitating symptoms and a high risk of evolution into acute leukaemia. It originates in clonal haematopoietic stem cells which are transformed by hyperactivation of JAK/STAT pathway resulting from *JAK2*, *CALR* or *MPL* mutations. The disease progresses through a complex network of contributors, which include the bone marrow and spleen microenvironment, non-clonal haematopoietic cells and an abnormal inflammatory background. The modern therapy of MF is ruxolitinib, a JAK2 inhibitor. However, this drug is only able to reduce the symptom burden and the splenomegaly, without significantly modifying the disease course and overall survival. In view of this, there is an urgent need for new therapeutic strategies.

In order to identify the genes essential for the survival of MPN cells and those that protect them against ruxolitinib, we applied pooled-shRNA library screening on HEL cells, an MPN cell model, and primary CD34+ cells from MF patients. While the latter proved to be technically very challenging, mainly due to the limited transduction efficiency of the lentiviral system and did not lead to statistically significant candidates, the screen of HEL cells revealed several potential targets. Among the top hits, the most represented were the genes encoding for the ubiquitin-proteasome family, which were essential for HEL cell survival in the presence and absence of ruxolitinib and microenvironment-mimicking conditioned medium derived from HS-5 cells.

This finding was validated through the exposure of both HEL cells and primary MF cells to the proteasome inhibitors (PI) carfilzomib (CFZ) and bortezomib (BTZ), which were both effective in inhibiting cell proliferation. Considering the pharmacokinetic profile of BTZ and its lack of clinical efficacy as monotherapy in MF, CFZ was chosen for investigation of primary MF cells. Pulsed-exposure experiments confirmed that adding CFZ to ruxolitinib augmented the growth inhibition, the extent of apoptosis and the reduction of clonogenicity of MF CD34+ cells, compared to ruxolitinib alone. Gene set enrichment analysis showed that ruxolitinib downregulated the expression of proteasome family genes in MF CD34+ cells, suggesting that this mechanism could make these cells more sensitive to PI.

We also provided preliminary evidence that CFZ alone and its combination with ruxolitinib decrease the activation of NF-κB canonical pathway in MF CD34+ cells, which, if confirmed

by a larger study, may constitute another important disease-promoting pathway targeted by CFZ.

In summary, starting from the pooled-shRNA screening on HEL cells identifying proteasome genes among the top hits, we found that CFZ enhances the efficacy of ruxolitinib against primary MF CD34+ cells. Further research should investigate the exact mechanistic basis and consider further exploration of this combination as a potential new therapeutic strategy for MF.

Summary of contents

Abstract **8**

List of Tables **13**

List of Figures **15**

List of recurring acronyms **17**

CHAPTER 1 ..... **18**

1.1 Classical Ph-negative Chronic Myeloproliferative Neoplasms *18*

1.2 Myelofibrosis *20*

1.2.1 Clinical features of MF 20

1.2.2 Pathogenesis of MF – more than one protagonist 22

1.2.2.1 Haematopoietic stem cell 22

1.2.2.2 Megakaryocyte 22

1.2.2.3 Spleen 24

1.2.2.4 Monocyte 24

1.2.2.5 BM stroma, niche and chronic inflammation 26

1.2.2.6 Time 26

1.2.3 Modern therapy for MF 27

1.2.3.1 Ruxolitinib 27

1.2.3.2 Allogeneic haematopoietic stem cell transplantation 31

1.2.3.3 Experimental drugs 33

1.3 Project aims *37*

1.4 shRNA and pooled-shRNA screens for cancer pathways *37*

1.5 Stromal cell lines *40*

1.6 MPN Cell lines *41*

CHAPTER 2 ..... **42**

2.1 HEL cell *42*

2.1.1 HEL cell line 42

2.1.2 Fluorescence in situ hybridization and NGS panel screen of HEL cells 42

2.1.3 Viability assay 42

2.1.4 MTS assay 43

2.1.5 Apoptosis assay 43

2.1.6 Western Blot 43

2.2 HS-5 cell culture, transduction and conditioned medium *45*

2.3 Lentiviral production *46*

2.3.1 Bacterial transformation, plasmid amplification and extraction 46

2.3.2 Viral vector production 47

2.3.3 Multiplicity of infection 49

2.3.4 In vitro transduction and determination of lentiviral vector titre 49

2.4 Pooled shRNA screening pipeline *50*

2.5 Isolation of MF CD34+ cells from peripheral blood-derived mononuclear cells *53*

2.6 Lentiviral transduction and pooled-shRNA screening of primary cells *53*

2.7 DNA extraction *53*

2.8 shRNA barcode amplification, purification and isolation and NGS *54*
2.8.1 First-round PCR 54
2.8.2 Second-round PCR 55
2.9 Bioinformatic analysis of pooled-shRNA library screens *58*
2.10 MTS assay on primary cells *59*
2.10.1 Experiments on continuous-inhibitors exposure 59
2.10.2 Exposure to pulsed proteasome inhibitors 60
2.11 Apoptosis and cell cycle analysis on primary cells *61*
2.12 Experimental design for gene expression profiling of primary cells *61*
2.13 RNA extraction and sequencing *61*
2.14 Bioinformatic analysis of RNA-seq data *62*
2.15 RT-qPCR on primary cells *63*
2.16 NF-κB pathway low-density microarray on primary cells *64*
2.17 Colony formation assay on primary cells *66*
2.18 Western Blot on primary cells *66*
2.19 Additional MTS experiments on primary cells *67*

CHAPTER 3 68

3.1 HEL cell line pre-shRNA screen analysis *68*
3.1.1 Genomic characterization of the HEL cell line 68
3.1.2 Reduced sensitivity of the HEL cells to ruxolitinib in presence of CM mimicking BM microenvironment 69
3.2 Pooled-shRNA screen results on HEL *73*
3.3 Pooled-shRNA library screen results on primary cells *83*
3.4 Selection of the target for validation *88*
3.5 Chemical validation targeting proteasome on HEL cells *88*
3.6 Chemical validation targeting proteasome on primary cells *89*
3.6.1 PI CFZ reduce the number of viable MF cells 89
3.6.2 PI CFZ enhances inhibitory effect of ruxolitinib on MF cells 89
3.6.3 Ruxolitinib-CFZ combination increases apoptosis of MF cells compared to ruxolitinib alone 95
3.6.4 PI BTZ enhances the inhibitory effect of ruxolitinib on MF cells 95
3.6.5 Ruxolitinib-CFZ combination reduces colony formation of MF cells compared to ruxolitinib alone 95
3.7 Gene expression profile (GEP) on primary MF CD34+ cells *99*
3.7.1 Gene expression profile analysis 99
3.7.2 Gene set enrichment analysis 102
3.8 Additional potential targets from gene expression analysis which need further investigation *104*
3.8.1 *PTGDS* expression by MF and healthy CD34+ cells exposed to ruxolitinib 104
3.8.2 Effect of PDG2 and AT-56 +/- ruxolitinib on MF and healthy CD34+ cells 105
3.8.3 *ARG1* expression in MF CD34+ cells exposed to ruxolitinib 106
3.8.4 *FLT3* expression in CD34+ MF cells exposed to ruxolitinib 107
3.9 NF-κB pathway alteration in MF CD34+ cell exposed to inhibitors *107*
3.9.1 In vitro effects of pulsed CFZ with or without ruxolitinib on NF-κB pathway gene expression on MF CD34+ cells 108
3.9.2 Investigation of nuclear p65 in CD34+ MF cells does not support activation of NF-κB following CFZ treatment 112

CHAPTER 4 113

4.1 Interpretation of pooled-shRNA library screen results on HEL cell ... *113*
4.1.1 Advantages and limitations of the HEL cell line as MPN cell model ... 113
4.1.2 Top-depleted shRNAs in each experimental condition ... 114
4.1.2.1 Baseline (Setting 1) ... 114
4.1.2.2 Ruxolitinib alone (Setting 2) ... 115
4.1.2.3 Ruxolitinib + HS-5 CM in combination (Setting 3) ... 117
4.1.3 Top-depleted shRNAs in all 3 experimental settings ... 119
4.1.3.1 *RAN* ... 120
4.1.3.2 Proteasome gene family ... 120
4.1.3.3 *PHB2* ... 121
4.1.3.4 Genes involved in splicing ... 122
4.1.3.5 *NEDD8* ... 122
4.1.3.6 *JAK2* ... 123
4.1.3.7 Other genes targeted by the top-depleted shRNAs in all settings ... 123

4.3 Interpretation of pooled-shRNA library screen results on MF CD34+ cells ... *123*

4.4 Validation of pooled-shRNA library screen findings ... *126*
4.4.1 Chemical validation on HEL cells ... 126
4.4.2 Chemical validation on primary cells ... 126
4.4.2.1 Choice of CFZ as the PI to use for chemical validation ... 127
4.4.2.2 Interpretation of effects of CFZ on MF CD34+ cells and correlation with GEP results ... 128
4.4.2.3 Further arguments for the biological rational supporting JAK2 inhibitor/PI combinational therapy in myelofibrosis ... 134

4.5 Interpretation of NF-κB pathway alteration in MF CD34+ cells exposed to ruxolitinib +/- CFZ ... *136*

4.6 Interpretation of additional GEP findings (PTGDS, FLT3, ARG1) ... *140*

Conclusions ... *142*

References ... *143*

APPENDIX ... 176

Appendix References ... *234*

List of Tables

Chapter 1 - Introduction

Table 1.1. New agents under investigation for MF therapy (in monotherapy or combined with ruxolitinib). 34

Chapter 2 - Methods

Table 2.1. First-round PCR mix for shRNA barcode amplification. 54
Table 2.2. H_2O-genomic DNA ratios in the 1st-round PCR for shRNA barcode amplification. 55
Table 2.3. First-round PCR for shRNA barcode amplification: cycling conditions. 55
Table 2.4. PCR mix of the intermediate PCR for shRNA barcode amplification. 56
Table 2.5. Intermediate PCR for shRNA barcode amplification: cycling conditions. 56
Table 2.6. Second-round PCR mix for shRNA barcode amplification. 57
Table 2.7. Second-round PCR for shRNA barcode amplification: NRev Indexed Primers. 57
Table 2.8. Second-round PCR for shRNA barcode amplification: cycling conditions. 57
Table 2.9. Candidate target genes evaluated and TaqMan gene expression assay reference ID. 63
Table 2.10. RT-qPCR cycling conditions. 64
Table 2.11. Applied Biosystems® TaqMan® Array Human NF-kB Pathway 96-well Plate: list of genes. 65
Table 2.12. RT-qPCR cycling conditions for Applied Biosystems® TaqMan® Array Human NF-κB Pathway 96-well Plate. 65

Chapter 3 - Results

Table 3.1. Top essential genes for viability or proliferation of HEL cells under various conditions – Ranking approach 1 (RA1). 77
Table 3.2. HEL cell line pooled-shRNA library screen – Baseline setting (1) (analysis of 2 replicates according to ranking score 2, RA2). 80
Table 3.3. HEL cell line pooled-shRNA library screen – Ruxolitinib setting (2) (analysis of 2 replicates according to ranking score 2, RA2). 81
Table 3.4. HEL cell line pooled-shRNA library screen – Ruxolitinib + HS-5 CM setting (3) (analysis of 2 replicates according to ranking score 2, RA2). 82
Table 3.5. Summary of the pooled-shRNA library screen experiments on primary cells. 83
Table 3.6. RFP positivity at the end of the pooled-shRNA library screen of primary cells. 84
Table 3.7. List of the top 1% 2nd most depleted shRNAs in MF-3 (at day 14 post-transduction). 86
Table 3.8. Clinical characteristics of MF patients at the time of sample collection. 90

Chapter 4 - Discussion

Table 4.1. Other genes targeted by the top-depleted shRNAs in experimental setting 2. 116
Table 4.2. Other genes targeted by the top-depleted shRNAs in experimental setting 3. 119
Table 4.3. Genes targeted by the most depleted shRNAs in MF-3, of potential relevance in MPN. 125

Appendix

Table A1. Role of each shRNA construct cassette (from Cellecta website) 176
Table A2. List of the 59 genes targeted by shRNAs directed to a sequence no longer part of the mRNA sequence pertaining to that gene in RefSeqGene database 177
Table A3. List of the 96 TaqMan® gene expression assay ID and their disposition in the Applied Biosystems® TaqMan® Array Human NF-κB Pathway 96-well Plate. 180
Table A4. Pooled-shRNA library screen on HEL cell line and MF-3: list of 2nd most depleted shRNAs for each experiment (ranking approach 1, RA1). 181
Table A5. List of 143 genes for which there were ≥ 2 shRNAs having FC ≥ 3 or resulting among the top 2% depleted in BOTH replicates in one or more experimental conditions (alphabetical order). 217

Table A6. Top essential genes for viability or proliferation of HEL cells under various conditions – ranking approach 3 (RA3). 222
Table A7. Differentially expressed genes in CD34+ MF cells treated with ruxolitinib. 223
Table A8. Downregulated signalling pathways by ruxolitinib in CD34+ MF cells. 228
Table A9. Upregulated signalling pathways by ruxolitinib in CD34$^+$ MF cells. 230
Table A10. Negatively-enriched proteasome genes by ruxolitinib in CD34$^+$ MF cells – GSEA details. 231
Table A11. Genes of potential relevance in MPN whose expression is regulated by CFZ in MF-4 and MF-24. 232
Table A12. Genes downregulated by ruxolitinib, upregulated by CFZ and strongly upregulated by the treatment combination in MF-24 CD34+ cells. 233

List of Figures

Chapter 1 – Introduction

Figure 1.1. MPN driver mutations and their role in the activation of pro-survival downstream pathways. ...19
Figure 1.2. Potential therapeutical targets in MF and other MPN. 36
Figure 1.3. Types of RNAi constructs used for gene silencing. 38

Chapter 2 – Methods

Figure 2.1. DECIPHER pRSI12-U6-(sh)-HTS4-UbiC-TagRFP-2A-Puro 3rd generation transfer vector and 2nd generation lentivirus packaging system.....48
Figure 2.2. Lentiviral vector titre chart: relationship between transduced (RFP-positive) cells and MOI. (modified from Cellecta Manual, v9a 02/03/2016) 49
Figure 2.3. Pooled-shRNA library screen pipeline on HEL cell line. 52
Figure 2.4. Pulsed-PI in vitro exposure: experimental design. 60

Chapter 3 – Results

Figure 3.1. Fluorescence in situ hybridization of HEL cells. 68
Figure 3.2. Myeloid NGS panel applied to the HEL cell line. 70
Figure 3.3. HEL cell proliferation assay. 70
Figure 3.4. MTS assay on HEL cell line. 71
Figure 3.5. Ruxolitinib IC_{50} in HEL cell cultured in RF10 and HS-5 CM. 71
Figure 3.6. Effect of HS-5 CM on HEL cell apoptosis induced by ruxolitinib. 72
Figure 3.7. Effect of ruxolitinib on phosphorylated-STAT5 in HEL cell line. 72
Figure 3.8. Pooled-shRNA library screen of HEL cell line. 76
Figure 3.9. The correlation between the replicates of pooled-shRNA library screen on HEL cell line. 78
Figure 3.10. Second most depleted shRNAs: comparison of single replicates across different treatment conditions. 79
Figure 3.11. Pooled-shRNA library screen of CD34+ cells purified from peripheral blood of a patient with MF. 85
Figure 3.12. Genes targeted by the most depleted shRNAs in cell line and primary MF CD34+ which belong to the MPL receptor intracellular cascade.....87
Figure 3. 13. Fold-depletion of shRNAs targeting proteasome machinery in the pooled-shRNA library screen of MF-3 CD34+ cells. 87
Figure 3.14. Proteasome inhibitors (PI) IC_{50} and effect of ruxolitinib-CFZ combo on HEL cells. 88
Figure 3.15. In vitro effect of CFZ 50-1000 nM on MF CD34+ cells. 91
Figure 3.16. In vitro effect of CFZ 10/50 nM with or without ruxolitinib on MF CD34+ cells. 92
Figure 3.17. In vitro effect of ruxolitinib with or without 1h-pulsed CFZ on MF CD34+ cells and MF MNCs. ..94
Figure 3.18. Apoptosis and cell-cycle analysis of MF CD34+ cells after exposure to ruxolitinib, 1-h pulsed CFZ and their combination. 96
Figure 3.19. In vitro effect of ruxolitinib with or without 1h-pulsed BTZ on MF CD34+ cells and MF MNCs. .97
Figure 3.20. Colony formation assay on MF CD34+ cells exposed to of ruxolitinib with or without CFZ (continuous or 1h-pulsed). 98
Figure 3.21. MF CD34+ cells expansion in cytokine-rich medium, with and without ruxolitinib. 100
Figure 3.22. Differential GEP in MF CD34+ cells after in vitro exposure to ruxolitinib 300 nM. 100
Figure 3.23. Differential gene expression analysis on MF CD34+ cells treated in vitro with ruxolitinib or vehicle ("control"). 101
Figure 3.24. Proteasome gene set is negatively-enriched in MF CD34+ cells treated with ruxolitinib. 102
Figure 3.25. Gene set enrichment analysis in MF CD34+ cells treated in vitro with ruxolitinib: top-10 negatively-enriched pathways.....103
Figure 3.26. PTGDS upregulation in MF and healthy CD34+ cells exposed in vitro to ruxolitinib. 105
Figure 3.27. Effect of PDG2 and AT-56 on proliferation of MF CD34+ cells. 106
Figure 3.28. ARG1 upregulation in MF CD34+ cells exposed in vitro to ruxolitinib 300 nM. 106

Figure 3.29. FLT3 upregulation in MF CD34+ cells exposed in vitro to ruxolitinib 300 nM. 107
Figure 3.30. Effect of ruxolitinib and CFZ on the NF-κB pathway gene expression profile in MF-4 CD34+ cells. 109
Figure 3.31. Effect of ruxolitinib +/- CFZ on the NF-κB pathway gene expression profile in MF-24 CD34+ cells. 110
Figure 3.32. NF-κB pathway genes with discordant expression change induced by CFZ or ruxolitinib in MF-24 and MF-4 CD34+ cells in vitro. 111
Figure 3.33. Measurement of NF-κB activation on MF-19 CD34+ cells following in vitro treatment with ruxolitinib +/- 1h-pulsed CFZ. 112

Chapter 4 – Discussion

Figure 4.1. 26S proteasome structure and genes targeted by the most depleted shRNAs. 121
Figure 4.2. Grb2 and PHB1-PHB2 complex in the signal transduction from growth factor receptor to Ras/Raf/MEK/ERK pathway. 122
Figure 4.3. The UPR pathways. 130
Figure 4.4. PERK is associated with and phosphorylated by JAK1 and, likely, other JAKs. 132
Figure 4.5. Rationale for further investigation of the ruxolitinib-CFZ combination in myelofibrosis. 133
Figure 4.6. Canonical and non-canonical pathways of NF-κB activation and their inhibitors. 137
Figure 4.7. Model of JAK-STAT induced NF-kB activation. 138
Figure 4.8. Reflection on the observed effect of ruxolitinib and CFZ on NF-kB pathway in MF CD34+ cells. . 138

Appendix

Figure A1. Lentiviral titration on K562 cells. 176
Figure A2. Pooled-shRNA library screen result for the “control” shRNAs for the first replicate in each experimental setting. 178
Figure A3. Pooled-shRNA library screen result for the “control” shRNAs for the second replicate in each experimental setting. 179

List of recurring acronyms

ALL	acute lymphoblastic leukaemia
AML	acute myeloid leukaemia
APL	acute promyelocytic leukaemia
ARG1	arginase 1
ASCT	allogeneic haematopoietic stem cell transplant
Bcl-2	B-cell lymphoma 2
Bcl-xL	B-cell lymphoma extra-large
BM	bone marrow
BTZ	bortezomib
CALR	calreticulin
CDK	cyclin-dependent kinase
CFZ	carfilzomib
CHOP	C/EBP homologous protein
CM	conditioned medium
EMH	extramedullary haemopoiesis
ER	endoplasmic reticulum
ERK	extracellular signal-regulated kinase
ET	essential thrombocythaemia
FC	fold change (only when referred to the pooled-shRNA library screen analysis)
FLT3	fms-like tyrosine kinase 3
GFP	green fluorescent protein
GRB2	grow factor receptor-binding protein 2
HS-5	human stromal cell clone 5
HSC	haematopoietic stem cells
HSPC	haematopoietic stem and precursor cells
IC50	inhibitory concentration leading to 50% reduction of cell proliferation/viability
INF	interferon
JAK2	janus kinase 2
MAPK	mitogen-activated protein kinase
MCL-1	myeloid cell leukaemia-1
MF	myelofibrosis
MK	megakaryocyte
MM	multiple myeloma
MNCs	mononuclear cells
MPL	myeloproliferative leukaemia virus (thrombopoietin receptor gene)
MPN	classical Philadelphia (Ph)-negative chronic myeloproliferative neoplasms
NGS	next generation sequencing
PERK	protein kinase R-like endoplasmic reticulum kinase
PI	proteasome inhibitor
PIM	proviral integration site of Moloney murine leukaemia virus
PI3K	phosphoinositide 3-kinase
PP2A	protein phosphatase 2
PTGDS	glutathione-independent prostaglandin D synthase
PV	polycythaemia vera
RAN	Ras-related nuclear protein
RAS	Rat sarcoma (gene)
RFP	red fluorescent protein
shRNA	short hirpin RNA
STAT	signal transducer and activator of transcription
TLR	toll-like receptor
TPO	thrombopoietin
UPR	unfolded protein response

CHAPTER 1

Introduction

1.1 Classical Ph-negative Chronic Myeloproliferative Neoplasms

The classical Philadelphia (Ph)-negative chronic myeloproliferative neoplasms (MPN) include polycythaemia vera (PV), essential thrombocythaemia (ET) and primary or post-ET/PV myelofibrosis (MF). MPN are long-term haematopoietic stem cell (HSC) clonal disorders characterized by uncontrolled proliferation of one or more myeloid lineages with preserved cell differentiation and variable predisposition for leukaemic evolution.

The main feature of MPN is marrow hypercellularity affecting all lineages, associated with a variable degree of leucocytosis, erythrocytosis and thrombocytosis depending on the subtype. Splenomegaly is a classical manifestation in these conditions, more common in MF. PV and ET, sometimes clinically overlapping, can evolve in MF (post-ET and post-PV MF)(1). Although the course of MPN is chronic and can last for several decades, especially for ET and PV, these conditions have a high propensity to thrombosis and bleeding and, ultimately, evolution into acute leukaemia. While the thrombotic complications are more frequent in the proliferative stages of MPN (ET and PV)(2), with a cumulative rate of thrombosis of 3% per year (3), leukemic transformation is by far most common in MF, with an incidence of 10-20% in the first 10 years (4). Haemorrhagic events are another important cause of comorbidity and mortality in MPN, especially in ET and in MF, with one study reporting a rate of major bleeding of 0.79% and 1.79% per year, respectively (5).

Pre-fibrotic MF identifies a fourth recently recognized distinct clinicopathological entity (6), characterized histologically by megakaryocytic and granulocytic proliferation, with atypical megakaryocyte morphology, but without any significant bone marrow (BM) fibrosis, and clinically by a lower incidence of cytopenia and splenomegaly, lower circulating blast percentage and higher incidence of thrombocytosis compared to overt MF (7).

Since the discovery of the V617F mutation in the exon 14 of janus kinase 2 (*JAK2*) gene in virtually all cases of PV (95%) and in a considerable proportion of ET and MF patients (40-50%), important advances have been made in the discovery of mechanisms underpinning the pathogenesis of these diseases and their clinical behaviour (8). Somatic mutations in exon 12 of *JAK2* have been found in the rare cases of *JAK2*^{V617F}-negative PV (9). Several gain of function mutations in exon 10 of the thrombopoietin (TPO) receptor gene *MPL*

(myeloproliferative leukaemia virus) have been discovered in up to 15% of *JAK2*^{V617F}-negative ET and MF (10, 11). More recently, whole exome sequencing led in two independent studies to the identification of a new mutation in the exon 9 of calreticulin (*CALR*) gene in the 50-70% of ET and MF patients with wild type *JAK2* and *MPL* (12, 13).

So far, scientific research into the molecular pathogenesis of MPN has focused on understanding how three mutually exclusive oncogenic mutations in *JAK2*, *MPL* and *CALR* could be linked to different disease phenotype and evolution.

The only clear evidence is that hyperactivation of the JAK/STAT pathway is the common mechanism in all three forms of MPN (14), with the recent finding of a different modality of JAK/STAT pathway activation between *JAK2*- and *CALR*-mutated neoplasms (15).

Figure 1.1 summarises the mechanism of receptor activation by each of the 3 driver mutations with the consequent effect on downstream survival pathways.

Figure 1.1. MPN driver mutations and their role in the activation of pro-survival downstream pathways.
(adapted from Guijarro-Hernández A. and Vizmanos JL. Cancers (Basel) 2021 Feb 26;13(5):984)

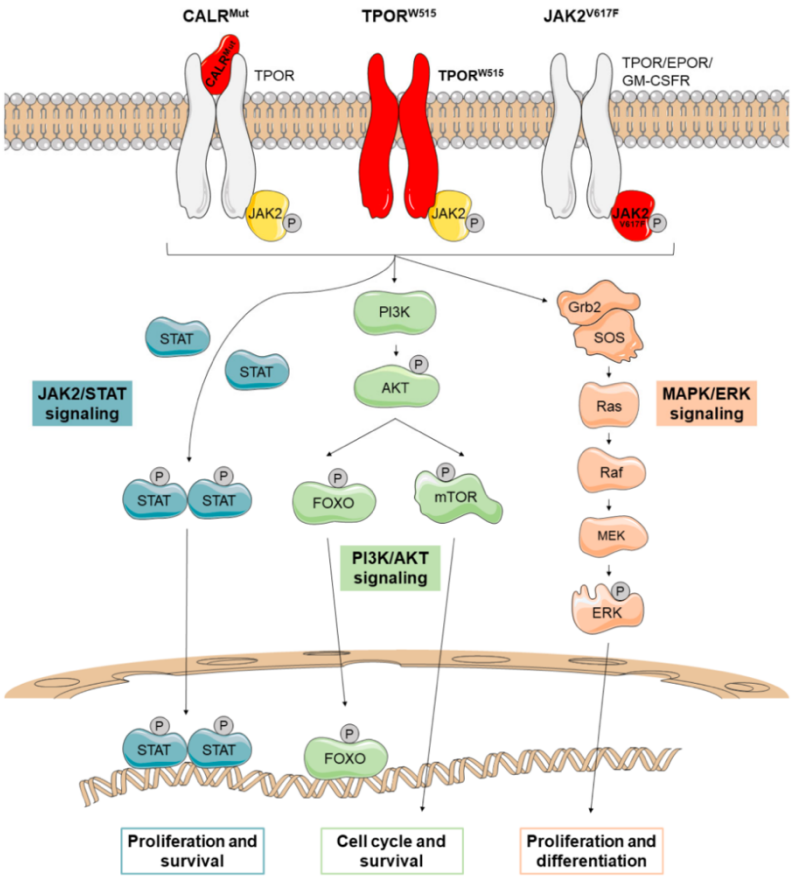

Although *JAK2*^{V617F} is also found in 50% to 60% of those with MF, the additional factors determining the phenotype of this clinically heterogeneous disorder are less clear. It is likely

that additional mutations in MPN are important and they are more common in MF than in PV or ET and frequently coexist with *JAK2*^{V617F} (16, 17). These mutations affect either epigenetic regulators or components of the spliceosome machinery. The most frequent genetic events of the former group include *TET2*, *ASXL1*, *DNMT3A* and, more rarely, *IDH1/2* and *EZH2* mutations, while *SF3B1, SRSF2* and *U2AF1* mutations belong to the latter.

Some of these genetic alterations, often occurring together with *JAK2*^{V617F}, might contribute to development of a specific disease phenotype, conferring dominance to the HSC clone and contributing to the evolution towards MF. Spliceosome machinery mutations occur preferentially in *CALR*-unmutated MPN (18) and usually in patients with MF (19). In a recent study by Ortman at al. (20), the order in which *TET2* and *JAK2* mutations are acquired in MPN emerged as an important factor in determining the disease phenotype, clinical behaviour, response to targeted therapy, biology and the clonal evolution of stem and progenitor cells.

Further research is needed to determine the genesis of different MPN and to distinguish more indolent diseases from more aggressive forms prone to rapid evolution.

This would help in finding more effective therapeutic interventions as the current ones are still non-specific and of limited activity, especially in MF (discussed below).

1.2 Myelofibrosis

MF is the most severe form of MPN. It can evolve from ET and PV or be diagnosed as a *de novo* condition. Its clinical features, pathogenesis and therapeutic strategies are discussed below.

1.2.1 Clinical features of MF

The reported incidence of MF is between 0.5-2 /100.000 persons per year, with a prevalence of 0.5-6 cases per 100.000 individuals, a male predominance (ratio male:female of 1.3-4) and a median age at diagnosis ranging from 65 to76 years (21-29).

MF is the most complex disorder among MPN, as the clonal myeloproliferation is accompanied by BM fibrosis, neoangiogenesis, abnormal inflammatory cytokine production and extramedullary haematopoiesis, an intricate scenario reflecting the multifactorial pathogenesis (see below). Clinically, the consequences of this derangement of the haematopoietic stem cell and microenvironment in MF are abnormal blood counts (severe anaemia; leucocytosis/leukopenia; thrombocytopenia), marked hepatosplenomegaly and constitutional symptoms (weight loss, fatigue, night sweats), often accompanied by other symptoms such as

bone pain and pruritus. In addition, complications such as thrombotic events, variceal bleeding and ascites from portal hypertension are not uncommon.

The causes of severe anaemia in MF involve many factors such as the displacement of erythropoietic tissue by the marrow fibrotic process, the suboptimal milieu found by migrating erythropoietic tissue in sites of extramedullary haematopoiesis (EMH), the dilutional anaemia induced by splenomegaly, the systemic inflammation and the deranged iron metabolism from increased circulating hepcidin (30). Anaemia is one of the most debilitating aspect of MF and often leads to transfusion-dependency, which in turns produces iron overload and the related pathological consequences.

The mechanisms underlying the splenic and non-splenic EMH are still not fully understood. It is thought that contributing factors are the altered homing of HSC and the altered host immune response (31, 32), aberration of the CXCL12/CXCR4 pathway (33) and GATA1 upregulation in megakaryocytes (34).

Patients diagnosed with MF have an average estimated survival of 4-7 years, with 35%-46% of them expected to be alive at 5 years from diagnosis, which is the shortest survival among MPN (35-39). Interestingly, the advent of JAK2 inhibitors has not led to a significant improvement of the survival in MF (27).

Prognostic scores help in tailoring the therapeutic strategy for MF, providing different survival group estimates based on clinical and molecular characteristics. These include age at diagnosis or age at clinical assessment, degree of anaemia, thrombocytopenia and leucocytosis, presence of constitutional symptoms, percentage of circulating blasts, driver or other mutations and karyotypic abnormalities. Several prognostic scores have been proposed to date, which use different combinations of the above variables: the International Prognostic Scoring System (IPSS) (40), the Dynamic IPSS (DIPSS) (41), the DIPSS-plus (42), the genetically inspired prognostic scoring system (GIPSS) (43), and the mutation-enhanced IPSS (MIPSS70) version 2.0 (44). In addition, MYSEC-PM, a specific score designed for post-PV and post-ET MF has been developed recently (45).

However, the long-term treatment plan for patients with MF remains challenging for two main reasons: the high degree of variability in survival (reflected in the prognostic tools developed so far) and the lack of disease-eradicating pharmacological therapies, which implies that the clinician has the hard task of identifying the best candidate and the best timing for allogeneic haematopoietic stem cell transplant (ASCT), the only potentially curative option so far available for MF.

1.2.2 Pathogenesis of MF – more than one protagonist

1.2.2.1 Haematopoietic stem cell

All MPN originate from the pluripotent HSC (46, 47). Experience from murine models demonstrated that the introduction of any of the three driver mutations (*JAK2*^{V617F}, *MPL*^{W515L} and *CALR*^{del52}) in haematopoietic precursors was sufficient to recapitulate the MPN disease spectrum with evolution into MF (10, 48-53). Furthermore, these studies defined the role of the allele burden of *JAK2*^{V617} mutation in determining the disease phenotype and the degree of BM fibrosis (50). Interestingly, in a mouse model of MF induced by the retroviral expression of *MPL*^{W515L} in haematopoietic stem and progenitor cells (HSPC) (10), activation of JAK/STAT pathway and abnormal cytokine production were found also in non-malignant haematopoietic cells, including the more differentiated ones (54). This suggests that the genetic lesion in the HSC can transform the non-mutated haematopoietic compartment which in turn contributes to disease pathogenesis. In the same work, the authors described similar findings in a *JAK2*^{V617F} knock-in mouse model.

Two recent single-cell studies support the critical role of mutant HSC in the pathogenesis of MF. One work showed a bias toward megakaryocyte (MK) differentiation (and the MK plays a determinant role in MF, as discussed in the next section) originating in early multipotent stem cells and that mutant HSPC had increased expression of MK-associated genes, observations which were found across all clinical and molecular patient subgroups (55). The second work revealed that pro-inflammatory gene signatures are evident already in malignant HSPC of *CALR*-mutated MF (56).

Finally, a third single-cell study demonstrated that high heterogeneity exists in HSPC within individual patients from both the genetic and transcriptomic points of view (57).

1.2.2.2 Megakaryocyte

Extensive literature has confirmed the important role of MKs in MPN and MF pathogenesis and progression. These cells are increased in the BM of MF patients and are characterized by dysplastic features, reflecting a profound abnormality in their maturation process. The latter seems to be associated with a combination of enhanced proliferative capacities, reduced apoptotic functions and altered epigenetic control (58, 59).

MK in MPN are cardinal players in the process of sustaining the myeloproliferation, contributing to the inflammatory background typical of MF and promoting the development of BM fibrosis.

Two studies using a mouse model of MK-restricted expression of *JAK2*^{V617} demonstrated that the first effect is mediated by the JAK/STAT hyperactivation in the mutant MK which in turn leads to increased quiescence and repopulating capacity of wild-type HSPC (60); interestingly, the expansion of the wild-type hematopoietic compartment was found to be mediated by the secretion of proinflammatory cytokines by the mutant MK (61). Woods et al showed that MK depletion in both *JAK2*^{V617} and *MPL*^{W515L} MPN mouse models significantly blunted the disease phenotype in both (61), suggesting that the contribution of MK to myeloproliferation is not driver-mutation specific and that MK are essential for the maintenance of the MPN phenotype in vivo.

With respect to MK contribution to inflammation in MPN, recent work applying gene set enrichment analysis found that MK precursors in MF have enriched inflammatory pathways compared to healthy donor counterparts (55). MK in MF secrete a wide range of cytokines which enhance the typical MF proinflammatory background, which in turn is a potent stimulator of megakaryopoiesis (62-64).

Closely related to the last point, some of the cytokines released by MF MK are major determinants of fibrosis. Among them, the most relevant are TGF-β (65-67), platelet-derived growth factor (PDGF) (68, 69) and CXCL4 (PF4) (70). Other contributors include fibroblast growth factor (FGF) (71), vascular endothelial growth factor (VEGF) (72), thrombospondin-1 (73), interleukin-8 (63), lipocalin-2 (LCN2) (74), oncostatin M (75) and bone morphogenic proteins (76, 77).

In addition to cytokines, the fibrosis-induction and promotion by MK is mediated by expression of extracellular matrix components (78) and enzymes that regulate its composition. In particular, MF MK overexpress lysil-oxidase (LOX) (79), a copper-dependent amine oxidase leading to cross-linking of collagen and elastin and regulating the matrix elasticity; also, they show deranged expression of metalloproteinases and their inhibitors, with the final effect of reduced matrix degradation (80). Direct MK interaction with other cellular BM components (fibroblasts (81), mesenchymal stem cells (82) and polymorphonuclear leukocytes (83, 84)) is a third mechanism cooperating in the fibrotic process in MF.

As mentioned in the next section, spleen-resident MK in MF are important contributors to MF pathogenesis and progression, but they might have different roles in this process as suggested by the difference in their ultrastructural abnormalities compared to their BM-resident counterpart (85).

Abnormal MK in MF might also exert indirectly their influence on disease progression through platelets. A recent study demonstrated that MF MK have increased expression of *B4GALT1*,

which encodes for β-1,4-galactosyltransferase 1 (β4GalT1), leading to abnormal platelet glycosylation. The latter was found to be responsible for the increased hepatic TPO synthesis regardless of the platelet mass (86). Also, platelets can directly contribute to the abnormal inflammation in MPN (87).

Finally, in support of the peculiar cellular derangement and disease-promoting role of MK in MF, a recent study showed that MK isolated from the BM of MPN patients frequently demonstrate additional somatic mutations not shared by the other haematopoietic cells, with the greatest allelic burden observed in MF patients (88).

1.2.2.3 Spleen

Splenomegaly in MF results directly from splenic EMH, which transforms this organ into an important contributor to MF pathogenesis. In fact, spleen endothelial cells (EC) from patients with MF contain the *JAK2*^{V617F} mutation, likely because these cells derive from differentiation of MF HSC into EC (89). In a vicious circle, mutant EC alter the splenic vascular niche which favours increased migratory behaviour and enhanced differentiating potential of MF HSPC (90, 91). Furthermore, EC in both BM and spleen, through cross-talk with MK, undergo mesenchymal phenotype transformation, thus participating in the development of pathological BM and splenic haematopoietic niches (92). In addition, Avanzini et al. demonstrated the existence of functionally and genetically abnormal splenic mesenchymal cells which sustain the abnormal EMH in the spleen (93). Finally, the spleen in MF might play an important role in the generation of abnormal cellular clones leading to disease progression, through its ability to alter the functional and genetic properties of splenic MF HSC compared to HSC derived from the peripheral blood of the same patient (91).

1.2.2.4 Monocyte

The monocyte is another example of how in MF each cell type exerts its own contribution to the pathogenesis and that both malignant and non-malignant counterparts participate in this process.

Elevated monocytes are a poor prognostic marker in MF (94). In MPN the monocytes have an activated phenotype compared to healthy subjects, and they secrete pro-fibrotic cytokines and pro-thrombotic factors (95, 96). Also, monocytes in MPN have been recently shown to bear a defect in the negative regulation of toll-like receptor (TLR) signalling, leading to abnormal production of TNF-α upon TLR activation. Interestingly, not only was this functional abnormality found in both clonal and non-clonal monocytes, but it was also shown in the

healthy twin of an MPN patient. The authors speculated that this dysfunction might constitute at the same time a pathogenetic mechanism and a potential predisposition to MPN (97).

Others have shown that monocytes are the cell population most responsible for elevated circulating cytokine levels in MF, including TNF, TGF-β, and IL-10, and that this extends to all the monocyte phenotypes ("classical" CD14+CD16−, "inflammatory" CD14+CD16+ and "non-classical" CD14−CD16+ monocytes) (98).

In addition to a direct pathogenetic role of monocytes, recent research has discovered that fibrocytes, derived from a subpopulation of CD14+ monocytes (99, 100), are crucial players in MF. Data from a murine model of MF showed that the activation of the TPO receptor promotes fibrocyte differentiation from their precursor clonal monocytes and macrophages, and that elimination of the latter reverse the MF phenotype. Based on these findings the authors speculated that the origin of BM fibrosis comes from both malignant and reactive fibrocytes, the latter stimulated by increased TPO levels. Additionally, in the same work, they identified the SLAMF7^{high} MPL^{high} monocyte subtype as the possible precursor of fibrocytes in human peripheral-blood derived mononuclear cells (MNCs) and that this cellular subset is increased in MF patients compared to healthy subjects (101). In a subsequent work, the same authors further studied this monocyte subset in MPN patients, showing that it was increased in *JAK2*^{V617F}-mutated MF compared to other MPN subtypes and healthy controls. Furthermore, targeting these cells with elotuzumab, an anti-SLAMF7 antibody, inhibited their differentiation into fibrocytes in vitro and reduced BM fibrosis and splenomegaly in a murine xenograft model (102).

A further study found that BM of MF patients is rich in clonal fibrocytes producing collagen and fibronectin, which are key constituents of fibrous tissue in the BM of MF, and that transplanting MF patients' BM cells into immunocompromised mice induced an MF-like phenotype. Importantly, treatment of the xenograft mice with serum amyloid P (pentraxin 2), a fibrocyte inhibitor, prolonged survival and slowed the fibrotic process (103). Lately, authors from the same group confirmed their initial finding by transplanting purified BM-derived fibrocyte-precursor CD14+/CD34- monocytes from MF patients into immunocompromised mice, leading to a MF-like phenotype characterized by splenomegaly, reticulin fibrosis and MK clustering (104).

Finally, in line with these findings, a very recent study on a *JAK2*^{V617F} transgenic MF mouse model demonstrated that neoplastic fibrocytes are the major contributors to BM fibrosis in MF and that TGF-β1 is required for their differentiation from their precursors, the neoplastic monocytes (105).

1.2.2.5 BM stroma, niche and chronic inflammation

Further to the intrinsic leukaemic stem cell derangement, the microenvironment has a crucial role in the development of MPN (106-114). The BM is a specialized organ where normal haematopoiesis takes place and is a sanctuary in which malignant cells from a variety of haematological disorders proliferate and out-compete their normal counterparts (115). The supportive effect of the BM is mediated by secretion of soluble factors, like cytokines, but also through direct cellular contact between the leukaemic cells and the stromal marrow cells (116-118).

In fact, the BM stroma has been implicated in the cytoprotection of leukaemic cells from a variety of pharmacological compounds (119-122). In the context of MPN, the BM microenvironment protected MPN cells from the cytotoxic action of the JAK inhibitor atiprimod (123). Furthermore, BM-derived human stromal cell clone 5 (HS-5, see below) can protect MPN-derived cell lines and MPN patient-derived BM cells from the cytotoxic effects of ruxolitinib and the histone deacetylase inhibitor vorinostat (124). This protective effect is mediated, at least in part, by the secretion of soluble factors from the BM stroma and correlates with the activation of signalling pathways important for cellular homeostasis (such as JAK/STAT, PI3K, JNK, MEK/ERK and NF-κB). Interestingly, pharmacological inhibition of JNK and PI3K pathways completely abrogated the protective effect exerted by the presence of these stromal cells.

In a recent interesting study, BM stromal cells (BM-MSC) derived from healthy subjects (HD) were compared with those derived from MPN patients (MPN-MSC) (125). The gene expression profile showed a total of 169 genes that were differentially expressed. The ability of BM-MSC to support the growth and survival of HSPC was significantly higher for the MPN-MSC. Furthermore, MPN-MSC showed alterations in the expression of genes associated with the maintenance of haematopoiesis.

Finally, there is large body of evidence that the stromal cells in MPN are transformed into a pro-neoplastic supportive phenotype able to maintain the leukaemic stem cell clone and confer resistance to therapy (103, 126, 127).

1.2.2.6 Time

MF pathogenesis and progression result from an extremely complex interaction of multiple cellular and molecular players. Especially for this reason, it is fascinating how 3 different driver mutations create such an intricate scenario leading to the same disease and, on the other hand, the same driver mutation gives rise to three different MPN phenotypes of ET, PV and MF.

In view of this, it is acceptable to speculate that time is another crucial pathogenetic factor in MF, as the effect exerted by this intricate crosstalk on the disease evolution might depend on its prosecution over time. In support of this hypothesis there are findings of a long-term follow-up analysis of COMFORT-I study, which demonstrated that ruxolitinib induced greater *JAK2*^{V617F} allele burden reductions in patients with shorter disease durations (128). Furthermore, it has recently been shown that driver mutations in MPN can originate before birth (129).

MF is a chronic disease, which might last up to more than 10 years, so it is reasonable to think that the reiterated intra- and extracellular consequences of the driver mutations (or other unknown genetic lesions in triple-negative MF) finally lead to a biological derangement which is more profound when there is a longer time lapse from diagnosis. Any screening and testing of therapeutic targets will need to consider the dynamic aspect of this disease, impossible to recapitulate on cell line models or animal models.

1.2.3 Modern therapy for MF

1.2.3.1 Ruxolitinib

Ruxolitinib is the first JAK inhibitor developed for MF. It is type-I JAK1-2 inhibitor, that is an ATP-competitor binding to the kinase-active conformation of both wild-type and mutant-JAK2 (130), explaining its activity also in *CALR*- and *MPL*-mutated MF.

Two large phase 3 trials (COMFORT-I and COMFORT-II) compared ruxolitinib to placebo or best available therapy, respectively, in patients with IPSS intermediate-2 and high-risk MF. Ruxolitinib showed positive results in reduction of massive splenomegaly and resolution of constitutional symptoms (131, 132), which led to FDA approval in 2011.

Furthermore, ruxolitinib resulted effective in controlling the haematocrit, reducing the spleen volume, and improving symptoms in PV (133, 134), leading to its FDA approval in 2014 for the treatment of PV patients resistant or intolerant to hydroxycarbamide therapy. The use of ruxolitinib in ET has been more limited so far and preliminary data do not support any advantage compared to best available therapy (135).

The efficacy of ruxolitinib in MF, however, is not of the same magnitude as that resulting from BCR-ABL1 inhibition in chronic myeloid leukaemia and is considered palliative rather than curative (136).

In fact, ruxolitinib, like other clinically tested JAK2 inhibitors (137, 138), is unable to appreciably reduce the burden of *JAK2*-mutant allele in patients and thus cannot eradicate the

disease. Furthermore, ruxolitinib increases the probability of stabilisation of BM fibrosis in some patients but does not induce reversal (139, 140). Although a recent pooled analysis of COMFORT-I and COMFORT-II data showed a survival benefit for ruxolitinib in interemediate-2 and high-risk MF (132), this finding is not universally accepted (141). No data exist about the ability of ruxolitinib to prevent or delay disease progression to acute leukaemia. In addition, long-term follow-up of these clinical trials showed that 50% of patients had lost their response and more than 70% had discontinued the drug for disease progression and/or intolerance, within 5 years of starting treatment (131, 142). Finally, ruxolitinib is not free from significant serious toxicity, including a withdrawal syndrome upon its sudden discontinuation and risk of severe opportunistic infections and non-melanoma skin cancers (142-146).

Response to JAK inhibitors and predictive factors

Although the status of stable or progressive disease is well defined by the revised IWG-MRT and ELN response criteria (147), there is no universally accepted definition of clinical resistance to JAK inhibitors, as demonstrated by the variability of criteria used across clinical trials (JAKARTA-2 (148); FREEDOM [NCT03755518] and FREEDOM-2 [NCT03952039]). One possible reason could be that it is still unknown how responses such as "stable" disease or "improvement in anaemia", "reduction in spleen size" or "decreased symptomatic burden" while on JAK inhibitors impact on long term outcomes (i.e. duration of response, leukemic evolution, overall survival). A universal definition of JAK inhibitor failure is of particular relevance in the management of young patients, for whom a prompt decision on when to abandon the JAK inhibitor treatment and proceed to ASCT is of extreme importance. It is also relevant for clinical research, as it would facilitate comparisons of results from clinical studies investigating new therapies in patients failing ruxolitinib.

Although limited, there are some factors which might predict response to ruxolitinib. A recent analysis from the phase 3b prospective expanded-access study (JUMP), including 2233 MF patients treated with ruxolitinib, found that patients with lower IPSS scores and those receiving ruxolitinib as first-line treatment experienced higher spleen response rates and that higher ruxolitinib doses were more likely to induce better spleen volume reductions, although not symptom improvement (149). However, the authors could not identify any association between baseline clinical characteristics and the total ruxolitinib daily dose at week 12, such that the only useful predictor of ruxolitinib success is early intervention. A similar conclusion came from an independent retrospective multicentre analysis of 408 patients, where higher IPSS

scores, longer time from diagnosis to ruxolitinib start and lower ruxolitinib doses were negatively associated with spleen response (150).

Some evidence suggests that a MF molecular "fingerprint" at diagnosis might predict response to ruxolitinib. Analysis of the COMFORT-II study showed that when patients were defined as high molecular (according to the presence of any mutation in *ASXL1*, *EZH2*, *SRSF2*, and *IDH1–2*) and low molecular risk (151), this did not affect the likelihood of obtaining a >35% spleen volume reduction or symptomatic improvement (152). However, subsequent analysis of phase 1-2 studies on MF patients found that the presence of three or more mutations was associated with a worse spleen response and shorter time to ruxoltinib discontinuation (153). A recent study demonstrated that the presence of *ASXL1* or *EZH2* was independently associated with shorter time to ruxolitinib failure (154). Finally, in a very recent retrospective study, among 61 MF patients treated with JAK2 inhibitors (which was ruxolitinib in 57 of them) multivariate analysis revealed that *RAS*/*CBL* mutations were associated with significantly inferior symptom and spleen response, higher rate of evolution into acute leukaemia and inferior survival (155). Furthermore, the authors found that the absence of a *JAK2* mutation was associated with lower probability of symptom response, while presence of *ASXL1* mutation was associated with lower probability of spleen response.

During ruxolitinib therapy, some factors can predict outcome. One small study found that an increase in mutation burden while on ruxolitinib treatment correlated with higher rate of therapy discontinuation and/or death, while reduction of $JAK2^{V617F}$ allele burden was associated with spleen response (156). Another study showed that decreasing platelet count and the acquisition of additional mutations while on ruxolitinib were markers of poor prognosis (157).

Finally, after ruxolitinib failure, life expectancy is short, in particular in those patients who discontinued the drug at disease progression (158).

Biological resistance to JAK inhibitors

Despite the lack of validated baseline predictors of ruxolitinib response, increasing evidence is accumulating about the biological reasons of resistance. The hope is that surrogate markers of such resistance mechanisms could be soon found and introduced in clinical practice, in order to allow the identification of patients who may benefit the most from JAK inhibitor therapy and those who should proceed straight to alternative treatment, either experimental drugs or ASCT.

Currently, it is known that resistance to JAK inhibitors can either be acquired and occurring on exposure to the drug, or be intrinsic to the cell.

To the first group belong the acquired mutations in the JAK2 kinase domain and the mechanism of JAK2 heterodimer formation. Interestingly, the former has been found to confer resistance to ruxolitinib and other type-I inhibitors only in vitro in the context of mutagenesis screens (159-161), but they have never been detected in patients (162). As postulated by some researchers, this finding could derive from the fact that the submaximal target inhibition exerted by these agents, which would also explain the minimal effect on the allele burden, does not favour genetic escape (163). In contrast, the second phenomenon seems to explain the clinical observation that patients losing their response to ruxolitinib can regain sensitivity to this agent after temporary treatment interruptions (164), the effectiveness of which has been recently corroborated by mathematical modelling (165). After prolonged exposure to type-I JAK inhibitors (ruxolitinib, momelotinib, fedratinib), JAK2 can form heterodimers with other family members, which include JAK1 and TYK2 (JAK2-tyrosine kinase), with the consequent reactivation of JAK2 and persistence of JAK/STAT signalling, but this event is reversible upon treatment discontinuation (166-168). Also, this mechanism does not occur with the modern type-II JAK inhibitors (169), which bind and stabilise the inactive JAK kinase conformation. Interestingly, one of these inhibitors, CHZ868, exerts preferential targeting of the mutated MPN clone in mouse models (167). Additionally, this type-II JAK inhibitor is predicted not to be associated with JAK inhibitor withdrawal syndrome (common with type-I inhibitors), as the mechanism of this clinical manifestation has been strictly linked with the JAK-activation-loop hyperphosphorylation induced only by type-I inhibitors, which in turn is another possible functional mechanism of resistance to these agents (168, 170).

The newer type-II JAK inhibitors, along with JAK-mutant specific inhibitors (still in development)(171), have not yet entered clinical trials but represent a notable promise for the more effective targeting of JAK kinase.

With respect to intrinsic mechanisms of resistance, a recent study described how the *JAK2*^{V617F} mutation is able to induce ligand-independent homodimerization of type-I cytokine-receptor, through a mechanism which is not affected by ruxolitinib (172). Also, among the most studied mechanisms of intrinsic resistance to JAK inhibitor is the activation of alternative intracellular signalling pathways, which include both PI3K/AKT and MAPK pathways, and the contribution of deranged microenvironment components in concert with the abnormal inflammatory background characteristic of MF (173). In addition, as discussed above, MF patients with multiple genetic mutations seem to have inferior responses to ruxolitinib, and more than a third

of patients acquire such mutations during ruxolitinib treatment, which affect *ASXL1*, *TET2*, *EZH2*, *IDH1-2*, *TP53*, *DNMT3A* and other (174-176).

JAK2 has also been defined by some as a epigenetic "writer" (177), meaning that, apart from through JAK/STAT activation, JAK2 itself can sustain cell survival through direct control on epigenetic regulation (178), leading to intrinsic resistance to JAK inhibitor treatment (179).

A final thought is the possible role on disease progression and treatment resistance of ruxolitinib(or other JAK inhibitors)-induced immunosuppression (180), the latter being the basis of its success in inflammatory/autoimmune diseases such as graft versus host disease (GvHD) (181), rheumatoid arthritis, psoriasis (182), haemophagocytic lymphohistiocytosis (183) and COVID-19 (184). A recent single-cell study also showed that ruxolitinib induced suppression of interferon (INF) signalling in MF cells which was associated with inhibition of apoptosis (176). So, although no study has so far directly explored this possibility, the effect of ruxolitinib on the immune system could contribute to disease escape and treatment failure.

Finally, additional factors, independent from driver mutation allele burden and cytokines, should be explored in order to explain the observed peculiar and cell-intrinsic resistance to JAK2 inhibitors observed in MF compared to PV and ET cells (185).

Fedratinib is the only other type-I JAK2 inhibitor recently approved by FDA for the treatment of patients intolerant or resistant to ruxolitinib and it has led to response in approximately one third of subjects (148). No other agent is available outside clinical trials after ruxolitinib failure in MF.

1.2.3.2 Allogeneic haematopoietic stem cell transplantation

Apart from supportive treatment (blood product transfusion) and poorly effective conventional therapies (hydroxycarbamide, danazol, androgens, immunomodulatory drugs, prednisolone, splenectomy or others)(186), the only therapeutic choices after JAK inhibitor failure are either enrolment into clinical trials of new experimental agents (see next section) or ASCT for eligible patients.

The latter is the only potentially curative option for MF. Among the most important factors affecting the outcome of ASCT in MF is age (187). Age is no longer a limiting factor in view of the availability of reduced-intensity conditioning regimens (RIC), which allow an increased number of patients to benefit from this strategy. However, RIC ASCT seems to lead a poorer outcome compared to myeloablative conditioning (MAC) ASCT, with significantly lower 10-year overall and disease-free survivals (188). Donor type is also another important determinant, as matched related donors are usually considered the best choice compared to matched

unrelated (MUD) and mismatched related donors (MMRD)(189-192). However, with recent improvements in the conditioning platforms (193), prevention and treatment of GvHD and increased expertise in mismatched donor transplant management, the overall survival after ASCT has improved in recent years (194). The largest cohort study reported so far on MMRD ASCT in MF showed encouraging outcomes, suggesting that this strategy is feasible in this context and allows the extension of the transplant option to more patients. Also, the stem cell source affects the ASCT outcome in MF. Although there is no evidence to date to support the use of peripheral blood- vs bone marrow-derived HSC, the former are associated with faster neutrophil recovery (187, 192, 195, 196) and usually more GvHD and increased transplant-related mortality (TRM), while umbilical cord blood has led to worse results, due to high relapse rate and TRM (197-199).

On the other hand, disease-related characteristics play a role in determining the results of ASCT in MF. Mutational status might independently affect transplant outcome in MF, where *CALR* mutations appear to be associated with better results (200, 201). Current MF prognostic scores, which reflect the severity of the disease and estimate the risk of death, regardless of the treatment, have been used to select patients expected to have a significant survival benefit from transplant (202). A large retrospective study on patients younger than 65 years found that patients with intermediate-2 and high-risk DPISS clearly benefited from ASCT, while the low-risk group benefited from non-transplant therapy. The authors recommended individual counselling for subjects classified in the intermediate-1 risk group, for which the relative risk of death from ASCT was not significantly different compared to that from alternative treatment (203). For the latter group, the ELN/EBMT consensus recommends that patients up to the age 65 years should also be considered candidates for ASCT if they have either refractory, transfusion-dependent anaemia, >2% of blasts in the peripheral blood, adverse cytogenetics, or absence of *JAK2*/*CALR*/*MPL* mutations and/or *ASXL1* mutation-positive status (204).

In order to gain more insight into the expected ASCT outcome and to more appropriately choose the best management approach in patients eligible to intensive therapy, attempts have been made to develop transplant-specific prognostic scores. In the earliest, originating in the pre-ruxolitinib era, patients had poor survival after ASCT if they had at least two of these variables: having received more than 20 red blood cell unit transfusions before transplant, a spleen size >22 cm on ultrasound and a non-HLA-matched sibling donor (190). In the latest, the Myelofibrosis Transplant Scoring System (MTSS), four different survival groups were derived from the presence of some combination of the following poor-outcome factors: leukocytes >25 × 10^9/L, platelets <150 × 10^9/L, Karnofsky scale <90%, age >57 years,

presence of *ASXL1* mutation, *JAK2*-mutated or triple-negative status and transplant from a mismatched unrelated donor (205).

An additional prognostic factor is a good response to ruxolitinib, which has been associated with better transplant outcomes (206, 207), a finding that supports the recommendation to proceed to transplant even if the patient has a good response to ruxolitinib, whenever the cure is the final goal (208, 209). Also, some reports suggest that ruxolitinib pre-treatment might improve transplant outcomes (210, 211).

1.2.3.3 Experimental drugs

Given the heterogeneity of pathogenesis in MF, there is increasing interest in combination therapies, where, along with JAK inhibition, additional aspects of the disease are targeted; in parallel, new agents are under investigation as monotherapy for MF.

A summary of all experimental therapies under current investigation in MF are listed in Table 1.1. Figure 1.2 represents the intra- or extra-cellular targets of these treatments.

Some alternative therapies, such as histone deacetylase (HDAC)-inhibitors (212, 213), telomerase inhibitors (214), HSP90 inhibitors (215, 216) immunomodulatory drugs (217), have demonstrated limited efficacy as monotherapy, and are currently being explored in combination with ruxolitinib.

Agents targeting the PI3K/Akt/mTOR pathway dose-dependently inhibited *JAK2*^{V617F}-mutated cell lines and reduced the clonogenic activity of haematopoietic progenitors from patients with MPN (218). However, the first study assessing the combination of buparlisib (an oral pan-PI3K inhibitor) with ruxolitinib failed to show any improvement over ruxolitinib alone (219). Other PI3K inhibitors are at the moment under investigation for combinational therapy. Of note, justifying the need of further search for agents targeting this pathway, everolimus, an mTOR inhibitor, showed notable clinical activity as monotherapy in a phase1/2 trial in MF patients refractory to ruxolitinib, with reduction of splenomegaly >30% and complete resolution of symptoms in almost half and in 69% of patients, respectively (220).

Finally, certain new molecules failed to show a significant clinical benefit on MF patients, despite promising pre-clinical data, which include Hedgehog pathway inhibitors (sonidegib and vismodegib) (221, 222), inhibitors of angiogenesis (bevacizumab and sunitinib) (223, 224), and the antagonist of lysil-oxidase-like-2 protein (LOX2)(simtuzumab) (225).

Table 1.1. New agents under investigation for MF therapy (in monotherapy or combined with ruxolitinib).

Target		Agent	Monotherapy (phase)	+ Ruxolitinib (phase)	Trial number
Membrane receptor	JAK1	Itacitinib	2	2	NCT01633372 & NCT03144687
	JAK1/2	Momelotinib vs ruxolitinib	3	-	NCT01969838
	JAK1/2	NS-018	1/2	-	NCT01423851
	JAK2	Pacritinib	2,3	-	NCT03165734, NCT03645824
	JAK2	Fedratinib	3	-	NCT03755518
	JAK2	LY2784544	2	-	NCT01594723
	Interferon-α receptor	Peg-IFN-α-2a/-2b	3	-	NCT01387763
	Interferon-α receptor	Peg-IFN-α-2a	2	2	NCT00452023, NCT02742324 & EudraCT2013003295-12
	Interferon-α receptor	Ropeg-IFN-α-2b (P1101)	2	-	NCT02370329
	P-selectin	Crizanlizumab	-	1/2	NCT04097821
	PD-1	Pembrolizumab	2	-	NCT03065400
	TIM-3 + TGF-β	MBG453 + NIS793	1	-	NCT04283526
	CD123	Tagraxofusp (SL-401)	2	-	NCT02268253
	TGF-β	Sotatercept	2	-	NCT01712308
	TGF-β	Luspatercept	2	-	NCT03194542
	TGF-β	TGF-β trap (AVID200)	1/2b	-	NCT03895112
	TIM-3	MBG453	-	1/2	NCT04097821
	SLAMF7	Elotuzumab	2	-	NCT04517851
Intracellular enzyme/mediator	PIM kinase	TP-3654	1	-	NCT04176198
	PIM kinase	PIM447	-	1	NCT02370706
	CDK4/6	LEE011	-	1	NCT02370706
	Aurora kinase	Alisertib	1	-	NCT02530619
	HSP90	PU-H71	1	1	NCT03935555 & NCT03373877
	IDH2	Enasidenib	-	2	NCT04281498
	BCL-2/BCL-xL	Navitoclax	-	1,2	NCT04041050, NCT03222609
	PI3K	Idelalisib	-	1	NCT02436135
	PI3K	Parsaclisib	-	2	NCT02718300
	PI3K	Umbralisib	-	1	NCT02493530
	GSK-3β	9-ING-41	-	2	NCT04218071
	NEDD8	Pevonedistat	-	1	NCT03386214
	MDM2	KRT-232	2	-	NCT03662126
	MDM2	Siremadlin	-	1/2	NCT04097821
	SMAC mimetic	LCL161	-	2	NCT02098161
	MEK	Selumetinib + azacitidine	1	-	NCT03326310

Table 1.1. (continues from previous page)

	Target	Agent	Monotherapy (phase)	+ Ruxolitinib (phase)	Trial number
Nuclear effectors	Exportin 1	Selinexor	2	-	NCT03627403
	HDAC	Givinostat	2	-	NCT01761968
	HDAC	Panobinostat	-	1	NCT01693601, NCT01433445
	BET/BRD4	INCB057643	1	x	NCT04279847
	BET/BRD4	CPI-0610	-	1/2	NCT02158858
	DNA methyltransferase	Azacitidine	-	2	NCT01787487
	Telomerase	Imetelstat	2	-	NCT02426086
	histone demethylase specific for H3K4 (LSD1)	Bomedemstat	2	-	NCT03136185
other	Multiple targets	Thalidomide	-	2	NCT03069326
	Multiple targets	Pomalidomide	-	1/2	NCT01644110
	Multiple targets	PRM-151	x	2	NCT01981850

Figure 1.2. Potential therapeutical targets in MF and other MPN.
(adapted from Brkic S and Meyer SC, Hemasphere. 2020 Dec 29;5(1):e516)

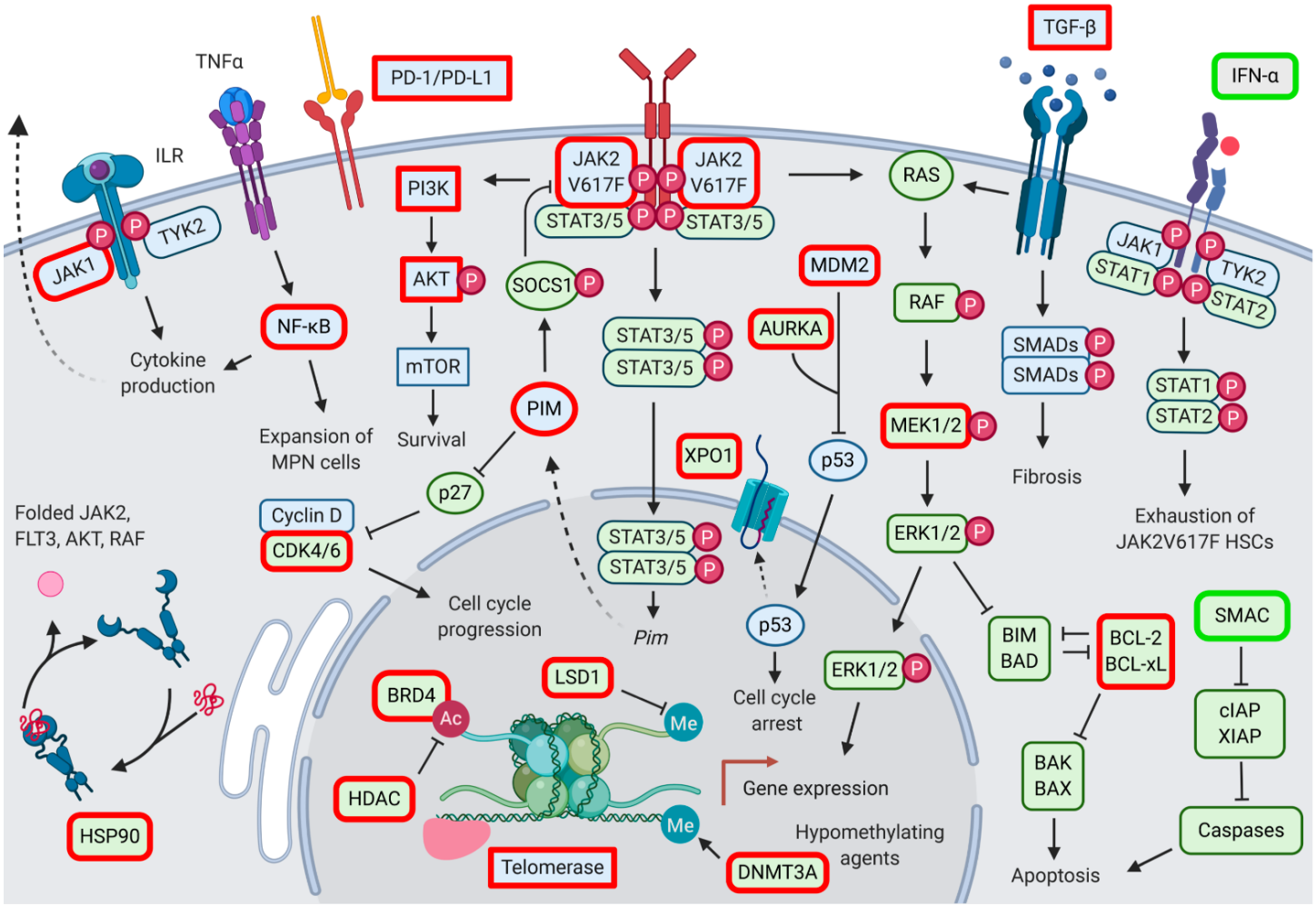

1.3 Project aims

As described in the above sections, MF pathogenesis and progression derive from an intricated network of players. However, the clonal HSC is probably the ideal target of therapies aimed at disease eradication.

The hypothesis of my work is that the survival of MF HSC might rely on cellular pathways not directly part of the JAK/STAT signalling cascade, which could also be responsible for the resistance to JAK2 inhibitors, and that their identification might constitute a ground for future more effective therapeutics.

The aim of the present doctoral project was to identify molecular pathways essential for the survival and resistance to JAK2 inhibition of the MPN leukemic stem/progenitor cells using the pooled-shRNA library screen, a function-first high-throughput method for this type of investigation (described below).

The first part of the work focused on identifying such targets and pathways using the human erythroleukaemia (HEL) cell line which is a commonly used model for *JAK2*^{V617F} positive neoplasm.

In order to explore the underlying mechanism of MPN expansion and survival following exposure to JAK2 inhibitors in the presence or absence of microenvironment, the pooled-shRNA library screen of the top depleted shRNAs was performed in three different settings:

1) Baseline (no ruxolitinib and no conditioned media [CM, described in the Methods])
2) Ruxolitinib
3) Ruxolitinib and CM.

Subsequently, the pooled-shRNA library screen was applied on CD34+ cells from patients with MF.

In the third part of the project, I performed gene expression analysis of CD34+ cells exposed to ruxolitinib in order to identify molecular alterations induced by the JAK2 inhibitor, and compared this with the results from the pooled-shRNA screen. The validated candidates derived from the integration of these results could identify potential targets for novel and more effective therapies.

1.4 shRNA and pooled-shRNA screens for cancer pathways

RNA interference (RNAi), a cellular process that regulates gene expression, has emerged as a powerful genetic strategy to interrogate the function of a gene or genes by suppressing the messenger RNA (mRNA). Small regulatory RNAs (siRNAs) and microRNAs (miRNAs) bind

to the enzymatic RNAi machinery and reduce the expression level of the complementary mRNAs (226). This process can be experimentally controlled to knock down the expression of any specific gene. The action of siRNAs is transient, lasting from 3 to 7 days, making this approach unsuitable for studying the long-term effects of gene silencing. The search for a sustained gene-silencing resulted in development of a class of RNAi called short hairpin RNAs (shRNAs). Integration of the plasmids expressing shRNAs into the cell genome establishes a stable gene-silencing through continuous supply of shRNA (227) (Figure 1.3).

Figure 1.3. Types of RNAi constructs used for gene silencing.
(adapted from Perwitasari O et al., Pharmaceuticals 2013, 6, 124-160).

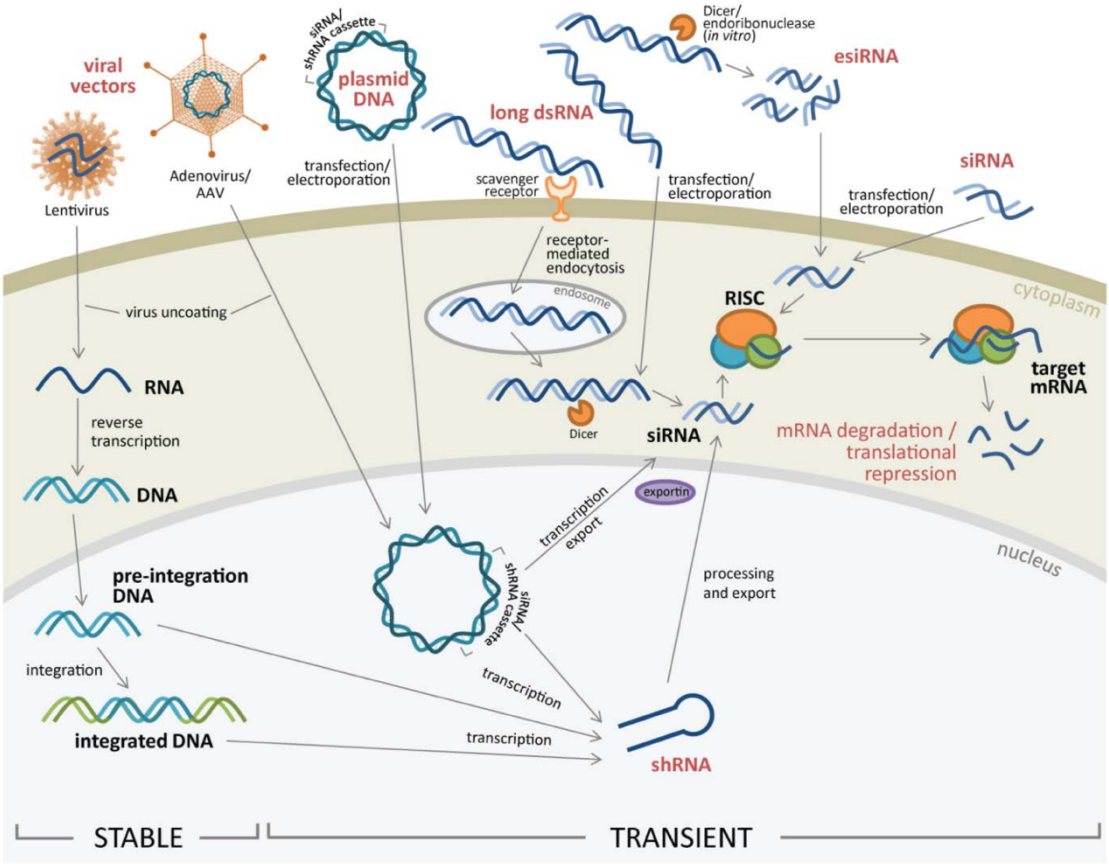

The synthetic or endogenously processed siRNA molecules are incorporated into the RNA-induced silencing complex (RISC) and mediate gene silencing through target mRNA cleavage (if perfect sequence complementarity exists between the target mRNA and the siRNA) or translational interference (if the complementarity is partial) (228).

There are two main approaches for applying a large-scale functional genomic screen to mammalian cells through siRNA: cell-based assays and pooled screens. In cell-based assays, cells are transfected with individual siRNAs or shRNAs and screened in a multi-well format

for the activation or repression of a reporter, biochemical activity, increased or decreased cell proliferation. In this approach, one individual gene is suppressed per well and analysis is carried out in a high-throughput manner using a robotic platform. However, this method is expensive, labour intensive, and time consuming. On the other hand, pooled screening allows the ability to analyse the effects of the whole library at one time. For example, if suppression of a particular gene by shRNA confers resistance to an inhibitor, the representation of that shRNA will increase in the pool in the presence of the inhibitor (positive selection) during the selection period (culture period). In contrast if a given shRNA sensitizes a cell population to the inhibitor, the relative abundance of this shRNA will diminish during the selection period (negative selection). Application of pooled-RNAi libraries provides the opportunity to investigate partial or entire genome in a loss-of-function approach. The RNAi library can be used for either positive or negative selection screens, in both of which the first step is the delivery and the integration of shRNAs into the target cells using a vehicle (i.e. lentiviral particles). In a positive screen, the shRNAs which give proliferative or survival advantage to the target cell are enriched at the end of the selection. In a negative screen, the shRNAs that are underrepresented after the selection period are the significant ones.

Single-copy integration, or low multiplicity of infection (MOI), is of critical importance for pooled screening to avoid combinatorial phenotypes deriving from simultaneous silencing of multiple genes per cell (229). This is achieved through limiting dilution where only a fraction of cells become infected upon exposure to the viral pool, and most infected cells integrate only a single shRNA construct. Uninfected cells are subsequently eliminated by puromycin selection as the construct contains a puromycin-resistant gene. As it was described earlier, the pooled-lentiviral shRNA screening strategy relies upon readout of the changes in the abundance of each shRNA clone in a pool of cells over a defined period of time, which is the selection period. A decline in representation of specific clones infers that their target mRNA is essential to cell viability (230, 231).

Pooled-shRNA library screen has led to important discoveries in cancer therapy and has been investigated in many haematological neoplasms, with interesting and promising results (232, 233).

However, despite their great scientific potential, RNAi screens, like all screening approaches, can be affected by false discovery (false-positive and false-negative results). For RNAi, false positives due to sequence-specific off-target effect are the main concern. siRNAs can induce silencing of non-target mRNAs with limited sequence complementarity, often via interactions with the 3′UTR (234). These interactions occur when short regions of the mRNA 3′-UTR

contain imperfect matches to the small RNA, triggering translational repression and/or degradation. Through this mechanism and depending on the sequence, a single siRNA can repress up to hundreds of transcripts (235). Interestingly, these off-target effects seem to be dosage dependent and the resulting phenotypes can dominate over the on-target phenotypes (236).

In addition to sequence specific off-target effects, there are non-sequence specific ones. In fact, the artificial siRNAs and shRNAs use a natural pathway that regulates cellular gene expression levels, where the system is governed by endogenous miRNAs which, as a result, can be displaced from RISC. This can lead to the impairment of gene transcript levels and consequently to off-target phenotypes (237).

1.5 Stromal cell lines

Two human stromal cell lines, HS-5 and BM-derived human stromal cells clone 27a (HS-27a), represent functionally distinct components of the BM microenvironment (238-240). They are derived from human BM stromal cells immortalised with replication-defective recombinant retrovirus containing the human papilloma virus E6/E7 genes. HS-27a supports cobblestone area formation by early haematopoietic progenitors. One study showed their capability to enhance erythroid commitment (241). HS-5, instead, is fibroblastoid and secretes multiple cytokines that support the proliferation of committed progenitors. Among the produced cytokines there are granulocyte colony-stimulating factor (G-CSF), granulocyte-macrophage-CSF (GM-CSF), Kit ligand, interleukin-6 (IL-6), interleukin-8 (IL-8), interleukin-11 (IL-11) and CLXCL10 (239).

The growth of haematopoietic progenitors is supported when they are co-cultured in CM obtained from HS-5 cells, and HS-5 CM induces the growth of significantly more colonies from human CD34+ CD38+ than a cocktail of recombinant cytokines (239). The capability of these cells to support and stimulate the growth of haematopoietic progenitors is probably responsible for the described ‘protective’ effect on haematopoietic neoplastic disorders (242-244), already discussed above for MPN. Several *in vitro* studies have depicted their role at inducing chemotherapy resistance in AML cell lines (245, 246) and primary AML cells (247).

1.6 MPN Cell lines

Many cell lines containing the *JAK2*^{V617F} mutation are available (248). Among them, the HEL cell line was established in 1982 from a patient with erythroleukaemia (FAB M6) (249). It is capable of spontaneous globin synthesis.

HEL cells are extensively used as a model for myeloproliferative neoplasms for *in vitro* biological and pharmacological research (250). Furthermore, HEL is the *JAK2*^{V617F} positive cell line with highest number of *JAK2* gene copies (251, 252).

CHAPTER 2

Methods

2.1 HEL cell

2.1.1 HEL cell line

Human erythroleukaemia cells (HEL) with homozygous expression of *JAK2*^{V617F} were purchased from Leibniz Institute DSMZ (German Collection of Microorganisms and Cell Cultures). They were grown in RF10 which is RPMI media (Thermo Fisher Scientific, USA) supplemented with 10% FBS (Thermo Fisher Scientific, USA), 1% penicillin/streptomycin (Thermo Fisher Scientific, USA) and 1% L-glutamine (Thermo Fisher Scientific, USA), as previously described (253-255).

During the normal culture condition and the pooled-shRNA library screening, a maximum density of 1.5 x 10^6 cells/mL was never exceeded, as recommended by the manufacturer.

2.1.2 Fluorescence in situ hybridization and NGS panel screen of HEL cells

To characterise the alterations of the *JAK2* gene in HEL cells, fluorescence in situ hybridization (FISH) was performed using two probes crossing the *JAK2* gene region, purchased from Kreatech, Leica Biosystems to measure *JAK2* copy numbers. Next-generation sequencing (NGS) of the DNA extracted from HEL cells was done through a Custom AmpliSeq for Illumina Myeloid Panel (Illumina, USA) targeting hot spots in 54 genes commonly mutated in myeloid malignancies.

Both FISH and NGS screens of HEL cells were performed at Molecular Pathology Laboratory at Hammersmith Hospital.

2.1.3 Viability assay

HEL cells were cultured in RF10 on a 6-well plate and seeded at a density of 0.5 x 10^6 cells/mL. Different concentration of ruxolitinib (Santa-Cruz Biotechnology, Texas, USA) were added to each well (0 nM, 150 nM, 300 nM, 500 nM, 750 nM). Cell viability was assessed by Trypan-blue exclusion at different time points and cells were counted using an automated cell counter (Countess II FL, Thermo Fisher Scientific, USA).

2.1.4 MTS assay

3-(4,5-dimethylthiazol-2-yl)-5-(3-carboxymethoxyphenyl)-2-(4-sulfophenyl)-2H-tetrazolium inner salt (MTS) assay was used to analyse cell proliferation under different treatment conditions. The CellTiter 96® AQueous Non-Radioactive Cell Proliferation Assay kit (Promega, UK) was utilised for this purpose. This is a metabolic assay which can identify viable cells based on their capability to reduce the yellow tetrazolium salt to a formazan product.

HEL cells (3 x 10^3) were suspended in 100 µL RF10 (plate A) or HS-5 CM (plate B). Cells were incubated with different concentrations of ruxolitinib: 0 nM, 50 nM, 100 nM, 150 nM, 300 nM, 500 nM, 750 nM, 1000 nM. Each plate contained 10 technical replicates and the experiment was repeated 3 times. Each plate was left for 72 hours in a 5% CO_2 incubator at 37 °C. Following the incubation period, 20 µL of PMS-MTS solution mix (ratio 1:20) was pipetted to each well of the 96-well plate containing 100 µL of cell suspension in either RF10 or HS-5 CM. The plate was incubated from 1-4 hours in a 5% CO_2 incubator at 37 °C and checked every 30 minutes until the colour of the medium in the control sample changed from yellow to dark brown (corresponding to high proportion of viable cells).

Viable cells were quantified by measuring absorbance in each well at 491 nm wavelength using Multiscan GO Microplate Spectrophotometer (Thermo Fisher Scientific, USA).

Statistical software Prism GraphPad (v.8; La Jolla, CA) was used to perform statistical analysis and graphs.

2.1.5 Apoptosis assay

HEL cells were seeded on a six-well plate at a density of 2.5 x 10^5/mL and grown in RF10 (plate A) and in HS-5 CM (plate B).

Apoptosis was assessed by staining with FITC-conjugated Annexin V (Miltenyi Biotec, Germany) in combination with DAPI (Miltenyi Biotec, Germany). Cells were analysed for fluorescence through flow-cytometry and analysed at 24h after the addiction of ruxolitinib 150 nM.

2.1.6 Western Blot

HEL cells were cultured at a density of 1 x 10^6/mL in RF10 with 0 nM, 150 nM, 300 nM and 600 nM ruxolitinib. At 3h and 27h 1-3 x 10^6 cells were collected and total cell lysates prepared. Cells were precipitated in a 15 ml centrifuge tube and kept on ice. A lysis buffer was prepared by adding protease and phosphatase inhibitor (Thermo Fisher Scientific, USA) to

Radioimmunoprecipitation assay (RIPA) buffer (Sigma-Aldrich, USA). Thirty µL of lysis buffer were added to 1 x 10^6 cells and transferred to 1.5 mL Eppendorf tubes. Cells were vortexed at highest speed for 15 seconds and incubated on ice for 10 minutes and this step was repeated for a total of 30 minutes. Finally, the tube was centrifuged for 5 minutes at 16000 G at 4 °C and supernatant collected in new Eppendorf tube and stored at -80 °C.

Protein lysates were quantified using Bradford's assay though DC Protein Assay kit (BioRad, USA), containing reagent A, B and S. Reagent A' was made of 20 µL of reagent S and 1 mL of reagent A. Protein concentrations of cell line extracts were determined against a standard curve produced using bovine serum albumin (BSA) (Sigma-Aldrich, USA), after preparation of serial dilution of BSA in lysis buffer (2 mg/mL, 1 mg/mL, 0.5 mg/mL, 0.25 mg/mL, 0.125 mg/mL). Five µL of protein standards and samples were pipetted into 96-well microplates (VWR, USA). Twenty-five µL of reagent A' and 200 µL of reagent B were added sequentially into each well. After 15 minutes incubation, absorbances were measured at 750 nm wavelength using Multiscan GO Microplate Spectrophotometer (Thermo Fisher Scientific, USA).

The level of the protein concentration was balanced between each treatment condition through appropriate dilution of the protein lysate in lysis buffer according to the calculated concentration of each sample, in order to ensure equal loading of proteins into the gel.

Equal amounts of proteins were aliquoted in 1.5 mL centrifuge tubes according to their concentration at a final volume of 30 µL. Ten µL of SDS NuPage sample buffer (Thermo Fisher Scientific, USA) were added to each of the sample tubes. These were then transferred on a 100 °C Dri-Block Heater (Techne, UK) and left for 7 minutes. The components of XCell SureLock Mini-Cell Kit (Thermo Fisher Scientific, USA) were assembled into the upper and lower buffer chambers and Nupage Bis-Tris 4-12% (Thermo Fisher scientific, USA) gel cassette set in place for electrophoretic protein separation. Running buffer was prepared by mixing 50 mL 20X MES SDS running buffer in 950 mL of distilled water and the required volume to fill the void between the gel cassette and cover the wells was transferred in, while 200 mL added to the lower buffer chamber. Fifteen µL of Novex sharp pre-stained protein ladder (Thermo Fisher Scientific, USA) was added in the first well, while 16-25 µL of sample buffer mix (corresponding to at least 50 µg of protein lysate) was pipetted into the following wells. The run lasted 90 minutes at 200 V.

The gel was then transferred through XCell II Blot Module (Thermo Fisher Scientific, USA). A transfer buffer was prepared mixing 50 mL of 20X NuPage transfer buffer (Thermo Fisher Scientific, USA), 150 mL methanol (VWR, USA), 1 mL Nupage antioxidant (Thermo Fisher Scientific, USA) and 849 mL deionised water. Bloating pads (Thermo Fisher scientific, USA)

were immersed in 700 mL of transfer buffer until saturated. Filter papers (Thermo Fisher Scientific, USA) and a transfer membrane polyvinylidene difluoride PVDF (Sigma-Aldrich, USA) were soaked 30 seconds in methanol, then rinsed quickly in water, soaked few minutes in transfer buffer sequentially. Transfer sandwich was made of 3 blotting pads, 2 filter papers, the gel, transfer membrane, 2 filter papers and 3 blotting pads, with PVDF positioned closer to the cathode respect to the gel. The transfer sandwich was positioned in the XCell II Blot Module, which was then filled with transfer buffer and 600 mL of deionised water in the outer chamber. The transfer duration from the gel onto the PVDF was 90 minutes at 30 V.

The PVDF membrane was then blocked using blocking buffer (phosphate buffered saline [PBS] [Thermo Fisher Scientific, USA] + 5% BSA [Sigma-Aldrich, USA] + 0.05% Tween [VWR, USA]) and left on an orbital shaking machine for 1 hour at room temperature.

The PVDF membranes were transferred and rolled in 20 mL tube (Sterilin, UK) with a primary antibody (anti-phospho-STAT5 [Y694] rabbit mAb and anti-β-tubulin rabbit mAb, from Cell Signalling Technology, USA) diluted in blocking buffer and incubated on roller machine overnight at 4 °C. Following overnight incubation and 4-times washing with washing buffer (PBS + 0.05% Tween), membranes were incubated with secondary antibody (swine anti-rabbit IgG HRP-linked; from Dako, Agilent Technologies, UK) in blocking buffer for 2h at room temperature on a roller machine. The washing steps were repeated 3 times with washing buffer and one last time with PBS only before imaging carried out with chemiluminescence using Amersham ECL kit (LifeSciences, UK). The reagent mix was distributed evenly on the membrane, rolled with a roller to avoid any air bubbles and left for 5 minutes in dark container, followed by visualizing the bands using ChemiDoc imaging system (BioRad, USA). Images were captured after a time of exposure range between 15 and 600 seconds.

Protein bands were analysed semi-quantitatively by densitometry using Image J software (version 1.52t; NIH, USA). The density of the protein bands was deducted from the density of the background and densitometric ratios (protein of interest/β-tubulin) were calculated and compared to the control sample.

2.2 HS-5 cell culture, transduction and conditioned medium

HS-5 cell lines were purchased from ATCC (Virginia, USA) and were cultured in RF10. In order to co-culture HS-5 cells with the primary cells which had been transduced with the shRNA construct containing puromycin-resistant gene, HS-5 cells were made resistant to

puromycin by transforming them with a pGIPZ lentivirus construct (Addgene, USA) carrying both a GFP marker and a puromycin resistance gene.

The construct was packaged in combination with vesicular stomatitis virus glycoprotein (VSV-G) (Clontech, Mountain View, CA) and psPAX2 (2nd generation packaging vector, Addgene, USA) using the ProFection® Mammalian Transfection System (Promega, Madison, WI) in 293FT cells (kindly donated by Prof. Michael Deininger, University of Utah) as recommended by the manufacturer. Transduction was performed when the confluency of the HS-5 cells reached 70%. Before transduction, the medium was replaced with fresh RF10, followed by adding polybrene (1 µg/mL) and pGIPZ lentivirus. The medium was replaced again after 18h. To purify transduced cells puromycin was added to the culture 72h after transduction at concentration of 2 µg/mL and maintained for 1 week. The percentage of fluorescing cells was assessed under a fluorescent microscope (Leica Microsystems). Conditioned medium (CM) from non-transduced HS-5 was harvested 24h after the achievement of 70-80% of confluence in a 75 mL flask, clarified by centrifugation and stored at -80 ºC.

2.3 Lentiviral production

2.3.1 Bacterial transformation, plasmid amplification and extraction

The packaging plasmid psPAX2 and vesicular stomatitis virus glycoprotein, pCMV-VSV-G (both purchase by Addgene, USA), were amplified using one Shot™ TOP10 Chemically Competent E. Coli (purchased from Thermo Fisher Scientific, USA), following a chemical transformation protocol which included heat shock at 42 ºC for 30 seconds. Afterwards, 50 µL of the transformation mixture were plated on 10 cm plates containing LB Agar (Sigma-Aldrich, UK), supplemented with 100 µg/mL ampicillin, and incubated overnight at 37ºC.

A single bacterial colony from each plate was selected and grown in 3 mL of LB medium supplemented with 100 µg/mL ampicillin, on a 37 ºC shacking incubator overnight. Finally, the culture was expanded on 300 mL of the same medium and grown again overnight in the same conditions.

The plasmid was then extracted using PureYieldTM Plasmid Maxiprep System kit (Promega, USA), as recommended by the manufacturers. The concentration of each plasmid was then measured using NanoDrop Lite spectrophotometer (Thermo Fisher Scientific, USA).

2.3.2 Viral vector production

The Human Module 1 (HM1) lentiviral shRNA library containing 27500 shRNAs targeting 5043 genes (5-6 shRNAs per gene) involved in cell signalling was purchased from Cellecta (http://www.cellecta.com/index.php). The lentiviral expression vector contains a puromycin-resistance gene (PuroR) and a red fluorescent protein (RFP) marker (TagRFP)(Figure 2.1). Each shRNA is linked to a unique 18-bp barcode identifiable by sequencing (see Appendix, Table A1 for specifications).

Second generation replication-defective lentiviral particles were generated by transient co-transfection of 293T cells with the two plasmids (psPAX2 and pCMV-VSV-G) and the lentiviral expression vector, using a $Ca_3(PO_4)_2$ precipitation method.

293T cells were grown in 75 mL flasks with Dulbecco's modified Eagle medium (DMEM)(Thermo Fisher Scientific, USA), supplemented with 10% FBS, 1% non-essential amino acids, 1% sodium-pyruvate, 1% penicillin-streptomycin, 1% L-glutamine. Immediately before transfection, DMEM was removed from each flask and replaced with the same fresh medium. The transfection mix included: 6 µg pCMV-VSV-G, 9 µg psPAX2, 9 µg shRNA construct, 186 µL 2 M $CaCl_2$, 1.5 mL ddH_2O and 1.5 mL 2 M HEPES buffer.

This solution (incubated for 20 minutes at room temperature) was then added dropwise into 30 mL DMEM cell suspension and all the mixture incubated at 37 ºC and 5% CO_2. At 24h the medium was changed.

The medium was harvested 48h post-transfection, centrifuged at low speed to remove cell debris. Subsequently, 30 mL of supernatant was added to each polypropylene ultra-centrifugation tube (6 × 30 mL), and ultra-centrifuged at 26000 rpm for 1h and 40 min at 4 °C (CP100NX ultracentrifuge, HITACHI, Japan). After centrifugation, the tubes were promptly removed and supernatant decanted. The viral pellet was resuspended in 0.3 mL of DMEM and snap-frozen at -80 °C.

Figure 2.1. DECIPHER pRSI12-U6-(sh)-HTS4-UbiC-TagRFP-2A-Puro 3rd generation transfer vector and 2nd generation lentivirus packaging system.

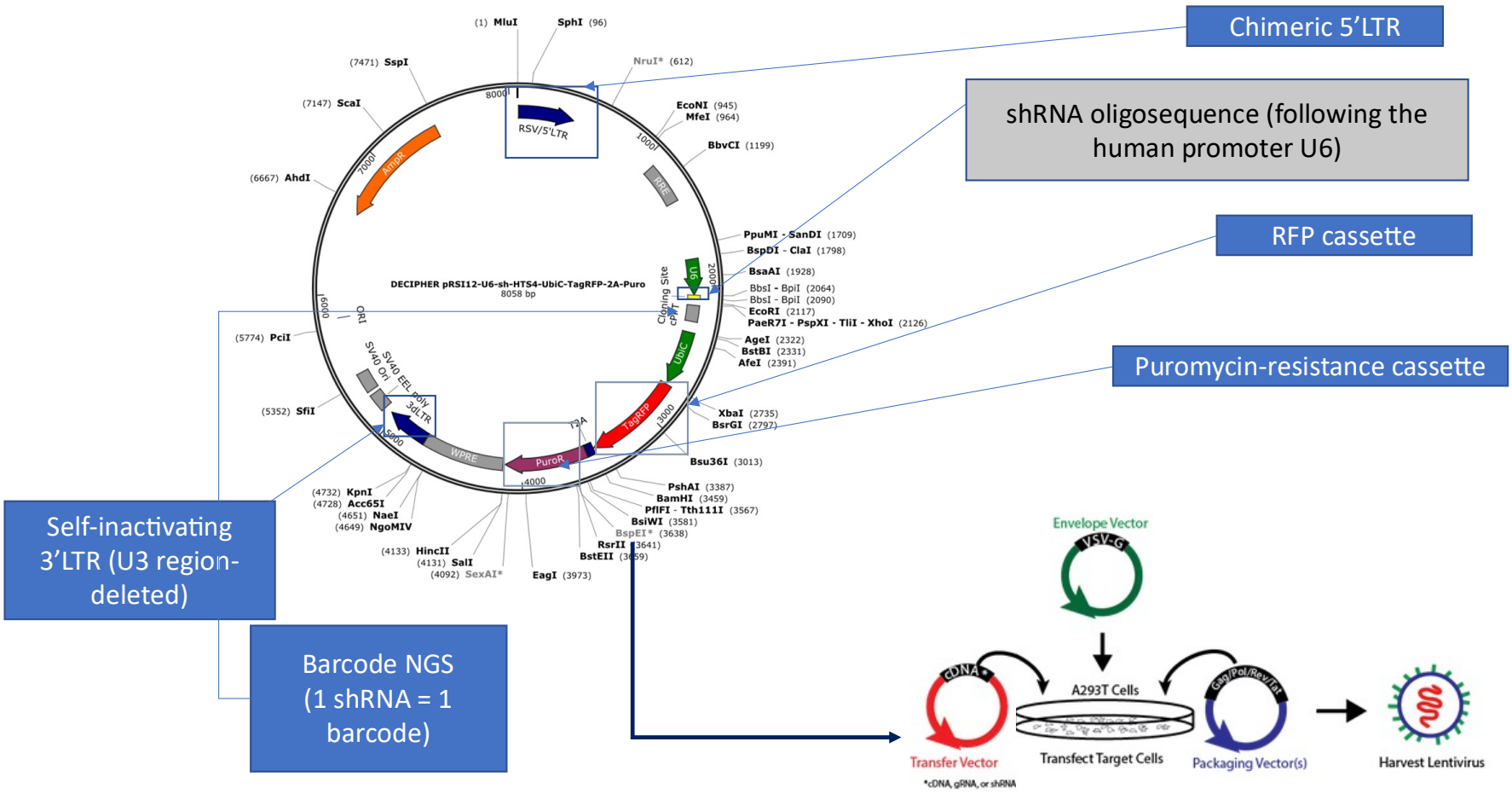

adapted from www.cellecta.com

adapted from www.addgene.org

2.3.3 Multiplicity of infection

The multiplicity of infection (MOI, which expresses the ratio between the number of viral particles to the number of target cells) of 0.3 was designed to ensure that the majority of transduced cells carry only one integrated provirus (as per Poisson's distribution formula, which describes the stochastic event of viral integration at a given MOI(256)), corresponding to ~30% of RFP-positive cells (as illustrated by the titre chart reported in Figure 2.2, from Cellecta Manual, v9a 02/03/2016).

For shRNA screens the number of cells stably transduced with the shRNA library at the time of transduction should exceed the complexity of the shRNA library by at least 200 fold (257). Given that the library contained 27500 shRNAs, the required transduced cell number was calculated to be at least 5.5 million cells. In order to reach the target of ~30% RFP-positive cells the total number of cells at transduction should be >16.5 million cells, explaining the choice for a HEL cell number at transduction of 20 x 10^6 (see section 2.6).

Figure 2.2. Lentiviral vector titre chart: relationship between transduced (RFP-positive) cells and MOI. *(modified from Cellecta Manual, v9a 02/03/2016)*

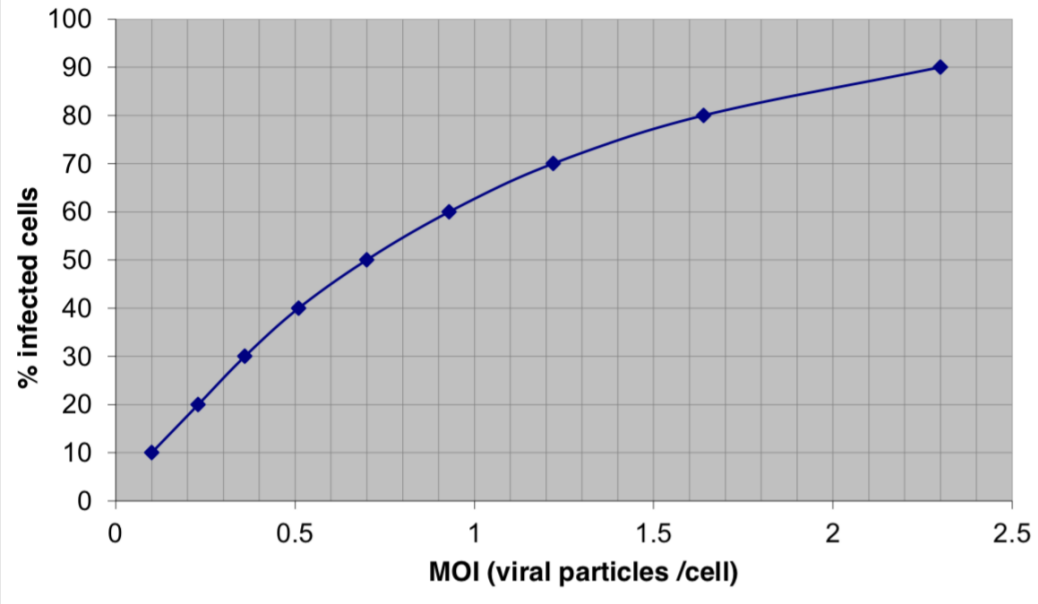

2.3.4 In vitro transduction and determination of lentiviral vector titre

K562 cells are used routinely to determine lentiviral particle titration in our laboratory. Cultured K562 cells were grown and maintained at a density of 5 x 10^5 cells/mL and transduced with serially diluted and concentrated viral vector stocks (as per manufacturer's instructions, Cellecta Manual, v.9a 2/3/2006). Seventy-two hours after transduction, RFP-positive

fluorescent cells were estimated by flow cytometry. The viral vector titre in TU (transducing units/µL; 1 TU produces one integration event per target cell) was determined as follows:

$$\text{Virus TU/µL} = \text{n cells at transduction} * \text{MOI/µL of vector inoculum at transduction.}$$

Once obtained the lentiviral titer, the amount of viral stock to use for each experiment was calculated as follows:

$$\text{Vector inoculum to be used (µL)} = \text{n of cells at transduction} * \text{desired MOI/virus TU.}$$

2.4 Pooled shRNA screening pipeline

The classical pipeline for a negative pooled-shRNA screening is illustrated in Figure 2.3. HEL cells were seeded at 1.5 x 10^6/mL in 6-well plates. All experiments were run in duplicate, with a total starting cell number of 20 x 10^6 cells per replicate. Cell transduction was performed by adding 1 M HEPES buffer, polybrene 8 µg/mL and lentivirus at a MOI of 0.3 to each well containing cultured HEL cells. Soon after, cell plates underwent spinoculation (1800 rpm, at 32 °C for 90 minutes) and were incubated at 37 °C, 5% CO_2. Within 12-18h the medium was replaced. At 72h post-transduction, cells were analysed for RFP expression, and one-third was snap frozen to be used later as baseline control. Experiments with a transduction efficiency of >40% and < 10% were considered as failures and not brought forward to the screening phase. The remaining two-thirds of cells was cultured for 9 days with maintaining puromycin at a concentration of 2 µg/µL, in order to selectively favour the growth of transduced cells (puromycin-resistant).

Cells were cultured in three different settings:

1) RF10
2) RF10 + ruxolitinib (maintaining the concentration of 150 nM)
3) HS-5 CM only + ruxolitinib (added daily at a concentration of 150 nM) for the first 3 days, followed by the combination of HS-5 CM (50% of the volume) and RF10 (50% of the volume) + ruxolitinib.

The combination of CM with RF10 for the last 6 days of culture in setting 3 was to avoid the depletion of the medium from metabolic components.

After 9 days, cells were collected and the cell pellet was stored at -80 ^{o}C for future DNA extraction. DNA extraction was performed through phenol–chloroform extraction method, as described in section 2.7 and as per previously applied protocol (232).

After the amplification of the shRNA barcodes and the NGS (discussed in the next sections), shRNA barcode abundance between day-0 and day-9 samples was compared by means of bioinformatic analysis and the top depleted shRNAs were identified through a previously established pipeline (232). The finding from the pooled-shRNA screen was validated in HEL cells and primary cells isolated from patients with MF.

Figure 2.3. Pooled-shRNA library screen pipeline on HEL cell line.

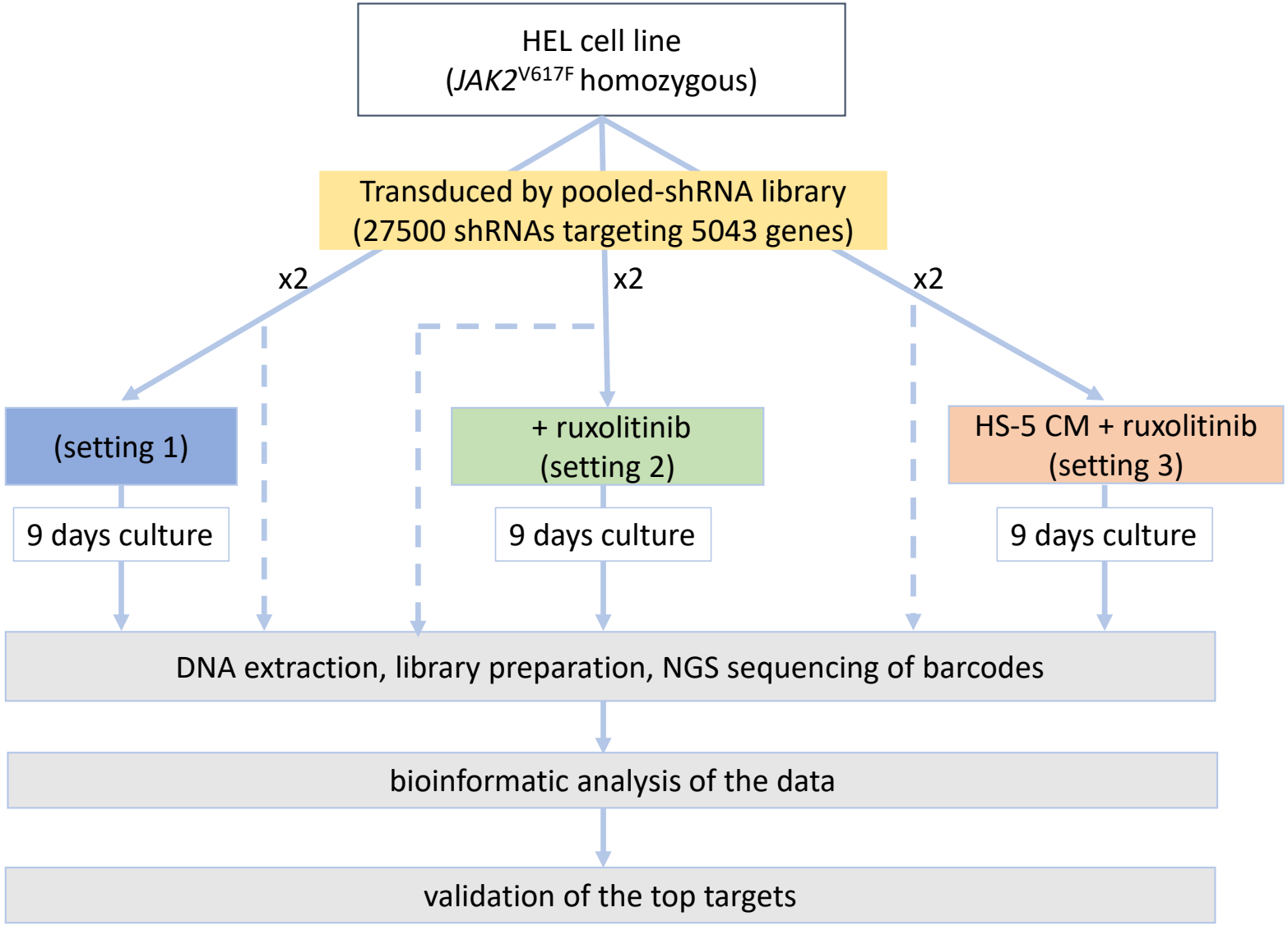

2.5 Isolation of MF CD34+ cells from peripheral blood-derived mononuclear cells

Patients gave written informed consent for research (in accordance with MPN-JK-16-003 ethical approval from Imperial College Tissue Bank). Mononuclear cells were obtained from 15-20 mL of fresh peripheral blood through density gradient separation using LymphoprepTM (StemCell Technologies, Canada). Subsequently, CD34+ positive cells were isolated using magnetic beads selection as recommended by the manufacturer (anti-CD34 antibody-conjugated supermagnetic microbeads and MACS columns purchased from Myltenyi Biotec, Germany).

2.6 Lentiviral transduction and pooled-shRNA screening of primary cells

Peripheral blood-derived CD34+ cells from patients diagnosed with primary or secondary MF were cultured and expanded in RF10 supplemented with 10 µL/mL CC100 human recombinant cytokine cocktail containing FLT3L, SCF, IL-3 and IL-6 (Stem Cell Technologies, Canada) in a 24-well plate, at a density of 1 x 10^6 cells/mL. After 3 days in culture, cells were counted, checked for CD34+ fraction at flow cytometry and transduced with lentiviral vector through the same process described above for HEL cells. After 72h from transduction, RFP-positivity was assessed through flow cytometry. On the same day, after collection of one-third of cells as a baseline sample, the remaining cells were transferred on top of puromycin-resistant HS-5 cells (prepared 24h before in a 6-well plate, at a density of 3 x 10^5 cells/mL) and co-cultured for 9 days, with daily replacement of medium and addition of puromycin 2 µg/µL. On day-9 of co-culture, RFP+ cells underwent fluorescence activated cell sorting (FACS) and stored at -80^{o}C for subsequent analysis.

The flow cytometry analysis on both HEL cell and primary CD34+ cell experiments and the FACS were performed at Centre for Haematology, Department of Immunology and Inflammation and MRC-BRC Flow Cytometry Facility, Imperial College, respectively.

2.7 DNA extraction

Cell pellets collected at baseline and after the selection period were lysed for DNA extraction, using the following steps. One mL of Qiagen RLT buffer (from Qiagen DNA extraction kit, Qiagen, Germany) was added to ≤ 1 x 10^7 cells and the cell pellet was dissolved. Then SDS 20% at one-twentieth of cell suspension volume was added and left for 5 minutes, after which

the content was mixed with 21-G syringe for 10-15 times. Phenol chloroform 1:1 volume was added and the solution vortexed. After centrifuging the mixture for 20 minutes at 12000 rpm, 0.1:1 and 0.8:1 volumes of 3 M NaOAc and isopropanolol were added, respectively, and the tube was inverted repeatedly multiple times until strings of DNA became visible. After new centrifugation at 12000 rpm for 10 minutes, the supernatant was discarded and the pellet mixed with 1 mL of 70% ethanol and centrifuged for 5 minutes at 12000 rpm. Finally, 56 µL of DEPC-treated water (Thermo Fisher Scientific, USA) was added to the pellet and the tube was put at 55 °C for 5 minutes, after which the DNA content was measured through NanoDrop Lite spectrophotometer (Thermo Fisher Scientific, USA). An A260/A280 ratio between 1.8 and 2 was considered satisfactory.

2.8 shRNA barcode amplification, purification and isolation and NGS

Extracted DNA was used to amplify the 27500 shRNA barcodes using LNGS-101, NGS Prep Kit for shRNA Libraries in pRSI12 (DECIPHER).

2.8.1 First-round PCR

For each sample a total of 50 µg of genomic DNA was used for 1st-round PCR. A PCR mix was prepared as shown in Table 2.1.

Table 2.1. First-round PCR mix for shRNA barcode amplification.

Volume x1	Volume x8*	Component	Primer sequence
10 µL	80 µL	Taq Polymerase buffer	
2 µL	16 µL	dNTP Mix	
3 µL	24 µL	Forward 1st-round PCR primer	5'-TTCTCTGGCAAGCAAAAGACGGCATA-3'
3 µL	24 µL	Reverse 1st-round PCR primer	5'-TAGCCAACGCATCGCACAAGCCA-3'
2 µL	16 µL	Taq Polymerase	
20 µL	**160 µL**	**Total volume**	

Table legend: * = the table provides an example, where for given 6 samples and 1 negative control the PCR mix was prepared for 8 volumes considering the possible volume loss during pipetting; dNTP = deoxynucleotide triphosphate.

The PCR mix was prepared and centrifuged gently and then split in 7 PCR tubes (6 samples plus 1 negative control (N.C.), 20 µl in each tube, to which was then added PCR-grade water (H_2O) and genomic DNA in the proportion reported in Table 2.2.

Table 2.2. H_2O-genomic DNA ratios in the 1st-round PCR for shRNA barcode amplification.

	H_20 in PCR (µL)	Genomic DNA in PCR (µL)
1	60	20
2	55	25
3	55	25
4	55	25
5	30	50
6	25	55
N.C.	80	-

The PCR mix was then performed according to the cycling conditions reported in Table 2.3.

Table 2.3. First-round PCR for shRNA barcode amplification: cycling conditions.

Temperature	Time	nº of cycles
94 ºC	2 minutes	1
94 ºC **65 ºC** **72 ºC**	45 seconds 15 seconds 30 seconds	16
72 ºC	2 minutes	1

2.8.2 Second-round PCR

The goal of the 2nd-round PCR was to significantly reduce genomic DNA carryover into the NGS step, and to add the P5 and P7 sequences that are complementary to the immobilized primers in the NGS Illumina Flow Cells.

An analytical PCR was performed independently to establish the optimised conditions for the 2nd-round PCR step (i.e. to find the optimal cycle number for the 2nd-round PCR in order to avoid overcycling of PCR reactions and to assess the adequacy of the starting amount of the 1st-round PCR product to use for the 2nd-round PCR).

For this intermediate PCR, PCR mix was prepared as shown in the table below (in the second column is reported the total mix volume for a given 7 PCR reactions):

Table 2.4. PCR mix of the intermediate PCR for shRNA barcode amplification.

Volume x1	Volume x8*	Component	Primer sequence
36.1 µL	288.8 µL	H_2O	
5 µL	40 µL	Taq Polymerase Buffer	
0.4 µL	3.2 µL	dNTP Mix	
2.5 µL	20 µL	NFwd primer	5'-CAAGCAGAAGACGGCATACGAGA-3'
2.5 µL	20 µL	NRev primer	5'-AATGATACGGCGACCACCGAGA-3'
1 µL	8 µL	Taq Polymerase	
47.5 µL	**380 µL**	**Total volume**	

Table legend: * = as for Table 2.1; dNTP = deoxynucleotide triphosphate; NFwd primer = nested forward primer; NRev primer = nested reverse primer.

The PCR mix was mixed and centrifuged gently and then split in 7 PCR tubes (6 sample + 1 negative control, N.C.), 20 µl in each to which was then added 2.5 µL of the 1st-round PCR product.

The PCR was then performed with the following cycling conditions:

Table 2.5. Intermediate PCR for shRNA barcode amplification: cycling conditions.

Temperature	Time	nº of cycles
94 ºC	2 minutes	1
94 ºC **65 ºC** **72 ºC**	45 seconds 15 seconds 30 seconds	12
72 ºC	2 minutes	1

The amplified barcodes were analysed on a 3.5% agarose-1x TAE gel to verify band brightness. Based on the results we adjusted the number of PCR cycles to use on the 2nd-round PCR (ranging from 10 to 14 cycles) and the amount of 1st-round PCR product. For example, in case the amplified band had a very weak appearance after the analytical intermediate PCR step, two reactions were run for that sample instead of one, in order to obtain more amplified barcode DNA to sequence at the end of 2nd-round PCR.

For the 2nd-round of PCR, an aliquot of 5 µL of the 1st-round PCR product for each sample was used. The components of the PCR mix for the 2nd-round PCR are shown in Table 2.6.

Table 2.6. Second-round PCR mix for shRNA barcode amplification.

Volume x1	Volume x8*	Component	Primer sequence
71 µl	568 µl	H_2O	
10 µl	80 µl	Taq Polymerase buffer	
2 µl	16 µl	dNTP Mix	
5 µl	40 µl	NFwd primer	5'-CAAGCAGAAGACGGCATACGAGA-3'
2 µl	16 µl	Taq Polymerase	
90 µl	**720 µl**	**Total volume**	

Table legend: * = as for Table 2.1; dNTP = deoxynucleotide triphosphate; NFwd primer = nested forward primer.

As the NGS Illumina sequencing was carried out in multiplex (multiple samples per lane), reverse indexed primers were used (each identified by one letter, see below Table 2.7).
After mixing gently and centrifuging briefly, 90 µL of the above mixture were put in each tube, which were labelled with the letter corresponding to the specific reverse indexed-primer, as per the below table. To each tube were added 5 µL of the reverse indexed primer (or 5 µL H_2O for the N.C.) and 5 µL of the amplified DNA from 1st-round PCR:

Table 2.7. Second-round PCR for shRNA barcode amplification: NRev Indexed Primers.

ID	NRev Index Primer	Index sequence
1	A	TACGAC
2	B	CTGATG
3	C	GCATCA
4	D	AGTCGT
5	E	TCGCAT
6	F	CATAGC

The 2nd-round PCR was performed according the following cycling conditions (* for primary cell experiments 16 cycles were used):

Table 2.8. Second-round PCR for shRNA barcode amplification: cycling conditions.

Temperature	Duration	n^{o} of cycles
94 °C	2 minutes	1
94 °C **65 °C** **72 °C**	45 seconds 15 seconds 30 seconds	10-14*
72 °C	2 minutes	1

After the PCR, the amplified DNA from each tube (and in case of two tubes for the same sample, the PCR product was mixed in a new single tube) was purified using the QIAquick PCR purification kit (Qiagen, Germany) following the manufacturer's protocol.
Finally, 30 µL of purified PCR product from each sample was run on a 3.5% agarose-1x TAE-gel (110 V for 20 minutes). The remaining PCR products were stored at 4° C for further use, if needed.
The band were read under UV lamp, then cut from the gel and put in a tube for DNA isolation. The amplified DNA in each electrophoretic band was extracted from the gel using the QIAquick gel purification kit (Qiagen, Germany). DNA was then measured through Qubit 2.0 Fluorometer (Invitrogen, USA).
Samples were randomized prior to sequencing on a NextSeq 500 (Illumina, USA) to avoid potential biases associated with variable sequencing depths and other NGS-related artefacts (258).

2.9 Bioinformatic analysis of pooled-shRNA library screens

Bioinformatic analyses and fold change (FC) calculations were performed by our research collaborator Clinton Mason (Department of Pediatrics, Division of Pediatric Hematology and Oncology, University of Utah, Salt Lake City, UT, USA) as previously described (232, 259).
In summary, the barcodes for each shRNA were identified in the sequencing data for each sample. Tallying and subsequent normalization of shRNA read counts allowed for FC calculations to assess the degree of depletion compared to baseline for each shRNA in live cells. Comparison of reads at baseline and follow-up controlled against the possibility of FC bias, which may happen due to dissimilar shRNA incorporation when a surrogate baseline control is used. Out of the 27500 shRNAs, 563 were excluded from the analysis due to their being either "control" shRNA (210 shRNAs, as per manufacturer's instruction) or targeting a sequence no longer part of the mRNA sequence pertaining to their respective gene in RefSeqGene database (353 shRNAs)(Table A2). The "control" shRNAs targeted the following genes: *EIF3A*, *ACTB*, *GAPDH*, *KIF11*, *PLK1*, *POLR2B*, *RBL2*, *RBX1* and *ACTA1* ("positive controls", supposed to be essential for cell survival) and *LUC* (luciferase, "negative control"). The "control" shRNAs were not included in the analysis because of the limitations associated with using the genes targeted by them for proving the goodness of mRNA-based screens. These limitations comprise the diversity in tissue-specific expression and role of these genes (260-262) and the existence of pseudogenes (263, 264). Figure A2 and A3 report the outcome of the

performance of the "control" shRNAs in our pooled-shRNA library screen. Although *LUC*- and *RBX1*-, *EIF3A*-, *KIF11*-targeting shRNAs behaved on average as "controls" (i.e. showing a median FC ≅ 1 ["negative control"] or a relatively high median FC ["positive control"], respectively), we found overall an high degree of result variability, especially in the sets of shRNAs targeting the "positive control" genes.

In view of this, the reproducibility of shRNA read counts between biological replicates was taken into account as alternative method for assessing the data quality. Statistical analyses of the data were performed in SAS (version 9.1).

2.10 MTS assay on primary cells

2.10.1 Experiments on continuous-inhibitors exposure

For the MTS assay, 2-5 x 10^4 CD34+ cells isolated from healthy donor cells (obtained from G-CSF-stimulated leukapheresis) were suspended in 100 µL StemSpan medium supplemented with CC100 (Stem Cell Technologies, Canada) in each well of 96-well plate, after 24-48h expansion in absence of drug. Similarly, 2-5 x 10^4 CD34+ cells isolated from peripheral blood from MF patients were suspended in 100 µL of StemSpan medium supplemented with CC100 in each well of 96-well plate and were expanded for 24-48h.

Different concentrations of carfilzomib (Abcam, UK) (CFZ) were tested with and without 300 nM ruxolitinib. This ruxolitinib concentration was chosen because it is in between the ruxolitinib C_{max} of 1000 nM in human plasma after a single oral dose of 25 mg and the concentration of 45.6 nM after 12h (when a new dose is given in a twice daily regimen)(265). Experiments were done in triplicate and analysed after 24-72h of incubation in a 5% CO_2 incubator at 37 °C.

For the Trypan Blue viability assay CD34+ cells were seeded in each well of a 24-well plate at a concentration of 0.25-0.5 x 10^6/mL in StemSpan medium supplemented with CC100 and were expanded for 24h-48h in the absence of any drug. Cells were counted with automated cell counter (Countess II FL, Thermo Fisher Scientific, USA). Different concentrations of CFZ were then tested, with and without 300 nM ruxolitinib. Experiments were done in triplicate and analysed after 24-72h of incubation in a 5% CO_2 incubator at 37 °C.

2.10.2 Exposure to pulsed proteasome inhibitors

In order to recapitulate the *in vivo* pharmacokinetic of proteasome inhibitors (PI), the effects on cell viability of pulsed-PI alone or in the presence of ruxolitinib were assessed on both MNCs and CD34+ cells derived from peripheral blood of MF patients (as shown in Figure 2.4).

Figure 2.4. Pulsed-PI in vitro exposure: experimental design.

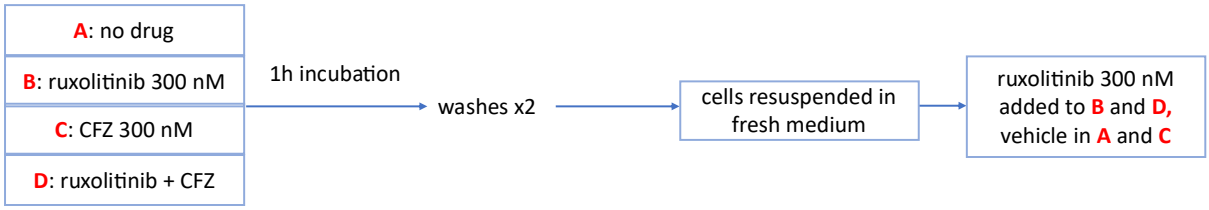

For MF MNCs, cells were seeded in a 24-well plate at a density of 0.3 x 10^6/mL in StemSpan and transferred in a 5% CO_2 incubator at 37 °C for 1h after the addition of (A) medium with no drug; (B) ruxolitinib 300 nM; (C) CFZ 300 nM; and (D) combination of the two drugs. Then, after 1-2 washes with phosphate-buffered saline (PBS, Thermo Fisher Scientific, USA) cells from the above conditions were resuspended in StemSpam supplemented with CC100 and treated with (A) no drug; (B) ruxolitinib 300 nM; (C) no drug; and (D) ruxolitinib 300 nM. Trypan blue viability assay was performed after 48h or 72h incubation.

For MF CD34+, cells were exposed for 1h to CFZ 300 nM +/- ruxolitinib 300 nM (following the same procedure described above for MNCs). Then, after washing with PBS, two experiments were carried out: 1) 2.5-3 x 10^4 cells were seeded in each well of a 96-well plate in 100 µL StemSpan + CC100 and treated respectively with (A) no drug; (B) ruxolitinib 300 nM; (C) no drug; and (D) ruxolitinib 300 nM and cell viability was assessed using MTS assay at 24h-72h; 2) cells were resuspended in StemSpam + CC100 in a 24-well plate (0.3-0.5 x 10^6 cells/mL) with (A) no drug; (B) ruxolitinib 300 nM; (C) no drug and (D) ruxolitinib 300 nM respectively, followed by Trypan blue viability assay after 24-48h.

As for the continuous exposure experiments, for Trypan blue assays, cells were counted with automated cell counter (Countess II FL, Thermo Fisher Scientific, USA).

Following the same scheme described above, a limited number of experiments were also done with bortezomib (BTZ)(Axon MedChem, Netherlands) instead of CFZ.

2.11 Apoptosis and cell cycle analysis on primary cells

Apoptosis on primary cells was assessed by staining with FITC-conjugated Annexin V in combination with propidium iodide as per company recommendations (Miltenyi Biotec, Germany). Cells were re-suspended in 100 µL PBS and stained with Annexin V, incubated for 15 minutes in dark and then stained with propidium iodide immediately before flow-cytometric analysis.

For the cell cycle assay, cells were stained with Hoechst 33342 dye (Thermo Fisher Scientific, USA) at a concentration of 10 µM, and prepared in PBS (Thermo Fisher Scientific, USA). Flow-cytometry analysis was performed after 1h incubation in darkness.

2.12 Experimental design for gene expression profiling of primary cells

In order to explore the molecular pathways important for the survival of MF leukemic stem cells on exposure to JAK2 inhibitor, CD34+ cells were isolated from peripheral blood of MF patients and expanded for 2 days in StemSpan medium supplemented with CC100. Cells were then split in two different experimental settings: in the absence (A) or presence (B) of ruxolitinib 300 nM. After 48h, cells were collected and total RNA extracted with RNeasy Mini kit (Qiagen, Germany) for total RNA-Seq.

2.13 RNA extraction and sequencing

Total RNA extracts from CD34+ cell of MF patients were separated using RNeasy Mini kit. Up to 5 x 10^6 cells were pelleted in 15 mL centrifuge tubes after spinning at 1500 rpm for 5 minutes and lysed with 350 µL of RNeasy Lysis buffer (RLT buffer) by pipetting ~20 times. Then, 350 µL of 70% ethanol was added to the same volume of lysate and mixed. The resulting 700 µL of lysate mix were transferred to RNeasy eliminator spin column (Qiagen, Germany), placed in 2 mL collection tube (Qiagen, Germany) and centrifuged at 12000 rpm for 15 seconds.

DNase digestion with RNase-Free DNase set (Qiagen, Germany) was performed at this stage, adding 80 µL of the solution mix DNase stock solution-buffer RDD (ratio 1:7) to the RNeasy spin column and left for 15 minutes at room temperature.

After this, 350 µL of RW1 buffer were added to the spin column, centrifuged at 12000 rpm for 15 seconds. Five-hundred µL of RPE buffer were added to the spin column and centrifuged at 12000 rpm for 15 seconds. This step was repeated to wash the spin column membrane but

centrifugation prolonged to 2 minutes. The spin column was placed in a new 2 mL collection tube, centrifuged at full speed for 1 minute and placed in a new 1.5 mL collection tube. Thirty-fifty µL RNase- free water were added and the spin column was centrifuged at 12000 rpm for 1 minute to elute the RNA. RNA concertation was quantified using NanoDrop Lite spectrophotometer (Thermo Fisher Scientific, USA). The RNA extracts were incubated in the heating block at 65 °C for 10 minutes and then stored a -80 °C.

Messenger-RNA was sequenced through HiSeq 4000 (Illumina, USA) in BRC Genomic Facility at Imperial College London, using 75bp paired-end DNA sequencing and dual index libraries (to reduce sample mix-ups when multiplexing samples on the same lane). Ten samples (5 patients, 2 conditions) were pooled in order to reduce the batch effect and then run over two lanes (5 samples per lane), with a predicted 70-80 million reads per sample.

2.14 Bioinformatic analysis of RNA-seq data

Bioinformatic analysis of RNA-seq data was performed by the research collaborator Andrea Bianchi, with the support of Prof. Antinisca De Marco (both from Department of Information Engineering, University of L'Aquila, Italy) and Cristina Pellegrini (from Department of Biotechnological and Applied Clinical Science, University of L'Aquila, Italy).

RNA-seq data were generated from $CD34^+$ cells of 3 MF patients after 48h of *in vitro* treatment with 300 nM ruxolitinib or vehicle for each sample.

In order to identify gene regions matching the read sequences, sequencing alignment was performed by using the human genome as reference (GRCh38.p13; https://www.ensembl.org/Homo_sapiens/Info/Index).

The alignment was performed with STAR (https://github.com/alexdobin/STAR version '2.7.5a') tool, with the '*--twopassMode Basic*' parameter enabled. The genome index was created from scratch with reference to the GRCh38 genome (ftp://ftp.ensembl.org/pub/release-100/fasta/homo_sapiens/dna/, primary assembly version). In order to quantify gene expression, we counted the number of reads that map to each gene using 'featureCounts' (http://subread.sourceforge.net/ version '2.0.1'). The reads were normalised and the differential expression analysis was performed by using the 'DESeq2' package (version '1.26.0'). Heat maps were produced using the 'pheatmap' package on R3.6.0 and included only genes showing adjusted p values <0.05 and log fold change > 1 in absolute value.

The Gene Set Enrichment Analysis (GSEA) was performed on all differentially expressed genes (not filtered by thresholds on padj and fold change), by using the 'GSEA' software

(https://www.gsea-msigdb.org/gsea/index.jsp version '4.0.3') with the '*Collapse/Remap to gene symbols*' parameter enabled in 'No_Collapse' mode. We used canonical pathways from KEGG and BIOCARTA as the reference database (version '7.1') in GSEA analysis. Other parameters were used with default settings: 10 as min number of members, 500 as max number of members, and 1000 as permutations.

2.15 RT-qPCR on primary cells

After RNA extraction, complementary DNA (cDNA) was synthesized by reverse transcription, using M-MLV Reverse Transcriptase (Invitrogen, USA) and random primers (random hexadeoxynucleotides) (Promega, USA). RNAsin (Progmega, USA) and M-MLV Reverse Transcriptase (Invitrogen, USA) were added to 25 mM dNTPs (dATP, dCTP, dGTP and dTTP) (Promega, USA) and mixed gently. This cDNA mix was then transferred to each RNA extract, and the tubes were left at 37 °C for 2h, followed by incubation at 65 °C for 10 minutes to inactivate the reverse transcriptase. cDNA samples were stored at -20 °C.

The quantitative reverse transcription polymerase chain reaction (RT-qPCR) was performed in StepOnePlusTM Real- Time PCR System from Applied Biosystems (Thermo Fisher Scientific, USA). The reaction volume was 10 µL composed by: 5 µL of TaqMan fast master mix (2x) from Applied Biosystems (Thermo Fisher Scientific, USA), 1 µL of sample cDNA, 3.5 µL of RNase-free water and 0.5 µL from each primer TaqMan gene expression assays from Applied Biosystems (Thermo Fisher Scientific, USA) (Table 2.9) per each reaction. Each sample was run in triplicate for both gene of interest and control gene (*GUSB*).

Table 2.9. Candidate target genes evaluated and TaqMan gene expression assay reference ID.

Gene symbol	Product number TaqMan gene expression assay
ARG1	Hs00163660
FLT3	Hs00174690
PTGDS	Hs00168748
GUSB	Hs00939627

Master mix for each gene was loaded into 96-well TaqMan qPCR plate (Thermo Fisher Scientific, USA), one reaction per well. The RT-qPCR reaction settings are shown in the Table 2.10.

Table 2.10. RT-qPCR cycling conditions.

Temperature	Time	nº of cycles
72 ºC	2 minutes	1
95 ºC	2 minutes	1
95 ºC **60ºC**	15 seconds 20 seconds	45

The StepOnePlusTM Real-Time PCR software was used to obtain cycle threshold (CT) values and amplification plots. Samples for which there was a difference >0.5 in the CT value across triplicates were excluded from the analysis. Gene expression fold change between treated and untreated samples was calculated according to the following formula:

$$\text{Gene expression fold change for } PTGDS = 2^{-\Delta CT\ (treated)} / 2^{-\Delta CT\ (untreated)}$$

where $\Delta CT = PTGDS_{CT\ average} - GUSB_{CT\ average}$, and
CT average = sum of CT values for 3 replicates for each sample/3.
Statistical analysis was performed through Prism GraphPad (v.8; La Jolla, CA).

2.16 NF-κB pathway low-density microarray on primary cells

Applied Biosystems® TaqMan® Array Human NF-κB Pathway 96-well Plate (Thermo Fisher Scientific, USA) was used to analyse the differential expression profile of a set of genes belonging to the NF-κB pathway, between different treatment conditions of the pulsed experiment on primary cells (please refer to section 2.10.2). The panel of assays in this plate targets genes codifying for 5 proteins of the Rel/NF-κB family: NFKB1, NFKB2, REL A, REL B, and REL; genes from IκB kinase, IκBs (inhibitor of κB), Toll-like receptor (TLR), Tumor Necrosis Factor (TNF), Tumor Necrosis Factor Receptors (TNFR), and Tumor Necrosis Factor Receptor Associated Factor (TRAF) families; genes associated with NF-κB function in apoptosis, immune/inflammation responses and genes codifying for chemokines and cytokines part of the general NF-κB pathway. Each plate contains high-quality Applied Biosystems® TaqMan® gene expression preloaded assays (for both target genes and endogenous controls) dried-down in the bottom of each well. Table 2.11 shows the full list of genes' assays contained in each reaction well and their disposition across the plate (for the list of TaqMan® gene expression assay ID for each gene please refer to the Appendix), where in pink are highlighted the control genes.

Table 2.11. Applied Biosystems® TaqMan® Array Human NF-kB Pathway 96-well Plate: list of genes.

	1	2	3	4	5	6	7	8	9	10	11	12
A	18S	GAPDH	HPRT1	GUSB	TLR4	TLR8	PTGS2	NFKBIA	RELA	MYC	IRAK1	LTBR
B	ICAM1	NOS2	IL1R1	IL12A	RIPK1	CCL20	CSF2	SELE	IL10	IL1A	IL1B	IL8
C	IL2	TNF	IL6	CSF1	NFKB2	IKBKG	IRAK2	MAP3K7	MAP3K14	TBK1	BCL3	FASLG
D	MYD88	NFKBIB	BTRC	TRAF5	TRAF2	ZFP36	TNFRSF11A	CD83	TRAF4	TRAF1	MAP3K7IP1	ENPP2
E	CREB1	CREBBP	RELB	IL12B	CCL2	NFKBIE	TNFAIP3	STAT1	CXCL1	TRAF3	TNFSF11	PTAFR
F	TNFRSF10A	TLR6	IER3	TNFSF15	TLR1	CARD14	VCAM1	TNFRSF10B	CARD10	EDARADD	TLR9	NKIRAS2
G	NKIRAS1	MAP3K1	IKBKB	IRAK1BP1	FADD	TRADD	ZNF675	BCL2	TLR7	PTGES	CSF3	NFKB1
H	IL2RA	BCL10	REL	BIRC5,EPR1	CHUK	TNFRSF1A	MALT1	TLR2	LTA	AKT1	CD40	TLR3

Quantitative PCR volume reaction was 10 µL, made of: 5 µL of TaqMan™ Fast Advanced Master Mix and 5 µL of the sample cDNA + nuclease-free water, ensuring that the final cDNA concentration per well was between 5-50 ng. After mixing gently, the master mix was combined with the sample cDNA in a 1.5 mL Eppendorf. The tube was vortexed and then centrifuged briefly. The mixture of Master Mix and cDNA-nuclease free water was distributed in each well with automatic pipette. Then the plate was sealed with MicroAmp™ Optical Adhesive Film, and then centrifuged before being read though StepOnePlusTM Real-Time PCR System from Applied Biosystems (Thermo Fisher Scientific, USA). The thermal protocol used was the following:

Table 2.12. RT-qPCR cycling conditions for Applied Biosystems® TaqMan® Array Human NF-κB Pathway 96-well Plate.

Temperature	Time	nº of cycles
50 ºC	2 minutes	1
95 ºC	20 seconds	1
95 ºC **60 ºC**	1 second 20 seconds	40

The StepOnePlusTM Real-Time PCR software was used to obtain cycle threshold CT values and amplification plots. Analysis of CT values and fold changes followed the same method described in the previous section.

2.17 Colony formation assay on primary cells

CD34+ cells isolated from peripheral blood of patients with MF were exposed to inhibitors as described in section 2.10. Two types of approaches were used:

- continuous drug exposure: cells were plated in a medium containing the inhibitors
- pulsed exposure: after the 1h-pulsed exposure step (refer to section 2.10.2), cells were plated with the addition of ruxolitinib in the group B and D.

Eleven µL StemSpan CC100 human cytokine cocktail was added to a 15 mL Falcon tube, to which was added 440 µL of a StemSpan cell suspension having a cellular density of 5000 cells/mL, supplemented with inhibitors where needed.

Finally, 1.8 mL of Methocult H4434 Classic (StemCell Technologies), pre-warmed for 2-4h, were aspirated from the bottle using a 3 mL syringe connected to a blunt-end needle and were added to the cell medium and mixed thoroughly 15-20 times, trying to avoid bubbles. One mL of this new mixture was plated into each of 2 small 35 mm x 10 mm round dishes. The latter were incubated inside a large round dish at 37 °C and 5% CO_2 for 13-14 days, after creating a moist chamber with soaked paper towel and a 35 mm open dish full of sterile water, placed at the centre of the chamber. Each experiment was run in duplicate. Colonies were manually counted under microscope, using a 35 mm gridded scoring dish as a guide.

2.18 Western Blot on primary cells

For western blot experiments, 2 x 10^6 $CD34^+$ cells isolated from peripheral blood of a patient with MF were treated for 24h with ruxolitinib 300 nM, 1 h-pulsed CFZ 300 nM and combination of the two (as illustrated in Figure 2.2). Cells were then lysate with NE-PER™ nuclear and cytoplasmic extraction kit (Thermo Fisher Scientific, USA), according to manufacturer protocol. Protein lysates were quantified using Bradford's assay though DC Protein Assay kit (BioRad, USA). Absorbances were measured at 750 nm wavelength using Multiscan GO Microplate Spectrophotometer (Thermo Fisher Scientific, USA). Twenty-seven µL of protein lysate solution from each sample was loaded into Nupage Bis-Tris 4-12% (Thermo Fisher Scientific, USA) gel cassette and run into XCell SureLock Mini-Cell kit (Thermo Fisher Scientific, USA) and the gel was then transferred utilising XCell II Blot Module (Thermo Fisher Scientific, USA) on to PDVF membranes (Thermo Fisher Scientific, USA). These were sequentially incubated with primary antibodies (anti-Phospho-NF-κB p65 [Ser536] rabbit mAb, anti-β-tubulin rabbit mAb, anti-NF-κB p65 [D14E12] XP rabbit mAb

and anti-lamin B1 rabbit mAb; from Cell Signalling Technology, USA) and secondary antibodies (rabbit anti-mouse IgG HRP-linked and swine anti-rabbit IgG HRP-linked; from Dako, Agilent Technologies, UK). Imaging was carried out with chemiluminescence using Amersham ECL kit (Life Sciences, UK). Western blot bands were visualised using ChemiDoc imaging system (Bio-Rad, USA). Images were captured after a time of exposure range between 30 and 1200 seconds. Protein bands were analysed semi-quantitatively by densitometry using Image J software (version 1.52t; NIH, USA). The density of the protein bands was deducted from the density of the background and densitometric ratios (protein of interest/β-tubulin or lamin B1) were calculated and compared to the control sample.

2.19 Additional MTS experiments on primary cells

Following the same procedure described in section 2.10.1 for MTS, CD34+ cells from healthy donor and from MF patients were exposed to PDG2 (prostaglandin-2, product of lipocalin-type prostaglandin-D2 synthase [L-PTGDS]; from Cayman Chemical Company, USA) 5 μM and AT-56 (a potent and selective inhibitor of L-PTGDS; from Tocris Bioscience, UK) 100 μM in order to further explore results of gene expression profile experiment.

CHAPTER 3

Results

3.1 HEL cell line pre-shRNA screen analysis

3.1.1 Genomic characterization of the HEL cell line

FISH was performed on HEL cell line through the use of a double probe system crossing the *JAK2* gene region (Figure 3.1). FISH confirmed that this cell line bears multiple copies of *JAK2*, as previously reported (266).

Figure 3.1. Fluorescence in situ hybridization of HEL cells.

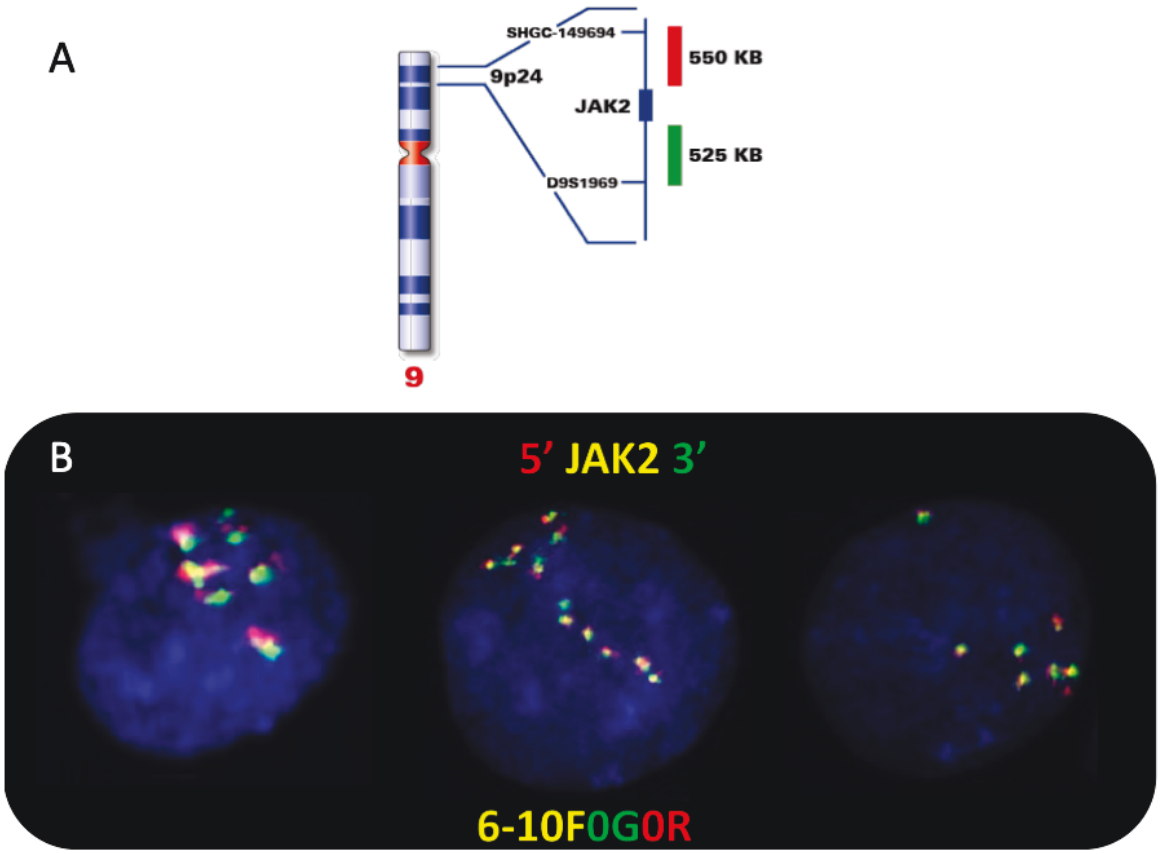

Figure 3.1. A: positions of probes in the *JAK2* gene region on the short arm of chromosome 9. B: FISH on HEL cell line. The yellow-coloured signal indicates that both probes (green and red) are very close each to the other, indicating that the *JAK2* is not involved in chromosomal translocation/deletion. The number of the yellow signals (6-10F, where F= fusion signal, G= green signal, R = red signal) equals the number of integer *JAK2* gene copies per cell.

In order to confirm the presence of *JAK2*^{V617F} mutation in this cell line, we applied a NGS panel containing 54 genes commonly mutated in myeloid neoplasm. This revealed the presence of homozygous V167F mutation in exon 14 of *JAK2* and homozygous M133L mutation in exon 5 of *TP53*. Figure 3.2 illustrates the NGS panel and the sequencing results in detail.

3.1.2 Reduced sensitivity of the HEL cells to ruxolitinib in presence of CM mimicking BM microenvironment

The proliferation assay of HEL cells exposed to increasing ruxolitinib concentrations showed that 150 nM was the least effective in inhibiting the cell proliferation (Figure 3.3). This was confirmed by the MTS assay, in which 300 nM was the lowest concentration able to significantly reduce the number of viable cells (Figure 3.4). However, in the presence of microenvironment, the lowest effective dose causing a statistically significant reduction in viability was 750 nM. When directly comparing the two conditions, concentrations of 300, 500, 750 and 1000 nM were significantly more effective in reducing the cell viability in the absence of HS-5 CM (p <0.001, 0.013, 0.016 and <0.001, respectively, from two-way ANOVA).

In fact, in line with previous observations (124), the HEL cell line cultured in HS-5-derived CM was protected from the suppressive action of ruxolitinib: the IC50s of HEL cells in RF10 or in the presence of CM were 1.2 µM and 3.4 µM, respectively (Figure 3.5).

The protective effect of the microenvironment was reflected by a reduction of the apoptotic cells compared to RF10 alone (Figure 3.6). However, even a concentration of ruxolitinib as low as 150 nM was able to reduce the activation of JAK/STAT pathway (Figure 3.7). On the basis of this evidence, this 150 nM was the concentration chosen for the pooled-shRNA screening phase on HEL cells, with the aim of inhibiting the JAK/STAT pathway without affecting markedly the cell survival.

Figure 3.2. Myeloid NGS panel applied to the HEL cell line.

Gene	Target Region (exon)	Gene	Target Region (exon)	Gene	Target Region (exon)	Gene	Target Region (exon)
ABL1	4–6	*DNMT3A*	full	*KDM6A*	full	*RAD21*	full
ASXL1	12	*ETV6/TEL*	full	*KIT*	2, 8–11, 13 + 17	*RUNX1*	full
ATRX	8-10 and 17–31	*EZH2*	full	*KRAS*	2 + 3	*SETBP1*	4 (partial)
BCOR	full	*FBXW7*	9 + 10 + 11	*MLL*	5–8	*SF3B1*	13–16
BCORL1	full	*FLT3*	14 + 15 + 20	*MPL*	10	*SMC1A*	2, 11, 16 + 17
BRAF	15	*GATA1*	2	*MYD88*	3–5	*SMC3*	10, 13, 19, 23, 25 + 28
CALR	9	*GATA2*	2–6	*NOTCH1*	26-28 + 34	*SRSF2*	1
CBL	8 + 9	*GNAS*	8 + 9	*NPM1*	12	*STAG2*	full
CBLB	9, 10	*HRAS*	2 + 3	*NRAS*	2 + 3	*TET2*	3–11
CBLC	9, 10	*IDH1*	4	*PDGFRA*	12, 14, 18	*TP53*	2–11
CDKN2A	full	*IDH2*	4	*PHF6*	full	*U2AF1*	2 + 6
CEBPA	full	*IKZF1*	full	*PTEN*	5 + 7	*WT1*	7 + 9
CSF3R	14–17	*JAK2*	12 + 14	*PTPN11*	3 + 13	*ZRSR2*	full
CUX1	full	*JAK3*	13				

JAK2 Exon 14
c1849G>T
p.(Val617Phe)
- allele depth 35119
- total read depth 35129
- variant read frequency: 99.9%

TP53 Exon 5
c398T>A
p.(Met133Lys)
- allele depth 1195
- total read depth 1200
- variant read frequency: 99.58%

Figure 3.3. HEL cell proliferation assay.

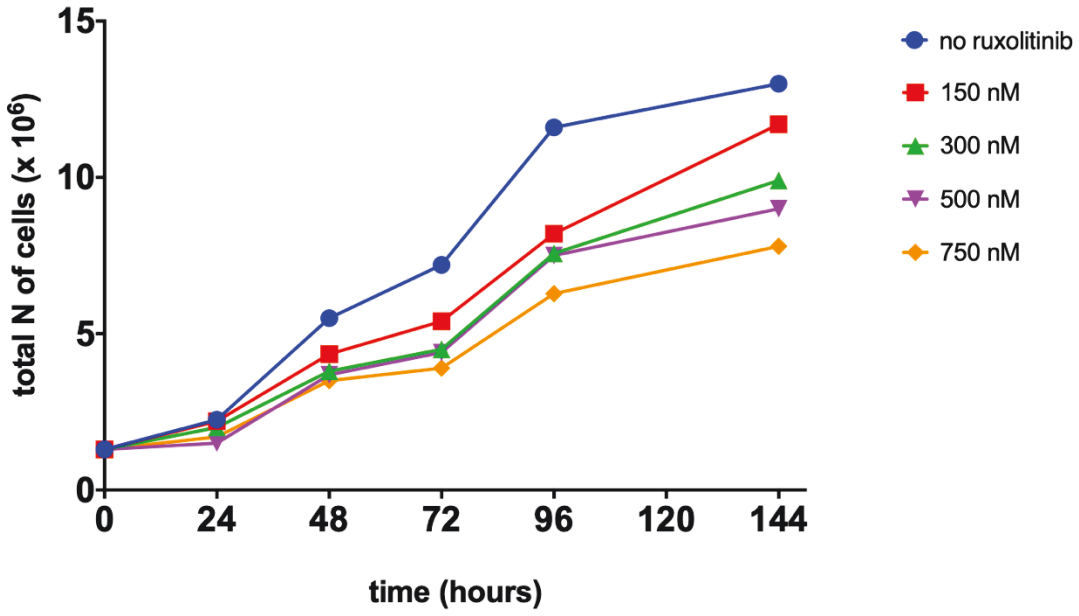

Figure 3.3. Each line refers to cells cultured at specific ruxolitinib concentrations (see colour code), where each dot indicates the total number of viable cells assessed through Trypan blue assay. The graph illustrate data from a single representative experiment (please refer to Methods for details).

Figure 3.4. MTS assay on HEL cell line.

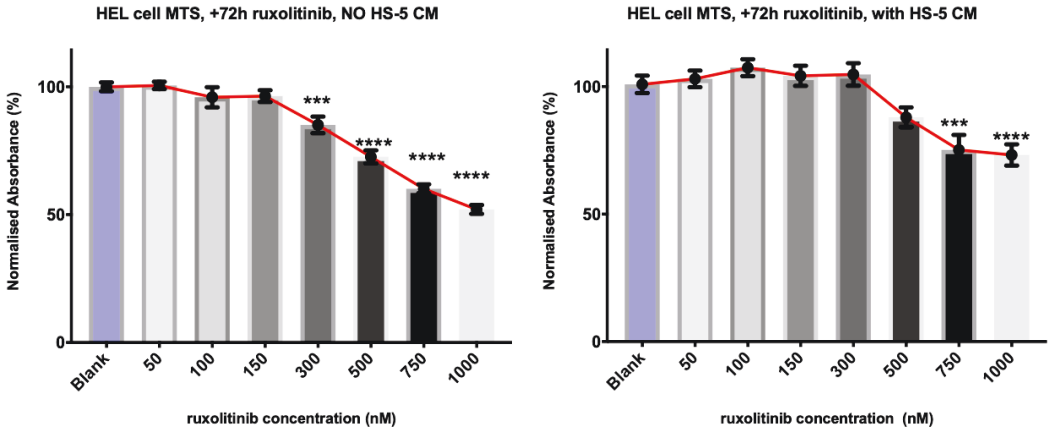

Figure 3.4: The MTS assay was performed with the same conditions for each setting: HEL cells cultured in RF10 + increasing concentration of ruxolitinib vs HEL cells cultured in HS-5 CM (10 wells for the control and for each drug concentration were read). In the figure is reported the normalised absorbance compared to the mean absorbance of the untreated control (Blank), after removing the absorbance values of the cell-free mixture of medium-MTS. Bars indicate the mean ± SEM of three different experiment replicates for each of the setting (culture in RF10 vs culture in HS-5 CM). Asterisks express the statistical significance from one-way ANOVA of the comparison of each treatment condition vs the untreated control (where **= p<0.01, ***= p<0.001 and ****= p<0.0001).

Figure 3.5. Ruxolitinib IC_{50} in HEL cell cultured in RF10 and HS-5 CM.

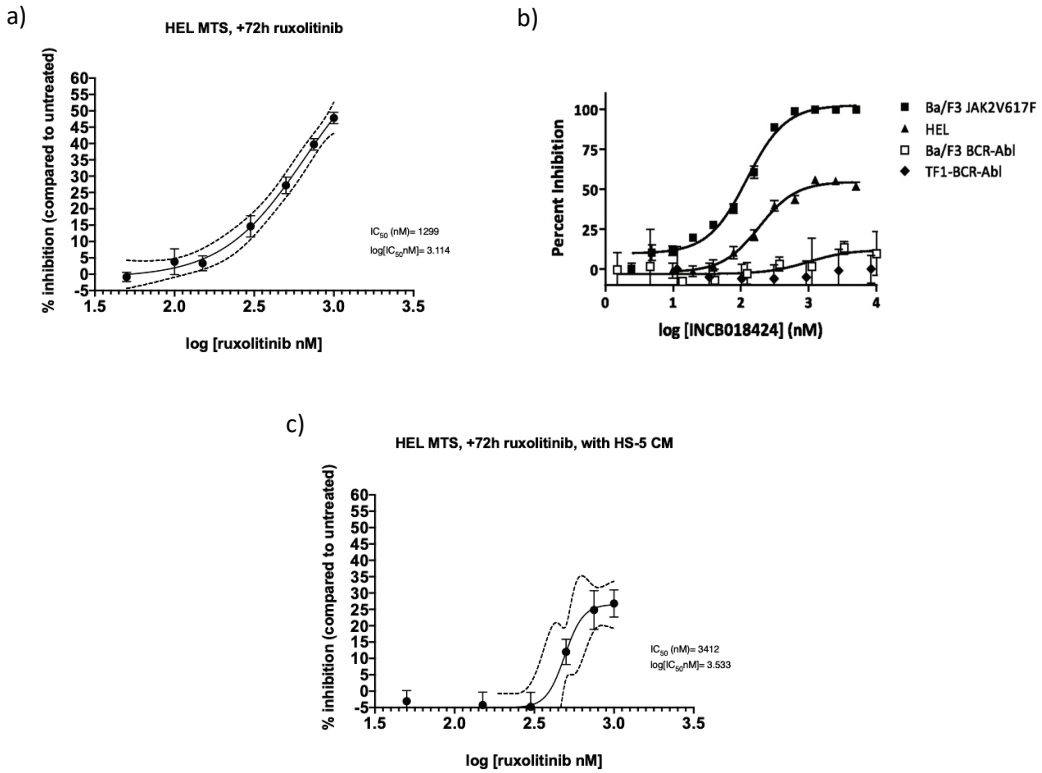

Figure 3.5. The plot in a) shows the % inhibition of proliferation (compared to the untreated control) by increasing concentration of ruxolitinib on HEL cell line cultured in RF10, derived from 3 representative MTS assays. Each point on the continuous black line represents the mean ± SEM (vertical bars); dotted lines sows 95% confidence interval. The obtained IC_{50} is comparable to that reported by Quintás-Cardama A. et al. (Blood 2010;115 [15]: 3109–3117), reported in b). The plot c) shows the protective effect of HS-5 CM on the proliferation of HEL cells exposed to the increasing ruxolitinib concentrations. In this case, the IC_{50} resulted to be more the doubled as compared to RF10 only (3.4 µM versus 1.2 µM, respectively).

Figure 3.6. Effect of HS-5 CM on HEL cell apoptosis induced by ruxolitinib.

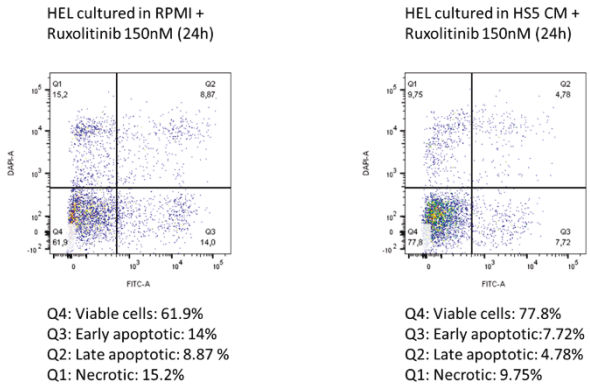

Figure 3.6. Annexin V/DAPI staining after 24h of ruxolitinib exposure. Cells were cultured in RF10 (left) or HS-5 CM (right). Results showed a significant protective effect of HS-5 medium on viability of HEL cell line under exposure to ruxolitinib (viable vs non-viable cells between experiments: p = 0.02, Fisher's exact test).

Figure 3.7. Effect of ruxolitinib on phosphorylated-STAT5 in HEL cell line.

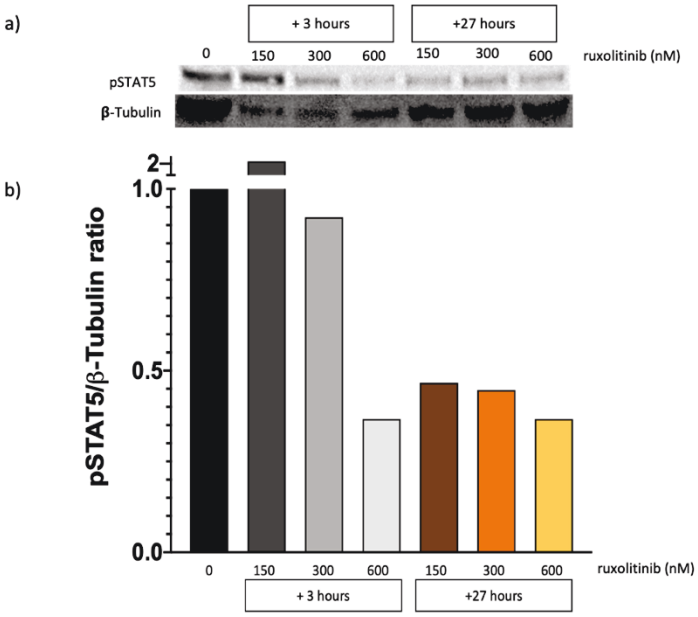

Figure 3.7. In a) is reported the Western Blot on HEL cells of phospho-STAT5 (pSTAT5) and β-tubulin at 3h and 27h from ruxolitinib 150nM, 300nM and 600nM exposure. In b), the bar chart shows the ratio pSTAT5/β-tubulin obtained from densitometry analysis of the Western Blot bands, per each condition. The experiment was run on a single biological replicate.

3.2 Pooled-shRNA screen results on HEL

Two replicates were run for pooled-shRNA screening per condition (no ruxolitinib, ruxolitinib, ruxolitinib + HS-5 CM). Figure 3.8 shows the flow-cytometry analysis of RFP positivity 72h from transduction of the HEL cell line with the pooled-shRNA library. Out of a total of 11 experiments run, 6 were successful with appropriate RFP positivity at 72h (refer to the Methods).

After bioinformatic analysis of the shRNA barcode abundancy between the pre- (72h after transduction) and post-selection (9 days after puromycin selection) samples, different ranking approaches (RA) were used in order to explore the most depleted shRNAs.

NGS of the shRNA barcodes showed the recovery of nearly all 27,500 unique barcodes in each experiment, consistent with complete representation of the shRNAs library. The average number of total reads per sample was 24.7 million (range: 19.1 to 34.8 million).

Figure 3.9 shows the correlation of FC between experimental replicates for no ruxolitinib (setting 1), ruxolitinib (setting 2), and ruxolitinib plus HS-5 CM (setting 3). The FC is calculated as described in the Methods, showing the change in reads present between baseline and at the end of the selection period for each of the 26,937 shRNAs targeting 4,973 genes. The Spearman's correlations were for setting 1: r = 0.635, p <0.0001; setting 2: r = 0.720, p <0.0001; setting 3: r = 0.574, p <0.0001. This means that results of the pooled-shRNA screening had a very good correlation between the replicates within each condition, suggesting that the experiments were technically successful and confirming the reproducibility of the screen.

First of all, for each replicate, the shRNA with the 2nd highest FC was taken into account in order to increase the reliability of the analysis, based on the fact that there is another shRNA with higher fold depletion targeting the same gene.

The 2nd highest shRNA was ranked in descending order (ranking approach 1, RA1) (Table 3.1; for the full list please refer to Appendix, Table A4): FC represents the change in reads observed between baseline and follow-up, with a FC >1 indicating a depletion from baseline in observed cells having incorporated the shRNA for each gene, as explained in the Methods.

The target genes among the top 1% candidates across the three settings codified mainly for the following cellular components: ribosome-translation complex, ubiquitin-proteasome, spliceosome machinery, DNA/RNA enzymes and transcription factors.

A total of 34 proteasomal genes were among the 4,973 targeted in the shRNA library. Of these, 8, 9, and 10 genes were present in the top 25 in experimental setting 1, setting 2 and setting 3, respectively.

Additional observations of proteasomal gene family members beyond the top 25 but within the top 1% for each setting were: setting 1: *PSMD3*, *PSMD7*, *PSMB3*, *PSMC6*, *PSMD2*; setting 2: *PSMB7*, *PSMA4*, *PSMB2*, *PSMD11*, *SHFM1*, *PSMD6*, *PSMD2*, *PSMD1*, *PSMC6*; setting 3: *PSMA3*, *PSMB1*, *PSMD2*, *PSMB4*, *PSMD11*, *PSMD6*, *PSMB1*. *JAK2* and *MPL*, which are crucial drivers of MPN pathogenesis, ranked within the top 1.25% of fold depletions for at least one of the replicates for all settings. Three genes which were in the top 1% of both replicates for setting 3 were not in the top 1% of any replicate for settings 1 and 2: *PSMB1*, *SNRPA1*, *SIN3A*; similarly, unique to setting 2 was only one gene: *AQR*; and similarly, unique to setting 1 were two genes: *GTF2F1*, *RACK1*.

Figure 3.10 shows comparisons of FC of the 2nd most depleted shRNA, taking into account the first replicate per each condition, between pairs of experimental settings, where gene of proteasome machinery are among the most recurrent ones across different conditions.

For 143 genes there were ≥ 2 shRNAs having either FC ≥ 3 or being in the top 2% positions for both replicates of at least one experimental condition (Appendix, Table A5). Starting from this group of highly depleted shRNAs, in order to better identify those more relevant in one treatment condition then in the others (so that a comparison among experimental conditions could be attempted), a second ranking approach (RA2) was used. In RA2, the two replicates for each experimental setting were compared and most depleted shRNAs were ranked (Tables 3.2, 3.3, 3.4) based on the sum of the following scores:

- for each gene, the number of shRNAs (out of 5 or 6) being in the top 2% of shRNAs in both replicates

  (so, if **5** *RAN* shRNAs met the above criteria for both replicates, score = **5**)

and

- for each gene, the number of shRNAs (out of 5 or 6) with 3 ≥ fold depletion in both replicates

(so, if 2 *RAN* shRNA met the above criteria for both replicates, score = **2**)

RA2 score for shRNAs targeting RAN gene: 5 + 2 = **7**

Only the shRNAs with a score ≥1 for at least one of the above criteria were included in the lists and a RA2 score ≥3.

Two findings are immediately evident: 1) genes unique to each condition were identified in the top ranked position, highlighting the different experimental settings (in red) 2) there were many

recurring genes shared by all tables (in blue) or by 2 tables (in black): in particular, there is abundancy of shRNAs targeting the proteasome machinery genes (in bold).

Given the finding of many shared genes across the different treatment conditions, a final ranking approach (RA3) was applied, in order to identify the essential genes for the HEL cell survival, regardless of the experimental setting.

The RA3 used the following criteria: we included only genes for which there were at least 2 targeting shRNAs in the top 2% for both replicates of each couple and/or 2 targeting shRNAs which had at least 3-fold change in both replicates of each couple, and in all the experimental settings. Then, in order to rank the genes included in this list, a score was applied counting the number of times each of these criteria was satisfied for the gene across the 3 experimental conditions (minimum 3 = only one criteria satisfied in 3 experimental settings; maximum 6 = both criteria satisfied for that gene and in all 3 experimental conditions).

Again, among the 22 genes identified (Appendix, Table A6) the proteasome genes resulted the most represented and also in the top positions.

Figure 3.8. Pooled-shRNA library screen of HEL cell line.

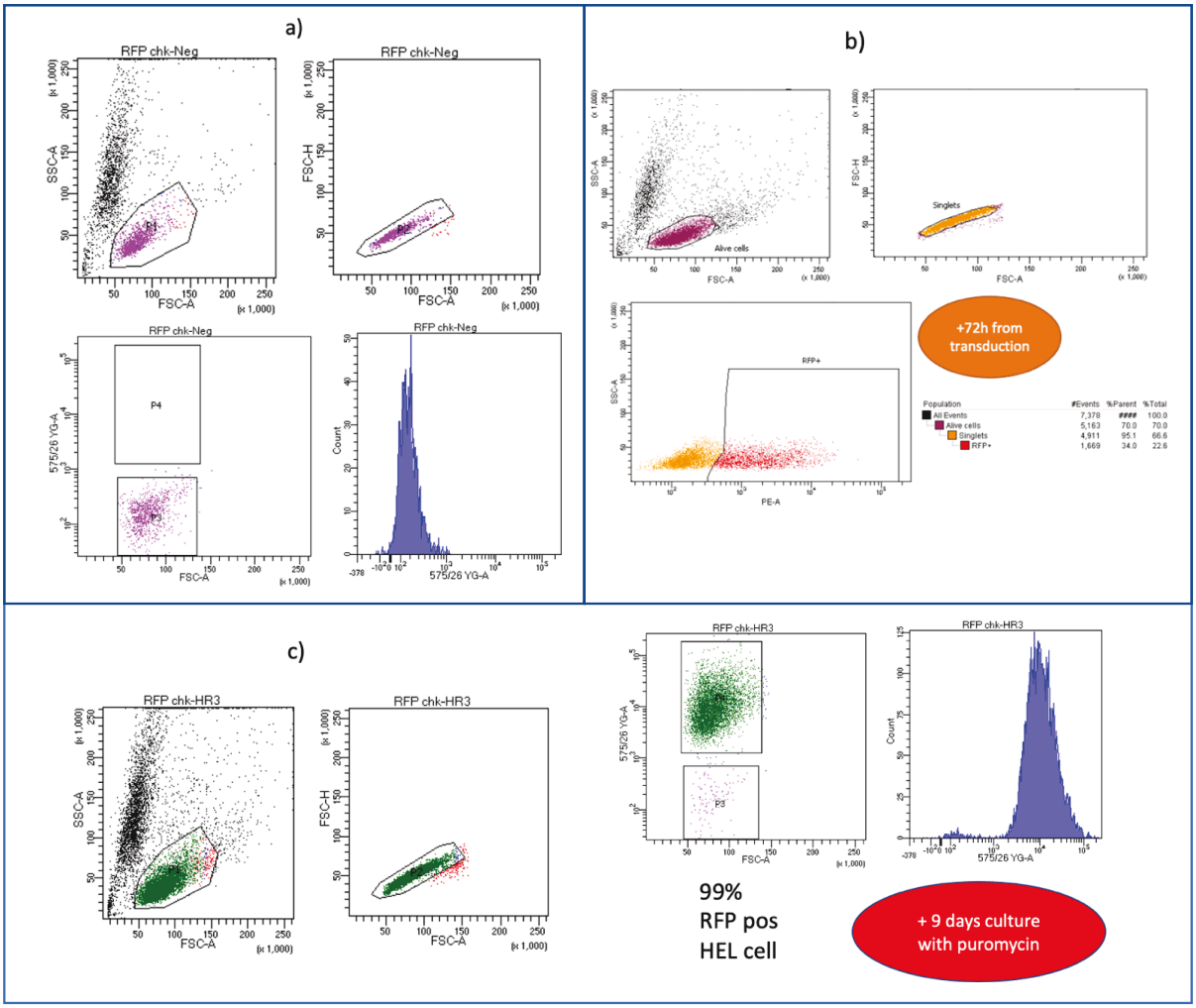

Figure 3.8. Flow cytometry plots of RFP positivity determination on HEL cells (a): RFP determination of HEL cell line at baseline (pre-transduction); (b): assessment at 72h post-transduction with pooled-shRNA library, where the RFP+ cells constituted 34% of the total alive cells; c): post-puromycin selection determination (+ 9 days of culture) where 99% of the cells were RFP-positive, confirming effective selection of transduced cells.

Table 3.1. Top essential genes for viability or proliferation of HEL cells under various conditions – Ranking approach 1 (RA1).

	No ruxolitinib (setting 1)				Ruxolitinib (setting 2)				Ruxolitinib + CM (setting 3)			
	Experiment 1		Experiment 2		Experiment 1		Experiment 2		Experiment 1		Experiment 2	
Rank	Gene	Fold Change	Gene	Fold Change	Gene	Fold Change	Gene	Fold Change	Gene	Fold Change	Gene	Fold Change
1	*CSE1L*	4.1	***PSMD1***	8.7	***PSMA2***	12.7	*RAN*	11.7	*ABCB5*	11.4	*RTF1*	9.2
2	*RRM1*	4	***PSMB2***	7.7	*RPS6*	12	***PSMC1***	9.7	***PSMD3***	9	***PSMB7***	8.6
3	*SNRPN*	3.9	***PSMA2***	7.4	*RAN*	11.3	***PSMB2***	9.7	*PRDX2*	8.4	***PSMA2***	8.1
4	***PSMA2***	3.9	*SNRPN*	6.6	*EIF2S2*	10.6	***PSMA2***	9.7	***PSMD1***	8.3	*RAN*	7.6
5	*RAN*	3.7	*RRM1*	6.3	***PSMC1***	9.2	*RPS13*	9.6	*SNRNP200*	8.2	*SNRPN*	7.5
6	***PSMD1***	3.6	*SNRPD2*	6.2	*TUBA1C*	9.1	***PSMD11***	9.1	*PHB2*	8.2	*RPS13*	7
7	*RTF1*	3.6	*HSPE1*	5.5	*RUVBL2*	9	***PSMA3***	9	***PSMA2***	8.1	***PSMA3***	6.9
8	***PSMB2***	3.5	*TUBA1C*	5.4	***PSMB4***	9	*SNRPD2*	8.9	*GATA1*	8	***PSMD1***	6.5
9	***PSMA3***	3.2	*RPS13*	5.4	*SNRPD2*	8.9	*RRM1*	8.6	*RRM1*	7.9	*RRM1*	6.3
10	*EEF2*	3	***PSMA3***	5.1	*RPL14*	8.8	*HSPE1*	8.4	*RPL11*	7.9	*RPL12*	6.1
11	*MPL*	3	*SNRNP200*	4.9	*RPS11*	8.6	*INPP4A*	8.3	*TUBA1C*	7.7	*RPS3A*	5.9
12	*RPS13*	3	***PSMB7***	4.9	*RTF1*	8.6	*RTF1*	7.9	*SIN3A*	7.6	*SNRPD2*	5.9
13	*SNRPD2*	2.9	*RAN*	4.7	***PSMA3***	8.6	*RPL12*	7.7	*RAN*	7.4	***PSMB2***	5.8
14	*EIF2S2*	2.9	*EEF2*	4.6	***PSMD1***	8.4	*SNRNP200*	7.6	***PSMB2***	7.3	*RPL10*	5.7
15	*JAK2*	2.8	***PSMB4***	4.6	***PSMD6***	7.9	*RPL4*	7.5	*MPL*	7.2	***PSMC6***	5.6
16	*RPL12*	2.8	*BCL2L1*	4.4	*HSPA9*	7.9	*EIF2S2*	7.4	*EIF2S2*	7.2	*SNRNP200*	5.5
17	***SHFM1***	2.7	*RPL14*	4.3	*RPL12*	7.7	*HSPA9*	7.4	*RUVBL2*	7	*KPNB1*	5.3
18	*NEDD8*	2.7	*EIF2S2*	4.3	*RPS13*	7.7	*MPL*	7.3	*BCL2L1*	6.8	*TUBA1C*	5.2
19	*PHKB*	2.7	*RPL13*	4.3	*ACTA2*	7.6	*FLI1*	7.2	***PSMA4***	6.7	*RPS11*	5.2
20	*CCNG1*	2.7	*RPSA*	4.3	*PRPF40A*	7.6	*RPS6*	7.2	***PSMB7***	6.6	*RPL8*	5.1
21	*SNRNP200*	2.7	*RTF1*	4.2	*RPSA*	7.5	*PRPF40A*	7	*STX1A*	6.4	*RPL11*	5
22	*CDC40*	2.7	*KPNB1*	4.1	*PHB2*	7.3	*OGDH*	7	*INPP4A*	6.4	*RUVBL2*	5
23	*FLI1*	2.7	***PSMD6***	4.1	*SNRNP200*	7.3	*JAK2*	6.9	*DDX23*	6.2	*PRDX2*	4.7
24	*PAFAH1B1*	2.7	*PHB2*	4.1	*EIF1AX*	7.3	***PSMB7***	6.9	*RPS13*	6.2	***PSMA7***	4.7
25	*RPS11*	2.7	*CSE1L*	4	*AQR*	7.2	*PDHX*	6.8	*CD247*	6	***PSMC3***	4.7

The table lists the top 25 essential genes for the viability or proliferation of HEL cells in the presence or absence of ruxolitinib and HS-5 conditioned medium (CM) as identified by a pooled-shRNA library targeting 4,973 genes (control genes excluded) for two experimental replicates of each condition.

Figure 3.9. The correlation between the replicates of pooled-shRNA library screen on HEL cell line.

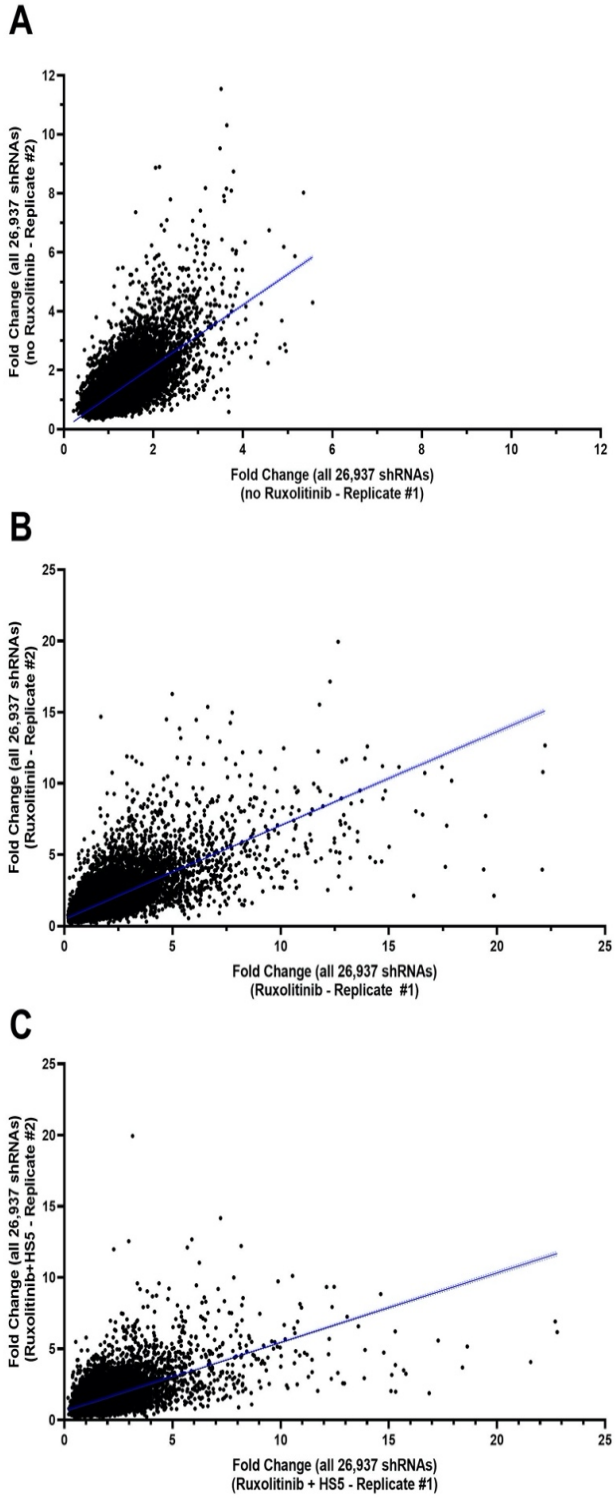

Figure 3.9. The plots show the correlation of fold changes between biological replicates for each experimental setting: (**A**) no ruxolitinib (setting 1), (**B**) ruxolitnib (setting 2), and (**C**) ruxolitinib + HS-5 CM (setting 3). The fold change is calculated as described in the Methods, showing the change in reads present between baseline and at the end of the selection period for each of the 26,937 shRNAs targeting 4,974 genes ("control" shRNA probes being excluded). The X and Y axes represent the frequency of the normalised shRNA for replicate 1 and 2 for each setting. The Spearman correlations were for setting 1: r = 0.635, p <0.0001; setting 2: r = 0.720, p <0.0001; setting 3: r = 0.574, p <0.0001.

Figure 3.10. Second most depleted shRNAs: comparison of single replicates across different treatment conditions.

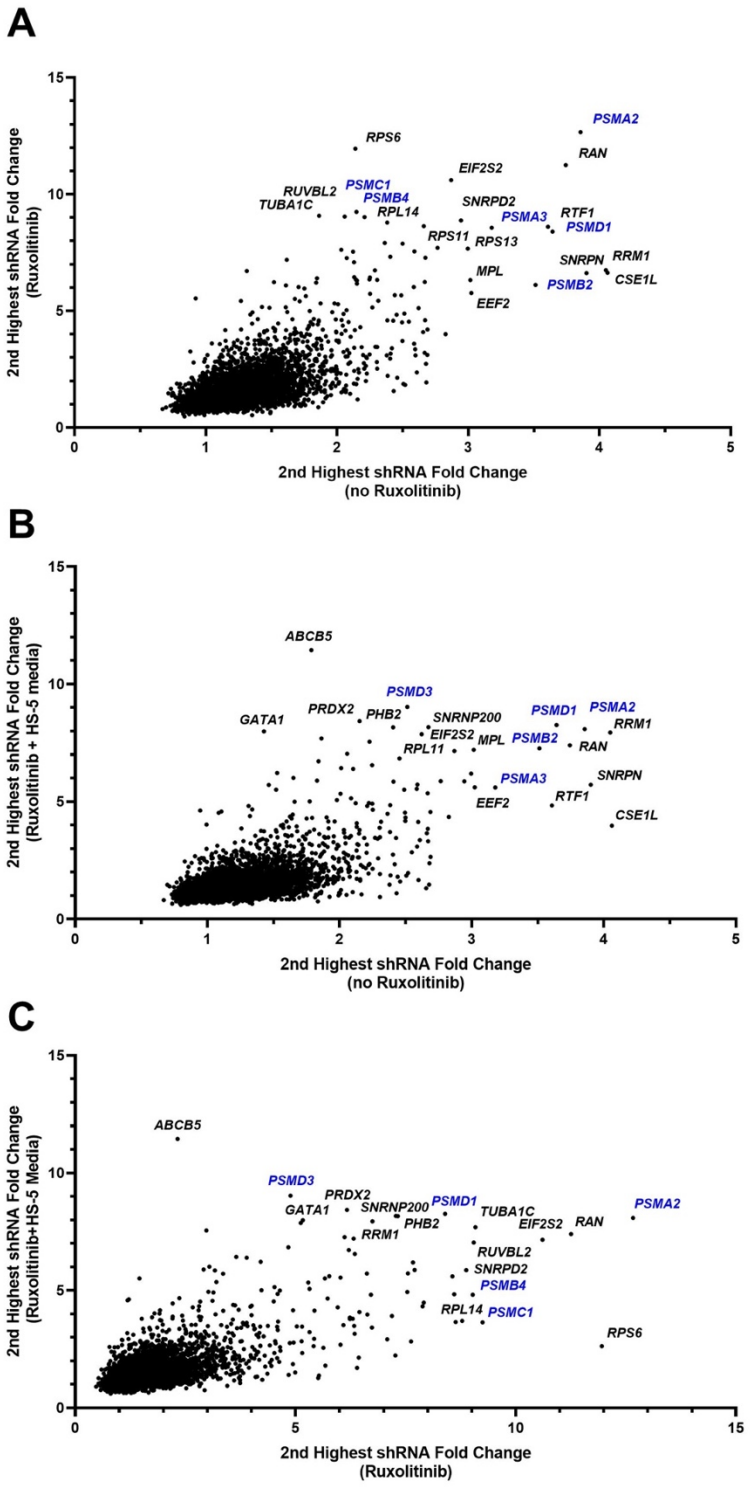

Figure 3.10. The plots show the comparison between single biological replicates of different experimental setting: (**A**) no ruxolitinib (X axis) vs ruxolitinib (Y axis); (**B**) no ruxolitnib (X axis) vs ruxolitinib + HS-5 CM (Y axis) and (**C**) ruxolitinib (X axis) vs ruxolitinib + HS-5 CM (Y axis). On each axis is reported the 2nd-highest fold change for the indicated shRNA (black dots); the dots which correspond a gene label indicate those genes with high fold depletion in either one or both settings. In blue are genes belonging to the proteasome gene family.

Table 3.2. HEL cell line pooled-shRNA library screen – Baseline setting (1) (analysis of 2 replicates according to ranking score 2, RA2).

Gene symbol	also in setting 2	also in setting 3	N of shRNAs with ≥ 3FC in both replicates	N of shRNAs in the top 2% in both replicates	sum (= ranking score 2)
PSMA2	x		4	4	8
RAN	x		2	5	7
PSMB2	x		2	4	6
CSE1L	x		3	3	6
PSMA3	x		2	4	6
PSMD1	x		3	3	6
RRM1	x		3	3	6
RTF1	x		2	3	5
RPS13	x		1	3	4
BCL2L1		x	1	3	4
EEF2		x	2	2	4
RPL11		x	1	2	3
ASCC3L1	x	x	1	2	3
EIF2S2	x	x	1	2	3
JAK2	x	x	1	2	3
PRPF40A	x	x	1	2	3
SNRPN	x	x	1	2	3
HSPA9	x		1	2	3
NEDD8	x	x	1	2	3
RPS3A	x	x	1	2	3
SNW1	x	x	1	2	3

Table 3.3. HEL cell line pooled-shRNA library screen – Ruxolitinib setting (2) (analysis of 2 replicates according to ranking score 2, RA2).

Gene symbol	also in setting 1	also in setting 3	N of shRNAs with ≥ 3FC in both replicates	N of shRNAs in the top 2% in both replicates	sum (= ranking score 2)
RAN	x	x	6	4	10
PSMA2	x	x	5	5	10
PSMB2	x	x	5	3	8
RPS13	x	x	4	4	8
RRM1	x	x	4	4	8
PHB2		x	4	3	7
PSMB7		x	4	3	7
PSMC1			4	3	7
PSMD1	x	x	4	3	7
PSMD6		x	4	3	7
SNRPD2		x	4	3	7
RUVBL2		x	5	1	6
CSE1L	x		4	2	6
PSMA3	x	x	3	3	6
PSMD11		x	4	2	6
RPL14			3	3	6
SNRPN	x	x	3	3	6
FLI1			4	1	5
RPL4	x	x	4	1	5
ASCC3L1	x	x	3	2	5
CDC2L1			3	2	5
DDX41		x	3	2	5
EIF2S2	x	x	3	2	5
PRPF40A	x	x	3	2	5
PSMB4		x	3	2	5
RPL10			3	1	4
JAK2	x	x	3	1	4
PSMA4		x	3	1	4
PSMC6		x	3	1	4
PSMD2		x	3	1	4
RANBP1			3	1	4
RIPK3			3	1	4
RPL12		x	3	1	4
RPL6		x	3	1	4
RPS11			3	1	4
RPSA			3	1	4
RTF1	x	x	2	2	4
ANAPC2		x	2	2	4
AQR		x	2	2	4
HSPA9	x		2	2	4
RPS6			2	2	4
SNW1	x	x	2	2	4
SULT1B1			2	2	4
TUBA1C		x	2	2	4
CAPN5			2	1	3
EFTUD2		x	2	1	3
ACOX3			2	1	3
ACTA2		x	2	1	3
CCL20			2	1	3
CDC40			2	1	3
CLDN2			2	1	3
DNAJB2		x	2	1	3
GNB2L1			2	1	3
HTR1B			2	1	3
IL12RB1			2	1	3
INPP4A			2	1	3
KPNB1		x	2	1	3
MAPKAPK5			2	1	3
NEDD8	x	x	2	1	3
NLN			2	1	3
PAX2			2	1	3
PDHX		x	2	1	3
POLR2F		x	2	1	3
PRKAB2			2	1	3
PSMD13			2	1	3
PSMD3		x	2	1	3
RANBP2			2	1	3
RBM8A		x	2	1	3
RPA1		x	2	1	3
RPL15			2	1	3
RPL8			2	1	3
RPS3A	x	x	2	1	3
SARS			2	1	3
SHFM1			2	1	3
WNT8A			2	1	3

Table 3.4. HEL cell line pooled-shRNA library screen – Ruxolitinib + HS-5 CM setting (3) (analysis of 2 replicates according to ranking score 2, RA2).

Gene symbol	also in setting 1	also in setting 2	N of shRNAs with ≥ 3FC in both replicates	N of shRNAs in the top 2% in both replicates	sum (= ranking score 2)
PSMA2	x	x	5	5	10
RAN	x	x	5	4	9
PSMB2	x	x	4	4	8
RPL11	x		5	3	8
PSMA3	x	x	4	3	7
PSMB7		x	4	3	7
RUVBL2		x	3	3	6
PSMD6		x	4	2	6
RRM1	x	x	4	2	6
RTF1	x	x	3	3	6
SNRPN	x	x	3	3	6
PHB2		x	3	2	5
PSMD11		x	3	2	5
RPS13	x	x	3	2	5
ASCC3L1	x	x	3	2	5
EEF2	x		3	2	5
PRPF40A	x	x	3	2	5
PSMD1	x	x	2	2	4
SNRPD2		x	2	2	4
EFTUD2		x	3	1	4
EIF2S2	x	x	3	1	4
MPL			3	1	4
PSMA4		x	2	2	4
PSMB4		x	2	2	4
RPL12		x	2	2	4
ABCB5			2	2	4
ANAPC2		x	2	2	4
GSR			2	2	4
KPNB1		x	2	2	4
NEDD8	x	x	2	2	4
PRDX2			2	2	4
SIN3A			2	2	4
SNW1	x	x	2	2	4
TUBA1C		x	2	2	4
BCL2L1	x		2	1	3
DDX41		x	2	1	3
JAK2	x	x	2	1	3
PSMC6		x	2	1	3
PSMD2		x	2	1	3
AQR		x	2	1	3
CD247			2	1	3
CYP51A1			2	1	3
DNAJB2		x	2	1	3
PDHX		x	2	1	3
POLR2F		x	2	1	3
PSMB1			2	1	3
PSMC3			2	1	3
PSMD3		x	2	1	3
RBM8A		x	2	1	3
RPA1		x	2	1	3
RPS3A	x	x	2	1	3
RUVBL1			2	1	3
SNRPA1			2	1	3

3.3 Pooled-shRNA library screen results on primary cells

The aim of this experiment was to explore the possibility of performing pooled shRNA library screen in primary cells.

Four experiments were performed on peripheral blood-derived CD34+ cells, donated by 4 patients with MF. Figure 3.11 shows the essential steps of one representative experiment (please refer to the Methods).

The challenges encountered in these experiments were several. First of all, the starting cell number was relatively limited, ranging from 1-5 x 10^6 of CD34+ cells (Table 3.5) after magnetic beads separation (please refer to the Methods), obtained from an average of 30-40mL of peripheral blood. The target cell number to start with for HEL cell line, was of at least ~16 x 10^6 CD34+ cells.

The second challenge was by far the most relevant. In fact, primary cells were very difficult to transduce. The target RFP-positivity of 20-30% was never achieved in any of the four samples, even after >72h from transduction: only 2 samples showed RFP positivity of 2.5% and 7.1% at 120h (Table 3.5).

Table 3.5. Summary of the pooled-shRNA library screen experiments on primary cells.

Primary cells sample	N of CD34+ cells isolated from peripheral blood MNCs	length of expansion (days)	N of alive cells at T	72h RFP	120h RFP	days from T to CC	days from isolation to CC	CC length	days from T to collection	days from isolation to collection
MF-1	4.3 x 10^6	3	7.1 x 10^6	0.1	nd	7	10	8	15	18
MF-2	3.9 x 10^6	3	6 x 10^6	0	nd	9	12	9	18	21
MF-3	3.7 x 10^6	2	5.6 x 10^6	nd	7.1%	6	8	8	14	16
MF-4	1.2 x 10^6	4	4 x 10^6	1.4%	2.5%	5	9	8	13	17

Table 3.5 illustrates for each experiment (MF1-MF4) the details regarding (from left to right): the starting CD34+ cell number, the length of CD34+ cell expansion after positive selection through magnetic beads, the number of cells on the day of transduction (T), the RFP-positivity after 72h and 120h, the time from transduction to the transfer on top of HS-5 layer and start of co-culture (CC), the time from CD34+ isolation to the start of co-culture, the length of co-culture, the time between transduction and end of pooled-shRNA library screen (collection), and the time between CD34+ cell isolation to the end of the screening (nd= not determined).

Table 3.6. RFP positivity at the end of the pooled-shRNA library screen of primary cells.

Primary cells sample	Total number of alive cells on suspension at collection day	GFP-negative fraction at collection day	RFP-positive cells (of GFP-negative fraction) at collection day
MF-1	1 x 10^6	10.3%	**44.7%***
MF-2	nd (failed)	nd (failed)	nd (failed)
MF-3	2.7 x 10^6	21.5%	**18.4%**
MF-4	7.3 x 10^6	55%	**72%**

Table 3.6 shows data related to the collection day (end of the pooled-shRNA library screen). GFP-positive cells are the HS-5 puromycin-resistant cells. The first column provides the total number of alive cells in the cell suspension. In the second column is shown the % of GFP-negative cells in the cell suspension, representing the primary cells, of which is provided the % of RFP-positive cells in the third column. * includes a mixture of trypsinized cells (rich in HS-5) and the cells in the suspension (rich in primary cells). The sorting step was introduced to MF-3 and MF-4. MF-2 failed due to contamination during co-culture.

At the end of the co-culture, the barcode amplification showed no amplification for MF-1 and MF-2, while amplification was observed for MF-3 post-selection sample and MF-4 baseline sample only.

To explore the shRNA depletion in MF-3, the MF-4 shRNA content at baseline was taken into account, assuming a homogeneous and similar representation of shRNA transduction in the baseline cell population between samples of same cellular and disease type. Table 3.6 shows the top 1% 2nd most depleted shRNA in MF-3 (for the full list refer to the Appendix, Table A4). The shRNAs targeting genes involved in the MPL receptor intracellular cascade were among the most depleted ones (Figure 3.12). Figure 3.13 shows the fold depletion of shRNAs targeting genes of the proteasome family in MF-3; among them the shRNAs targeting PSMC1 was the most depleted.

In conclusion, further improvement and modifications of the technique is needed in order to obtain data with strong confidence from pooled-shRNA library screen of primary cells (as it will be discussed in Chapter 4).

In view of the time-consuming process of optimization and application of this technology for primary cells and taking into account the available resources, I decided to move to the validation of the findings obtained in HEL cells.

Figure 3.11. Pooled-shRNA library screen of CD34+ cells purified from peripheral blood of a patient with MF.

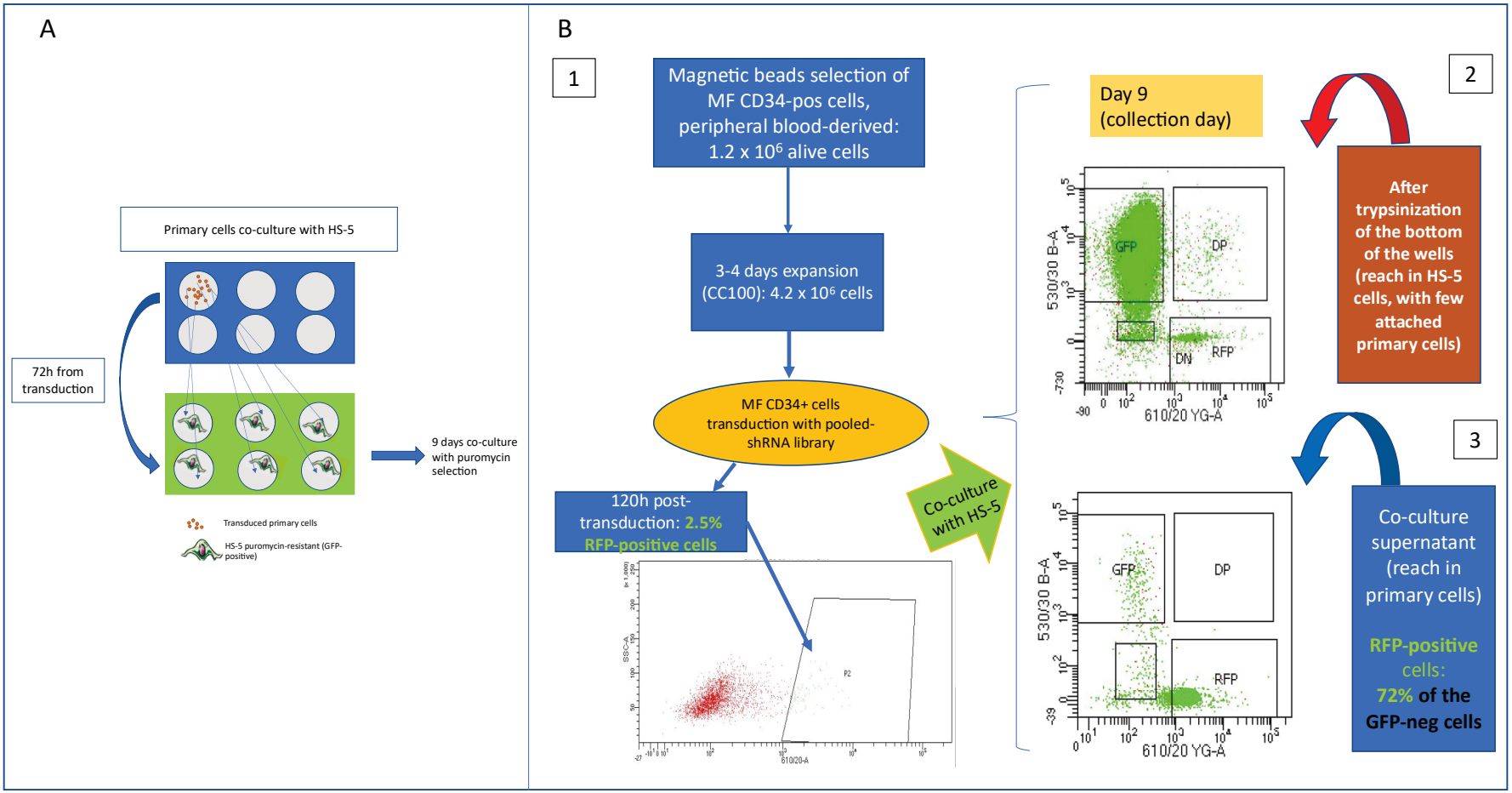

Figure 3.11. A: schematic representation of pooled-shRNA library screen experimental design on primary MF cells. 72h after transduction, MF cells were transferred on top of puromycin-resistant HS-5, in a 6-well plate and co-cultured for 9-days in presence of puromycin. B: flow-cytometric assessments for the pooled-shRNA library experiments on primary cells: (1) after selection and expansion of MF CD34+ cell on cytokine enriched medium (CC100), determination of RFP positivity was carried out 72h after pooled-shRNA library transduction (showing the low-transduction efficiency); this was followed by 9 days co-culture on top of the adherent puromycin-resistant HS-5 cells. On the collection day, the supernatant containing the RFP-positive cells was collected. To obtain the RFP-positive cells attached to HS-5 the plates were treated with trypsin, which led to suspension of HS-5 cells and primary cells (RFP-positive and RFP-negative). Cell sorting of RFP-positive cells was performed to separate RFP-positive primary cells from HS-5 cells (2). The sorted RFP-positive cells were added to the cell collected from the supernatant (3) and stored for later DNA extraction.

Table 3.7. List of the top 1% 2nd most depleted shRNAs in MF-3 (at day 14 post-transduction).

Targeted gene	Fold depletion
EIF5A2	39.91081
CX3CL1	24.9414063
CREB3L2	20.6469964
DUSP14	20.3579444
SCLY	19.6393095
STAT5A	19.4367129
TFPI	18.127799
PIGG	17.3360391
GRM8	16.9942939
ASNS	16.7478798
MYO1C	16.4059554
GJD2	16.3641548
ICAM5	16.2550515
RGS5	16.1300952
SYN3	16.0708956
TLE1	15.8082583
EIF2AK4	15.7622232
FSHR	15.7381013
GDF10	15.6243515
SULT1C4	15.5469014
ATP5G1	15.38057
KLRK1	14.9867799
GNPDA1	14.9806777
ITPK1	14.5299695
CASR	14.1681408
SALL4	14.0926578
PRKG2	14.0611436
DNMT3L	13.7878763
PLCE1	13.7420382
TNF	13.7395217
HSD17B2	13.7028602
FOXC2	13.5937786
COL4A5	13.5444958
ATG7	13.4787605
PLCG1	13.4174698
FABP2	13.4161426
ALAS2	13.4111874
T	13.392588
RPL13A	12.9848706
MAFB	12.8449386
DYRK1A	12.7066877
LEPR	12.6983456
PGM3	12.6601214
KREMEN1	12.608122
SSTR2	12.608122
GLB1	12.5095563
HPD	12.4586265
NCF1	12.4109907
CCNA1	12.1565218
FRAT1	11.8837538

Figure 3.12. Genes targeted by the most depleted shRNAs in cell line and primary MF CD34+ which belong to the MPL receptor intracellular cascade.

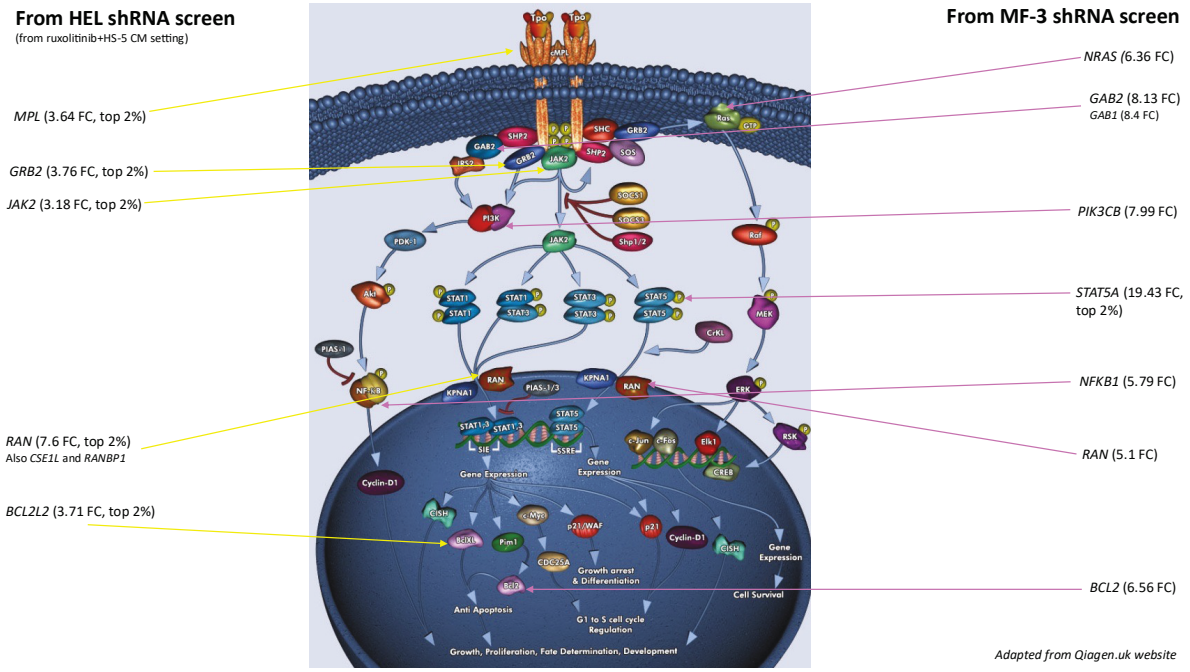

Figure 3.12. The picture is adapted from the Qiagen website (quiagen.uk) and shows the TPO/MPL pathway. It is interesting to note that several top-depleted shRNAs in both HEL cell line and primary MF-3 CD34+ cells belong to this pathway, which has a crucial role in the pathogenesis of MF (the targeted gene is shown; FC=fold change; top 2%= the shRNA with the 2nd-highest fold-change targeting the indicated gene ranked in the top 2% positions among all the 2nd-highest depleted shRNA targeting 4974 genes).

Figure 3. 13. Fold-depletion of shRNAs targeting proteasome machinery in the pooled-shRNA library screen of MF-3 CD34+ cells.

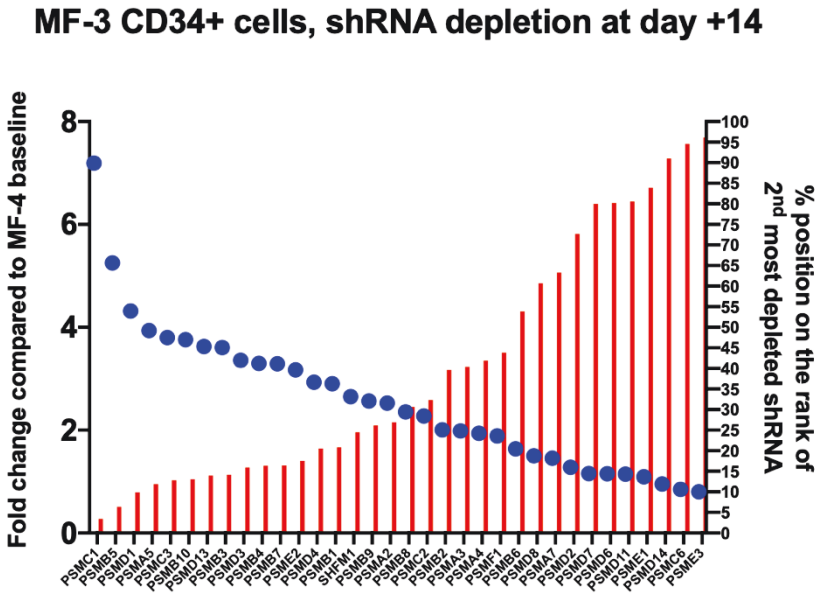

Figure 3.13. The plot shows 2nd most depleted shRNAs targeting genes of the proteasome family in the pooled-shRNA library screen of MF-3. Left Y axis reports the fold change, to which the blue dots refer; the right Y axis shows the percentile position of the gene-targeting shRNA in the list of the 4974 2nd most depleted shRNAs, indicated by the red vertical line.

3.4 Selection of the target for validation

Given the results of the pooled-shRNA library screen on HEL cells showing an abundance of shRNAs targeting proteasome machinery amongst the most depleted ones and regardless of the treatment conditions, we chose the proteasome as the target for validation. In vitro chemical validation using proteasome inhibitors (PI) bortezomib (BTZ) and carfilzomib (CFZ) was then performed on both the cell line and primary cells.

3.5 Chemical validation targeting proteasome on HEL cells

The IC_{50} for BTZ and CFZ on HEL cell line was measured using MTS assay after 72h of continuous drug exposure (Figure 3.14 A).

HEL cells were sensitive to PI, with IC_{50} of 7.3 nM and 41.3 nM for BTZ and CFZ, respectively.

The combination of ruxolitinib with CFZ at 10 or 20 nM significantly increased inhibition of proliferation compared to either only ruxolitinib ($p = 0.01$ and $p = 0.02$, respectively) or CFZ ($p = 0.001$ and $p = 0.008$, respectively) after 72 hours (Figure 3.14 B). The inhibitory effect of CFZ 50 or 100 nM alone or in combination with ruxolitinib compared to control was significant ($p < 0.001$).

Figure 3.14. Proteasome inhibitors (PI) IC_{50} and effect of ruxolitinib-CFZ combo on HEL cells.

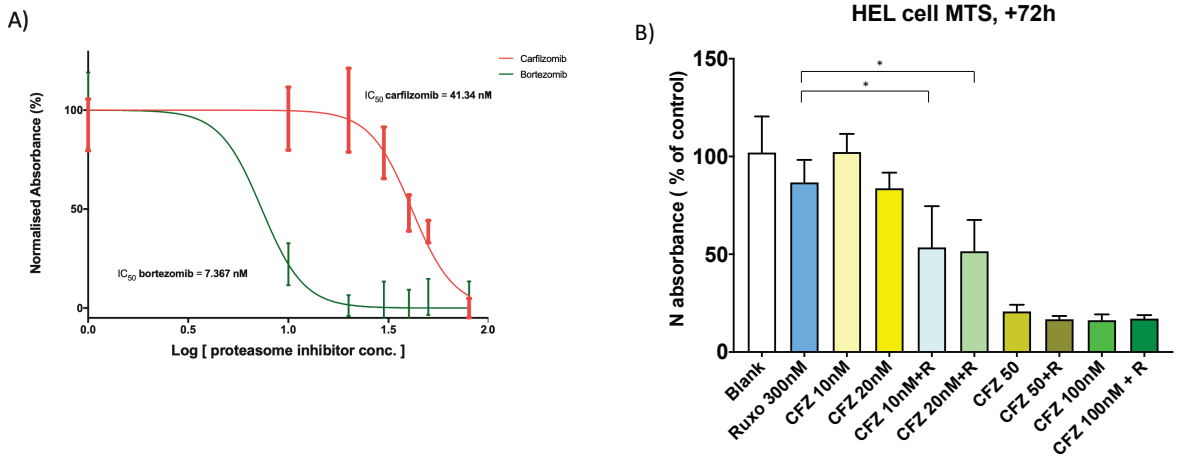

Figure 3.14. (A) MTS assay on HEL cells at 72h from exposure to CFZ or BTZ at concentrations ranging from 5 to 80 nM. The shown data were derived from 7 technical replicates for each treatment condition and each point on curves is the mean with SD (bars). (B) MTS assay of HEL cells after 72h exposure to ruxolitinib (Ruxo) 300 nM and/or CFZ either alone or in combination. Bars indicates mean with SD from 4 technical replicates. * represents $p < 0.05$ for the comparison between the combination therapy to either treatments (from one-way ANOVA). In (A) and (B), the Y axis reports the normalized (N) absorbance to the mean absorbance of the untreated control.

3.6 Chemical validation targeting proteasome on primary cells

Following chemical validation of the findings from pooled-shRNA library screen on HEL cells, the same was carried out on MNCs and CD34+ cells isolated from peripheral blood of patients with MF.

Table 3.8 shows patients' clinical characteristics at the time of sample collection.

3.6.1 PI CFZ reduce the number of viable MF cells

The first experiment was carried out on a patient with triple-negative post-ET MF (MF-9), clinically refractory to ruxolitinib. CFZ concentrations used were 100-1000 nM. Trypan blue assay at 24h and MTS assay at 48h from drug exposure showed a significant reduction of viable CD34+ cells starting at a concentration of 100 nM (p <0.0001) (Figure 3.15). Consequently, lower concentrations were investigated, ranging from 50 to 90 nM in another sample. On MF-12 (*CALR*^{mut}-positive patient), CFZ 50nM (and higher concentrations) significantly reduced the number of viable cells after 96h (p <0.0001) (Figure 3.15).

3.6.2 PI CFZ enhances inhibitory effect of ruxolitinib on MF cells

Subsequently, $CD34^+$ cells from 4 other MF patients were exposed for 24h to CZF in the range of 10-50nM (for MF-3 and MF-14 the viability of the cells at 50 nM CFZ was also measured at 72h). CFZ induced effective reduction of the number of viable cells at 24h, even at low concentrations (10 nM) for all but one patient sample (MF-14), p <0.0001, <0.0001, 0.006 and <0.0001 for MF-10, MF-3, MF-9 and MF-15, respectively (Figure 3.16).

For MF-10, MF-9, MF-15, MF-3 and MF-14 the addition of CFZ 50 nM to ruxolitinib 300 nM significantly reduced the number of viable cells compared to ruxolitinib alone (Figure 3.16).

In a separate experiment on MF-10, the addition of CFZ 20 nM to the higher ruxolitinib concentration of 1 μM increased the efficacy of ruxolitinib alone (p = 0.04).

Table 3.8. Clinical characteristics of MF patients at the time of sample collection.

	Diagnosis	Sex, Age	Mutation status (VAF)	Therapy at sample collection ?	Ongoing therapies	WCC (x 10^9/L)	Hb (g/L) & Plts (x10^9/L)	Spleen size (cm)/response (y/n/pr)	Symptom response
MF-3	Primary MF	F, 76	***JAK2*^{V617F}** (94%) ***TET2*^{Pro419LeufsTer8}** *(44%)*	Yes	Momelotinib	23.1	90 & 375	16.1/n	no
MF-4	Primary MF	F, 69	***JAK2*^{V617F}** (75%)	No	None	20.1	127	24/NA	NA
MF-5	Primary MF	M, 75	***JAK2*^{V617F}** (36%)	No	Ruxolitinib (stopped 3 weeks before)	13.6	94 & 34	NA*	no
MF-8	Primary MF	M, 53	***MPL*^{W515L}** (74%) ***ASXL1*^{Gly646TrpfsTer12}** *(34.4%)*	Yes	Ruxolitinib	14.6	121 & 191	28/n	no
MF-9	Post-ET MF	M, 66	**Triple-NEG** ***ASXL1*^{Gly646TrpfsTer12}** *(36%)*	Yes	Ruxolitinib	14.6	99 & 262	20.1/n	no
MF-10	Primary MF	M, 80	***JAK2*^{V617F}** (48%)	Yes	Ruxolitinib	23	133 & 138	17/n	yes
MF-12	Primary MF	M, 40	***CALR* type-2** (34%)	No	None	7.3	136 & 765	14.7/NA	NA
MF-14	Post-PV MF	F, 75	***JAK2*^{V617F}** (nd)	Yes	Ruxolitinib	11.7	137 & 250	19/n	no
MF-15	Primary MF	M, 83	***JAK2*^{V617F}** (80%)	Yes	Ruxolitinib	15.9	109 & 221	Normal/c	no
MF-19	Primary MF	F, 75	***JAK2*^{V617F}** (83%) ***ASXL1*^{Arg693Ter}** *(10%)*	Yes	Ruxolitinib	23.2	75 & 130	23/pr	no
MF-20	Post-ET MF	F, 60	***JAK2*^{V617F}** (94%)	Yes	Ruxolitinib	22.3	130 & 91	30/pr	yes
MF-21	Primary MF	M, 62	***JAK2*^{V617F}** (nd)	Yes	Ruxolitinib	8.5	156 & 99	28/pr	yes
MF-23	Post-ET MF	M, 62	***CALR* type-2** (43%)	No	none	3	109 & 389	20.4	NA
MF-24	Primary MF	F, 62	***JAK2*^{V617F}** (nd)	Yes	Ruxolitinib	20.7	98 & 179	17/pr	no
MF-28	Post-PV MF	M, 77	***JAK2*^{V617F}** (94%)	No	None	59.8	117 & 278	17/NA	NA

Table legend: VAF = variant allele frequency; WCC = white cell count; Hb = haemoglobin; Plts = platelets; spleen response: c = complete, n = none, pr = progressive splenomegaly. Reported spleen size derives from abdomen ultrasound study. NA = not applicable; nd = not determined. * = patient previously splenectomised. Both spleen response and symptom burden response to treatment are according to the revised IWG-MRT and ELN response criteria (147).

Figure 3.15. In vitro effect of CFZ 50-1000 nM on MF CD34+ cells.

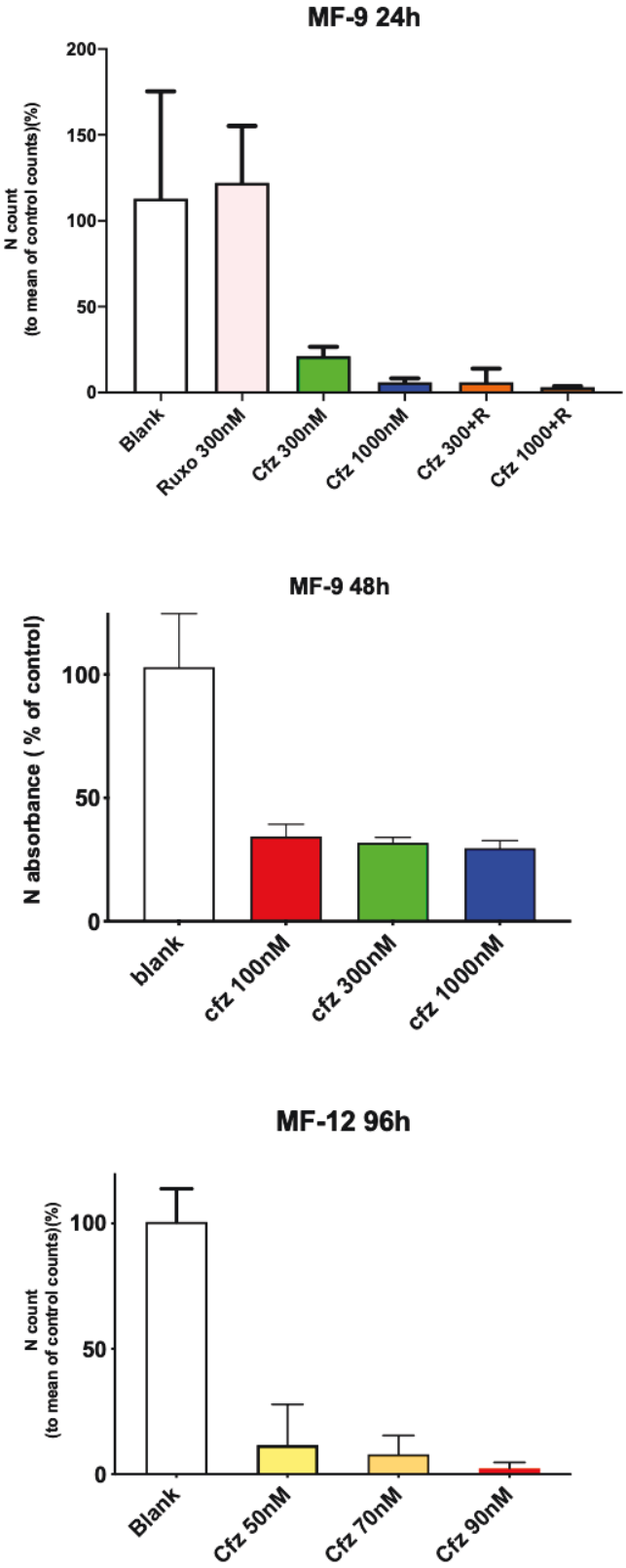

Figure 3.15. Y axis represent the normalized (N) absorbance (for MTS) or count (for Trypan blue assay) relative to the mean absorbance/count of the untreated control (Blank); quantitative results are shown as mean with SD of at least 3 technical replicates; *, $p < 0.05$, from one-way ANOVA). In the top chart, Ruxo, R = ruxolitinib.

Figure 3.16. In vitro effect of CFZ 10/50 nM with or without ruxolitinib on MF CD34+ cells.

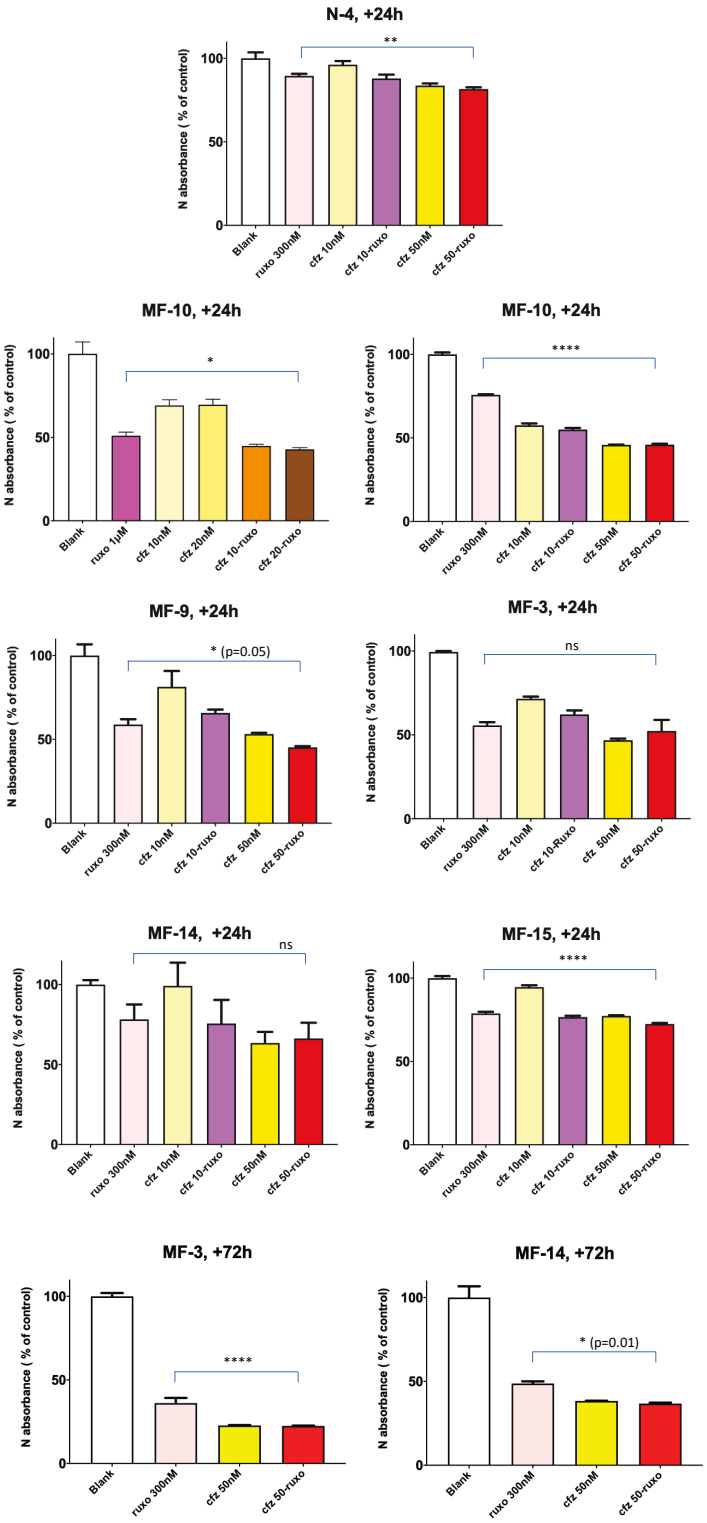

Figure 3.16. Y axis represent the normalized (N) absorbance to the mean absorbance of the untreated control (Blank); quantitative results are shown as mean with SD of at least 3 technical replicates and were analyzed by 1-way ANOVA. *, $p < 0.05$; **, $p \leq 0.01$; ***, $p \leq 0.001$; ****, $p \leq 0.0001$). For MF-10 there were two separate experiments, each testing a different concentration of ruxolitinib (ruxo). The fact that these are biological rather than technical replicates explains the variability of the inhibitory effect observed for CFZ 10 nM and 20 nM in one (left bar chart) compared to CFZ 10 nM on the other experiment (right bar chart).

In order to recapitulate the pharmacokinetic prolife of CFZ, characterized by a very short half-life after intravenous infusion, additional experiments were performed in which MF CD34+ cells or MNCs were exposed to 1h-pulsed CZF. MTS or Trypan blue assays were performed at different time points from drug exposure (24-72h). The results are illustrated in Figure 3.17. At 72h, 1h-pulsed 300 nM CFZ, but not 100 nM CFZ, effectively reduced the number of viable cells of MF-10, compared to untreated control ($p = 0.006$); the addition of ruxolitinib increased the suppressive effect over ruxolitinib alone (means of normalized absorbances: 54.1% vs 68.09%, respectively); although the reduction was not statistically significant ($p = 0.07$) (Figure 3.17a).

At 48 h, 1h-pulsed CFZ at 300 nM was able to reduce the number of viable cells of MF-4 compared to control ($p = 0.0009$); combination treatment had an additional effect compared to ruxolitinib alone in ($p = 0.08$; means 44.8% vs 70.7%, respectively).

At 24h, 1h-pulsed CFZ at 300 nM significantly reduced the number of viable cells of MF-10 ($p = 0.002$), but it did not on MF-21, MF-9 and MF-24. However, on the latter sample, the combination with ruxolitinib resulted more effective then ruxolitinib or CFZ alone ($p = 0.0014$ and $p = 0.045$, respectively) (Figure 3.17c).

For MNCs from MF-19, the inhibitory effect of combination treatment was pronounced and superior to ruxolitinib alone at 72h and was already apparent at 24h from drug exposure ($p < 0.0001$). This was also true for MNCs from MF-3 at 48h ($p=0.02$). At 72h, the combination arm showed ~50% reduction of mean normalized absorbance compared to ruxolitinib-only arm (27.6% vs 59.8%, respectively; p not significant) (Figure 3.17d).

Figure 3.17. In vitro effect of ruxolitinib with or without 1h-pulsed CFZ on MF CD34+ cells and MF MNCs.

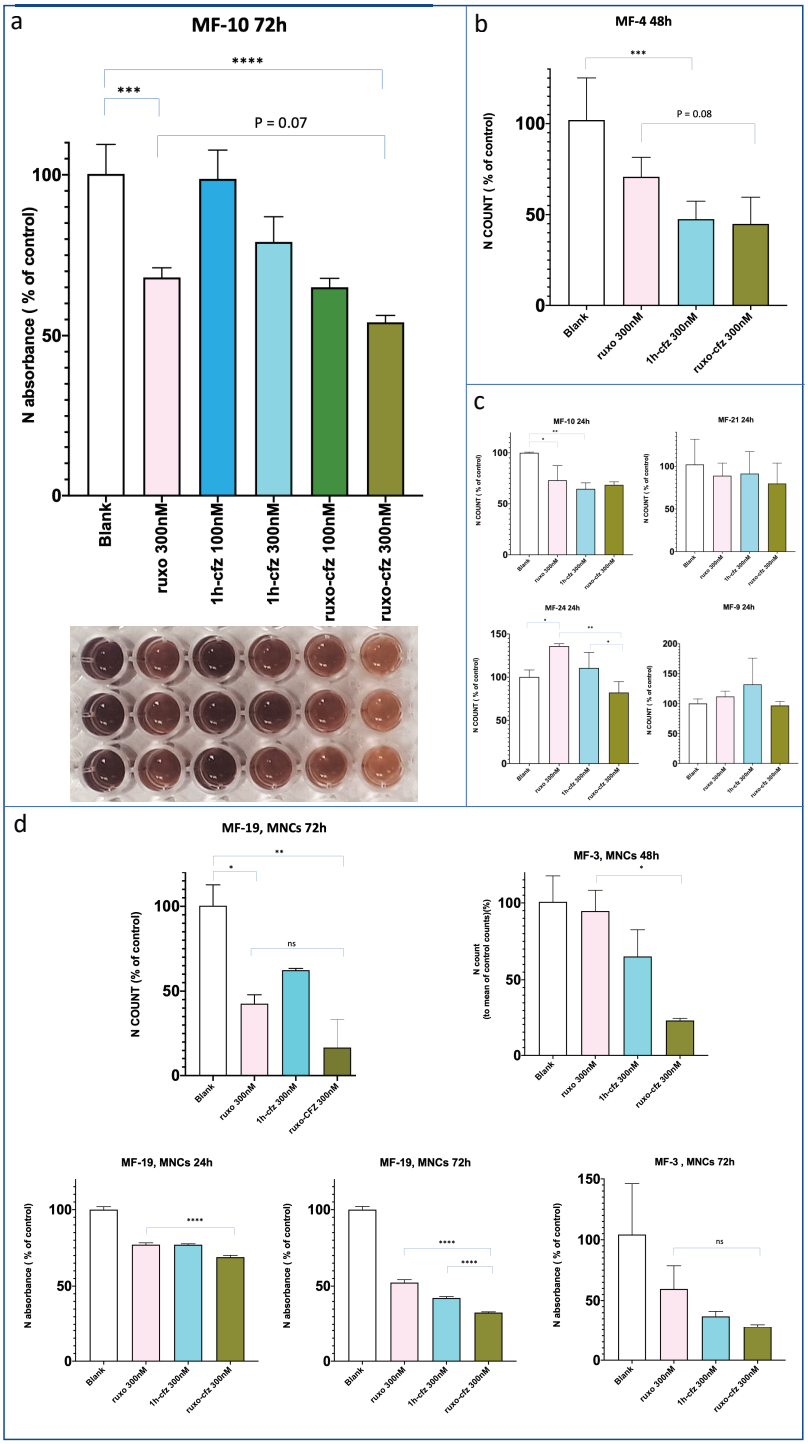

Figure 3.17. a) MTS result on MF-10, after 72h from drug exposure. The image below the bar chart is the picture of the 96-well plate of MF-10 containing 3 technical replicates for each condition (represented by a column of wells and corresponding to the condition indicated by the above X-axis of the bar chart). The picture was taken at 2h from adding MTS dye: darker colour means higher number of viable cells.
b) Trypan blue assay on MF-4 CD34+ cells at 48h from drug exposure; c) Trypan blue assay at 24h on MF CD34+ cells from 4 other patients; d) MTS or Trypan blue assay results on MF MNCs from 2 other patients, at different time points (24-,48- and 72h).
All experiments had at least 3 technical replicates. Y axis for MTS assays bar chart is the absorbance normalised (N) to the mean absorbance of the untreated control (Blank); Y axis for Trypan blue assays bar chart is the absolute count of viable cells normalised to the mean count of the untreated control. *, **, ***, **** = p value <0.05, <0.01, <0.001, <0.0001, respectively, from one-way ANOVA analysis. Bars indicate mean with SD.

3.6.3 Ruxolitinib-CFZ combination increases apoptosis of MF cells compared to ruxolitinib alone

The effect of pulsed CFZ on apoptosis and cell cycle was studied on MF-19 CD34+ cells at 24h. This experiment revealed the 1h-pulsed CFZ 300 nM, either alone or in combination with ruxolitinib, was able to significantly increase the number of apoptotic cells compared to ruxolitinib alone ($p = 0.02$ and $p = 0.0001$, respectively; Figure 3.18A), although to a minor extent. With respect to the cell cycle, CFZ alone did not affect the cell cycle compared to control at 24h; in the ruxolitinib arms there was instead a higher proportion of cells in G0/G1 compared to control and CFZ alone (Figure 3.18B). The proportion of cells arrested in sub-G0 was equal across the four treatment arms (0.5%, 0.7%, 0.7% and 0.9% for control, ruxolitinib, CFZ and combination, respectively).

3.6.4 PI BTZ enhances the inhibitory effect of ruxolitinib on MF cells

In order to see if a similar effect could be obtained with a different PI, the first-generation PI BTZ was used (Figure 3.19). On MF-20 MNCs, 1h-pulsed BTZ 300 nM showed a more pronounced efficacy then CFZ; however, this is at a dose never reached in patient plasma (where it is lower, please refer to Discussion, section 4.4.2.1) and was used in this experiment only to allow comparison with CFZ. Interestingly, on MF-20 CD34+ the combination of BTZ and ruxolitinib showed an at least additive effect at a prolonged time point (168h).

3.6.5 Ruxolitinib-CFZ combination reduces colony formation of MF cells compared to ruxolitinib alone

To explore the effect of PI on the long-term clonogenic potential of CD34+ MF cells, we performed colony formation assays. These showed that CFZ has a significant inhibitory impact on stem/progenitor cells at 50 nM which was increased several times by the combination with ruxolitinib (for both MF-9 and MF-28); pulsed CFZ in combination with ruxolitinib was able to exert a higher inhibitory effect compared to ruxolitinib alone in MF-28 ($p = 0.008$) (Figure 3.20).

Figure 3.18. Apoptosis and cell-cycle analysis of MF CD34+ cells after exposure to ruxolitinib, 1-h pulsed CFZ and their combination.

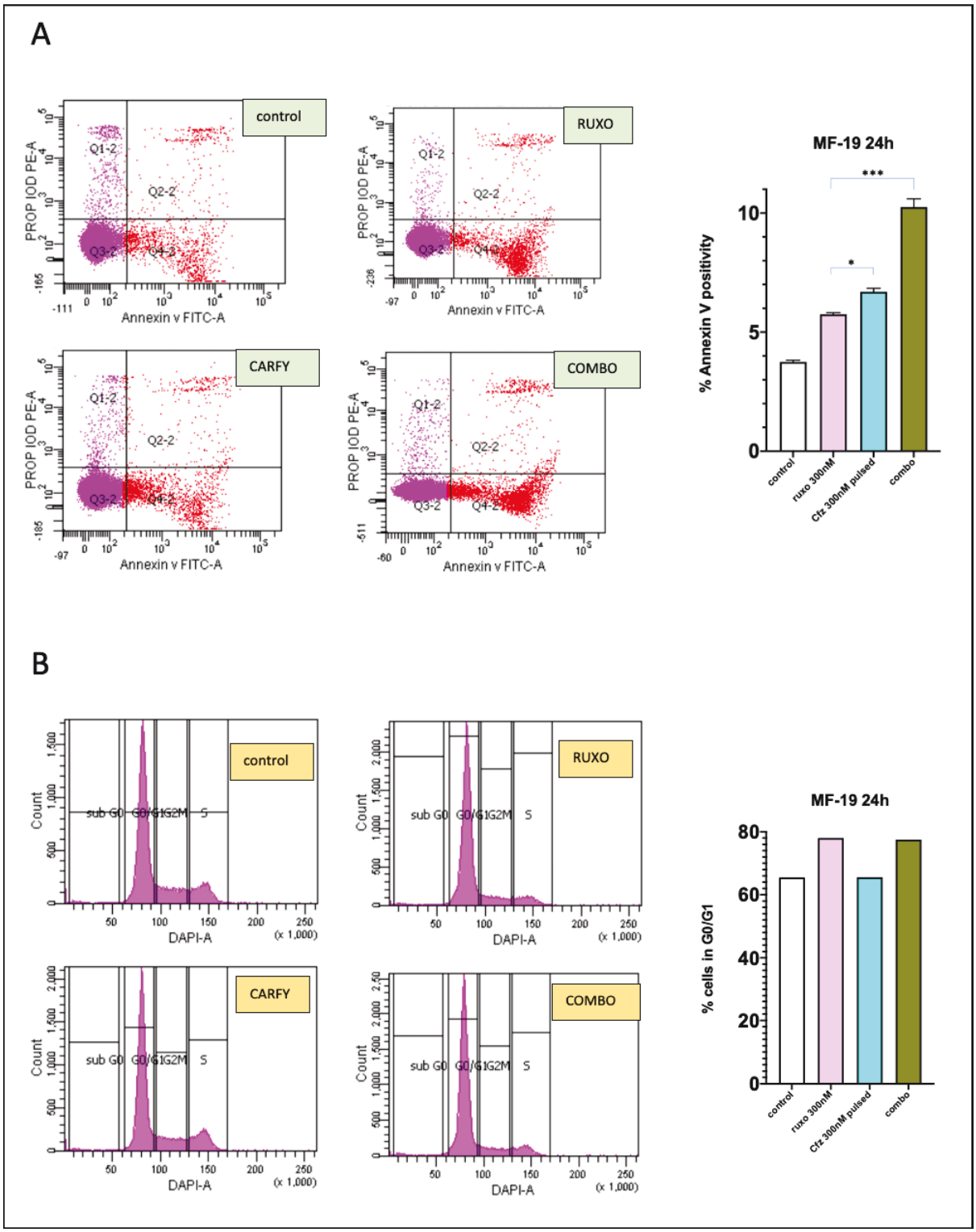

Figure 3.18. Apoptosis (A) and cell cycle (B) studies on CD34+ MF-19 cells at 24h from exposure to 1h-pulsed carfilzomib 300 nM (CARFY, cfz) +/- ruxolitinib (RUXO) 300 nM. *, *** = $p<0.05$, <0.001, respectively, from one-way ANOVA. The apoptosis assay was run on two technical replicates and bar chart reports mean with SD.

Figure 3.19. In vitro effect of ruxolitinib with or without 1h-pulsed BTZ on MF CD34+ cells and MF MNCs.

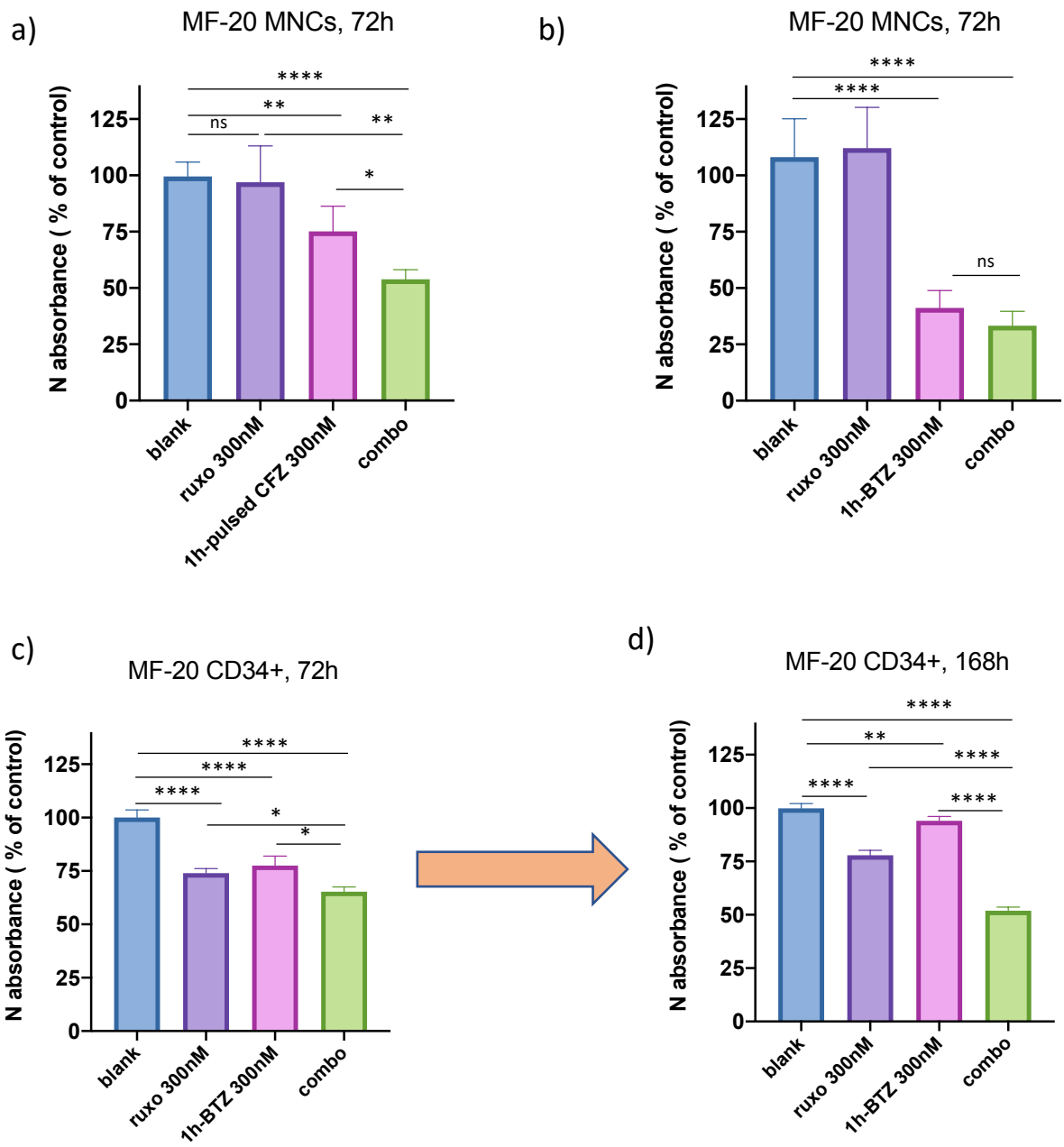

Figure 3.19. MF-20 MNCs were treated in vitro with either 1h-pulsed CFZ 300 nM (a) or 1h-pulsed BTZ 300 nM (b), with or without ruxolitinib (ruxo) 300 nM. Both PI significantly reduced the cell viability assessed through MTS after 72h from pulsed exposure.
CD34+ cells from the same patient were then exposed to pulsed BTZ and assessed through MTS at 72h and 168h. Y axis of bar charts indicates the absorbance normalised (N) to the mean absorbance of the untreated control (blank). Bars represent the mean with SD of 6 technical replicates for each of the MNCs experiments and of 4 technical replicates for the CD34+ cell experiment (*, **, ****: *p* value <0.05, <0.01 and <0.0001, respectively, from one-way ANOVA). Prolongation of the exposure time increased the efficacy of the combination treatment.

Figure 3.20. Colony formation assay on MF CD34+ cells exposed to of ruxolitinib with or without CFZ (continuous or 1h-pulsed).

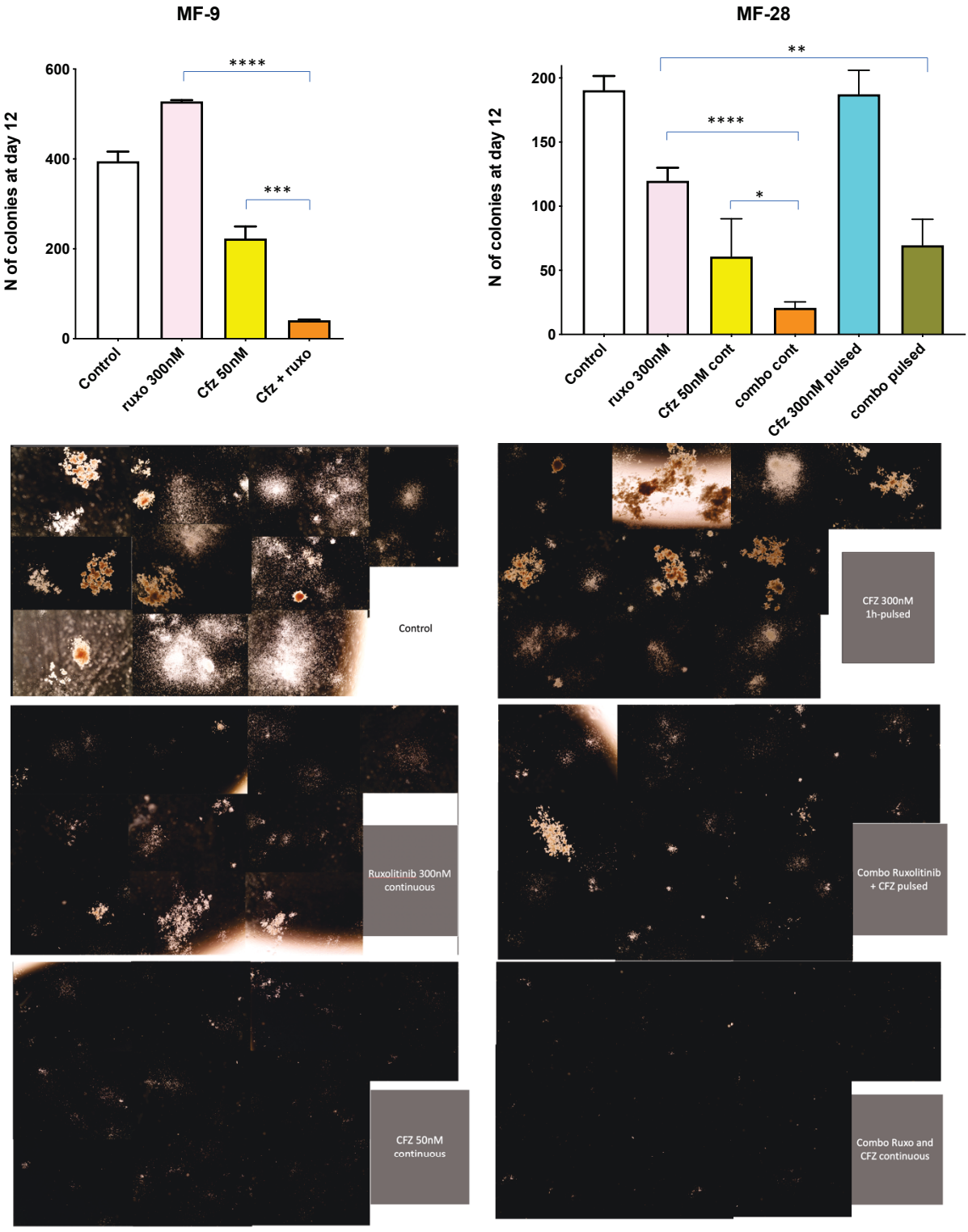

Figure 3.20. In the upper part of the figure are shown the bar charts representing the number (indicated by N, Y axis) of total haematopoietic colonies for each condition in MF-9 (left) and MF-28 (right), after 12 and 14 days, respectively. Data were obtained by reading the number of colonies from 4 dishes per each treatment condition (there were 2 dishes in each of 2 experiment replicates) and presented as mean with SD (*, **, ***, ****: *p* value <0.05, <0.01, <0.001, <0.0001, respectively; one-way ANOVA test). The lower part of the figure shows 10 representative pictures (those with the highest number of colonies visible) at microscope, taken from the two dishes of each treatment condition for each replicate (MF-28), at same magnification (25X). Ruxo = ruxolitinib.

3.7 Gene expression profile (GEP) on primary MF CD34+ cells

In order to explore the molecular alterations in leukemic stem/progenitor cells in MF following exposure to JAK2-inhibitor, CD34+ cells were isolated from the peripheral blood of 5 patients with MF (day 0) and expanded for 2 days in cytokine enriched medium (StemSpan medium supplemented with CC100, StemCell Technologies). On day 2, cells were split in two different experimental settings: A, to continue in cytokine-supplemented culture (vehicle); B, to continue in cytokine-supplemented culture together with ruxolitinib 300 nM. The reason for the choice of this ruxolitinib concentration is because it is intermediate between ruxolitinib C_{max} plasma concentration (1100 nM) and its concentration after 12h (45.6 nM) from administration of oral dose of 25 mg (265).

On day 4 cells were collected and total RNA extracted. Gene expression analysis of primary MF $CD34^{+}$cells was performed to identify genes most affected by ruxolitinib and to define a list of genes of interest to further interrogate using gene set enrichment analysis (GSEA)(267, 268).

Figure 3.21 shows the expansion of CD34+ cell after 4 days in culture, in both experimental conditions.

The differential GEP was investigated in the best 3 samples i.e. MF-3, MF-8, MF-10 (MF-5 and MF-9 were excluded because they failed to pass the quality metrics required for RNAseq analysis).

3.7.1 Gene expression profile analysis

Gene expression analysis resulted in the identification of 17,435 differentially expressed genes. In detail, by following threshold described in the Methods, 186 genes were found to be significantly differentially expressed, of which 46 were upregulated (log2 fold change > 1 in absolute value) and 140 were downregulated (log2 fold change < 1 in absolute value) in treated cells compared to untreated cells (Appendix, Table A7). The Volcano plot in Figure 3.22 shows the differential GEP between treated and untreated samples, where on the *x* axis is the log2 fold change and on the *y* axis is the log10 adjusted *p* value (padj). The top 30 differential expressed genes are shown in Fig 3.23. Most of the genes in the heatmap are downregulated by ruxolitinib, the majority of which are involved in the immune-inflammation process and oxidative phosphorylation.

Figure 3.21. MF CD34+ cells expansion in cytokine-rich medium, with and without ruxolitinib.

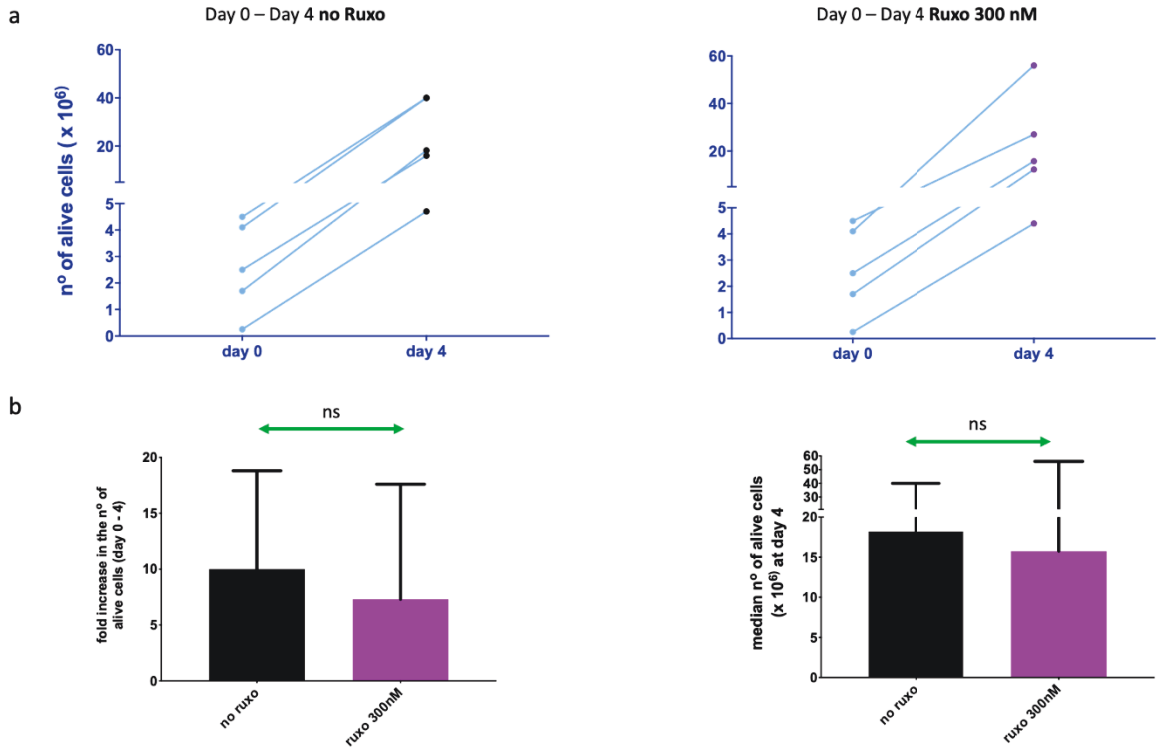

Figure 3.21. a) change in the number of viable cells after 4 days of culture in CC100-supplemented medium (day 0 corresponds to the day of CD34+ selection and day 4 to the collection day and RNA extraction; ruxolitinib was added to one group of cells on day 2). b) on the left, the fold change in the number of viable cells compared to day 0 without or with ruxolitinib exposure; on the right, the median number of viable cells at day 4 across all 5 samples, for both untreated and treated groups. Ns = not statistically significant, from unpaired t-test.

Figure 3.22. Differential GEP in MF CD34+ cells after in vitro exposure to ruxolitinib 300 nM.

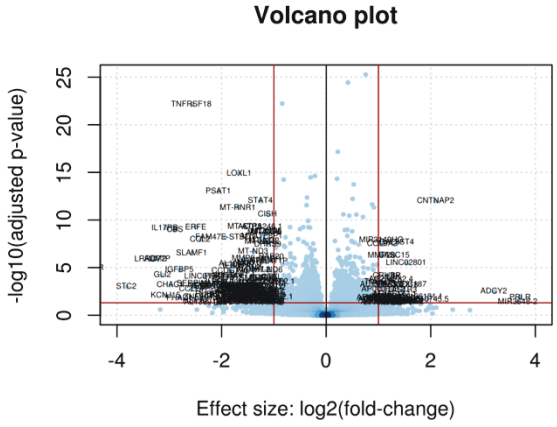

Figure 3.22. The Volcano plot shows the differentially-expressed genes in the ruxolitinib-treated MF CD34+ cells compared to untreated control. CD34+ cells from 3 MF patients were included in the analysis (MF-3, MF-8 and MF-10). On X axis is reported the log2 fold-change of gene expression, while on the Y axis the -log10 adjusted *p* value. Vertical red lines correspond to -1 and + 1 log2 fold change, while horizontal red lines to padj <0.05.

Figure 3.23. Differential gene expression analysis on MF CD34+ cells treated in vitro with ruxolitinib or vehicle ("control").

Figure 3.23. The heatmap shows the 30 most statistically relevant genes (adjusted *p* value, padj) that are differentially-expressed between ruxolitinib-treated cells and untreated control, listed according to padj (the first gene having the smallest padj). The heatmap is divided into two parts: the first 6 columns at the left side of the heatmap, indicated by the grey bar at the top of the heatmap, represent untreated samples; the remaining 6 columns of the heatmap, indicated by green bar at the top, represent the treated samples. The colour scale refers to the gene expression log2 fold change.

3.7.2 Gene set enrichment analysis

The list of differentially expressed genes providing input for the gene set enrichment analysis (GSEA) was ranked using the following metrics: $-log_{10}(pvalue)*sign(log\ fold\ change)$ (269). The full list of positively- and negatively-enriched **gene sets** is given in the Appendix (Tables A8 and A9). The proteasome family was among the top 10 negatively-enriched gene sets in MF CD34+ cells treated with ruxolitinib (Figure 3.24), suggesting that ruxolitinib treatment has an inhibitory effect on the gene expression of this pathway. The full list of enriched genes for the proteasome family is provided in the Appendix (Table A10).

Other negatively-enriched gene sets there were oxidative phosphorylation, spliceosome components, DNA replication, cytokine-receptor interaction (Figure 3.25).

Of note, only the negatively-enriched gene sets showed a significant enrichment according their FDR (which was <0.25 for 46 gene sets, <0.1 for 34 and <0.01 for 21), suggesting that ruxolitinib induced mostly a suppressive effect on gene expression.

Figure 3.24. Proteasome gene set is negatively-enriched in MF CD34+ cells treated with ruxolitinib.

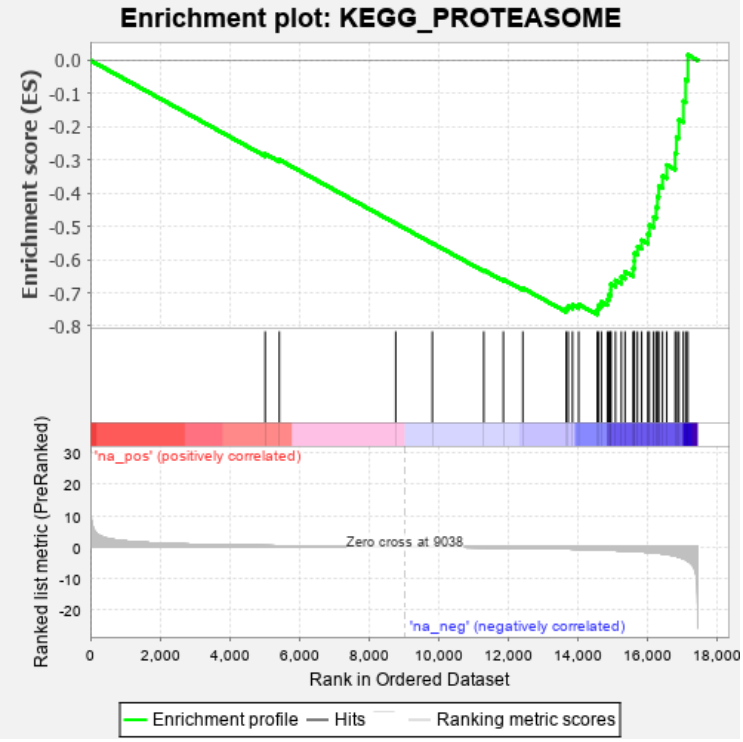

Figure 3.24. The figure illustrates the Enrichment plot of the proteasome gene set members, from KEGG gene set enrichment analysis. The gene set members are represented as black bars. They are listed in order of ES, genes on the left are the most upregulated, those on the right side are downregulated. The figure shows that most of the dysregulated genes in the proteasome pathway (gene set) are downregulated in ruxolitinib-treated MF CD34+ cells compared to untreated control.

Figure 3.25. Gene set enrichment analysis in MF CD34+ cells treated in vitro with ruxolitinib: top-10 negatively-enriched pathways.

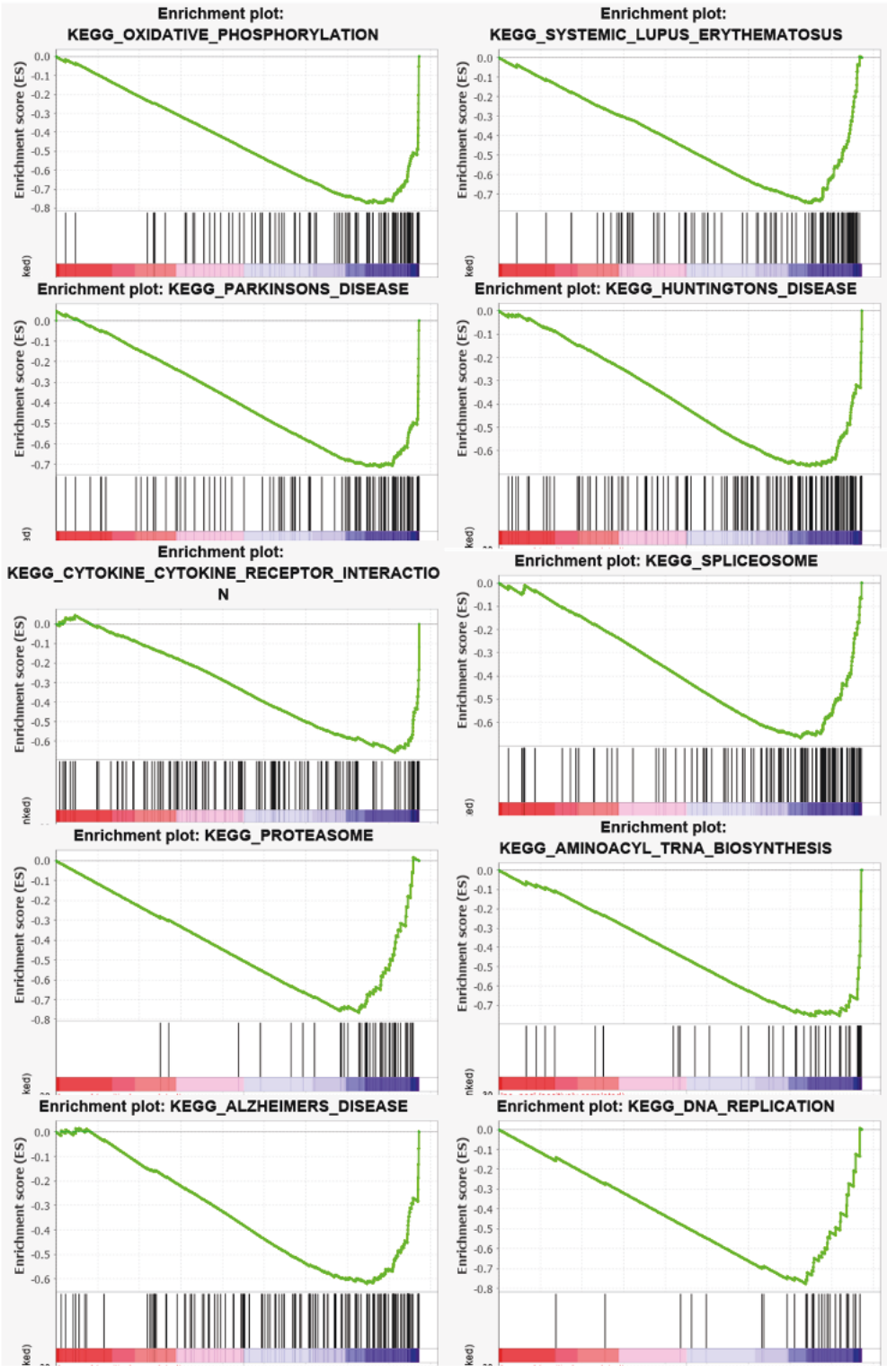

Figure 3.25. The figure illustrates the enrichment plots of top-10 negatively-enriched pathways in ruxolitinib-treated MF CD34+ cells, ranked by NOM-p value, from KEGG and BIOCARTA databases gene set enrichment analysis. Gene sets are ordered in descending order from the 1st (smallest NOM-p value) to the 10th (from left to right and starting from the top).

3.8 Additional potential targets from gene expression analysis which need further investigation

In a preliminary differential gene expression analysis (data not shown), upregulated genes were identified that were not investigated functionally. However, RT-qPCR revealed that some of these genes (*PTGDS* and *ARG1*) were upregulated in the same CD34+ MF samples treated with ruxolitinib. The reason for choosing these two targets for further validation with RT-qPCR was the presence of their shRNAs among the top depleted ones from the pooled-shRNA library screen of MF-3, suggesting a possible important role for them in viability of MF CD34+ cells. The other gene of which I measured expression in MF samples was *FLT3,* which is present among the 46 upregulated genes by ruxolitinib (Appendix, Table A7) and in view of its role in activation of STAT5 (please refer to the Discussion, section 4.6).

3.8.1 *PTGDS* expression by MF and healthy CD34+ cells exposed to ruxolitinib

Figure 3.26 shows the upregulation of *PTGDS* expression in the MF CD34+ from all 5 patients studied in the GEP experiment. In MF-10 the *PTGDS* expression level increased 12.8 folds compared to the untreated control. In order to investigate whether this finding was specific to MF CD34+, the expression of *PTGDS* was also measured in healthy donor CD34+ cells and was found to be upregulated following treatment with ruxolitinib but at a significantly lower degree: the median fold change in MF samples was 7.7 vs 1.7 in healthy controls, $p = 0.02$). Although no comparison can be done across driver mutations, it is worth nothing that the 3 patients with highest fold change are all *JAK2*-mutated MF, while MF-9 is triple-negative, MF-8 *MPL*-mutated and MF-23 *CALR* type 2-mutated.

Figure 3.26. *PTGDS* upregulation in MF and healthy CD34+ cells exposed in vitro to ruxolitinib.

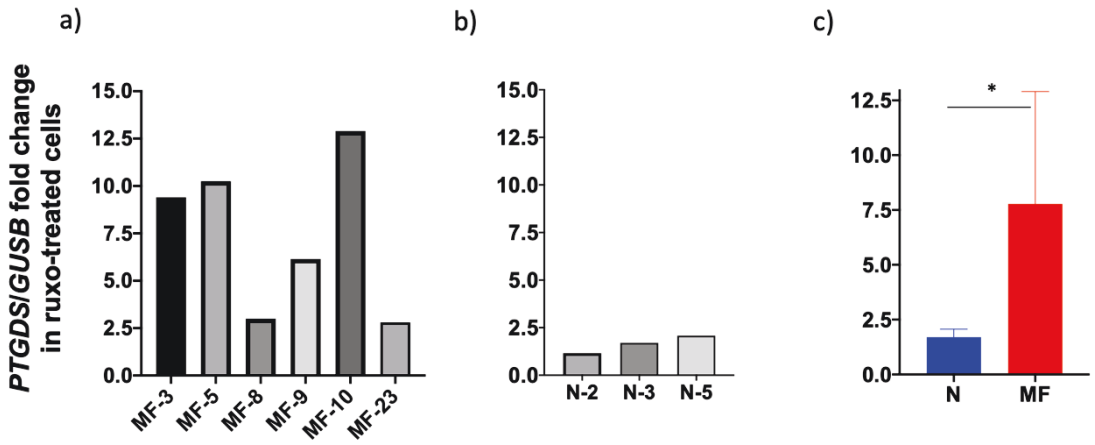

Figure 3.26. Fold change of *PTGDS* expression in MF (a) and healthy control (b) CD34+ cells treated with ruxolitinib (ruxo) 300 nM for 48h, compared to the untreated sample; and the comparison of the *PTGDS* fold changes (c) (bars express median with range) between healthy control (N) and myelofibrosis (MF) groups. * is for p <0.05, Mann-Withney test.

3.8.2 Effect of PDG2 and AT-56 +/- ruxolitinib on MF and healthy CD34+ cells

AT-56 is a potent and selective inhibitor of lipocalin-type prostaglandin D2 synthase (L-PTGDS). PDG2 is the product of *PTGDS*. In order to explore the effect of the exposure to these compounds on MF CD34+ cells, MTS assay was used in absence or presence of ruxolitinib 300 nM. Data showed no significant differences of the combination treatments compared to ruxolitinib alone nor any significant effect of PDG2 and AT-56 on cell proliferation (Figure 3.27).

Figure 3.27. Effect of PDG2 and AT-56 on proliferation of MF CD34+ cells.

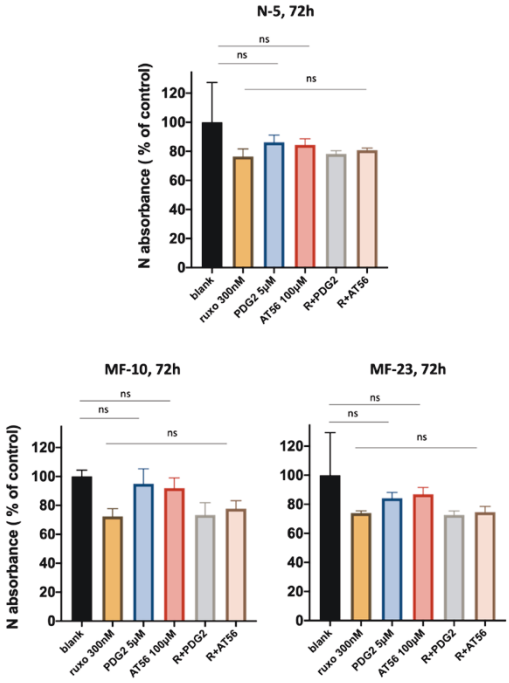

Figure 3.27. MTS assay of healthy donor (N-5) and MF CD34+ cells (from 2 patients, MF-10 and MF-23) exposed for 72h to ruxolitinib (ruxo) 300nM, prostaglandin D2 (PDG2) 5 µM, L-PTGDS selective inhibitor AT-56 100 µM and combo treatments ruxolitinib-PDG2 (R+PDG2) and ruxolitinib-AT-56 (R+AT56). Y axis reports the normalised (N) absorbance to the mean absorbance of the untreated control (blank). Bar chart represent mean with SD.

3.8.3 *ARG1* expression in MF CD34+ cells exposed to ruxolitinib

The RT-qPCR for *ARG1* showed more diverse results, with increased expression in some samples and no difference for others (Figure 3.28). Of note, a 7.8-fold change gene expression level was found in MF-3, the sample which was studied by the pooled-shRNA library experiment. In the latter, the 2nd most depleted *ARG1*-targeting shRNA had 5.17-fold depletion.

Figure 3.28. *ARG1* upregulation in MF CD34+ cells exposed in vitro to ruxolitinib 300 nM.

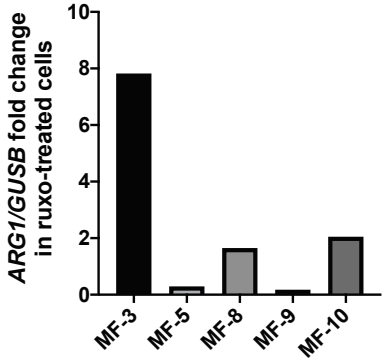

Figure 3.28. RT-qPCR gene expression fold change of ARG1 in MF CD34+ cells exposed to ruxolitinib (ruxo) 300 nM for 48h, compared to the untreated sample.

3.8.4 *FLT3* expression in CD34+ MF cells exposed to ruxolitinib

Among the 46 upregulated genes identified by the differential gene expression analysis reported in section 3.7.1, *FLT3* emerged as an interesting target to further explore given the well-known pathogenic role of its point mutations in AML and the clinically available FLT3-inhibitors. RT-qPCR validated this finding, showing an increased expression ranging between 1.6 to 5.7-fold change compared to the untreated control (Figure 3.29).

Figure 3.29. *FLT3* upregulation in MF CD34+ cells exposed in vitro to ruxolitinib 300 nM.

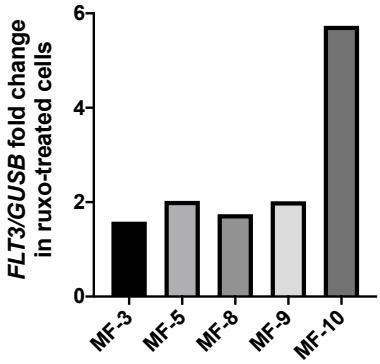

Figure 3.29. RT-qPCR gene expression fold change of *FLT3* in MF CD34+ cells exposed to ruxolitinib (ruxo) 300 nM for 48h, compared to the untreated sample.

Further studies on a larger number of samples are needed to explore the role of *PTGDS, ARG1* and *FLT3* in MF.

3.9 NF-κB pathway alteration in MF CD34+ cell exposed to inhibitors

Myelofibrosis is characterised by NF-κB pathway hyperactivation, which is a crucial pathogenetic player as it drives sustained inflammatory response and promotes leukemic cell survival (270). Although limited, evidence exists about a suppressive effect of ruxolitinib on this pathway (271, 272).

In view of the importance of proteasome in the regulation of NF-κB activation (273), we investigated the alteration induced by ruxolitinib and its combination with CFZ on this pathway, first of all at gene expression level (next section) and then at protein level (section 3.8.2).

3.9.1 In vitro effects of pulsed CFZ with or without ruxolitinib on NF-κB pathway gene expression on MF CD34+ cells

CD34+ cells separated from the peripheral blood of two patients with MF (MF-4, and MF-24) were exposed in vitro to pulsed treatment experiments as described in the Methods, and RNA was extracted and analysed using low-density microarray for 92 genes of the NF-κB pathway. The Trypan-blue assay data for each sample is shown in Figure 3.17 b) and c), respectively.

For statistical analysis, Kruskal-Wallis test was applied to the entire set of genes across treatment conditions, taking into account the gene expression fold change compared to the untreated control. Each patient experiment was analysed separately.

Overall, ruxolitinib induced a downregulation of most genes (p <0.0001 for both MF-4 and MF-24); CFZ, on the contrary, induced an upregulation of most genes compared to control, and the effect was far more diffuse and pronounced in MF-24 (ruxolitinib-treated patient) than in MF-4 (ruxolitinib-naïve patient) (CFZ vs control: p <0.0001 and 0.05, respectively) (Figure 3.30 and 3.31).

Although the general pattern across treatment arms was similar between MF-4 and MF-24, there were some groups of genes for which the direction of the change in the gene expression (up- vs downregulation) differed: group 1, genes whose expression was upregulated or unchanged in MF-24 while it resulted unchanged or downregulated in MF-4, compared to control; group 2, genes whose expression was upregulated or unchanged in MF-4 while it resulted unchanged or downregulated in MF-24, compared to control; and group 3, genes for which the exposure to ruxolitinib caused a discordant change in the gene expression between the 2 patients (as shown in Figure 3.32).

Finally, looking at MF-24 only, the difference between the combination of the two drugs and CFZ alone was not significant (p = 0.9). This could be related to the fact that the addition of ruxolitinib produced 3 different effects on the gene expression compared to the CFZ-alone arm: no effect, reduction of the upregulation or increase in the upregulation. The last event is the most interesting, given most genes were downregulated by ruxolitinib. The following genes were downregulated by ruxolitinib and upregulated by the combination CFZ-ruxolitinib, more than by CFZ alone: *TLR4*, *TLR8*, *NOS2*, *ILR1*, *IL12A*, *IL1A*, *IRAK2*, *TBK1*, *TNFRSF11A*, *TLR6*, *IER3*, *TNFSF15*, *CARD10*, *EDARADD*, *TLR9*, *NKIRAS2*, *ZNF675*, *TLR7*, *CSF3*, *TNFRSF1A*, *TLR3*. Reflection on these findings will follow in the Discussion, section 4.5.

Figure 3.30. Effect of ruxolitinib and CFZ on the NF-κB pathway gene expression profile in MF-4 CD34+ cells.

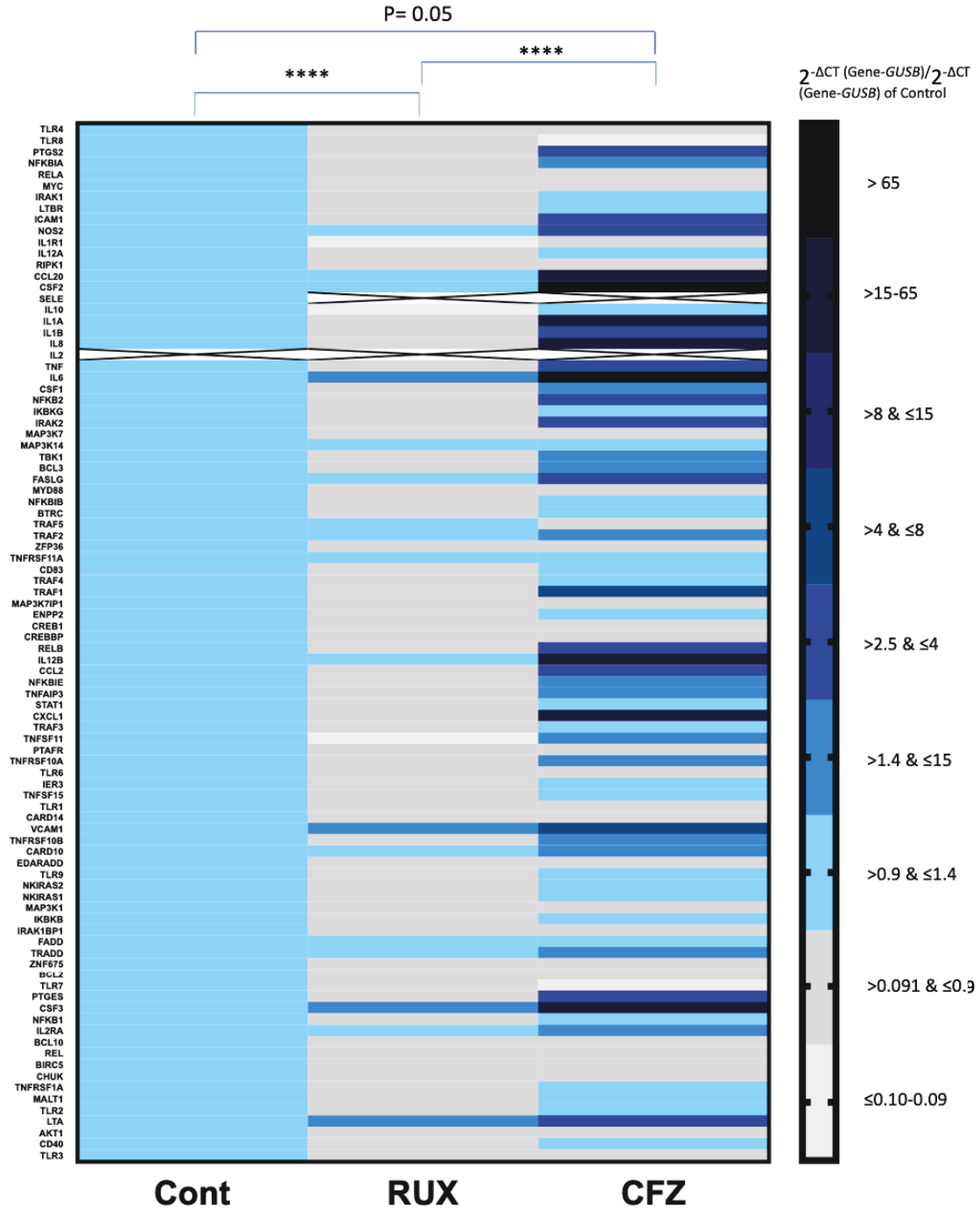

Figure 3.30. The heat map shows the gene expression fold change in each treatment arm (RUX = ruxolitinib; CFZ = carfilzomib) compared to the untreated control (Cont) derived from the ratio of the $2^{-\Delta CT(\text{gene of interest-}GUSB)}$ of the treatment arm analysed to the $2^{-\Delta CT(\text{gene of interest-}GUSB)}$ of the control. RNA was extracted from CD34+ cells derived from peripheral blood of MF-4 (treatment-naïve patient), 48h after the exposure to 1h-pulsed CFZ 300 nM or continuous ruxolitinib 300 nM. Low-density microarray was performed using Applied Biosystems® TaqMan® Array Human NFkB Pathway 96-well Plate. "X" in some cells means that reaction in the respective gene well failed. Kruskal-Wallis test with Dunn's multiple comparisons post hoc test was carried out across the treatment arms and *,**,***,**** are for p <0.05, <0.01, <0.001, <0.0001, respectively.

Figure 3.31. Effect of ruxolitinib +/- CFZ on the NF-κB pathway gene expression profile in MF-24 CD34+ cells.

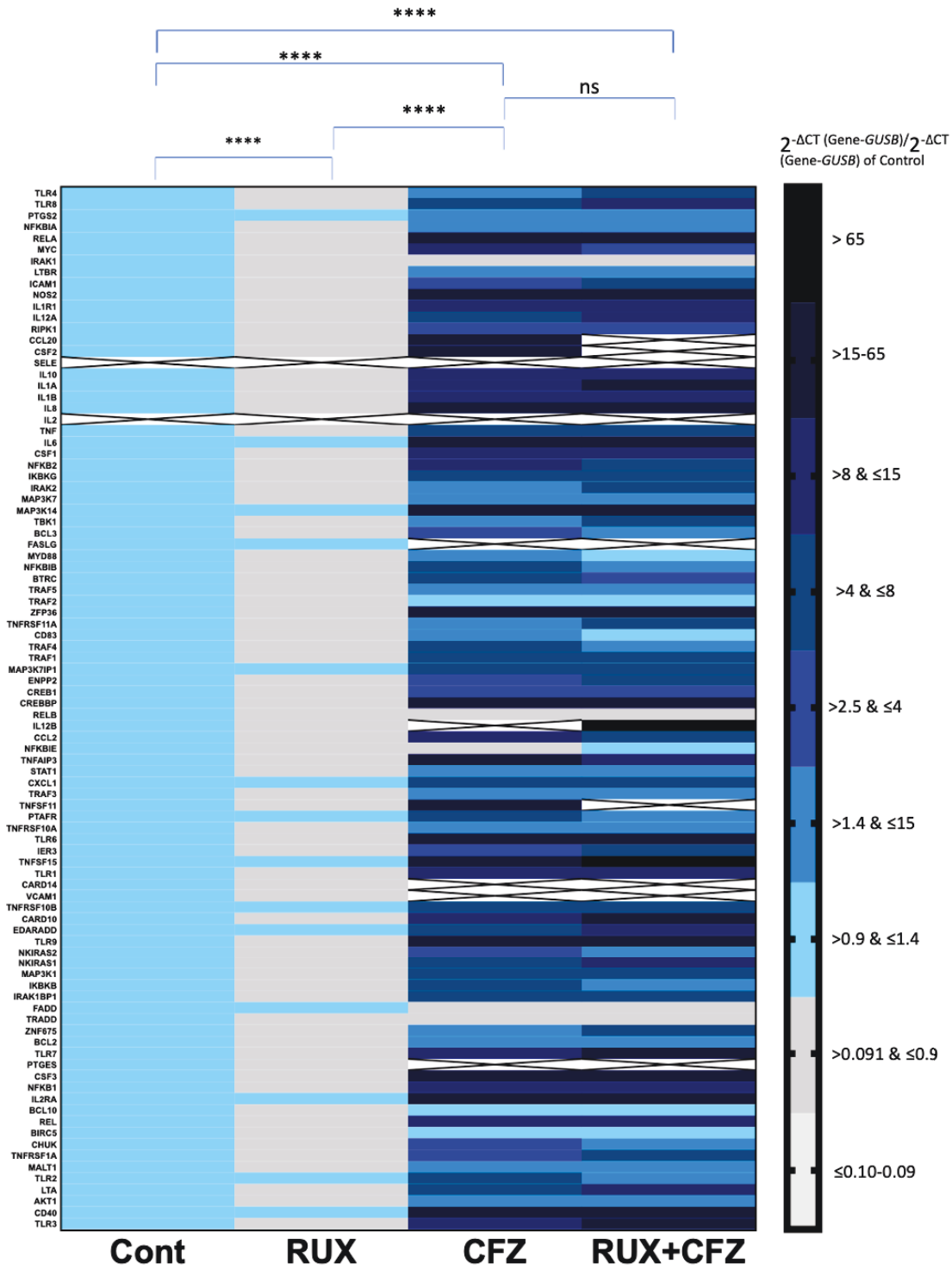

Figure 3.31. The heat map shows the gene expression fold change in each treatment arm (RUX = ruxolitinib; CFZ = carfilzomib; RUX+CFZ = combination treatment) compared to the untreated control (Cont) derived from the ratio of the $2^{-\Delta CT(\text{gene of interest-GUSB})}$ of the treatment arm analysed to the $2^{-\Delta CT(\text{gene of interest-}GUSB)}$ of the control. RNA was extracted from CD34+ cells derived from peripheral blood of MF-24 (ruxolitinib-refractory patient), 24h after the exposure to 1-h pulsed CFZ 300nM +/- continuous ruxolitinib 300 nM. Low-density microarray was performed using Applied Biosystems® TaqMan® Array Human NFkB Pathway 96-well Plate. "X" in some cells means that reaction in the respective gene well failed. Kruskal-Wallis test with Dunn's multiple comparisons post hoc test was carried out across the treatment arms and *,**,***,**** are for p <0.05, <0.01, <0.001, <0.0001, respectively.

Figure 3.32. NF-κB pathway genes with discordant expression change induced by CFZ or ruxolitinib in MF-24 and MF-4 CD34+ cells in vitro.

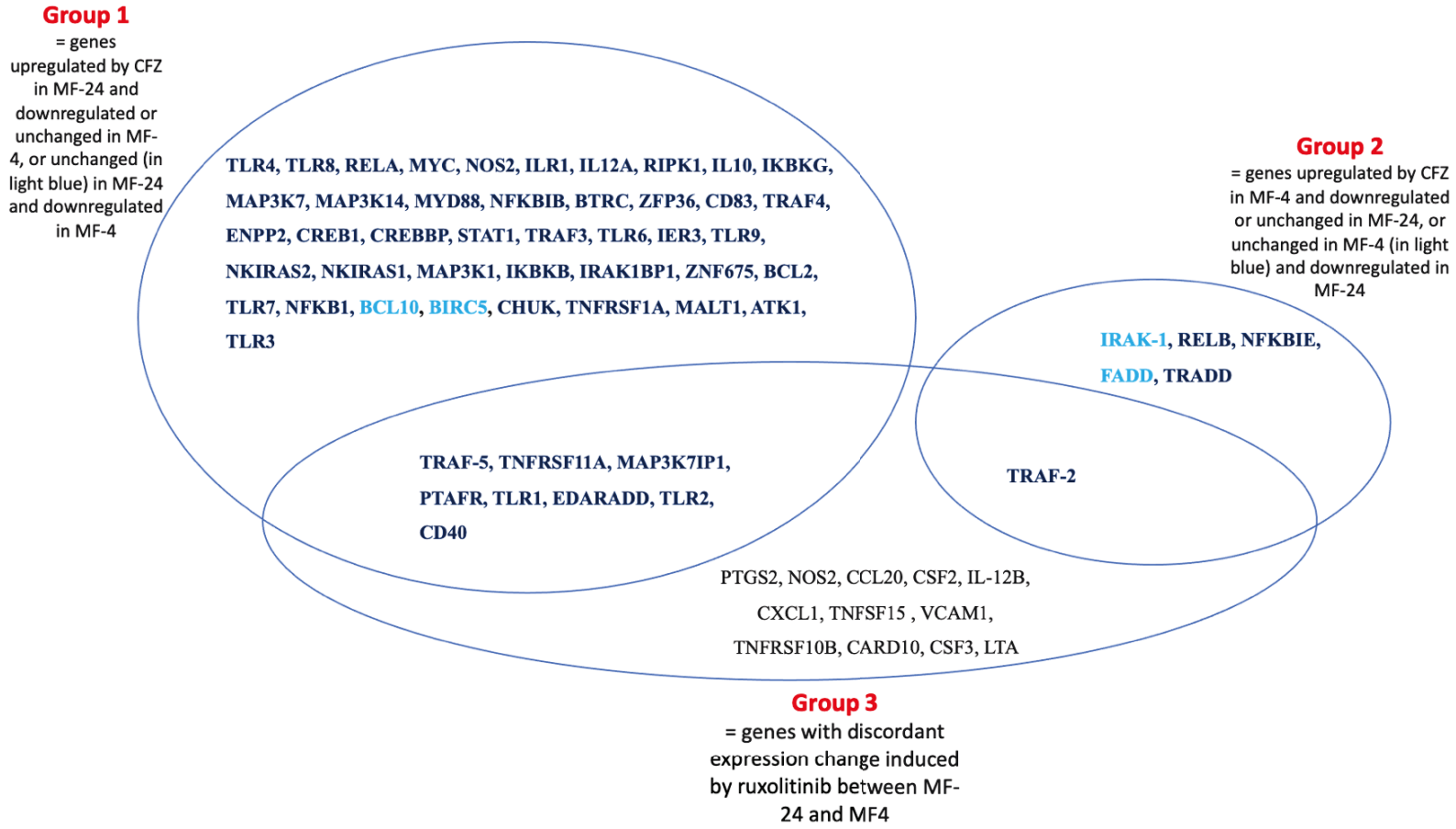

Figure 3.32. The figure shows groups of genes with discordant expression change between MF-4 and MF-24 in respect to each treatment arm, either carfilzomib (CFZ) (group 1 and group 2) or ruxolitinib (group 3). Some of these genes are shared between group 1 and 2 and 2 and 3. The experiment to which the Figure refers is the NF-κB pathway gene expression analysis through Applied Biosystems® TaqMan® Array Human NF-κB Pathway 96-well Plate, performed on CD34+ cells of 2 patients with MF (refer to text for further detail).

3.9.2 Investigation of nuclear p65 in CD34+ MF cells does not support activation of NF-κB following CFZ treatment

Following the low-density microarray experiment reported in the above section, we wonder whether the upregulation of the NF-κB pathway induced by CFZ at gene expression level was reflected also at protein level in MF CD34+ cells.

The Western Blot analysis of the extracted protein from nuclear and cytoplasmic fractions of CD34+ cells from MF-19 is shown in Figure 3.33.

The experiment showed that 1h in vitro exposure to CFZ significantly reduced the activation of NF-κB pathway in MF CD34+ cells (p65/lamin B1 ratio means were 1.05 vs 0.403 in untreated control and 1h-pulsed CFZ arms, respectively, $p = 0.03$), at least as effectively as ruxolitinib (mean p65/lamin B1 ratio in ruxolitinib arm was 0.582, difference not statically significant compared to untreated control). However, the addition of the latter did not lead to any additive effect compared to pulsed CFZ alone. The mean p65/lamin B1 ratio for the combo arm was 0.488, with a statistically significant difference compared to control ($p = 0.04$).

Figure 3.33. Measurement of NF-κB activation on MF-19 CD34+ cells following in vitro treatment with ruxolitinib +/- 1h-pulsed CFZ.

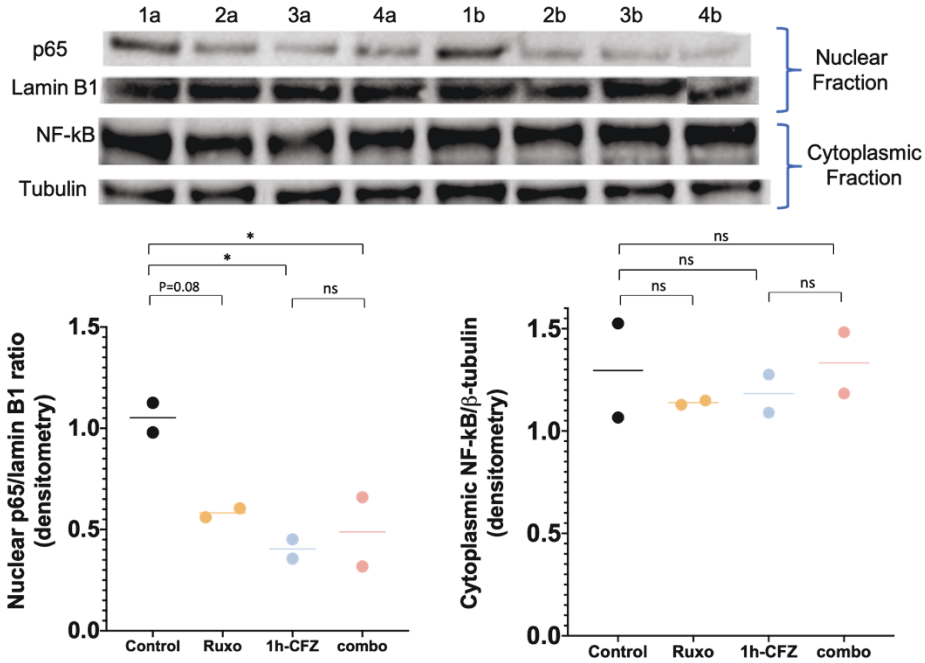

Figure 3.33. In the upper part of the figure is shown the Western Blot images of nuclear p65 (activated NF-κB) versus total NF-κB in cytoplasmic fraction of MF-19 CD34+ cells treated with inhibitors. 1, 2, 3 and 4 represent untreated (control), 24h-continuous ruxolitinib 300 nM, 1h-pulsed CFZ 300 nM and combined 1h-pulsed CFZ plus 24h-continuous ruxolitinib, respectively. The experiment was performed in duplicate (1a, 1b; 2a, 2b; 3a, 3b; 4a, 4b). The density of the bands was measured using Image J software (version 1.52t; NIH, USA). In the lower part, the left chart shows the p65/lamin B1 ratio across treatment arms, while the right chart the cytoplasmic NF-κB/β-tubulin ratio. Coloured dots represent the ratios obtained from each of the 2 technical replicates for each condition and the bar indicates the mean. * is for $p < 0.05$ and ns = not statistically significant, from one-way ANOVA analysis.

CHAPTER 4

Discussion

4.1 Interpretation of pooled-shRNA library screen results on HEL cell

In this section I will reflect on the findings of the pooled-shRNA library screen on the HEL cell line, after a brief comment on the pre-screening findings in the HEL cell line (section 4.1.1).

The bioinformatic analysis of post-selection barcode abundancy revealed shRNAs more depleted in one experimental setting (section 4.1.2) and shRNAs recurrently top-depleted across all 3 settings (section 4.1.3).

My discussion will be focused mainly on those genes, targeted by these shRNA, for which an extensive literature search highlighted a potential relationship with the JAK/STAT pathway, and other molecular alternations characteristic of MPN and MF or with cancer in general, making them possible targets for future research.

In 4.1.3.2 I will discuss the proteasome gene family, found in the group of genes targeted by recurrent highly-depleted shRNA and on which the validation phase on both HEL cell line and primary MF cells has been centred.

4.1.1 Advantages and limitations of the HEL cell line as MPN cell model

We chose to use the HEL cell line as it is widely accepted as a cell model of myeloproliferative neoplasms (274), and is dependent on hyperactivation of the JAK/STAT pathway (275) which renders it a good candidate for high throughput knockout screen of genetic vulnerabilities of MPN.

We confirmed the presence of the homozygous *JAK2*^{V617F} mutation and, most importantly, amplification of the mutated *JAK2* gene with 6-10 *JAK2* copies found by FISH. The 72h IC_{50} for ruxolitinib was >1 μM, which in presence of HS-5 CM increased by almost three fold. This supports a protective role of the microenvironment on leukemic cell survival and justifies the use of HS-5 CM in the pooled-shRNA screen as a tool to recapitulate the in vivo effect.

However, it is important to acknowledge an important limitation. HEL cells have other genetic abnormalities, including the *TP53*^{M133K} missense mutation (276) (as confirmed by our genomic analysis), which are responsible for additional pro-survival and anti-apoptotic pathways (277).

Mutation of *TP53* are rare events in chronic phase MPNs, including MF, while they are more frequent in secondary AML evolving from MPNs (278). However, *TP53* mutations have recently been found at low levels in a minority (14.7%) of MPN patients (279). In view of this, caution should be exercised in extending the findings of the pooled-shRNA library screen to primary MF cells. This is however a general concern with cell lines and applies to the other two commonly used *JAK2*^{V617}-positive human cell lines, SET2 (megakaryoblastic cell line, bearing complex karyotype along with two point mutations in *TP53* and *DNMT3A*)(276, 280) and UKE1 (having multiple structural chromosomal abnormalities)(281).

4.1.2 Top-depleted shRNAs in each experimental condition

4.1.2.1 Baseline (Setting 1)

Referring to Table 3.2 of Results, which lists the top-depleted genes in setting 1 (no ruxolitinib, no CM), it is interesting to note that all genes are shared by the other two experimental settings. This is not unexpected, as the addition of ruxolitinib in the presence or absence of microenvironment-mimicking medium should not impact the genes essential for HEL cell survival but can reveal additional targets important for survival under these conditions (refer to next sections). A gene of possible relevance in setting 1 is *CDC2*, as there was 1 shRNA with FC $\geq$ 3 and 1 shRNA in top 2% position for both replicates (while there were 3 shRNA with FC $\geq$ 3 in the setting 2, but none in the top 2% positions, and there was no shRNA satisfying any of these criteria for setting 3 [Appendix, Table A5]). *CDC2* codes for cyclin-dependent kinase-1 (CDK1), a protein involved in the transition from G2 to M phase and positively-regulated by JAK/STAT pathway (282). Interestingly, CDK1 interacts with Aurora kinase A, a crucial player in cell-cycle progression and control, that was recently shown to be a potential target in MPN (283). Also, CDK1 is negatively-regulated by protein phosphatase 2 (PP2A) (284), which in turn is a known phosphatase whose activity is suppressed in MPNs (285). Finally, an interesting gene for which there are 3 shRNAs resulting in the top 2% depleted for both replicates in this experimental setting is *BCL2L1* (Figure 3.12 and Table A5) which codes for Bcl-2-like protein, also known as Bcl-xL (Bcl-extra large). Bcl-xL is a member of the anti-apoptotic Bcl-2 protein family, which is overexpressed in MPN as a consequence of JAK/STAT hyperactivation (286). ShRNAs targeting *BCL2L1* are also among the top-depleted in the other two experimental settings, although the number of shRNAs satisfying the above criteria for both replicates was lower (Table A5).

Up-regulation of Bcl-xL in MF megakaryocytes is a key element in the perturbation of differentiation and proliferation (287), which in turn contribute to the pathogenesis of MF (288). In preclinical mice models, navitoclax, a BH3-mimetic drug able to inhibit Bcl-2, Bcl-xL and Bcl-w, synergistically induced apoptosis with ruxolitinib, prevented fibrosis, and overcame resistance to a JAK2 inhibitor (289). The combination of navitoclax and ruxolitinib was tested in a phase 2 clinical trial in MF patients already treated with ruxolitinib (NCT03222609) and provided encouraging results, including meaningful reductions in spleen size, reduction of symptoms and driver mutation allelic burden and some improvement in the degree of bone marrow fibrosis (290). In our pooled-shRNA screen of the HEL cell line only shRNAs targeting *BCL2L1* were the most depleted, whereas those targeting other Bcl-2 family members were not (Appendix, Table A4). This might suggest a more specific role for Bcl-xL compared to other Bcl-2 proteins in the survival of HEL cells. Very recently, *BCL2L1* expression was shown to be highest in MF compared to PV and ET (291). In the same study, the authors showed that the combination of ABT-737, a BH3-mimetic with high BcL-xL affinity, and a JAK2 inhibitor exerted a synergistic pro-apoptotic effect on HEL cells and primary MF cells, as previously suggested (292). The finding of *BCL2L1* along with *JAK2* and, indirectly, *MPL* (via JAK/STAT pathway), amongst the most important genes for the survival of HEL cells, is evidence of the reliability of the pooled-shRNA screening results, as Bcl-xL is a known important key regulator of cell survival in HEL cells (293). In summary, based on our pooled-shRNA results and independent evidence from the literature, it would be reasonable to further explore more selective Bcl-xL inhibitors (such as the potent A-1331852) in combination with ruxolitinib in MF.

4.1.2.2 Ruxolitinib alone (Setting 2)

ShRNAs with the highest RA2 rank in presence of ruxolitinib targeted 31 genes (Results, Table 3.3, genes highlighted in red).

Ribosomal protein genes were among the most represented in the top positions in this experimental condition (*RPL 14, 10, 15, 8 and RPS11, RPS6 and RPSA*). Upregulation of the ribosomal pathway was also seen in MF CD34+ cells treated with ruxolitinib (Appendix, Table A9). Of note, mutated *RPL10* can activate the JAK/STAT pathway in T-ALL (294).

MAPKAPK5 (Mitogen-Activated Protein Kinase-Activated Protein Kinase-5 or MAPK-activated Protein Kinase-5 [MK5]) is a downstream component of the Ras/Raf/MEK/ERK/MAPK pathway, whose compensatory activation is a possible mechanism of resistance to ruxolitinib (155, 293, 295, 296). Furthermore, MK5 activates HPS27, (297) a

small heat shock protein recently shown to be a potential therapeutic target in MF as it prevents STAT5 de-phosphorylation and might favour the interaction between JAK2 and STAT5 (298). Finally, *FLI1* encodes for Fli1, a transcription factor member of the ETS family of transcription factors, which is a known positive regulator of *MPL* expression (299). *FLI1* expression is upregulated by activation of JAK/STAT signalling (300). Very recently, Fli1 has been implicated in the pathogenesis of *CALR*-mutated MPN, where the mutated calreticulin binds to Fli1 and increases its chromatin localization and occupancy genome wide, with enriched recruitment of the *MPL* promoter and resulting increased *MPL* expression (301). Table 4.1 summarises the other genes targeted by the most depleted shRNAs preferentially in the presence of ruxolitinib, along with a brief explanation of their role and, if any, their possible relevance in MPN obtained from the available literature.

Table 4.1. Other genes targeted by the top-depleted shRNAs in experimental setting 2.

Gene name	Protein	Cellular function and possible relevance in MPN
PSMC1	26S proteasome regulatory subunit 4	proteasome genes will be discussed in section 4.1.3.2
CDC2L1	cell division cycle 2-like 1	a cyclin-dependent kinase involved in the activation of Hedgehog Signal Transduction (302)
RANBP1	RAN binding protein 2	refer to discussion in section 4.1.3.1 about *RAN* gene
RIPK3	receptor-interacting serine/threonine protein kinase-3	it promotes necroptosis downstream in the TNF-pathway (303)
SULT1B1	sulfotransferase family 1B member 1	one study showed differential expression of this gene in polymorphonuclear cells of patients with PV compared to healthy controls (304)
CAPN5	calpain-5	a protease which activates multiple cellular pathways (305) including inflammatory cell death
ACOX3	pristanoyl-CoA oxidase	involved in peroxisomal fatty-acid oxidation found to be upregulated in cancer (306)
CCL20	CC chemokine ligand (CCL) 20	is expressed and favours the growth how many cancers; the CCL20/CCR6 (its receptor) axis is an autocrine mechanism of growth of lung cancer cells (307); CCL20 secretion is induced by activation of JAK/STAT pathway in cancer (308). In acute lymphoblastic leukaemia (ALL), STAT5A activation favours the expression of CCR6 and pre-B cell growth in a CCL20-dependent manner (309)
CDC40	pre-mRNA-processing factor 17	key role in cell cycle progression and pre-mRNA splicing, found to be upregulated in gastric cancer (310)
CLDN2	claudin-2	a membrane-bound protein involved in cellular permeability and whose expression is induced by activation of JAK/STAT pathway (311)
GNB2L1	receptor for activated C kinase 1 (RACK1)	a scaffold protein involved in various signalling pathways that might contribute to the survival of leukemic cells, especially in acute promyelocytic leukaemia (APL) (312)
HTR1B	5-Hydroxytryptamine (serotonine) Receptor 1B	serotonine receptor play an important role in cancer; HTR1B can activate both Ras and ERK pathways (313)

IL12RB1	interleukin-12 receptor	components of heterodimeric receptor can contribute to the activation of mutatant JAK2V617F (314)
INPP4A	inositol Polyphosphate-4-Phosphatase Type I A	it is involved in JAK2/STAT3 activation in lung cancer (315)
NLN	neurolysin	a mitochondrial peptidase, recently found to be essential for AML viability and a possible therapeutic target (316)
PAX2	paired box 2	a transcription factor belonging to the same family as PAX5, whose loss-of-function mutations are pathogenic in ALL (317)
PRKAB2	β-subunit of AMP-activated protein kinase (AMPK)	frequently amplified in tumour cells (318)
PSMD13	26S proteasome non-ATPase regulatory subunit 13	proteasome genes will be discussed in section 4.1.3.2
RANBP2	RAN Binding Protein 2	refer to discussion in section 4.1.3.1 about *RAN* gene
SARS	seryl-tRNA synthetase	belongs to the group of Aminoacyl-tRNA synthetases (ARSs), which are involved in tumourigenesis (319)
SHFM1	26S proteasome subunit DSS1	proteasome genes will be discussed in section 4.1.3.2
WNT8A	Wnt Family Member 8A	it is a Wnt ligand. Wnt/β-Catenin pathway is deranged in myelofibrosis (320)

4.1.2.3 Ruxolitinib + HS-5 CM in combination (Setting 3)

Eleven genes were the target of the top-ranked shRNAs in presence of ruxolitinib and HS-5-CM (Results, Table 3.4, genes highlighted in red). Among them, some are associated with JAK/STAT pathway, MPN and/or known to be important in cancer.

MPL encodes the TPO receptor, a key player in the pathogenesis of MPN (60, 321). In addition, osteoblasts derived from mesenchymal stromal cells from patients with AML, protect HEL cells through the secretion of TPO (322). With respect to my work, it would be useful to know if the HS-5 cells secrete TPO, which has not been reported previously. Work investigating targeting TPO receptor in MPN is ongoing by other groups (323).

ABCB5 encodes a drug efflux ATP-binding cassette (ABC)-transporter, mediating the ATP-dependent transport of various anticancer drugs. It seems to identify cancer stem-like cells in some cancers (324-326) and is associated with tumour progression and resistance to therapy (327). In a recent study in melanoma, ABCB5 was shown to drive the secretion of IL-1β, revealing oncogenic properties outside its drug-transporter function (328). The gene was also found to be overexpressed in human leukaemia cells (329). Hou et al. performed whole-exome single-cell sequencing of 90 cells from a *JAK2*-negative MPN patient and, from a total of 71 genes harbouring nonsynonymous somatic mutations, identified *ABCB5* and other 7 genes as those with the highest likelihood of being involved in ET initiation and/or progression (330). Recently, Kondo et al demonstrated that ABCB5, through still unknown mechanisms, leads to overexpression of STAT1 (331). Another group have demonstrated that genetic inactivation of

ABCB1, coding for a transporter belonging to the same family of ABCB5, increases the inhibition of proliferation induced by ruxolitinib in HEL cells (332). Further evidence that these drug transporters might be important in MPN and in their response to ruxolitinib comes from very recent work demonstrating that *ABCG2* is overexpressed in MPN red cells and facilitates intracellular transport of ruxolitinib. In addition, its inhibition hampered the lethal effect of ruxolitinib on both cell lines and primary cells (333).

Finally, a gene worthy of mention is *GRB2*, for which there were 2 shRNAs having FC ≥ 3 for both replicates (but none in the top 2% positions for both replicates: so not identified in either RA1 and RA2). *GRB2* encodes growth-factor receptor-bound protein-2 (Grb2), a widely expressed adaptor protein which is strongly expressed in the haematopoietic system (334). It has a crucial role in signal transduction from oncogenic tyrosine kinases such as BCR-ABL1 (335-337), c-KIT (338) and JAK2 (339, 340) (Figure 3.12). Grb2 associates with SOS to activate the RAS-ERK1/2 pathway (341) (Figure 4.1). As Grb2 lacks enzymatic activity, it has been difficult to find an effective inhibitor and to date there has been no clinical translation (342). Recently, however, a liposomal *GRB2* antisense nucleotide (BP1001) has shown activity in relapsed/refractory haematological malignancies (343). Of note, p27, a CDK-inhibitory protein and a negative Grb2 regulator, is expressed at lower levels in CD34+ cells from patients with MF compared to healthy controls (344). Interestingly, Grb2 has a negative regulatory function on p27 (345). If an effective inhibitor for Grb2 can be found, this pathway could be further explored in MPN.

The remaining genes resulted top-depleted in this experimental setting are listed in Table 4.2.

Table 4.2. Other genes targeted by the top-depleted shRNAs in experimental setting 3.

Gene name	Protein	Cellular function and possible relevance in MPN
GSR	glutation reductase	antioxidant enzyme; it mediates therapy resistance in glioblastoma (346)
PRDX2	peroxiredoxin 2	a member of the peroxiredoxin family, which attenuates oxidative stress and is upregulated in some cancers (347)
SIN3A	SIN3 Transcription Regulator Family Member A	part of a transcription-regulator complex including DNMT and HDAC, binds to activated STAT3 and induce repression of tumour suppressor genes; evidence suggests that the STAT3-SIN3a axis might be an important target of STAT3-addicted tumours (348)
CD247	T cell receptor complex ζ chain	Expressed on T-cell, no known association with cancer or MPN
CYP51A1	Cytochrome P450 Family 51 Subfamily A Member 1	lanosterol 14α-demethylase, is a cytochrome P450 involved in cholesterol biosynthesis. This enzyme is under investigation as anti-cancer target (349). Lung cancer cells upregulate CYP51A1 and its inhibition overcome TKI-resistance (350)
PSMB1	proteasome 20S subunit β6	proteasome genes will be discussed in section 4.1.3.2
PSMC3	proteasome 26S regulatory subunit 6A	proteasome genes will be discussed in section 4.1.3.2
RUVBL1	pontin	an ATPase-associated protein with various cellular activities, including chromatin remodelling, transcription regulation, DNA damage response and repair and biogenesis of small nuclear ribonucleoproteins (351). This protein complexes with its partner RUVBL2 (RuvB-like 2, also known as Reptin) and both are overexpressed in a variety of malignancies (352), including specific subtypes of AML (353, 354), and, for this reason, are emerging as potential targets in cancer therapy. Sorafenib, a FLT3-inhibitor used in AML, is also an inhibitor of RUVBL2 (355). Recently, a selective inhibitor of RUVBL2-RUVBL1 complex has been developed, with promising anti-cancer activity (356)
SNRPA1	small nuclear ribonucleoprotein polypeptide A	a spliceosome component responsible for processing of pre-mRNA into mRNA, is an oncogene whose high expression correlates with poor prognosis in some cancers (357)

4.1.3 Top-depleted shRNAs in all 3 experimental settings

Table A6 of the Appendix contains a list of the 22 top-depleted shRNAs recurring in all 3 experimental conditions (according to RA3; Results, section 3.2), considered to be essential for the survival of HEL cells even in the presence of ruxolitinib and microenvironment-mimicking CM. Most of these target genes can be grouped within a specific cellular function; among these, the most populated group is the proteasome gene family.

A brief discussion about some of the other genes is provided below, presented in descending RA3 score, as they could have potential relevance in MPN.

4.1.3.1 *RAN*

RAN encodes a small GTPase involved in nucleo-cytoplasmic transport of molecules, including STATs, through its interaction with nuclear exportins (shuttling macromolecules from nucleus to cytoplasm) and importins (shuttling macromolecules from cytoplasm to nucleus). Extensive literature exists on the association of its overexpression and cancer (358). Increased expression of *RAN* is of prognostic relevance in cancer (359, 360), including lymphoma (360). Of note, mutation of Exportin 1 (XPO1), has been found in B-cell haematological malignancies (361). *RAN* has been previously found to be among the top-depleted in the pooled-shRNA library screening of the HEL cell line by another group (362). The authors also found that *RAN* knock-down or pharmacological inhibition of nucleo-cytoplasmic transport were effective *in vitro* against CD34+ cells from MF patients and in a mouse-model of MF.

Evidence that inhibition of members of the exportin family have clinical efficacy has been shown using Selinexor (KPT-330), a first-in class XPO1 inhibitor that has been FDA-approved for the treatment of relapsed/refractory multiple myeloma. It has also shown promising activity against relapsed/refractory DLBCL (363) and in combination with standard chemotherapy in AML (364). This compound has also some activity in advanced solid cancers (365-367).

4.1.3.2 Proteasome gene family

As reported above, shRNAs targeting proteasome genes were among the most depleted in each experimental setting and they were (listed in order of RA3 score): *PSMA2*, *PSMB2*, *PSMA3*, *PSMD1*, *PSMD6*. In addition, shRNAs targeting other proteasome genes were among the most depleted shared by the ruxolitinib and ruxolitinib-HS5 CM settings (refer to the Results, Table 3.3 and Table 3.4): *PSMB7*, *PSMD11*, *PSMB4*, *PSMA4*, *PSMC6*, *PSMD2*, *PSMD3*.

Six of the above 12 genes belong to the catalytic subunit (20S) of the 26S proteasome, and *PSMB7* codes for the subunit β2, which is one of the three subunits with peptide-hydrolysis enzymatic activity (more specifically, trypsin-like activity). Figure 4.2 shows the components of the proteasome machinery and their respective genes.

Despite the identification of the many other potential targets, highlighted in the previous and in the following sections, in view of the abundance of the members of the proteasome gene family across all experimental settings of pooled-shRNA library screen, we decided to continue the validation phase through chemical inhibition of the proteasome activity in both HEL cell line and primary MF CD34+ cells.

Figure 4.1. 26S proteasome structure and genes targeted by the most depleted shRNAs.

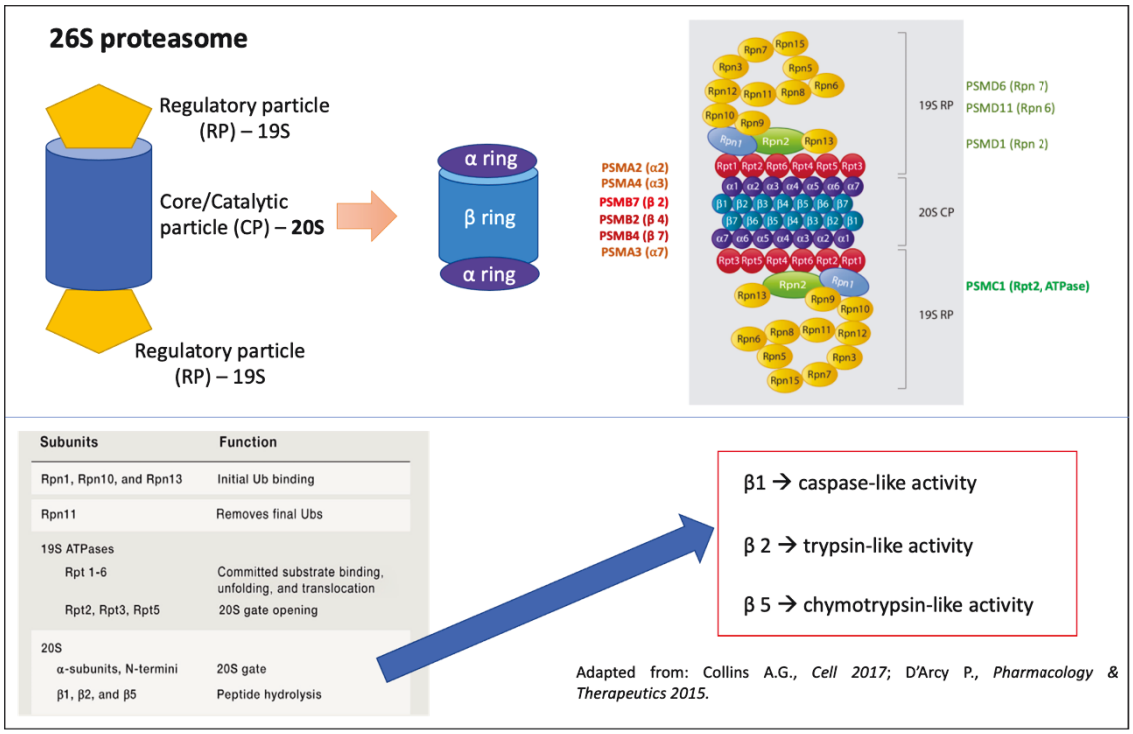

4.1.3.3 *PHB2*

The *PHB2* gene encodes for prohibitin-2 protein, a homolog of prohibitin-1 (PHB1). Human prohibitins are highly conserved proteins, ubiquitously expressed in many cell types and located in mitochondria, nucleus and plasma membranes. Prohibitins act as both monomers or PHB1-PHB2 heterodimers and control multiple cellular functions including signal transduction, energy metabolism, mitochondrial oxidative stress and genome stabilization, cell proliferation and apoptosis (368). In view of the variety of processes in which prohibitins are involved, they are increasingly explored as potential targets for inflammatory and metabolic disease and cancer (369). Among the most studied prohibitin roles is the activation of the Ras/Raf/MEK/ERK pathway. In fact, the PHB1-PHB2 complex in the plasma membrane is a crucial player in the signal transduction from the growth factor receptors, which include TPO and EPO receptors, through Grb2 and Ras (Figure 4.2)(370, 371). Of note, effective inhibitors of the association of CRaf with PHB1-PHB2 complex exist (rocaglamides)(372). The Ras pathway is deranged in MPN (373): Ras mutations have prognostic impact in myelofibrosis (374) and are associated with ruxolitinib-resistance (155, 293). This may suggest PHB2 as a potential new target deserving further study in MPN.

Figure 4.2. Grb2 and PHB1-PHB2 complex in the signal transduction from growth factor receptor to Ras/Raf/MEK/ERK pathway.
(adapted from Polier G. et al., Chemistry & Biology 19, 1093–1104, September 21, 2012)

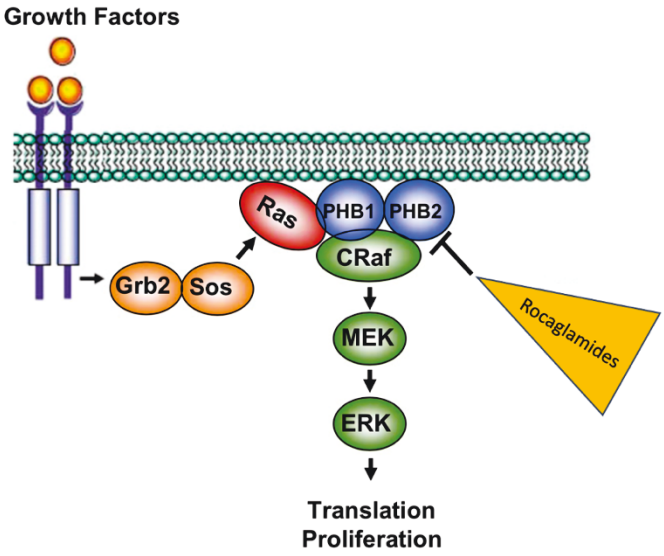

4.1.3.4 Genes involved in splicing

SNRPD2, SNRPN, ASCC3L1, PRPF40A and *SNW1* are genes encoding proteins involved in pre-mRNA processing and splicing, i.e. small nuclear ribonucleoprotein D2, small nuclear ribonucleoprotein-associated polypeptide N, U5 small nuclear ribonucleoprotein 200 kDa helicase, pre-mRNA Processing Factor 40 Homolog A and SNW1-containing protein 1, respectively. The latter, in addition to its role as a regulator of splicing, has been recently described as an important transcription regulator of the NF-κB pathway (375).

Spliceosome-associated mutations are common in haematological malignancies, including MF (376). Very recently, targeting of the splicing factor YBX1 in combination with the pharmacological inhibition of JAK2 has emerged has a therapeutic combination able to eradicate the JAK2-mutant MPN clone (377).

Interestingly, *SNRPD2* and other spliceosome genes are negatively-enriched in the ruxolitinib-treated CD34+ MF cell in the present work (refer to the Results, section 3.7.2 and; Appendix, table A8).

4.1.3.5 *NEDD8*

NEDD8 codes for the neuronal precursor cell-expressed developmentally down-regulated protein 8, an ubiquitin-like protein, which is the main player in neddylation. The latter is a reversible covalent conjugation of NEDD8 to a lysine residue on a substrate protein (378).

Overall, binding of NEDD8 molecules to target proteins can affect their stability, subcellular localization, conformation and function. Protein neddylation processes have been found elevated in many malignancies and, for this reason, inhibition of neddylation is regarded as an intriguing new strategy of cancer therapy (379), with a possible application also in leukaemia (380, 381).

4.1.3.6 *JAK2*

The fact that *JAK2* was a target of the recurrently most depleted shRNAs confirms the dependency of HEL cells on JAK/STAT pathway and corroborates their use for the screening of additional vulnerabilities in MPN, in which a hyperactive JAK/STAT pathway is a common feature. This result is also in line with the findings of a study showing that JAK2 knockdown through small interfering RNA suppresses HEL cell growth (382).

4.1.3.7 Other genes targeted by the top-depleted shRNAs in all settings

The other genes targeted by the most depleted shRNA shared by all 3 experimental setting code for ribosomal proteins (*RPS13*, ribosomal protein S13; *RPL11,* 60S ribosomal protein L11; RPL12, 60S ribosomal protein L11; *RPS3A*, ribosomal protein S3A), for proteins involved in translation (*EEF2*, Eukaryotic elongation factor 2; *EIF2S2*, Eukaryotic translation initiation factor 2 subunit 2) and for proteins involved in RNA synthesis (*RRM1*, ribonucleotide reductase; *RTF1*, RNA-polymerase-associated protein RTF1 homolog).

Apart from the discussion in section 4.1.2.2 for other ribosomal proteins, the ribosome plays an important role in the acquisition and maintenance of cancer stem cell phenotype (383). In regards to EEF2 and EIF2S2, they are both well-known promoters of tumorigenesis (384-386), while RRM1 is a potential therapeutic target in multiple myeloma (MM) (387).

4.3 Interpretation of pooled-shRNA library screen results on MF CD34+ cells

The application of the pooled-shRNA-library screen to primary cells proved to be very challenging. The original objective was to transduce CD34+ cells from patients with MF with the pooled-shRNA library in order to identify genes important for their survival. However, none of the four screens carried out was successful. All four MF samples studied were characterised by very low transduction efficiency (2 samples had an RFP positivity at 72h

<0.5%, 1 sample 1.4%; and 7.1% at 120h in the final sample), 1 sample (MF-2) did not survive the long-term co-culture on HS-5. Furthermore, only 1 sample (MF-4) had successful shRNA barcode amplification at baseline (pre-transduction) and only 1 sample (MF-3) was successful in the post-screening sample (day 14 post-transduction).

The two main reasons that might explain the lack of success of the pooled-shRNA library approach on primary cells are the relatively low starting cell number (discussed in the Results) and the low transduction efficiency.

Considering these challenges, a long optimization process would be needed to solve them. This might include, for example, the use of smaller pooled-shRNA libraries, in order to decrease the library complexity and, consequently, reduce the target number of infected cells required to obtain a full representation of the library. Alternatively, in order to obtain a higher starting cell number, I should have processed larger volumes of peripheral blood and/or prolonged the number of days of culture before the lentiviral transduction. The first strategy would involve collecting additional blood from patients often anaemic due to MF and/or its treatment. In regards to the second solution, I thought that it was not appropriate in view of possible biases that might be introduced by the long *ex vivo* permanence of primary cells and by the likely increased cellular differentiation of CD34+ cells.

The low transduction efficiency is also a difficult obstacle to overcome. Possible solutions could be the use of additional positively-charged polycations such as protamine sulphate (aimed at reducing the strong electrostatic repulsion between the negatively-charged cell and the positively-charged approaching enveloped virus)(388), to use smaller viral vectors (as the vector size >6000 bp has been found to be a crucial determinant of the transduction efficiency of primary cells (389)) and the use of retronectin-coated plates in order to increase the interaction between the viral particle and the primary cells (388-390).

In an attempt to explore shRNA depletion for MF-3, we assumed a similar distribution of shRNA in the transduced cells at baseline between the two MF samples and compared the post-selection MF-3 sample with the baseline MF-4 sample. We considered this a better approach than comparing post-selection barcode abundancy with the plasmid library itself, as it allowed us to compare the results in the same cellular background.

Although no definite conclusions can be drawn from the analysis, there were some genes of potential relevance in MPN among those targeted by the most-depleted shRNA, listed in Table 4.3.

Table 4.3. Genes targeted by the most depleted shRNAs in MF-3, of potential relevance in MPN.

Gene	Protein	Function	Possible relevance in MPN
EIF5A2	**Eukaryotic translation initiation factor 5A-2.**	- Involved in cancer development and progression (391-394). - Recent report of an EIF5A2/MCL-1 axis, where MCL-1 (myeloid-cell leukaemia-1 protein, member of the Bcl-2 family proteins) is positively regulated by EIF5A2 and drives leukemic cell survival (395).	- MCL-1 is an important player in MPN, and is upregulated by JAK/STAT pathway activation (396). - in a study on bladder cancer, EIF5A2 has been shown to upregulate TGF-β1 (397), which in turn is key mediator of fibrosis in MF. - interestingly, in the pooled-shRNA library screen of HEL cell line shRNA targeting EIF5S2 (another translation/elongation factor) emerged among the most depleted (Appendix, Table A6).
CX3CL1	**Fractalkine,** a chemokine which exists in soluble form and as a membrane-bound protein, and has different roles according to its form: chemotaxis and cell adhesion. Its receptor, CX3CR1, is expressed in monocytes, dendritic cells, macrophages, T and NK cells and in the microglia.	Binding of CX3CL1 to its receptor activates AKT, MAPK and NF-κB pathways (398, 399). Its expression can be induced by NF-κB activation (400, 401). The CX3CL1-CX3CR1 axis plays several important roles: - in monocytes, it induces survival pathways and protects them from apoptosis (402) - CX3CL1 protects against apoptosis through the upregulation of anti-apoptotic proteins Bcl-2 and Bcl-xL (403) - it activates a pro-tumoural response leading to proliferation, migration, invasion and increased cellular survival (404-409) - Fractalkine receptor is overexpressed in primary AML cells (410) - CX3CL1 can promote angiogenesis (411), and might be involved in the recruitment of pro-inflammatory infiltrate and in the fibrotic process (412, 413).	- This protein is involved in MAPK and NF-κB signalling. Also, it upregulates Bcl family proteins.
CREB3L2	**CREB protein 3-like 2**, a member of the CREB3 family of endoplasmic reticulum (ER)-localised transmembrane transcription factors, involved in the: - the adaptative arm of the unfolded protein response (UPR)(414) - regulation of collagen production - process of hepatic stellate cells activation and liver fibrosis upon TGF-β1-induced signalling (415).	CREB3L2 belongs to an ATF5 pro-survival pathway starting from Ras and PI3K activation and ending in the anti-apoptotic MCL-1 activation (416).	- Ras and PI3K are known mediators of ruxolitinib-resistance (285, 293, 417) - MCL-1 is a key downstream effector of the $JAK2^{V617F}$-induced pro-survival pathway (396). CREB protein 3-like 1 (another member of the same protein family), which resides in the ER and acts as a transducer of the UPR, has been recently found to be overexpressed in MPN patients and identified to be a potential diagnostic marker of MPN (418) - CREB3L2 is involved in UPR (relevance of UPR in MPN will be discussed in the following sections) and in fibrosis.
STAT5A	**Signal transducer and activator of transcription 5A.** STAT proteins act as transcriptional activators upon phosphorylation of a conserved tyrosine residue at the C terminus followed by translocation into the nucleus, where they bind to DNA and activate target gene transcription.	STATs hyperactivation is the direct and main pathogenic consequence of JAK2 activation. - JAK2/STAT3-mediated cytokine production from malignant and non-malignant cells contributes to MPN pathogenesis (54) - Overexpression of constitutively active STAT5A gives rise to multilineage leukaemia (419) - STAT5 has a critical role in the transforming activity of $JAK2^{V617F}$ and TEL-JAK2 in murine bone marrow transplant models (420, 421).	Increased levels of constitutively phosphorylated STAT5 (p-STAT5) in haematopoietic cells is a characteristic finding in MPN: - only p-STAT5 levels were constitutively higher in CD34+ cells of MF patients than in controls (as compared to p-STAT3 levels)(422) - STAT5 activation persists after exposure to ruxolitinib, through JAK2-dependent and -independent mechanisms (185, 423, 424) - selective STAT5 inhibitors (including AC-4-130, recently shown to suppress AML growth in vitro and in vivo (425)) inhibits the growth of JAK2-mutated cell lines (426).
MPL pathway genes	Among others: -GAB2, **GRB2 Associated Binding Protein 2,** mediator in the MPL pathway -PIK3CB, class I **phosphoinositide 3-kinase (PI3K) catalytic subunit p110β,** mediator in the MPL pathway.	-GAB2 is the haematopoietic cell-specific scaffolding protein mediating the cytokine-induced PIK3-AKT pathway activation (known to mediate ruxolitinib resistance, as mentioned above) -genetic knockdown of PIK3CB is able to attenuate some features of the *PTPN11*-mutated form of juvenile myelomonocytic leukaemia, a form of myeloproliferative neoplasm, including leucocytosis, splenomegaly and progression into AML in mice (427).	- MPL (TPO-receptor) pathway is crucial in the pathogenesis of MPN - Among the top 5% depleted shRNAs in the pooled shRNA screen of MF-3, there were eight whose targets code for downstream effectors in the MPL pathway (STAT5A, GAB2, GAB1, PIK3CB, NRAS, BCL-2, NRas and NFKB1). Also, shRNA targeting RAN, one of the crucial genes emerging from the HEL cell line screening, was found among the most depleted.
Proteasome genes	Among others (refer to Figure 3.13): PSMB5, codifying for the **β5 chymotrypsine-like catalytic subunit**.	Proteasome genes are upregulated in MPN (428, 429).	Relevance of proteasome and its inhibition in MPN will be discussed in the next sections.

4.4 Validation of pooled-shRNA library screen findings

As discussed in previous sections, shRNAs targeting several genes encoding for members of the ubiquitin-proteasome gene family were the most depleted across all the experimental conditions of pooled-RNA library screen on HEL cells. In view of this, I chose the proteasome as the target to explore through chemical validation with the use of proteasome inhibitors (PI), first on HEL cells and then on primary MF CD34+ cells, of which findings are commented in the next sections.

4.4.1 Chemical validation on HEL cells

PI are the backbone of treatment for MM, a haematological neoplasm in which clonal plasma cells produce enormous amounts of immunoglobulin and heavily rely on the perfect function of the ubiquitin-proteasome system to avoid proteotoxic stress, the latter leading to the activation of the unfolded protein response (UPR) and apoptosis.

Bortezomib (BTZ) was the first PI approved for MM (430). It is a peptide boronate which reversibly binds the 26S proteasome. Carfilzomib (CFZ), a newer class of PI, is an epoxyketone-type PI and binds irreversibly the proteasome. Both PIs mainly target the β5 (PSMB5) subunit, while ixazomib, a new boronate-based orally-available PI, has a slightly higher preference for the β1 (PSMB6) subunit. The epoxyketone-based PI oprozomib, the boronate-based PI delanzomib, and the irreversibly proteasome binding β-lactone PI marizomib are newer PIs are under investigation in clinical trials.

The HEL cell line was sensitive to relatively low concentrations of both BTZ and CFZ, with IC_{50} of 7.36 nM and 41.34 nM, respectively, after continuous 72h-exposure. For comparison, the IC_{50} of PIs on HEL cells were either equal to (for BTZ) or between 4-9 times higher (for CFZ) than those reported for PI-sensitive MM cell lines (431, 432). Furthermore, the combination of CFZ at 10 nM and 20 nM increased the growth-inhibitory effect on HEL cells of ruxolitinib.

These findings validate the pooled-shRNA library screen results, although no specific experiment was carried out to confirm a reduction in the function of the proteasome machinery on exposure to PIs.

4.4.2 Chemical validation on primary cells

The in vitro assays conducted on primary cells showed that CFZ is effective in inhibiting the growth of MF CD34+ cells, either alone or in combination with ruxolitinib. However, in

regards to the mechanism of the CFZ effect, functional studies aimed at the verification of the decreased proteasome activity in MF cells are lacking in the present work.

The MTS experiments on cells from multiple patients did not show the same degree of inhibition induced by CFZ. Possible explanations include the cellular source (MNCs vs CD34+), the methods used (MTS vs Trypan blue assay), the drug exposure time, the number of technical replicates and last, but not least, the clinical patient variability.

Some assays, like the Annexin V and cell cycle analysis, have only been performed in a single patient, and further work, in terms of numbers of patients and replicates of experiments will be required to confirm the results. Other valuable studies would include additional clonogenic assays on normal and MF patients CD34+ cells in the presence of CFZ.

Finally, although the data are in keeping with an increased in vitro inhibitory activity of the CFZ-ruxolitinib combination compared to ruxolitinib alone, further studies are needed to explore the effect of the combination at different concentrations of each drug and to calculate the combination index (as per Chou-Talalay method(433)).

4.4.2.1 Choice of CFZ as the PI to use for chemical validation

Both BTZ and CFZ were effective in inhibiting the growth of the HEL cell line. The choice of CFZ over BTZ for the chemical validation on primary cells was based on the following reasons:

1. BTZ lacks efficacy in monotherapy in patients with MF (discussed below);
2. The evidence of the β2-inhibitory ability of CFZ at clinically therapeutic ranges and the efficacy of CFZ in BTZ-refractory MM patients, makes it a more attractive PI (discussed below).

BTZ is not effective as monotherapy in MF

BTZ was shown to reduce marrow and spleen fibrosis, myeloproliferation and to prolong survival in a TPO^{high} murine model of myelofibrosis (434). This effect was thought to be mediated by the inhibitory effect of BTZ on NF-κB pathway activation and the consequent decrease in TGF- β1 levels.

Subsequent work showed that BTZ inhibits proliferation and induces apoptosis of the megakaryoblastic cell line, M-O7e, it sequesters NF-κB in the cytoplasm of these cells and reduces the number of megakaryocyte colony forming units from BM-derived MNCs of patients with MF (435). The same groups found that BTZ reduces angiogenesis in half of MF patients *ex vivo*, but had no effect on cellularity or fibrosis (436).

This preclinical evidence suggests that BTZ has an inhibitory effect on the megakaryocyte lineage (of note, one of the most common haematological toxicities of BTZ is thrombocytopenia) and exerts anti-proliferative and anti-fibrotic changes in a non-JAK2-driven mouse model of MF.

Based on these findings, two clinical trials, both carried out in the pre-ruxolitinib era, tested the efficacy of BTZ monotherapy in patients with MF. In the phase-1/2 study (437), none of 22 patients treated with standard dose BTZ (of whom 18 received up to 4 cycles) experienced a clinical benefit. The two main changes induced by BTZ were reduction of angiogenesis (decrease in the density of bone marrow microvessels in 6 of 15 patients studied) and downregulation of CXCR4 surface expression on circulating CD34+ cells. As the latter is already a characteristic aspect of MF and results in the abnormal mobilization and homing of CD34+ cells (438), the authors hypothesized that BTZ could worsen this cellular phenomenon, which is associated with disease activity and progression (439). In another smaller phase-1 study, none of 9 patients receiving BTZ monotherapy had any clinical benefit (440).

CFZ co-inhibitory effect on proteasome subunits and its superior efficacy in MM over BTZ

In order to reach a higher functional PI activity and cytotoxic effect, co-inhibition of both β5 and β1 subunits (achieved by BTZ at 1h-pulsed concentrations of 100-1000 nM) or β5 and β2 (PSMB7) subunits (achieved by CFZ at 1h-pulsed concentrations of 300-3000 nM) is required: the latter combination is particularly effective against PI-refractory MM cell lines or primary MM cells (431).

CFZ is the only available PI able to achieve combined inhibition of the β5 and β2 subunits after intravenous administration (431). This seems to explain the superior activity of CFZ over BTZ when high-dose regimens are used (≥ 56 mg/m^2 weekly), leading to its approval for relapsed/refractory MM (441, 442). In fact, the BTZ C_{max} after an intravenous bolus of 1.3 mg/m^2 is ~130 nM (443) which then declines to < 100 nM (not high enough for β5 and β1 co-inhibition, see above), while a 30 minutes infusion of CFZ 56 mg/m^2 produces a C_{max} of 2.89 μM (444), the latter being a concentration allowing β5 and β2 co-inhibition.

4.4.2.2 Interpretation of effects of CFZ on MF CD34+ cells and correlation with GEP results

I showed that CFZ reduces *in vitro* the viability of CD34+ cells from patients with MF and increases the inhibitory effect induced by ruxolitinib. This effect was confirmed by a pulsed-exposure experiment, at the minimum dose (300 nM) at which CFZ is able to induce co-

inhibition of β5 and β2 subunits (see above). Also, CFZ pulsed-treatment increased the proportion of apoptotic cells assessed at 24h, compared to ruxolitinib-only treated MF CD34+ cells. The inhibitory effect of CFZ on MF CD34+ cells was even more pronounced when assessed through colony formation assay.

Importantly, the enhanced *in vitro* inhibition of MF cells by combined CFZ and ruxolitinib was achieved at lower concentrations than those observed in patients' plasma after therapeutic CFZ doses. This suggests that a stronger inhibitory effect on MF cells might be observed at higher CFZ doses. Interestingly, the few experiments run using BTZ, at a dose of 300nM (chosen as it falls within the optimal range for double catalytic subunit inhibition [as discussed above] and to allow comparison with CFZ), showed similar results. Although no conclusion can be drawn from a limited number of assays, it could be at least hypothesised that effective proteasome inhibition (obtained with any PI) combined with ruxolitinib potentiates the anti-leukemic effect of the latter. However, this tested BTZ concertation is never reached in patient plasma after therapeutic dosing, making CFZ preferred for further validation studies (as discussed above).

Ruxolitinib reduces the expression of proteasome genes

Recent analysis of microarray data from 34 MF patients in comparison to healthy controls (428) and an earlier study (429) have shown upregulation of the proteasome degradation pathway in MF $CD34^+$ cells.

STAT3 is activated by JAK2 phosphorylation in the JAK/STAT pathway and upregulates the expression of proteasome genes (445). Also, activation of JAK2 through INF-gamma receptors 1 and 2 or the receptor of advance glycation end products (RAGE) leads to STAT1-induced expression of the inducible proteasome genes (i11S and i20S)(446).

Ruxolitinib inhibits the IL-6/JAK/STAT3 pathway (447, 448), which may explain the reduced transcription of proteasome genes as observed in our study.

In mammalian cells oxidative phosphorylation controls the transcription of proteasome genes leading to their upregulation as an adaptive response to prolonged exposure to oxidative stress (449-451). In MF, reactive oxygen species are increased and responsible for a proliferative advantage and DNA-damage leading to disease evolution (452-454) and this could be another trigger for proteasome gene upregulation in MF.

The oxidative phosphorylation signalling is among the top negatively-enriched pathways in ruxolitinib-treated MF $CD34^+$ cells in our study (Appendix, Table A8). This may be another mechanism for downregulation of the proteasome gene family by ruxolitinib in MF $CD34^+$ cells.

JAK/STAT inhibition negatively modulates the adaptive arm of UPR

UPR is a complex mechanism elicited in the endoplasmic reticulum (ER) by stress which derives from a variety of causes such as hypoxia, altered protein glycosylation and folding, redox imbalances and alteration in Ca^{2+} homeostasis. As shown in Figure 4.3, activation of the UPR may result in either an adaptive response to stress promoting cell survival (characterised by the increased production of chaperons, such as immunoglobulin heavy chain chaperone protein Bip, other key mediators of protein folding, redox balance components, and by stimulation of autophagy), or a pro-apoptotic response, via prolonged activation of PERK (protein kinase RNA-like endoplasmic reticulum kinase), which regulates the translational response of UPR, and induction of expression of CHOP (C/EBP homologous protein), a transcription factor that controls genes mediating apoptosis. Among the latter, CHOP downregulates the anti-apoptotic *BCL-2*; interestingly, this gene is upregulated by JAK/STAT activation in MPN (286), and could be a possible source of UPR dysfunction in MPN.

Figure 4.3. The UPR pathways.
(adapted from Judith A. Smith Frontiers in Immunology 2018; Mar 5;9:422)

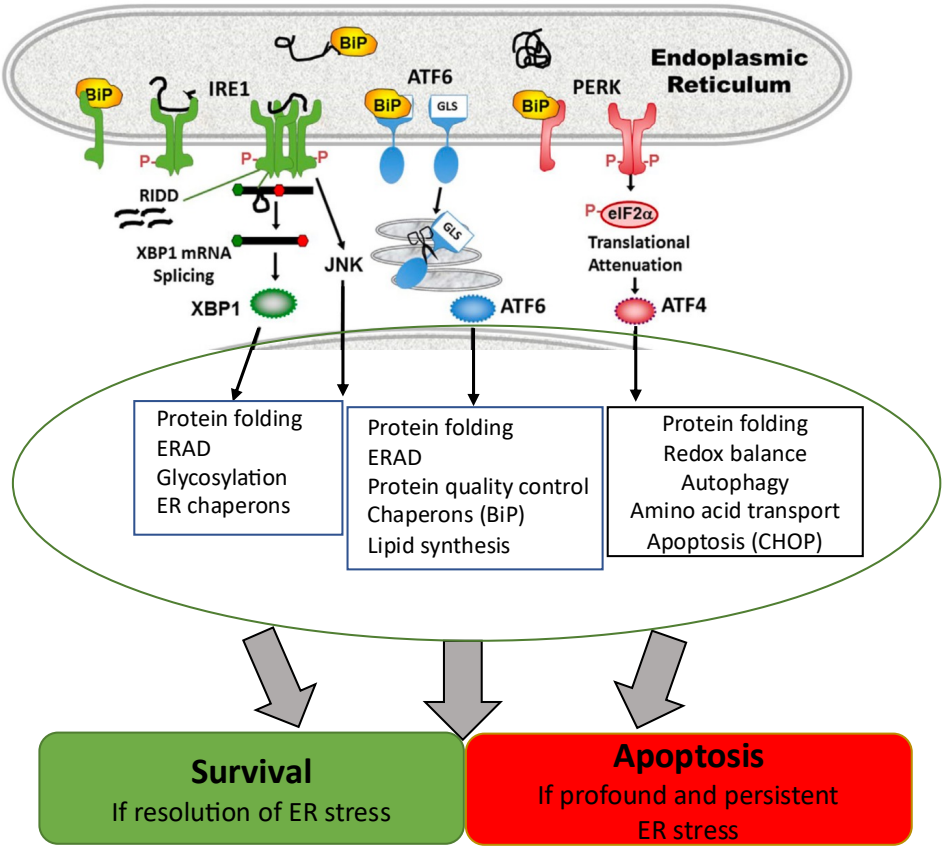

UPR is an increasingly studied process emerging as a potential novel vulnerability of cancer cells. In particular, extensive data demonstrate that UPR is an essential pathogenic mechanism

in acute and chronic leukaemias, including CML, through the upregulation of its adaptive and pro-survival branch (455).

JAK2 inhibition is known to suppress the adaptive arm of UPR. JAK2/STAT3 activation via exogenous berberine treatment is protective in myocardial ischemia/reperfusion-induced apoptosis in a rat model, possibly through the attenuation of ER stress, evidenced by reduction of myocardial PERK and eIF2α phosphorylation levels and the expression of ATF4 and CHOP. The effect is abrogated by co-treatment with the JAK2 inhibitor AG490, and suggests that the JAK2/STAT3 axis is involved in the modulation of the ER stress, towards cellular adaptation and survival (456). Also, other groups have found that ER stress has the capability to prolong the phosphorylation of JAK2 and the DNA binding of STAT5 in response to growth hormone (GH) in rat liver cells and they concluded that cellular stress may modulate transcription through JAK/STAT pathway (457). Similarly, in astrocytes PERK-dependent activation of JAK1/STAT3 axis is responsible for neuro-inflammation in a mouse model of multiple sclerosis. The authors provided evidence that, in presence of ER stress, PERK may function as a typo-I and type-II cytokine receptor associated with JAK1 and, upon dimerization induced by ER stress, it is phosphorylated by JAK1 and finally activates STAT3, inducing a non-apoptotic robust inflammatory transcription program. They also showed that PERK phosphorylation and STAT3-dependent inflammatory response can be inhibited by the JAK1/2 inhibitor AZD1480. The model they proposed is shown in Figure 4.4 and they hypothesized that PERK can be phosphorylated also by other JAKs (458). Of note, 2 studies have demonstrated that JAK2 is a resident tyrosine kinase in ER (459, 460), where it also functions as a chaperone protein: it would be very interesting to investigate whether and how a constitutively active JAK2 (i.e. due to *JAK2*^{V617F} mutation) can affect ER functions, including direct perturbation of UPR.

Figure 4.4. PERK is associated with and phosphorylated by JAK1 and, likely, other JAKs.
(adapted from Meares GP et al., Molecular and Cellular Biology 2014).

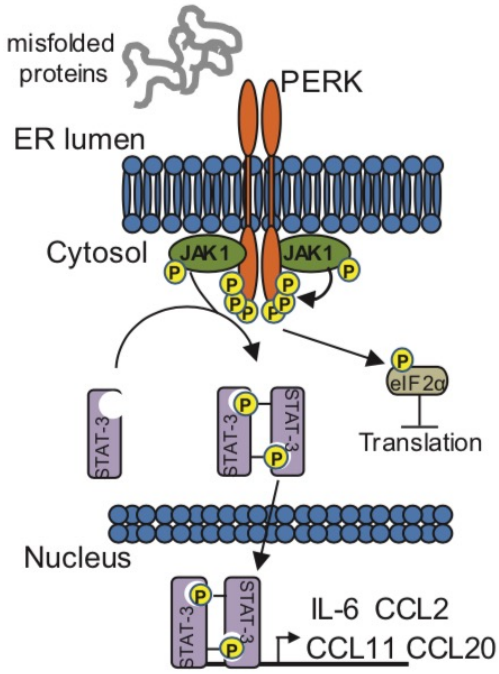

Additional evidence for a role of the JAK/STAT pathway in ER stress comes from work showing that, in the Drosophila intestinal stem cells (ISC), JAK/STAT pathway activation from cytokine released by surrounding ER-stressed intestinal epithelial cell leads to activation of PERK, which in turns activates the pros-survival branch of UPR and stimulates ISC proliferation (461).

Other groups have found that dipyridamole potentiates the ER stress-induced apoptosis caused by bortezomib in several cell lines of leukaemia and lymphoma; they found that biological basis of the increased cytotoxicity came at least in part from the dipyridamole-induced downregulation of JAK2 phosphorylation (462).

Of note, the upregulated expression of proteasome genes is part of the adaptative arm of UPR (463). In this context, their downregulation in CD34+ MF cells treated with ruxolitinib could be related to a potential suppressive effect exerted by this drug on the UPR pro-survival branch.

Finally, in a pre-B Ph+ acute lymphoblastic leukaemia (ALL) mouse model, the ALL cells had particularly high levels of XBP1 (UPR downstream pro-survival effector) and its expression and activity was positively-regulated by STAT5, AKT and ERK signalling (464). In summary, it seems that the JAK/STAT pathway might have a role in modulating the response of ER to stress.

In MPN, there are no data associating the UPR and *JAK2*-mutated MF, but two recent reports have suggested that the UPR might be deranged in *CALR*-mutated MPN, with both downregulation of the pro-apoptotic pathway (465) and upregulation of the pro-survival pathway (56). In the latter study, the UPR was found to be the predominant outcome of *CALR* mutations in megakaryocyte progenitors (MkPs), with a robust upregulation of IRE1 in both ET and MF. Furthermore, they also showed upregulation of *TGFB1* expression in MF MkPs, which correlated with the degree of fibrosis in the bone marrow of the patient. Interestingly, severe or prolonged UPR is the pathogenic mechanism in some chronic disorders characterised by fibrosis (466).

In summary, the lack of BTZ efficacy in MF patients (discussed above) could be due to the use of the drug as a monotherapy (which leaves the JAK/STAT pathway active and eventually potentiates it, in a vicious circle with UPR), and/or to the lack of double catalytic subunit inhibition at clinical concentrations, which, although not essential for a disease highly-dependent on proteasome like MM, might instead be important in MF to achieve effective proteasome inhibition and apoptosis.

The mechanistic hypothesis supporting the utility of further investigation of the ruxolitinib-CZF combination in MF is summarized in Figure 4.5: ruxolitinib inhibits the UPR adaptive pathway and decreases the number of proteasome units, so that CFZ can exert an apoptotic effect on MF cells.

Figure 4.5. Rationale for further investigation of the ruxolitinib-CFZ combination in myelofibrosis.

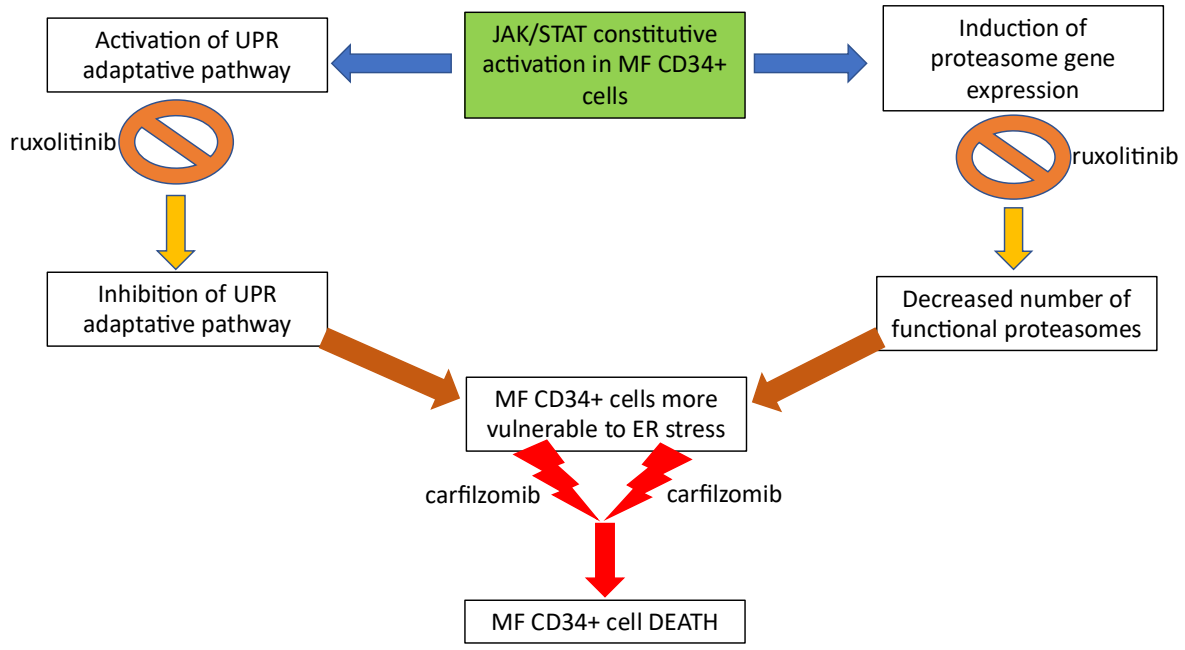

4.4.2.3 Further arguments for the biological rational supporting JAK2 inhibitor/PI combinational therapy in myelofibrosis

Other PI-induced effects of potential relevance in MF

PI can affect other targets important for cell survival and apoptosis. Some of these targets might be relevant in MF, as they are involved in disease pathogenesis and/or ruxolitinib-resistance.

CFZ is an indirect mTOR complex 1 (mTORC1) inhibitor (467) and has been shown to induce leukaemia cell apoptosis via downregulation of cellular inhibitor of PP2A (CIP2A) and increased PP2A activity (468). The latter effect of CFZ seems not to be cell-specific, as it is responsible for the CFZ-induced cardiotoxicity (469). Interestingly, pan-PIM kinase inhibitors, that inhibit mTOR, have synergistic activity with ruxolitinib in MPN (470-472).

Restoration of the activity of PP2A is a potential therapeutic strategy in MPN (473, 474). PP2A is a tumour suppressor and is an ubiquitously expressed phosphatase responsible for a large proportion of phosphatase activity in eukaryotic cells. PP2A activity is downregulated in MPN cells (474) while CIP2A (allosteric inhibitor of PP2A) is overexpressed in *JAK2*^{V617F}-mutated cell lines and downregulated in MF patients with clinical responses to mTOR inhibitors (285). Overexpression of CIP2A may be the result of activation of PI3K/mTOR pathway and PI3K and mTOR inhibitors increase the efficacy of ruxolitinib in *JAK2*^{V617F}-mutated cells line, in primary MF cells and in *JAK2*^{V617F} knock-in mice (285).

Furthermore, CFZ has a direct effect on PIM-1 in MM downregulating its expression (475).

If this also occurs in MF cells, this could be relevant as the anti-apoptotic PIM-1 is overexpressed in MF cells (476, 477) and is regarded as a contributor to the resistance to JAK2 inhibitors (470).

Another interesting protein targeted by CFZ is MCL-1 (myeloid cell leukemia-1), an anti-apoptotic protein known as a potential therapeutic target in MPN (396). CFZ has been shown to inhibit MCL-1 in MM cells through the upregulation of its repressor NOXA (478); a similar CFZ-induced effect on NOXA has been shown in primary CLL lymphocytes (479).

PI-combinational therapies in other haematological cancers

Apart from their great success in MM, PI as single agents have shown activity in non-Hodgkin lymphoma (480, 481) and some leukaemias (482, 483). Compared to BTZ, CFZ has shown superior activity in vitro against ALL cells (484) and in AML (485), where it preferentially induces apoptosis of primary AML CD34+ cells over normal CD34+ cells (486).

However, PI efficacy in most cases is observed in combination with either chemotherapy or tyrosine kinase inhibitors (487-490). The combination of CFZ and the Bruton's kinase-

inhibitor ibrutinib has promising additive or synergistic activity in CLL (479) and mantle cell lymphoma (491), in both *in vitro* and/or *in vivo* models and in patient cells.
Furthermore, ruxolitinib acts synergistically with BTZ against cutaneous T-cell lymphoma primary cells (492).

CXCL12/CXCR4 axis in MF and its inhibition by ruxolitinib

The phase 1 study of BTZ monotherapy in MF revealed that BTZ further downregulates the surface expression of CXCR4 on MF cells, so worsening the mechanism responsible for the abnormal mobilization and homing of CD34+ cells (see above). This effect has also been shown by CFZ in MM (493), and is mediated by decreased phosphorylation of CXCR4 induced by CFZ through downregulation of the expression of its kinase PIM-1 (475).
However, in hypothesising that CFZ monotherapy leads to the same cellular effect on MF CD34+ cells, this could be counteracted by the reported suppressive effect of ruxolitinib on the CXCL12/CXCR4 axis, where JAK2 inhibition is effective in decreasing the chemotactic response of CD34+ MF cell to CXCL12 (494).

JAK2 inhibitors enhance the effect of PI in MM

In MM, a disease characterised by high dependency on proteasome pathway, there is increasing evidence for efficacy of JAK2 inhibitors in both monotherapy or in combination with other MM regimens, including PI (495, 496).
Some groups have shown that the JAK1-2 inhibitor INCB16562 potentiates the growth-inhibitory effect of BTZ on myeloma xenografts in mice (497). Another recent study found that ruxolitinib enhances the anti-tumour activity of BTZ (498). Possible explanations for the activity of JAK1-2 inhibitors in MM are several, including inhibition of an overactive JAK/STAT pathway (499) and direct effect on the microenvironment (497), such as the reduction of the proportion of tumour-stimulatory M2 macrophages (500). The final result of these, and possibly other JAK inhibitors effects, are the inhibition of cell cycle progression and induction of apoptosis in MM cell lines and primary MM plasma cells (496). Furthermore, ruxolitinib blocks PD-L1 expression in the MM cells, increasing the anti-tumour effects of T cells (501).
A recent clinical trial reported an overall response rate of 38% by treatment with ruxolitinib-lenalidomide-dexamethasone scheme in MM patients refractory to previous lenalidomide/corticosteroids and PI combinations (502).

A PV patient on ruxolitinib who had developed MM from MGUS did not respond to lenalidomide and methylprednisolone; however, the addition of low-dose ruxolitinib to the latter agents was effective as anti-myeloma therapy (503).
CFZ is currently being investigated in combination with ruxolitinib and dexamethasone in the treatment of relapsed/refractory MM patients (clinical trial.gov, NCT03773107).

4.5 Interpretation of NF-κB pathway alteration in MF CD34+ cells exposed to ruxolitinib +/- CFZ

The assessment of NF-κB pathway gene expression was performed on CD34+ cells of 2 MF patients (one naïve, MF-4, not yet on treatment, and one, MF-24, refractory to ruxolitinib), whereas the Western Blot analysis of NF-κB canonical pathway (phosphorylated p65 translocated in the nucleus; Figure 4.6) was performed on another patient (MF-19, refractory to ruxolitinib). In view of the limited number of experiments and the lack of parallel assessment through these two different methods on the same patient, it is impossible to draw any definite conclusion. However, I think is useful to highlight some aspects of the results which can motivate future investigation.
First, in both patients, 1h-pulsed CFZ induced significant upregulation of most of the genes, while ruxolitinib, on the contrary, induced downregulation. In MF-24, exposure to the combination ruxolitinib-CFZ did not significantly change the effects induced by CFZ alone.
In contrast, the Western Blot analysis performed on cells from a third patient (MF-19) revealed that 1h-pulsed CFZ induced effective inhibition of activation of NF-κB pathway, slightly more than with ruxolitinib alone (although the difference did not reach statistical significance) and this effect persisted with the combined treatment. If this is confirmed also in MF-4 and MF-24 at protein level, it would suggest that the gene expression upregulation induced by CFZ, especially pronounced in the ruxolitinib-refractory patient (MF-24), is either a compensatory effect of its inhibition at protein level (through possible regulatory loops) or the result of reduced proteasomal degradation of the proteins which induce NF-κB gene expression.

Figure 4.6. Canonical and non-canonical pathways of NF-κB activation and their inhibitors.
(adapted from Felicity D. Herrington et al. Journal of Biomolecular Screening 2016, Vol. 21(3) 223–242).

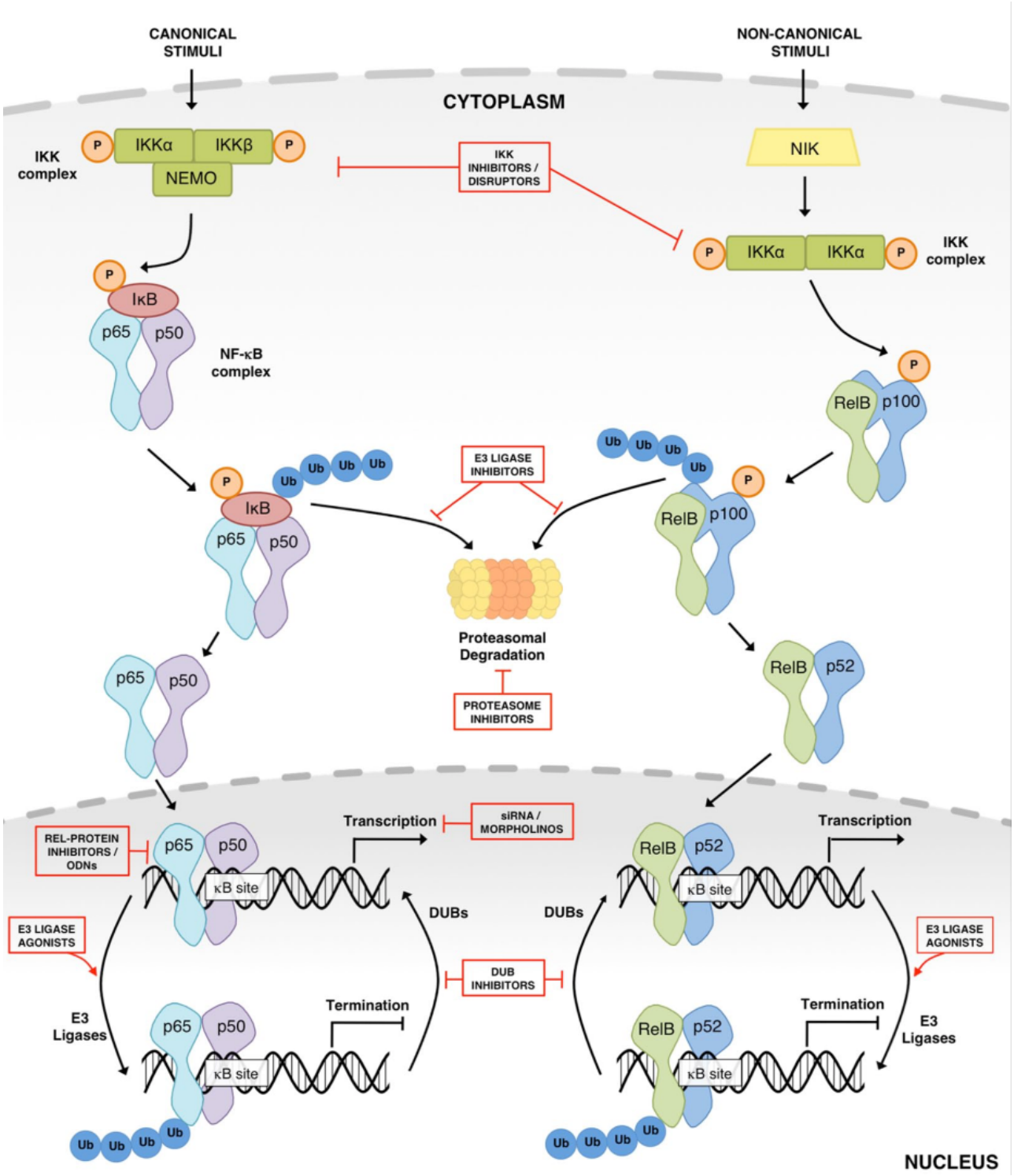

It is relevant to note at this point that the effect of ruxolitinib and CFZ on the NF-κB pathway are different: the JAK/STAT pathway activates NF-κB through both direct interaction with NF-κB (although the precise mechanism is not yet fully understood) (504, 505) and an indirect effect from the reduction of STAT3/5-mediated upregulation of genes encoding NF-κB activators or regulated by NF-κB itself (as NF-κB might interact with STATs at DNA-binding sites) (506-508): ruxolitinib might exert an NF-κB inhibitory effect at both protein and gene level as shown in Figure 4.7 (270); CFZ, prevents the activation of NF-κB via translocation p65 into the nucleus, as reported in other malignancies (509, 510), so its effect might be exerted mainly at the protein level.

Figure 4.8 provides a graphical summary of the explanatory hypothesis of the above experimental results, based on the available literature describing the effect of ruxolitinib and CFZ on NF-κB pathway. However, NF-κB pathway regulation is complex (511) and varies according to the cell and disease type (512-514) and the experiments performed in this work are too limited in number. Further studies are needed to understand the effect of JAK2 inhibition combined with proteasome inhibition on this pathway.

Figure 4.7. Model of JAK-STAT induced NF-kB activation.
(adapted from Fisher D et al. Leukemia. 2017 September; 31(9): 1962–1974)

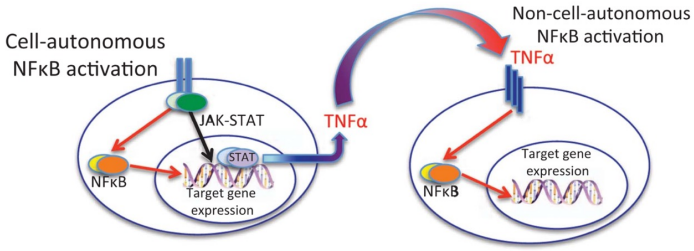

Figure 4.8. Reflection on the observed effect of ruxolitinib and CFZ on NF-kB pathway in MF CD34+ cells.

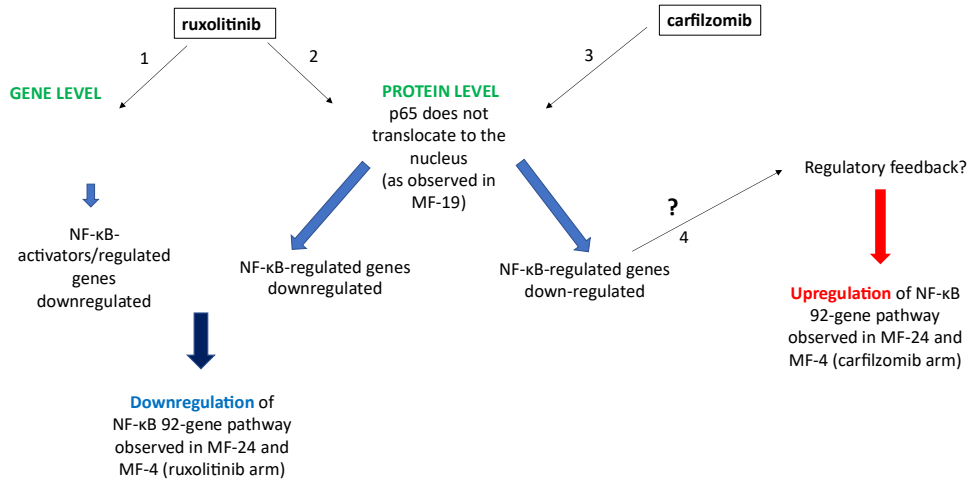

Secondly, although the overall pattern of differential gene expression is maintained between the two patients across treatment arms, there were some groups of genes with different behaviours (group 1 to 3, please refer to the Results) and, overall, CFZ upregulated more genes in the ruxolitinib-refractory patient that in the naïve individual. The explanation of these differences is difficult as there is no matched experiment run on the same samples to study the respective protein levels. However, it could be related to the differentially deranged NF-κB pathway in MF-24 and/or more pronounced inhibitory effect of CFZ at protein level, with a higher rebound upregulation of the gene expression, as compared to MF-4.

In Table A11 (Appendix) are listed some of the genes which could have a particular relevance in MF pathogenesis and progression, whose gene expression is altered by CFZ (either concordantly or discordantly between MF-4 and MF-24).

Finally, focusing on the MF-24 experiment, the addition of ruxolitinib to CFZ either attenuated or it did not change the upregulatory effect of CFZ for 21 genes (Table A12); however, despite ruxolitinib downregulating or not affecting their expression, when combined with CFZ it potentiated the upregulatory effect of CZF. This is an interesting effect that would deserve further investigation as it could suggest a synergistic effect of the drug combination on the upregulation of these genes. Most of these genes encode activators of NF-κB pathway, so, if the result is confirmed on several patient samples, it would be important to clarify whether the higher gene upregulation caused by the combination treatment corresponds to an increased or suppressed NF-κB activity in MF CD34+ cells. In the latter case the potentiated upregulating effect at gene level might be a regulatory feed-back from a profound NF-κB inhibition at protein level exerted by both drugs (similarly to what discussed above, please refer to Figure 4.8). In order to answer to this question, combined Western blot and gene expression analyses should be run on the same samples.

Proteasome activity is required for NF-κB activity (273, 515) and constitutive NF-κB activity has been shown in MF cells (270), which protects them against apoptosis (270, 516-518).

The apoptotic activity of CFZ in MF cells might be due to its role in suppressing NF-κB as demonstrated before for other haematological malignancies (509, 519). In conclusion, although the regulation of NF-κB pathway and the function of each of its subunits is a complex scenario (520), if further studies confirm that CFZ inhibits the canonical NF-κB activity in MF CD34+ cells it is reasonable to think that CFZ may also reinforce ruxolitinib efficacy against MF inflammatory background and clonal expansion. In support of this, recent studies showed that the addition of an inhibitor of NF-κB activity to ruxolitinib enhances its therapeutical potential in MF (270, 521).

4.6 Interpretation of additional GEP findings (*PTGDS*, *FLT3*, *ARG1*)

The finding of increased *PTGDS* expression in MF CD34+ cells treated with ruxolitinib is of interest and deserves further investigation. The upregulation of this gene by ruxolitinib was also found in three healthy controls, but the fold change was significantly greater in MF samples. *PTGDS* encodes the glutathione-independent prostaglandin D synthase, which catalyses the conversion of prostaglandin H2 (PGH2) to prostaglandin D2 (PGD2), a pro-inflammatory mediator. The limited in vitro experiments with PGD2 and its inhibitor AT-56 on MF CD34+ cells were unable to confirm a functional effect of PGD2. However, PTGDS and PDG2 might still be worthy of further study for some reasons. PDG2 through its receptor participates in the PDG2/SOX9 axis, a pathway shown to lead to invasion and migration of testis and ovarian cancers (522, 523). Also, SOX9 transcription factor is a well-recognized oncogenic driver in other cancer types (524) and a mediator of fibrosis (525-528). Interestingly, IL-6/JAK/STAT3 pathway inhibition increased expression of *SOX9* in chondrocytes (529).
PDG2 might exert its effect on and through the participation of microenvironment and/or it might have other targets, such as immune cells. APL blasts release a large amount of PDG2 which finally leads to the stimulation of monocytic myeloid-derived suppressor cells (530).
Ruxolitinib, through STAT3 inhibition, has been shown to upregulate *PTGS2* (which encodes for the enzyme COX-2) in tumour-infiltrating macrophages, and the consequential increase in PGE2 (prostaglandin E2, produced by COX-2) is responsible for ruxolitinib resistance in both *in vitro* and *in vivo* models of breast cancer (531). PGE2 may also favour immune escape by the impairment of NK and cytotoxic T cell functions (532). *PTGS2* is a JAK1-dependent UPR gene (533) and is found to be overexpressed in ET (534). Furthermore, a recent work identified *PTGS2* among the most upregulated genes in HSPC in advanced phase MF compared to earlier disease stages, in a patient progressed to secondary AML during treatment with ruxolitinib (176).
Altogether, the above evidence suggests that prostaglandins might be relevant in the pathogenesis of MF through participating in the inflammatory background and fibrotic process, immune-evasion and disease progression. Also, they might contribute to ruxolitinib failure in eradicating the MF clone through taking part into its well-known immunomodulatory/immunosuppressive action, accounting for ruxolitinib success in inflammatory and autoimmune conditions (535-539).
Similarly, the upregulation of *ARG1* induced by ruxolitinib observed in MF samples is a very preliminary finding, as it was found only in 3 of 5 patients and the fold change was >2 only in

2 patients. If confirmed by future studies, it might represent an immune escape-favouring event. *ARG1* codifies for arginase 1, an enzyme that metabolises arginine in ornithine and urea and a known immunosuppressive mediator, of particular importance in AML (540). Furthermore, ornithine, stimulates cell proliferation and collagen deposition (541).

Finally, *FLT3* was found upregulated in all the 5 MF patients studied. *FLT3* encodes the fms-like tyrosine kinase 3 (Flt3), a receptor tyrosine kinase whose mutation in one the most recurrent in AML and associated with poor prognosis (542). Of note, 15 cases of *FLT3*-rearranged myeloid/lymphoid neoplasms have been reported until 2020, of which most are myeloproliferative neoplasms without other genetic lesions (543). Activation of FLT3 tyrosine kinase potentiates the JAK/STAT signalling (544, 545) and increased p-STAT5 are present in AML with *FLT3* ITD mutation (546-548), so *FLT3* overexpression found in the present study might deserve further investigation.

Conclusions

This study revealed that the HEL cell line is vulnerable to genetic knockdown of the proteasome gene family and that PI are effective in inhibiting its proliferation at relatively low doses.

The extension of these results on primary MF CD34+ cells revealed that CFZ, a second-generation PI, is able to inhibit their proliferation and to induce apoptosis in vitro.

The addition of CFZ to the JAK2 inhibitor ruxolitinib increased the efficacy of ruxolitinib alone and this finding was confirmed also on pulsed-CFZ experiments, although the degree of this effect varied across MF samples and was more significant only on long-term clonogenic assays.

We then provided evidence that the proteasome gene set is negatively-enriched in MF CD34+ cells treated with ruxolitinib and we hypothesised that this mechanism would render these cells even more vulnerable to PI. Indirectly, this finding, along with the different pharmacokinetic and pharmacodynamic properties of CFZ, could be a possible explanation for the lack of clinical activity of BTZ as a monotherapy for patients with MF.

Furthermore, we provided a very preliminary observation about the negative effect of CFZ on the activation of NF-κB canonical pathway in one MF sample, which, if confirmed by further studies, might represent an additional point in favour of the investigation of CFZ in MF therapy. In this regard, additional work is needed to understand the mechanism underlying the upregulation of NF-κB pathway gene expression induced by CFZ in MF cells.

Based on the above findings, we think that the combination of JAK2 inhibitor and CFZ could be a potential new therapy to further explore in MF.

Additionally, the high throughput genetic approach used to screen for genetic vulnerabilities in HEL cells revealed several genes connected in different ways to the JAK/STAT pathway or other pathways relevant in MPN, which might be interesting candidates for future research.

Similarly, the data obtained from the gene expression analysis of MF CD34+ cells treated with ruxolitinib needs to be exploited as they might reveal novel clues to alternative pathways to be targeted in combination with JAK/STAT in order to improve current MF therapeutics.

Finally, this work showed that pooled-shRNA library screen is a highly informative technique but its application on primary cells remains challenging and needs optimization. The very limited amount of data resulted from the post-selection barcode abundancy of one MF sample, however, are of some interest and could to justify further efforts in developing this method on MF CD34+ cells.

References

1. Barosi G, Mesa RA, Thiele J, Cervantes F, Campbell PJ, Verstovsek S, et al. Proposed criteria for the diagnosis of post-polycythemia vera and post-essential thrombocythemia myelofibrosis: a consensus statement from the International Working Group for Myelofibrosis Research and Treatment. Leukemia. 2008;22(2):437-8.
2. Kaifie A, Kirschner M, Wolf D, Maintz C, Hanel M, Gattermann N, et al. Bleeding, thrombosis, and anticoagulation in myeloproliferative neoplasms (MPN): analysis from the German SAL-MPN-registry. J Hematol Oncol. 2016;9:18.
3. McMahon B, Stein BL. Thrombotic and bleeding complications in classical myeloproliferative neoplasms. Semin Thromb Hemost. 2013;39(1):101-11.
4. Vallapureddy RR, Mudireddy M, Penna D, Lasho TL, Finke CM, Hanson CA, et al. Leukemic transformation among 1306 patients with primary myelofibrosis: risk factors and development of a predictive model. Blood Cancer J. 2019;9(2):12.
5. Finazzi G, Carobbio A, Thiele J, Passamonti F, Rumi E, Ruggeri M, et al. Incidence and risk factors for bleeding in 1104 patients with essential thrombocythemia or prefibrotic myelofibrosis diagnosed according to the 2008 WHO criteria. Leukemia. 2012;26(4):716-9.
6. Arber DA, Orazi A, Hasserjian R, Thiele J, Borowitz MJ, Le Beau MM, et al. The 2016 revision to the World Health Organization classification of myeloid neoplasms and acute leukemia. Blood. 2016;127(20):2391-405.
7. Guglielmelli P, Pacilli A, Rotunno G, Rumi E, Rosti V, Delaini F, et al. Presentation and outcome of patients with 2016 WHO diagnosis of prefibrotic and overt primary myelofibrosis. Blood. 2017;129(24):3227-36.
8. Baxter EJ, Scott LM, Campbell PJ, East C, Fourouclas N, Swanton S, et al. Acquired mutation of the tyrosine kinase JAK2 in human myeloproliferative disorders. Lancet. 2005;365(9464):1054-61.
9. Scott LM, Tong W, Levine RL, Scott MA, Beer PA, Stratton MR, et al. JAK2 exon 12 mutations in polycythemia vera and idiopathic erythrocytosis. N Engl J Med. 2007;356(5):459-68.
10. Pikman Y, Lee BH, Mercher T, McDowell E, Ebert BL, Gozo M, et al. MPLW515L is a novel somatic activating mutation in myelofibrosis with myeloid metaplasia. PLoS Med. 2006;3(7):e270.
11. Pardanani AD, Levine RL, Lasho T, Pikman Y, Mesa RA, Wadleigh M, et al. MPL515 mutations in myeloproliferative and other myeloid disorders: a study of 1182 patients. Blood. 2006;108(10):3472-6.
12. Nangalia J, Massie CE, Baxter EJ, Nice FL, Gundem G, Wedge DC, et al. Somatic CALR mutations in myeloproliferative neoplasms with nonmutated JAK2. N Engl J Med. 2013;369(25):2391-405.
13. Klampfl T, Gisslinger H, Harutyunyan AS, Nivarthi H, Rumi E, Milosevic JD, et al. Somatic mutations of calreticulin in myeloproliferative neoplasms. The New England journal of medicine. 2013;369(25):2379-90.
14. Anand S, Stedham F, Gudgin E, Campbell P, Beer P, Green AR, et al. Increased basal intracellular signaling patterns do not correlate with JAK2 genotype in human myeloproliferative neoplasms. Blood. 2011;118(6):1610-21.
15. Lau WW, Hannah R, Green AR, Gottgens B. The JAK-STAT signaling pathway is differentially activated in CALR-positive compared with JAK2V617F-positive ET patients. Blood. 2015;125(10):1679-81.
16. Tefferi A. Novel mutations and their functional and clinical relevance in myeloproliferative neoplasms: JAK2, MPL, TET2, ASXL1, CBL, IDH and IKZF1. Leukemia. 2010;24(6):1128-38.

17. Stein BL, Williams DM, O'Keefe C, Rogers O, Ingersoll RG, Spivak JL, et al. Disruption of the ASXL1 gene is frequent in primary, post-essential thrombocytosis and post-polycythemia vera myelofibrosis, but not essential thrombocytosis or polycythemia vera: analysis of molecular genetics and clinical phenotypes. Haematologica. 2011;96(10):1462-9.
18. Tefferi A, Lasho TL, Finke CM, Knudson RA, Ketterling R, Hanson CH, et al. CALR vs JAK2 vs MPL-mutated or triple-negative myelofibrosis: clinical, cytogenetic and molecular comparisons. Leukemia. 2014;28(7):1472-7.
19. Hautin M, Mornet C, Chauveau A, Bernard D, Corcos L, Lippert E. Splicing Anomalies in Myeloproliferative Neoplasms: Paving the Way for New Therapeutic Venues. Cancers (Basel). 2020;12(8).
20. Ortmann CA, Kent DG, Nangalia J, Silber Y, Wedge DC, Grinfeld J, et al. Effect of mutation order on myeloproliferative neoplasms. The New England journal of medicine. 2015;372(7):601-12.
21. Roaldsnes C, Holst R, Frederiksen H, Ghanima W. Myeloproliferative neoplasms: trends in incidence, prevalence and survival in Norway. Eur J Haematol. 2017;98(1):85-93.
22. Mehta J, Wang H, Iqbal SU, Mesa R. Epidemiology of myeloproliferative neoplasms in the United States. Leuk Lymphoma. 2014;55(3):595-600.
23. Moulard O, Mehta J, Fryzek J, Olivares R, Iqbal U, Mesa RA. Epidemiology of myelofibrosis, essential thrombocythemia, and polycythemia vera in the European Union. Eur J Haematol. 2014;92(4):289-97.
24. Byun JM, Kim YJ, Youk T, Yang JJ, Yoo J, Park TS. Real world epidemiology of myeloproliferative neoplasms: a population based study in Korea 2004-2013. Ann Hematol. 2017;96(3):373-81.
25. Selinger HA, Ma X. Jakking up tumor registry reporting of the myeloproliferative neoplasms. Am J Hematol. 2009;84(2):124-6.
26. Johansson P. Epidemiology of the myeloproliferative disorders polycythemia vera and essential thrombocythemia. Semin Thromb Hemost. 2006;32(3):171-3.
27. Shallis RM, Wang R, Davidoff A, Ma X, Podoltsev NA, Zeidan AM. Epidemiology of the classical myeloproliferative neoplasms: The four corners of an expansive and complex map. Blood Rev. 2020;42:100706.
28. Baade PD, Ross DM, Anderson LA, Forsyth C, Fritschi L. Changing incidence of myeloproliferative neoplasms in Australia, 2003-2014. Am J Hematol. 2019;94(4):E107-E9.
29. Titmarsh GJ, Duncombe AS, McMullin MF, O'Rorke M, Mesa R, De Vocht F, et al. How common are myeloproliferative neoplasms? A systematic review and meta-analysis. Am J Hematol. 2014;89(6):581-7.
30. Naymagon L, Mascarenhas J. Myelofibrosis-Related Anemia: Current and Emerging Therapeutic Strategies. Hemasphere. 2017;1(1):e1.
31. Barraco D, Lasho TL, Gangat N, Finke C, Elala YC, Pardanani A, et al. Leukocytosis and presence of CALR mutation is associated with non-hepatosplenic extramedullary hematopoiesis in primary myelofibrosis. Blood Cancer J. 2016;6:e436.
32. Hart C, Klatt S, Barop J, Muller G, Schelker R, Holler E, et al. Splenic pooling and loss of VCAM-1 causes an engraftment defect in patients with myelofibrosis after allogeneic hematopoietic stem cell transplantation. Haematologica. 2016;101(11):1407-16.
33. Bogani C, Ponziani V, Guglielmelli P, Desterke C, Rosti V, Bosi A, et al. Hypermethylation of CXCR4 promoter in CD34+ cells from patients with primary myelofibrosis. Stem Cells. 2008;26(8):1920-30.
34. Song MK, Park BB, Uhm JE. Understanding Splenomegaly in Myelofibrosis: Association with Molecular Pathogenesis. Int J Mol Sci. 2018;19(3).

35. Maynadie M, De Angelis R, Marcos-Gragera R, Visser O, Allemani C, Tereanu C, et al. Survival of European patients diagnosed with myeloid malignancies: a HAEMACARE study. Haematologica. 2013;98(2):230-8.
36. Tefferi A, Guglielmelli P, Larson DR, Finke C, Wassie EA, Pieri L, et al. Long-term survival and blast transformation in molecularly annotated essential thrombocythemia, polycythemia vera, and myelofibrosis. Blood. 2014;124(16):2507-13; quiz 615.
37. Visser O, Trama A, Maynadie M, Stiller C, Marcos-Gragera R, De Angelis R, et al. Incidence, survival and prevalence of myeloid malignancies in Europe. Eur J Cancer. 2012;48(17):3257-66.
38. Cervantes F, Dupriez B, Passamonti F, Vannucchi AM, Morra E, Reilly JT, et al. Improving survival trends in primary myelofibrosis: an international study. J Clin Oncol. 2012;30(24):2981-7.
39. Hultcrantz M, Kristinsson SY, Andersson TM, Landgren O, Eloranta S, Derolf AR, et al. Patterns of survival among patients with myeloproliferative neoplasms diagnosed in Sweden from 1973 to 2008: a population-based study. J Clin Oncol. 2012;30(24):2995-3001.
40. Cervantes F, Dupriez B, Pereira A, Passamonti F, Reilly JT, Morra E, et al. New prognostic scoring system for primary myelofibrosis based on a study of the International Working Group for Myelofibrosis Research and Treatment. Blood. 2009;113(13):2895-901.
41. Passamonti F, Cervantes F, Vannucchi AM, Morra E, Rumi E, Pereira A, et al. A dynamic prognostic model to predict survival in primary myelofibrosis: a study by the IWG-MRT (International Working Group for Myeloproliferative Neoplasms Research and Treatment). Blood. 2010;115(9):1703-8.
42. Gangat N, Caramazza D, Vaidya R, George G, Begna K, Schwager S, et al. DIPSS plus: a refined Dynamic International Prognostic Scoring System for primary myelofibrosis that incorporates prognostic information from karyotype, platelet count, and transfusion status. J Clin Oncol. 2011;29(4):392-7.
43. Tefferi A, Guglielmelli P, Nicolosi M, Mannelli F, Mudireddy M, Bartalucci N, et al. GIPSS: genetically inspired prognostic scoring system for primary myelofibrosis. Leukemia. 2018;32(7):1631-42.
44. Tefferi A, Guglielmelli P, Lasho TL, Gangat N, Ketterling RP, Pardanani A, et al. MIPSS70+ Version 2.0: Mutation and Karyotype-Enhanced International Prognostic Scoring System for Primary Myelofibrosis. J Clin Oncol. 2018;36(17):1769-70.
45. Passamonti F, Giorgino T, Mora B, Guglielmelli P, Rumi E, Maffioli M, et al. A clinical-molecular prognostic model to predict survival in patients with post polycythemia vera and post essential thrombocythemia myelofibrosis. Leukemia. 2017;31(12):2726-31.
46. Skoda RC, Duek A, Grisouard J. Pathogenesis of myeloproliferative neoplasms. Exp Hematol. 2015;43(8):599-608.
47. Kralovics R, Skoda RC. Molecular pathogenesis of Philadelphia chromosome negative myeloproliferative disorders. Blood Rev. 2005;19(1):1-13.
48. Wernig G, Mercher T, Okabe R, Levine RL, Lee BH, Gilliland DG. Expression of Jak2V617F causes a polycythemia vera-like disease with associated myelofibrosis in a murine bone marrow transplant model. Blood. 2006;107(11):4274-81.
49. Lacout C, Pisani DF, Tulliez M, Gachelin FM, Vainchenker W, Villeval JL. JAK2V617F expression in murine hematopoietic cells leads to MPD mimicking human PV with secondary myelofibrosis. Blood. 2006;108(5):1652-60.
50. Shide K, Shimoda HK, Kumano T, Karube K, Kameda T, Takenaka K, et al. Development of ET, primary myelofibrosis and PV in mice expressing JAK2 V617F. Leukemia. 2008;22(1):87-95.
51. Xing S, Wanting TH, Zhao W, Ma J, Wang S, Xu X, et al. Transgenic expression of JAK2V617F causes myeloproliferative disorders in mice. Blood. 2008;111(10):5109-17.

52. Akada H, Yan D, Zou H, Fiering S, Hutchison RE, Mohi MG. Conditional expression of heterozygous or homozygous Jak2V617F from its endogenous promoter induces a polycythemia vera-like disease. Blood. 2010;115(17):3589-97.
53. Marty C, Pecquet C, Nivarthi H, El-Khoury M, Chachoua I, Tulliez M, et al. Calreticulin mutants in mice induce an MPL-dependent thrombocytosis with frequent progression to myelofibrosis. Blood. 2016;127(10):1317-24.
54. Kleppe M, Kwak M, Koppikar P, Riester M, Keller M, Bastian L, et al. JAK-STAT pathway activation in malignant and nonmalignant cells contributes to MPN pathogenesis and therapeutic response. Cancer Discov. 2015;5(3):316-31.
55. Psaila B, Wang G, Rodriguez-Meira A, Li R, Heuston EF, Murphy L, et al. Single-Cell Analyses Reveal Megakaryocyte-Biased Hematopoiesis in Myelofibrosis and Identify Mutant Clone-Specific Targets. Mol Cell. 2020;78(3):477-92 e8.
56. Nam AS, Kim KT, Chaligne R, Izzo F, Ang C, Taylor J, et al. Somatic mutations and cell identity linked by Genotyping of Transcriptomes. Nature. 2019;571(7765):355-60.
57. Rodriguez-Meira A, Buck G, Clark SA, Povinelli BJ, Alcolea V, Louka E, et al. Unravelling Intratumoral Heterogeneity through High-Sensitivity Single-Cell Mutational Analysis and Parallel RNA Sequencing. Molecular cell. 2019;73(6):1292-305 e8.
58. Malherbe JA, Fuller KA, Mirzai B, Kavanagh S, So CC, Ip HW, et al. Dysregulation of the intrinsic apoptotic pathway mediates megakaryocytic hyperplasia in myeloproliferative neoplasms. J Clin Pathol. 2016.
59. Malherbe JA, Fuller KA, Arshad A, Nangalia J, Romeo G, Hall SL, et al. Megakaryocytic hyperplasia in myeloproliferative neoplasms is driven by disordered proliferative, apoptotic and epigenetic mechanisms. J Clin Pathol. 2016;69(2):155-63.
60. Zhang Y, Lin CHS, Kaushansky K, Zhan H. JAK2V617F Megakaryocytes Promote Hematopoietic Stem/Progenitor Cell Expansion in Mice Through Thrombopoietin/MPL Signaling. Stem Cells. 2018;36(11):1676-84.
61. Woods B, Chen W, Chiu S, Marinaccio C, Fu C, Gu L, et al. Activation of JAK/STAT Signaling in Megakaryocytes Sustains Myeloproliferation In Vivo. Clin Cancer Res. 2019;25(19):5901-12.
62. Badalucco S, Di Buduo CA, Campanelli R, Pallotta I, Catarsi P, Rosti V, et al. Involvement of TGFbeta1 in autocrine regulation of proplatelet formation in healthy subjects and patients with primary myelofibrosis. Haematologica. 2013;98(4):514-7.
63. Emadi S, Clay D, Desterke C, Guerton B, Maquarre E, Charpentier A, et al. IL-8 and its CXCR1 and CXCR2 receptors participate in the control of megakaryocytic proliferation, differentiation, and ploidy in myeloid metaplasia with myelofibrosis. Blood. 2005;105(2):464-73.
64. Haas S, Hansson J, Klimmeck D, Loeffler D, Velten L, Uckelmann H, et al. Inflammation-Induced Emergency Megakaryopoiesis Driven by Hematopoietic Stem Cell-like Megakaryocyte Progenitors. Cell Stem Cell. 2015;17(4):422-34.
65. Le Bousse-Kerdiles MC, Chevillard S, Charpentier A, Romquin N, Clay D, Smadja-Joffe F, et al. Differential expression of transforming growth factor-beta, basic fibroblast growth factor, and their receptors in CD34+ hematopoietic progenitor cells from patients with myelofibrosis and myeloid metaplasia. Blood. 1996;88(12):4534-46.
66. Campanelli R, Rosti V, Villani L, Castagno M, Moretti E, Bonetti E, et al. Evaluation of the bioactive and total transforming growth factor beta1 levels in primary myelofibrosis. Cytokine. 2011;53(1):100-6.
67. Vannucchi AM, Bianchi L, Paoletti F, Pancrazzi A, Torre E, Nishikawa M, et al. A pathobiologic pathway linking thrombopoietin, GATA-1, and TGF-beta1 in the development of myelofibrosis. Blood. 2005;105(9):3493-501.

68. Yoon SY, Tefferi A, Li CY. Cellular distribution of platelet-derived growth factor, transforming growth factor-beta, basic fibroblast growth factor, and their receptors in normal bone marrow. Acta Haematol. 2000;104(4):151-7.
69. Bock O, Loch G, Busche G, von Wasielewski R, Schlue J, Kreipe H. Aberrant expression of platelet-derived growth factor (PDGF) and PDGF receptor-alpha is associated with advanced bone marrow fibrosis in idiopathic myelofibrosis. Haematologica. 2005;90(1):133-4.
70. Schneider RK, Mullally A, Dugourd A, Peisker F, Hoogenboezem R, Van Strien PMH, et al. Gli1(+) Mesenchymal Stromal Cells Are a Key Driver of Bone Marrow Fibrosis and an Important Cellular Therapeutic Target. Cell Stem Cell. 2017;20(6):785-800 e8.
71. Martyre MC, Le Bousse-Kerdiles MC, Romquin N, Chevillard S, Praloran V, Demory JL, et al. Elevated levels of basic fibroblast growth factor in megakaryocytes and platelets from patients with idiopathic myelofibrosis. Br J Haematol. 1997;97(2):441-8.
72. Boiocchi L, Vener C, Savi F, Bonoldi E, Moro A, Fracchiolla NS, et al. Increased expression of vascular endothelial growth factor receptor 1 correlates with VEGF and microvessel density in Philadelphia chromosome-negative myeloproliferative neoplasms. J Clin Pathol. 2011;64(3):226-31.
73. Muth M, Engelhardt BM, Kroger N, Hussein K, Schlue J, Busche G, et al. Thrombospondin-1 (TSP-1) in primary myelofibrosis (PMF) - a megakaryocyte-derived biomarker which largely discriminates PMF from essential thrombocythemia. Ann Hematol. 2011;90(1):33-40.
74. Lu M, Xia L, Liu YC, Hochman T, Bizzari L, Aruch D, et al. Lipocalin produced by myelofibrosis cells affects the fate of both hematopoietic and marrow microenvironmental cells. Blood. 2015;126(8):972-82.
75. Hoermann G, Cerny-Reiterer S, Herrmann H, Blatt K, Bilban M, Gisslinger H, et al. Identification of oncostatin M as a JAK2 V617F-dependent amplifier of cytokine production and bone marrow remodeling in myeloproliferative neoplasms. FASEB J. 2012;26(2):894-906.
76. Bock O, Hoftmann J, Theophile K, Hussein K, Wiese B, Schlue J, et al. Bone morphogenetic proteins are overexpressed in the bone marrow of primary myelofibrosis and are apparently induced by fibrogenic cytokines. Am J Pathol. 2008;172(4):951-60.
77. Garimella R, Kacena MA, Tague SE, Wang J, Horowitz MC, Anderson HC. Expression of bone morphogenetic proteins and their receptors in the bone marrow megakaryocytes of GATA-1(low) mice: a possible role in osteosclerosis. J Histochem Cytochem. 2007;55(7):745-52.
78. Malara A, Currao M, Gruppi C, Celesti G, Viarengo G, Buracchi C, et al. Megakaryocytes contribute to the bone marrow-matrix environment by expressing fibronectin, type IV collagen, and laminin. Stem Cells. 2014;32(4):926-37.
79. Eliades A, Papadantonakis N, Bhupatiraju A, Burridge KA, Johnston-Cox HA, Migliaccio AR, et al. Control of megakaryocyte expansion and bone marrow fibrosis by lysyl oxidase. J Biol Chem. 2011;286(31):27630-8.
80. Bock O, Neuse J, Hussein K, Brakensiek K, Buesche G, Buhr T, et al. Aberrant collagenase expression in chronic idiopathic myelofibrosis is related to the stage of disease but not to the JAK2 mutation status. Am J Pathol. 2006;169(2):471-81.
81. Wickenhauser C, Schmitz B, Baldus SE, Henze F, Farahmand P, Frimpong S, et al. Selectins (CD62L, CD62P) and megakaryocytic glycoproteins (CD41a, CD42b) mediate megakaryocyte-fibroblast interactions in human bone marrow. Leuk Res. 2000;24(12):1013-21.
82. El Agha E, Kramann R, Schneider RK, Li X, Seeger W, Humphreys BD, et al. Mesenchymal Stem Cells in Fibrotic Disease. Cell Stem Cell. 2017;21(2):166-77.

83. Schmitt A, Drouin A, Masse JM, Guichard J, Shagraoui H, Cramer EM. Polymorphonuclear neutrophil and megakaryocyte mutual involvement in myelofibrosis pathogenesis. Leuk Lymphoma. 2002;43(4):719-24.
84. Centurione L, Di Baldassarre A, Zingariello M, Bosco D, Gatta V, Rana RA, et al. Increased and pathologic emperipolesis of neutrophils within megakaryocytes associated with marrow fibrosis in GATA-1(low) mice. Blood. 2004;104(12):3573-80.
85. Zingariello M, Rosti V, Vannucchi AM, Guglielmelli P, Mazzarini M, Barosi G, et al. Shared and Distinctive Ultrastructural Abnormalities Expressed by Megakaryocytes in Bone Marrow and Spleen From Patients With Myelofibrosis. Front Oncol. 2020;10:584541.
86. Di Buduo CA, Giannini S, Abbonante V, Rosti V, Hoffmeister KM, Balduini A. Increased B4GALT1 expression is associated with platelet surface galactosylation and thrombopoietin plasma levels in MPNs. Blood. 2021;137(15):2085-9.
87. Marin Oyarzun CP, Heller PG. Platelets as Mediators of Thromboinflammation in Chronic Myeloproliferative Neoplasms. Front Immunol. 2019;10:1373.
88. Guo BB, Allcock RJ, Mirzai B, Malherbe JA, Choudry FA, Frontini M, et al. Megakaryocytes in Myeloproliferative Neoplasms Have Unique Somatic Mutations. Am J Pathol. 2017;187(7):1512-22.
89. Rosti V, Villani L, Riboni R, Poletto V, Bonetti E, Tozzi L, et al. Spleen endothelial cells from patients with myelofibrosis harbor the JAK2V617F mutation. Blood. 2013;121(2):360-8.
90. Massa M, Campanelli R, Lupo L, Fois G, Viarengo G, Jemos V, et al. Splenectomy produces a rapid but transient decrease of the frequency of circulating CD34+ haematopoietic progenitor cells in primary myelofibrosis. Br J Haematol. 2011;152(5):665-7.
91. Wang X, Prakash S, Lu M, Tripodi J, Ye F, Najfeld V, et al. Spleens of myelofibrosis patients contain malignant hematopoietic stem cells. J Clin Invest. 2012;122(11):3888-99.
92. Erba BG, Gruppi C, Corada M, Pisati F, Rosti V, Bartalucci N, et al. Endothelial-to-Mesenchymal Transition in Bone Marrow and Spleen of Primary Myelofibrosis. Am J Pathol. 2017;187(8):1879-92.
93. Avanzini MA, Abbonante V, Catarsi P, Dambruoso I, Mantelli M, Poletto V, et al. The spleen of patients with myelofibrosis harbors defective mesenchymal stromal cells. Am J Hematol. 2018;93(5):615-22.
94. Elliott MA, Verstovsek S, Dingli D, Schwager SM, Mesa RA, Li CY, et al. Monocytosis is an adverse prognostic factor for survival in younger patients with primary myelofibrosis. Leuk Res. 2007;31(11):1503-9.
95. Rameshwar P, Denny TN, Stein D, Gascon P. Monocyte adhesion in patients with bone marrow fibrosis is required for the production of fibrogenic cytokines. Potential role for interleukin-1 and TGF-beta. J Immunol. 1994;153(6):2819-30.
96. Goette NP, Lev PR, Heller PG, Kornblihtt LI, Korin L, Molinas FC, et al. Monocyte IL-2Ralpha expression is associated with thrombosis and the JAK2V617F mutation in myeloproliferative neoplasms. Cytokine. 2010;51(1):67-72.
97. Lai HY, Brooks SA, Craver BM, Morse SJ, Nguyen TK, Haghighi N, et al. Defective negative regulation of Toll-like receptor signaling leads to excessive TNF-alpha in myeloproliferative neoplasm. Blood Adv. 2019;3(2):122-31.
98. Fisher DAC, Miner CA, Engle EK, Hu H, Collins TB, Zhou A, et al. Cytokine production in myelofibrosis exhibits differential responsiveness to JAK-STAT, MAP kinase, and NFkappaB signaling. Leukemia. 2019;33(8):1978-95.
99. Abe R, Donnelly SC, Peng T, Bucala R, Metz CN. Peripheral blood fibrocytes: differentiation pathway and migration to wound sites. J Immunol. 2001;166(12):7556-62.

100. Pilling D, Fan T, Huang D, Kaul B, Gomer RH. Identification of markers that distinguish monocyte-derived fibrocytes from monocytes, macrophages, and fibroblasts. PLoS One. 2009;4(10):e7475.
101. Maekawa T, Osawa Y, Izumi T, Nagao S, Takano K, Okada Y, et al. Myeloproliferative leukemia protein activation directly induces fibrocyte differentiation to cause myelofibrosis. Leukemia. 2017;31(12):2709-16.
102. Maekawa T, Kato S, Kawamura T, Takada K, Sone T, Ogata H, et al. Increased SLAMF7(high) monocytes in myelofibrosis patients harboring JAK2V617F provide a therapeutic target of elotuzumab. Blood. 2019;134(10):814-25.
103. Verstovsek S, Manshouri T, Pilling D, Bueso-Ramos CE, Newberry KJ, Prijic S, et al. Role of neoplastic monocyte-derived fibrocytes in primary myelofibrosis. J Exp Med. 2016;213(9):1723-40.
104. Manshouri T, Verstovsek S, Harris DM, Veletic I, Zhang X, Post SM, et al. Primary myelofibrosis marrow-derived CD14+/CD34- monocytes induce myelofibrosis-like phenotype in immunodeficient mice and give rise to megakaryocytes. PLoS One. 2019;14(9):e0222912.
105. Ozono Y, Shide K, Kameda T, Kamiunten A, Tahira Y, Sekine M, et al. Neoplastic fibrocytes play an essential role in bone marrow fibrosis in Jak2V617F-induced primary myelofibrosis mice. Leukemia. 2021;35(2):454-67.
106. Arranz L, Sanchez-Aguilera A, Martin-Perez D, Isern J, Langa X, Tzankov A, et al. Neuropathy of haematopoietic stem cell niche is essential for myeloproliferative neoplasms. Nature. 2014;512(7512):78-81.
107. Ramos TL, Sanchez-Abarca LI, Redondo A, Hernandez-Hernandez A, Almeida AM, Puig N, et al. HDAC8 overexpression in mesenchymal stromal cells from JAK2+ myeloproliferative neoplasms: a new therapeutic target? Oncotarget. 2017;8(17):28187-202.
108. Schneider RK, Ziegler S, Leisten I, Ferreira MS, Schumacher A, Rath B, et al. Activated fibronectin-secretory phenotype of mesenchymal stromal cells in pre-fibrotic myeloproliferative neoplasms. Journal of hematology & oncology. 2014;7:92.
109. Schepers K, Pietras EM, Reynaud D, Flach J, Binnewies M, Garg T, et al. Myeloproliferative neoplasia remodels the endosteal bone marrow niche into a self-reinforcing leukemic niche. Cell stem cell. 2013;13(3):285-99.
110. Martinaud C, Desterke C, Konopacki J, Pieri L, Torossian F, Golub R, et al. Osteogenic Potential of Mesenchymal Stromal Cells Contributes to Primary Myelofibrosis. Cancer research. 2015;75(22):4753-65.
111. Wang L, Zhang H, Rodriguez S, Cao L, Parish J, Mumaw C, et al. Notch-dependent repression of miR-155 in the bone marrow niche regulates hematopoiesis in an NF-kappaB-dependent manner. Cell stem cell. 2014;15(1):51-65.
112. Hermouet S, Bigot-Corbel E, Gardie B. Pathogenesis of Myeloproliferative Neoplasms: Role and Mechanisms of Chronic Inflammation. Mediators of inflammation. 2015;2015:145293.
113. Hermouet S. Pathogenesis of myeloproliferative neoplasms: More than mutations. Experimental hematology. 2015;43(12):993-4.
114. Hinz B, Phan SH, Thannickal VJ, Prunotto M, Desmouliere A, Varga J, et al. Recent developments in myofibroblast biology: paradigms for connective tissue remodeling. The American journal of pathology. 2012;180(4):1340-55.
115. Colmone A, Amorim M, Pontier AL, Wang S, Jablonski E, Sipkins DA. Leukemic cells create bone marrow niches that disrupt the behavior of normal hematopoietic progenitor cells. Science. 2008;322(5909):1861-5.
116. Lataillade JJ, Pierre-Louis O, Hasselbalch HC, Uzan G, Jasmin C, Martyre MC, et al. Does primary myelofibrosis involve a defective stem cell niche? From concept to evidence. Blood. 2008;112(8):3026-35.

117. Meads MB, Hazlehurst LA, Dalton WS. The bone marrow microenvironment as a tumor sanctuary and contributor to drug resistance. Clinical cancer research : an official journal of the American Association for Cancer Research. 2008;14(9):2519-26.
118. Smith JN, Calvi LM. Concise review: Current concepts in bone marrow microenvironmental regulation of hematopoietic stem and progenitor cells. Stem cells. 2013;31(6):1044-50.
119. Tesfai Y, Ford J, Carter KW, Firth MJ, O'Leary RA, Gottardo NG, et al. Interactions between acute lymphoblastic leukemia and bone marrow stromal cells influence response to therapy. Leukemia research. 2012;36(3):299-306.
120. Weisberg E, Wright RD, McMillin DW, Mitsiades C, Ray A, Barrett R, et al. Stromal-mediated protection of tyrosine kinase inhibitor-treated BCR-ABL-expressing leukemia cells. Molecular cancer therapeutics. 2008;7(5):1121-9.
121. Weisberg E, Liu Q, Nelson E, Kung AL, Christie AL, Bronson R, et al. Using combination therapy to override stromal-mediated chemoresistance in mutant FLT3-positive AML: synergism between FLT3 inhibitors, dasatinib/multi-targeted inhibitors and JAK inhibitors. Leukemia. 2012;26(10):2233-44.
122. Zhang B, Li M, McDonald T, Holyoake TL, Moon RT, Campana D, et al. Microenvironmental protection of CML stem and progenitor cells from tyrosine kinase inhibitors through N-cadherin and Wnt-beta-catenin signaling. Blood. 2013;121(10):1824-38.
123. Manshouri T, Estrov Z, Quintas-Cardama A, Burger J, Zhang Y, Livun A, et al. Bone marrow stroma-secreted cytokines protect JAK2(V617F)-mutated cells from the effects of a JAK2 inhibitor. Cancer research. 2011;71(11):3831-40.
124. Cardoso BA, Belo H, Barata JT, Almeida AM. The Bone Marrow-Mediated Protection of Myeloproliferative Neoplastic Cells to Vorinostat and Ruxolitinib Relies on the Activation of JNK and PI3K Signalling Pathways. PloS one. 2015;10(12):e0143897.
125. Ramos TL, Sanchez-Abarca LI, Roson-Burgo B, Redondo A, Rico A, Preciado S, et al. Mesenchymal stromal cells (MSC) from JAK2+ myeloproliferative neoplasms differ from normal MSC and contribute to the maintenance of neoplastic hematopoiesis. PloS one. 2017;12(8):e0182470.
126. Pieri L, Guglielmelli P, Bogani C, Bosi A, Vannucchi AM, Myeloproliferative Disorders Research C. Mesenchymal stem cells from JAK2(V617F) mutant patients with primary myelofibrosis do not harbor JAK2 mutant allele. Leukemia research. 2008;32(3):516-7.
127. Maekawa T, Osawa Y, Izumi T, Nagao S, Takano K, Okada Y, et al. Myeloproliferative leukemia protein activation directly induces fibrocyte differentiation to cause myelofibrosis. Leukemia. 2017.
128. Deininger M, Radich J, Burn TC, Huber R, Paranagama D, Verstovsek S. The effect of long-term ruxolitinib treatment on JAK2p.V617F allele burden in patients with myelofibrosis. Blood. 2015;126(13):1551-4.
129. Williams N LJ, Moore L, Baxter JE, Hewinson J, Dawson KJ, Menzies A, Godfrey AL, R Green AR, Campbell PJ, Nangalia J. Driver Mutation Acquisition in Utero and Childhood Followed By Lifelong Clonal Evolution Underlie Myeloproliferative Neoplasms. Blood. 2020;136 (Supplement_2): LBA-1.
130. Quintas-Cardama A, Kantarjian H, Cortes J, Verstovsek S. Janus kinase inhibitors for the treatment of myeloproliferative neoplasias and beyond. Nat Rev Drug Discov. 2011;10(2):127-40.
131. Verstovsek S, Mesa RA, Gotlib J, Gupta V, DiPersio JF, Catalano JV, et al. Long-term treatment with ruxolitinib for patients with myelofibrosis: 5-year update from the randomized, double-blind, placebo-controlled, phase 3 COMFORT-I trial. Journal of hematology & oncology. 2017;10(1):55.

132. Verstovsek S, Gotlib J, Mesa RA, Vannucchi AM, Kiladjian JJ, Cervantes F, et al. Long-term survival in patients treated with ruxolitinib for myelofibrosis: COMFORT-I and -II pooled analyses. J Hematol Oncol. 2017;10(1):156.
133. Vannucchi AM, Kiladjian JJ, Griesshammer M, Masszi T, Durrant S, Passamonti F, et al. Ruxolitinib versus standard therapy for the treatment of polycythemia vera. N Engl J Med. 2015;372(5):426-35.
134. Passamonti F, Griesshammer M, Palandri F, Egyed M, Benevolo G, Devos T, et al. Ruxolitinib for the treatment of inadequately controlled polycythaemia vera without splenomegaly (RESPONSE-2): a randomised, open-label, phase 3b study. Lancet Oncol. 2017;18(1):88-99.
135. Gunawan A, Harrington P, Garcia-Curto N, McLornan D, Radia D, Harrison C. Ruxolitinib for the Treatment of Essential Thrombocythemia. Hemasphere. 2018;2(4):e56.
136. Tefferi A. JAK inhibitors for myeloproliferative neoplasms: clarifying facts from myths. Blood. 2012;119(12):2721-30.
137. Gupta V, Mesa RA, Deininger MW, Rivera CE, Sirhan S, Brachmann CB, et al. A phase 1/2, open-label study evaluating twice-daily administration of momelotinib in myelofibrosis. Haematologica. 2017;102(1):94-102.
138. Mesa RA, Vannucchi AM, Mead A, Egyed M, Szoke A, Suvorov A, et al. Pacritinib versus best available therapy for the treatment of myelofibrosis irrespective of baseline cytopenias (PERSIST-1): an international, randomised, phase 3 trial. The Lancet Haematology. 2017;4(5):e225-e36.
139. Breccia M, Molica M, Colafigli G, Alimena G. Improvement of bone marrow fibrosis with ruxolitinib: will this finding change our perception of the drug? Expert review of hematology. 2015;8(4):387-9.
140. Kvasnicka HM, Thiele J, Bueso-Ramos CE, Sun W, Cortes J, Kantarjian HM, et al. Long-term effects of ruxolitinib versus best available therapy on bone marrow fibrosis in patients with myelofibrosis. J Hematol Oncol. 2018;11(1):42.
141. Cervantes F, Pereira A. Does ruxolitinib prolong the survival of patients with myelofibrosis? Blood. 2017;129(7):832-7.
142. Harrison CN, Vannucchi AM, Kiladjian JJ, Al-Ali HK, Gisslinger H, Knoops L, et al. Long-term findings from COMFORT-II, a phase 3 study of ruxolitinib vs best available therapy for myelofibrosis. Leukemia. 2016;30(8):1701-7.
143. Kiladjian JJ, Zachee P, Hino M, Pane F, Masszi T, Harrison CN, et al. Long-term efficacy and safety of ruxolitinib versus best available therapy in polycythaemia vera (RESPONSE): 5-year follow up of a phase 3 study. Lancet Haematol. 2020;7(3):e226-e37.
144. Heine A, Brossart P, Wolf D. Ruxolitinib is a potent immunosuppressive compound: is it time for anti-infective prophylaxis? Blood. 2013;122(23):3843-4.
145. Tsukamoto Y, Kiyasu J, Tsuda M, Ikeda M, Shiratsuchi M, Ogawa Y, et al. Fatal Disseminated Tuberculosis during Treatment with Ruxolitinib Plus Prednisolone in a Patient with Primary Myelofibrosis: A Case Report and Review of the Literature. Intern Med. 2018;57(9):1297-300.
146. Eyal O, Flaschner M, Ben Yehuda A, Rund D. Varicella-zoster virus meningoencephalitis in a patient treated with ruxolitinib. Am J Hematol. 2017;92(5):E74-E5.
147. Tefferi A, Cervantes F, Mesa R, Passamonti F, Verstovsek S, Vannucchi AM, et al. Revised response criteria for myelofibrosis: International Working Group-Myeloproliferative Neoplasms Research and Treatment (IWG-MRT) and European LeukemiaNet (ELN) consensus report. Blood. 2013;122(8):1395-8.
148. Harrison CN, Schaap N, Vannucchi AM, Kiladjian JJ, Jourdan E, Silver RT, et al. Fedratinib in patients with myelofibrosis previously treated with ruxolitinib: An updated

analysis of the JAKARTA2 study using stringent criteria for ruxolitinib failure. Am J Hematol. 2020;95(6):594-603.
149. Gupta V, Griesshammer M, Martino B, Foltz L, Tavares R, Al-Ali HK, et al. Analysis of predictors of response to ruxolitinib in patients with myelofibrosis in the phase 3b expanded-access JUMP study. Leuk Lymphoma. 2021;62(4):918-26.
150. Palandri F, Palumbo GA, Bonifacio M, Tiribelli M, Benevolo G, Martino B, et al. Baseline factors associated with response to ruxolitinib: an independent study on 408 patients with myelofibrosis. Oncotarget. 2017;8(45):79073-86.
151. Vannucchi AM, Lasho TL, Guglielmelli P, Biamonte F, Pardanani A, Pereira A, et al. Mutations and prognosis in primary myelofibrosis. Leukemia. 2013;27(9):1861-9.
152. Guglielmelli P, Biamonte F, Rotunno G, Artusi V, Artuso L, Bernardis I, et al. Impact of mutational status on outcomes in myelofibrosis patients treated with ruxolitinib in the COMFORT-II study. Blood. 2014;123(14):2157-60.
153. Patel KP, Newberry KJ, Luthra R, Jabbour E, Pierce S, Cortes J, et al. Correlation of mutation profile and response in patients with myelofibrosis treated with ruxolitinib. Blood. 2015;126(6):790-7.
154. Spiegel JY, McNamara C, Kennedy JA, Panzarella T, Arruda A, Stockley T, et al. Impact of genomic alterations on outcomes in myelofibrosis patients undergoing JAK1/2 inhibitor therapy. Blood Adv. 2017;1(20):1729-38.
155. Coltro G, Rotunno G, Mannelli L, Mannarelli C, Fiaccabrino S, Romagnoli S, et al. RAS/CBL mutations predict resistance to JAK inhibitors in myelofibrosis and are associated with poor prognostic features. Blood Adv. 2020;4(15):3677-87.
156. Pacilli A, Rotunno G, Mannarelli C, Fanelli T, Pancrazzi A, Contini E, et al. Mutation landscape in patients with myelofibrosis receiving ruxolitinib or hydroxyurea. Blood Cancer J. 2018;8(12):122.
157. Newberry KJ, Patel K, Masarova L, Luthra R, Manshouri T, Jabbour E, et al. Clonal evolution and outcomes in myelofibrosis after ruxolitinib discontinuation. Blood. 2017;130(9):1125-31.
158. Palandri F, Breccia M, Bonifacio M, Polverelli N, Elli EM, Benevolo G, et al. Life after ruxolitinib: Reasons for discontinuation, impact of disease phase, and outcomes in 218 patients with myelofibrosis. Cancer. 2020;126(6):1243-52.
159. Deshpande A, Reddy MM, Schade GO, Ray A, Chowdary TK, Griffin JD, et al. Kinase domain mutations confer resistance to novel inhibitors targeting JAK2V617F in myeloproliferative neoplasms. Leukemia. 2012;26(4):708-15.
160. Weigert O, Lane AA, Bird L, Kopp N, Chapuy B, van Bodegom D, et al. Genetic resistance to JAK2 enzymatic inhibitors is overcome by HSP90 inhibition. J Exp Med. 2012;209(2):259-73.
161. Hornakova T, Springuel L, Devreux J, Dusa A, Constantinescu SN, Knoops L, et al. Oncogenic JAK1 and JAK2-activating mutations resistant to ATP-competitive inhibitors. Haematologica. 2011;96(6):845-53.
162. Andreoli A VE, Robin M, Raffoux E, Zini J, Rousselot P, Socié G, Rea D, Parquet N, Giraudier S, Chomienne C, Cassinat B, Jean-Jacques Kiladjian J. Clinical Resistance To Ruxolitinib Is More Frequent In Patients Without MPN-Associated Mutations and Is Rarely Due To Mutations In The JAK2 Kinase Drug-Binding Domain. Blood. 2013;122 (21): 1591.
163. Meyer SC. Mechanisms of Resistance to JAK2 Inhibitors in Myeloproliferative Neoplasms. Hematol Oncol Clin North Am. 2017;31(4):627-42.
164. Gisslinger H, Schalling M, Gisslinger B, Skrabs C, Mullauer L, Kralovics R. Restoration of response to ruxolitinib upon brief withdrawal in two patients with myelofibrosis. Am J Hematol. 2014;89(3):344-6.

165. Shank K, Dunbar A, Koppikar P, Kleppe M, Teruya-Feldstein J, Csete I, et al. Mathematical modeling reveals alternative JAK inhibitor treatment in myeloproliferative neoplasms. Haematologica. 2020;105(3):e91-e4.
166. Koppikar P, Bhagwat N, Kilpivaara O, Manshouri T, Adli M, Hricik T, et al. Heterodimeric JAK-STAT activation as a mechanism of persistence to JAK2 inhibitor therapy. Nature. 2012;489(7414):155-9.
167. Meyer SC, Keller MD, Chiu S, Koppikar P, Guryanova OA, Rapaport F, et al. CHZ868, a Type II JAK2 Inhibitor, Reverses Type I JAK Inhibitor Persistence and Demonstrates Efficacy in Myeloproliferative Neoplasms. Cancer Cell. 2015;28(1):15-28.
168. Andraos R, Qian Z, Bonenfant D, Rubert J, Vangrevelinghe E, Scheufler C, et al. Modulation of activation-loop phosphorylation by JAK inhibitors is binding mode dependent. Cancer Discov. 2012;2(6):512-23.
169. Wu SC, Li LS, Kopp N, Montero J, Chapuy B, Yoda A, et al. Activity of the Type II JAK2 Inhibitor CHZ868 in B Cell Acute Lymphoblastic Leukemia. Cancer Cell. 2015;28(1):29-41.
170. Tvorogov D, Thomas D, Liau NPD, Dottore M, Barry EF, Lathi M, et al. Accumulation of JAK activation loop phosphorylation is linked to type I JAK inhibitor withdrawal syndrome in myelofibrosis. Sci Adv. 2018;4(11):eaat3834.
171. Leroy E, Constantinescu SN. Rethinking JAK2 inhibition: towards novel strategies of more specific and versatile Janus kinase inhibition. Leukemia. 2017;31(5):1023-38.
172. Wilmes S, Hafer M, Vuorio J, Tucker JA, Winkelmann H, Lochte S, et al. Mechanism of homodimeric cytokine receptor activation and dysregulation by oncogenic mutations. Science. 2020;367(6478):643-52.
173. Brkic S, Meyer SC. Challenges and Perspectives for Therapeutic Targeting of Myeloproliferative Neoplasms. Hemasphere. 2021;5(1):e516.
174. Mylonas E, Yoshida K, Frick M, Hoyer K, Christen F, Kaeda J, et al. Single-cell analysis based dissection of clonality in myelofibrosis. Nat Commun. 2020;11(1):73.
175. Lundberg P, Karow A, Nienhold R, Looser R, Hao-Shen H, Nissen I, et al. Clonal evolution and clinical correlates of somatic mutations in myeloproliferative neoplasms. Blood. 2014;123(14):2220-8.
176. Parenti S, Rontauroli S, Carretta C, Mallia S, Genovese E, Chiereghin C, et al. Mutated clones driving leukemic transformation are already detectable at the single-cell level in CD34-positive cells in the chronic phase of primary myelofibrosis. NPJ Precis Oncol. 2021;5(1):4.
177. He J, Zhang Y. Janus kinase 2: an epigenetic 'writer' that activates leukemogenic genes. J Mol Cell Biol. 2010;2(5):231-3.
178. Dawson MA, Bannister AJ, Gottgens B, Foster SD, Bartke T, Green AR, et al. JAK2 phosphorylates histone H3Y41 and excludes HP1alpha from chromatin. Nature. 2009;461(7265):819-22.
179. Quintas-Cardama A, Verstovsek S. Molecular pathways: Jak/STAT pathway: mutations, inhibitors, and resistance. Clin Cancer Res. 2013;19(8):1933-40.
180. Elli EM, Barate C, Mendicino F, Palandri F, Palumbo GA. Mechanisms Underlying the Anti-inflammatory and Immunosuppressive Activity of Ruxolitinib. Front Oncol. 2019;9:1186.
181. Escamilla Gomez V, Garcia-Gutierrez V, Lopez Corral L, Garcia Cadenas I, Perez Martinez A, Marquez Malaver FJ, et al. Ruxolitinib in refractory acute and chronic graft-versus-host disease: a multicenter survey study. Bone Marrow Transplant. 2020;55(3):641-8.
182. Fragoulis GE, McInnes IB, Siebert S. JAK-inhibitors. New players in the field of immune-mediated diseases, beyond rheumatoid arthritis. Rheumatology (Oxford). 2019;58(Suppl 1):i43-i54.

183. Wang J, Wang Y, Wu L, Wang X, Jin Z, Gao Z, et al. Ruxolitinib for refractory/relapsed hemophagocytic lymphohistiocytosis. Haematologica. 2020;105(5):e210-e2.
184. Capochiani E, Frediani B, Iervasi G, Paolicchi A, Sani S, Roncucci P, et al. Ruxolitinib Rapidly Reduces Acute Respiratory Distress Syndrome in COVID-19 Disease. Analysis of Data Collection From RESPIRE Protocol. Front Med (Lausanne). 2020;7:466.
185. Kalota A, Jeschke GR, Carroll M, Hexner EO. Intrinsic resistance to JAK2 inhibition in myelofibrosis. Clin Cancer Res. 2013;19(7):1729-39.
186. Tefferi A. Primary myelofibrosis: 2021 update on diagnosis, risk-stratification and management. Am J Hematol. 2021;96(1):145-62.
187. Kroger N, Holler E, Kobbe G, Bornhauser M, Schwerdtfeger R, Baurmann H, et al. Allogeneic stem cell transplantation after reduced-intensity conditioning in patients with myelofibrosis: a prospective, multicenter study of the Chronic Leukemia Working Party of the European Group for Blood and Marrow Transplantation. Blood. 2009;114(26):5264-70.
188. Robin M, de Wreede LC, Wolschke C, Schetelig J, Eikema DJ, Van Lint MT, et al. Long-term outcome after allogeneic hematopoietic cell transplantation for myelofibrosis. Haematologica. 2019;104(9):1782-8.
189. Rondelli D, Goldberg JD, Isola L, Price LS, Shore TB, Boyer M, et al. MPD-RC 101 prospective study of reduced-intensity allogeneic hematopoietic stem cell transplantation in patients with myelofibrosis. Blood. 2014;124(7):1183-91.
190. Bacigalupo A, Soraru M, Dominietto A, Pozzi S, Geroldi S, Van Lint MT, et al. Allogeneic hemopoietic SCT for patients with primary myelofibrosis: a predictive transplant score based on transfusion requirement, spleen size and donor type. Bone Marrow Transplant. 2010;45(3):458-63.
191. Patriarca F, Bacigalupo A, Sperotto A, Isola M, Soldano F, Bruno B, et al. Allogeneic hematopoietic stem cell transplantation in myelofibrosis: the 20-year experience of the Gruppo Italiano Trapianto di Midollo Osseo (GITMO). Haematologica. 2008;93(10):1514-22.
192. Gupta V, Malone AK, Hari PN, Ahn KW, Hu ZH, Gale RP, et al. Reduced-intensity hematopoietic cell transplantation for patients with primary myelofibrosis: a cohort analysis from the center for international blood and marrow transplant research. Biol Blood Marrow Transplant. 2014;20(1):89-97.
193. Luznik L, O'Donnell PV, Symons HJ, Chen AR, Leffell MS, Zahurak M, et al. HLA-haploidentical bone marrow transplantation for hematologic malignancies using nonmyeloablative conditioning and high-dose, posttransplantation cyclophosphamide. Biol Blood Marrow Transplant. 2008;14(6):641-50.
194. Bregante S, Dominietto A, Ghiso A, Raiola AM, Gualandi F, Varaldo R, et al. Improved Outcome of Alternative Donor Transplantations in Patients with Myelofibrosis: From Unrelated to Haploidentical Family Donors. Biol Blood Marrow Transplant. 2016;22(2):324-9.
195. Robin M, Tabrizi R, Mohty M, Furst S, Michallet M, Bay JO, et al. Allogeneic haematopoietic stem cell transplantation for myelofibrosis: a report of the Societe Francaise de Greffe de Moelle et de Therapie Cellulaire (SFGM-TC). Br J Haematol. 2011;152(3):331-9.
196. Samuelson S, Sandmaier BM, Heslop HE, Popat U, Carrum G, Champlin RE, et al. Allogeneic haematopoietic cell transplantation for myelofibrosis in 30 patients 60-78 years of age. British journal of haematology. 2011;153(1):76-82.
197. Murata M, Takenaka K, Uchida N, Ozawa Y, Ohashi K, Kim SW, et al. Comparison of Outcomes of Allogeneic Transplantation for Primary Myelofibrosis among Hematopoietic Stem Cell Source Groups. Biol Blood Marrow Transplant. 2019;25(8):1536-43.
198. Robin M, Giannotti F, Deconinck E, Mohty M, Michallet M, Sanz G, et al. Unrelated cord blood transplantation for patients with primary or secondary myelofibrosis. Biology of

blood and marrow transplantation : journal of the American Society for Blood and Marrow Transplantation. 2014;20(11):1841-6.
199. Murata M, Nishida T, Taniguchi S, Ohashi K, Ogawa H, Fukuda T, et al. Allogeneic transplantation for primary myelofibrosis with BM, peripheral blood or umbilical cord blood: an analysis of the JSHCT. Bone marrow transplantation. 2014;49(3):355-60.
200. Panagiota V, Thol F, Markus B, Fehse B, Alchalby H, Badbaran A, et al. Prognostic effect of calreticulin mutations in patients with myelofibrosis after allogeneic hematopoietic stem cell transplantation. Leukemia. 2014;28(7):1552-5.
201. Kroger N, Panagiota V, Badbaran A, Zabelina T, Triviai I, Araujo Cruz MM, et al. Impact of Molecular Genetics on Outcome in Myelofibrosis Patients after Allogeneic Stem Cell Transplantation. Biol Blood Marrow Transplant. 2017;23(7):1095-101.
202. Gagelmann N, Eikema DJ, de Wreede LC, Koster L, Wolschke C, Arnold R, et al. Comparison of Dynamic International Prognostic Scoring System and MYelofibrosis SECondary to PV and ET Prognostic Model for Prediction of Outcome in Polycythemia Vera and Essential Thrombocythemia Myelofibrosis after Allogeneic Stem Cell Transplantation. Biol Blood Marrow Transplant. 2019;25(6):e204-e8.
203. Kroger N, Giorgino T, Scott BL, Ditschkowski M, Alchalby H, Cervantes F, et al. Impact of allogeneic stem cell transplantation on survival of patients less than 65 years of age with primary myelofibrosis. Blood. 2015;125(21):3347-50; quiz 64.
204. Kroger NM, Deeg JH, Olavarria E, Niederwieser D, Bacigalupo A, Barbui T, et al. Indication and management of allogeneic stem cell transplantation in primary myelofibrosis: a consensus process by an EBMT/ELN international working group. Leukemia. 2015;29(11):2126-33.
205. Gagelmann N, Ditschkowski M, Bogdanov R, Bredin S, Robin M, Cassinat B, et al. Comprehensive clinical-molecular transplant scoring system for myelofibrosis undergoing stem cell transplantation. Blood. 2019;133(20):2233-42.
206. Shanavas M, Popat U, Michaelis LC, Fauble V, McLornan D, Klisovic R, et al. Outcomes of Allogeneic Hematopoietic Cell Transplantation in Patients with Myelofibrosis with Prior Exposure to Janus Kinase 1/2 Inhibitors. Biol Blood Marrow Transplant. 2016;22(3):432-40.
207. Stubig T, Alchalby H, Ditschkowski M, Wolf D, Wulf G, Zabelina T, et al. JAK inhibition with ruxolitinib as pretreatment for allogeneic stem cell transplantation in primary or post-ET/PV myelofibrosis. Leukemia. 2014;28(8):1736-8.
208. Gupta V, Hari P, Hoffman R. Allogeneic hematopoietic cell transplantation for myelofibrosis in the era of JAK inhibitors. Blood. 2012;120(7):1367-79.
209. Bose P, Verstovsek S. JAK Inhibition for the Treatment of Myelofibrosis: Limitations and Future Perspectives. Hemasphere. 2020;4(4):e424.
210. Jaekel N, Behre G, Behning A, Wickenhauser C, Lange T, Niederwieser D, et al. Allogeneic hematopoietic cell transplantation for myelofibrosis in patients pretreated with the JAK1 and JAK2 inhibitor ruxolitinib. Bone Marrow Transplant. 2014;49(2):179-84.
211. Salit RB, Scott BL, Stevens EA, Baker KK, Gooley TA, Deeg HJ. Pre-hematopoietic cell transplant Ruxolitinib in patients with primary and secondary myelofibrosis. Bone Marrow Transplant. 2020;55(1):70-6.
212. Amaru Calzada A, Pedrini O, Finazzi G, Leoni F, Mascagni P, Introna M, et al. Givinostat and hydroxyurea synergize in vitro to induce apoptosis of cells from JAK2(V617F) myeloproliferative neoplasm patients. Experimental hematology. 2013;41(3):253-60 e2.
213. Mascarenhas J, Lu M, Li T, Petersen B, Hochman T, Najfeld V, et al. A phase I study of panobinostat (LBH589) in patients with primary myelofibrosis (PMF) and post-polycythaemia vera/essential thrombocythaemia myelofibrosis (post-PV/ET MF). British journal of haematology. 2013;161(1):68-75.

214. Tefferi A, Lasho TL, Begna KH, Patnaik MM, Zblewski DL, Finke CM, et al. A Pilot Study of the Telomerase Inhibitor Imetelstat for Myelofibrosis. N Engl J Med. 2015;373(10):908-19.
215. Vannucchi AM, Harrison CN. Emerging treatments for classical myeloproliferative neoplasms. Blood. 2017;129(6):693-703.
216. Hobbs GS, Hanasoge Somasundara AV, Kleppe M, Litvin R, Arcila M, Ahn J, et al. Hsp90 inhibition disrupts JAK-STAT signaling and leads to reductions in splenomegaly in patients with MPNs. Haematologica. 2017.
217. Tefferi A, Verstovsek S, Barosi G, Passamonti F, Roboz GJ, Gisslinger H, et al. Pomalidomide is active in the treatment of anemia associated with myelofibrosis. J Clin Oncol. 2009;27(27):4563-9.
218. Bogani C, Bartalucci N, Martinelli S, Tozzi L, Guglielmelli P, Bosi A, et al. mTOR inhibitors alone and in combination with JAK2 inhibitors effectively inhibit cells of myeloproliferative neoplasms. PLoS One. 2013;8(1):e54826.
219. Durrant ST, Nagler A, Guglielmelli P, Lavie D, le Coutre P, Gisslinger H, et al. Results from HARMONY: an open-label, multicenter, 2-arm, phase 1b, dose-finding study assessing the safety and efficacy of the oral combination of ruxolitinib and buparlisib in patients with myelofibrosis. Haematologica. 2019;104(12):e551-e4.
220. Guglielmelli P, Barosi G, Rambaldi A, Marchioli R, Masciulli A, Tozzi L, et al. Safety and efficacy of everolimus, a mTOR inhibitor, as single agent in a phase 1/2 study in patients with myelofibrosis. Blood. 2011;118(8):2069-76.
221. Gupta V, Wolleschak D, Hasselbalch H, Vannucchi AM, Koschmieder S, Cervantes F, et al. Safety and efficacy of the combination of sonidegib and ruxolitinib in myelofibrosis: a phase 1b/2 dose-finding study. Blood Adv. 2020;4(13):3063-71.
222. Couban S, Benevolo G, Donnellan W, Cultrera J, Koschmieder S, Verstovsek S, et al. A phase Ib study to assess the efficacy and safety of vismodegib in combination with ruxolitinib in patients with intermediate- or high-risk myelofibrosis. J Hematol Oncol. 2018;11(1):122.
223. Mesa RA, Silver RT, Verstovsek S, Mascarenhas J, Kessler CM, Rondelli D, et al. Single agent bevacizumab for myelofibrosis: results of the Myeloproliferative Disorders Research Consortium Trial. Haematologica. 2013;98(9):1421-3.
224. Apostolidou E, Kantarjian H, Thomas D, Burger I, Borthakur G, Verstovsek S. Phase II study of sunitinib in patients with primary or post-polycythemia vera/essential thrombocythemia myelofibrosis. Clin Lymphoma Myeloma Leuk. 2010;10(4):281-4.
225. Verstovsek S, Savona MR, Mesa RA, Dong H, Maltzman JD, Sharma S, et al. A phase 2 study of simtuzumab in patients with primary, post-polycythaemia vera or post-essential thrombocythaemia myelofibrosis. Br J Haematol. 2017;176(6):939-49.
226. Mohr S, Bakal C, Perrimon N. Genomic screening with RNAi: results and challenges. Annual review of biochemistry. 2010;79:37-64.
227. Mohr SE, Smith JA, Shamu CE, Neumuller RA, Perrimon N. RNAi screening comes of age: improved techniques and complementary approaches. Nature reviews Molecular cell biology. 2014;15(9):591-600.
228. Agrawal N, Dasaradhi PV, Mohmmed A, Malhotra P, Bhatnagar RK, Mukherjee SK. RNA interference: biology, mechanism, and applications. Microbiology and molecular biology reviews : MMBR. 2003;67(4):657-85.
229. Echeverri CJ, Perrimon N. High-throughput RNAi screening in cultured cells: a user's guide. Nat Rev Genet. 2006;7(5):373-84.
230. Schlabach MR, Luo J, Solimini NL, Hu G, Xu Q, Li MZ, et al. Cancer proliferation gene discovery through functional genomics. Science. 2008;319(5863):620-4.
231. Root DE, Hacohen N, Hahn WC, Lander ES, Sabatini DM. Genome-scale loss-of-function screening with a lentiviral RNAi library. Nature methods. 2006;3(9):715-9.

232. Khorashad JS, Eiring AM, Mason CC, Gantz KC, Bowler AD, Redwine HM, et al. shRNA library screening identifies nucleocytoplasmic transport as a mediator of BCR-ABL1 kinase-independent resistance. Blood. 2015;125(11):1772-81.
233. Alvarez-Calderon F, Gregory MA, DeGregori J. Using functional genomics to overcome therapeutic resistance in hematological malignancies. Immunol Res. 2013;55(1-3):100-15.
234. Carthew RW, Sontheimer EJ. Origins and Mechanisms of miRNAs and siRNAs. Cell. 2009;136(4):642-55.
235. Sigoillot FD, King RW. Vigilance and validation: Keys to success in RNAi screening. ACS Chem Biol. 2011;6(1):47-60.
236. Franceschini A, Meier R, Casanova A, Kreibich S, Daga N, Andritschke D, et al. Specific inhibition of diverse pathogens in human cells by synthetic microRNA-like oligonucleotides inferred from RNAi screens. Proc Natl Acad Sci U S A. 2014;111(12):4548-53.
237. Khan AA, Betel D, Miller ML, Sander C, Leslie CS, Marks DS. Transfection of small RNAs globally perturbs gene regulation by endogenous microRNAs. Nat Biotechnol. 2009;27(6):549-55.
238. Torok-Storb B, Iwata M, Graf L, Gianotti J, Horton H, Byrne MC. Dissecting the marrow microenvironment. Ann N Y Acad Sci. 1999;872:164-70.
239. Roecklein BA, Torok-Storb B. Functionally distinct human marrow stromal cell lines immortalized by transduction with the human papilloma virus E6/E7 genes. Blood. 1995;85(4):997-1005.
240. Iwata M, Sandstrom RS, Delrow JJ, Stamatoyannopoulos JA, Torok-Storb B. Functionally and phenotypically distinct subpopulations of marrow stromal cells are fibroblast in origin and induce different fates in peripheral blood monocytes. Stem Cells Dev. 2014;23(7):729-40.
241. Belay E, Hayes BJ, Blau CA, Torok-Storb B. Human Cord Blood and Bone Marrow CD34+ Cells Generate Macrophages That Support Erythroid Islands. PLoS One. 2017;12(1):e0171096.
242. Le Y, Fraineau S, Chandran P, Sabloff M, Brand M, Lavoie JR, et al. Adipogenic Mesenchymal Stromal Cells from Bone Marrow and Their Hematopoietic Supportive Role: Towards Understanding the Permissive Marrow Microenvironment in Acute Myeloid Leukemia. Stem Cell Rev. 2016;12(2):235-44.
243. Bulycheva E, Rauner M, Medyouf H, Theurl I, Bornhauser M, Hofbauer LC, et al. Myelodysplasia is in the niche: novel concepts and emerging therapies. Leukemia. 2015;29(2):259-68.
244. Moses BS, Slone WL, Thomas P, Evans R, Piktel D, Angel PM, et al. Bone marrow microenvironment modulation of acute lymphoblastic leukemia phenotype. Exp Hematol. 2016;44(1):50-9 e1-2.
245. Chen P, Jin Q, Fu Q, You P, Jiang X, Yuan Q, et al. Induction of Multidrug Resistance of Acute Myeloid Leukemia Cells by Cocultured Stromal Cells via Upregulation of the PI3K/Akt Signaling Pathway. Oncol Res. 2016;24(4):215-23.
246. Karimpoor M, E II, Reid AG, Claudiani S, Edirisinghe M, Khorashad JS. Development of artificial bone marrow fibre scaffolds to study resistance to anti-leukaemia agents. British journal of haematology. 2017.
247. Garrido SM, Appelbaum FR, Willman CL, Banker DE. Acute myeloid leukemia cells are protected from spontaneous and drug-induced apoptosis by direct contact with a human bone marrow stromal cell line (HS-5). Exp Hematol. 2001;29(4):448-57.
248. Quentmeier H, MacLeod RA, Zaborski M, Drexler HG. JAK2 V617F tyrosine kinase mutation in cell lines derived from myeloproliferative disorders. Leukemia. 2006;20(3):471-6.

249. Martin P, Papayannopoulou T. HEL cells: a new human erythroleukemia cell line with spontaneous and induced globin expression. Science. 1982;216(4551):1233-5.
250. Quintas-Cardama A, Vaddi K, Liu P, Manshouri T, Li J, Scherle PA, et al. Preclinical characterization of the selective JAK1/2 inhibitor INCB018424: therapeutic implications for the treatment of myeloproliferative neoplasms. Blood. 2010;115(15):3109-17.
251. Nauroy P, Delhommeau F, Baklouti F. JAK2V617F mRNA metabolism in myeloproliferative neoplasm cell lines. Blood Cancer J. 2014;4:e222.
252. Minnucci G, Amicarelli G, Salmoiraghi S, Spinelli O, Guinea Montalvo ML, Giussani U, et al. A novel, highly sensitive and rapid allele-specific loop-mediated amplification assay for the detection of the JAK2V617F mutation in chronic myeloproliferative neoplasms. Haematologica. 2012;97(9):1394-400.
253. Wang Y, Fiskus W, Chong DG, Buckley KM, Natarajan K, Rao R, et al. Cotreatment with panobinostat and JAK2 inhibitor TG101209 attenuates JAK2V617F levels and signaling and exerts synergistic cytotoxic effects against human myeloproliferative neoplastic cells. Blood. 2009;114(24):5024-33.
254. Fiedler W, Henke RP, Ergun S, Schumacher U, Gehling UM, Vohwinkel G, et al. Derivation of a new hematopoietic cell line with endothelial features from a patient with transformed myeloproliferative syndrome: a case report. Cancer. 2000;88(2):344-51.
255. Fiskus W, Verstovsek S, Manshouri T, Rao R, Balusu R, Venkannagari S, et al. Heat shock protein 90 inhibitor is synergistic with JAK2 inhibitor and overcomes resistance to JAK2-TKI in human myeloproliferative neoplasm cells. Clinical cancer research : an official journal of the American Association for Cancer Research. 2011;17(23):7347-58.
256. Knipe DM HP. Fields virology, 6th edition.: Philadelphia: Wolters Kluwer/Lippincott Williams & Wilkins Health; 2013.
257. Sims D, Mendes-Pereira AM, Frankum J, Burgess D, Cerone MA, Lombardelli C, et al. High-throughput RNA interference screening using pooled shRNA libraries and next generation sequencing. Genome biology. 2011;12(10):R104.
258. Mason CC. Four study design principles for genetic investigations using next generation sequencing. BMJ. 2017;359:j4069.
259. Mason CC, Fiol CR, Baker MJ, Nadal-Melsio E, Yebra-Fernandez E, Bicalho L, et al. Identification of genetic targets in acute myeloid leukaemia for designing targeted therapy. Br J Haematol. 2020.
260. Hara MR, Agrawal N, Kim SF, Cascio MB, Fujimuro M, Ozeki Y, et al. S-nitrosylated GAPDH initiates apoptotic cell death by nuclear translocation following Siah1 binding. Nat Cell Biol. 2005;7(7):665-74.
261. Radonic A, Thulke S, Mackay IM, Landt O, Siegert W, Nitsche A. Guideline to reference gene selection for quantitative real-time PCR. Biochem Biophys Res Commun. 2004;313(4):856-62.
262. Butterfield DA, Hardas SS, Lange ML. Oxidatively modified glyceraldehyde-3-phosphate dehydrogenase (GAPDH) and Alzheimer's disease: many pathways to neurodegeneration. J Alzheimers Dis. 2010;20(2):369-93.
263. Liu YJ, Zheng D, Balasubramanian S, Carriero N, Khurana E, Robilotto R, et al. Comprehensive analysis of the pseudogenes of glycolytic enzymes in vertebrates: the anomalously high number of GAPDH pseudogenes highlights a recent burst of retrotrans-positional activity. BMC Genomics. 2009;10:480.
264. Kalyana-Sundaram S, Kumar-Sinha C, Shankar S, Robinson DR, Wu YM, Cao X, et al. Expressed pseudogenes in the transcriptional landscape of human cancers. Cell. 2012;149(7):1622-34.

265. Verstovsek S, Yeleswaram S, Hou K, Chen X, Erickson-Viitanen S. Sustained-release ruxolitinib: Findings from a phase 1 study in healthy subjects and a phase 2 study in patients with myelofibrosis. Hematol Oncol. 2018;36(4):701-8.
266. Mackinnon RN, Wall M, Zordan A, Nutalapati S, Mercer B, Peverall J, et al. Genome organization and the role of centromeres in evolution of the erythroleukaemia cell line HEL. Evol Med Public Health. 2013;2013(1):225-40.
267. Subramanian A, Tamayo P, Mootha VK, Mukherjee S, Ebert BL, Gillette MA, et al. Gene set enrichment analysis: a knowledge-based approach for interpreting genome-wide expression profiles. Proc Natl Acad Sci U S A. 2005;102(43):15545-50.
268. Mootha VK, Lindgren CM, Eriksson KF, Subramanian A, Sihag S, Lehar J, et al. PGC-1alpha-responsive genes involved in oxidative phosphorylation are coordinately downregulated in human diabetes. Nat Genet. 2003;34(3):267-73.
269. Faure A, Hayes M, Sugden B. How Kaposi's sarcoma-associated herpesvirus stably transforms peripheral B cells towards lymphomagenesis. Proc Natl Acad Sci U S A. 2019;116(33):16519-28.
270. Fisher DAC, Malkova O, Engle EK, Miner CA, Fulbright MC, Behbehani GK, et al. Mass cytometry analysis reveals hyperactive NF Kappa B signaling in myelofibrosis and secondary acute myeloid leukemia. Leukemia. 2017;31(9):1962-74.
271. Abaza Y, Hidalgo-Lopez JE, Verstovsek S, Jabbour E, Ravandi F, Borthakur G, et al. Phase I study of ruxolitinib in previously treated patients with low or intermediate-1 risk myelodysplastic syndrome with evidence of NF-kB activation. Leuk Res. 2018;73:78-85.
272. Held S HA, Wolf D, Brossart P. Ruxolitinib Inhibits Dendritic Cell Function By Interfering With The MAP-Kinase/NF-Kb Signalling Pathways. Blood. 2013;122 (21): 3463.
273. Chen ZJ. Ubiquitin signalling in the NF-kappaB pathway. Nat Cell Biol. 2005;7(8):758-65.
274. Bartalucci N, Bogani C, Vannucchi AM. Preclinical models for drug selection in myeloproliferative neoplasms. Current hematologic malignancy reports. 2013;8(4):317-24.
275. Verstovsek S, Manshouri T, Quintas-Cardama A, Harris D, Cortes J, Giles FJ, et al. WP1066, a novel JAK2 inhibitor, suppresses proliferation and induces apoptosis in erythroid human cells carrying the JAK2 V617F mutation. Clin Cancer Res. 2008;14(3):788-96.
276. Zhao W, Du Y, Ho WT, Fu X, Zhao ZJ. JAK2V617F and p53 mutations coexist in erythroleukemia and megakaryoblastic leukemic cell lines. Exp Hematol Oncol. 2012;1(1):15.
277. Zong H, Gozman A, Caldas-Lopes E, Taldone T, Sturgill E, Brennan S, et al. A Hyperactive Signalosome in Acute Myeloid Leukemia Drives Addiction to a Tumor-Specific Hsp90 Species. Cell Rep. 2015;13(10):2159-73.
278. Harutyunyan A, Klampfl T, Cazzola M, Kralovics R. p53 lesions in leukemic transformation. N Engl J Med. 2011;364(5):488-90.
279. Kubesova B, Pavlova S, Malcikova J, Kabathova J, Radova L, Tom N, et al. Low-burden TP53 mutations in chronic phase of myeloproliferative neoplasms: association with age, hydroxyurea administration, disease type and JAK2 mutational status. Leukemia. 2018;32(2):450-61.
280. Quentmeier H, Pommerenke C, Dirks WG, Fahnrich S, Hauer V, Uphoff CC, et al. DNMT3A R882H mutation in acute myeloid leukemia cell line SET-2. Leuk Res. 2020;88:106270.
281. Buors C, Douet-Guilbert N, Morel F, Lecucq L, Cassinat B, Ugo V. Clonal evolution in UKE-1 cell line leading to an increase in JAK2 copy number. Blood Cancer J. 2012;2(4):e66.
282. Su Y, Li G, Zhang X, Gu J, Zhang C, Tian Z, et al. JSI-124 inhibits glioblastoma multiforme cell proliferation through G(2)/M cell cycle arrest and apoptosis augment. Cancer Biol Ther. 2008;7(8):1243-9.

283. Wen QJ, Yang Q, Goldenson B, Malinge S, Lasho T, Schneider RK, et al. Targeting megakaryocytic-induced fibrosis in myeloproliferative neoplasms by AURKA inhibition. Nat Med. 2015;21(12):1473-80.
284. Millward TA, Zolnierowicz S, Hemmings BA. Regulation of protein kinase cascades by protein phosphatase 2A. Trends Biochem Sci. 1999;24(5):186-91.
285. Bartalucci N, Calabresi L, Balliu M, Martinelli S, Rossi MC, Villeval JL, et al. Inhibitors of the PI3K/mTOR pathway prevent STAT5 phosphorylation in JAK2V617F mutated cells through PP2A/CIP2A axis. Oncotarget. 2017;8(57):96710-24.
286. Tognon R, Gasparotto EP, Neves RP, Nunes NS, Ferreira AF, Palma PV, et al. Deregulation of apoptosis-related genes is associated with PRV1 overexpression and JAK2 V617F allele burden in Essential Thrombocythemia and Myelofibrosis. J Hematol Oncol. 2012;5:2.
287. Masselli E, Carubbi C, Gobbi G, Mirandola P, Galli D, Martini S, et al. Protein kinase Cvarepsilon inhibition restores megakaryocytic differentiation of hematopoietic progenitors from primary myelofibrosis patients. Leukemia. 2015;29(11):2192-201.
288. Ciurea SO, Merchant D, Mahmud N, Ishii T, Zhao Y, Hu W, et al. Pivotal contributions of megakaryocytes to the biology of idiopathic myelofibrosis. Blood. 2007;110(3):986-93.
289. Waibel M, Solomon VS, Knight DA, Ralli RA, Kim SK, Banks KM, et al. Combined targeting of JAK2 and Bcl-2/Bcl-xL to cure mutant JAK2-driven malignancies and overcome acquired resistance to JAK2 inhibitors. Cell Rep. 2013;5(4):1047-59.
290. Harrison C GJ, Mesa RA, Somervaille TCP, Komrokji RS, Pemmaraju N et al. . Results from a Phase 2 Study of Navitoclax in Combination with Ruxolitinib in Patients with Primary or Secondary Myelofibrosis. Blood. 2019;134 (Supplement_1): 671.
291. Petiti J, Lo Iacono M, Rosso V, Andreani G, Jovanovski A, Podesta M, et al. Bcl-xL represents a therapeutic target in Philadelphia negative myeloproliferative neoplasms. J Cell Mol Med. 2020;24(18):10978-86.
292. Lu M ZW, Wang J, Li Y, Wang X, Yoo D et al. Treatment in Vitro with a Combination of Bcl-Xl Inhibitor-ABT-737 and a JAK2 Inhibitor Selectively Eliminates JAK2V617F MPN Progenitor Cells. Blood. 2009;114 (22): 752.
293. Winter PS, Sarosiek KA, Lin KH, Meggendorfer M, Schnittger S, Letai A, et al. RAS signaling promotes resistance to JAK inhibitors by suppressing BAD-mediated apoptosis. Sci Signal. 2014;7(357):ra122.
294. Girardi T, Vereecke S, Sulima SO, Khan Y, Fancello L, Briggs JW, et al. The T-cell leukemia-associated ribosomal RPL10 R98S mutation enhances JAK-STAT signaling. Leukemia. 2018;32(3):809-19.
295. Kong G, Wunderlich M, Yang D, Ranheim EA, Young KH, Wang J, et al. Combined MEK and JAK inhibition abrogates murine myeloproliferative neoplasm. J Clin Invest. 2014;124(6):2762-73.
296. Stivala S, Codilupi T, Brkic S, Baerenwaldt A, Ghosh N, Hao-Shen H, et al. Targeting compensatory MEK/ERK activation increases JAK inhibitor efficacy in myeloproliferative neoplasms. J Clin Invest. 2019;129(4):1596-611.
297. Kostenko S, Dumitriu G, Laegreid KJ, Moens U. Physiological roles of mitogen-activated-protein-kinase-activated p38-regulated/activated protein kinase. World J Biol Chem. 2011;2(5):73-89.
298. Sevin M, Kubovcakova L, Pernet N, Causse S, Vitte F, Villeval JL, et al. HSP27 is a partner of JAK2-STAT5 and a potential therapeutic target in myelofibrosis. Nat Commun. 2018;9(1):1431.
299. Deveaux S, Filipe A, Lemarchandel V, Ghysdael J, Romeo PH, Mignotte V. Analysis of the thrombopoietin receptor (MPL) promoter implicates GATA and Ets proteins in the coregulation of megakaryocyte-specific genes. Blood. 1996;87(11):4678-85.

300. Thaler R, Agsten M, Spitzer S, Paschalis EP, Karlic H, Klaushofer K, et al. Homocysteine suppresses the expression of the collagen cross-linker lysyl oxidase involving IL-6, Fli1, and epigenetic DNA methylation. J Biol Chem. 2011;286(7):5578-88.
301. Pronier E, Cifani P, Merlinsky TR, Berman KB, Somasundara AVH, Rampal RK, et al. Targeting the CALR interactome in myeloproliferative neoplasms. JCI Insight. 2018;3(22).
302. Evangelista M, Lim TY, Lee J, Parker L, Ashique A, Peterson AS, et al. Kinome siRNA screen identifies regulators of ciliogenesis and hedgehog signal transduction. Sci Signal. 2008;1(39):ra7.
303. Samson AL, Garnish SE, Hildebrand JM, Murphy JM. Location, location, location: A compartmentalized view of TNF-induced necroptotic signaling. Sci Signal. 2021;14(668).
304. Wong CL IA, Ma B, Gerrard G, Norziha ZA , Cheong SK Leong CF, Bee PC, Sathar J, Lye SF, Foroni L, Aitman T , Liang L, Gil J , Laffan M. Differential Expression of Genes Associated with Oncogene-Induced Senescence and Senescence Associated Secretory Phenotype in the Absence of Differential Expression of High Molecular Risk Genes and Genes Associated with JAK-STAT Pathway in Sorted Cells of Patients with Polycythemia Vera and Primary Myelofibrosis. Blood. 2016;128 (22): 4283.
305. Zatz M, Starling A. Calpains and disease. N Engl J Med. 2005;352(23):2413-23.
306. Zha S, Ferdinandusse S, Hicks JL, Denis S, Dunn TA, Wanders RJ, et al. Peroxisomal branched chain fatty acid beta-oxidation pathway is upregulated in prostate cancer. Prostate. 2005;63(4):316-23.
307. Wang B, Shi L, Sun X, Wang L, Wang X, Chen C. Production of CCL20 from lung cancer cells induces the cell migration and proliferation through PI3K pathway. J Cell Mol Med. 2016;20(5):920-9.
308. Beider K, Abraham M, Begin M, Wald H, Weiss ID, Wald O, et al. Interaction between CXCR4 and CCL20 pathways regulates tumor growth. PLoS One. 2009;4(4):e5125.
309. Tsuruyama T, Hiratsuka T, Aini W, Nakamura T. STAT5A Modulates Chemokine Receptor CCR6 Expression and Enhances Pre-B Cell Growth in a CCL20-Dependent Manner. J Cell Biochem. 2016;117(11):2630-42.
310. Zhu F, Li H, Ding F, Guo H, Mou H, Ma J. MiR-422a in gastric cancer cells directly targets CDC40 and modulates cell proliferation. Am J Transl Res. 2020;12(8):4693-701.
311. Sayoc-Becerra A, Krishnan M, Fan S, Jimenez J, Hernandez R, Gibson K, et al. The JAK-Inhibitor Tofacitinib Rescues Human Intestinal Epithelial Cells and Colonoids from Cytokine-Induced Barrier Dysfunction. Inflamm Bowel Dis. 2020;26(3):407-22.
312. Wu H, Liu J, Huang X, Pian L, Cheng Q, Wang Q, et al. RACK1 deficiency synergizes with all-trans retinoic acid to induce apoptosis in human acute promyelocytic leukemia cells. Mol Cell Biochem. 2019;451(1-2):155-63.
313. Karmakar S, Lal G. Role of serotonin receptor signaling in cancer cells and anti-tumor immunity. Theranostics. 2021;11(11):5296-312.
314. Pradhan A, Lambert QT, Reuther GW. Transformation of hematopoietic cells and activation of JAK2-V617F by IL-27R, a component of a heterodimeric type I cytokine receptor. Proc Natl Acad Sci U S A. 2007;104(47):18502-7.
315. Zhang M, Tian H, Li R, Yan W, Xu R. MicroRNA-4286 promotes esophageal carcinoma development by targeting INPP4A to evoke the JAK2/STAT3 pathway activation. Pharmazie. 2018;73(6):342-8.
316. Mirali S, Botham A, Voisin V, Xu C, St-Germain J, Sharon D, et al. The mitochondrial peptidase, neurolysin, regulates respiratory chain supercomplex formation and is necessary for AML viability. Sci Transl Med. 2020;12(538).
317. Coyaud E, Struski S, Prade N, Familiades J, Eichner R, Quelen C, et al. Wide diversity of PAX5 alterations in B-ALL: a Groupe Francophone de Cytogenetique Hematologique study. Blood. 2010;115(15):3089-97.

318. Ross FA, MacKintosh C, Hardie DG. AMP-activated protein kinase: a cellular energy sensor that comes in 12 flavours. FEBS J. 2016;283(16):2987-3001.
319. Zhou Z, Sun B, Huang S, Yu D, Zhang X. Roles of aminoacyl-tRNA synthetase-interacting multi-functional proteins in physiology and cancer. Cell Death Dis. 2020;11(7):579.
320. Lucijanic M, Livun A, Tomasovic-Loncaric C, Stoos-Veic T, Pejsa V, Jaksic O, et al. Canonical Wnt/beta-Catenin Signaling Pathway Is Dysregulated in Patients With Primary and Secondary Myelofibrosis. Clin Lymphoma Myeloma Leuk. 2016;16(9):523-6.
321. Fujita M, Oda Y, Yamashita S, Kaneda K, Kaneko T, Suehiro E, et al. Early-Stage Hyperoxia Is Associated with Favorable Neurological Outcomes and Survival after Severe Traumatic Brain Injury: A Post-Hoc Analysis of the Brain Hypothermia Study. Journal of neurotrauma. 2017.
322. Dong-Feng Z, Ting L, Yong Z, Cheng C, Xi Z, Pei-Yan K. The TPO/c-MPL pathway in the bone marrow may protect leukemia cells from chemotherapy in AML Patients. Pathol Oncol Res. 2014;20(2):309-17.
323. Wang X, Haylock D, Hu CS, Kowalczyk W, Jiang T, Qiu J, et al. A thrombopoietin receptor antagonist is capable of depleting myelofibrosis hematopoietic stem and progenitor cells. Blood. 2016;127(26):3398-409.
324. Schatton T, Murphy GF, Frank NY, Yamaura K, Waaga-Gasser AM, Gasser M, et al. Identification of cells initiating human melanomas. Nature. 2008;451(7176):345-9.
325. Cheung ST, Cheung PF, Cheng CK, Wong NC, Fan ST. Granulin-epithelin precursor and ATP-dependent binding cassette (ABC)B5 regulate liver cancer cell chemoresistance. Gastroenterology. 2011;140(1):344-55.
326. Wilson BJ, Schatton T, Zhan Q, Gasser M, Ma J, Saab KR, et al. ABCB5 identifies a therapy-refractory tumor cell population in colorectal cancer patients. Cancer Res. 2011;71(15):5307-16.
327. Chartrain M, Riond J, Stennevin A, Vandenberghe I, Gomes B, Lamant L, et al. Melanoma chemotherapy leads to the selection of ABCB5-expressing cells. PLoS One. 2012;7(5):e36762.
328. Wilson BJ, Saab KR, Ma J, Schatton T, Putz P, Zhan Q, et al. ABCB5 maintains melanoma-initiating cells through a proinflammatory cytokine signaling circuit. Cancer Res. 2014;74(15):4196-207.
329. Frank NY, Frank MH. ABCB5 gene amplification in human leukemia cells. Leuk Res. 2009;33(10):1303-5.
330. Hou Y, Song L, Zhu P, Zhang B, Tao Y, Xu X, et al. Single-cell exome sequencing and monoclonal evolution of a JAK2-negative myeloproliferative neoplasm. Cell. 2012;148(5):873-85.
331. Kondo S, Kato Y, Minagawa S, Sugimoto Y. STAT1 upregulates glutaminase and modulates amino acids and glutathione metabolism. Biochem Biophys Res Commun. 2020;523(3):672-7.
332. Ebert C, Perner F, Wolleschak D, Schnoder TM, Fischer T, Heidel FH. Expression and function of ABC-transporter protein ABCB1 correlates with inhibitory capacity of Ruxolitinib in vitro and in vivo. Haematologica. 2016;101(3):e81-5.
333. Buks R, Brusson M, Cochet S, Galochkina T, Cassinat B, Nemazanyy I, et al. ABCG2 Is Overexpressed on Red Blood Cells in Ph-Negative Myeloproliferative Neoplasms and Potentiates Ruxolitinib-Induced Apoptosis. Int J Mol Sci. 2021;22(7).
334. Cheng AM, Saxton TM, Sakai R, Kulkarni S, Mbamalu G, Vogel W, et al. Mammalian Grb2 regulates multiple steps in embryonic development and malignant transformation. Cell. 1998;95(6):793-803.

335. Johnson KJ, Griswold IJ, O'Hare T, Corbin AS, Loriaux M, Deininger MW, et al. A BCR-ABL mutant lacking direct binding sites for the GRB2, CBL and CRKL adapter proteins fails to induce leukemia in mice. PLoS One. 2009;4(10):e7439.
336. Gillis LC, Berry DM, Minden MD, McGlade CJ, Barber DL. Gads (Grb2-related adaptor downstream of Shc) is required for BCR-ABL-mediated lymphoid leukemia. Leukemia. 2013;27(8):1666-76.
337. Modi H, Li L, Chu S, Rossi J, Yee JK, Bhatia R. Inhibition of Grb2 expression demonstrates an important role in BCR-ABL-mediated MAPK activation and transformation of primary human hematopoietic cells. Leukemia. 2011;25(2):305-12.
338. Sun J, Pedersen M, Bengtsson S, Ronnstrand L. Grb2 mediates negative regulation of stem cell factor receptor/c-Kit signaling by recruitment of Cbl. Exp Cell Res. 2007;313(18):3935-42.
339. Chauhan D, Kharbanda SM, Ogata A, Urashima M, Frank D, Malik N, et al. Oncostatin M induces association of Grb2 with Janus kinase JAK2 in multiple myeloma cells. J Exp Med. 1995;182(6):1801-6.
340. Giorgetti-Peraldi S, Peyrade F, Baron V, Van Obberghen E. Involvement of Janus kinases in the insulin signaling pathway. Eur J Biochem. 1995;234(2):656-60.
341. Lowenstein EJ, Daly RJ, Batzer AG, Li W, Margolis B, Lammers R, et al. The SH2 and SH3 domain-containing protein GRB2 links receptor tyrosine kinases to ras signaling. Cell. 1992;70(3):431-42.
342. Fretz H, Furet P, Garcia-Echeverria C, Schoepfer J, Rahuel J. Structure-based design of compounds inhibiting Grb2-SH2 mediated protein-protein interactions in signal transduction pathways. Curr Pharm Des. 2000;6(18):1777-96.
343. Ohanian M, Tari Ashizawa A, Garcia-Manero G, Pemmaraju N, Kadia T, Jabbour E, et al. Liposomal Grb2 antisense oligodeoxynucleotide (BP1001) in patients with refractory or relapsed haematological malignancies: a single-centre, open-label, dose-escalation, phase 1/1b trial. Lancet Haematol. 2018;5(4):e136-e46.
344. Pardanani A, Tefferi A, Guglielmelli P, Bogani C, Bartalucci N, Rodriguez J, et al. Evaluation of plitidepsin in patients with primary myelofibrosis and post polycythemia vera/essential thrombocythemia myelofibrosis: results of preclinical studies and a phase II clinical trial. Blood Cancer J. 2015;5:e286.
345. Sugiyama Y, Tomoda K, Tanaka T, Arata Y, Yoneda-Kato N, Kato J. Direct binding of the signal-transducing adaptor Grb2 facilitates down-regulation of the cyclin-dependent kinase inhibitor p27Kip1. J Biol Chem. 2001;276(15):12084-90.
346. Zhu Z, Du S, Du Y, Ren J, Ying G, Yan Z. Glutathione reductase mediates drug resistance in glioblastoma cells by regulating redox homeostasis. J Neurochem. 2018;144(1):93-104.
347. Nicolussi A, D'Inzeo S, Capalbo C, Giannini G, Coppa A. The role of peroxiredoxins in cancer. Mol Clin Oncol. 2017;6(2):139-53.
348. Gambi G, Di Simone E, Basso V, Ricci L, Wang R, Verma A, et al. The Transcriptional Regulator Sin3A Contributes to the Oncogenic Potential of STAT3. Cancer Res. 2019;79(12):3076-87.
349. Hargrove TY, Friggeri L, Wawrzak Z, Sivakumaran S, Yazlovitskaya EM, Hiebert SW, et al. Human sterol 14alpha-demethylase as a target for anticancer chemotherapy: towards structure-aided drug design. J Lipid Res. 2016;57(8):1552-63.
350. Howell MC, Green R, Khalil R, Foran E, Quarni W, Nair R, et al. Lung cancer cells survive epidermal growth factor receptor tyrosine kinase inhibitor exposure through upregulation of cholesterol synthesis. FASEB Bioadv. 2020;2(2):90-105.
351. Jha S, Dutta A. RVB1/RVB2: running rings around molecular biology. Mol Cell. 2009;34(5):521-33.

352. Mao YQ, Houry WA. The Role of Pontin and Reptin in Cellular Physiology and Cancer Etiology. Front Mol Biosci. 2017;4:58.
353. Breig O, Bras S, Martinez Soria N, Osman D, Heidenreich O, Haenlin M, et al. Pontin is a critical regulator for AML1-ETO-induced leukemia. Leukemia. 2014;28(6):1271-9.
354. Osaki H, Walf-Vorderwulbecke V, Mangolini M, Zhao L, Horton SJ, Morrone G, et al. The AAA+ ATPase RUVBL2 is a critical mediator of MLL-AF9 oncogenesis. Leukemia. 2013;27(7):1461-8.
355. Nano N, Ugwu F, Seraphim TV, Li T, Azer G, Isaac M, et al. Sorafenib as an Inhibitor of RUVBL2. Biomolecules. 2020;10(4).
356. Assimon VA, Tang Y, Vargas JD, Lee GJ, Wu ZY, Lou K, et al. CB-6644 Is a Selective Inhibitor of the RUVBL1/2 Complex with Anticancer Activity. ACS Chem Biol. 2019;14(2):236-44.
357. Yuan P, Ling L, Gao X, Sun T, Miao J, Yuan X, et al. Identification of RNA-binding protein SNRPA1 for prognosis in prostate cancer. Aging (Albany NY). 2021;13(2):2895-911.
358. Yuen HF, Chan KK, Grills C, Murray JT, Platt-Higgins A, Eldin OS, et al. Ran is a potential therapeutic target for cancer cells with molecular changes associated with activation of the PI3K/Akt/mTORC1 and Ras/MEK/ERK pathways. Clin Cancer Res. 2012;18(2):380-91.
359. Abe H, Kamai T, Shirataki H, Oyama T, Arai K, Yoshida K. High expression of Ran GTPase is associated with local invasion and metastasis of human clear cell renal cell carcinoma. Int J Cancer. 2008;122(10):2391-7.
360. Hartmann E, Fernandez V, Moreno V, Valls J, Hernandez L, Bosch F, et al. Five-gene model to predict survival in mantle-cell lymphoma using frozen or formalin-fixed, paraffin-embedded tissue. J Clin Oncol. 2008;26(30):4966-72.
361. Camus V, Miloudi H, Taly A, Sola B, Jardin F. XPO1 in B cell hematological malignancies: from recurrent somatic mutations to targeted therapy. J Hematol Oncol. 2017;10(1):47.
362. Yan D, Pomicter AD, Tantravahi S, Mason CC, Senina AV, Ahmann JM, et al. Nuclear-Cytoplasmic Transport Is a Therapeutic Target in Myelofibrosis. Clin Cancer Res. 2019;25(7):2323-35.
363. Kalakonda N, Maerevoet M, Cavallo F, Follows G, Goy A, Vermaat JSP, et al. Selinexor in patients with relapsed or refractory diffuse large B-cell lymphoma (SADAL): a single-arm, multinational, multicentre, open-label, phase 2 trial. Lancet Haematol. 2020;7(7):e511-e22.
364. Sweet K, Komrokji R, Padron E, Cubitt CL, Turner JG, Zhou J, et al. Phase I Clinical Trial of Selinexor in Combination with Daunorubicin and Cytarabine in Previously Untreated Poor-Risk Acute Myeloid Leukemia. Clin Cancer Res. 2020;26(1):54-60.
365. Vergote IB, Lund B, Peen U, Umajuridze Z, Mau-Sorensen M, Kranich A, et al. Phase 2 study of the Exportin 1 inhibitor selinexor in patients with recurrent gynecological malignancies. Gynecol Oncol. 2020;156(2):308-14.
366. Subhash VV, Yeo MS, Wang L, Tan SH, Wong FY, Thuya WL, et al. Anti-tumor efficacy of Selinexor (KPT-330) in gastric cancer is dependent on nuclear accumulation of p53 tumor suppressor. Sci Rep. 2018;8(1):12248.
367. Abdul Razak AR, Mau-Soerensen M, Gabrail NY, Gerecitano JF, Shields AF, Unger TJ, et al. First-in-Class, First-in-Human Phase I Study of Selinexor, a Selective Inhibitor of Nuclear Export, in Patients With Advanced Solid Tumors. J Clin Oncol. 2016;34(34):4142-50.
368. Peng YT, Chen P, Ouyang RY, Song L. Multifaceted role of prohibitin in cell survival and apoptosis. Apoptosis. 2015;20(9):1135-49.
369. Theiss AL, Sitaraman SV. The role and therapeutic potential of prohibitin in disease. Biochim Biophys Acta. 2011;1813(6):1137-43.

370. Liu S, Wang W, Brown LE, Qiu C, Lajkiewicz N, Zhao T, et al. A Novel Class of Small Molecule Compounds that Inhibit Hepatitis C Virus Infection by Targeting the Prohibitin-CRaf Pathway. EBioMedicine. 2015;2(11):1600-6.
371. Rajalingam K, Wunder C, Brinkmann V, Churin Y, Hekman M, Sievers C, et al. Prohibitin is required for Ras-induced Raf-MEK-ERK activation and epithelial cell migration. Nat Cell Biol. 2005;7(8):837-43.
372. Polier G, Neumann J, Thuaud F, Ribeiro N, Gelhaus C, Schmidt H, et al. The natural anticancer compounds rocaglamides inhibit the Raf-MEK-ERK pathway by targeting prohibitin 1 and 2. Chem Biol. 2012;19(9):1093-104.
373. Socoro-Yuste N, Cokic VP, Mondet J, Plo I, Mossuz P. Quantitative Proteome Heterogeneity in Myeloproliferative Neoplasm Subtypes and Association with JAK2 Mutation Status. Mol Cancer Res. 2017;15(7):852-61.
374. Santos FPS, Getta B, Masarova L, Famulare C, Schulman J, Datoguia TS, et al. Prognostic impact of RAS-pathway mutations in patients with myelofibrosis. Leukemia. 2020;34(3):799-810.
375. Verma S, De Jesus P, Chanda SK, Verma IM. SNW1, a Novel Transcriptional Regulator of the NF-kappaB Pathway. Mol Cell Biol. 2019;39(3).
376. Scott LM, Rebel VI. Acquired mutations that affect pre-mRNA splicing in hematologic malignancies and solid tumors. J Natl Cancer Inst. 2013;105(20):1540-9.
377. Jayavelu AK, Schnoder TM, Perner F, Herzog C, Meiler A, Krishnamoorthy G, et al. Splicing factor YBX1 mediates persistence of JAK2-mutated neoplasms. Nature. 2020;588(7836):157-63.
378. Enchev RI, Schulman BA, Peter M. Protein neddylation: beyond cullin-RING ligases. Nat Rev Mol Cell Biol. 2015;16(1):30-44.
379. Zhou L, Zhang W, Sun Y, Jia L. Protein neddylation and its alterations in human cancers for targeted therapy. Cell Signal. 2018;44:92-102.
380. Leclerc GM, Zheng S, Leclerc GJ, DeSalvo J, Swords RT, Barredo JC. The NEDD8-activating enzyme inhibitor pevonedistat activates the eIF2alpha and mTOR pathways inducing UPR-mediated cell death in acute lymphoblastic leukemia. Leuk Res. 2016;50:1-10.
381. Bahjat M, de Wilde G, van Dam T, Maas C, Bloedjes T, Bende RJ, et al. The NEDD8-activating enzyme inhibitor MLN4924 induces DNA damage in Ph+ leukemia and sensitizes for ABL kinase inhibitors. Cell Cycle. 2019;18(18):2307-22.
382. Walz C, Crowley BJ, Hudon HE, Gramlich JL, Neuberg DS, Podar K, et al. Activated Jak2 with the V617F point mutation promotes G1/S phase transition. J Biol Chem. 2006;281(26):18177-83.
383. Bastide A, David A. The ribosome, (slow) beating heart of cancer (stem) cell. Oncogenesis. 2018;7(4):34.
384. Shi N, Chen X, Liu R, Wang D, Su M, Wang Q, et al. Eukaryotic elongation factors 2 promotes tumor cell proliferation and correlates with poor prognosis in ovarian cancer. Tissue & cell. 2018;53:53-60.
385. Oji Y, Tatsumi N, Fukuda M, Nakatsuka S, Aoyagi S, Hirata E, et al. The translation elongation factor eEF2 is a novel tumorassociated antigen overexpressed in various types of cancers. International journal of oncology. 2014;44(5):1461-9.
386. Zhang J, Li S, Zhang L, Xu J, Song M, Shao T, et al. RBP EIF2S2 Promotes Tumorigenesis and Progression by Regulating MYC-Mediated Inhibition via FHIT-Related Enhancers. Molecular therapy : the journal of the American Society of Gene Therapy. 2020;28(4):1105-18.
387. Sagawa M, Ohguchi H, Harada T, Samur MK, Tai YT, Munshi NC, et al. Ribonucleotide Reductase Catalytic Subunit M1 (RRM1) as a Novel Therapeutic Target in

Multiple Myeloma. Clinical cancer research : an official journal of the American Association for Cancer Research. 2017;23(17):5225-37.
388. Schimmer AD, Singh RP, Seneviratne AK, Thomas GE, MacLean N, Hurren R. Transduction of Primary AML Cells with Lentiviral Vector for In Vitro Study or In Vivo Engraftment. STAR Protoc. 2020;1(3):100163.
389. Cante-Barrett K, Mendes RD, Smits WK, van Helsdingen-van Wijk YM, Pieters R, Meijerink JP. Lentiviral gene transfer into human and murine hematopoietic stem cells: size matters. BMC Res Notes. 2016;9:312.
390. Hanenberg H, Xiao XL, Dilloo D, Hashino K, Kato I, Williams DA. Colocalization of retrovirus and target cells on specific fibronectin fragments increases genetic transduction of mammalian cells. Nat Med. 1996;2(8):876-82.
391. Luo JH, Hua WF, Rao HL, Liao YJ, Kung HF, Zeng YX, et al. Overexpression of EIF-5A2 predicts tumor recurrence and progression in pTa/pT1 urothelial carcinoma of the bladder. Cancer Sci. 2009;100(5):896-902.
392. Khosravi S, Martinka M, Zhou Y, Ong CJ. Prognostic significance of the expression of nuclear eukaryotic translation initiation factor 5A2 in human melanoma. Oncol Lett. 2016;12(5):3089-100.
393. Yang GF, Xie D, Liu JH, Luo JH, Li LJ, Hua WF, et al. Expression and amplification of eIF-5A2 in human epithelial ovarian tumors and overexpression of EIF-5A2 is a new independent predictor of outcome in patients with ovarian carcinoma. Gynecol Oncol. 2009;112(2):314-8.
394. Huang PY, Zeng TT, Ban X, Li MQ, Zhang BZ, Zhu YH, et al. Expression of EIF5A2 associates with poor survival of nasopharyngeal carcinoma patients treated with induction chemotherapy. BMC Cancer. 2016;16:669.
395. Liu Y, Lei P, Qiao H, Sun K, Lu X, Bao F, et al. miR-9 Enhances the Chemosensitivity of AML Cells to Daunorubicin by Targeting the EIF5A2/MCL-1 Axis. Int J Biol Sci. 2019;15(3):579-86.
396. Guo J, Roberts L, Chen Z, Merta PJ, Glaser KB, Shah OJ. JAK2V617F drives Mcl-1 expression and sensitizes hematologic cell lines to dual inhibition of JAK2 and Bcl-xL. PLoS One. 2015;10(3):e0114363.
397. Wei JH, Cao JZ, Zhang D, Liao B, Zhong WM, Lu J, et al. EIF5A2 predicts outcome in localised invasive bladder cancer and promotes bladder cancer cell aggressiveness in vitro and in vivo. Br J Cancer. 2014;110(7):1767-77.
398. Galan-Ganga M, Garcia-Yague AJ, Lastres-Becker I. Role of MSK1 in the Induction of NF-kappaB by the Chemokine CX3CL1 in Microglial Cells. Cell Mol Neurobiol. 2019;39(3):331-40.
399. Liu JF, Tsao YT, Hou CH. Fractalkine/CX3CL1 induced intercellular adhesion molecule-1-dependent tumor metastasis through the CX3CR1/PI3K/Akt/NF-kappaB pathway in human osteosarcoma. Oncotarget. 2017;8(33):54136-48.
400. Wang J, Zhang XS, Tao R, Zhang J, Liu L, Jiang YH, et al. Upregulation of CX3CL1 mediated by NF-kappaB activation in dorsal root ganglion contributes to peripheral sensitization and chronic pain induced by oxaliplatin administration. Mol Pain. 2017;13:1744806917726256.
401. Li D, Huang ZZ, Ling YZ, Wei JY, Cui Y, Zhang XZ, et al. Up-regulation of CX3CL1 via Nuclear Factor-kappaB-dependent Histone Acetylation Is Involved in Paclitaxel-induced Peripheral Neuropathy. Anesthesiology. 2015;122(5):1142-51.
402. White GE, McNeill E, Channon KM, Greaves DR. Fractalkine promotes human monocyte survival via a reduction in oxidative stress. Arterioscler Thromb Vasc Biol. 2014;34(12):2554-62.

403. Wang H, Cai J, Du S, Guo Z, Xin B, Wang J, et al. Fractalkine/CX3CR1 induces apoptosis resistance and proliferation through the activation of the AKT/NF-kappaB cascade in pancreatic cancer cells. Cell Biochem Funct. 2017;35(6):315-26.
404. Gaudin F, Nasreddine S, Donnadieu AC, Emilie D, Combadiere C, Prevot S, et al. Identification of the chemokine CX3CL1 as a new regulator of malignant cell proliferation in epithelial ovarian cancer. PLoS One. 2011;6(7):e21546.
405. Ren H, Zhao T, Sun J, Wang X, Liu J, Gao S, et al. The CX3CL1/CX3CR1 reprograms glucose metabolism through HIF-1 pathway in pancreatic adenocarcinoma. J Cell Biochem. 2013;114(11):2603-11.
406. Tardaguila M, Mira E, Garcia-Cabezas MA, Feijoo AM, Quintela-Fandino M, Azcoitia I, et al. CX3CL1 promotes breast cancer via transactivation of the EGF pathway. Cancer Res. 2013;73(14):4461-73.
407. Ren T, Chen Q, Tian Z, Wei H. Down-regulation of surface fractalkine by RNA interference in B16 melanoma reduced tumor growth in mice. Biochem Biophys Res Commun. 2007;364(4):978-84.
408. Yao X, Qi L, Chen X, Du J, Zhang Z, Liu S. Expression of CX3CR1 associates with cellular migration, metastasis, and prognosis in human clear cell renal cell carcinoma. Urol Oncol. 2014;32(2):162-70.
409. Ferretti E, Bertolotto M, Deaglio S, Tripodo C, Ribatti D, Audrito V, et al. A novel role of the CX3CR1/CX3CL1 system in the cross-talk between chronic lymphocytic leukemia cells and tumor microenvironment. Leukemia. 2011;25(8):1268-77.
410. Maiga A, Lemieux S, Pabst C, Lavallee VP, Bouvier M, Sauvageau G, et al. Transcriptome analysis of G protein-coupled receptors in distinct genetic subgroups of acute myeloid leukemia: identification of potential disease-specific targets. Blood Cancer J. 2016;6(6):e431.
411. Marchica V, Toscani D, Corcione A, Bolzoni M, Storti P, Vescovini R, et al. Bone Marrow CX3CL1/Fractalkine is a New Player of the Pro-Angiogenic Microenvironment in Multiple Myeloma Patients. Cancers (Basel). 2019;11(3).
412. Ishida Y, Kimura A, Nosaka M, Kuninaka Y, Hemmi H, Sasaki I, et al. Essential involvement of the CX3CL1-CX3CR1 axis in bleomycin-induced pulmonary fibrosis via regulation of fibrocyte and M2 macrophage migration. Sci Rep. 2017;7(1):16833.
413. Greiffo FR, Viteri-Alvarez V, Frankenberger M, Dietel D, Ortega-Gomez A, Lee JS, et al. CX3CR1-fractalkine axis drives kinetic changes of monocytes in fibrotic interstitial lung diseases. Eur Respir J. 2020;55(2).
414. Chevet E, Hetz C, Samali A. Endoplasmic reticulum stress-activated cell reprogramming in oncogenesis. Cancer Discov. 2015;5(6):586-97.
415. Tomoishi S, Fukushima S, Shinohara K, Katada T, Saito K. CREB3L2-mediated expression of Sec23A/Sec24D is involved in hepatic stellate cell activation through ER-Golgi transport. Sci Rep. 2017;7(1):7992.
416. Sheng Z, Evans SK, Green MR. An activating transcription factor 5-mediated survival pathway as a target for cancer therapy? Oncotarget. 2010;1(6):457-60.
417. Fiskus W, Verstovsek S, Manshouri T, Smith JE, Peth K, Abhyankar S, et al. Dual PI3K/AKT/mTOR inhibitor BEZ235 synergistically enhances the activity of JAK2 inhibitor against cultured and primary human myeloproliferative neoplasm cells. Mol Cancer Ther. 2013;12(5):577-88.
418. Morishita S, Yasuda H, Yamawaki S, Kawaji H, Itoh M, Edahiro Y, et al. CREB3L1 overexpression as a potential diagnostic marker of Philadelphia chromosome-negative myeloproliferative neoplasms. Cancer Sci. 2021;112(2):884-92.
419. Moriggl R, Sexl V, Kenner L, Duntsch C, Stangl K, Gingras S, et al. Stat5 tetramer formation is associated with leukemogenesis. Cancer Cell. 2005;7(1):87-99.

420. Walz C, Ahmed W, Lazarides K, Betancur M, Patel N, Hennighausen L, et al. Essential role for Stat5a/b in myeloproliferative neoplasms induced by BCR-ABL1 and JAK2(V617F) in mice. Blood. 2012;119(15):3550-60.
421. Schwaller J, Parganas E, Wang D, Cain D, Aster JC, Williams IR, et al. Stat5 is essential for the myelo- and lymphoproliferative disease induced by TEL/JAK2. Mol Cell. 2000;6(3):693-704.
422. Abba C, Campanelli R, Catarsi P, Villani L, Abbonante V, Sesta MA, et al. Constitutive STAT5 phosphorylation in CD34+ cells of patients with primary myelofibrosis: Correlation with driver mutation status and disease severity. PLoS One. 2019;14(8):e0220189.
423. Bartalucci N, Tozzi L, Bogani C, Martinelli S, Rotunno G, Villeval JL, et al. Co-targeting the PI3K/mTOR and JAK2 signalling pathways produces synergistic activity against myeloproliferative neoplasms. J Cell Mol Med. 2013;17(11):1385-96.
424. Choong ML, Pecquet C, Pendharkar V, Diaconu CC, Yong JW, Tai SJ, et al. Combination treatment for myeloproliferative neoplasms using JAK and pan-class I PI3K inhibitors. J Cell Mol Med. 2013;17(11):1397-409.
425. Wingelhofer B, Maurer B, Heyes EC, Cumaraswamy AA, Berger-Becvar A, de Araujo ED, et al. Pharmacologic inhibition of STAT5 in acute myeloid leukemia. Leukemia. 2018;32(5):1135-46.
426. Hadzijusufovic E, Keller A, Berger D, Greiner G, Wingelhofer B, Witzeneder N, et al. STAT5 is Expressed in CD34(+)/CD38(-) Stem Cells and Serves as a Potential Molecular Target in Ph-Negative Myeloproliferative Neoplasms. Cancers (Basel). 2020;12(4).
427. Liu W, Yu WM, Zhang J, Chan RJ, Loh ML, Zhang Z, et al. Inhibition of the Gab2/PI3K/mTOR signaling ameliorates myeloid malignancy caused by Ptpn11 (Shp2) gain-of-function mutations. Leukemia. 2017;31(6):1415-22.
428. Di Rosa M, Giallongo C, Romano A, Tibullo D, Li Volti G, Musumeci G, et al. Immunoproteasome Genes Are Modulated in CD34(+) JAK2(V617F) Mutated Cells from Primary Myelofibrosis Patients. International journal of molecular sciences. 2020;21(8).
429. Skov V, Larsen TS, Thomassen M, Riley C, Jensen MK, Bjerrum OW, et al. Increased Expression of Proteasome-Related Genes In Patients with Primary Myelofibrosis. Blood. 2010;116(21):4117-.
430. Kouroukis TC, Baldassarre FG, Haynes AE, Imrie K, Reece DE, Cheung MC. Bortezomib in multiple myeloma: systematic review and clinical considerations. Curr Oncol. 2014;21(4):e573-603.
431. Besse A, Besse L, Kraus M, Mendez-Lopez M, Bader J, Xin BT, et al. Proteasome Inhibition in Multiple Myeloma: Head-to-Head Comparison of Currently Available Proteasome Inhibitors. Cell Chem Biol. 2019;26(3):340-51 e3.
432. Kuhn DJ, Chen Q, Voorhees PM, Strader JS, Shenk KD, Sun CM, et al. Potent activity of carfilzomib, a novel, irreversible inhibitor of the ubiquitin-proteasome pathway, against preclinical models of multiple myeloma. Blood. 2007;110(9):3281-90.
433. Chou TC. Drug combination studies and their synergy quantification using the Chou-Talalay method. Cancer Res. 2010;70(2):440-6.
434. Wagner-Ballon O, Pisani DF, Gastinne T, Tulliez M, Chaligne R, Lacout C, et al. Proteasome inhibitor bortezomib impairs both myelofibrosis and osteosclerosis induced by high thrombopoietin levels in mice. Blood. 2007;110(1):345-53.
435. Galimberti S, Canestraro M, Pacini S, Fazzi R, Orciuolo E, Trombi L, et al. PS-341 (Bortezomib) inhibits proliferation and induces apoptosis of megakaryoblastic MO7-e cells. Leuk Res. 2008;32(1):103-12.
436. Galimberti S, Canestaro M, Ciancia E, Fazzi R, Marasca R, Petrini M. Bortezomib is able to reduce angiogenesis in half of patients affected by idiopathic myelofibrosis: an ex vivo study. Leuk Res. 2008;32(8):1324-5.

437. Barosi G, Gattoni E, Guglielmelli P, Campanelli R, Facchetti F, Fisogni S, et al. Phase I/II study of single-agent bortezomib for the treatment of patients with myelofibrosis. Clinical and biological effects of proteasome inhibition. Am J Hematol. 2010;85(8):616-9.
438. Wang X, Cho SY, Hu CS, Chen D, Roboz J, Hoffman R. C-X-C motif chemokine 12 influences the development of extramedullary hematopoiesis in the spleens of myelofibrosis patients. Exp Hematol. 2015;43(2):100-9 e1.
439. Rosti V, Massa M, Vannucchi AM, Bergamaschi G, Campanelli R, Pecci A, et al. The expression of CXCR4 is down-regulated on the CD34+ cells of patients with myelofibrosis with myeloid metaplasia. Blood Cells Mol Dis. 2007;38(3):280-6.
440. Mesa RA, Verstovsek S, Rivera C, Pardanani A, Hussein K, Lasho T, et al. Bortezomib therapy in myelofibrosis: a phase II clinical trial. Leukemia. 2008;22(8):1636-8.
441. Dimopoulos MA, Moreau P, Palumbo A, Joshua D, Pour L, Hajek R, et al. Carfilzomib and dexamethasone versus bortezomib and dexamethasone for patients with relapsed or refractory multiple myeloma (ENDEAVOR): a randomised, phase 3, open-label, multicentre study. Lancet Oncol. 2016;17(1):27-38.
442. Dimopoulos MA, Roussou M, Gavriatopoulou M, Psimenou E, Ziogas D, Eleutherakis-Papaiakovou E, et al. Cardiac and renal complications of carfilzomib in patients with multiple myeloma. Blood Adv. 2017;1(7):449-54.
443. Liston DR, Davis M. Clinically Relevant Concentrations of Anticancer Drugs: A Guide for Nonclinical Studies. Clin Cancer Res. 2017;23(14):3489-98.
444. Papadopoulos KP, Siegel DS, Vesole DH, Lee P, Rosen ST, Zojwalla N, et al. Phase I study of 30-minute infusion of carfilzomib as single agent or in combination with low-dose dexamethasone in patients with relapsed and/or refractory multiple myeloma. J Clin Oncol. 2015;33(7):732-9.
445. Vangala JR, Dudem S, Jain N, Kalivendi SV. Regulation of PSMB5 protein and beta subunits of mammalian proteasome by constitutively activated signal transducer and activator of transcription 3 (STAT3): potential role in bortezomib-mediated anticancer therapy. J Biol Chem. 2014;289(18):12612-22.
446. Hohn TJ, Grune T. The proteasome and the degradation of oxidized proteins: part III-Redox regulation of the proteasomal system. Redox Biol. 2014;2:388-94.
447. Kusoglu A, Bagca BG, Ozates Ay NP, Saydam G, Avci CB. Ruxolitinib Regulates the Autophagy Machinery in Multiple Myeloma Cells. Anticancer Agents Med Chem. 2020.
448. Caocci G, La Nasa G. Could ruxolitinib be effective in patients with COVID-19 infection at risk of acute respiratory distress syndrome (ARDS)? Ann Hematol. 2020;99(7):1675-6.
449. Pickering AM, Koop AL, Teoh CY, Ermak G, Grune T, Davies KJ. The immunoproteasome, the 20S proteasome and the PA28alphabeta proteasome regulator are oxidative-stress-adaptive proteolytic complexes. Biochem J. 2010;432(3):585-94.
450. Ding Q, Reinacker K, Dimayuga E, Nukala V, Drake J, Butterfield DA, et al. Role of the proteasome in protein oxidation and neural viability following low-level oxidative stress. FEBS Lett. 2003;546(2-3):228-32.
451. Aiken CT, Kaake RM, Wang X, Huang L. Oxidative stress-mediated regulation of proteasome complexes. Mol Cell Proteomics. 2011;10(5):R110 006924.
452. Hurtado-Nedelec M, Csillag-Grange MJ, Boussetta T, Belambri SA, Fay M, Cassinat B, et al. Increased reactive oxygen species production and p47phox phosphorylation in neutrophils from myeloproliferative disorders patients with JAK2 (V617F) mutation. Haematologica. 2013;98(10):1517-24.
453. Bjorn ME, Hasselbalch HC. The Role of Reactive Oxygen Species in Myelofibrosis and Related Neoplasms. Mediators Inflamm. 2015;2015:648090.

454. Rossi C, Zini R, Rontauroli S, Ruberti S, Prudente Z, Barbieri G, et al. Role of TGF-beta1/miR-382-5p/SOD2 axis in the induction of oxidative stress in CD34+ cells from primary myelofibrosis. Mol Oncol. 2018;12(12):2102-23.
455. Khateb A, Ronai ZA. Unfolded Protein Response in Leukemia: From Basic Understanding to Therapeutic Opportunities. Trends Cancer. 2020;6(11):960-73.
456. Zhao GL, Yu LM, Gao WL, Duan WX, Jiang B, Liu XD, et al. Berberine protects rat heart from ischemia/reperfusion injury via activating JAK2/STAT3 signaling and attenuating endoplasmic reticulum stress. Acta Pharmacol Sin. 2016;37(3):354-67.
457. Flores-Morales A, Fernandez L, Rico-Bautista E, Umana A, Negrin C, Zhang JG, et al. Endoplasmic reticulum stress prolongs GH-induced Janus kinase (JAK2)/signal transducer and activator of transcription (STAT5) signaling pathway. Mol Endocrinol. 2001;15(9):1471-83.
458. Meares GP, Liu Y, Rajbhandari R, Qin H, Nozell SE, Mobley JA, et al. PERK-dependent activation of JAK1 and STAT3 contributes to endoplasmic reticulum stress-induced inflammation. Mol Cell Biol. 2014;34(20):3911-25.
459. Huang LJ, Constantinescu SN, Lodish HF. The N-terminal domain of Janus kinase 2 is required for Golgi processing and cell surface expression of erythropoietin receptor. Mol Cell. 2001;8(6):1327-38.
460. Lavoie C, Chevet E, Roy L, Tonks NK, Fazel A, Posner BI, et al. Tyrosine phosphorylation of p97 regulates transitional endoplasmic reticulum assembly in vitro. Proc Natl Acad Sci U S A. 2000;97(25):13637-42.
461. Wang L, Ryoo HD, Qi Y, Jasper H. PERK Limits Drosophila Lifespan by Promoting Intestinal Stem Cell Proliferation in Response to ER Stress. PLoS Genet. 2015;11(5):e1005220.
462. Goda AE, Erikson RL, Sakai T, Ahn JS, Kim BY. Preclinical evaluation of bortezomib/dipyridamole novel combination as a potential therapeutic modality for hematologic malignancies. Mol Oncol. 2015;9(1):309-22.
463. Digaleh H, Kiaei M, Khodagholi F. Nrf2 and Nrf1 signaling and ER stress crosstalk: implication for proteasomal degradation and autophagy. Cell Mol Life Sci. 2013;70(24):4681-94.
464. Kharabi Masouleh B, Geng H, Hurtz C, Chan LN, Logan AC, Chang MS, et al. Mechanistic rationale for targeting the unfolded protein response in pre-B acute lymphoblastic leukemia. Proc Natl Acad Sci U S A. 2014;111(21):E2219-28.
465. Salati S, Genovese E, Carretta C, Zini R, Bartalucci N, Prudente Z, et al. Calreticulin Ins5 and Del52 mutations impair unfolded protein and oxidative stress responses in K562 cells expressing CALR mutants. Sci Rep. 2019;9(1):10558.
466. Kropski JA, Blackwell TS. Endoplasmic reticulum stress in the pathogenesis of fibrotic disease. J Clin Invest. 2018;128(1):64-73.
467. Nogami A, Okada K, Ishida S, Akiyama H, Umezawa Y, Miura O. Inhibition of the STAT5/Pim Kinase Axis Enhances Cytotoxic Effects of Proteasome Inhibitors on FLT3-ITD-Positive AML Cells by Cooperatively Inhibiting the mTORC1/4EBP1/S6K/Mcl-1 Pathway. Transl Oncol. 2019;12(2):336-49.
468. Liu CY, Hsieh FS, Chu PY, Tsai WC, Huang CT, Yu YB, et al. Carfilzomib induces leukaemia cell apoptosis via inhibiting ELK1/KIAA1524 (Elk-1/CIP2A) and activating PP2A not related to proteasome inhibition. Br J Haematol. 2017;177(5):726-40.
469. Efentakis P, Kremastiotis G, Varela A, Nikolaou PE, Papanagnou ED, Davos CH, et al. Molecular mechanisms of carfilzomib-induced cardiotoxicity in mice and the emerging cardioprotective role of metformin. Blood. 2019;133(7):710-23.
470. Mazzacurati L, Lambert QT, Pradhan A, Griner LN, Huszar D, Reuther GW. The PIM inhibitor AZD1208 synergizes with ruxolitinib to induce apoptosis of ruxolitinib sensitive and

resistant JAK2-V617F-driven cells and inhibit colony formation of primary MPN cells. Oncotarget. 2015;6(37):40141-57.
471. Mazzacurati L, Collins RJ, Pandey G, Lambert-Showers QT, Amin NE, Zhang L, et al. The pan-PIM inhibitor INCB053914 displays potent synergy in combination with ruxolitinib in models of MPN. Blood Adv. 2019;3(22):3503-14.
472. Rubert J, Qian Z, Andraos R, Guthy DA, Radimerski T. Bim and Mcl-1 exert key roles in regulating JAK2V617F cell survival. BMC Cancer. 2011;11:24.
473. Kawashima I, Kirito K. Metformin inhibits JAK2V617F activity in MPN cells by activating AMPK and PP2A complexes containing the B56alpha subunit. Exp Hematol. 2016;44(12):1156-65 e4.
474. Oaks JJ, Santhanam R, Walker CJ, Roof S, Harb JG, Ferenchak G, et al. Antagonistic activities of the immunomodulator and PP2A-activating drug FTY720 (Fingolimod, Gilenya) in Jak2-driven hematologic malignancies. Blood. 2013;122(11):1923-34.
475. Waldschmidt JM WD, Müller SJ, Simon A, Decker S , Follo M, Duyster J, Wäsch R, Engelhardt M. PIM1-Mediated CXCR4 Phosphorylation: A Potentially Class-Distinct Therapeutic Target of Next Generation Proteasome Inhibitors in Multiple Myeloma. Blood. 2016;128 (22): 2774.
476. Nath D DA, Yang Y, Whatcott C, Warner S, Mohi G. The PIM Kinase Inhibitor TP-3654 in Combination with Ruxolitinib Exhibits Marked Improvement of Myelofibrosis in Murine Models. Blood. 2018;132 (Supplement 1): 54.
477. Norfo R, Zini R, Pennucci V, Bianchi E, Salati S, Guglielmelli P, et al. miRNA-mRNA integrative analysis in primary myelofibrosis CD34+ cells: role of miR-155/JARID2 axis in abnormal megakaryopoiesis. Blood. 2014;124(13):e21-32.
478. Ponder KG, Matulis SM, Hitosugi S, Gupta VA, Sharp C, Burrows F, et al. Dual inhibition of Mcl-1 by the combination of carfilzomib and TG02 in multiple myeloma. Cancer Biol Ther. 2016;17(7):769-77.
479. Lamothe B, Cervantes-Gomez F, Sivina M, Wierda WG, Keating MJ, Gandhi V. Proteasome inhibitor carfilzomib complements ibrutinib's action in chronic lymphocytic leukemia. Blood. 2015;125(2):407-10.
480. Lee HJ, Badillo M, Romaguera J, Wang M. A phase II study of carfilzomib in the treatment of relapsed/refractory mantle cell lymphoma. Br J Haematol. 2019;184(3):460-2.
481. Gu JJ, Hernandez-Ilizaliturri FJ, Kaufman GP, Czuczman NM, Mavis C, Skitzki JJ, et al. The novel proteasome inhibitor carfilzomib induces cell cycle arrest, apoptosis and potentiates the anti-tumour activity of chemotherapy in rituximab-resistant lymphoma. Br J Haematol. 2013;162(5):657-69.
482. Sarlo C, Buccisano F, Maurillo L, Cefalo M, Di Caprio L, Cicconi L, et al. Phase II Study of Bortezomib as a Single Agent in Patients with Previously Untreated or Relapsed/Refractory Acute Myeloid Leukemia Ineligible for Intensive Therapy. Leuk Res Treatment. 2013;2013:705714.
483. Wartman LD, Fiala MA, Fletcher T, Hawkins ER, Cashen A, DiPersio JF, et al. A phase I study of carfilzomib for relapsed or refractory acute myeloid and acute lymphoblastic leukemia. Leuk Lymphoma. 2016;57(3):728-30.
484. Liu H, Westergard TD, Cashen A, Piwnica-Worms DR, Kunkle L, Vij R, et al. Proteasome inhibitors evoke latent tumor suppression programs in pro-B MLL leukemias through MLL-AF4. Cancer Cell. 2014;25(4):530-42.
485. van der Helm LH, Bosman MC, Schuringa JJ, Vellenga E. Effective targeting of primitive AML CD34+ cells by the second-generation proteasome inhibitor carfilzomib. Br J Haematol. 2015;171(4):652-5.

486. Guzman ML, Swiderski CF, Howard DS, Grimes BA, Rossi RM, Szilvassy SJ, et al. Preferential induction of apoptosis for primary human leukemic stem cells. Proc Natl Acad Sci U S A. 2002;99(25):16220-5.
487. Mato AR, Feldman T, Goy A. Proteasome inhibition and combination therapy for non-Hodgkin's lymphoma: from bench to bedside. Oncologist. 2012;17(5):694-707.
488. Orlowski RZ, Voorhees PM, Garcia RA, Hall MD, Kudrik FJ, Allred T, et al. Phase 1 trial of the proteasome inhibitor bortezomib and pegylated liposomal doxorubicin in patients with advanced hematologic malignancies. Blood. 2005;105(8):3058-65.
489. Attar EC, De Angelo DJ, Supko JG, D'Amato F, Zahrieh D, Sirulnik A, et al. Phase I and pharmacokinetic study of bortezomib in combination with idarubicin and cytarabine in patients with acute myelogenous leukemia. Clin Cancer Res. 2008;14(5):1446-54.
490. Howard DS, Liesveld J, Phillips GL, 2nd, Hayslip J, Weiss H, Jordan CT, et al. A phase I study using bortezomib with weekly idarubicin for treatment of elderly patients with acute myeloid leukemia. Leuk Res. 2013;37(11):1502-8.
491. Axelrod M, Ou Z, Brett LK, Zhang L, Lopez ER, Tamayo AT, et al. Combinatorial drug screening identifies synergistic co-targeting of Bruton's tyrosine kinase and the proteasome in mantle cell lymphoma. Leukemia. 2014;28(2):407-10.
492. Yumeen S, Mirza FN, Lewis JM, King ALO, Kim SR, Carlson KR, et al. JAK inhibition synergistically potentiates BCL2, BET, HDAC, and proteasome inhibition in advanced CTCL. Blood Adv. 2020;4(10):2213-26.
493. Waldschmidt JM, Simon A, Wider D, Muller SJ, Follo M, Ihorst G, et al. CXCL12 and CXCR7 are relevant targets to reverse cell adhesion-mediated drug resistance in multiple myeloma. Br J Haematol. 2017;179(1):36-49.
494. Abdelouahab H, Zhang Y, Wittner M, Oishi S, Fujii N, Besancenot R, et al. CXCL12/CXCR4 pathway is activated by oncogenic JAK2 in a PI3K-dependent manner. Oncotarget. 2017;8(33):54082-95.
495. Ramakrishnan V, Kimlinger T, Haug J, Timm M, Wellik L, Halling T, et al. TG101209, a novel JAK2 inhibitor, has significant in vitro activity in multiple myeloma and displays preferential cytotoxicity for CD45+ myeloma cells. American journal of hematology. 2010;85(9):675-86.
496. Monaghan KA, Khong T, Burns CJ, Spencer A. The novel JAK inhibitor CYT387 suppresses multiple signalling pathways, prevents proliferation and induces apoptosis in phenotypically diverse myeloma cells. Leukemia. 2011;25(12):1891-9.
497. Li J, Favata M, Kelley JA, Caulder E, Thomas B, Wen X, et al. INCB16562, a JAK1/2 selective inhibitor, is efficacious against multiple myeloma cells and reverses the protective effects of cytokine and stromal cell support. Neoplasia. 2010;12(1):28-38.
498. de Oliveira MB, Fook-Alves VL, Eugenio AIP, Fernando RC, Sanson LFG, de Carvalho MF, et al. Anti-myeloma effects of ruxolitinib combined with bortezomib and lenalidomide: A rationale for JAK/STAT pathway inhibition in myeloma patients. Cancer Lett. 2017;403:206-15.
499. Podar K, Chauhan D, Anderson KC. Bone marrow microenvironment and the identification of new targets for myeloma therapy. Leukemia. 2009;23(1):10-24.
500. Chen H SE, Li M, Wang C, Gillespie A, Shvartsur A, Vardanyan S, Harutyunyan N, Garzio G, Tang G, Bonavida B, Berenson J. Increased M2 Macrophages in Multiple Myeloma Patients with Progressive Disease and Down-Regulated Polarization with the JAK2 Inhibitor Ruxolitinib. Blood. 2014;124(21): 4106. .
501. Chen H, Li M, Ng N, Yu E, Bujarski S, Yin Z, et al. Ruxolitinib reverses checkpoint inhibition by reducing programmed cell death ligand-1 (PD-L1) expression and increases anti-tumour effects of T cells in multiple myeloma. Br J Haematol. 2021;192(3):568-76.

502. Berenson J TJ, Spektor T, Martinez D, Sanchez A, Ghermezi M, Turner C, Swift R, Benjamin M, Eades B, Schwartz G, Eshaghian S, Stampleman L, Moss R, Nassir Y, Patel R, Bessudo A, Lim S, Vescio R. A phase I trial of ruxolitinib, lenalidomide, and methylprednisolone for patients with relapsed/refractory multiple myeloma (MM). J Clin Oncol. 2019;37(15):8048.
503. Chen H SE, Li M, Wang C, Gillespie A, Shvartsur A, Vardanyan S, Harutyunyan N, Garzio G, Tang G, Bonavida B, Berenson J. Anti-Myeloma Activity by the Combination of the JAK2 Inhibitor Ruxolitinib with Lenalidomide and Corticosteroids. Blood. 2014;124(21): 2114.
504. Funakoshi-Tago M, Tago K, Sato Y, Tominaga S, Kasahara T. JAK2 is an important signal transducer in IL-33-induced NF-kappaB activation. Cell Signal. 2011;23(2):363-70.
505. Wang Q, Zhou X, Yang L, Zhao Y, Chew Z, Xiao J, et al. The Natural Compound Notopterol Binds and Targets JAK2/3 to Ameliorate Inflammation and Arthritis. Cell Rep. 2020;32(11):108158.
506. Lee H, Herrmann A, Deng JH, Kujawski M, Niu G, Li Z, et al. Persistently activated Stat3 maintains constitutive NF-kappaB activity in tumors. Cancer Cell. 2009;15(4):283-93.
507. Gao SP, Mark KG, Leslie K, Pao W, Motoi N, Gerald WL, et al. Mutations in the EGFR kinase domain mediate STAT3 activation via IL-6 production in human lung adenocarcinomas. J Clin Invest. 2007;117(12):3846-56.
508. Grivennikov S, Karin M. Autocrine IL-6 signaling: a key event in tumorigenesis? Cancer Cell. 2008;13(1):7-9.
509. Zhang YL, Guang MH, Zhuo HQ, Min XH, Yao Q, Gu AQ, et al. Carfilzomib Inhibits Constitutive NF-kappaB Activation in Mantle Cell Lymphoma B Cells and Leads to the Induction of Apoptosis. Acta Haematol. 2017;137(2):106-12.
510. Guan S, Zhao Y, Lu J, Yu Y, Sun W, Mao X, et al. Second-generation proteasome inhibitor carfilzomib sensitizes neuroblastoma cells to doxorubicin-induced apoptosis. Oncotarget. 2016;7(46):75914-25.
511. Hoesel B, Schmid JA. The complexity of NF-kappaB signaling in inflammation and cancer. Mol Cancer. 2013;12:86.
512. Mussbacher M, Salzmann M, Brostjan C, Hoesel B, Schoergenhofer C, Datler H, et al. Cell Type-Specific Roles of NF-kappaB Linking Inflammation and Thrombosis. Front Immunol. 2019;10:85.
513. Park MH, Hong JT. Roles of NF-kappaB in Cancer and Inflammatory Diseases and Their Therapeutic Approaches. Cells. 2016;5(2).
514. Tilstra JS, Clauson CL, Niedernhofer LJ, Robbins PD. NF-kappaB in Aging and Disease. Aging Dis. 2011;2(6):449-65.
515. Kravtsova-Ivantsiv Y, Ciechanover A. The ubiquitin-proteasome system and activation of NF-kappaB: involvement of the ubiquitin ligase KPC1 in p105 processing and tumor suppression. Mol Cell Oncol. 2015;2(4):e1054552.
516. Xia ZB, Meng FR, Fang YX, Wu X, Zhang CW, Liu Y, et al. Inhibition of NF-kappaB signaling pathway induces apoptosis and suppresses proliferation and angiogenesis of human fibroblast-like synovial cells in rheumatoid arthritis. Medicine (Baltimore). 2018;97(23):e10920.
517. Wang CY, Mayo MW, Korneluk RG, Goeddel DV, Baldwin AS, Jr. NF-kappaB antiapoptosis: induction of TRAF1 and TRAF2 and c-IAP1 and c-IAP2 to suppress caspase-8 activation. Science. 1998;281(5383):1680-3.
518. Bours V, Bentires-Alj M, Hellin AC, Viatour P, Robe P, Delhalle S, et al. Nuclear factor-kappa B, cancer, and apoptosis. Biochem Pharmacol. 2000;60(8):1085-9.
519. Vrabel D, Pour L, Sevcikova S. The impact of NF-kappaB signaling on pathogenesis and current treatment strategies in multiple myeloma. Blood Rev. 2019;34:56-66.

520. Perkins ND. The diverse and complex roles of NF-kappaB subunits in cancer. Nat Rev Cancer. 2012;12(2):121-32.
521. Kleppe M, Koche R, Zou L, van Galen P, Hill CE, Dong L, et al. Dual Targeting of Oncogenic Activation and Inflammatory Signaling Increases Therapeutic Efficacy in Myeloproliferative Neoplasms. Cancer Cell. 2018;33(4):785-7.
522. Malki S, Bibeau F, Notarnicola C, Roques S, Berta P, Poulat F, et al. Expression and biological role of the prostaglandin D synthase/SOX9 pathway in human ovarian cancer cells. Cancer Lett. 2007;255(2):182-93.
523. Wu CC, Shyu RY, Wang CH, Tsai TC, Wang LK, Chen ML, et al. Involvement of the prostaglandin D2 signal pathway in retinoid-inducible gene 1 (RIG1)-mediated suppression of cell invasion in testis cancer cells. Biochim Biophys Acta. 2012;1823(12):2227-36.
524. Aguilar-Medina M, Avendano-Felix M, Lizarraga-Verdugo E, Bermudez M, Romero-Quintana JG, Ramos-Payan R, et al. SOX9 Stem-Cell Factor: Clinical and Functional Relevance in Cancer. J Oncol. 2019;2019:6754040.
525. Pritchett J, Harvey E, Athwal V, Berry A, Rowe C, Oakley F, et al. Osteopontin is a novel downstream target of SOX9 with diagnostic implications for progression of liver fibrosis in humans. Hepatology. 2012;56(3):1108-16.
526. Hanley KP, Oakley F, Sugden S, Wilson DI, Mann DA, Hanley NA. Ectopic SOX9 mediates extracellular matrix deposition characteristic of organ fibrosis. J Biol Chem. 2008;283(20):14063-71.
527. Bennett MR, Czech KA, Arend LJ, Witte DP, Devarajan P, Potter SS. Laser capture microdissection-microarray analysis of focal segmental glomerulosclerosis glomeruli. Nephron Exp Nephrol. 2007;107(1):e30-40.
528. Sumi E, Iehara N, Akiyama H, Matsubara T, Mima A, Kanamori H, et al. SRY-related HMG box 9 regulates the expression of Col4a2 through transactivating its enhancer element in mesangial cells. Am J Pathol. 2007;170(6):1854-64.
529. Legendre F, Dudhia J, Pujol JP, Bogdanowicz P. JAK/STAT but not ERK1/ERK2 pathway mediates interleukin (IL)-6/soluble IL-6R down-regulation of Type II collagen, aggrecan core, and link protein transcription in articular chondrocytes. Association with a down-regulation of SOX9 expression. J Biol Chem. 2003;278(5):2903-12.
530. Trabanelli S, Chevalier MF, Martinez-Usatorre A, Gomez-Cadena A, Salome B, Lecciso M, et al. Tumour-derived PGD2 and NKp30-B7H6 engagement drives an immunosuppressive ILC2-MDSC axis. Nat Commun. 2017;8(1):593.
531. Irey EA, Lassiter CM, Brady NJ, Chuntova P, Wang Y, Knutson TP, et al. JAK/STAT inhibition in macrophages promotes therapeutic resistance by inducing expression of protumorigenic factors. Proc Natl Acad Sci U S A. 2019;116(25):12442-51.
532. Yakar I, Melamed R, Shakhar G, Shakhar K, Rosenne E, Abudarham N, et al. Prostaglandin e(2) suppresses NK activity in vivo and promotes postoperative tumor metastasis in rats. Ann Surg Oncol. 2003;10(4):469-79.
533. Sims SG, Meares GP. Janus Kinase 1 Is Required for Transcriptional Reprograming of Murine Astrocytes in Response to Endoplasmic Reticulum Stress. Front Cell Neurosci. 2019;13:446.
534. Puigdecanet E, Espinet B, Lozano JJ, Sumoy L, Bellosillo B, Arenillas L, et al. Gene expression profiling distinguishes JAK2V617F-negative from JAK2V617F-positive patients in essential thrombocythemia. Leukemia. 2008;22(7):1368-76.
535. Damsky W, Peterson D, Ramseier J, Al-Bawardy B, Chun H, Proctor D, et al. The emerging role of Janus kinase inhibitors in the treatment of autoimmune and inflammatory diseases. J Allergy Clin Immunol. 2021;147(3):814-26.
536. Pan J, Deng B, Ling Z, Song W, Xu J, Duan J, et al. Ruxolitinib mitigates steroid-refractory CRS during CAR T therapy. J Cell Mol Med. 2021;25(2):1089-99.

537. D'Alessio A, Del Poggio P, Bracchi F, Cesana G, Sertori N, Di Mauro D, et al. Low-dose ruxolitinib plus steroid in severe SARS-CoV-2 pneumonia. Leukemia. 2021;35(2):635-8.
538. Borg MA, Shalabi RA, Childs R, Wells BC. Alopecia Universalis and Chronic Graft-vs-Host Disease Treated With Ruxolitinib. JAMA Dermatol. 2018;154(11):1357-8.
539. Keenan C, Nichols KE, Albeituni S. Use of the JAK Inhibitor Ruxolitinib in the Treatment of Hemophagocytic Lymphohistiocytosis. Front Immunol. 2021;12:614704.
540. Barrett AJ. Acute myeloid leukaemia and the immune system: implications for immunotherapy. Br J Haematol. 2020;188(1):147-58.
541. Rodriguez PC, Ochoa AC, Al-Khami AA. Arginine Metabolism in Myeloid Cells Shapes Innate and Adaptive Immunity. Front Immunol. 2017;8:93.
542. Dohner H, Estey E, Grimwade D, Amadori S, Appelbaum FR, Buchner T, et al. Diagnosis and management of AML in adults: 2017 ELN recommendations from an international expert panel. Blood. 2017;129(4):424-47.
543. Zhou X, Yang C, Zou Z, Lang X, Chen P, Chen S, et al. ZBTB44-FLT3 fusion in a patient with a myeloproliferative neoplasm. Br J Haematol. 2020;191(2):297-301.
544. Verstovsek S, Komrokji RS. A comprehensive review of pacritinib in myelofibrosis. Future Oncol. 2015;11(20):2819-30.
545. Komrokji RS, Seymour JF, Roberts AW, Wadleigh M, To LB, Scherber R, et al. Results of a phase 2 study of pacritinib (SB1518), a JAK2/JAK2(V617F) inhibitor, in patients with myelofibrosis. Blood. 2015;125(17):2649-55.
546. Spiekermann K, Bagrintseva K, Schwab R, Schmieja K, Hiddemann W. Overexpression and constitutive activation of FLT3 induces STAT5 activation in primary acute myeloid leukemia blast cells. Clin Cancer Res. 2003;9(6):2140-50.
547. Yoshimoto G, Miyamoto T, Jabbarzadeh-Tabrizi S, Iino T, Rocnik JL, Kikushige Y, et al. FLT3-ITD up-regulates MCL-1 to promote survival of stem cells in acute myeloid leukemia via FLT3-ITD-specific STAT5 activation. Blood. 2009;114(24):5034-43.
548. Seedhouse CH, Pallis M, Grundy M, Shang S, Russell NH. FLT3-ITD expression levels and their effect on STAT5 in AML with and without NPM mutations. Br J Haematol. 2009;147(5):653-61.

APPENDIX

Table A1. Role of each shRNA construct cassette (from Cellecta website).

DECIPHER pRSI12-U6-sh-UbiC-TagRFP-2A-Puro-W Vector Features

Feature	Location	Function	Source
Rous Sarcoma Virus (RSV) enhancer/promoter	7 - 233	Allows Tat-independent production of viral mRNA (Dull et al., 1998).	Rous sarcoma virus
HIV-1 truncated 5' LTR	233 - 413	Permits viral packaging and reverse transcription of the viral mRNA (Luciw, 1996).	HIV-1
HIV-1 psi (ψ) packaging signal	569 - 922	Allows viral packaging (Luciw, 1996).	HIV-1
HIV-1 Rev response element (RRE)	1072 - 1370	Permits Rev-dependent nuclear export of unspliced viral mRNA (Kjems et al., 1991; Malim et al., 1989).	HIV-1
U6	1803 - 2064	Human U6 promoter drives RNA Polymerase III transcription for generation of shRNA transcripts.	Human
cPPT	2138 - 2255	Central polypurine tract, cPPT, improves transduction efficiency by facilitating nuclear import of the vector's preintegration complex in the transduced cells.	HIV-1
UbiC promoter	2336 - 2734	Ubiquitin C promoter drives expression of TagRFP and PuroR	Human
TagRFP	2748 - 3458	TagRFP fluorescent protein (Evrogen) serves as an indicator of successful transduction	sea anemone *Entacmaea quadricolor*
2A (T2A)	3465 - 3518	Thosea asigna virus 2A translational cleavage site containing 18 amino acid residues. Cleavage occurs via a co-translational ribosome skipping mechanism between the C-terminal Glycin and Prolin residues, leaving 17 residues attached to the end of copGFP and 1 residue to the start of the puromycin resistance marker	Thosea asigna virus
PuroR	3525 - 4121	Puromycin-resistant marker for selection of the transduced cells	*Streptomyces alboniger*
WPRE	4137 - 4727	Woodchuck hepatitis virus posttranscriptional regulatory element—enhances the stability of viral transcripts.	Woodchuck hepatitis virus
ΔU3/HIV-1 truncated 3' LTR	4734 - 5047	3' Self-inactivating long terminal repeat. Allows viral packaging but self-inactivates the 5' LTR for biosafety purposes (Dull et al., 1998). The element also contains a polyadenylation signal for transcription termination and polyadenylation of mRNA in transduced cells. Required for viral reverse transcription; self- inactivating 3' LTR with deletion in U3 region prevents formation of replication-competent viral particles after integration into genomic DNA	HIV-1
SV40 polyadenylation signal	5104 - 5235	Allows transcription termination and polyadenylation of mRNA.	SV40
SV40 Ori	5265 - 5411	Allows for episomal replication of plasmid in eukaryotic cells	SV40
AmpR	6594 – 7454 (c)	Ampicillin resistance gene (β-lactamase) for selection of plasmid in bacterial cells	bacterium *Salmonella paratyphi*
pUC ori	5835 (c)	pUC bacterial origin of replication.	pUC

** (c): element on complementary strand*

Figure A1. Lentiviral titration on K562 cells.

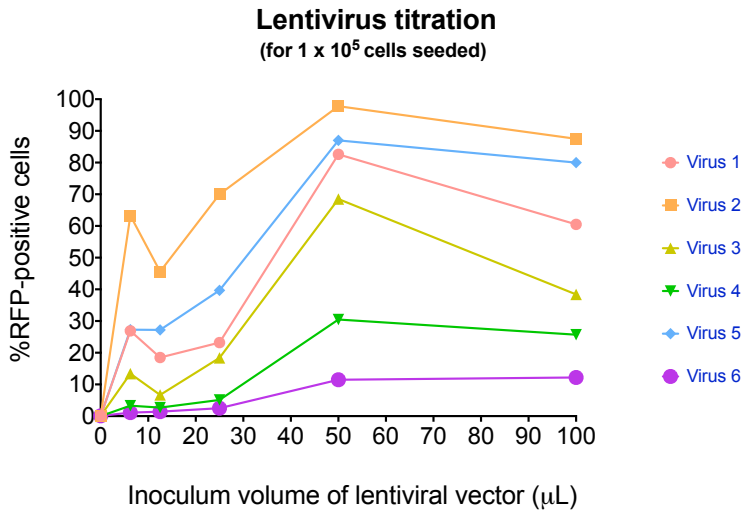

Table A2. List of the 59 genes targeted by shRNAs directed to a sequence no longer part of the mRNA sequence pertaining to that gene in RefSeqGene database

ABI2
ADRA2C
ANAPC1
ATP1B3
ATP4B
ATP6V0C
ATR
BRUNOL4
CCS
CDAN1
CHRNA7
CLK2
CNGA4
CPN2
CRLF2
DDB1
ELSPBP1
GGTL3
GNAT3
GPSM1
GRAP
HIP1R
HLA-DQA1
INPP5A
KCNG2
KLF11
LAMA1
LOC283398
LOC283412
LOC284064
LOC284288
LOC285053
LOC347292
LOC388720
LOC390876
LOC391656

LOC400652
LOC439992
LOC441996
LOC643224
LOC654264
LOC728919
LTC4S
MGAM
MGC5139
MIB2
MUC5AC
NAT1
NR1D2
PDZK1
PSMD12
PTPN9
SDC3
SFTPA2
SLC25A20
THOC4
TIMP2
ULK1
UNC13A

Figure A2. Pooled-shRNA library screen result for the "control" shRNAs for the first replicate in each experimental setting.

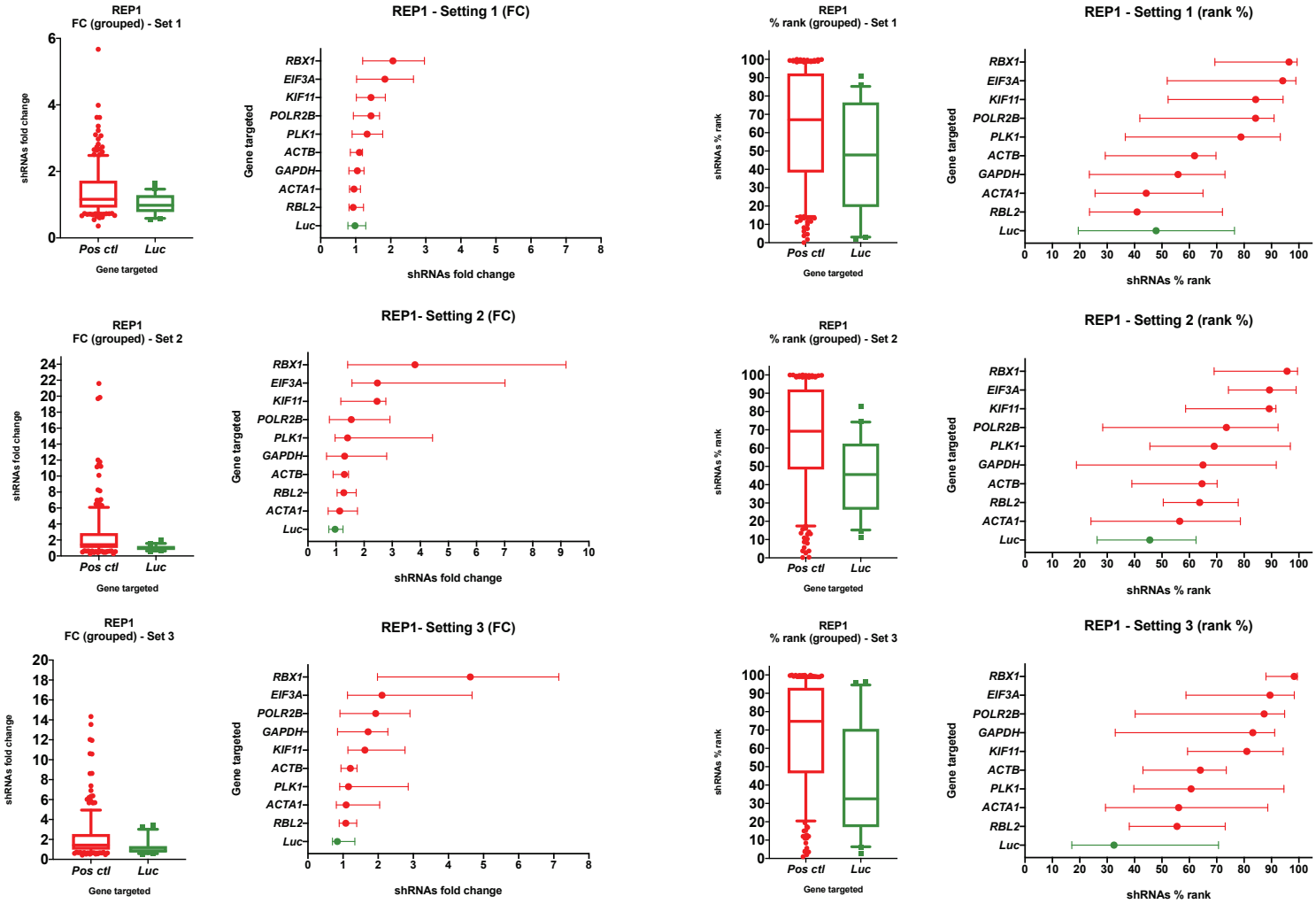

Legend to Figure A2: The figure illustrates the performance of the shRNAs considered to be "control" (as per manufacturer's instructions) in the pooled-shRNA library screen on HEL cells, for replicate 1 (REP1) of each experimental setting (Set or Setting). Each gene was targeted by 21 shRNAs, for a total of 210 "control" shRNAs. The charts on the left half of the image show to the absolute fold change (FC) of the "control" shRNAs compared to the baseline sample (pre-selection). shRNAs are presented either grouped for the "positive controls" (Pos ctl), where the box plots depicts the 10-90 percentile of the results for all the "control" shRNAs and the dots indicate the result for a single shRNA (*Pos ctl*, n=189, *LUC* = 21; the boxes and solid line within them refer to the interquartile interval and the median, respectively); or per each targeted gene, where the dots represent the median (with the interquartile range) of the results for all the shRNAs targeting the gene indicated on the Y axis. The charts on the right half of the image, instead, show the percentile ranking (% rank) of FC of the "control" shRNAs, presented again as grouped or per sets of gene-targeting shRNAs (100% meaning the highest FC relatively to the rank of the total of 27500 shRNAs of the library, 0% meaning the least FC). For both REP1 and REP2 (replicate 2, shown in Figure A3), although *LUC*- and *RBX1*-, *EIF3A*-, *KIF11*-targeting shRNAs behaved on average as "control" shRNAs (i.e. showing a median FC ≅ 1 ["negative control"] or a relatively high median FC ["positive control"], respectively), we found overall an high degree of result variability, especially in the sets of shRNAs targeting the "positive control" genes.

Figure A3. Pooled-shRNA library screen result for the "control" shRNAs for the second replicate in each experimental setting.

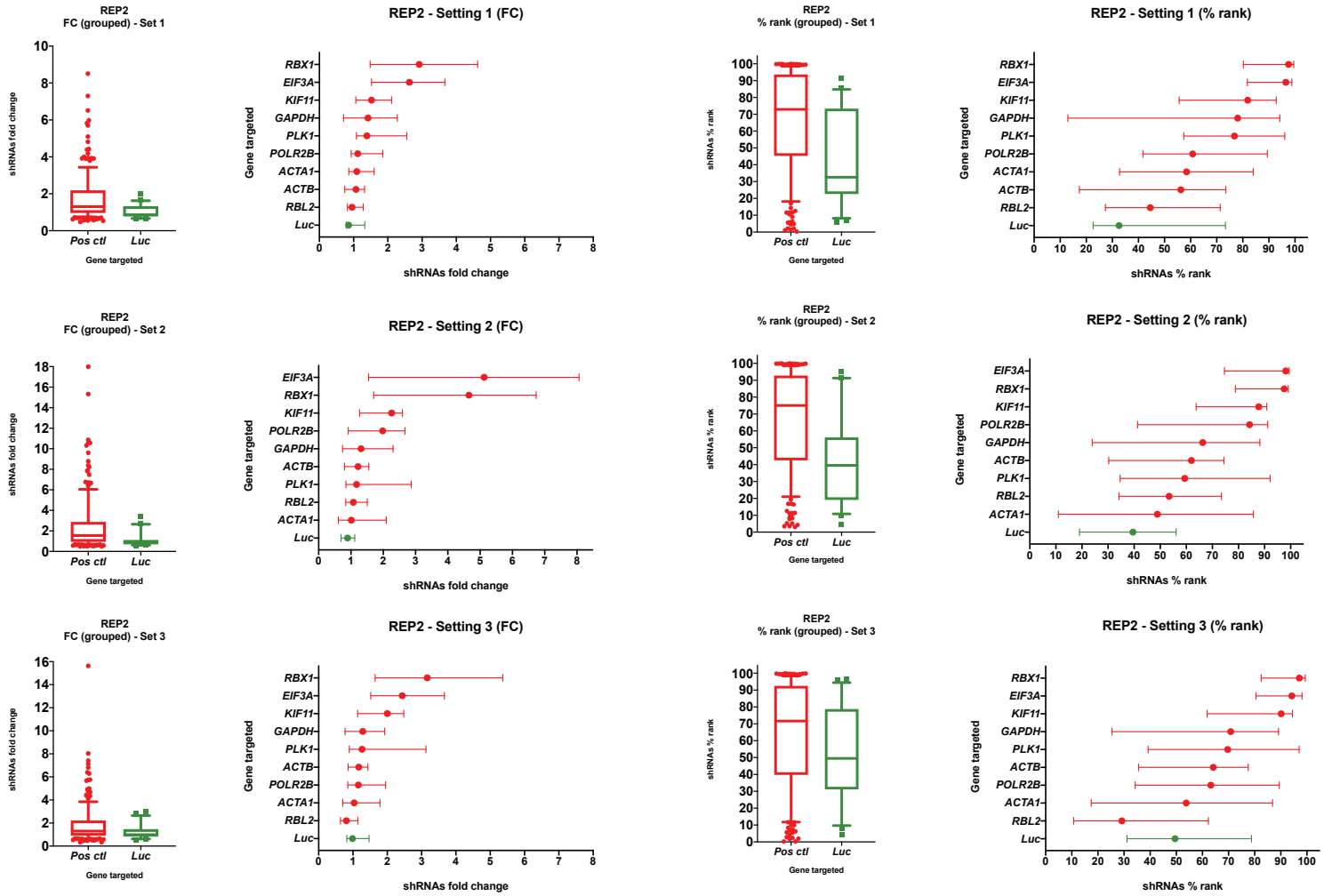

Legend to Figure A3: refer to Legend to Figure A2 (previous page).

Table A3. List of the 96 TaqMan® gene expression assay ID and their disposition in the Applied Biosystems® TaqMan® Array Human NF-κB Pathway 96-well Plate.

Well Position	Assay ID	Gene Symbol
A01	Hs99999901_s1	18S
A02	Hs99999905_m1	GAPDH
A03	Hs99999909_m1	HPRT1
A04	Hs99999908_m1	GUSB
A05	Hs00152939_m1	TLR4
A06	Hs00607866_mH	TLR8
A07	Hs00153133_m1	PTGS2
A08	Hs00153283_m1	NFKBIA
A09	Hs00153294_m1	RELA
A10	Hs00153408_m1	MYC
A11	Hs00155570_m1	IRAK1
A12	Hs00158922_m1	LTBR
B01	Hs00164932_m1	ICAM1
B02	Hs00167248_m1	NOS2
B03	Hs00168392_m1	IL1R1
B04	Hs00168405_m1	IL12A
B05	Hs00169407_m1	RIPK1
B06	Hs00171125_m1	CCL20
B07	Hs00171266_m1	CSF2
B08	Hs00174057_m1	SELE
B09	Hs00174086_m1	IL10
B10	Hs00174092_m1	IL1A
B11	Hs00174097_m1	IL1B
B12	Hs00174103_m1	IL8
C01	Hs00174114_m1	IL2
C02	Hs00174128_m1	TNF
C03	Hs00174131_m1	IL6
C04	Hs00174164_m1	CSF1
C05	Hs00174517_m1	NFKB2
C06	Hs00415849_m1	IKBKG
C07	Hs00176394_m1	IRAK2
C08	Hs00177373_m1	MAP3K7
C09	Hs00177695_m1	MAP3K14
C10	Hs00179410_m1	TBK1
C11	Hs00180403_m1	BCL3
C12	Hs00181225_m1	FASLG
D01	Hs00182082_m1	MYD88
D02	Hs00182115_m1	NFKBIB
D03	Hs00182707_m1	BTRC
D04	Hs00182979_m1	TRAF5
D05	Hs00184186_m1	TRAF2
D06	Hs00185658_m1	ZFP36
D07	Hs00187192_m1	TNFRSF11A
D08	Hs00188486_m1	CD83
D09	Hs00188755_m1	TRAF4
D10	Hs00194638_m1	TRAF1
D11	Hs00196143_m1	MAP3K7IP1
D12	Hs00196470_m1	ENPP2
E01	Hs00231713_m1	CREB1
E02	Hs00231733_m1	CREBBP
E03	Hs00232399_m1	RELB
E04	Hs00233688_m1	IL12B
E05	Hs00234140_m1	CCL2
E06	Hs00234431_m1	NFKBIE
E07	Hs00234713_m1	TNFAIP3
E08	Hs00234829_m1	STAT1
E09	Hs00236937_m1	CXCL1
E10	Hs00237035_m1	TRAF3
E11	Hs00243522_m1	TNFSF11
E12	Hs00265399_s1	PTAFR
F01	Hs00269492_m1	TNFRSF10A
F02	Hs00271977_s1	TLR6
F03	Hs00277234_s1	IER3
F04	Hs00353710_s1	TNFSF15
F05	Hs00413978_m1	TLR1
F06	Hs00364499_m1	CARD14
F07	Hs00365486_m1	VCAM1
F08	Hs00366272_m1	TNFRSF10B
F09	Hs00367225_m1	CARD10
F10	Hs00369830_m1	EDARADD
F11	Hs00152973_m1	TLR9
F12	Hs00383387_m1	NKIRAS2
G01	Hs00384611_m1	NKIRAS1
G02	Hs00394890_m1	MAP3K1
G03	Hs00233284_m1	IKBKB
G04	Hs00418138_m1	IRAK1BP1
G05	Hs00538709_m1	FADD
G06	Hs00182558_m1	TRADD
G07	Hs00603247_m1	ZNF675
G08	Hs00608023_m1	BCL2
G09	Hs00152971_m1	TLR7
G10	Hs00610420_m1	PTGES
G11	Hs00738431_g1	CSF3
G12	Hs00765730_m1	NFKB1
H01	Hs00907779_m1	IL2RA
H02	Hs00184839_m1	BCL10
H03	Hs00968436_m1	REL
H04	Hs00977611_g1	BIRC5,EPR1
H05	Hs00989507_m1	CHUK
H06	Hs01042313_m1	TNFRSF1A
H07	Hs00198984_m1	MALT1
H08	Hs00152932_m1	TLR2
H09	Hs00236874_m1	LTA
H10	Hs00178289_m1	AKT1
H11	Hs00374176_m1	CD40
H12	Hs00152933_m1	TLR3

Table A4. Pooled-shRNA library screen on HEL cell line and MF-3: list of 2nd most depleted shRNAs for each experiment (ranking approach 1, RA1).

	NO ruxolitinib (setting 1)				Ruxolitinib (setting 2)				Ruxolitinib + CM (setting 3)				MF-3			
	Experiment 1		Experiment 2		Experiment 1		Experiment 2		Experiment 1		Experiment 2					
Rank	Gene	Fold change	Gene	Fold change	Gene	Fold change	Gene	Fold change	Gene	Fold change	Gene	Fold change	Gene	Fold change	Rank	Gene
1	CSE1L	4,06154967	PSMD1	8,74263884	PSMA2	12,6655983	RAN	11,6959923	ABCB5	11,4474564	RTF1	9,22238088	EIF5A2	39,91081	71	DDX56
2	RRM1	4,0489743	PSMB2	7,74385383	RPS6	11,953435	PSMC1	9,73018238	PSMD3	9,03286024	PSMB7	8,6017039	CX3CL1	24,9414063	72	NCAM1
3	SNRPN	3,90129433	PSMA2	7,36153258	RAN	11,2537732	PSMB2	9,71953631	PRDX2	8,42763783	PSMA2	8,14061646	CREB3L2	20,6469964	73	PSMB4
4	PSMA2	3,85505597	SNRPN	6,59902018	EIF2S2	10,6065337	PSMA2	9,69127171	PSMD1	8,25842025	RAN	7,60252684	DUSP14	20,3579444	74	GRB2
5	RAN	3,74365697	RRM1	6,34705148	PSMC1	9,2468826	RPS13	9,64890676	ASCC3L1	8,17038045	SNRPN	7,52565368	SCLY	19,6393095	75	PSMA5
6	PSMD1	3,64174345	SNRPD2	6,20506142	TUBA1C	9,08302072	PSMD11	9,06442675	PHB2	8,16537979	RPS13	6,97537328	STAT5A	19,4367129	76	CDC2L2
7	RTF1	3,6076494	HSPE1	5,48603009	RUVBL2	9,04651997	PSMA3	8,95326079	PSMA2	8,08732013	PSMA3	6,86687794	TFPI	18,127799	77	CIRBP
8	PSMB2	3,51276808	TUBA1C	5,4479302	PSMB4	9,02627889	SNRPD2	8,9446861	GATA1	7,99243293	PSMD1	6,46615799	PIGG	17,3360391	78	CCNK
9	PSMA3	3,17906315	RPS13	5,409382	SNRPD2	8,87741259	RRM1	8,64937014	RRM1	7,9440672	RRM1	6,28211745	GRM8	16,9942939	79	NCOR2
10	EEF2	3,02386515	PSMA3	5,12048466	RPL14	8,78645381	HSPE1	8,35751601	RPL11	7,87008932	RPL12	6,12974083	ASNS	16,7478798	80	B4GALT5
11	MPL	3,0162	ASCC3L1	4,91795763	RPS11	8,63593317	INPP4A	8,294707	TUBA1C	7,69098996	RPS3A	5,93561333	MYO1C	16,4059554	81	NPR2
12	RPS13	2,99630927	PSMB7	4,88446673	RTF1	8,60549885	RTF1	7,86842346	SIN3A	7,55295535	SNRPD2	5,87784083	GJD2	16,3641548	82	FMO1
13	SNRPD2	2,94381826	RAN	4,73276488	PSMA3	8,56442241	RPL12	7,70912801	RAN	7,4021948	PSMB2	5,81195395	ICAM5	16,2550515	83	PRDX2
14	EIF2S2	2,86962007	EEF2	4,6217269	PSMD1	8,39708048	ASCC3L1	7,61657012	PSMB2	7,2684541	RPL10	5,68541749	RGS5	16,1300952	84	WNT8A
15	JAK2	2,82783566	PSMB4	4,57312948	PSMD6	7,91334062	RPL4	7,4597753	MPL	7,20391148	PSMC6	5,59909678	SYN3	16,0708956	85	PSMC1
16	RPL12	2,76578647	BCL2L1	4,41621794	HSPA9	7,88638062	EIF2S2	7,38560384	EIF2S2	7,1542251	ASCC3L1	5,48920062	TLE1	15,8082583	86	FOXN1
17	SHFM1	2,68944486	RPL14	4,31201846	RPL12	7,70407747	HSPA9	7,36436	RUVBL2	7,03670962	KPNB1	5,31999254	EIF2AK4	15,7622232	87	SARS
18	NEDD8	2,68837519	EIF2S2	4,30980812	RPS13	7,66920046	MPL	7,30906242	BCL2L1	6,83809651	TUBA1C	5,17348802	FSHR	15,7381013	88	RPS6
19	PHKB	2,68083863	RPL13	4,30431476	ACTA2	7,6241126	FLI1	7,24359589	PSMA4	6,71793612	RPS11	5,16516675	GDF10	15,6243515	89	CAPN5
20	CCNG1	2,67813947	RPSA	4,25893543	PRPF40A	7,55463194	RPS6	7,20037558	PSMB7	6,55395223	RPL8	5,09076812	SULT1C4	15,5469014	90	CIP29
21	ASCC3L1	2,67321691	RTF1	4,20607596	RPSA	7,53921559	PRPF40A	7,03062855	STX1A	6,42380646	RPL11	5,02191138	ATP5G1	15,38057	91	DDX41
22	CDC40	2,67129539	KPNB1	4,12142439	PHB2	7,32421298	OGDH	6,99915291	INPP4A	6,38993514	RUVBL2	4,97133942	KLRK1	14,9867799	92	WNT7A
23	FLI1	2,66855018	PSMD6	4,08096133	ASCC3L1	7,27842657	JAK2	6,86716646	DDX23	6,21969	PRDX2	4,72304881	GNPDA1	14,9806777	93	ALDOC
24	PAFAH1B1	2,66655899	PHB2	4,07918227	EIF1AX	7,26909487	PSMB7	6,85636805	RPS13	6,19113293	PSMA7	4,70266031	ITPK1	14,5299695	94	ATP1A1
25	RPS11	2,66097659	CSE1L	3,9814893	AQR	7,19084498	PDHX	6,83991017	CD247	6,00845436	PSMC3	4,68742262	CASR	14,1681408	95	RPSA
26	ALG10B	2,65587444	RPS6	3,95866933	ALDOC	7,08475891	ANAPC2	6,82858824	TCF7	5,8944393	PRPF40A	4,67284489	SALL4	14,0926578	96	INPP4A
27	RPL11	2,62180995	RPL12	3,7962984	RRM1	6,74711575	PSMD6	6,75653011	RPL12	5,87314451	CDC2L1	4,61330438	PRKG2	14,0611436	97	AVPR1B
28	POLR2A	2,60824286	SLC2A4	3,7877751	CDC2L1	6,73723628	KPNB1	6,73160892	SNRPD2	5,86219949	NEDD8	4,61193254	DNMT3L	13,7878763	98	BLK
29	SHMT1	2,597976	RPL11	3,78426188	POLR2F	6,71413535	RPL6	6,72633744	KPNB1	5,85162026	EIF2S2	4,5243803	PLCE1	13,7420382	99	CDC2
30	GNB2L1	2,59605382	HLA-DQB2	3,7326847	CSE1L	6,63409738	SNW1	6,71339967	PRPF40A	5,7253982	PSMD2	4,47416223	TNF	13,7395217	100	ACCN3
31	PRPF40A	2,58934047	RBM8A	3,70365195	SNRPN	6,62260162	PHB2	6,71129209	SNRPN	5,7203996	PHB2	4,41404792	HSD17B2	13,7028602	101	XPO1
32	RPS3A	2,58736928	CYP51A1	3,64883367	DDX41	6,45038672	SHFM1	6,70992532	GMPPA	5,71033644	CSE1L	4,34346462	FOXC2	13,5937786	102	GPLD1
33	ANAPC2	2,58503781	PRPF40A	3,60697899	GABRA6	6,43581829	POLA	6,59275479	EEF2	5,60672069	SNRPA1	4,31813883	COL4A5	13,5444958	103	STX19
34	RPL8	2,54779226	CIRBP	3,60282408	PRKAB2	6,40102147	RPL14	6,45668814	PSMA3	5,60149888	PSMB4	4,28919323	ATG7	13,4787605	104	EIF1AX
35	GOS2	2,51902471	HSPA9	3,58396954	PSMB7	6,34917376	SNRPN	6,42450622	ANAPC2	5,54294469	HSPE1	4,20823684	PLCG1	13,4174698	105	HNRPK
36	PSMD3	2,51285293	SNW1	3,57224467	SARS	6,34415717	TUBA1C	6,39883195	SNW1	5,51070779	RPSA	4,17936254	FABP2	13,4161426	106	HLA-DQB2
37	POLR2C	2,50544144	NEDD8	3,57166388	RPL10	6,3321979	RPL10	6,19747818	NDUFS2	5,50862821	POLR2J	4,1741096	ALAS2	13,4111874	107	PIGM
38	HSPA9	2,49919567	RPL10	3,56346032	MPL	6,32366361	CSE1L	6,14328901	PAFAH1B1	5,35792422	RPS6	4,09074507	T	13,392588	108	PENK
39	NUDT1	2,49826737	PSMC6	3,53674046	WNT8A	6,30015132	PSMD2	6,12549249	RPL4	5,33575469	PSMD11	4,07468849	RPL13A	12,9848706	109	IL17F
40	PSMD7	2,49615331	CAPN5	3,48979634	FLI1	6,23861641	PSMD1	5,99935695	ACCN3	5,14028197	PSMD6	4,03733475	MAFB	12,8449386	110	RANBP2
41	SNW1	2,48953875	FLI1	3,48604019	DNAJB2	6,23569757	RPS3A	5,97205246	PSMB1	5,06605467	RPL13A	4,02470664	DYRK1A	12,7066877	111	NDUFA10
42	GTF2F1	2,45815088	GTF2F1	3,44959564	PSMA4	6,21259236	RUVBL1	5,89318754	SNRPA1	5,01108048	EEF2	3,94754	LEPR	12,6983456	112	RUVBL2
43	BCL2L1	2,45331051	RPS11	3,43613913	PRDX2	6,16993261	CDC2L1	5,81177549	SUPT6H	4,9998023	ANAPC2	3,93580699	PGM3	12,6601214	113	GNB3
44	RANBP1	2,44026822	PSMD2	3,42784357	PSMB2	6,11532152	NPPA	5,67667981	ATP5C1	4,9391653	PSMB1	3,90903467	KREMEN1	12,608122	114	PSMD4
45	CHPF	2,43166689	EFTUD2	3,36262494	RPL13A	6,09049608	PSMC6	5,57195201	RPSA	4,93549925	SIN3A	3,9037769	SSTR2	12,608122	115	PORCN
46	RPL6	2,4274517	GNB2L1	3,32903742	MAPKAPK5	6,02174714	RPA1	5,55174914	GSR	4,91390359	RBM8A	3,90043497	GLB1	12,5095563	116	P2RY12
47	PSMB3	2,41837633	PRKAB2	3,29637961	ANAPC2	6,02111317	NEDD8	5,54123412	RPA1	4,84941311	RPL4	3,82205321	HPD	12,4586265	117	HSPE1
48	KPNB1	2,40818747	EIF1AX	3,28749045	PSMD11	5,95953349	SULT1B1	5,44122478	RTF1	4,8400844	FLI1	3,7956599	NCF1	12,4109907	118	PSMD2
49	PHB2	2,40587476	SARS	3,28324147	EEF2	5,76656207	AQR	5,42229839	POLR2F	4,81832467	RPL6	3,77994312	CCNA1	12,1565218	119	CA1
50	PSMB6	2,40438862	NDUFS2	3,2744656	PSCA	5,73023292	CDC40	5,41826496	PSMB4	4,81279467	GRB2	3,7652254	FRAT1	11,8837538	120	TLE1
51	PRKCD	2,38571547	ALG10B	3,24954265	RANBP1	5,67733096	BCL2L1	5,35541936	PAG1	4,6683889	GSR	3,75526657	ENTPD5	11,8345586	121	ACTA2
52	RPA1	2,3832499	NDUFA10	3,23944387	SNW1	5,66696174	RUVBL2	5,33850583	PSCA	4,65414604	SNW1	3,71757438	NFATC2	11,7490661	122	CDK6
53	RPL14	2,38238584	RUVBL2	3,2230595	PSMD13	5,63461703	POLR2F	5,24091836	SCN2A	4,61885165	BCL2L1	3,715642	RAD54B	11,7126585	123	GTF2H3
54	NDUFA11	2,37808673	MAP2K5	3,22062571	PLCB3	5,53545081	ACCN3	5,15644341	PKMYT1	4,58140517	AQR	3,69354552	MYEF2	11,6415194	124	STX1A
55	PSMD6	2,3643196	POLR2D	3,21094517	TREM2	5,51440588	XPO1	5,1430034	NEDD8	4,55713302	ABCB5	3,69261561	LDHAL6A	11,5829648	125	MTMR6
56	PSMC3	2,31407419	CDC2	3,20496271	PSMC3	5,43182017	EFTUD2	5,06868066	PSMD7	4,53407324	PSMA4	3,66203132	SULT1A4	11,5731826	126	SUV39H1
57	ALAS1	2,30622213	JAK2	3,17477345	ID2	5,42498222	CYP2F1	5,0589045	PIK3CD	4,52554487	DDX41	3,66110367	CD2BP2	11,4731078	127	RPL4
58	MEF2B	2,30594581	POLR2A	3,16523545	CCL20	5,4131928	CAPN5	5,05475965	PSMD6	4,48607991	PSMD3	3,6604957	CIR	11,4106197	128	SDHA
59	RPL10	2,30523929	CDC2L1	3,16378862	PSMB1	5,32106449	DDX41	5,00764649	RFC5	4,44885542	MPL	3,64104475	DNMT3B	11,3681769	129	C10ORF110
60	RPL13	2,30336509	PSMD11	3,14632794	SULT1B1	5,32039638	PSMB4	4,98526984	PDHX	4,38210466	PSMC1	3,63671475	EIF2S2	11,3025416	130	NCSTN
61	SHMT2	2,29187449	RPS3A	3,12278817	RPL4	5,29004567	ABAT	4,88087698	RPA3	4,36211266	CAPN5	3,62272718	FGL2	11,3025416	131	GPR35
62	CDC2L1	2,2891737	POLA	3,10995604	GATA1	5,16754008	RPS11	4,82711953	JAK2	4,35328579	CCL20	3,61356521	E2F5	11,2774856	132	PSMD14
63	EFTUD2	2,26921956	RPL4	3,04865153	FADS2	5,15388133	ACTA2	4,78600993	SAP18	4,33175936	RPL14	3,58499843	STX19	11,0445319	133	TNFRSF11B
64	PSCA	2,2515437	AQR	3,02950606	EFTUD2	5,14797249	RPL15	4,75932074	HSPA9	4,32249267	ANAPC4	3,52106745	GSTM5	11,0037013	134	OGDH
65	GABRA6	2,25086588	GAP43	3,00602305	CASP12	5,13840811	EIF4G3	4,73612106	EARS2	4,30574125	ACOX3	3,49945009	IFI44	10,8504982	135	SIRT5
66	GSR	2,24762727	RPL15	2,99078461	RPL11	5,11852951	PRDX2	4,71577406	PSMD11	4,28003038	PSMD13	3,46128391	GALNT17	10,7641867	136	ACOX3
67	PSMB7	2,2460858	POLR2G	2,98745942	HNRPK	5,02974049	STX1A	4,71442704	TACC3	4,27951259	HNRPK	3,45624108	DPPA3	10,7447374	137	DCI
68	SIN3A	2,22736864	RPA3	2,98593164	JUN	4,99618751	AMT	4,71315533	NUDT1	4,17836114	POLR2F	3,445631	SEC22B	10,6781531	138	ACYP2
69	NCF1	2,22708755	MPL	2,98064241	CHST7	4,9573215	RIPK3	4,7105478	PSMC6	4,15761783	RPL15	3,44311452	EMX2	10,6201194	139	PSMB1
70	ATP5C1	2,22200163	CDC14B	2,9408383	PSMC6	4,94465815	NDUFA10	4,70086598	HSD17B4	4,15755106	RPA1	3,36817192	NR1D1	10,5382431	140	MYL1

	NO ruxolitinib (setting 1)				Ruxolitinib (setting 2)				Ruxolitinib + CM (setting 3)				MF-3	
	Experiment 1		Experiment 2		Experiment 1		Experiment 2		Experiment 1		Experiment 2			
Rank	Gene	Fold change	Gene	Fold change	Gene	Fold change	Gene	Fold change	Gene	Fold change	Gene	Fold change	Gene	Fold change
71	DDX56	2,21973096	MEF2B	2,93950142	RAD23B	4,94282527	IL12RB1	4,68944869	NACA	4,15654032	SFN	3,36674239	ADRA1D	10,474961
72	NCAM1	2,21898611	HNRPK	2,92155443	PSMD3	4,88745021	RPSA	4,65700008	PSMC3	4,14354014	SHFM1	3,36381606	CDKN1B	10,4653168
73	PSMB4	2,20939374	CDK4	2,90074541	PORCN	4,8739722	SNRPA1	4,62909432	GNB2L1	4,13762216	CD247	3,35852974	C1QA	10,4231486
74	GRB2	2,20704182	SIN3A	2,8928645	IL9R	4,84496244	MAPKAPK5	4,6290844	DDX41	4,07868737	CDC40	3,33950637	CHRM5	10,3903946
75	PSMA5	2,20535935	ANAPC2	2,88475384	BCL2L1	4,8393485	SYNGR1	4,61377335	TLR2	4,02770015	EFTUD2	3,31589587	H19	10,3318157
76	CDC2L2	2,19822185	POLR2F	2,87331587	SOS1	4,65791936	GALNTL4	4,59427833	PROM2	4,01962902	COL8A1	3,27198132	NAT6	10,28516
77	CIRBP	2,18773134	PSMC3	2,8724445	IL1A	4,64987148	LAMP2	4,56482296	PAPOLA	3,98387717	DNAJB2	3,27120438	RARB	10,2250404
78	CCNK	2,17821594	RANBP2	2,87182326	SUPT6H	4,64521568	CDC2	4,56089351	CSE1L	3,9739665	NPPA	3,25429549	MMP14	10,0549294
79	NCOR2	2,16593453	OGDH	2,86714478	ACOX3	4,63372422	EEF2	4,51498288	OSBPL3	3,94693834	OGDH	3,24000472	RAP1B	10,0154105
80	B4GALT5	2,16164881	ZMYM2	2,86602429	PSMD2	4,60518645	CCL20	4,49661103	WNT7A	3,9258574	SAP18	3,20278353	SPP1	9,96014419
81	NPR2	2,15729224	PPP2R1A	2,86328336	CDC40	4,59795862	PSMA4	4,4910935	AQR	3,91301832	ACTA2	3,19955175	UBE2E3	9,95817608
82	FMO1	2,15638394	PSMC1	2,83403213	RPA1	4,59416522	SARS	4,48156299	CDK4	3,88884506	RAD51	3,19088882	SSTR3	9,86487314
83	PRDX2	2,15182032	INPP4A	2,83051698	NDUFS1	4,58427264	C7ORF16	4,47569774	RPL13	3,88296059	JAK2	3,1863599	VCL	9,85951406
84	WNT8A	2,15156962	CA1	2,82503547	RPL6	4,58304713	DDX23	4,4534859	PAF1	3,86398945	PSMB6	3,18053881	GTF2F1	9,84386404
85	PSMC1	2,14808422	DNAJB2	2,82114645	PSMA7	4,54899554	MEN1	4,4346376	RPE	3,85921962	RUVBL1	3,1621595	MYST3	9,82640804
86	FOXN1	2,14718235	XPO1	2,80449049	RPL8	4,54058087	ATP5C1	4,4163872	FLI1	3,8460078	NDUFA10	3,1463405	HLA-DQB1	9,77029855
87	SARS	2,14302865	ATP5L	2,79997094	ACCN3	4,52501161	SHMT1	4,34530001	HSPA12A	3,80619591	PTPN7	3,09562739	IL13RA1	9,76939986
88	RPS6	2,13921774	NSMCE2	2,78440941	PAX2	4,52193149	EFNB1	4,27893655	TLE1	3,79690876	SARS	3,09431281	UBE2L6	9,73025526
89	CAPN5	2,13605126	PSMD3	2,7796289	PSMD7	4,50718289	SIN3A	4,26000655	WNT8A	3,79447983	CYP51A1	3,07258797	ST3GAL6	9,60186935
90	CIP29	2,13083027	GRM5	2,77570509	CLDN2	4,46362504	IARS2	4,21644957	DNAJB2	3,78678823	ITK	3,06900646	ST6GAL1	9,58358336
91	DDX41	2,13038309	H19	2,76587151	RBBP4	4,45442809	NACA	4,20383773	FANCG	3,7636468	POLR2I	3,05317969	RAB4A	9,52940573
92	WNT7A	2,1303048	PRDX2	2,762206	CLYBL	4,42286142	GALNT3	4,17202553	CARS	3,73873189	RPL13	3,0524244	RPL12	9,50745425
93	ALDOC	2,13012091	CDC40	2,75165469	IARS2	4,41930481	EIF1AX	4,15103496	IL28B	3,73731695	ST3GAL1	3,01823021	PIGO	9,50348935
94	ATP1A1	2,12781442	RPA1	2,74920462	HSPE1	4,37437458	ABCB5	4,13502242	GTF2IRD1	3,72204091	PDHX	3,00737454	SPRY4	9,48549682
95	RPSA	2,12273847	PTPN7	2,74538427	CLEC5A	4,36184209	RANBP1	4,13319594	HRAS	3,71770142	SULT1B1	3,00386702	PES1	9,43834393
96	INPP4A	2,10384285	PAFAH1B1	2,74400762	AKAP13	4,31253604	IL28B	4,10721088	RPL14	3,7029006	HK2	2,99820269	GPAM	9,42542301
97	AVPR1B	2,09971725	HRAS	2,73734075	CCNK	4,30361616	RPL11	4,08484272	PSMD2	3,67402149	TUBE1	2,98523435	JUP	9,42180508
98	BLK	2,09951798	LAMP2	2,73247933	EIF2S1	4,27581367	HNRPK	4,08085496	RPS11	3,6577997	CUGBP1	2,97672594	FLNA	9,40945288
99	CDC2	2,09364678	IGF2R	2,6972906	FARS2	4,24758073	P2RY12	4,07907839	PSMC1	3,64037888	KARS	2,97662074	ALS2	9,3168731
100	ACCN3	2,08749545	FIGF	2,69610309	SNRPA1	4,22852415	RBM8A	4,05992128	RIPK3	3,624656	PAFAH1B1	2,95968169	RAC2	9,30977565
101	XPO1	2,08615757	POLS	2,68897516	DDX23	4,20895748	COL9A3	4,05909825	CYP51A1	3,61818875	MAPKAPK5	2,95095185	ANKFY1	9,30617237
102	GPLD1	2,08050541	EFNB1	2,68876176	SHFM1	4,20440267	PSMD3	4,0386304	TUBG1	3,58306301	TNNT1	2,94457454	IL28RA	9,28648092
103	STX19	2,07801861	SHFM1	2,67944756	POLR2D	4,2018248	PSCA	4,02749123	EFNB1	3,55810643	PTGER1	2,93305651	HRK	9,25688954
104	EIF1AX	2,07443546	TNNT1	2,66880445	RBM8A	4,19946519	IGF2R	4,01183066	PPP2R1A	3,55020096	EIF4G3	2,927763	CA12	9,25549145
105	HNRPK	2,0730081	DTNBP1	2,65597229	CAPN5	4,18002584	GTF2F1	4,00488794	SMC4	3,54444002	PFKFB3	2,91844034	CHRNA6	9,25427273
106	HLA-DQB2	2,07009575	LOC402057	2,65545482	ENG	4,17587476	KARS	3,97628783	XPO1	3,53596317	BHMT2	2,91381555	YES1	9,10037234
107	PIGM	2,06872849	RIPK3	2,65514339	LCK	4,17507854	PSMA7	3,95382655	RELB	3,53246378	API5	2,89514176	CCNG1	9,06764346
108	PENK	2,06859885	PDHX	2,64846451	WNT3A	4,16157595	GTF2A1L	3,95342457	RPL13A	3,52178002	GTF2F1	2,87379325	SNIP1	9,02560518
109	IL17F	2,0670617	ACTA2	2,64000226	NDUFA10	4,156367	PSMC3	3,94717385	EIF1AY	3,52169513	CDC2	2,85882373	GDF3	8,93560477
110	RANBP2	2,06537307	GALNTL4	2,63663416	COL24A1	4,13018014	EDNRA	3,94689392	CYP2F1	3,51680793	BMPR1A	2,84472592	CACNA1F	8,84615261
111	NDUFA10	2,06442713	CDC2L2	2,62630795	LRP8	4,12919991	GBP1	3,94221898	CDC14B	3,50447832	FOXP1	2,81802274	SLC33A1	8,83616182
112	RUVBL2	2,05845019	CAV3	2,6198601	OGDH	4,11634421	ACOX3	3,93103067	HSPE1	3,49270973	TOLLIP	2,81753859	HNRPK	8,75024529
113	GNB3	2,05324713	NDE1	2,61472995	NDE1	4,10571902	NCAM1	3,91563252	RPL10	3,48909865	IL10RB	2,81697458	NFE2L2	8,73057118
114	PSMD4	2,04991003	PSMA4	2,60576006	ALG10B	4,09465501	CIRBP	3,89951457	RUVBL1	3,48223088	OPRM1	2,8132104	ARRB1	8,71477841
115	PORCN	2,04926983	ITK	2,59924161	TNFRSF11B	4,08241153	TCF7	3,87681591	KARS	3,48068239	ACCN3	2,78741342	EMP1	8,71477841
116	P2RY12	2,04568993	MTHFD1L	2,59873292	GBP1	4,07896924	CLDN2	3,87033248	HNRPK	3,47044032	SLC9A1	2,78297571	OPRM1	8,69886121
117	HSPE1	2,04333419	RPL8	2,59457359	PTPRC	4,07325919	BNIP1	3,86373741	EFTUD2	3,46408567	FBL	2,75696656	PPP1CC	8,69178364
118	PSMD2	2,03461788	ACOX3	2,58942356	BUB1B	4,06688573	CAV3	3,86319194	RBM8A	3,46371276	SPTLC2	2,74853676	POLR2K	8,68138948
119	CA1	2,03427554	ABCB5	2,58875722	RPL15	4,06596808	RPL13	3,86038637	RPL6	3,45818182	NACA	2,73250833	FRMD8	8,65309857
120	TLE1	2,03311736	MYL1	2,57877579	CYP2F1	4,04479447	WNT8A	3,8518311	CIRBP	3,45276495	GALNT3	2,72457258	TUBA4	8,63570876
121	ACTA2	2,03165716	SAP18	2,56589769	CA1	4,02051707	SLC2A4	3,83452803	CDC2L1	3,41950603	CD226	2,71767563	GPX1	8,61333558
122	CDK6	2,02730343	ATP2A2	2,55421212	GRM5	4,01007856	RANBP2	3,81589921	SLC9A1	3,41874177	DDX23	2,70641771	MYF6	8,50532484
123	GTF2H3	2,01517996	CASP12	2,54470974	JAK2	4,00631661	PSMD13	3,78719858	ZMYM2	3,41199874	ENG	2,69447283	ADH1B	8,44177739
124	STX1A	2,01290531	HNRNPC	2,54386087	OSBPL3	4,00206144	NDE1	3,77687286	FH	3,40976496	MYCBP	2,69428486	AP3B1	8,4348715
125	MTMR6	2,01169667	AK2	2,53328926	SRP19	3,99256258	POLR2A	3,76788777	PSMC2	3,39401883	CFD	2,69283006	GAB1	8,40279444
126	SUV39H1	2,01096121	SPTLC1	2,5268564	DEFB4	3,98358689	PSMB1	3,75905611	GBP1	3,37408268	HELLS	2,69160113	YAP1	8,38212208
127	RPL4	2,00748359	CTNNA1	2,51645354	EARS2	3,976245	UGT1A7	3,75199084	MTFMT	3,36984956	CCNK	2,6905073	GFPT2	8,36053891
128	SDHA	2,00362559	VAMP1	2,51565601	SNCB	3,94556546	PSMA5	3,74956647	POLR2A	3,36244748	CD151	2,68838641	CLDN19	8,26532217
129	C10ORF110	1,99736618	WISP1	2,51425881	NLN	3,94367879	RPS6KB1	3,74871432	NSMCE2	3,35071718	PRTN3	2,6847677	ABCB5	8,19469357
130	NCSTN	1,99584499	RPL13A	2,50771236	KARS	3,91059366	VAMP1	3,74773648	BUB1B	3,34878685	POLR2A	2,68458281	SIRT5	8,16078079
131	GPR35	1,99541078	RFC5	2,50652046	INPP4A	3,89373685	DNAJB2	3,74452608	SPAM1	3,33658412	PIGX	2,6817536	CBR1	8,15441672
132	PSMD14	1,99520718	UCN	2,50041907	RIPK3	3,8923947	TSLP	3,72585912	SCN8A	3,32342315	C7ORF16	2,67795561	GAB2	8,13533389
133	TNFRSF11B	1,99439695	POLR2J	2,48854198	CTNNA1	3,88025067	ARHGAP5	3,71641478	CDC40	3,31936204	GAP43	2,67757582	PPP3R2	8,1256677
134	OGDH	1,99267828	NCOR2	2,48412921	PPP2R1A	3,84270648	PIGX	3,68657737	CALM2	3,28193486	FVT1	2,67713792	MAN2B1	8,07480705
135	SIRT5	1,99260776	CLDN2	2,48353462	APOA5	3,83038004	SCTR	3,67070054	CARD14	3,2737328	DEFB4	2,67396494	TOP3A	8,05880239
136	ACOX3	1,99055723	DDX50	2,48161899	EFNB1	3,82176757	SAP18	3,6619411	EIF4G2	3,2545931	CALM2	2,67169621	GAA	8,02481878
137	DCI	1,9882161	WNT7A	2,47915721	TKT	3,81750115	CAPNS1	3,65984026	ITK	3,22745722	SOX2	2,66795337	PIK3CB	7,99441105
138	ACYP2	1,98539107	CCNG1	2,47381

Table A4. Pooled-shRNA library screen on HEL cell line and MF-3: list of 2nd most depleted shRNAs for each experiment (ranking approach 1, RA1).

	NO ruxolitinib (setting 1)				Ruxolitinib (setting 2)				Ruxolitinib + CM (setting 3)				MF-3				NO ruxolitinib (setting 1)				Ruxolitinib (setting 2)				Ruxolitinib + CM (setting 3)				MF-3	
	Experiment 1		Experiment 2		Experiment 1		Experiment 2		Experiment 1		Experiment 2						Experiment 1		Experiment 2		Experiment 1		Experiment 2		Experiment 1		Experiment 2					
Rank	*Gene*	*Fold change*	*Gene*	*Fold change*	*Gene*	*Fold change*	*Gene*	*Fold change*	*Gene*	*Fold change*	*Gene*	*Fold change*	*Gene*	*Fold change*	*Rank*	*Gene*	*Fold change*	*Gene*	*Fold change*	*Gene*	*Fold change*	*Gene*	*Fold change*	*Gene*	*Fold change*	*Gene*	*Fold change*	*Gene*	*Fold change*	*Gene*	*Fold change*
141	MAOA	1,96800826	CCL20	2,46291556	DNAJB4	3,77413839	HES6	3,60993387	TOP1	3,20349689	VARS	2,63671621	COL4A2	7,85428898	211	CTGF	1,83557724	BNIP1	2,24416656	POLS	3,2209958	TCP1	3,18024064	SPTAN1	2,74646136	MYF5	2,41260382	LMNB2	6,39690054
142	GATA6	1,96592248	TLR9	2,46278302	FH	3,76709024	B4GALT6	3,59731622	ARFIP2	3,20306703	POLR2D	2,63525265	NSF	7,84703065	212	AKAP12	1,83232391	GPR45	2,24365863	EIF1AY	3,31689342	APEX2	3,17491419	NAIP	2,74362956	ODC1	2,41171443	SMARCD1	6,38314688
143	PSMC6	1,96288242	PORCN	2,45810136	RAD21	3,761313	NLN	3,595273	CAPN5	3,18828706	RUNX1	2,63057866	PEMT	7,81818832	213	AKAP4	1,83212662	NAT2	2,24318305	EIF2S3	3,31262722	LDHC	3,17284167	TNFSF8	2,74084321	EPS15	2,41091272	BAG5	6,37642474
144	HPSE2	1,96264658	DDX41	2,44497561	PIGX	3,7510934	GNB2L1	3,58533034	CTNNBIP1	3,18602209	GK2	2,62770398	ZBTB32	7,81383015	214	FGFR3	1,83118598	MAPKAPK5	2,24032944	PIK3C2A	3,31218159	BLK	3,17137278	TAL1	2,73270036	KCNA4	2,40751121	NRAS	6,36884613
145	POLR2G	1,9606323	ACTR2	2,44018813	CFB	3,74507806	GTF2B	3,57712419	EDNRA	3,18002069	RAPSN	2,62275791	TUBB2C	7,80459774	215	TCF7	1,82969109	TUBE1	2,23263147	HYAL2	3,30239838	RFC5	3,1676724	CHRNA10	2,72066151	RETN	2,40541168	GRK1	6,3568096
146	EIF1AY	1,95678525	NR4A1	2,44017364	MGMT	3,74166683	TSG101	3,56763717	POLR2J	3,17878134	GATA1	2,62106886	GRIN3A	7,79240216	216	CDC37	1,82327811	TOB1	2,23142228	SPTLC2	3,2908429	GATA1	3,1669807	ALDH1A2	2,71997587	CLDN22	2,40409312	ATP6V1B2	6,33791261
147	NR4A1	1,95552582	DAAM1	2,4354255	EIF4B	3,74034995	WNT7A	3,54524832	OXSM	3,17765586	IGF1R	2,61902364	TUBA3C	7,77643803	217	NSF	1,82289692	DDX56	2,23141925	UBE1	3,28675873	HDAC3	3,1611504	SLC6A1	2,71811956	TNFSF8	2,40191085	TCIRG1	6,30340123
148	MYCBP	1,95508897	SNCA	2,43533626	TUBG2	3,73937184	B4GALT5	3,53826523	GRB2	3,17244076	POLR2L	2,6152549	LRRC41	7,66211443	218	SOS1	1,82231301	EIF1AY	2,23025501	HARS	3,26231277	ID2	3,15559698	SSRP1	2,71647003	MYST3	2,40016982	SPCS3	6,26394788
149	CARD14	1,95417396	ALDH1A2	2,43325157	GPR35	3,73210504	HSD17B1	3,51756313	ACYP2	3,16174066	EIF4G2	2,61296023	OTX2	7,6596445	219	KCNA4	1,82112039	PPP1R12B	2,22980355	EPS15	3,25955366	PNKP	3,15003235	IL17F	2,7137985	HSF1	2,39481324	APOB	6,25495202
150	NXT1	1,95368353	TYROBP	2,42700554	SUV39H1	3,72287212	CLEC5A	3,51400641	POLA	3,15919664	PSMD7	2,61029033	MMAB	7,64255874	220	ATP5H	1,82070747	GNPNAT1	2,22907297	API5	3,24129512	NT5E	3,14887674	STRA6	2,71244058	WISP1	2,3939685	DAXX	6,21486981
151	MSH6	1,95304335	RPL6	2,42690098	NARS	3,71835378	PSMD7	3,51215037	E2F5	3,15874123	PES1	2,60357255	FUT6	7,60066472	221	GTF2A1L	1,82007511	EIF2S3	2,22891939	FLOT1	3,23975238	PGAM1	3,14196253	HIST3H3	2,71162183	HTR2C	2,39139672	HYAL1	6,20695759
152	FVT1	1,95014052	FBL	2,42641693	IMMT	3,71710975	IL23A	3,51062579	SARS	3,15824378	IDH3B	2,60158139	ATP5L	7,58977226	222	CLTC	1,81877104	MEN1	2,22741617	PSMD4	3,23807849	IL10RB	3,14195419	HARS	2,70959672	TKT	2,38385477	NAPG	6,19954803
153	SRP68	1,95008894	NUDT1	2,42407521	HAT1	3,71386026	CEL	3,50723461	EFNA4	3,15470483	MARS	2,5979205	GDNF	7,57761786	223	CLYBL	1,81614235	CD247	2,22610628	UBE2E3	3,22779007	GFRA1	3,14080752	MASP2	2,70625705	PROCR	2,38368682	HRH1	6,1813887
154	HLA-DQA2	1,93287186	FSHR	2,42142516	NUDT1	3,71152879	DEFB4	3,50706145	NF1	3,12247015	TOP1	2,59658306	IL1RN	7,5620928	224	BCL2L11	1,81605549	ANAPC4	2,22292591	DTNBP1	3,22061566	KCNJ5	3,13341841	RETN	2,70397221	CDK4	2,38315108	MAP3K5	6,1800294
155	TBX2	1,92533687	PSMD13	2,41701546	CEL	3,69601819	STX19	3,50692277	RAD9A	3,12006728	PSMB3	2,59498291	VLDLR	7,55626211	225	ABCA10	1,81506821	DLG7	2,22162094	COL9A3	3,21079681	FUT4	3,13250864	ITGA3	2,70073498	EIF2S3	2,38107732	RAD23A	6,15839542
156	SLC6A12	1,92073953	ATP5C1	2,41614026	CAPNS2	3,6944474	PAX2	3,50564092	OGDH	3,11733349	GPR45	2,5877441	PNPO	7,5480982	226	NEU3	1,81009565	HGF	2,22095074	VAMP1	3,20865328	TLR9	3,12767174	PSAP	2,69426211	DEGS2	2,37933045	SRC	6,15632799
157	PAF1	1,91704554	TACR1	2,41214898	HLA-DQA2	3,68680088	FADD	3,49449557	MAX	3,11644436	SELE	2,57039528	NQO2	7,53245207	227	UBB	1,8086293	EIF4G2	2,21860931	PAFAH1B1	3,20601316	CAD	3,12382118	MAPKAPK5	2,69111534	ITGA2	2,37873431	VNN2	6,13324365
158	CYP2A7	1,91655686	CLK3	2,40909863	PSMC2	3,67390096	RETN	3,48787516	ITCH	3,11481534	RAD21	2,56852955	PRKACA	7,52604763	228	HSPA12A	1,80839262	RUVBL1	2,21469948	KRT17	3,20364511	CCL16	3,11315188	IRF6	2,69012956	CCNG1	2,37786291	TCP1	6,13125774
159	KARS	1,91563162	NCF1	2,39990659	STX1A	3,65564025	GSTA5	3,47817515	RPS3A	3,08629468	ATP5L	2,55846432	KCNA7	7,48647537	229	CYP11B1	1,80443216	STX19	2,211015	TWIST1	3,20314739	PSMC2	3,10773245	HSD17B1	2,68824806	PTGS1	2,37270321	PANK2	6,12610215
160	NACA	1,9149352	ESRRA	2,39701815	RAMP1	3,64058998	POLR2D	3,47480836	HDGF	3,07694334	SMN1	2,55612732	GRK4	7,47352757	230	HTR1B	1,79994364	VARS	2,21002374	MAP4K2	3,19375811	CTSL1	3,10090614	FUCA2	2,68532275	CXCL3	2,37138554	NR1H3	6,11376299
161	GGPS1	1,91207196	PIGK	2,39377263	STXBP4	3,64058998	CD3D	3,47372911	CA7	3,07366428	H19	2,5555431	SIGIRR	7,44049867	231	PAX2	1,798787	USP9X	2,20983119	CDC2	3,19356976	SFN	3,09866596	IGFBP5	2,68249428	WNK1	2,35533773	PRC1	6,11360463
162	COX10	1,90999912	MYST3	2,39116333	PSME1	3,63985539	CD151	3,46859563	CAPNS1	3,06388019	GMPPA	2,55355175	GORASP1	7,38414199	232	HGF	1,7953706	EIF2S1	2,20854153	IGF2R	3,19189933	PTPN7	3,09087332	BMPR1A	2,68183684	FAM132A	2,34573416	RBKS	6,10151902
163	CA7	1,90961122	NR1D1	2,38056541	TNNT1	3,63261273	C15ORF15	3,46763151	ARG2	3,06281021	CCNC	2,54952432	AK1	7,36051055	233	EARS2	1,79328181	CBS	2,20605179	PAPOLA	3,18775304	GRIN1	3,08639031	IFNA2	2,6764207	CTNNAL1	2,34341338	RTN4	6,0804933
164	HS3ST2	1,90664238	HSD17B4	2,37939556	RPA3	3,62844633	FASN	3,46611177	EIF2S1	3,04590835	RANBP1	2,54851971	CD244	7,34854526	234	FLNA	1,79208104	EHMT1	2,20157988	XRCC6	3,17374592	MAP3K7IP2	3,07689332	VLDLR	2,67636738	SLC6A12	2,33857131	MDH1	6,07492949
165	GABARAP	1,90648802	PSCA	2,37049843	ANP32B	3,62415702	APH1B	3,44144038	KRT17	3,01872602	CDC14B	2,54627298	NR3C1	7,33897149	235	C9	1,79199879	ILK	2,19961448	DEFA1	3,17311685	CALM2	3,07340556	DLAT	2,67489685	CHRNA10	2,33802673	FRZB	6,06119763
166	FMO3	1,90582634	EP300	2,36304284	TPP2	3,61792773	MCM6	3,4400021	WNT3A	3,01709302	RPA3	2,54134092	LAMC1	7,33833763	236	JUN	1,79196243	NDUFS1	2,19954485	DIDO1	3,17263772	TRIM14	3,07252433	ALG5	2,67434472	KCNMB3	2,33421058	RSAD2	6,05912804
167	ACOT12	1,90464012	ACOT12	2,3625904	PPP2R5D	3,60911296	COL8A1	3,43858663	CCL3	3,00759129	HCK	2,54106966	NOD1	7,33485916	237	MAT2A	1,7900521	CHPF	2,19775313	KPNB1	3,17174622	IL22RA2	3,06233344	IL4R	2,67410209	IL1A	2,33419991	DMD	6,02136477
168	SAP18	1,90271756	PIGX	2,35660278	HSD17B3	3,60839983	SLC6A12	3,43481924	CCL19	3,00246105	ID2	2,53730876	SLC22A12	7,30305492	238	POLA	1,79002074	HYAL2	2,19725038	PGAM1	3,17083296	CARD14	3,05310414	PIWIL3	2,67299229	APOA5	2,33182451	AVPR2	6,01920858
169	CCL15	1,89859101	TRPM7	2,35512302	GPHN	3,59958245	CDK4	3,43455622	MYL1	2,99458827	L1CAM	2,53538541	COL4A3BP	7,27328022	239	LOC402057	1,78996244	CCNK	2,19706374	CD3D	3,1688999	EIF2S1	3,04341743	IARS2	2,66281328	ARRB1	2,32919229	XRCC2	6,01044041
170	WARS	1,89748986	DDX23	2,3548191	RPS3A	3,59618082	RUNX1	3,42313359	HES7	2,99256629	ALAS1	2,53193969	BNIP1	7,2362935	240	HMGCR	1,78914918	EIF4B	2,19464096	ABCB7	3,16865172	CTSA	3,03835109	LTB4R	2,65316321	COX10	2,32460247	CD69	6,00079809
171	HSPG2	1,89398942	KARS	2,35029255	PDHX	3,5843753	XRCC6	3,42186711	PRPF19	2,99230735	SELP	2,52858758	IL27RA	7,22965564	241	POLR1E	1,78853745	IL17D	2,19406888	VSNL1	3,16659945	PORCN	3,03495356	BLK	2,65151404	PAX2	2,32454029	PTGER2	5,99553421
172	RBM8A	1,8912155	ABAT	2,33955214	CFHR5	3,58109607	AGA	3,41231979	FOXP1	2,99186146	HMGCS2	2,52661356	GNAI1	7,19914354	242	ABCB5	1,78687284	STX1A	2,1933198	NR1D1	3,15124898	SMN1	3,03043529	C1QL4	2,64978488	CTNNA1	2,32049197	PPARBP	5,98676942
173	CHAF1A	1,88893267	INPP5E	2,33564026	FANCG	3,57864728	CYP51A1	3,40458177	UCN	2,95129679	ALDH1A2	2,52532734	PSMC1	7,19021261	243	CLEC5A	1,78618445	IDH2	2,1910162	ITGA3	3,15055375	PLEKHA8	3,02857182	OBFC1	2,64912756	PSMD4	2,31907881	CACNA1D	5,98146166
174	E2F5	1,8887742	GRIP1	2,33480804	COL4A3	3,5779266	NUDT1	3,39562512	ID2	2,93816904	POLR2G	2,51767431	IKZF3	7,17199052	244	RPS6KB1	1,78611977	ADCY8	2,19061621	PSCD2	3,14901716	ISLR	3,02801531	SHFM1	2,64856038	EARS2	2,3181033	CCKBR	5,96194675
175	CDC14B	1,88386851	APOA5	2,33314314	DAD1	3,57017349	DUT	3,38092136	ANAPC7	2,93639232	HGFAC	2,51691616	CGN	7,16886603	245	POLR2L	1,78488332	RPA2	2,1902923	POLA	3,14640302	MYST3	3,02787362	KLRD1	2,64797425	CDK6	2,31149094	IRF4	5,91781009
176	HNRNPC	1,88299988	DDX18	2,33294331	EDNRA	3,5618516	SULT2B1	3,37055123	PPP1CC	2,93412848	P2RY12	2,51466756	MMP10	7,1511876	246	AKAP13	1,78475307	PRKAA1	2,18812468	GSR	3,13773974	PDE6G	3,02685741	PDE6A	2,63952691	NSD1	2,30591408	LDLR	5,90672673
177	IL23A	1,88029398	PSMD7	2,33206518	GRIN1	3,54546304	ZMYM2	3,36653042	CASP4	2,92391648	CHPF	2,51440553	CCR2	7,13772783	247	POLR2H	1,78474958	WNT3A	2,18781257	CSF2RB	3,13189714	WNT3A	3,02014047	BMP7	2,63855971	LDB1	2,30502523	UBTF	5,90565707
178	HLA-DRB1	1,87989603	HNF4G	2,32969751	TUBG1	3,5424622	SOS1	3,3601928	ALDOC	2,92177687	WNT8A	2,51221657	CYP17A1	7,12776921	248	CAV3	1,78441137	RBBP4	2,18741168	SNCA	3,13135554	PRKAA1	3,01508199	FVT1	2,63746412	BMP7	2,3032354	PRIM1	5,89727781
179	EIF4B	1,87881242	GALNAC4S-6S	2,32830737	CANT1	3,53805852	ARG2	3,34634888	FBL	2,91228083	HES6	2,50974069	PRKAR2A	7,12521711	249	B3GALT6	1,78280342	SH3GLB2	2,18634328	IL12RB1	3,1264941	GGPS1	3,00978722	PRKAG1	2,63486032	CANT1	2,30281961	PON3	5,89655745
180	L1CAM	1,87537679	NPPA	2,3271877	GTF2A1L	3,52934846	PTPRB	3,33871734	PLEKHA8	2,90079037	XYLT2	2,50143326	TUBB4	7,10769292	250	DNM2	1,77995115	BID	2,18174107	TOLLIP	3,1234112	EIF4G2	3,00314972	POLR2D	2,63209269	RIPK3	2,30239999	HK1	5,89621501
181	SULT1B1	1,87438127	WNT8A	2,31713096	FBL	3,52102546	GRM5	3,32927782	RANGAP1	2,89567159	NT5E	2,49750297	PTGDS	7,08939295	251	CAPNS2	1,77496108	GPHN	2,1803545	PTPN7	3,11967804	COL4A6	2,99865795	RPS6	2,62980793	EIF4B	2,30231093	OXCT2	5,8791198
182	DNMT3B	1,87379602	LSM8	2,31670347	IL23A	3,51755683	KTN1	3,32679486	ADH5	2,88633123	CHAF1A	2,496015	LEP	7,08633847	252	WNK1	1,77461284	CYP11B1	2,17446125	BMP7	3,11953861	UCN	2,99286782	CCL20	2,62850507	C15ORF15	2,30126624	COL11A2	5,86599401
183	CSF3	1,87130038	COL4A3	2,3136616	AKAP12	3,48766752	HK2	3,31808878	AASDH	2,88084148	WNT7A	2,49539808	PTPRB	7,00597403	253	SNRPA1	1,77445305	ODC1	2,17213382	NEDD8	3,11677734	PPP1R12B	2,98857711	FOXN1	2,6270305	HTR7	2,30050842	INPP1	5,85220332
184	TKT	1,86714039	PRKAR1A	2,30557912	TOP1	3,47940889	IL17F	3,30702835	HNRNPC	2,87907789	CEL	2,49374705	EIF4A2	6,96263632	254	PRKAR1A	1,77335839	GOS2	2,17021223	C1GALT1C1	3,110937	SLC9A1	2,98430346	GDF5	2,62233497	EDG7	2,29962723	NODAL	5,82264532
185	BID	1,86688151	GPD2	2,30363101	OPRD1	3,46518624	MEOX2	3,30112661	CYP1A1	2,87101116	USP11	2,4896797	CTSA	6,94204014	255	HRAS	1,77331359	FABP2	2,16928572	PKM2	3,11030016	HDGF	2,96369935	PDE6G	2,6177005	RANGAP1	2,29929125	AZI2	5,81240173
186	TUBA1C	1,86384114	SNRPA1	2,30172666	SHMT2	3,46297277	HGFAC	3,30067867	AGA	2,87053832	NUP214	2,48661424	AKR1B1	6,92964788	256	TOP1	1,77320439	P2RY12	2,16871955	CDC2L2	3,10562177	CAMK4	2,95913084	NKX2-2	2,61674679	CYGB	2,29457324	NFKB1	5,79333942
187	PTPN7	1,86365008	C15ORF15	2,30169695	MEF2B	3,45402843	NCSTN	3,29956603	TCP1	2,86971928	TUBA4	2,48476864	CD83	6,91295204	257	DCTN1	1,77141906	PRMT5	2,16866735	POLR2G	3,10287565	MAP3K7	2,9576644	KRT1	2,61542192	AVPR1B	2,29449167	GPX3	5,77777403
188	CLK1	1,8617091	IRF4	2,30139062	INHBB	3,44884058	EP300	3,2986278	ATG7	2,85144774	GPD2	2,48299781	SLC6A11	6,90026198	258	CCL1	1,77000649	KCNC4	2,16527978	CMKLR1	3,09706916	WAS	2,94935404	EHMT1	2,61527037	CCL17	2,29127703	MYL1	5,77751726
189	NDUFS1	1,86064836	ABCB8	2,30085648	CIRBP	3,44556781	HPSE2	3,28528405	RPL8	2,84193633	DHRSX	2,4794758	DAG1	6,89031869	259	GRM5	1,76953555	FOXN1	2,16373212	SHMT1	3,09431234	MEF2B	2,94454157	ACAT1	2,6143283	PSMC2	2,29006045	GRWD1	5,76867236
190	PSMA7	1,86034334	XRCC6	2,29871674	PIGT	3,42871386	ENG	3,27660751	ONECUT1	2,84147109	ABCB6	2,46629575	TEP1	6,87865921	260	ATM	1,76707917	ATM	2,16311519	NDUFA11	3,09347845	NCOR2	2,94447694	GCS1	2,60261122	UNC5B	2,28972783	CFHR5	5,76407953
191	NFYB	1,86008656	TUBA4	2,29813921	CIP29	3,41672775	PDE7B	3,27275399	CASP12	2,83929865	DCI	2,46554539	KCNMA1	6,85101931	261	ABCA3	1,76308326	PGK2	2,16151065	NAT2	3,09345005	SPTAN1	2,94212596	TNFSF18	2,60207296	MAP1LC3A	2,28725586	PCSK1	5,75714168
192	VNN2	1,85728516	SP1	2,296871	CAV3	3,41419059	RPL8	3,27189187	PIGX	2,83144982	PRKAB2	2,46004329	IGF1	6,76323439	262	PSMD13	1,76214144	GRB2	2,15807632	WNK1	3,09136475	CNTN1	2,93765138	HIP2	2,59867484	MEN1	2,28201137	PTPN22	5,74747093
193	XBP1	1,85689301	ABCC2	2,29529763	FOXP1	3,40959492	CCNH	3,2677652	ACTA2	2,83016507	PTPRB	2,45899405	ITPA	6,6800863	263	PLD1	1,75704725	RAD23B	2,15779448	VIM	3,08908675	SF1	2,93568258	CA1	2,59388938	ANGPTL6	2,28025879	IL1R2	5,7435886
194	MCFD2	1,85674531	COX5B	2,29265717	CD74	3,40418794	POLR2J	3,26632945	NR1D1	2,82908055	DDX56	2,45453239	CLCF1	6,67349822	264	OCIAD1	1,75670277	LHB	2,15728358	SLC22A12	3,08756977	PRPF40B	2,93247986	FABP3	2,59264641	PYGM	2,2783133	LEF1	5,74303297
195	IARS2	1,85364311	RPS6KB1	2,29170694	PSMB3	3,39783165	DDX18	3,26051243	PSMA5	2,82364379	TLR9	2,45372439	NR1I3	6,65451927	265	ATG12	1,75633097	TOP1	2,15377614	NPY2R	3,06692017	PSCD4	2,932161	GALNT7	2,59176325	CDC2L2	2,27506061	MUS81	5,73723599
196	SC4MOL	1,85083763	PSMB3	2,2907905	C15ORF15	3,38841403	MYL1	3,25588362	ACAD8	2,81853278	CNGA3	2,44877187	PYGL	6,65260305	266	SPTLC1	1,75531214	ANAPC7	2,15210188	ARMETL1	3,05582618	ARF5	2,92898854	SHMT2	2,58851152	PKMYT1	2,27496289	CFHR2	5,70753509
197	NDUFB2	1,84991333	MCM7	2,28721221	HNRNPC	3,38486505	HTR1B	3,24825356	C9	2,81547183	ZMYM2	2,44379302	TANK	6,63841276	267	CUGBP1	1,7537922	ITGA3	2,14902551	GPLD1	3,05329083	RAD54L	2,92836347	LSM8	2,58548261	CLDN2	2,27458543	MAL	5,68463773
198	TUBE1	1,84812359	ACSL6	2,28665714	PTGS1	3,3836799	GPHN	3,24447821	ADSSL1	2,8145996	POLR2C	2,43739747	JPH3	6,61574032	268	SLC22A12	1,75339924	GRIN1	2,14779398	YARS	3,04845262	HOXB6	2,92807988	CCND2	2,58543734	NCK1	2,27447514	POLR2D	5,67408382
199	DIABLO	1,84754056	SULT1B1	2,28360303	CLCN2	3,37038288	GPD2	3,22964327	FASN	2,81144095	HSPA9	2,43724243	COX6C	6,58452162	269	UBE2C	1,7526302	DGKH	2,14736774	HTR2A	3,04692949	DAD1	2,91500823	BCL11B	2,5853064	CDC16	2,27257322	BIN1	5,66687472
200	ABCB9	1,84698088	CDC16	2,27857411	PHF1	3,36944614	SHMT2	3,22467846	ANAPC4	2,80594535	NAT2	2,43469542	MAP3K7IP1	6,57861031	270	KDELR3	1,75191944	THBS2	2,14732209	CD247	3,04652307	ASL	2,91439607	IL1A	2,58386976	CCL15	2,27198787	SLC34A1	5,66252921
201	CYP51A1	1,84694732	IARS2	2,27708199	ODC1	3,36839657	CCNG1	3,22199542	GTF2A1L	2,79549443	GALNAC4S-6S	2,43221491	MTRR	6,57649694	271	PSMD11	1,75120925	SMN1	2,14668914	RANBP2	3,04519354	CDC2L2	2,90723702	ADRA1D	2,58061835	INPP4A	2,271425	ENTPD6	5,65924292
202	PRKAB2	1,84672881	EDNRA	2,27342944	DIABLO	3,36111289	PRMT5	3,2178373	BID	2,78979685	NRIP1	2,43084737	VHL	6,56694134	272	RIPK3	1,75053164	SRP19	2,14195641	HSPB2	3,04194715	RCHY1	2,90720763	NR2F2	2,57661439	PRMT5	2,27080067	MCHR1	5,65506189
203	RAD9A	1,84633747	CHST7	2,27052353	GNB2L1	3,35831649	ALG10B	3,21647865	CHST7	2,78430495	RPS6KB1	2,43007054	BCL2	6,56465845	273	GRIP1	1,74978632	GTF2H1	2,14175316	CDC16	3,03947935	EARS2	2,90270182	B4GALT1	2,57606715	CAV3	2,26851689	ITGB7	5,6379405
204	ANP32B	1,84513807	SMARCC1	2,26958949	GMPPA	3,35530941	BID	3,21636846	LRRC41	2,78190358	CIT	2,42846335	KDR	6,51690091	274	ALPP	1,74946815	PDE6G	2,14128342	GPD2	3,03847933	BMPR1A	2,90199128	POLR2G	2,5751304	NGB	2,2682946	RAB27A	5,62415167
205	GPR45	1,8419198	ACADS	2,26698618	DAAM1	3,35427755	CARS	3,21328305	HSF1	2,76829169	PSMA5	2,42639403	PICALM	6,49705104	275	ACADS	1,74496007	PIK3C2B	2,13778965	NXT1	3,0377511	GGA1	2,90180929	GOT1	2,57358585	NR1D1	2,26370015	POLR2F	5,62246524
206	INPP5B	1,84161105	NUMA1	2,2640236	GALNT3	3,34940409	HMGCR	3,20874966	PIGK	2,76543305	GRIN2A	2,42346554	CDC34	6,48553662	276	FCGR3A	1,74431243	LDB1	2,13421005	CD207	3,03704194	ARSB	2,89767594	CDC2	2,57150759	STX1A	2,25806797	ATG4B	5,61987164
207	ARRB1	1,84131983	RNF4	2,2638811	UBE2I	3,34435122	EFNA4	3,20492659	PORCN	2,76320188	NR2F2	2,42205677	DISC1	6,45569894	277	CRP	1,74378565	WNK1	2,13375294	CA7	3,03562407	FMN2	2,89672851	NCSTN	2,57081421	CAD	2,25143158	ITGB6	5,61813649
208	PSMA4	1,84102324	CA7	2,26337738	STX19	3,33261626	PRKAB2	3,20430095	CLTB	2,75427837	NDE1	2,42112208	ST3GAL4	6,43346394	278	WDR1	1,7424133	POLR2L	2,13083957	POLR2I	3,03381624	LCK	2,89644631	ARPC2	2,56927932	FLNC	2,24925531	MARS2	5,58104868
209	GRIN1	1,83862877	NT5C1A	2,26045876	HTR1B	3,3282333	GCS1	3,20358533	PSMA7	2,74803081	DPYSL2	2,41883174	MST1R	6,42122563	279	PLCE1	1,74214246	RALA	2,12727397	MCM7	3,03212662	LSM8	2,89399717	PLAT	2,56524501	ALG10B	2,24847172	DDX41	5,54447437
210	HNF4G	1,83848393	API5	2,24440057	LHB	3,32800496	TUBA4	3,19686369	PSMB6	2,74761713	SRP19	2,41595254	FABP3	6,42090745	280	EGF	1,74135629	PYGM	2,12696361	PYGO1	3,02937667	ATP5G1	2,88748593	PSMD13	2,56106115	MGST1	2,24719284	SNAI1	5,53745093

Table A4. Pooled-shRNA library screen on HEL cell line and MF-3: list of 2nd most depleted shRNAs for each experiment (ranking approach 1, RA1).

	NO ruxolitinib (setting 1)				Ruxolitinib (setting 2)				Ruxolitinib + CM (setting 3)				MF-3			NO ruxolitinib (setting 1)				Ruxolitinib (setting 2)				Ruxolitinib + CM (setting 3)				MF-3	
	Experiment 1		Experiment 2		Experiment 1		Experiment 2		Experiment 1		Experiment 2					Experiment 1		Experiment 2		Experiment 1		Experiment 2		Experiment 1		Experiment 2			
Rank	Gene	Fold change	Gene	Fold change	Gene	Fold change	Gene	Fold change	Gene	Fold change	Gene	Fold change	Gene	Fold change	Rank	Gene	Fold change	Gene	Fold change	Gene	Fold change	Gene	Fold change	Gene	Fold change	Gene	Fold change	Gene	Fold change
281	RNASEN	1,74125141	BMPR1A	2,12668112	CIT	3,02236897	CCNK	2,88125445	PRDM1	2,55838017	TFEB	2,24582822	HDAC1	5,53435083	351	NCOR1	1,69578247	CUGBP1	2,03110661	G6PC	2,82422998	WNT1	2,72351836	RING1	2,3870257	ADIPOR2	2,1185358	IFI16	5,03777497
282	SLC9A1	1,74104891	NLN	2,12388018	ATP5C1	3,02181687	IL1A	2,88070701	C5AR1	2,5564044	SUPT6H	2,24506604	BCL2L14	5,53346896	352	PEMT	1,69527786	UBB	2,03066545	ERBB3	2,82292419	LY96	2,72207873	CAMK4	2,38549008	DKC1	2,11720498	NDUFA11	5,03503128
283	AKR1A1	1,74061777	AURKA	2,12261986	ABCA3	3,01857101	ITCH	2,87981864	ANAPC5	2,55482064	LIAS	2,24360079	MAFG	5,53205825	353	KCNJ5	1,69392379	EIF4E	2,02957041	CPSF1	2,8221525	WNT7B	2,72183016	LRP8	2,38354811	GTF2A1L	2,10719798	GFPT1	5,03084715
284	PSMC2	1,74042708	CADM1	2,12113567	ACSL6	3,01836799	CHRM1	2,87574317	CCL17	2,54837268	CARD14	2,24162862	NGFR	5,530958	354	BUB1B	1,6933439	NEK1	2,02944895	FOXA3	2,81418499	CYGB	2,72123716	NDRG2	2,38188166	FANCG	2,10706562	ITGA6	5,02834669
285	API5	1,73978811	ARG2	2,12083913	GTF2H1	3,01672814	PAPOLA	2,8693263	CANT1	2,54396067	HLA-DQB2	2,23955862	NR2F6	5,52826124	355	LXN	1,6913845	RAD21	2,02750615	SAP18	2,81244189	LRP8	2,71879646	IL12RB1	2,37961898	PAX4	2,10617398	RCHY1	5,02707353
286	CAMK4	1,73877194	SPN	2,11996305	RUVBL1	3,01250711	SLC22A12	2,86913555	DAAM1	2,53830533	ITGB1	2,23724304	C9ORF95	5,52161591	356	VSIG4	1,6900047	CDH1	2,02668866	RPL13	2,8118597	FUCA2	2,71771325	SMN1	2,37929829	ATP5B	2,10592906	NACA	5,01567395
287	GNPNAT1	1,73809236	SYNGR1	2,11902519	ESCO2	3,01126479	CD2AP	2,8663262	GRIP1	2,53745444	SUV39H1	2,23372616	FOXA2	5,50030609	357	POLS	1,68965797	CYP21A2	2,02586275	MYBPC3	2,8082787	GRB2	2,71670113	INHBB	2,378783	CA1	2,10542586	CDO1	5,00884517
288	MEST	1,73770466	CFHR3	2,11763688	HEY1	3,00483345	ARFIP2	2,86422868	FLNA	2,5371488	TYROBP	2,23313932	CHST6	5,49653781	358	WISP1	1,6893664	PLA2G1B	2,02552279	EHMT1	2,80385124	PLAT	2,71582083	PHKB	2,3778277	CASP12	2,10356751	PELI2	4,99249326
289	NRIP1	1,7366375	WARS2	2,11753887	MASP2	3,00369267	CAV1	2,85446946	ACOX1	2,52937315	H2AFY	2,23009911	NEDD4L	5,47024616	359	POFUT1	1,68853005	PPP2R5D	2,0218051	NACA	2,80206436	PLCE1	2,7129923	NDUFA10	2,37738016	NOTCH2	2,10212526	MX1	4,97496059
290	CPS1	1,73582291	EDG7	2,11739988	CAV1	3,00172541	GPR35	2,85282166	FOXO4	2,52885537	PKM2	2,22359474	COL13A1	5,46715423	360	TUBA4	1,68775735	TPP2	2,02158288	CDO1	2,80195182	WIF1	2,71253567	GPHN	2,37129141	DKK4	2,10179987	HLA-DPB1	4,9521483
291	FGF9	1,73490844	MYO1C	2,1086159	PKLR	2,9979745	OCRL	2,84724933	TSG101	2,52316676	TACC3	2,22208381	MT3	5,46231495	361	IGF2R	1,68731679	CCNH	2,01945145	ALS2	2,80027406	GNPNAT1	2,71249506	GNPNAT1	2,37093109	GDF5	2,10177852	PHKA2	4,94439475
292	CLDN22	1,73420507	MEOX2	2,10711946	APPL1	2,99672763	SRP19	2,84468833	B3GAT2	2,52285599	GDNF	2,22017214	INPP4A	5,45558316	362	GPHN	1,68715338	PAFAH2	2,01604089	PTK2	2,80004178	CLK3	2,71206986	CYP27B1	2,36842116	GOS2	2,10087346	WDR61	4,9287969
293	NNMT	1,73301066	TFEB	2,10616034	RAD54L	2,99390677	PSMB6	2,84204774	CCNH	2,51638235	MGAT1	2,21884252	SOST	5,4547418	363	EPRS	1,68642228	RANBP1	2,01551773	TLR4	2,79990623	VARS	2,71017603	WNT7B	2,36684919	UBB	2,10086442	BYSL	4,9285731
294	MLL	1,73213825	PAG1	2,10553435	OCIAD1	2,99201468	ALAS1	2,84124156	CREB3	2,51221175	LCK	2,21881471	ADAM9	5,45348147	364	LAT2	1,68539146	SUMO2	2,01333769	PRPF19	2,79986035	GRIP1	2,70645478	TRAF6	2,36264111	NFKBIA	2,098354	IL12RB2	4,9284285
295	CIR	1,73093551	DKK2	2,10456595	TNIP1	2,9887616	PIWIL3	2,8407137	PRKD1	2,51019988	GLI2	2,2133504	HDC	5,4281126	365	NDE1	1,68518196	PIK3C2A	2,01229329	C5AR1	2,79913802	PTGER1	2,70638541	CD19	2,35607225	CD81	2,09787691	MCM10	4,92260521
296	TGFBR2	1,73058528	COL4A5	2,10339713	CCNH	2,98807791	PLA2G1B	2,84023561	GNA13	2,50697303	ATP6AP1	2,21279562	CYP1B1	5,42613661	366	HAT1	1,68361598	NQO1	2,00918393	CES1	2,79409755	CXCL12	2,70584922	PIK3C2A	2,3549708	PAF1	2,09520545	NRG1	4,92171225
297	SCN9A	1,73035869	LTB4R	2,10163735	ANGPTL6	2,98687043	SLC6A1	2,83995869	CGN	2,50589335	NCOR2	2,21196604	CD7	5,41752381	367	MCM2	1,68317627	GGA3	2,00902533	BLK	2,79402278	HGSNAT	2,70435928	DKK2	2,3542435	RAD9A	2,095068	EEA1	4,90459331
298	NLN	1,72925333	MLXIPL	2,10078196	GFRA1	2,98418225	PGM1	2,83459057	APOA5	2,50491464	B3GNT6	2,21137419	ALG14	5,41400711	368	SNX6	1,68285194	AACS	2,00896173	SDHB	2,79099083	TNIP1	2,70055825	PTGS1	2,3541735	RXRA	2,09468578	KLRC2	4,90237429
299	HLA-E	1,72894681	SOCS3	2,10002672	C7ORF16	2,98246718	FOXA3	2,83298866	PELI2	2,49970236	SMARCC1	2,21034272	POSTN	5,41361269	369	RAPSN	1,68224239	CFL1	2,00890676	HOXA11	2,78196643	SUV39H1	2,69917227	MLH3	2,3519865	COL27A1	2,09439152	SUOX	4,90026954
300	RPS6KB2	1,72890087	TSLP	2,09997134	SIN3A	2,98074738	DARC	2,82985794	WNT9A	2,49934864	TPP2	2,20936854	NCAM1	5,41158411	370	DOCK1	1,68176534	EARS2	2,00650915	PRKACG	2,78032522	NXT1	2,69895097	HSPG2	2,35091879	EIF2S1	2,09245915	CDC2L1	4,89919843
301	PRTN3	1,72833941	ALS2	2,09918751	GSTA5	2,97978914	CLCN2	2,82885392	TNKS1BP1	2,4948769	IL17A	2,20738874	MGAT1	5,39765508	371	SLC6A1	1,68169816	DNAJB4	2,00549804	PDHA1	2,77543907	UBE2G1	2,69640704	NCF1	2,35041342	CD3D	2,08828459	KRT17	4,89694987
302	NT5C1B	1,72829113	C7ORF16	2,09805145	SPTLC1	2,97708089	RPA2	2,82341879	POLR2I	2,49481547	EP300	2,2068821	PLA2G4A	5,38470989	372	GK2	1,68062291	FANCG	2,00548162	APH1B	2,77203534	PES1	2,69325507	ACADS	2,350062	GAD1	2,08795545	AHCY	4,88143831
303	MTIF2	1,7281287	DEFA1	2,09765844	EFNA4	2,97238009	BUB1B	2,82030631	COL8A1	2,48710442	XPO1	2,20437931	HMGCS2	5,38164012	373	GALNTL4	1,68052889	RAD51	2,00509254	PFKM	2,76288148	SELP	2,69077115	ADA	2,34946879	ALB	2,08739379	VAV2	4,87193778
304	MVP	1,72764897	B3GNT2	2,09710656	SLC2A4	2,97019645	WISP1	2,81990265	RAD54L	2,48519627	NAIP	2,20412452	PPP1R12B	5,38059269	374	RDH14	1,68034959	GCNT1	2,00458736	PSMA5	2,76165089	CFL1	2,69039584	HGF	2,34570094	SSRP1	2,08264111	CD28	4,86990368
305	NBL1	1,72681722	ARD1A	2,09631772	FMN2	2,96831953	UNC5B	2,81425806	CD58	2,48134446	ALDH1A3	2,2037797	FANCL	5,34172504	375	CARS	1,67911656	AKAP4	2,00292479	IGFBP2	2,76052727	GTF2IRD1	2,68894783	NEU3	2,34450553	LAT2	2,0800952	ZBTB7A	4,86874372
306	HSD17B1	1,72612464	APH1B	2,09482995	IGF1	2,96779868	ABCB7	2,81143291	PTPRC	2,47528813	PPARG	2,19900876	GLS	5,34172062	376	ANGPTL6	1,6781811	IL17F	2,00196069	ARG2	2,7575918	FGFR3	2,68809334	CD52	2,34121731	MEF2B	2,07976637	NOLA2	4,85849419
307	RBKS	1,72574354	PGM1	2,09196604	PSMB6	2,95472157	TKT	2,81083799	CD3D	2,47278087	CIRBP	2,19735288	CLDN10	5,33525126	377	TREM2	1,67815013	C9ORF47	2,00167961	PIK3CB	2,7537294	ADD1	2,68672884	GSTA5	2,34090152	ARRB2	2,07911587	TUBA1A	4,85723659
308	CCL19	1,72551417	CALM2	2,09149822	CS	2,9511693	PIK3C3	2,80870396	CAMK2A	2,47024652	RANBP2	2,19131564	PDE11A	5,32598638	378	FARS2	1,67809165	PDCD2	2,00035595	RRM2B	2,75112258	ESCO2	2,68558747	PAX2	2,33559602	ACSL3	2,07872172	SCSDL	4,85556132
309	GALNAC4S-6S	1,72543393	CAPNS1	2,08465613	PIGK	2,94744003	POLR2C	2,8082693	ATP6V0A2	2,46772266	DEFA1	2,19044753	EIF2B1	5,32425372	379	DNAJB4	1,67688822	KDR	1,99437535	HOXB6	2,74997496	IFI27	2,68464679	FADS2	2,33509434	RBKS	2,07864648	SULT2A1	4,84580567
310	CYP11B2	1,7247937	GALC	2,08441615	GPR45	2,94606631	CLTB	2,80560875	EIF2S3	2,46378257	IDI1	2,18997819	SIRPA	5,32343139	380	HSP90AA1	1,67592787	PYGO1	1,99353943	ITK	2,74627284	LGMN	2,68454098	PSMB3	2,3343079	CAST	2,0766794	PKMYT1	4,84363587
311	CYP2F1	1,72344116	PTPRC	2,08236377	EIF4G2	2,94292096	TNKS1BP1	2,80186781	IGF1R	2,46197482	TRIM14	2,18933793	NME2	5,31887317	381	OSBPL3	1,67590809	STAR	1,99322475	NDUFV2	2,7451126	NTRK1	2,68123158	HEY1	2,33168203	IL12RB1	2,0750766	MGST1	4,83544705
312	VIM	1,72307799	SULT2B1	2,08172483	CTGF	2,93930008	CDC23	2,80047611	EGF	2,46147981	LRRC41	2,18925102	PIN1	5,31426311	382	PPP2R5C	1,67573535	SNX4	1,99240122	MPO	2,74502812	LIAS	2,67795357	RUNX1	2,33112282	EHMT1	2,07427698	TP73	4,82939144
313	AASDH	1,72204994	POLQ	2,08112032	CASP6	2,9382685	COX10	2,79533821	WNK1	2,46036683	IL27RA	2,1887962	TPI1	5,31177564	383	PLA2G7	1,67534822	PIGA	1,99218202	NGB	2,74299636	IDH2	2,67491311	HYOU1	2,32893958	SIRT5	2,07399054	WWP2	4,82813375
314	TFEB	1,72159953	ILVBL	2,07972578	HES7	2,93770351	FARS2	2,79493017	MC3R	2,45944741	POLS	2,18411414	AES	5,29710384	384	RFC1	1,67447252	HOXB6	1,9911171	LAT2	2,74136331	ACCN2	2,67434217	CSF1R	2,32652043	KDELR3	2,07354347	TRAF5	4,82433775
315	ANAPC7	1,72115777	CHAF1A	2,07957898	CRTC1	2,92971674	ANP32B	2,794888	CYC1	2,45673636	HIST3H3	2,18200859	ITGAM	5,28306311	385	RPL15	1,67443129	CIT	1,98952686	MKI67	2,74126889	RPA3	2,67004052	EDG7	2,32508346	SOS1	2,07216077	KL	4,82255771
316	MEF2D	1,71957136	CXCL2	2,07904035	RCHY1	2,9214	ALLC	2,79229619	FOSL2	2,45367584	SH3GLB1	2,18096154	MSLN	5,27484552	386	TNFRSF11A	1,67423474	DTX3L	1,98930138	XCL1	2,73744037	APOL2	2,66674815	MEOX2	2,32416255	BID	2,07175168	FDFT1	4,82188451
317	PSEN2	1,71873748	TOLLIP	2,07792793	PDE7B	2,91743282	C1QC	2,79141755	HOXB6	2,45325784	STRA6	2,18011102	EPHB3	5,27009586	387	SSTR2	1,67394373	SC4MOL	1,98910427	NDNL2	2,7367929	RPL13A	2,66473197	CHAF1A	2,32362577	IFNA2	2,07054026	ACMSD	4,81420964
318	SC5DL	1,71815963	WDR1	2,0765996	TCF7	2,91577941	DOCK1	2,79097308	PRKAA1	2,45272521	PAK6	2,17959561	CASK	5,25582776	388	SFRS12IP1	1,67370971	TRAF6	1,98878702	XPO1	2,73387663	CELSR3	2,66186486	BIK	2,3225627	NNMT	2,06608256	EGR4	4,80634313
319	PPP1R12B	1,71809139	AGA	2,07619372	PPP1R12B	2,91556934	KDELR3	2,78801911	COL10A1	2,45064369	RAD54L	2,17645781	PSMB5	5,25233939	389	PTPRC	1,67242403	FGB	1,98860843	MAP3K7IP2	2,7338175	KCNMB3	2,66073573	DNMT3B	2,31868733	HNRNPC	2,0658938	MKI67	4,78792602
320	FLAD1	1,71654656	PSMA5	2,0746485	CCL3	2,89925653	SELE	2,78593353	TNFRSF11B	2,45047932	MEOX2	2,17576365	GPR132	5,24787883	390	TBK1	1,67204636	PER1	1,98578391	IFIH1	2,73344241	CHAF1A	2,65451714	NNMT	2,31849446	CLOCK	2,06449272	GLI3	4,78776018
321	MSTN	1,71647258	SUCLG2	2,07088291	APOBEC3F	2,89410429	MMAB	2,7810018	PSMD4	2,44707517	COL24A1	2,17402002	GALT	5,24627221	391	STAR	1,67204445	PIK3CB	1,9852475	PCYT1A	2,73132503	BACE1	2,65330145	POLR2K	2,31660323	CYP2A7	2,06373549	VCAM1	4,78676668
322	POLR2J	1,71589793	PTPRH	2,06978253	PDE6G	2,88633737	PAF1	2,77864986	ATP1B1	2,44504355	TRADD	2,17388745	SMC4	5,2393064	392	TCF7L1	1,67113182	WNT7B	1,98493352	CCNG1	2,73110218	HAT1	2,65253371	PRKAA2	2,30611864	ANXA4	2,06179087	CAPN5	4,78414821
323	CCL20	1,71574432	PSMA7	2,06964073	PTGDR	2,88350901	CDC14B	2,77615049	GAD1	2,44080298	XCR1	2,17249679	ATP12A	5,21578023	393	PDE7A	1,67110255	HTR1B	1,98188441	ACOX1	2,72964309	BBS2	2,64623221	B4GALT5	2,30486483	BNIP2	2,06071269	SLC18A1	4,78303716
324	CCR2	1,71534963	TNFRSF11B	2,06508269	RANGAP1	2,88261073	MAX	2,77489319	HSPB2	2,43605564	XRCC6	2,17132691	ARHGEF7	5,21569745	394	PSMF1	1,67101478	RUNX1	1,98183107	CHRND	2,72878088	CHST7	2,64501608	H2AFX	2,30441914	DCTN1	2,06012561	ACTR2	4,77808697
325	APPBP2	1,71368048	GOSR1	2,06479648	RPS6KB1	2,88008365	CCL15	2,77454379	SOS1	2,43441645	MC3R	2,16956434	CUL2	5,20839497	395	ACCN2	1,66986378	OPRM1	1,97888347	E2F5	2,72784687	CCL17	2,64438359	POLS	2,3042113	LRP8	2,05922861	RPL6	4,77350601
326	DGKH	1,71313647	ARL4D	2,06445855	PF4	2,87756958	CLYBL	2,76768377	CHRNE	2,43356049	INPP5E	2,16919456	PCSK2	5,20586924	396	AKT3	1,66951755	ABCB7	1,9788728	PIK3R3	2,72237483	LEP	2,64423279	MTHFD1L	2,30161054	PSMD14	2,05824088	DCI	4,76565836
327	ATIC	1,71258718	FLNA	2,06397403	FGFR3	2,87710209	CTNNA1	2,7661227	PES1	2,42591042	ABAT	2,1688395	PLD3	5,20206445	397	CYC1	1,66813213	IFIT3	1,97770331	UNC5B	2,71902778	CUGBP1	2,63852088	C1GALT1C1	2,30128332	SHMT1	2,0580216	FAS	4,7591016
328	BMP7	1,71249355	FARS2	2,06167174	WAS	2,87646212	COL5A2	2,76470213	PRTN3	2,42552428	GOSR1	2,16505101	FUT8	5,198698	398	ABCB8	1,66670214	REXO2	1,97666482	ACADS	2,71875967	GPR45	2,63644937	DDX56	2,3008387	GALC	2,05324101	CLDN2	4,75052727
329	TNFSF4	1,71022013	GSR	2,06102929	MCM2	2,87500379	CASP6	2,76382993	CIT	2,42251933	HARS	2,15768721	OPRS1	5,18156738	399	CD226	1,6659594	ATP6V0A2	1,97616692	CDX4	2,71669648	PPP2R1A	2,63558281	GPR45	2,30000816	GPHN	2,05311187	HTR6	4,74007891
330	RBL1	1,70822558	PRTN3	2,05909943	AREG	2,8741694	DNMT3L	2,76283685	TUBA4	2,42015129	RABGAP1L	2,15618521	RPS6KA1	5,18156738	400	OPRM1	1,66570903	CDC27	1,97531172	CDK7	2,71264344	FBL	2,63378483	NR4A2	2,29613424	FUCA2	2,05060473	CDH2	4,73466046
331	GRIN3A	1,70795924	NAGA	2,05224728	NEK2	2,87334604	TNNT1	2,76276285	CRTAM	2,41998984	GBP1	2,15322159	AHR	5,18140047	401	MAPK9	1,66413106	DHRSX	1,97443766	ALB	2,70949525	PIGK	2,63361419	LMO2	2,29596094	HSD17B4	2,04940206	RAD18	4,73224824
332	FABP2	1,70782295	WDR79	2,05070819	HSF1	2,87309327	CIR	2,76207165	CALB1	2,41983995	ATIC	2,150736	ARG1	5,17802999	402	IGFBP3	1,66295832	NACA	1,97223859	TNFSF8	2,70519092	TYROBP	2,6334241	CYP11B1	2,2920718	PTK2	2,04707678	ARHGDIA	4,73190309
333	ESCO2	1,70763055	HSF1	2,04962113	SPRY1	2,86681302	RAD23B	2,76086451	PER3	2,41769469	CDX4	2,1494881	CXCR3	5,17795761	403	NAT2	1,66263538	VAMP7	1,97174872	CXCL2	2,70126697	PSMB3	2,62905175	DNTT	2,29143833	FOXA3	2,04488581	G6PC2	4,72792407
334	WIF1	1,70750265	ALDOC	2,04765703	SPCS1	2,86369792	NPR2	2,75917975	GAS1	2,41157295	UGT1A7	2,14743972	AK2	5,17765047	404	MMRN1	1,66172432	ZFP42	1,96879984	PTPRH	2,69009671	JUN	2,62781674	CAPN1	2,29090022	GNPNAT1	2,04097908	TUBG2	4,72286915
335	MAPKAPK5	1,70682874	PLA2G4D	2,04725485	PAF1	2,86174717	CSTF2T	2,75188682	PTGER1	2,41084902	CYP2F1	2,14292787	ATP6V0E1	5,16753241	405	PRMT3	1,66156586	SHMT2	1,96820576	LGALS1	2,68993268	ABCC2	2,62415887	CDK5RAP1	2,29016619	MEST	2,03924032	SYT1	4,71539611
336	RAD21	1,70474702	HLA-DQA2	2,04625394	DTX3L	2,86081555	NDUFS1	2,75089178	TOLLIP	2,40980218	FIGF	2,13710541	GYS2	5,16641462	406	SUPT6H	1,65992733	TKT	1,96537293	FOXO4	2,68230947	PDLIM4	2,6234527	HTR7	2,28947494	OSCAR	2,03853056	NKX6-1	4,71156621
337	CCL17	1,70455719	PPIE	2,0453385	HAL	2,85961751	ACSL3	2,75055026	GALNT3	2,40976694	GIPR	2,13707013	GBP1	5,14644955	407	FABP7	1,65957196	DICER1	1,96386674	HS6ST1	2,68150147	IL4R	2,62279776	SLC1A2	2,28518113	ENPP1	2,03831919	CTBP1	4,70974793
338	SPRY1	1,70428413	CHST4	2,04491076	CELSR3	2,85834181	CDH1	2,74973456	HK2	2,40954999	APH1B	2,13617006	HCLS1	5,14075506	408	UGCG	1,65921239	MAN1A1	1,96281728	ITGA6	2,68018077	GTF2H1	2,62245941	ACE2	2,28244983	C10ORF110	2,03830369	ASCC3	4,70470981
339	NR1D1	1,70425956	CACNA1B	2,04333849	PPIE	2,85707436	HLA-DRB1	2,74713328	ACE	2,4089357	LHX2	2,13595068	OXSM	5,12506727	409	LDHC	1,65912929	CAPN10	1,96020695	AK7	2,67783215	SSRP1	2,62173393	MCM2	2,2806998	NTRK1	2,0378099	ATP6V1B1	4,70125831
340	NP	1,70424446	IL1A	2,04226016	IL22	2,85668624	HSF1	2,74650211	CD151	2,40079659	ATG12	2,13543546	GRK5	5,11915466	410	VAMP5	1,65636342	RANGAP1	1,95959673	CLTC	2,67760127	CARD10	2,62101983	LCAT	2,27703111	CKMT1A	2,03659532	KLC1	4,68559937
341	MEOX2	1,70235416	ATP5H	2,04125784	AKAP4	2,8552767	CD226	2,74320329	HSF2	2,39827047	KCNJ5	2,13514228	RAN	5,10361516	411	HDGF	1,65619279	PIAS4	1,95806957	CES4	2,67702616	CXCL3	2,62071552	CFL1	2,27465364	AKAP3	2,03497335	FGF2	4,68408019
342	NT5E	1,70192904	ARRB1	2,04077942	RAD9A	2,85300008	EIF4B	2,74104538	SNAP25	2,39578754	PTGER2	2,13291069	G6PC	5,10152247	412	HMGCS2	1,65583121	APPL1	1,95734207	PPAP2B	2,6719424	PI4KB	2,61710309	VARS	2,2729435	REG1A	2,03480184	SOD1	4,67172007
343	KRT8	1,70111762	DNAJC4	2,04025556	EIF4G3	2,85037692	GBL	2,74039708	DDX18	2,39386693	PDE6G	2,13235914	PPARD	5,09903838	413	NAT5	1,65405721	PACAP	1,95722277	TACC3	2,66883283	PDE6A	2,61700943	NOTCH4	2,26918912	DPYSL5	2,03470803	SYNE1	4,66733646
344	ACOX1	1,70083284	CDC37	2,0390566	COX10	2,84905397	RELB	2,73916681	SKI	2,39030596	ATP6V1G1	2,13025611	AKAP5	5,09439564	414	SLC2A4	1,65366059	CD226	1,95683636	UBB	2,66327484	ATP1A1	2,61649068	CENTD3	2,26791002	RET	2,03360547	COL9A1	4,66589888
345	WNT7B	1,70057352	MXI1	2,03818155	NPY1R	2,8421528	REG1A	2,73886786	BECN1	2,3896833	IL23A	2,12845402	IGFBP3	5,08158018	415	RETN	1,65320152	SF1	1,95540514	ATIC	2,66306961	DIDO1	2,61192729	AVPR2	2,26199488	FADD	2,03263357	FLOT2	4,66193609
346	TNFRSF10A	1,70003724	PDE7B	2,03577908	CARS	2,84085733	COL4A3	2,73686473	AOX1	2,38918458	ARHGEF4	2,12598763	EGLN3	5,07759673	416	PSCD2	1,65250653	CCNC	1,95464823	CXCL6	2,6622921	WNT5B	2,60297986	NDE1	2,26003049	PCNA	2,03246567	HIF1A	4,66066146
347	INDO	1,69873354	TNIP1	2,03553535	C9ORF47	2,84014576	HNF4G	2,73665104	MUT	2,38897729	HRAS	2,12411296	A2M	5,07107626	417	DBP	1,65222816	DDIT3	1,95460671	TLR9	2,66148837	C5AR1	2,60120731	RAMP1	2,25791611	MAF	2,03230954	FMO1	4,65582764
348	ONECUT1	1,69847274	LEP	2,03257725	PIK3CD	2,84004634	API5	2,72885666	WNT1	2,38843692	BUB1B	2,12343894	CSNK1D	5,06099139	418	CD247	1,65178041	NR1I2	1,95423703	PRPF40B	2,65871113	CA5A	2,59720036	LIAS	2,25627153	EDNRA	2,03095058	GTF2A2	4,65360236
349	GORASP1	1,69686816	POLE2	2,03196878	IRF4	2,83854519	SC4MOL	2,72754136	ALLC	2,38795988	PRKACA	2,12117605	UCHL3	5,0585007	419	XRCC6	1,65072466	FVT1	1,95314147	UGCG	2,65859757	C8B	2,59585062	PTPN7	2,2548684	GALNTL4	2,0304092	ELOVL6	4,6521916
350	MAP4K2	1,69667672	AKAP12	2,03136644	CD81	2,8290134	MAT2A	2,72654311	MAP3K11	2,38759612	MTAP	2,11991533	NR1H4	5,04335909	420	CSMD1	1,65015452	C1QL4	1,95314055	F8	2,65609215	TOB1	2,59581161	HIP1	2,25293538	PDCD2	2,02811103	MAP3K3	4,6491613

Table A4. Pooled-shRNA library screen on HEL cell line and MF-3: list of 2nd most depleted shRNAs for each experiment (ranking approach 1, RA1).

	NO ruxolitinib (setting 1)				Ruxolitinib (setting 2)				Ruxolitinib + CM (setting 3)				MF-3			NO ruxolitinib (setting 1)				Ruxolitinib (setting 2)				Ruxolitinib + CM (setting 3)				MF-3	
	Experiment 1		Experiment 2		Experiment 1		Experiment 2		Experiment 1		Experiment 2					Experiment 1		Experiment 2		Experiment 1		Experiment 2		Experiment 1		Experiment 2			
Rank	*Gene*	*Fold change*	*Gene*	*Fold change*	*Gene*	*Fold change*	*Gene*	*Fold change*	*Gene*	*Fold change*	*Gene*	*Fold change*	*Gene*	*Fold change*	*Rank*	*Gene*	*Fold change*	*Gene*	*Fold change*	*Gene*	*Fold change*	*Gene*	*Fold change*	*Gene*	*Fold change*	*Gene*	*Fold change*	*Gene*	*Fold change*
421	CACNA1B	1,64823579	SLC22A12	1,94918232	GCS1	2,65535909	NNMT	2,59562649	ODC1	2,25015174	CFL1	2,02655915	ATP1A4	4,63876217	491	ICOSLG	1,61560393	PTPN1	1,87952734	PER3	2,52613543	HSPA12A	2,4885245	ERBB3	2,15722668	MTHFD1	1,95524974	EIF1AY	4,33481049
422	SH3GLB1	1,64753667	HIST3H3	1,94906239	CCNT2	2,65497702	GLI2	2,5921934	DEFB4	2,24903976	RFC5	2,02649055	GDF15	4,6386738	492	TRIM14	1,6145206	CSTF2T	1,87950657	GLRX	2,52578326	PYGO1	2,48694708	COL27A1	2,15702563	GPSN2	1,95435902	CXCL12	4,32855183
423	AREG	1,64674807	PERP	1,94823454	ATG4A	2,65302992	GNAL	2,59052221	CD37	2,24825601	CYP2E1	2,02631977	ACP1	4,61954284	493	HYAL2	1,61393537	SUV39H1	1,87744676	COX5A	2,52520576	GSR	2,48414764	PIK3C3	2,15695332	RAG1	1,95411497	CNGB1	4,32405152
424	SLCO1C1	1,64672429	IL1R1	1,9481179	C22ORF28	2,65166194	CCNC	2,58840127	SHC1	2,24735241	GNB2L1	2,02460875	IFT57	4,61399949	494	DGKE	1,61328822	ADARB1	1,87717191	DPYSL2	2,52407487	ACOX1	2,48302746	HPX	2,1546652	GADD45B	1,95402173	PSMD1	4,31651394
425	RFC5	1,64657684	EIF4G3	1,94716216	IRF6	2,65089999	FOXP1	2,5870186	ABCC8	2,24717268	TOB1	2,02459471	RFX5	4,59982366	495	NCK2	1,61277348	CCL15	1,87696781	AOC2	2,52398696	HOXC13	2,48295152	ACADL	2,15318396	PPP2R1A	1,95371855	GSTO1	4,3155421
426	MC4R	1,64529125	APOL2	1,94600463	LSM8	2,64539862	GALNT17	2,5863152	CSNK1A1L	2,24462121	SPTLC1	2,02453252	ARPC1A	4,59828187	496	ENG	1,61241991	ACYP2	1,87494914	GRB2	2,52192821	ADSS	2,4816469	STEAP3	2,15303706	TCP1	1,95320224	PDE6C	4,3152211
427	DEFB4	1,64510325	ANKRD1	1,9456302	CDK8	2,64448847	CSF2	2,5848851	HTR1B	2,24343531	CDK3	2,02391934	JAM2	4,59122233	497	EP300	1,6110916	FOXA3	1,87490169	COL5A2	2,51961272	PABPC1	2,48112237	XBP1	2,1528499	EEF1D	1,95244672	SNCA	4,31355333
428	DNMT3L	1,64418052	TXLNA	1,94423068	ACCN2	2,6442972	AOC3	2,58325665	FRAT1	2,24261913	VAMP1	2,02269879	CHRNA1	4,58913879	498	RPL13A	1,61088656	DHDDS	1,87319207	TLX3	2,51882103	EHMT1	2,48092801	VAMP1	2,15093734	KTN1	1,95238476	LNPEP	4,31289275
429	MYF5	1,64348302	AGTR2	1,94412498	OXSM	2,64389394	CASP12	2,58155093	IGF2R	2,24103808	LHB	2,02011402	TSPAN7	4,58085911	499	CD74	1,61077484	CES1	1,87196074	GPR171	2,51823565	NDUFS2	2,48023195	RPS6KA3	2,1507216	FUT2	1,95226523	COL1A2	4,3115116
430	IMMT	1,64299642	BPTF	1,9430854	DDX56	2,64375136	WIPI1	2,58014978	TOB1	2,23693403	AKR1C4	2,01830155	SLC18A2	4,57851989	500	CAMK2A	1,61034074	PSMB1	1,87119437	SULT2B1	2,51756337	KCNA4	2,47833974	CYP2E1	2,14959543	PLP1	1,95184537	NFYB	4,30510734
431	PFKP	1,64095842	FASN	1,9418773	RELB	2,63867281	SMAD7	2,57984624	MMP10	2,23647166	ORC2L	2,01659594	ARFGAP3	4,57788627	501	FADS2	1,60961885	CFHR5	1,8711461	GATA6	2,51528345	ARPC2	2,47760727	HPSE2	2,14895432	SLC25A4	1,95114918	E2F3	4,30081159
432	SYNGR1	1,64055352	TUBG2	1,94185122	WARS	2,6372072	SPRY1	2,57776217	CXCL13	2,23635842	BCL9	2,01596528	PDE3B	4,57686625	502	CHRM2	1,60954377	TCF1	1,87052864	DKC1	2,51511097	APOBEC1	2,47354058	SUV39H1	2,14804345	SLC22A12	1,95080768	PGK2	4,3007164
433	SULT1A3	1,6403672	IRF6	1,94178023	HGF	2,63654654	CACNA1B	2,57509785	DDX47	2,23364957	CAPN11	2,01550331	FMO3	4,57596058	503	ADRB3	1,60788323	TNKS1BP1	1,86999621	CARD14	2,51375511	POLR2G	2,47054393	PPP2R5D	2,14649123	NKD2	1,94947686	RAD51C	4,2829275
434	JAG1	1,63925895	ANP32B	1,9413512	CDA	2,62945687	RASAL1	2,57389527	EIF1AX	2,23160721	TIFA	2,01226102	KIAA1394	4,57043116	504	FZD5	1,60785706	PTCH1	1,86998657	ARFIP2	2,51347862	DTNBP1	2,47008509	SPRY4	2,14634611	PLAGL1	1,94912505	VPREB1	4,28083039
435	MC3R	1,63905141	ELOVL5	1,94108682	DNTT	2,62553562	PRMT3	2,5725109	SYN3	2,22964885	WARS2	2,01080898	SPDEF	4,56674543	505	PRKAB1	1,60784769	AVP	1,8668184	HES6	2,5134151	CLDN15	2,46935511	MAPK8IP3	2,14571627	PELP1	1,94887486	GYG1	4,28024532
436	EFNB1	1,63892718	IGFBP3	1,9410232	GRM4	2,62391233	CELSR2	2,57250143	APOBEC3F	2,22953238	ARPC3	2,00872621	GNAI3	4,56241377	506	CLTA	1,60781519	PKM2	1,86575475	TIMP3	2,51168489	PFN2	2,46668977	GABRA6	2,14547953	HAL	1,94781689	RGS16	4,27450958
437	CD24	1,63890953	ACAD8	1,93979902	CAPNS1	2,62193131	RANGAP1	2,57228258	NXT1	2,22926151	TUBG2	2,00835122	NEDD8	4,56200751	507	IRF1	1,60696003	PFKFB3	1,86402003	CLDN7	2,51137765	ACYP2	2,46419589	PHF1	2,13950015	ITGAL	1,94743731	VAV3	4,27072554
438	FLOT1	1,63778723	CAMK2D	1,93687116	ATP6V0A2	2,62186541	ALDOC	2,57164517	ZFP36	2,22909391	CLCN2	2,00569726	C5	4,55943322	508	C1QC	1,60679533	AP2M1	1,86354361	GLUD1	2,50949765	CFB	2,4629709	FZD4	2,13786728	PDE5A	1,9470654	CDK5	4,27043625
439	LIPA	1,63777187	ARFIP2	1,93684951	SIRT5	2,62058485	GDF10	2,5703438	IL8RA	2,22818816	PSCA	2,00534712	MRPL19	4,55428485	509	GUCA1A	1,60538733	ID2	1,86311263	C1QL4	2,50801611	ALKBH3	2,46294298	PTGER2	2,13735977	ONECUT1	1,94678699	HS3ST3B1	4,26796744
440	TACC3	1,63741821	CDH5	1,93655467	POLR2J	2,61964633	GABRA6	2,56868103	AIFM1	2,22613462	CXCL12	2,00404206	COQ5	4,55177238	510	CENTD3	1,60526396	RETN	1,86278563	ACYP2	2,50639394	CIT	2,46226617	GRM5	2,13705885	NRG3	1,94382357	GRIA4	4,2492685
441	MCL1	1,63658694	ATP5A1	1,93494457	WISP1	2,61722978	SMARCC2	2,5669618	UGT2B15	2,22370765	IL15	2,00123382	SLC9A1	4,53782919	511	SH3BGRL	1,60503364	WBSCR22	1,86234818	RBL1	2,50444053	AKAP12	2,46149958	MSLN	2,1355152	EIF4G1	1,94360718	PROC	4,24827845
442	CYP21A2	1,63565009	SNX13	1,93484345	SVIL	2,61598053	ALDH1A3	2,56611809	CCNK	2,22300541	GFRA1	1,99946499	PTK6	4,53575072	512	SENP2	1,60427147	DPYD	1,86162418	PLA2G1B	2,50425174	TPP2	2,46127237	CDC16	2,13229879	MYH8	1,9418226	IL17RC	4,24712945
443	CARD6	1,63515009	ACOX1	1,93426246	VKORC1	2,61295007	UBB	2,56385514	IMMT	2,22133443	BTLA	1,99935837	ZMAT3	4,53446715	513	PPP2R1A	1,60403844	GATA6	1,86145463	ALPI	2,5032146	HLA-DQA2	2,46007883	CCNB3	2,13162454	HLA-DQA2	1,94159999	KERA	4,23905742
444	TARS	1,63343443	PSMC2	1,9327598	IRAK2	2,61163623	CYP2A7	2,56311274	MTHFD1	2,22076456	TCERG1	1,99796862	CDKSR2	4,5302418	514	VAMP1	1,60333722	NDUFA11	1,86103918	SSRP1	2,50305217	FIGF	2,45599287	FMN2	2,13129777	POFUT1	1,94142056	PAG1	4,23378748
445	IL7R	1,63298619	ATP6V1A	1,93192911	STRAP	2,61049425	COL5A1	2,56159525	DPPA3	2,2201213	SH3GLB2	1,99651222	DGKD	4,52992414	515	GRIA3	1,60266139	CARD14	1,86027414	CSF1	2,50299399	AGXT2	2,45315668	DEGS2	2,12729883	HSD3B2	1,94129057	SHH	4,22794742
446	PRMT6	1,63184167	COL5A2	1,93110319	KCNH7	2,60979812	BPNT1	2,55964513	UBE1	2,22010337	DBP	1,99599489	MAPK9	4,52889992	516	FMN2	1,60258931	WARS	1,85880956	NSMCE2	2,50231697	ICAM1	2,45296749	SELL	2,12621813	LRP5	1,94115126	BLK	4,2220392
447	MAX	1,63076506	TPK1	1,93048315	CSF3	2,60780081	CBS	2,55956023	XCR1	2,21720584	CAMP	1,99271792	HGS	4,5263216	517	ITCH	1,60224682	RING1	1,85576519	C10ORF110	2,50226726	VIM	2,45220041	HLA-DRB1	2,1260428	IMMT	1,94093444	COX5B	4,21842758
448	IRF4	1,63072648	LPL	1,9289596	CD151	2,60444569	CDX4	2,5575616	IL22	2,21416997	ACOX1	1,99219074	NPPA	4,51859688	518	COL21A1	1,60079694	PMVK	1,85546692	MAPK7	2,50151024	CASK	2,44968702	HK3	2,12563127	VIP	1,94074854	PLAT	4,21571217
449	MALT1	1,63059667	IL15	1,92790596	PDXK	2,60414471	PAFAH1B1	2,54926297	RNASEN	2,213376	ME2	1,99056651	PRKDC	4,5106228	519	GALC	1,60044297	ERAF	1,85544995	B4GALT5	2,50137401	NDNL2	2,44768572	SUCLG1	2,12206101	DKK3	1,94035527	DCT	4,21521304
450	COPS5	1,63019466	KCNA4	1,92777976	OSCAR	2,59997413	CES4	2,54774199	PRKAR2B	2,21155887	SLC18A1	1,98746245	SLC15A1	4,50020331	520	PIGT	1,60004293	L1CAM	1,85526365	RETN	2,4980028	OSBPL3	2,44494447	NDUFS1	2,12153432	POLR2H	1,93933291	APBA1	4,21116796
451	APOA1	1,62970795	ACCN2	1,92486894	BBS2	2,59872687	CDC25A	2,54557316	KCNJ5	2,20618105	FADS2	1,98741654	PDHB	4,49202801	521	PRKCI	1,59940108	ISL1	1,85406404	APOL2	2,49506771	MAP2K5	2,44008445	RANBP2	2,12141492	KRT17	1,93930071	PYGO1	4,20511619
452	SSR4	1,62947626	BUB1B	1,92316736	IFNA14	2,59807572	LRRK2	2,53997626	DUT	2,20590294	CCNH	1,98707058	CPE	4,49148078	522	HSD17B4	1,59920138	DNMT3L	1,85394053	IL17D	2,49452002	IL9	2,43893704	NUMA1	2,11953912	H2AFX	1,93866433	ELA1	4,20438104
453	FADS1	1,62938442	CLEC5A	1,92304672	SMN1	2,5960581	GALNAC4S-6	2,53739957	MCM7	2,20525092	UGCG	1,98673227	PLEKHA8	4,48290158	523	PMVK	1,59810378	NTSR1	1,85353745	CD83	2,49386046	ARMETL1	2,43871139	UBE2G1	2,11953236	UBE2G1	1,93819421	LTBR	4,20190933
454	ACAT1	1,62885973	COL9A3	1,92294349	CLTB	2,59568295	GCKR	2,53601301	TPP2	2,20520769	FLNA	1,98664477	TNFRSF1B	4,47785482	524	CALM2	1,59764778	IFNA5	1,85322513	GSTM4	2,49360223	PIK4CA	2,43731518	OCIAD1	2,11758153	ACADL	1,93800361	ACACB	4,19903374
455	ALK	1,62873999	MSH5	1,92237145	AK2	2,5917457	NR1D1	2,53440625	MCFD2	2,20365676	CTSG	1,98607385	DPF2	4,46890167	525	AMY2A	1,59756491	SRP68	1,85306603	MLL	2,49273594	ALB	2,43572397	TFEB	2,11741976	ADAR	1,93624331	BCL9	4,19532304
456	BAG1	1,6283944	DOCK1	1,92157384	FGF20	2,58973503	ADH5	2,5339636	PRIM2	2,20298969	AQP1	1,98607038	CASP4	4,46578236	526	FLT1	1,59647675	UBE2I	1,85253708	PLA2G6	2,49029113	CXCL13	2,43335168	APEX2	2,11684935	BHLHB3	1,93558934	KCNMB1	4,19313855
457	CXCL12	1,62805996	GALNT3	1,92066386	HHEX	2,58235963	ONECUT1	2,53203408	ACTN1	2,20255343	CYP8B1	1,98571276	CYP2C8	4,46470941	527	GPR109B	1,59636802	PAF1	1,85235673	CXCR6	2,48536988	TFEB	2,43086714	CES4	2,11201046	NLN	1,93520186	PDGFB	4,18740578
458	IGF1R	1,62757225	CLYBL	1,91906991	WNT7B	2,58184889	NFYB	2,52885375	MRPL19	2,2010065	CXCL13	1,98547868	UBE2J2	4,45397511	528	KCNK3	1,59603842	DEDD2	1,85206246	JAG2	2,48459595	CTSG	2,42888896	CXCR3	2,11199665	PRMT3	1,93203438	CD68	4,18534218
459	IRF6	1,62717654	XYLT2	1,91719705	ARSB	2,58085556	WARS2	2,52836524	TNFRSF1A	2,19597589	HGF	1,9849374	DYRK1B	4,45009885	529	PKLR	1,59587627	PAX2	1,8515703	LRIG1	2,48410659	ANAPC7	2,42853286	DHODH	2,11003934	MAP3K2	1,93053924	ACACA	4,18295843
460	DSP	1,62711709	IFNA7	1,91686755	CCL17	2,58023904	CBX2	2,52829962	CCL15	2,19496787	LOC402057	1,98462759	CTSD	4,44923617	530	IL8RA	1,59579146	IFIT2	1,85097287	CACNA2D2	2,48247875	FLNA	2,42793794	RPL15	2,10911091	THBS2	1,9298138	DHRS7	4,17915503
461	COX5A	1,62709958	ATIC	1,91617219	IDH3G	2,57992033	IMMT	2,52454092	WDR79	2,19300313	XRCC5	1,98412851	GLUD1	4,4463475	531	GAB1	1,59549835	ST6GALNAC6	1,84847201	ITGAV	2,48106511	GPR18	2,42776366	FABP2	2,10836374	DAAM1	1,92843888	SLCO1A2	4,17747791
462	CELSR2	1,62697916	PSME1	1,91546704	DSP	2,57962921	STEAP3	2,52204711	NCKAP1	2,19145025	PRKAA1	1,98358237	ACOX1	4,44578214	532	FZD9	1,59230027	HRK	1,84825959	CDC2L6	2,48081515	CD247	2,42771606	NUDT4	2,1074245	MAN2C1	1,9205868	HLA-DQA2	4,17671473
463	MTAP	1,62609173	CD83	1,91501799	RAB3B	2,57802684	NT5C1B	2,52185788	SMARCC1	2,18922851	GAS6	1,9826514	CSRP1	4,44168333	533	SNX4	1,59112883	SHMT1	1,84805028	EIF4E	2,47813524	NOX1	2,42441722	PCYT1A	2,10661998	PENK	1,91864039	SKP2	4,17409935
464	RPA3	1,62588629	PKMYT1	1,91463458	ORC3L	2,57757407	LSS	2,5205425	FPGT	2,18750725	MASP2	1,98231989	GCG	4,44140457	534	IFNA2	1,591069	AILC	1,84679138	HIST3H3	2,47542452	TGFBR3	2,42363334	ACP1	2,10276815	PTCH2	1,91822659	IDH1	4,17187884
465	XCL1	1,62501234	SMAD4	1,9132091	CD40LG	2,57655262	CREB3L3	2,51793497	HMGCR	2,18147102	CMKLR1	1,98208731	SH3KBP1	4,43992838	535	CES4	1,59077656	NSF	1,84671372	ADCYAP1R1	2,4750739	NR3C2	2,42293038	PER1	2,10091571	COL9A3	1,91791897	ASAH3L	4,1717692
466	EDG7	1,62493456	SMAD7	1,9128089	NR1H3	2,57510628	PAFAH2	2,51788239	SMAD7	2,17880935	PRPF19	1,9818625	GRIA1	4,43632008	536	CAPN1	1,59075806	POFUT1	1,84646065	IL8RB	2,47405121	IGF1	2,42132854	CAPN10	2,10030252	TBX2	1,91601151	YARS2	4,15995323
467	B3GNT2	1,6247392	NCK2	1,91085266	CCNC	2,57454146	AOC2	2,5178215	SPRY3	2,17721698	NR3C2	1,98178049	PRDX4	4,43451746	537	NAGA	1,59021175	MCHR1	1,84349656	PRKAA2	2,47340882	PSMD4	2,41655233	NUP153	2,09924647	MPST	1,91531263	CDS2	4,15946052
468	IL8RB	1,62458737	RASAL1	1,91004738	RENBP	2,57437196	NAGA	2,51694782	PRDM2	2,17610266	ALPI	1,98131569	ATP5J	4,42894704	538	STAT6	1,5901028	SHBG	1,84252691	DDX47	2,47228315	GTF2H3	2,41639428	PKM2	2,09897781	ACE2	1,91518245	MYD88	4,152848
469	DHX58	1,62427395	SLC6A1	1,90905361	IFI27	2,5723339	SULT1A3	2,51463486	PELP1	2,17552535	SLC2A4	1,98121831	NBN	4,42638352	539	MAGI1	1,59005239	GPR18	1,84137946	LY96	2,46878151	ITGAL	2,41456478	EGLN3	2,09791142	RSAD2	1,91510457	PBEF1	4,14370653
470	FASN	1,62373733	PAPOLA	1,90890587	FRAT1	2,56806964	HSP90AA1	2,51230451	CTSA	2,17518117	DDX18	1,98027927	PHKA1	4,42177164	540	TUBG1	1,58980177	VIM	1,84026363	CDC14B	2,4658238	MEF2D	2,41325743	COL9A1	2,09630027	TPK1	1,91395384	PIK3C2B	4,13015532
471	HRK	1,62315109	TAT	1,90714014	PAX1	2,5665729	ITGB1	2,51202247	SRP19	2,17452471	APEX1	1,97909684	AMPD2	4,41007277	541	AOC2	1,58840127	SPTAN1	1,8373896	PGDS	2,4640598	GRK5	2,41294444	DNMT3L	2,096231	HOXC13	1,91373864	IDH3A	4,12921138
472	TAGLN	1,62289335	FH	1,90513455	COL8A1	2,56190523	DDOST	2,51143795	CIR	2,1725122	NOV	1,97568175	CD96	4,40849634	542	POU2F2	1,58802206	CASK	1,83712129	REG1A	2,46174731	SPCS3	2,41176691	EIF2AK2	2,09497452	CR2	1,91363895	WARS2	4,1243588
473	EHMT1	1,62257932	NLK	1,90439634	DGKQ	2,56056586	FGF3	2,50941363	VSIG4	2,1725122	SRD5A2	1,97509459	NR0B1	4,40603638	543	SFN	1,5872453	RAD9A	1,83686819	SLC6A12	2,45514789	SERPINA10	2,41160042	LPHN3	2,09466207	TLR4	1,91303164	UST	4,11695971
474	SNX2	1,62159998	OSBPL3	1,90391261	B4GALNT1	2,559504	HES3	2,50858776	RPN2	2,17213162	IFNA7	1,97432385	TNFRSF1A	4,39907398	544	IGFBP2	1,58706474	CLTB	1,83659869	LOC402057	2,45137947	TDGF1	2,41126557	ENTPD7	2,0945315	VNN1	1,91173246	DCK	4,11441494
475	TOB1	1,62135158	CMKLR1	1,90315748	ARHGAP5	2,55887351	CTNNAL1	2,50847473	PCNA	2,17199875	GLRX	1,97318333	DGKZ	4,39772289	545	BPTF	1,58649718	GABRA3	1,83653384	CDK3	2,44964319	TNFRSF18	2,41035227	GALNTL4	2,09351571	REV3L	1,91139752	ISG15	4,10360407
476	HTR7	1,62076297	MCM10	1,90104756	PRTN3	2,55547439	CYP4F2	2,50676158	CAP1	2,17135631	F2R	1,97257488	RAD9A	4,39591259	546	GDF3	1,58632102	ATG3	1,83644443	VEGFA	2,44927595	DTX3L	2,41034021	LHB	2,09274747	EFNB1	1,91131252	H6PD	4,10241439
477	TLX3	1,62073369	AASDH	1,9000481	GRIP1	2,55455066	OSCAR	2,50455003	RHOA	2,17100498	CAPNS2	1,97073057	S100A12	4,38841731	547	LTB4R	1,58623358	MERTK	1,83638846	ALG3	2,44732094	FZD1	2,40767029	CSTF2T	2,09214228	ARNT	1,91042681	GLP2R	4,10194028
478	UBE3A	1,62045028	DIABLO	1,8963753	TCERG1	2,55080785	PIGA	2,50436025	BACE1	2,16994937	ACYP2	1,96912493	SESN1	4,38103996	548	COL9A3	1,58585425	C10ORF110	1,83596683	BCL2	2,44663102	LMNB1	2,40693588	OXA1L	2,08929027	DUT	1,91026546	WASF2	4,10086181
479	C1QA	1,62024007	COL10A1	1,89445501	MYH6	2,55017616	IDI1	2,50325816	CDC2L2	2,16817532	FSHR	1,9684501	LCK	4,37939567	549	MAP2K7	1,58567179	DBP	1,83525374	GTF2IRD1	2,44569419	UGCG	2,40346552	LIPC	2,08709092	CCNA2	1,90919545	EFNB1	4,09656174
480	AGXT	1,61995269	TGFBI	1,89093027	LRP5	2,54808749	NCF1	2,50324127	NOXO1	2,1680979	ADRB2	1,96692264	SUV39H1	4,37180811	550	NOLA2	1,58393556	AGXT2	1,83499416	SRP68	2,44482293	ERCC3	2,40269061	FS	2,08620514	PARK7	1,90863778	GALNT5	4,08946735
481	POLE2	1,61993317	CDC2L6	1,88897577	SYNGR1	2,54773063	ANGPTL6	2,50287055	GYS2	2,1673033	CDK8	1,96503211	ST6GALNAC2	4,37015301	551	PSMB8	1,58391603	PER2	1,83493659	MEOX2	2,44474009	FLNC	2,40258794	CAV3	2,08541057	PROM2	1,9082971	IL21R	4,08711697
482	CHST7	1,61985534	TUBA1A	1,88844209	CHRM1	2,54563136	AL2	2,50110071	WAS	2,16671562	FGB	1,96175301	IVD	4,36799417	552	CYP2C9	1,58335007	SYN3	1,83211025	DDX19A	2,44451868	CYP27A1	2,40152294	IL6	2,08514385	CHRM1	1,90773884	MERTK	4,08595423
483	IDH1	1,61878235	TRRAP	1,88711627	GPR83	2,54465324	RENBP	2,50042509	AASS	2,16548927	NUDT1	1,96160705	ACSL4	4,36769571	553	RAD54L	1,58306872	PSMF1	1,8301181	ANAPC10	2,44406898	VLDLR	2,40102296	TUBB3	2,08514385	HOXD13	1,90738024	MEFV	4,08104013
484	PDHA1	1,61859136	GAS1	1,88458652	IDH2	2,54450477	C1QL4	2,4994541	PLCE1	2,16345226	PGA4	1,96102485	VCAN	4,3666386	554	IL22	1,583047	CYP2F1	1,82931713	PGA5	2,44395707	ACAT1	2,39734826	ENPP1	2,08476955	AGPAT2	1,90735855	IFNB1	4,06381653
485	HTR2C	1,61858627	PENK	1,88458652	HRG	2,53922416	MTHFD1L	2,4959619	NRIP1	2,16342017	SCN9A	1,96071034	FABP4	4,36582088	555	BMP6	1,58299286	CANT1	1,82931166	RUNX1	2,44364186	ALDH1A2	2,39613761	SQSTM1	2,08441448	UCN	1,90726271	SHC3	4,06332273
486	AQR	1,61641893	RBBP7	1,88457652	ALDH1L1	2,53620499	ZFP36	2,49484942	IFIT2	2,16145119	PPP2RSD	1,95926294	MYCBP	4,36260932	556	C15ORF15	1,5826971	CAV1	1,82771965	UCN	2,43814491	ITK	2,39582056	KERA	2,08364496	ARMETL1	1,90719802	BCKDK	4,05826192
487	LRPPRC	1,61598233	CHRNA10	1,88377108	ARF5	2,53540278	HMGCL	2,49400629	FLAD1	2,16132016	THY1	1,95898406	CA8	4,36001006	557	HGSNAT	1,5825728	EIF4G1	1,82749894	CR2	2,43721106	PYGM	2,39445485	CYP11B2	2,0825972	CENTD3	1,90711789	PLA2G12B	4,0576763
488	SNAI1	1,61583355	PES1	1,88353498	AKR1C2	2,53108763	APOA5	2,49231728	COL4A3	2,16068815	FMN2	1,9579413	CELSR3	4,34755511	558	POLR2K	1,58254623	RAB3B	1,82618849	SRPR	2,43682894	MTHFD1	2,39267584	PSME1	2,08220496	REPS2	1,90574463	RETN	4,0560823
489	PLAGL1	1,61583334	HLA-F	1,88279053	IFT172	2,52948074	RAB3B	2,49141402	SLC22A12	2,16013286	TPO	1,95636946	GALNT9	4,34266971	559	ACY3	1,58218451	CSRP3	1,82531582	PYGM	2,43630326	FTMT	2,39241093	BLVRB	2,08082123	RAP2B	1,90346821	TRAF3IP2	4,04777417
490	MIOX	1,61563149	COX10	1,88137902	ALAS1	2,5266142	CSMD1	2,4896223	MAP3K7IP2	2,15804142	YY1	1,95545409	YARS	4,33862682	560	PIK3R4	1,58185241	ESCO2	1,82474296	C1QBP	2,43336871	MCL1	2,39128073	HSD17B2	2,08027907	BGLAP	1,90313988	FOXD3	4,03968287

Table A4. Pooled-shRNA library screen on HEL cell line and MF-3: list of 2nd most depleted shRNAs for each experiment (ranking approach 1, RA1).

	NO ruxolitinib (setting 1)				Ruxolitinib (setting 2)				Ruxolitinib + CM (setting 3)				MF-3				NO ruxolitinib (setting 1)				Ruxolitinib (setting 2)				Ruxolitinib + CM (setting 3)				MF-3	
	Experiment 1		Experiment 2		Experiment 1		Experiment 2		Experiment 1		Experiment 2						Experiment 1		Experiment 2		Experiment 1		Experiment 2		Experiment 1		Experiment 2					
Rank	Gene	Fold change	Gene	Fold change	Gene	Fold change	Gene	Fold change	Gene	Fold change	Gene	Fold change	Gene	Fold change	Rank	Gene	Fold change	Gene	Fold change	Gene	Fold change	Gene	Fold change	Gene	Fold change	Gene	Fold change	Gene	Fold change	Gene	Fold change
561	PPP1CC	1,58085932	HGS	1,82323138	MAP2K5	2,43222801	NF1	2,39095172	EZH1	2,080228	ASL	1,90220166	CBX3	4,03267419	631	DTX3L	1,54801146	UST	1,77393048	SAT1	2,34809803	SOCS3	2,29502924	DDX54	2,00852511	MAPK8IP3	1,85356053	DDX20	3,81197773
562	GPD2	1,58014332	MAP3K2	1,82298043	STAT5A	2,42791471	SPTLC2	2,38660768	SMAD5	2,0796616	HES1	1,90192237	TAF1L	4,02650445	632	BAP1	1,54743675	TACC3	1,77266644	ATM	2,34771092	SLC2A3	2,29490025	ATP1A1	2,00847095	TUB	1,8532273	MPO	3,80771688
563	IFNA14	1,57905888	CENTD3	1,82294055	WNT7A	2,42718015	CYP11B1	2,38631061	PSMD14	2,07816672	NDUFS2	1,90123371	PPP2R5B	4,02394544	633	PPP1R13B	1,54738778	CYP2A7	1,77200289	ALK	2,34748875	MCAT	2,29214074	EIF4B	2,00764525	HLA-G	1,85056782	SHMT2	3,80760434
564	CSTF2T	1,57899412	RFC1	1,82149224	MYL1	2,42690153	POLR2I	2,38579783	TERF2IP	2,07788856	CST3	1,90109118	HLA-F	4,02263619	634	PELI2	1,5472674	HRG	1,77167404	MCHR1	2,34667489	PRIM2	2,29181787	RALA	2,00705609	POLG	1,84774955	IGFBP4	3,80370738
565	PER3	1,57817407	MAN2C1	1,82072274	KCNA4	2,42624276	GLI1	2,38524877	NOV	2,07703005	CS	1,90067586	ITGAX	4,01395875	635	KDR	1,54577148	B4GALNT1	1,77085019	LRRK2	2,34613631	G6PC	2,29179587	MAF	2,00704144	GCNT1	1,84774452	IFI30	3,80235048
566	ARHGEF11	1,57735134	DRD1	1,81942304	SNAI1	2,42382478	CA1	2,38152996	WISP1	2,07629727	HSPB2	1,9005035	MCM4	4,01364334	636	NEK2	1,54549602	GBP1	1,77056432	HLA-F	2,34375797	IGFBP5	2,29130801	ITGAV	2,0062666	EIF2AK1	1,84671001	UROS	3,80171077
567	NDUFS7	1,57689294	HGSNAT	1,81908063	GGA3	2,42313903	HS3ST3B1	2,38092013	DAD1	2,07595388	ACOT12	1,89916434	SCN3B	4,01064272	637	HELLS	1,54515669	WAS	1,77025218	LDHC	2,34345093	EIF2S3	2,29107793	IDUA	2,00515712	FZD10	1,84568507	ATG5	3,80165331
568	TUBA3C	1,57584441	CEL	1,81617838	NGFR	2,4230516	POLE2	2,37334228	CHRD	2,07537251	IGF1	1,8986254	CYP2E1	4,01029593	638	EFNA4	1,54510867	RNASEN	1,76938845	PRDM2	2,34255926	HGF	2,2905459	ACSL3	2,00443471	STXBP1	1,84477297	PSMC3	3,79866484
569	CAD	1,57569236	E2F5	1,81312072	AGPAT6	2,42151445	REXO2	2,37299907	BIRC5	2,07292615	CCNA1	1,89838038	SST	4,00958795	639	CACNA1C	1,54461572	RBL1	1,76927925	UBE2A	2,3425252	RRM2B	2,28984626	XRCC1	2,0033231	DLG7	1,844487	CSNK1A1	3,79810223
570	CD38	1,57549346	RCHY1	1,81274087	SELL	2,42139249	ARPC5L	2,37298602	ALPI	2,07071847	ISL1	1,8975568	ALG12	4,00592155	640	NEIL3	1,54456416	GTF2E2	1,76918358	AURKA	2,34040572	IFNA5	2,28889941	PIGM	2,00323944	STX18	1,84373045	CRADD	3,79805708
571	FSTL1	1,57542706	CD14	1,81220479	EPX	2,41992993	RAD17	2,37222612	ATP6V1G3	2,06985874	PRKD1	1,89648824	PRTN3	4,00464222	641	AKAP7	1,54415891	HDAC3	1,76888419	TYROBP	2,33884274	CSF1	2,28821981	SPTLC2	2,00008397	DFFB	1,84301707	CCNE1	3,79664553
572	BTG3	1,57532148	TNFAIP3	1,81208075	NCK2	2,41941847	PCK1	2,36845928	LEF1	2,06604195	MCM7	1,89616053	CHST1	4,00227726	642	ACACB	1,54388058	MUC1	1,76888419	PRMT3	2,33818043	NCK1	2,28651698	PSCD2	1,99947642	FBLN2	1,8428269	UGT1A6	3,78792204
573	CXCR6	1,57496116	IL22	1,81167981	TUBA3C	2,41643261	FOXN1	2,36819388	GPLD1	2,06293662	GAS1	1,89583438	MAP3K1	3,99712817	643	PDE6G	1,54301457	HRB	1,7687222	CD58	2,33809057	PCYT1A	2,2815974	CDC7	1,9994648	NCAM1	1,84031494	NDST1	3,78473378
574	CDK4	1,57486472	GGPS1	1,81091806	BID	2,41617254	PRKACA	2,36818135	RBBP7	2,06287314	GTF2IRD1	1,8953095	CRYAB	3,99432721	644	EPHB2	1,54299423	WIPI1	1,76858415	SFRS12IP1	2,33723036	LRIG1	2,28043173	GPR109B	1,99865843	OSBPL3	1,8393597	DERA	3,77761422
575	RANGAP1	1,57465076	UBE2G1	1,81020988	PRMT7	2,41578852	AK7	2,36672941	SFRP2	2,06094665	LY96	1,89482293	NPR1	3,99224607	645	OXCT1	1,54283565	PPP6C	1,7679418	NAE1	2,3350091	PKM2	2,27747188	IMPDH1	1,99747819	PIGM	1,83933152	ARHGEF5	3,77586134
576	SLC6A13	1,57434871	AMY1A	1,81009337	MYCBP	2,41565839	TUBA1A	2,36643891	PDLIM4	2,06061995	CHST3	1,89471351	PGAP1	3,99060236	646	C1QL4	1,54252598	F8	1,76791726	EFNA2	2,33388142	NCL	2,27740017	MTTP	1,99699141	ALDOA	1,83901554	ITGA1	3,77419353
577	GSTA5	1,57410119	CCL7	1,80978291	STX18	2,41359775	SPP1	2,36544255	PRKAR1A	2,06041437	SC4MOL	1,89443491	CREBBP	3,98955154	647	FZD1	1,5422017	TNFSF8	1,76790715	DDIT4	2,33317845	DDX56	2,27689177	GRIA2	1,99542643	NFKBIE	1,83803879	CACNA1H	3,77333011
578	CBS	1,57303966	ENPEP	1,80935618	CAD	2,41289491	ISL1	2,36420901	RPA2	2,06027021	EME2	1,89424625	COL8A1	3,98826264	648	CCNC	1,54219338	MMAB	1,76747709	DYRK1A	2,3321632	DAPK1	2,2763233	LAT2	1,99538238	CLU	1,83739188	RXRG	3,77292925
579	DISC1	1,57303966	GTF2IRD1	1,80868103	PRKAG1	2,41234781	CANT1	2,36406949	PENK	2,05903942	PDE7A	1,89424625	PPME1	3,98243555	649	RABGAP1L	1,54217648	MTHFD1	1,76568751	GRIA3	2,33159635	MAP4K2	2,27598852	MEF2D	1,99499178	ATP5G1	1,83623329	TAF1	3,768708
580	ACAA1	1,57297111	ADD1	1,8083891	NRAS	2,4107756	LMAN1	2,36088236	PABPC1	2,05788495	AGPAT6	1,89419315	TCF1	3,97988269	650	PIGU	1,54167843	DNAJB9	1,76544875	ISL1	2,33033995	TOLLIP	2,27580199	PTGER4	1,99408131	CDC37	1,83544495	C9	3,76851803
581	CD2BP2	1,57292583	PRKAR2B	1,80832279	VANGL2	2,41029563	PPP1R10	2,35824645	PKP4	2,05689632	PRKCQ	1,89286925	KDELR3	3,97490818	651	EIF2B2	1,54110693	PELP1	1,7645201	IL3RA	2,32904851	PARK7	2,27544803	SNCB	1,99349349	WIPI1	1,83539375	POU2F2	3,76718785
582	PROM2	1,57271161	C1QA	1,80649565	KNG1	2,40967342	APBA1	2,35626795	MTA3	2,05641586	SALL4	1,89024394	RAB3B	3,97450402	652	TNFRSF1B	1,54108948	HSD17B1	1,76365544	FSHR	2,32834382	EPHA4	2,27392605	XCL1	1,9917621	SERPINA4	1,83495404	SLC18A3	3,76636438
583	SLC23A1	1,57244663	ARHGAP5	1,80633683	ITGAL	2,40820314	ANKRD1	2,35565839	GBA3	2,05564885	CES2	1,88941098	SNAP23	3,97146433	653	SH3GLB2	1,54105724	ALDH1L1	1,76321238	NEDD4L	2,32777262	FGL2	2,27262249	CAD	1,99162584	FST	1,83427158	PSMB10	3,75989731
584	MAP1LC3A	1,57128973	SULT1A3	1,80588418	TNKS1BP1	2,40749481	KL	2,35381931	HLA-DQB2	2,05428786	RALA	1,88916336	GPSN2	3,97074829	654	TCF1	1,54058568	MAF	1,76305238	EIF4G1	2,32754031	IFT172	2,27187696	EPHB2	1,9915764	KRT1	1,8333613	GAS6	3,75535986
585	AK5	1,56983007	TGFBR2	1,80561657	HSPD1	2,40478119	CHGB	2,35150842	GNPDA2	2,0542617	MAP2K2	1,88885877	KTN1	3,95474779	655	HPX	1,54041782	CIP29	1,762882	RGS4	2,32687641	DEFA1	2,27019889	PRKCA	1,9912855	TFR2	1,83323126	PCYT1A	3,74861751
586	TLX1	1,56844168	FUT2	1,80476741	NRG1	2,40469856	UBE2M	2,35017732	GTF2H3	2,05282268	CELSR2	1,8868731	GNB2L1	3,95379888	656	PRDX5	1,54028532	PRDX4	1,76225418	CDK6	2,32624209	GRHPR	2,26942787	PTPN22	1,99014628	LGALS1	1,83186566	GCH1	3,74692486
587	CHRNA10	1,56822446	TEAD2	1,80359689	TPK1	2,40304618	FUT2	2,34981852	PDE10A	2,05113865	PKLR	1,88625781	PROS1	3,95287188	657	SLC6A11	1,54002876	SSRP1	1,76219224	MPST	2,32574264	ST6GALNAC6	2,26902736	ATP6V0D1	1,98953215	CHST7	1,83117206	UBE2G1	3,74667382
588	VARS	1,5665507	CYC1	1,80302993	LMO2	2,40231722	SPTLC1	2,34775618	CYP2A7	2,0510803	ELOVL5	1,88591182	GSTA5	3,94947197	658	DNAJB9	1,53967157	NRG3	1,76152283	SUOX	2,32567147	RUNX3	2,26897616	DLX3	1,98946502	PGK2	1,82970488	NES	3,74332511
589	CDX4	1,56524472	CARS	1,80284146	GDF10	2,40118392	ZFP42	2,34754347	THRB	2,05048205	NADSYN1	1,88457456	IRF7	3,94921385	659	PIGX	1,53917417	ABCB9	1,76094242	TFEB	2,3253681	VAMP7	2,26723983	EIF2AK4	1,98861869	CD58	1,82920133	IL6R	3,7411569
590	S100A9	1,56496314	LIG3	1,79939403	CBX2	2,39989017	PSCD2	2,34732478	MPO	2,0501314	SKP1A	1,88353628	ZIC1	3,93749784	660	PRDM2	1,53884427	IL6	1,75974454	ABCC2	2,32499142	MCM2	2,26718405	FGF9	1,98849471	SPCS3	1,82909888	CYP11B1	3,73493472
591	HLA-DMB	1,56356929	RFXANK	1,79871035	GAP43	2,39852906	CDC42	2,3467848	ADRB3	2,0500018	PPP1R12B	1,88230304	CKMT1B	3,93717002	661	SRPR	1,53877685	WNT1	1,75971859	ABCB5	2,32379473	LMO2	2,26624888	GALNAC4S-6S	1,98816212	XCL1	1,82860123	WNT10B	3,72898483
592	ABCB7	1,56345898	PIK3AP1	1,79817022	IL2RA	2,39766497	HNRNPC	2,34119961	LRP6	2,04979468	CHD8	1,88143212	ID3	3,9353327	662	UCN	1,53864527	CXCL3	1,75939447	SMAD4	2,31948361	ACE2	2,26539082	GALNT9	1,98677922	ELA3B	1,82838821	PFN1	3,72637666
593	DAAM1	1,56329153	GTF2A1L	1,79801901	NQO1	2,39720153	ELK4	2,34018631	DHRS2	2,04936841	IARS2	1,88130285	PSMA5	3,93508117	663	RAF1	1,5383248	XCL1	1,75899922	TEC	2,31916123	RAD51	2,26523594	ECE2	1,98639811	KRT19	1,82785831	GRIK3	3,72304128
594	ARF5	1,56317477	SIGIRR	1,79792136	CCL15	2,39690286	STK36	2,33907175	DOCK1	2,04875163	RAB5C	1,87836404	PGDS	3,93028772	664	CHRD	1,53663463	ACAT1	1,75748819	HTR2C	2,31888301	UBE1	2,26371865	UGT2B4	1,98378575	GRIA3	1,82758579	PPP2CA	3,71904857
595	FGA	1,56309392	STX2	1,79678454	POLR3H	2,3944209	SPO11	2,33741117	MYOD1	2,04832991	SF1	1,87687124	MBTPS2	3,92414798	665	PIGA	1,53658709	BACE1	1,75683402	ABCA1	2,31862088	BLVRB	2,26179912	PIK3CB	1,98271794	HYAL2	1,82688374	CSRP3	3,71664262
596	IFNA7	1,56254937	DCTN1	1,79673154	TAL1	2,39147051	GNPDA1	2,33683702	CLDN2	2,04822665	PTPRC	1,87663218	AASS	3,91605508	666	ITGA6	1,53626863	TSG101	1,75673099	MSH5	2,31787928	F8	2,26016671	PMCH	1,98271794	KIAA1394	1,82661963	SCN11A	3,70883605
597	WBSCR22	1,5625371	MAT2A	1,79628868	NFKBIE	2,39075842	GABPA	2,33633245	DGKZ	2,04719551	FARS2	1,8758884	NCOR2	3,91398733	667	PON3	1,53620808	MARS	1,7566552	ADA	2,31678011	MAP1LC3A	2,25860591	ASL	1,9810846	ATP1A1	1,82643672	NARS	3,70773302
598	GPC5	1,56246468	PIAS1	1,79555718	VARS	2,38720816	PKP4	2,33431813	FGF6	2,04679213	ARG2	1,87561531	LPIN3	3,90305606	668	PRIM2	1,53609568	BLVRA	1,75658203	IL15	2,31608601	CD58	2,25761013	RECQL4	1,98001194	EXO1	1,82598789	TREH	3,70668947
599	CHUK	1,56229314	VANGL2	1,79528458	ZFP36	2,38640848	PGA5	2,33137803	ENG	2,04439999	DAXX	1,87453047	GNA13	3,90228582	669	BCL2	1,53532742	CTSL1	1,75654234	NCF1	2,31534745	FOSL1	2,25753691	C15ORF15	1,97985984	ACADS	1,82538215	POLK	3,70514723
600	CHSY1	1,56194065	DFFB	1,79525268	NRG2	2,38627711	GK2	2,33081533	IFIH1	2,04269996	TRO	1,87383053	ALAS1	3,90212422	670	TBL1XR1	1,53522844	FCGR3A	1,75631499	COL4A2	2,31288125	TNFRSF19	2,25736998	PRMT3	1,97953194	DRD3	1,8252831	ITGAV	3,70398204
601	ZCCHC11	1,56189449	MYH2	1,79515653	MME	2,38569618	RBL1	2,33069019	AVP	2,04248874	ARHGAP5	1,87272933	PIGA	3,89954435	671	CXCL13	1,53498257	CAST	1,75551612	FGF6	2,31205098	CMKLR1	2,25627397	ATP6V1C2	1,97908229	ACYP1	1,82518367	TLX3	3,70267266
602	ANGPT2	1,56135567	UGT1A7	1,79494963	MAF	2,38326535	IL9R	2,32994871	TKT	2,04232214	HSP90AA1	1,87134134	PTPN1	3,88908	672	KCNC4	1,53497111	PRKCD	1,7554994	EIF2AK4	2,30882007	COL6A3	2,25340611	TDG	1,97835424	TIMELESS	1,82449318	CCR8	3,70056958
603	RBPJ	1,56107782	NME2	1,79475944	PRKACA	2,38197572	CENTD3	2,32789093	COL16A1	2,04173823	DGKZ	1,87061025	MASP2	3,88672521	673	HSPD1	1,53479193	NT5E	1,75368571	POLR2L	2,30763061	ACADL	2,2525485	AKAP1	1,97810417	ERAP1	1,82447682	IFIT2	3,69969431
604	C5AR1	1,56004998	FABP3	1,79267235	SDHA	2,38033308	MYCBP	2,32669716	IL15	2,0410081	FRAT1	1,87032712	MAP3K10	3,88373333	674	HSPB2	1,53473091	PTPN12	1,75265428	PSME3	2,30733905	MASP2	2,25064616	AK7	1,9778339	TRAF6	1,82437796	TGIF2	3,69553894
605	GRK4	1,55859536	KCNJ5	1,79262026	NRIP1	2,37921043	HLA-DQB2	2,32603582	ANKRD1	2,03820056	SLC13A5	1,87027128	CTSB	3,87879033	675	UBE1	1,53454506	BCL6	1,75253699	CDC25A	2,3073006	YWHAG	2,24945811	KPNA2	1,97721136	PLA2G5	1,82412665	GNGT1	3,69541799
606	CLCN2	1,55832751	CASA	1,79254772	FSCN2	2,37856687	CCNG2	2,3221473	LCK	2,03773728	VSIG4	1,87004672	MYT1	3,87479345	676	PLAT	1,53450241	RALB	1,75195148	MAP2K7	2,30688063	SNX6	2,24944488	GHSR	1,97521808	MEPE	1,82393002	FANCM	3,69515161
607	ALB	1,55756458	GPR161	1,79242151	CYP1A1	2,37683823	TKTL2	2,3221108	C7ORF16	2,03727683	PRKAR1A	1,8691362	DDX52	3,8718789	677	PACAP	1,53401475	LY6E	1,7515233	PUM2	2,30665807	AACS	2,24904935	ADAR	1,97394835	CASP1	1,82200572	CTNNA3	3,6933553
608	CHGB	1,55736356	LMO2	1,7913027	DFFB	2,37460607	SLC22A7	2,31808586	CFH	2,03692513	ATP6V0E1	1,86874046	IKZF2	3,86699479	678	ERCC3	1,53377148	RELB	1,75089714	MUSK	2,30577442	PSME1	2,24885777	CTSE	1,97324432	ALLC	1,82146148	GAD1	3,69330281
609	COL8A1	1,55674682	HGD	1,79114859	CDC34	2,37388324	MC3R	2,31799962	EMR2	2,03636138	EIF2AK2	1,867993	GCS1	3,86591785	679	PRKCB1	1,53348089	PDLIM4	1,74996211	RFXANK	2,30491145	WNT9A	2,24881254	MBTPS2	1,97225877	IGFBP2	1,82063929	ST3GAL3	3,68694328
610	GAB2	1,55668853	TWIST1	1,78947774	B3GAT3	2,37117507	EIF4G1	2,31771993	NCOA3	2,03475193	SQSTM1	1,86786691	PRDM1	3,86562312	680	DDX4	1,53341937	COL9A1	1,74972838	PLAGL1	2,30455629	THBD	2,24836554	SC4MOL	1,97203955	APOL2	1,81961101	PPP1R3A	3,68241458
611	PAPOLA	1,55651177	GFPT2	1,7884259	VLDLR	2,37044704	VISA	2,31664462	RECK	2,03316472	FGFR3	1,86754382	SCAP	3,86285959	681	VISA	1,53250236	NFKBIE	1,7482997	DPPA2	2,30449287	CD40LG	2,24823309	PDE7B	1,97116511	GPT2	1,81939272	ATP5B	3,68080078
612	EME2	1,55650797	ARMETL1	1,7872343	ALDH3A2	2,36963127	CDC26	2,31418874	CCL28	2,0313729	NMI	1,86714202	HBB	3,86134297	682	BMPR1A	1,53190776	C1ORF103	1,74808072	ST3GAL1	2,30365279	NOTCH4	2,24802291	DGKQ	1,96847567	PAFAH2	1,81927214	ACCN5	3,67859616
613	UCHL3	1,55576789	CELSR1	1,78682873	LEP	2,36834779	C10ORF110	2,3134987	GSTM4	2,03098134	SLC22A7	1,86605441	GIT1	3,85556111	683	UQCRC1	1,53181868	TCF7	1,74766154	ACOT12	2,30322562	PHKB	2,24736273	PTPRF	1,96841865	RUNX3	1,81726385	C3AR1	3,67095113
614	ITGB1	1,55572365	MBD4	1,78659873	CDK2	2,36826638	DYRK1A	2,31275667	AKAP3	2,03026545	GBL	1,86525374	KLK7	3,85499035	684	CDC16	1,53177526	GSTA5	1,74730436	ALLC	2,30301384	ALDH1B1	2,24630198	GLI2	1,96594161	LDHC	1,81663087	STAR	3,66833583
615	HCST	1,55570398	CDK8	1,78419793	POLR2A	2,36680786	HSD3B2	2,31111674	POLR1A	2,02596068	VLDLR	1,86438592	GMDS	3,84980717	685	MUSK	1,53177526	ADORA3	1,74649488	TUBA1A	2,30271591	HSPB2	2,24453546	HGS	1,96529146	ABCA12	1,81649008	PRDX5	3,66789222
616	DLG7	1,55526244	AGL	1,78201386	NDUFA1	2,3652023	B4GALNT1	2,3105595	GART	2,02225646	MTHFD1L	1,86213036	IL17F	3,84723251	686	HSP90AB1	1,53165621	CASP6	1,74645326	TRPM7	2,30268416	UBE2I	2,24389088	MCM6	1,96263692	OLA1	1,81508618	MADD	3,663026
617	ATP6AP1	1,55510222	UGCG	1,78092175	PAG1	2,36402254	ENTPD7	2,30666258	DKFZP434E11	2,02131978	CARS	1,86157344	SH2B2	3,84611783	687	ASPH	1,53156177	FGL2	1,74577865	CXCL6	2,30141662	ITGAL	2,24204313	ITGAL	1,96024239	TCF3	1,8149257	BST1	3,66230602
618	TAF10	1,55437433	PRDM2	1,78036629	CIR	2,36331598	XRCC5	2,30533266	POLR2L	2,01931246	C12ORF57	1,86157136	CYP27B1	3,84193188	688	NSMAF	1,53077729	PLA2G4A	1,74540998	BBS1	2,29974792	NRIP1	2,2416655	LUM	1,96005208	DTX3L	1,81274116	HLA-DOB	3,65518438
619	BTLA	1,55384124	ANAPC10	1,78035963	CLDN18	2,36040482	E2F5	2,30274909	ARHGAP5	2,01767383	SRP68	1,86154536	ACYP1	3,84143738	689	PIK3AP1	1,53075397	TKTL2	1,74538422	HRB	2,29958671	POLR1E	2,2401757	DLST	1,95970011	NQO1	1,81273099	PPM1D	3,6461565
620	SPRY4	1,55357464	CTH	1,77998674	CA5A	2,36027089	NT5C1A	2,30264113	EIF4G1	2,01740929	ZFP42	1,86022362	FDPS	3,84018767	690	RUVBL1	1,5306446	IDH3G	1,74523826	BNIP1	2,29882297	TOB2	2,23931938	AK2	1,95962249	PORCN	1,81233021	FOLR1	3,64524699
621	VAMP7	1,55280834	ACADL	1,77907692	GSTP1	2,36006527	HS6ST3	2,30244322	RAD21	2,01736543	LIFR	1,8600776	CCNE2	3,83992145	691	ARG2	1,53063121	STEAP3	1,74509993	CHAF1A	2,29837789	MAP3K7IP3	2,23914042	ACOX3	1,95940136	GRIP1	1,81193292	PRKAG2	3,64328052
622	PNKP	1,55270229	CCL19	1,7787133	MEF2D	2,35890192	AMY2A	2,3016604	FLT4	2,01733878	EIF4E2	1,85952925	FGF3	3,83775128	692	SLC22A7	1,52997776	ACCN3	1,7447314	MB	2,29803887	IL8RB	2,23904084	GOS2	1,95904459	HS3ST2	1,81164615	NTAD1	3,63657324
623	CLDN2	1,55136383	ANXA4	1,77847685	AASDH	2,35788984	PHKA2	2,29965881	MYBPC3	2,0164258	APPL1	1,85881618	RPS6KA5	3,83191775	693	COL18A1	1,52873991	FADS2	1,74412318	UBE2D1	2,29756522	PTGER2	2,2381123	RFX5	1,95892218	PER1	1,81110926	BHMT	3,63273493
624	GRIA2	1,55133813	AGPAT6	1,77839263	NCOR2	2,35625652	HYOU1	2,29929541	CHRNA2	2,01512168	MAP3K5	1,85850744	RPIA	3,82920262	694	ATG9A	1,52871938	TPH1	1,74409683	ACCN5	2,29675862	SC5DL	2,23782258	NOLA2	1,95859627	PYGO1	1,81093888	PSMD13	3,62714464
625	SELP	1,5504019	RAD17	1,77770943	CSF2	2,35617258	CD74	2,29883424	SLC1A1	2,01506225	NEU3	1,85701326	ANGPTL3	3,82823395	695	DDX23	1,52837467	APBA3	1,74406715	ERCC2	2,29598442	F2R	2,23707648	TSLP	1,95724791	SRP9	1,80982997	GADD45A	3,62657241
626	KNG1	1,54937757	CRTC1	1,77704814	GYS2	2,35580252	COQ2	2,29808487	CLDN18	2,01436564	TGIF2	1,85643169	DAZL	3,8268205	696	WNT1	1,52817049	MASP2	1,74332562	PTPN1	2,29483414	RNASE1	2,23695009	ABCB11	1,95576988	WNT3A	1,80935472	CDC37	3,62548074
627	RASAL1	1,54928571	NFYB	1,7761279	CHRNA2	2,35556497	TNK2	2,29763197	MYST3	2,01008422	CDK7	1,85537645	REM2	3,82572366	697	SREBF2	1,52789994	PIGT	1,74292991	GFPT1	2,2933858	CYP21A2	2,23689992	WIPI1	1,95253675	TNK2	1,8088147	PSCD4	3,62503316
628	CSNK1G3	1,54887423	PIK3R4	1,77604276	IFNA7	2,35427373	RIPK2	2,29641299	SULT2A1	2,0099495	C22ORF28	1,85517474	AICDA	3,81983114	698	EFNA2	1,52744614	MBL2	1,74108881	TACR1	2,29279458	RPN2	2,23499716	NRAS	1,95021705	SUCLG2	1,80822843	FANCC	3,62479525
629	CAMK2G	1,54859913	STX4	1,77603677	RPA2	2,35131937	TOP2B	2,29638475	NR3C2	2,00907565	COL16A1	1,85404292	CDH5	3,81416955	699	PRMT5	1,52736229	MYH6	1,73927926	RAD17	2,29105568	GPLD1	2,233541	CUGBP1	1,94990872	LRPPRC	1,80774303	FGF10	3,62312943
630	NR3C2	1,54819844	CRTAM	1,77580711	PRKD1	2,34888395	SLC2A1	2,29583655	TRIM14	2,00894799	PPP1CC	1,85380609	CD27	3,81332469	700	COL24A1	1,52651799	KREMEN1	1,73926441	C1QA	2,28906957	IFIT1	2,23351432	HBA2	1,94964015	FMOD	1,80767444	DLL4	3,62216841

Table A4. Pooled-shRNA library screen on HEL cell line and MF-3: list of 2nd most depleted shRNAs for each experiment (ranking approach 1, RA1).

	NO ruxolitinib (setting 1)				Ruxolitinib (setting 2)				Ruxolitinib + CM (setting 3)				MF-3					NO ruxolitinib (setting 1)				Ruxolitinib (setting 2)				Ruxolitinib + CM (setting 3)				MF-3	
	Experiment 1		Experiment 2		Experiment 1		Experiment 2		Experiment 1		Experiment 2							Experiment 1		Experiment 2		Experiment 1		Experiment 2		Experiment 1		Experiment 2			
Rank	*Gene*	*Fold change*	*Gene*	*Fold change*	*Gene*	*Fold change*	*Gene*	*Fold change*	*Gene*	*Fold change*	*Gene*	*Fold change*	*Gene*	*Fold change*	*Rank*		*Gene*	*Fold change*	*Gene*	*Fold change*	*Gene*	*Fold change*	*Gene*	*Fold change*	*Gene*	*Fold change*	*Gene*	*Fold change*	*Gene*	*Fold change*	*Gene*	*Fold change*
701	CTNNA1	1,52595271	CCR3	1,73883491	B4GALT1	2,2883751	PCNA	2,2324502	FOSL1	1,94942254	IRS4	1,80736724	NFYA	3,61586963	771		CD151	1,50643981	CSF1	1,70253595	HSPA12A	2,209597	IRF6	2,15698981	SESN1	1,88684999	PFKM	1,76696037	PTGDR	3,39966645
702	NKX2-2	1,52547223	NKRF	1,73857907	NCSTN	2,28836533	NTSR1	2,23124831	GPR18	1,94911614	LPHN3	1,80721108	KRT19	3,61344283	772		ITK	1,50604064	CAPN11	1,70251894	MUC1	2,20918409	CSF2RB	2,15689653	SPTLC1	1,88579272	CXCR6	1,76569263	LRIG1	3,39903268
703	KL	1,52447884	NARS	1,73855237	ATP6V1C1	2,28498326	DAAM1	2,22999471	IDI1	1,94719323	LALBA	1,80662993	BMP4	3,61297365	773		ALS2	1,50535392	DAPK1	1,7022045	CCDC6	2,2091126	NBL1	2,15571613	APOBEC1	1,8855926	HSD17B1	1,76355071	CCR3	3,39545397
704	TSLP	1,52421881	MAGI1	1,73854495	SNX4	2,28447423	BCL6	2,22803452	TUBA1A	1,94533122	AOX1	1,8058569	FOXA3	3,61038125	774		TACR2	1,50482744	ASAH3L	1,7019175	PDE6A	2,20813917	BCKDHA	2,15548026	NUDT12	1,88513931	NT5C3	1,76275544	ALKBH3	3,39433575
705	TAT	1,5240624	UBE2E3	1,73827954	APBA2	2,2827756	ITGB4BP	2,22791527	CS	1,94486081	SMPD1	1,80578919	PSMB3	3,60441713	775		FHL5	1,50475714	GMPPA	1,70001876	NSD1	2,20758741	CAPN11	2,15462077	AKAP12	1,88509849	LSM8	1,7617677	FSCN2	3,39298696
706	HIST3H3	1,52405016	CDC20	1,73760255	PER1	2,28050298	ELA3B	2,22659525	LDHB	1,94465144	NPR2	1,80550684	AMY1C	3,60163718	776		TYROBP	1,50411098	DCC	1,69981673	PLA2G2D	2,20670321	SPAM1	2,15457294	STXBP4	1,88498091	NOTCH4	1,76176601	EPOR	3,39271932
707	PELP1	1,52337107	NDUFS8	1,73706089	ABCB6	2,27904625	ATG9A	2,22652737	WARS2	1,94057002	PDE10A	1,80537241	EIF4G2	3,58987146	777		AURKA	1,50392714	APEX2	1,69875886	MEN1	2,20655153	ILK	2,15385457	PTPRB	1,88450833	LIG3	1,76106547	MIOX	3,39244325
708	GART	1,52319928	CHD8	1,73706073	CTH	2,27870922	MB	2,22521777	NCAM1	1,93933678	SCN4B	1,80494464	HES3	3,58938142	778		GALNT10	1,50392694	DDX47	1,69811343	KCNJ5	2,20380618	LRP6	2,15374449	DAXX	1,88387238	ANAPC7	1,75917357	C1QL1	3,39145629
709	PDE7B	1,52304091	HPX	1,7369546	NCF4	2,27736107	HPX	2,22371523	SCTR	1,93883725	DGKH	1,80399164	CTPS2	3,58936405	779		GALNT3	1,50381637	GABARAP	1,69775744	SC4MOL	2,20320599	WASL	2,15066379	CYP2S1	1,88341098	GALNT8	1,75906813	CDT1	3,39083466
710	FOXA3	1,52303104	IL17RC	1,73653427	GRIN3A	2,2773033	ARHGEF12	2,22279569	B3GNT2	1,93781032	PLCE1	1,80316233	SPTLC1	3,58927234	780		CISH	1,50324808	PSMD14	1,69698028	EIF5A2	2,20224577	KRT1	2,1491797	SULT1A3	1,88294535	ZMYND17	1,75763031	UQCRC2	3,38891493
711	CCBP2	1,5230147	ABCD2	1,73615741	PIWIL3	2,27669157	B3GALT1	2,22131787	BNIP1	1,93640641	BLR1	1,80315684	ACVRL1	3,58596961	781		PDE6H	1,50272821	MAT1A	1,69656464	IL10RB	2,20164214	IDI2	2,14781695	CTNNA1	1,88277488	HGSNAT	1,75708521	TNFSF14	3,38731148
712	DUSP14	1,52295886	OXCT1	1,73455216	PABPC1	2,27433023	IFNA17	2,22117675	CDC37	1,93568329	GUCA1A	1,80244519	SOCS6	3,58596961	782		BRCA2	1,50197551	INSIG2	1,69652068	PACRG	2,20105712	IRF9	2,14775399	TNFRSF18	1,88276207	GRM5	1,75481787	CHRNA3	3,38674939
713	DTYMK	1,52287102	HLA-G	1,73411996	TRIM14	2,27357901	PIK3C2B	2,220987	OAT	1,93470025	EEF1G	1,8024359	FOS	3,57979865	783		NT5C3	1,50170892	CHRD	1,69553671	HDAC11	2,20081321	APOD	2,14738906	ABL2	1,88049922	MAT1A	1,75451963	PPP3R1	3,38510989
714	ZFP42	1,52277475	SCTR	1,7326799	ATP6V1A	2,27208409	NR2E1	2,22002361	CLYBL	1,93392615	IFNA5	1,8018941	HSPD1	3,57828524	784		HSD11B2	1,50096762	BST2	1,69547274	BMI1	2,20075968	HS6ST1	2,14708001	CD74	1,8794076	SLC6A11	1,75396199	FOXP3	3,38362276
715	GTF2IRD1	1,52257294	FOXO4	1,7324286	ITGB1	2,27202226	FAU	2,21996468	IL17D	1,93338837	NR4A1	1,80085712	RASA1	3,57106565	785		ADAM12	1,50095472	SIRT5	1,69447551	SCTR	2,19678899	PGK2	2,14639625	VISA	1,87929759	PI3	1,75337776	DPYSL2	3,38237508
716	CARD11	1,52207204	LRRK2	1,73177459	RXFP1	2,2702578	LTB4R	2,21989212	DAPK1	1,93191869	CAV1	1,79952589	VNN3	3,57044139	786		CYP4F2	1,50046554	PTGS1	1,69396439	HS3ST3B1	2,19324866	CDX2	2,14607989	SIM1	1,87798629	RBBP4	1,75266924	CREM	3,38218637
717	HARS2	1,52177632	PSCD4	1,73128798	TRAF6	2,26999163	PPP2R5D	2,21729897	NFKBIE	1,93072203	LY9	1,79943255	PGA3	3,56806198	787		SUCLG2	1,50000915	COMP	1,69359751	PIK4CA	2,1925084	ADAM9	2,14326197	TNNT1	1,87736756	CACNA1C	1,7520828	PMVK	3,38115776
718	OAT	1,52098219	SNAI1	1,73102656	ARID1A	2,26957705	ATP6V0A2	2,2167534	EIF4A1	1,92672574	BFAR	1,79887917	DDX47	3,56780075	788		CSF1	1,49969719	BST1	1,6929491	ADAR	2,19135934	PPP6C	2,14283177	TLR9	1,87704014	PIK3R3	1,75185498	FH	3,3761253
719	NDUFS2	1,52047064	SNCB	1,73072364	VSIG4	2,26841906	UST	2,21547563	HTR2A	1,92641255	GABPA	1,79820532	IFNA17	3,55804258	789		UGT1A7	1,49953089	MTHFD2	1,69277533	SLC10A2	2,1901083	RNASEN	2,14258391	ENPEP	1,87433635	CPS1	1,75125904	PTPN6	3,37554782
720	DTNBP1	1,51977559	HARS	1,73070286	HLA-DQB2	2,26827181	SFRS12IP1	2,21520399	MAP2K5	1,92628139	ARPC1B	1,79805752	RTN4R	3,54658889	790		ADORA3	1,4990682	RPN2	1,69241675	SERPINB2	2,18970187	CYP39A1	2,1420605	BNIP2	1,873218	FEZ1	1,75093751	SOX2	3,36921612
721	DNAJB2	1,51938545	HMGCR	1,73002338	MYH8	2,26820274	ENPP1	2,21515852	DPPA2	1,92614649	KDELR2	1,79786418	CIRBP	3,53766202	791		NFKBIA	1,49878452	PDCD4	1,69137449	ANAPC4	2,1856796	PER1	2,14181913	GPD2	1,87320667	SERPINA6	1,75042063	MAT2A	3,36505113
722	CCL13	1,51927936	ALOX15B	1,72906181	NT5C3	2,26800905	NCK2	2,21361507	LPIN1	1,92579102	EPHB2	1,79719001	HS3ST2	3,5375807	792		CFD	1,49872768	ATG4B	1,69105303	CCL16	2,18515458	ARRB2	2,14002998	TPH1	1,87094539	MTA3	1,75019927	GRIN2B	3,3645715
723	BNIP2	1,51923691	NFATC3	1,72866677	HSD17B1	2,26577113	CD160	2,21162344	XK	1,92544813	HS3ST3B1	1,79683031	F13B	3,53551179	793		CCNH	1,49836639	APBB1	1,69074664	RABGAP1L	2,18284687	AKAP3	2,13996049	MUS81	1,8708734	AMY2A	1,74993236	DKK2	3,36310224
724	ACE	1,51904821	PIK3CD	1,72858859	PRKACB	2,26496082	PFKM	2,21122848	TNFSF4	1,92320654	SNCA	1,79516449	ORC5L	3,53319493	794		COPA	1,49815054	CHRNA5	1,68985912	H2AFY	2,18177698	FSHR	2,13941178	CSF2	1,87080155	RXRB	1,74847352	HDAC9	3,35814608
725	LMO2	1,51880422	SLC6A12	1,72720044	LPHN3	2,26308285	ADAM17	2,21095635	SERPINC1	1,92263461	NCF1	1,79313572	FBLN1	3,53247906	795		ALPI	1,49780701	LCK	1,68869704	SMCHD1	2,18100333	CDK3	2,13929452	GDF10	1,86928815	ERCC2	1,74773315	PSMD3	3,35810477
726	AGXT2	1,51845104	C22ORF28	1,72638309	PES1	2,26203879	RAD51C	2,20718658	ARRB1	1,92257469	STX19	1,79214742	DTX3	3,53118526	796		TOR1A	1,4973874	NCSTN	1,68868764	MSR1	2,1809842	SPRED1	2,13813178	RAD51	1,86888533	WARS	1,74704036	SELL	3,35549429
727	HSD3B2	1,51827819	IL12RB1	1,72581543	MAT1A	2,26047001	HTR2C	2,20698974	CLDN22	1,92206642	B3GAT2	1,79191843	CA14	3,53100299	797		AMT	1,49738375	BTLA	1,68730655	CXCL3	2,17977546	DSP	2,13749612	CR1	1,86826115	NT5C1B	1,74703663	CFTR	3,35490059
728	PLCB2	1,51817132	TNFRSF1A	1,7257764	DOCK1	2,25872003	ACOT12	2,20686216	CLCN2	1,92140718	ATG3	1,79165183	FADS2	3,52814027	798		B3GNT6	1,49727577	SDHB	1,68671773	AMT	2,17934784	SMPD2	2,13506427	MC5R	1,86792709	E2F5	1,74697279	PIK3CA	3,35010251
729	EPX	1,51798386	ADAM9	1,72505226	BCL11B	2,25516293	COQ7	2,2043342	CCNT2	1,91962764	LMO2	1,79162881	HYAL2	3,52553669	799		CTSG	1,49685594	KRT8	1,6863007	DDX18	2,17765888	MCFD2	2,13470329	PRKCD	1,86712434	AKAP6	1,74680161	FANCE	3,34989409
730	NFAT5	1,51725497	IL27	1,72421809	PFKFB3	2,25353744	EIF4EBP1	2,20334688	RPS6KB1	1,91866418	SPTAN1	1,7915059	GCA	3,52199298	800		F11R	1,49612704	IL12B	1,68565787	GALC	2,17695493	SUCLG2	2,13419822	GNAI2	1,86711553	NCOA3	1,74672059	HELLS	3,34966601
731	AGTR2	1,51715538	EIF2AK1	1,72412428	MLXIPL	2,2482475	CDK8	2,20223245	CREB3L2	1,91831404	GGA3	1,79129519	RPL13	3,51690501	801		GNAI1	1,49568398	TERF2IP	1,6833753	EDG7	2,17524017	POLR2H	2,13356612	ISL1	1,86663023	SNAP25	1,74638189	THTPA	3,34856577
732	RENBP	1,51707354	SLC25A4	1,72401968	NOXO1	2,24817049	ATP6V1G3	2,20162769	ALAS1	1,91817819	CD79B	1,79098048	PFKFB3	3,51630457	802		RPS6KA3	1,49539099	PTK2	1,68322931	CYC1	2,17447093	RAD9A	2,13323976	RAD23B	1,86661866	TCOF1	1,74562987	IL7	3,3466622
733	FOXO4	1,51690854	BCL2	1,72395699	RASGRP1	2,24778274	FGB	2,20134525	BCL9	1,91747917	IFNB1	1,79054119	RAB1B	3,5159666	803		NFKBIE	1,49486067	PEMT	1,68234136	GFAP	2,17412835	TARS	2,13323976	CDK2	1,86659167	MYL1	1,74522132	AARS2	3,34239793
734	LIPC	1,51671112	PPFIA4	1,72342684	HK2	2,24597402	LIG3	2,20019629	ABCB9	1,91701514	GCA	1,79039548	ATG16L1	3,51369846	804		CCNT2	1,49485855	CSNK1G3	1,6821329	G6PC2	2,17379726	AKAP13	2,13295909	PPARG	1,86496287	SMAD5	1,74476763	ATP6V1G3	3,34167769
735	MCM6	1,51639161	GABBR1	1,72328417	PTGIS	2,2451728	TGDS	2,20005073	IRAK3	1,91633221	SCD	1,79019173	BCL2A1	3,51219432	805		C7ORF16	1,49484306	FBP1	1,68180044	NR6A1	2,17335456	PIGO	2,13262559	LRP1	1,86361377	AURKB	1,744414	RPA1	3,34022261
736	CDKN2A	1,51549936	FANCE	1,72246459	BAP1	2,24485372	FVT1	2,19867785	FADD	1,91569156	PABPC1	1,78791293	ACSM1	3,51159824	806		NRG2	1,49443248	HK2	1,68153649	PIK3AP1	2,17316529	CAPNS2	2,13241112	PFKM	1,86360951	PLOD1	1,74407367	PTPN12	3,33561941
737	SPTLC2	1,51546637	HSD3B2	1,72216797	FLNA	2,24438626	DDO	2,19534265	EEF1B2	1,91525774	RHOA	1,78783848	ZCCHC11	3,50113518	807		AQP1	1,49420594	SUPT6H	1,6814211	CDC23	2,17255439	SNAI1	2,12981387	TIMP1	1,86284451	RAB3B	1,74356898	ACE	3,33476014
738	MTHFD1L	1,51526817	DPYSL2	1,72131287	DARS	2,24296919	B3GNT2	2,1948395	GCA	1,9148516	CTNNBIP1	1,7874245	MAP3K9	3,5005975	808		NR5A2	1,49399149	CSNK1E	1,68010098	HDAC1	2,17072469	PPARA	2,1297265	EP300	1,86274714	CAPNS1	1,74331306	TIAM1	3,33231434
739	CAPN11	1,5151054	FOXP1	1,72124492	ADAM9	2,24125629	PPP2R5B	2,19430737	BHLHB3	1,91206108	ANAPC10	1,78726976	BOK	3,49750298	809		POLR2I	1,49361141	HHIP	1,67966827	CACNA1B	2,17011084	GAS6	2,12970304	IL12B	1,86075866	GNAS	1,7432077	LTB4R	3,33043754
740	EIF2S1	1,51463523	CTGF	1,72123132	CD226	2,24107304	USP11	2,19368547	C1QA	1,91195191	FAU	1,78662747	ACCN4	3,49532766	810		VSNL1	1,49356401	TACR2	1,67959325	WNT9A	2,17009084	MSLN	2,12811803	CLDN7	1,8606713	CLK3	1,74316431	THY1	3,32885935
741	APOBEC1	1,51437398	CD74	1,72046378	DDX20	2,24082594	PDCD2	2,19326059	BUB1	1,90999081	CDH1	1,78448055	NFS1	3,49398943	811		ADH1B	1,49351138	HDGF	1,67939	FZD3	2,16979326	CYP7A1	2,12550304	NSD1	1,85932073	PRKAR2B	1,74316071	SH3GLB1	3,30761744
742	SCD	1,51405117	DKK3	1,71995452	PGM1	2,23864577	SOX2	2,19300948	SLC6A11	1,90993627	TUBA1A	1,7835631	PDE2A	3,49079839	812		SELE	1,49344367	DEGS2	1,6790897	IFNA10	2,1695736	CRP	2,12540567	DGKH	1,85813785	MGAT4B	1,74267506	ZEB2	3,30740618
743	TLR4	1,51369968	CLDN18	1,71981764	TOB1	2,23852961	CD37	2,19061099	CD68	1,90864895	PMVK	1,78292713	CAMKK1	3,48119177	813		LY9	1,49278497	LFNG	1,67868458	IDI1	2,1682393	MCM7	2,12522549	ATP6V0D2	1,8576997	LDHB	1,74266715	STH	3,30686061
744	SUMO2	1,51359449	COX5A	1,71835781	LY6E	2,23770703	FOXO4	2,19018076	TNFAIP3	1,90662614	FBP1	1,78286432	RPRM	3,48063418	814		TACR3	1,49231868	CDO1	1,67839833	COPS5	2,16681677	PIGM	2,12293729	NR1H3	1,85671952	IL17D	1,74201812	IFNAR1	3,30297614
745	PTK2	1,51343339	CD3D	1,71780906	SF1	2,23675486	DIABLO	2,18913621	NCK1	1,90649809	G6PC2	1,7812062	FGF9	3,47809435	815		CANT1	1,49197875	MYLK2	1,67772843	RBBP7	2,16677478	TUBG1	2,12290673	PYGO1	1,85671952	ATP6V0A2	1,74180648	PSMB4	3,29774928
746	FABP5	1,51331374	PCAF	1,71692622	MCL1	2,23468422	WBSCR22	2,1890205	PYGM	1,90606942	NCKAP1	1,78056257	ITK	3,47778477	816		CYP46A1	1,49129999	A1BG	1,67772807	CYP7A1	2,16484511	CDO1	2,12266893	RAB3B	1,85605799	ACE	1,74142602	CFH	3,29451022
747	NR1I3	1,51322353	B3GAT3	1,71632201	B3GNT2	2,23396179	HLA-DOB	2,18860991	ARMETL1	1,90582442	HDGF	1,77940969	DDEF2	3,47768315	817		POLD4	1,49127692	ASNA1	1,67727244	CARD6	2,16386989	GABARAP	2,12264413	ATP6V1F	1,85581885	GHSR	1,74128675	LMO2	3,29132911
748	CFLAR	1,51310207	F2R	1,71589301	POLR2H	2,2321651	POLS	2,18706801	NGB	1,90225608	PGM1	1,77906635	PMAIP1	3,47471343	818		DDX18	1,49109202	ACTG2	1,6753852	AOC3	2,16335316	PTH	2,12232517	MXI1	1,85518228	ACVR1C	1,7409969	PSMB7	3,28907413
749	CYGB	1,51195333	IL23A	1,71577758	CTSA	2,23207943	UCP2	2,18627401	ALDH1B1	1,9008526	CYP4F2	1,77882069	GLI4	3,47323765	819		NPPA	1,49107123	PFN2	1,67537445	NFE2L2	2,16291774	POLR2L	2,12169834	PSMF1	1,85405346	TLN1	1,74068196	POLM	3,28902409
750	COL5A2	1,51194395	MB	1,71524655	ATP6V1G1	2,23077744	ACSS2	2,18439966	DTX3L	1,89967491	FLT4	1,77881836	EIF2AK2	3,47322718	820		NUDT4	1,49103232	SSTR4	1,67537002	SLC2A1	2,16252888	AKAP6	2,11897785	FGF3	1,85341456	EIF4EBP2	1,74041621	PPP2R1A	3,28185577
751	ARFIP2	1,511723	SLC9A1	1,71337535	SLC13A5	2,23021193	SPRY3	2,18343644	TYROBP	1,89847161	RAMP1	1,77820422	NRCAM	3,47106768	821		PSMB10	1,49047257	INPP5B	1,67528807	XYLT2	2,16161857	TREX1	2,11822518	CD40LG	1,85311051	PTPRH	1,74033817	CYP21A2	3,28096288
752	PDCD2	1,511057	STRA6	1,71306329	TFR2	2,22773335	NDUFB2	2,18278474	CYP4F2	1,89818859	LY6E	1,77754112	AKR1C4	3,4706787	822		TNFRSF1A	1,49040805	ICOS	1,67523265	ABCD2	2,16090061	CARD11	2,11809545	AGK	1,8510412	ATG4C	1,74013651	COQ7	3,27970029
753	PRPF40B	1,51078955	IRAK1	1,71269397	IRF8	2,22688806	CD276	2,18222349	ADAM9	1,89723025	IL1R1	1,77685026	CD37	3,47021064	823		COL13A1	1,48993576	DARS	1,67514034	STAR	2,16085856	HOXA11	2,11794741	TICAM2	1,85084341	C1QBP	1,73962078	ATP6V0D1	3,27916749
754	UBE2L3	1,51052984	DDX54	1,712431	DDIT3	2,22686054	MGMT	2,18184206	PTPRH	1,89718451	RCHY1	1,77683014	TREM1	3,46507383	824		RAP2B	1,48977253	GADD45B	1,67408704	ACPP	2,15763425	C9ORF47	2,11783951	POLR2C	1,85067997	BAK1	1,73846691	OTC	3,27519
755	EIF4EBP1	1,51019436	CSTF3	1,71222311	IL1RAP	2,22606063	SH3GLB1	2,18142942	NOX1	1,89715454	ALS2	1,77665063	PFKM	3,45847551	825		GARS	1,48942622	RPS6KA1	1,67389982	PLA2G3	2,15763042	ST6GALNAC5	2,11711015	GADD45G	1,8498657	B3GALT1	1,73775981	ACSL1	3,27178591
756	B3GAT2	1,50943463	CCL1	1,71201964	FUT2	2,22574021	WNK1	2,1788647	DEFA1	1,89611494	GPR171	1,77611301	KLRD1	3,45730433	826		CASP1	1,48920959	MAP3K8	1,67354037	ADSS	2,15597238	ST3GAL1	2,11504461	EPB49	1,84842633	DNAJC5	1,73758907	RPN2	3,27043407
757	ABAT	1,5092416	AVPR2	1,71185668	F2RL3	2,22204961	ACSL6	2,17232985	KRT8	1,89516845	ANXA6	1,77578167	ALOX5	3,45352525	827		CASP2	1,48880645	IL27RA	1,67289697	DAB2	2,1539222	NDST4	2,1129995	ANGPTL6	1,847499	WNT9A	1,73704041	CTF1	3,26974037
758	MASP2	1,50896904	LDHC	1,71182289	TREX1	2,22004722	NR4A2	2,16981966	GK2	1,89492766	AREG	1,77490315	CLK3	3,44628571	828		GLB1	1,48808905	ARF5	1,67287987	TERT	2,15356527	AKR1C1	2,11267544	CDT1	1,8471935	NUMA1	1,73607308	DPPA2	3,26974037
759	PAX4	1,50884391	DNAJA3	1,71152345	ATP4A	2,21948318	MOG	2,16786699	XYLT2	1,89490638	KCNK3	1,77481697	MYL2	3,44470821	829		CDO1	1,48796898	TBX21	1,67271877	KCNMB3	2,1534944	CDKN2A	2,11218906	NTRK1	1,84688525	HEMK1	1,73604926	AK7	3,26563163
760	GUCY1B3	1,5085092	PON3	1,71147521	TUBA4	2,21709635	LMX1B	2,16486763	UST	1,89404955	DLL3	1,77453426	CSTF3	3,44084199	830		CDK7	1,48795405	MBTPS1	1,67142579	PPM1D	2,1524922	ITGA9	2,1113055	ERCC3	1,84528442	VISA	1,73598164	BCL2L11	3,26541795
761	REG1A	1,50836728	MTFMT	1,71108443	PRKCD	2,21704322	FGF13	2,16412596	AKAP6	1,89318322	NDUFS1	1,77413557	PLTP	3,44012537	831		RNF4	1,48737151	B4GALT3	1,67018925	NDRG2	2,15220357	SERPINB2	2,11062401	SCNN1A	1,84520643	DHODH	1,73509227	NR3C2	3,26502507
762	LMAN1	1,50835186	DLL3	1,70938097	PIK3C3	2,21682032	NCKAP1	2,16329676	NR2C2	1,8931778	UBE2I	1,77407513	PACRG	3,43644943	832		PF4	1,48724212	CTNNB1	1,67016375	ACAD8	2,15189517	EIF2B2	2,10967955	GGCX	1,84211146	GABBR1	1,73397124	TNFRSF13C	3,26468389
763	ATP2A3	1,50825748	ITGB1	1,70915863	TRADD	2,21676471	CDK5RAP1	2,16305165	ACSL6	1,89296449	ALG14	1,77407141	CHKA	3,43598051	833		HESX1	1,48714566	HOXA11	1,66976724	CAB39	2,1518541	PON3	2,109161	CSF1	1,84200411	ADH5	1,73237124	ARNT2	3,26007191
764	DYRK1A	1,50814079	MC4R	1,70814415	DBP	2,21674331	AIFM1	2,16262952	ACTR2	1,8914706	PTGIS	1,77092609	TAF4	3,43534321	834		NR3C1	1,48712479	FGFR4	1,66890071	PRKAA1	2,15118606	PPP2R5C	2,1064913	KRT7	1,84198601	TREM2	1,73234047	GPR37	3,25559507
765	PIGK	1,50712603	ATG10	1,70773007	C9ORF97	2,21636483	CYP8B1	2,16140513	VAMP7	1,89061808	GSTM4	1,77073764	SULT1A3	3,43339912	835		B4GALT3	1,48695399	GCNT2	1,66837877	FUT8	2,15097826	C19ORF40	2,10644021	GUCY1B3	1,84168888	TOP2A	1,7321125	FGF18	3,25455889
766	PPM1D	1,50703661	GRIN2A	1,70559022	AR	2,21524377	FABP2	2,15999876	PLP1	1,89053395	MTIF2	1,7707183	SCN3A	3,42159155	836		ST3GAL1	1,48686447	CXCL12	1,66814767	NDST2	2,14891049	CCL1	2,10507329	HTRA2	1,84134917	B4GALT1	1,73200244	SDHA	3,24845039
767	ACSL6	1,50669958	NEUROG1	1,70557819	CDK4	2,21496328	EDG7	2,15906359	EIF2AK1	1,89044655	ANKRD1	1,76880425	IGFBP1	3,42135903	837		UIN7A	1,4864875	PRKACA	1,6675233	TNFRSF18	2,14817834	GUCY1B3	2,10349981	HS6ST1	1,84118233	IFNA10	1,73151849	SRD5A2	3,24407159
768	ITGA9	1,50656358	MCM2	1,70495212	RFC5	2,21360241	MARS	2,15906004	EIF5A2	1,88989279	SULT1A3	1,76876035	VIPR1	3,41694195	838		TFPI	1,48629957	CASP1	1,66626995	MYLK2	2,14810257	UBE2A	2,10348971	UBE2C	1,84074169	MEF2D	1,7314543	TFR2	3,24230927
769	NUP153	1,50654756	FLNC	1,70480539	MALT1	2,21312761	DFFB	2,15808621	XRCC6	1,88735679	GSTZ1	1,76870141	ADSL	3,41503844	839		YARS	1,48625822	HTR2C	1,66589347	ABAT	2,14616344	CARD9	2,10285902	DKC1	1,83927659	TWIST1	1,73122802	GPR171	3,24207794
770	HARS	1,50646995	CD2AP	1,70329345	ILK	2,21285628	NR4A1	2,15749545	DDX20	1,88731528	LTB4R	1,76781805	CNR1	3,41441292	840		C1GALT1C1	1,48567969	EPS15	1,66521284	ATG10	2,14494103	COMP	2,10248178	CELSR2	1,83827399	PLA2G4D	1,73115488	RGS4	3,23889553

Table A4. Pooled-shRNA library screen on HEL cell line and MF-3: list of 2nd most depleted shRNAs for each experiment (ranking approach 1, RA1).

	NO ruxolitinib (setting 1)				Ruxolitinib (setting 2)				Ruxolitinib + CM (setting 3)				MF-3					NO ruxolitinib (setting 1)				Ruxolitinib (setting 2)				Ruxolitinib + CM (setting 3)				MF-3	
	Experiment 1		Experiment 2		Experiment 1		Experiment 2		Experiment 1		Experiment 2							Experiment 1		Experiment 2		Experiment 1		Experiment 2		Experiment 1		Experiment 2			
Rank	*Gene*	*Fold change*	*Gene*	*Fold change*	*Gene*	*Fold change*	*Gene*	*Fold change*	*Gene*	*Fold change*	*Gene*	*Fold change*	*Gene*	*Fold change*	*Rank*	*Gene*	*Fold change*	*Gene*	*Fold change*	*Gene*	*Fold change*	*Gene*	*Fold change*	*Gene*	*Fold change*	*Gene*	*Fold change*	*Gene*	*Fold change*	*Gene*	*Fold change*
841	LYN	1,48566539	CAPNS2	1,66355475	SLC6A1	2,14479989	CDA	2,10220279	GRIN3A	1,83792104	PDUM4	1,7309997	MME	3,23873923	911	WNT3A	1,4658451	OSCAR	1,62962751	STMN1	2,08413962	GDNF	2,04478627	PRKCE	1,80271744	KRAS	1,69167684	CDBB	3,09314838
842	TRAF6	1,48546678	CARD10	1,66344047	SRP9	2,14479989	LOC402057	2,10135943	ACOT12	1,83708081	HIP1	1,72996308	BAG4	3,23781719	912	PFKFB3	1,4654748	SERPINF2	1,62951413	GSK3A	2,08402602	GPX6	2,04403629	MTHFS	1,80250221	CTNNB1	1,6915075	DGKB	3,09260842
843	SMPD2	1,48510707	FABP1	1,66309223	HELB	2,14354279	SNCB	2,09888055	PRKX	1,83564696	CARD10	1,729302	ACOX3	3,23446495	913	IL15RA	1,46538408	CLDN22	1,62929375	NPPA	2,08270905	CDC16	2,04336178	CPSF2	1,80216134	GABARAP	1,69128635	KCNJ5	3,09110424
844	CASP12	1,48504295	TNFRSF11A	1,66286027	AACS	2,14319386	CAND1	2,09961082	HS3ST3B1	1,83547945	MAP2K5	1,72706132	BMP5	3,23292341	914	GMPPA	1,46513047	PIK4CA	1,6292271	CHST4	2,08255917	PROX1	2,04316911	TCERG1	1,80087288	HCLS1	1,69119291	LEFTY2	3,08552784
845	NSD1	1,48501198	HHEX	1,66262397	IFI16	2,14176997	MXI1	2,09777131	FUT5	1,83519356	PPP6C	1,72548113	BTG1	3,23089351	915	COMT	1,46471185	SPCS1	1,62875107	IGFBP3	2,08192644	IL27RA	2,04178362	CMKLR1	1,80081146	AOC3	1,68929148	ACAD8	3,0829453
846	ARG1	1,4847818	ARRB2	1,66234625	ISLR	2,14154818	COX15	2,09593004	CFTR	1,83493612	FABP2	1,72490949	ELK1	3,22786144	916	DPF2	1,46459437	CCNB3	1,62814842	MCM10	2,08187541	MAOA	2,03916997	STX5	1,80066579	OBFC1	1,68916072	C1ORF103	3,08130053
847	PRKAR2B	1,48468558	WRN	1,66205286	PLCB2	2,14143584	CASP1	2,09562129	POLR2H	1,83447406	GSK3A	1,72381536	MMP13	3,22765922	917	CTNND1	1,46413083	UNC13B	1,62769365	OSBPL1A	2,08160578	PER3	2,03777709	GCNT1	1,80047568	GLS	1,68824912	ZAP70	3,08041326
848	CLK4	1,48456889	GUCA1A	1,66162993	MTHFD1L	2,14133768	HELLS	2,09323491	GRM7	1,83431798	FHL5	1,72287478	MAS1	3,22459419	918	PRPF19	1,46407582	TEC	1,62710799	MAT2A	2,08113788	APPL1	2,03727448	STX19	1,80031238	HPD	1,688074	EED	3,08006382
849	FUT2	1,48449453	GLS	1,66099159	UXS1	2,14111668	ALPI	2,09222392	CUGBP2	1,8336565	ANGPT1	1,72282182	FLI1	3,22097385	919	KRT1	1,46368484	SELL	1,62677399	GBA3	2,08008325	BUB1	2,03247753	ACPP	1,79980213	CSTF2T	1,6871153	AGTR1	3,0768943
850	APOB	1,48320138	RASGRP3	1,66045864	VAMP7	2,13929796	CHPF	2,09221774	PARC	1,83360031	C1GALT1C1	1,72221769	ACAA1	3,2207739	920	ATP6V1A	1,4634392	MGAT1	1,62644723	C1QC	2,08006728	DDX19A	2,03244252	GPR35	1,79980079	EMR2	1,68696314	EFTUD2	3,07474374
851	RUNX1	1,48284819	PIWIL3	1,6599898	PSMF1	2,139012	ACO2	2,09195625	SSTR3	1,8332451	MX1	1,72210685	WASF1	3,21932836	921	EIF2AK1	1,46314879	REM2	1,62621925	GABPA	2,08003606	THBS2	2,03233685	RANBP1	1,79952905	KCNC4	1,686681	TRO	3,07271205
852	BCAR1	1,48257258	AHCY	1,65959072	LDHB	2,13823376	NME2	2,09104989	B4GALT7	1,83260431	CADM1	1,71936225	AKAP12	3,20948033	922	MECR	1,46268926	GRM4	1,62621627	SPIB	2,07961634	EPS15	2,03219144	ATP6AP1	1,79777154	COX5A	1,68599499	NADSYN1	3,07124899
853	GABPA	1,48230486	ASL	1,65950199	GTF2F1	2,13758858	HSD17B3	2,09000997	SFN	1,83146745	COL5A2	1,71815345	PTPRO	3,20886512	923	NGFR	1,46207535	GRIN3A	1,62596792	MYF5	2,07951742	TERT	2,03057802	ANKRD6	1,79670978	CYBA	1,68498	CDKSR1	3,06803092
854	FLCN	1,48200597	BIRC5	1,65878607	FOSL1	2,13691726	COL9A1	2,08916321	OGDHL	1,83128571	NXT1	1,71794475	WWP1	3,20797677	924	PRIM1	1,46164911	PDIA3	1,62535092	SLC6A11	2,07901202	DDX20	2,02947434	CFLAR	1,79551584	SHBG	1,68441891	DBP	3,06212773
855	CTH	1,48178998	FGF9	1,65850683	THBS2	2,13626145	GAB2	2,08915954	ABAT	1,8300779	SYNGR1	1,71760193	TGM3	3,20695825	925	MSX1	1,46147156	DUT	1,62530764	KTN1	2,07843298	MAFA	2,02929419	SMS	1,79503331	GNAI2	1,68378746	KEAP1	3,06145231
856	CSTF3	1,48176697	ADAR	1,65827314	HGSNAT	2,13322879	KITLG	2,08886267	CITED1	1,82991351	CD74	1,71690896	NFAM1	3,20573021	926	PAFAH2	1,46132726	MSLN	1,62460987	TIMP1	2,07803913	ABO	2,02862723	TCF7L1	1,7948995	MLL	1,68298481	CP	3,06008802
857	CTF1	1,48174371	HIP1	1,65753139	ARHGAP4	2,1326952	ABCA1	2,088558	TACR2	1,82899762	CES4	1,71673568	MYH8	3,20559899	927	DDOST	1,46128693	CDC42	1,6245784	DKFZP434E11	2,07758292	AREG	2,02628799	MAP2K1	1,79418098	FZD9	1,68170545	UGT2A3	3,05888172
858	COX15	1,48103561	PLP1	1,65713547	MAD1L1	2,13263756	LPIN1	2,08845977	CHRNG	1,82854422	TAF1	1,71613758	CD81	3,20083986	928	DAD1	1,46095368	POLR2K	1,62342135	SOCS6	2,07750559	FGF9	2,02531562	IL24	1,79359375	POLM	1,68131297	BGN	3,05574384
859	CCR3	1,48072622	BIK	1,65647463	PNKP	2,13191575	AOX1	2,0882833	RASGRP1	1,82753452	IL28B	1,71546726	LCAT	3,19794309	929	SOX2	1,46095125	SLC6A11	1,62328667	BCKDK	2,07603214	KDELR2	2,02521227	CASP6	1,79322295	ATP5H	1,68106742	POLR1D	3,05530087
860	RELB	1,48008254	VEGFA	1,65609641	SCN8A	2,13099178	IRAK2	2,08800246	ARHGEF12	1,82743312	SYT2	1,71544922	DOT1L	3,19791392	930	HS6ST1	1,46071856	CLU	1,62328021	CLK3	2,07252553	NOLA2	2,02446983	FDFT1	1,79280084	NDUFV2	1,68105976	LIPT1	3,05032857
861	C13ORF15	1,47943562	CDK4	1,65603846	PELI2	2,13094279	ADC	2,08656689	ESCO2	1,82532303	ORM1	1,71510807	GCNT1	3,19442733	931	PPBP	1,46028491	LRIG1	1,62322992	EGF	2,07214541	HRAS	2,02417788	SMAD4	1,79216269	IL24	1,68066241	MAP4K2	3,04511974
862	COQ3	1,47929541	ALAS1	1,65602983	ARHGEF4	2,13018943	FZR1	2,08646303	NPY1R	1,82516984	TCF7L1	1,71508763	CETP	3,1937871	932	DPYSL2	1,46016539	ACTN4	1,62280845	UBE2G1	2,07190293	SHC2	2,02309527	EXT2	1,79103898	BST1	1,67982074	OPRD1	3,04403351
863	FDFT1	1,47912116	CES2	1,65477043	YES1	2,12798008	GPR171	2,08627381	PPAP2C	1,82498465	ALDOC	1,71493433	NR6A1	3,19335483	933	SLC12A1	1,46007118	AQP1	1,62258608	TOP2A	2,07168362	ATP5H	2,02276384	RBBP4	1,79061392	ROR2	1,67879557	HYAL4	3,04397745
864	RDH12	1,47816545	FMO3	1,65448048	FBXW2	2,12686827	SKP1A	2,0847696	POLR1E	1,82484618	PAPOLA	1,71482196	CYP4A11	3,19309152	934	BCKDK	1,45998028	EGR2	1,62244907	CD38	2,07130791	PIAS1	2,02048148	TIMELESS	1,79056302	NSMCE2	1,67864026	IL23A	3,04190952
865	BPNT1	1,478113	CSAR1	1,65446355	ACAT1	2,1253735	GALC	2,08367785	CKS1B	1,8246803	COL4A3BP	1,71338059	KALRN	3,19009859	935	RPIA	1,45995218	CPS1	1,62230775	S100A12	2,07059929	TXNRD1	2,02007587	CDKN1C	1,79028837	TLE1	1,67751394	B4GALT4	3,04149572
866	CASP6	1,47786733	SELP	1,65435494	KCNMB1	2,1243676	FASLG	2,08032447	PROM1	1,82449785	ADAMTS13	1,71236364	CA3	3,18553422	936	GNAS	1,45982005	PPARG	1,6222823	OTC	2,07021572	EME1	2,01992274	COL11A2	1,79026422	CAMK2G	1,67745043	CHST14	3,03943644
867	PPP1R3A	1,47727729	SCYL1	1,6543218	ASPA	2,12389882	PRKACG	2,08003465	CXCL2	1,82436738	EIF1AX	1,7122087	GFI1	3,18416397	937	ARMETL1	1,45959852	RPE	1,62225804	SMPD2	2,06963422	IFNA7	2,01782093	CES1	1,79012227	PPP2R5C	1,67729698	SMS	3,03678754
868	DGAT2	1,47711598	EEF1D	1,65429832	PAK2	2,12200881	ADCYAP1R1	2,07973447	IRF2	1,82387903	CYP21A2	1,71203998	ENTPD1	3,18279982	938	PCAF	1,45935081	CYP8B1	1,62129718	SLC23A1	2,06927436	CD36	2,01756969	DGKI	1,79000962	SLC12A3	1,6772321	XPO1	3,03607355
869	NMI	1,476604	PCNA	1,65373583	L1CAM	2,12082988	PTPRC	2,07837913	CXCL6	1,82383579	GTF2H3	1,71141525	ABL1	3,18095868	939	TNFRSF18	1,4593416	MME	1,62072526	XRCC5	2,06832864	SELL	2,0174883	PIK4CA	1,78917312	SPRY1	1,67568582	WASL	3,03391556
870	EFNB2	1,47636525	ATP5B	1,65343682	IL23R	2,11969239	NSD1	2,07836673	STAG2	1,82361921	NAGA	1,71116821	PRMT1	3,18013933	940	NUMBL	1,45933127	GABRA6	1,62057617	PRKAB1	2,06795785	STON1	2,0174591	FGF12	1,78862648	PGAM1	1,67567622	SMURF1	3,03333601
871	MAP3K7IP3	1,47549747	VDR	1,65261179	GNA13	2,11943488	PTPRH	2,07805668	STX18	1,82317191	MMP10	1,71116701	CDKN1A	3,17809214	941	MOG	1,45923203	KIAA1394	1,62046237	CSNK2B	2,06693494	ABCB6	2,01720051	CDR1	1,78841715	FOXA2	1,67540187	MAP2K1	3,03243968
872	CD68	1,47529072	CDC26	1,65229346	SULT1A3	2,11905676	C9ORF97	2,07768836	CCL1	1,82185125	HARS2	1,71086881	TNFAIP1	3,17743158	942	MCM7	1,45915282	TCERG1	1,62021242	EEF1B2	2,06549829	IRS4	2,01561827	CD79B	1,78825998	BIK	1,67539468	TACR3	3,03221352
873	A1BG	1,47477821	SRP9	1,65209569	UGT2B10	2,11905183	ATP1A4	2,07717084	C12ORF57	1,82175905	ANAPC5	1,71071383	PSME2	3,16988576	943	CDC26	1,45909983	IGF1R	1,62011215	TGFBR2	2,06433523	SYT2	2,01547018	ABCA1	1,78769977	BNIP3	1,67474114	CNTFR	3,0287572
874	TEC	1,47477518	PTGER2	1,65114963	EFNB2	2,11724571	FLAD1	2,07658235	DARC	1,82098774	CD33	1,70996813	XPC	3,16982399	944	CDKN2C	1,45897301	ENPP1	1,61973895	GPC5	2,06313848	SCYL1	2,01526063	RFC1	1,78721642	TBXAS1	1,67466951	ARHGEF11	3,02841058
875	CDH1	1,47474978	GDF10	1,650655	CSRP3	2,11675252	TIMP3	2,07582869	DRD3	1,82084769	DNTT	1,70995038	IL2	3,16980795	945	AANAT	1,45880856	CEBPD	1,61868106	WNT1	2,0629043	DGAT1	2,01367334	NARS	1,78697929	CALM1	1,67447419	SOS2	3,02742561
876	CITED1	1,47467947	VLDLR	1,64963378	CELSR1	2,11442166	ARHGAP1	2,07552401	ALPL	1,82026881	LEFTY1	1,70958592	TPMT	3,16737437	946	IL4R	1,45850853	EGR4	1,61856071	STK36	2,06218286	CAMK2A	2,01293467	MAN2C1	1,7866136	ITGA3	1,67409866	GOT1	3,02571616
877	GHSR	1,47447165	TDGF1	1,64948283	CDC37	2,11301697	FOLH1	2,07515002	DYSF	1,81989595	PRDM2	1,70920078	GPR45	3,16574881	947	PIGS	1,4523002	MC3R	1,6183643	GSTA1	2,06074199	GSTA1	2,01292688	SKP1A	1,78588474	B3GAT3	1,67404221	FHIT	3,02547357
878	SOCS3	1,47430946	AMY2A	1,64945534	HTR3C	2,11163413	VDR	2,07512197	DNAJA1	1,81974125	CA7	1,70907374	HS3ST3A1	3,16382222	948	PTGER1	1,45806803	LPHN3	1,61836392	GART	2,06070716	SQSTM1	2,0127689	CD207	1,78584445	SSR4	1,67368656	MT2A	3,02417312
879	GSS	1,47430662	APPL2	1,64710542	CSTF2T	2,11160474	RAP2B	2,0722604	SELP	1,81959481	LTA	1,70898479	AGER	3,16361552	949	CGN	1,45788146	CHGB	1,61776792	ACYP1	2,0595503	PLA2G12B	2,01196387	AGXT	1,78568526	GRIK3	1,67347635	KCNQ5	3,02316269
880	CDH5	1,47398553	H2AFY	1,64624847	RIPK2	2,11097053	ACADS	2,0720057	GALNT6	1,81952974	VCAM1	1,70886612	PTGIR	3,15909427	950	G6PC2	1,45720383	NOTCH1	1,61766923	EIF2B2	2,05528046	NFKBIE	2,011929	CAND1	1,78467643	SHMT2	1,6732301	SRPR	3,01972717
881	COL4A6	1,47378203	LY96	1,646135	MBD4	2,1109102	PALB2	2,06977171	NFKBIA	1,81900458	TLK1	1,70829802	DRD2	3,15288974	951	RAMP1	1,4571451	PIK3C2G	1,6175248	LMAN1	2,05327355	UBTF	2,01101751	MOG	1,78352018	PELI2	1,67309179	NKRF	3,01941918
882	CELSR3	1,4737356	PELI2	1,64409105	DKK4	2,11077591	SETD2	2,06834778	C9ORF47	1,81885063	PPP1R13B	1,70753862	DNAJB2	3,15205898	952	ADCY8	1,45714317	CAPN1	1,61593636	PSME2	2,05266394	RFXANK	2,01048442	H19	1,78220476	DNAJB4	1,67300618	RNASEN	3,01885431
883	GDF10	1,4737013	GALNT5	1,64399812	TRO	2,10968721	INS	2,06439346	TAF1	1,81823123	NT5C1A	1,70730906	ARF4	3,15160288	953	KRT17	1,45650592	CLTA	1,61444919	ASL	2,05194665	DDX1	2,00993192	PGA4	1,78160056	SPN	1,67222755	GAL	3,01808374
884	F2RL3	1,47359837	BAP1	1,64398394	BTG2	2,10811623	ALK	2,06193553	HRG	1,81755519	DNAJC4	1,70687194	EPX	3,15122266	954	BACE1	1,45648027	AVPR1B	1,61385212	FZD5	2,05132431	GPR109B	2,00732109	AREG	1,78129445	IL4R	1,6720627	ARSE	3,01661227
885	ATXN1	1,47347037	DGAT1	1,64395632	ATG9A	2,10691232	NAT2	2,06171287	ZBTB16	1,81721592	GDF10	1,70647099	FOXL1	3,1485696	955	TPK1	1,45597054	FABP5	1,61379923	CASP4	2,05044989	NFKBIA	2,00390802	AGPAT1	1,78063937	STX4	1,67193236	PELP1	3,01640405
886	MAP3K14	1,47306778	HOXA4	1,64346064	KDELR3	2,10548159	IFNA2	2,06098283	ATP5A1	1,81591697	CD28	1,70332259	POLR3B	3,14656859	956	MAP2K5	1,45582436	RPS6KA3	1,61377517	CYP8B1	2,05028709	RAB5A	2,00382862	AKAP8	1,78051182	PIAS1	1,67075856	CES2	3,01598565
887	MAN2C1	1,4730336	PTPN22	1,64248132	IL19	2,10465254	CA6	2,06062338	CYP21A2	1,81542487	ADAM8	1,703142	NT5C1A	3,14632444	957	HMGN1	1,45570675	ENTPD7	1,6128978	SOCS3	2,05028664	MPPED2	2,00361529	UGDH	1,78026377	CSAR1	1,6704344	IL28B	3,01429847
888	GPX6	1,47181727	KPNA6	1,64191861	RBKS	2,10447512	HYAL2	2,05900397	SLC10A2	1,81535275	IL1RAP	1,70303116	ARPC3	3,14577184	958	AVPR2	1,45553359	RBKS	1,61262941	YY1	2,04823273	GADD45B	2,0010371	MAOA	1,7799738	DOCK1	1,66776112	EBF1	3,01422122
889	MUC1	1,47161155	CDK7	1,64078543	CNTN1	2,102862	NP	2,05887071	ENTPD3	1,8148479	AHCY	1,70291776	GTF2E2	3,14277865	959	AMHR2	1,4554051	NDUFA1	1,61245018	RAD51	2,0479144	TGFBR2	2,00051187	RPS6KA5	1,77958571	POLR1E	1,66771377	OTUB1	3,0126659
890	AK2	1,47121444	BNIP3	1,64037045	NOLA2	2,10265941	PRKAR1A	2,05812618	CXCL9	1,8136029	GPR18	1,7028684	DNTT	3,14037851	960	MAFA	1,45518134	CYP2C9	1,61227909	HMGCR	2,04739551	NLK	1,99890328	RAB3A	1,77950329	IGFBP7	1,66763995	CMKLR1	3,01263507
891	MCAT	1,4709017	RASGRF1	1,63996839	NNMT	2,10255493	AGPAT6	2,05726547	API5	1,8134316	NTSR1	1,70249709	RTF1	3,13613782	961	OLA1	1,45503214	SERPINC1	1,61050028	NFKBIA	2,04738507	PRTN3	1,99667226	CDC14A	1,7791013	TAGLN	1,6667427	HLA-DQB2	3,01075335
892	MYST3	1,47080349	UQCRC1	1,639141	RNF2	2,10081861	EGLN3	2,05684331	PTPRO	1,81221472	HSPA12A	1,70179436	CACNA2D2	3,13469885	962	MFGE8	1,4549857	MAPK13	1,6101589	INS	2,04720108	OXCT1	1,995727	EDN1	1,77887214	GABRG3	1,66598747	ERBB4	3,00966441
893	IL8	1,47077521	ERCC2	1,6380074	POLE2	2,10031994	F2RL3	2,05651496	NR4A1	1,81018425	PSME1	1,70116337	ADCY1	3,13177967	963	PES1	1,4545805	TREM2	1,60905423	TSLP	2,04565539	DDX50	1,99543478	SLC30A1	1,77868701	HTR3C	1,66598378	CDC2L2	3,00885163
894	GIPR	1,47064749	POLG	1,63798694	AQP1	2,09784104	TAT	2,05519013	CLK4	1,81012337	CR1	1,69964567	POLD1	3,1311639	964	MAP3K8	1,45454643	NUMBL	1,60880918	MOG	2,04494348	HRB	1,99512155	F8	1,7785856	ERBB3	1,66550758	HSD11B2	3,00846254
895	LIAS	1,47049211	NP	1,6371808	DPPA3	2,09694558	GAP43	2,05482675	ADRA1A	1,80866398	SVIL	1,6989874	CLDN17	3,12969049	965	IL1RAP	1,45434337	GDF5	1,60852619	BCHE	2,0445355	WARS	1,99496298	NEDD4L	1,77765668	IRS1	1,66469282	CCNT2	3,0084007
896	AOC3	1,47019151	MAP3K7IP2	1,63683098	PSMD14	2,09668148	CSNK2B	2,05469323	NGFR	1,80852538	EIF2AK3	1,69874202	GCKR	3,12638559	966	STON1	1,45399726	SCN2A	1,6074169	TERF2IP	2,04421425	AICDA	1,99491913	MBD4	1,77716879	ACSL4	1,66460112	SMAD3	3,00446703
897	GTF2E2	1,4700015	CYP7A1	1,63681484	MGAT4B	2,09615263	MSR1	2,05368452	FMO3	1,80753777	GNG3	1,69726674	DPP4	3,12562561	967	DDX20	1,45356286	FOXA1	1,60722999	IFNA2	2,04321372	ATP5B	1,99443771	GABBR1	1,77705233	NOXO1	1,6644351	SNX4	3,00423439
898	C1QB	1,46995993	CES4	1,63587675	PHF21A	2,09443644	LIPT1	2,05263306	NT5C3	1,80727159	UBE2E3	1,69712368	ISLR	3,125246	968	TREX1	1,45313959	PPP1CC	1,60687888	VTN	2,04241836	IDH3B	1,99345299	HTR3B	1,77690189	MVD	1,66395099	TNFRSF9	3,00226461
899	EIF2AK2	1,46961769	RAD51C	1,63586706	EFNA3	2,09367778	CALR	2,05262483	PDGFRB	1,80607529	TUBG1	1,69642142	NKD1	3,12252383	969	NSMCE2	1,45285986	TLR6	1,60678342	EXO1	2,04135295	LHB	1,99329812	CLDN10	1,77678923	APC	1,66353791	PIGW	3,00048154
900	KCNMB4	1,46904823	KRT17	1,63548435	CLDN22	2,091926	KCNE1	2,0519089	VCAM1	1,80588675	KLRD1	1,69627692	CSNK1G1	3,11812193	970	GTF2H1	1,45242819	SSTR3	1,60594831	TAF13	2,04073979	ABCB10	1,99204424	ADCY1	1,7761328	PF4	1,66323242	JAG1	3,0003019
901	CPO	1,4676542	FMN2	1,63534255	GARS	2,09185465	FABP1	2,05172478	AGPAT2	1,80519592	DSP	1,69598338	CCNH	3,11692781	971	PRKACA	1,45220794	GK2	1,60561606	TPH1	2,04004875	NAE1	1,99204424	ITGB2	1,77572544	FABP7	1,6632304	TFAP2C	2,99838682
902	SCNN1A	1,46761927	NPR2	1,63484956	ORC2L	2,0914799	BHLHB3	2,05038237	CD226	1,80499297	ABCD3	1,69585205	SOCS5	3,1168381	972	HOXD1	1,45213777	GARS	1,60541073	SPO11	2,03800312	SLC12A2	1,99067613	ERCC5	1,77513977	PECR	1,66229907	BTK	2,99813244
903	CDK8	1,46743686	MECP2	1,63473248	AKR1C4	2,09108637	KLRD1	2,0500511	LDB1	1,80472783	IDH2	1,69505214	LY75	3,1144734	973	FEZ1	1,45209818	CABIN1	1,60494843	LRP6	2,03796599	IFT57	1,98964282	GRAP2	1,77497396	BTG3	1,66133983	HTR4	2,99802031
904	MLXIPL	1,46721023	IL28B	1,63394259	CUGBP1	2,08883712	TCF7L1	2,04903539	MUC1	1,80422008	CHKA	1,69434502	CRY2	3,11385261	974	ATP6V0E1	1,45196593	CCL16	1,6048214	KCNA7	2,03792963	ADORA2B	1,98813907	MTAP	1,77446156	MKI67	1,66116007	LTB4R2	2,99724365
905	NKD2	1,46690936	CSF2RA	1,63377487	MYST3	2,08786853	APBA3	2,04878974	SUCLG2	1,80403312	PLLP	1,69378353	TNFRSF11B	3,11314924	975	DEGS2	1,4518924	ITGA6	1,60478843	ENPEP	2,03536257	PMM1	1,98595573	TUB	1,77440465	RNF4	1,66067742	CHST13	2,99667062
906	KCNE1	1,46682477	SFN	1,6334069	AOX1	2,08773008	CBR3	2,04730906	COL9A3	1,80395813	WIF1	1,69318056	APOL2	3,11266586	976	ACP1	1,45129549	VIP	1,60408358	DLL3	2,03463645	CHRNA3	1,98575453	TNFRSF10A	1,77389507	BST2	1,66010842	MTIF2	2,99646378
907	PGM1	1,46668149	ZMAT3	1,63226149	NPR2	2,08741427	EIF2AK4	2,04646873	CHRM1	1,80395048	INDO	1,69265464	CHUK	3,11018777	977	ECE2	1,44914756	HSPA12A	1,60404288	CA4	2,03394446	IRS1	1,98496856	SHB	1,7738095	HOXA4	1,6600065	ZMYM2	2,99585712
908	FASLG	1,46636442	CAND1	1,63135147	BTLA	2,08504515	TNKS2	2,04646766	PHKA2	1,80374531	COMP	1,69201762	NPM2	3,10205517	978	CREB3L3	1,44880924	MYLK	1,60388581	PPIA4	2,03382828	AP2M1	1,98306698	SP1	1,77234234	OPRD1	1,65987005	AMHR2	2,99507922
909	ABCA7	1,46616329	CDC34	1,63112923	PRIM2	2,08504515	PLLP	2,04562452	A1BG	1,80349552	PLCG1	1,6919489	FMOD	3,09696407	979	PGK2	1,44873403	YWHAQ	1,60333746	ACTG2	2,03345715	IFIT2	1,98267467	NT5C1A	1,77225963	DDIT4	1,65972403	RFNG	2,99407355
910	TAF1L	1,46595154	TNFRSF18	1,63005312	DHDDS	2,08428368	DLAT	2,04519857	SYNJ1	1,80284071	PLD3	1,69168398	SLC1A6	3,09452181	980	PRDX1	1,44845927	ATF4	1,60318266	SUCLG2	2,03345594	STX18	1,98253356	DTNBP1	1,77222867	MIF	1,65967798	LIAS	2,9910506

Table A4. Pooled-shRNA library screen on HEL cell line and MF-3: list of 2nd most depleted shRNAs for each experiment (ranking approach 1, RA1).

	NO ruxolitinib (setting 1)				Ruxolitinib (setting 2)				Ruxolitinib + CM (setting 3)				MF-3				NO ruxolitinib (setting 1)				Ruxolitinib (setting 2)				Ruxolitinib + CM (setting 3)				MF-3	
	Experiment 1		Experiment 2		Experiment 1		Experiment 2		Experiment 1		Experiment 2						Experiment 1		Experiment 2		Experiment 1		Experiment 2		Experiment 1		Experiment 2					
Rank	*Gene*	*Fold change*	*Gene*	*Fold change*	*Gene*	*Fold change*	*Gene*	*Fold change*	*Gene*	*Fold change*	*Gene*	*Fold change*	*Gene*	*Fold change*	*Rank*	*Gene*	*Fold change*	*Gene*	*Fold change*	*Gene*	*Fold change*	*Gene*	*Fold change*	*Gene*	*Fold change*	*Gene*	*Fold change*	*Gene*	*Fold change*	*Gene*	*Fold change*
981	ATP5A1	1,44832666	IL22RA2	1,60314608	CDH1	2,0330069	BCL2	1,98128791	MYOG	1,77206759	PIGT	1,65904967	HPX	2,99045349	1051	BLVRA	1,43243207	ADCY3	1,57526682	SMC4	1,98909838	NKD2	1,93957241	DHRSX	1,73820448	STAG2	1,62680259	HARS	2,88503499
982	ALLC	1,44824471	CNTFR	1,60307643	AKAP1	2,03295604	DLX3	1,98037797	MGAT1	1,77082168	HPR	1,65902259	POLD4	2,98736662	1052	TEAD2	1,43242396	MAP3K5	1,57493941	MMRN1	1,98894389	VIP	1,93917429	AGPAT4	1,73815458	JAG2	1,62657269	ALPP	2,88110587
983	B4GALT1	1,44823708	JAZF1	1,6030239	ATP5G1	2,03241594	LRPPRC	1,98009143	ADAMTS13	1,77064091	KIF3A	1,6586666	UGT1A3	2,98490341	1053	INPP5E	1,43223391	BCL2L11	1,57460449	HTR7	1,98681475	ADRB3	1,93880386	CDX4	1,73809574	EGR2	1,62640965	OAS1	2,8803161
984	CLEC7A	1,44821219	ALPI	1,60151351	MPPED2	2,03235136	GLB1	1,9798198	PERP	1,77060769	PNKP	1,65828744	GARS	2,98418518	1054	GPX3	1,432151	LARS	1,57409409	ASPH	1,9852747	B3GNT6	1,93845028	GP1BA	1,73808702	IRF9	1,62621728	CYP2C18	2,87966311
985	TCERG1	1,44771993	GPR35	1,60123909	TIMELESS	2,03229687	TNFSF8	1,9790819	GLS2	1,77001543	ATXN1	1,65816791	AVP	2,98105787	1055	PIR	1,43191908	SMAD5	1,57393385	ABLIM3	1,9849274	OPRS1	1,93811619	ST3GAL2	1,7380587	IFIT2	1,6252848	DUSP1	2,87958167
986	PPP2R5D	1,4476085	MAX	1,60110164	NCK1	2,0309609	SLC25A4	1,97901796	LPL	1,77000121	SETD2	1,65762749	ATG4D	2,98015926	1056	WIPI1	1,43170774	CD52	1,57334317	CALM2	1,98438674	RFK	1,93760552	ST8SIA2	1,73768234	SELL	1,6249337	APP	2,87897483
987	DFFB	1,44712721	HSPB2	1,60100137	NMI	2,02956991	STX4	1,97811518	FADS1	1,7698238	CHST2	1,65756076	KCNMB2	2,97911585	1057	ILVBL	1,43145094	PRPF19	1,57277513	VAMP5	1,98434685	PTGIS	1,93639211	DDEF2	1,73642113	ANKRD6	1,62492613	HNRNPC	2,87880951
988	ALKBH2	1,44677523	PDE1B	1,60098376	MAFA	2,02896751	HSD17B4	1,97770324	SORBS1	1,7695812	PIK4CA	1,65697253	PTGS1	2,97888024	1058	GRIN2A	1,43137115	IL4R	1,57275502	FUT9	1,98401733	CD40	1,93549213	SLC2A1	1,73635753	IKZF2	1,6246578	ITCH	2,87880951
989	CEL	1,44588484	TLR4	1,60056128	ALDH1A3	2,02867114	ARRB1	1,97764578	MCM10	1,76922841	NF1	1,65610793	CSF1R	2,97852501	1059	SLC12A3	1,43131292	COL6A1	1,57258248	CBB	1,98390099	SCARB1	1,93528757	CD8B	1,73550444	PACAP	1,624643	NRF1	2,87775928
990	CYP2J2	1,44528629	CTBS	1,60034508	ABCC8	2,02776511	KPNA6	1,97683215	CFD	1,76812746	DICER1	1,65588917	FKBP1A	2,9764355	1060	CPSF6	1,43112582	CDR1	1,5725058	NT5C1A	1,98377118	FRAT1	1,93527738	PSMB9	1,7347483	ABCD2	1,62450332	C1R	2,87558307
991	ITGAL	1,4451906	HTR4	1,60012199	GABRA3	2,02697587	NOXO1	1,97612743	TXLNA	1,76772816	DNMT3A	1,65570776	DGKH	2,97589724	1061	PRKAG1	1,43109614	HOXA1	1,57224309	ACSM1	1,98331469	XRCC4	1,9348732	ALDH2	1,73424312	NEFM	1,62267193	FGF8	2,87420735
992	CACNA1S	1,44496929	IFNB1	1,59971911	PTCH1	2,02686511	COL11A2	1,975013	VTN	1,76751784	OCIAD1	1,65532101	P2RY12	2,97562962	1062	SLC2A3	1,43067465	COL8A1	1,57175641	PACAP	1,98229547	ARPC1B	1,93456071	ARG1	1,73375271	HMGCR	1,62250713	WNT11	2,87310785
993	LRP8	1,44492152	NUDT4	1,59916384	CACNA1C	2,02681104	RPS6KA1	1,97334339	DIABLO	1,76699315	ATP5C1	1,65472788	RFXAP	2,97475077	1063	DYSF	1,43062059	WIF1	1,57165453	LRRC41	1,98226018	CA9	1,93367907	IRF1	1,73340358	TDG	1,62167908	PTK2B	2,87016543
994	SERPINA10	1,44450459	CHRNG	1,59812572	CYP26A1	2,02611185	ANAPC10	1,97326654	VDR	1,7660677	PIK3CD	1,65460445	AKAP1	2,9730652	1064	EBP	1,43034567	ROR2	1,57158374	DCLRE1B	1,98214452	HCK	1,93361142	VAMP5	1,73317157	RARS	1,62159663	UBE3A	2,86897624
995	GBP1	1,44439283	B3GALT1	1,59792281	SMARCB1	2,02575891	NT5C3	1,97318834	NT5C2	1,76598462	NRAS	1,6541829	PTPN7	2,9710362	1065	HLA-C	1,43028331	TNFRSF19	1,57143952	GAA	1,98212854	SNAP25	1,93315898	CYP4A11	1,73305007	TAL1	1,62151699	MYBPC3	2,86788894
996	B4GALT6	1,44419789	RAD18	1,59735604	VCAN	2,02566882	EPPK1	1,9730788	ADIPOR2	1,76596404	ATP5J	1,65401729	PACAP	2,96940312	1066	TUBA8	1,43015883	BP75	1,57107527	COX5B	1,98171312	SPRED2	1,93025793	CSF3	1,73208596	CCR8	1,62131947	HSD17B4	2,86044687
997	SRP54	1,44350938	UBE2D3	1,59673871	PTGER1	2,02489985	PRIM1	1,97260885	UBE2H	1,76564904	ZBTB32	1,65331872	BRD4	2,96919808	1067	TNFRSF19	1,42964083	PLLP	1,57075125	DRD3	1,98116475	PSEN1	1,93023613	ARHGAP4	1,73146816	GPX7	1,62130468	WNT3A	2,85922352
998	BST1	1,44333508	DDOST	1,59653476	IFIT2	2,02382636	BET1	1,97149658	IL1R1	1,76525901	RAD23B	1,65294981	SLC2A4	2,9676093	1068	EIF2AK4	1,42945885	IFI44	1,57062582	TLR10	1,9807826	MTFMT	1,92998078	TRIP12	1,73133399	ACP1	1,62082092	GATA1	2,85725572
999	CTNNBIP1	1,44330384	FST	1,59650747	F3	2,02337818	CHD8	1,97093431	DCK	1,76507632	MXI1	1,65224556	HBA2	2,96684713	1069	GNPDA1	1,4293786	DAD1	1,56952266	FOXA2	1,97822144	FBLN2	1,92952718	METTL6	1,73125709	ITGA2B	1,62059269	DIXDC1	2,8543803
1000	ENPP3	1,44322676	BBS2	1,5957288	TSG101	2,02068377	PRKCE	1,97022527	WDFY3	1,76460054	DDX4	1,65203145	GBA3	2,96681543	1070	CXCL11	1,42920834	SPO11	1,56870851	ACADL	1,97800402	INPP5E	1,92945916	TGFBR3	1,7306071	TRIM28	1,62035046	CHSY1	2,85397593
1001	GABBR1	1,44303606	PALB2	1,59547017	PPARA	2,01959914	RAD52	1,97019108	CBX2	1,76354084	ARPC5	1,65173376	SERPINB2	2,96599958	1071	HDAC1	1,42905015	JUNB	1,56752974	CXCL12	1,97731748	EZH1	1,92913018	TLR4	1,73054167	ACAA1	1,62013426	NLRP2	2,85170332
1002	TPP2	1,4430066	CLCN2	1,59515626	CARD11	2,01941248	BDKRB2	1,96910269	AKAP13	1,76305084	FASN	1,65071278	MAP2K2	2,96532235	1072	VIP	1,42897346	ATP6AP1	1,56740029	AK5	1,97705157	PFKFB3	1,92913018	POLQ	1,72962678	CDC42	1,61951557	IDI2	2,85120267
1003	TCP1	1,44298663	ST3GAL1	1,59512753	CHSY1	2,01918373	TRRAP	1,96847248	RRM2B	1,76206364	MAP4K2	1,65067508	CHAF1A	2,96014307	1073	ARPC2	1,42828801	FTO	1,56525574	CSMD1	1,97477056	CLTC	1,927066	CRLS1	1,72906358	MAP3K7IP2	1,61901548	CAMK4	2,85012159
1004	MYL4	1,44274652	GBL	1,59490764	RFC1	2,01880902	LRRTM3	1,96737923	FOXA1	1,76197115	CFHR3	1,65064491	RAG2	2,95685368	1074	CMKLR1	1,4282074	PRKX	1,56498968	SOX2	1,97419067	SUCLG1	1,92704618	ATP6V0B	1,7288208	RTKN	1,61827732	MDH2	2,84785013
1005	ERAF	1,44244542	SULT2A1	1,59339429	COL4A3BP	2,01840385	CXCL2	1,96676952	YY1	1,76183416	KERA	1,6502873	PAX4	2,95476329	1075	SHB	1,42808423	XRCC2	1,56494637	CASP1	1,97274887	PBEF1	1,92686328	LRMP	1,72881861	SFRS12IP1	1,61820299	EXTL3	2,84716296
1006	KLKB1	1,44142347	NRAS	1,59248849	LTB4R	2,0171237	TIMELESS	1,96659097	L1CAM	1,76148177	REV1	1,6501999	RDH14	2,95445176	1076	GATA1	1,42807204	ATG9A	1,56468182	CSF2RA	1,97259171	AANAT	1,92439175	RFXANK	1,72839523	FOXA1	1,61772896	ACADSB	2,84250229
1007	PCNA	1,44142208	ACTG1	1,59142967	ACO2	2,01703719	IFIT3	1,96656285	BET1	1,76003448	CRP	1,64946961	TLR7	2,95265062	1077	HDAC11	1,42796856	PRKRA	1,56411183	PARK7	1,97215611	RALB	1,9240058	CNTFR	1,72817469	RAD51C	1,61695818	PCK1	2,84238793
1008	XPA	1,44093285	UNC5B	1,59139354	AGPAT2	2,01684945	AMDHD1	1,96624967	H2AFY	1,7596491	MAPK7	1,64817103	FGA	2,95201167	1078	IL28B	1,42769858	CD207	1,56366461	RPS6KA3	1,97132205	DDX54	1,92226311	IRAK1	1,72785781	EIF1AY	1,61636963	CYP2F1	2,84063593
1009	METTL2B	1,44084671	POLR2C	1,59110909	KIAA1394	2,0164398	ZBTB16	1,96598147	CLTC	1,75801389	HELB	1,64809749	PLCG2	2,95190593	1079	CAPN2	1,42753501	PTGIS	1,56357437	KCNJ3	1,97064476	CKMT1A	1,92221368	INPP5B	1,72776319	EEF1B2	1,61557287	MGAT5	2,83655166
1010	ARHGEF4	1,44055773	IL1RAP	1,59009066	COPA	2,01640459	CYP4F12	1,96565297	FUT2	1,75761459	NP	1,64802698	IL4R	2,94618815	1080	CTNNAL1	1,42751266	CHSY1	1,56356337	PPP2R5C	1,97013175	CHGA	1,92120484	FSTL1	1,72722467	TNFAIP3	1,61493769	GSTM1	2,83637366
1011	CRTC1	1,44047593	NCL	1,58969901	EIF2AK2	2,01592884	FANCG	1,96502368	DCTN1	1,75723266	COL25A1	1,6476436	B3GNT3	2,94512232	1081	DLL3	1,42710719	CYP4A22	1,56353257	TFPI	1,96915626	CA7	1,92056276	IFT172	1,72666369	FAM59A	1,61410815	CALCA	2,83131988
1012	PPP6C	1,44046534	SMC4	1,5885489	CTBP2	2,0150991	EIF2AK3	1,96446087	IRS4	1,75674619	HSD11B2	1,64709415	PHPT1	2,94153473	1082	TANK	1,42691104	NUP214	1,56337722	SLC27A4	1,96888163	DICER1	1,92042189	ALOX15B	1,72534253	TREX1	1,61350602	IRAK4	2,83040185
1013	CDS1	1,44039911	TEK	1,5883677	TRRAP	2,01431877	MECP2	1,96263581	ICOS	1,75624545	WASF2	1,64630715	ANGPTL4	2,94141198	1083	XYLT2	1,42664678	ARHGEF11	1,56329069	NFYB	1,96854636	HDC	1,91989845	PGAM1	1,72412402	CAMKK2	1,61316608	UNC5CL	2,83038817
1014	ADCY3	1,44032745	MAOA	1,58822588	COL27A1	2,01325627	SUMO2	1,96212557	KCNJ2	1,75606378	NUMBL	1,64607299	COL24A1	2,93977284	1084	GCAT	1,42628929	CNTN1	1,56320239	JAZF1	1,96606024	HNF4A	1,91842681	PAPSS2	1,72381045	ARHGEF11	1,61261538	MMP3	2,82794722
1015	MAL	1,44012601	VKORC1	1,5880319	ATG12	2,01310125	C8A	1,95932314	PLLP	1,75447549	FZD1	1,64536219	NDE1	2,93898202	1085	ST6GALNAC5	1,42583192	HELLS	1,56316083	VNN1	1,96573862	DAXX	1,91808665	DVL2	1,72329182	TNKS1BP1	1,61141114	ADH6	2,82643764
1016	DAPK1	1,4400074	NSD1	1,58764766	TNFRSF13C	2,01107409	AK2	1,95846283	PPP2R5B	1,75423237	COL4A2	1,64530068	CDX4	2,93650407	1086	HYOU1	1,42478532	IGF1	1,56303012	NUDT4	1,96526204	TRPV6	1,91752607	ST3GAL1	1,72296755	PRKCD	1,6110976	DDX1	2,82524547
1017	IFNA5	1,43995509	ST6GALNAC4	1,58745107	BPNT1	2,01013924	PTGDR	1,95667883	ISG20	1,75394346	CXCL9	1,64516079	FPGT	2,93641312	1087	CRTAM	1,42476313	PRIM1	1,56272851	TNFAIP3	1,96517259	E2F2	1,9169335	SLC12A3	1,72247996	C1QL4	1,61097153	PAX3	2,82464266
1018	NCK1	1,43992181	IL10RB	1,58735613	HCST	2,00879786	PIK3R4	1,95642783	CDC6	1,75370329	ILK	1,64504798	PTPRH	2,93619471	1088	SSRP1	1,42391699	ACE2	1,56264142	ROR2	1,96516369	CD83	1,916667	HPD	1,72245056	PRKDC	1,61004682	AKR1C3	2,8240911
1019	GABRD	1,43990417	MARCO	1,58734467	CYP4A22	2,00865649	ABCD2	1,95609804	AGMAT	1,75345961	PDE6H	1,64436367	IL2RA	2,93518407	1089	GMPPB	1,42384653	ALDH1A3	1,56227489	OBFC1	1,96445685	VSIG4	1,91662195	ENDOG	1,72190321	DAG1	1,6100159	APPBP2	2,82334807
1020	FLT4	1,43982191	HSPG2	1,58675526	EEF1D	2,00849046	RAF1	1,95557145	OPRD1	1,75313584	PIK3AP1	1,64404442	IL23R	2,93384824	1090	ARD1A	1,42356662	PLCG1	1,5619374	AZIN1	1,96435783	XCL1	1,9165653	ACTN4	1,72009849	ARF5	1,60992921	NOV	2,82329762
1021	KDELR2	1,43959242	DPPA2	1,58643387	HGFAC	2,00717879	CDC2L6	1,95305731	ESRRA	1,75221165	FLOT1	1,64350306	OLIG2	2,93308869	1091	NFKB2	1,42332449	PARP1	1,56181025	BUB1	1,96427099	HAGH	1,91651153	TAT	1,71844563	AKAP4	1,60956491	ALG3	2,82260475
1022	MAP3K12	1,43921632	FBLN2	1,58643383	PPP5C	2,00664704	RGS4	1,95260121	RECQL	1,75216817	SLC12A1	1,64333503	SLC30A6	2,93189026	1092	ATG2A	1,42313239	UAS	1,56153787	LIF	1,96232389	OBFC2B	1,91634021	CIP29	1,71782725	POLR1A	1,60936549	MVD	2,82239316
1023	HLA-DPB1	1,43865239	NNMT	1,58627077	SOD2	2,00577457	PROM2	1,95138334	KEAP1	1,75213231	CNTN1	1,64315765	PSMD4	2,93106281	1093	DNTT	1,42296522	HPR	1,56147419	CARD10	1,96057685	MST1	1,91610047	PURA	1,71765795	DLX3	1,609287	APAF1	2,82191614
1024	TOLLIP	1,43861	EFNB2	1,585309	MMAB	2,00540993	DNAJB4	1,95064135	ITGA2B	1,75171494	CASP6	1,64308434	AMY2B	2,93016618	1094	SMN1	1,42289769	PHF1	1,56145173	NKX2-2	1,9603879	MYL4	1,9159243	HES6	1,71704249	CLTC	1,60918581	ACY1	2,81981926
1025	ISL1	1,43798915	PNKP	1,5851792	CPO	2,00447716	BPTF	1,95039982	PIP3-E	1,75107849	FCGR3B	1,64264811	HLA-A	2,92799813	1095	GAST	1,4226911	MYBPC1	1,56010103	MIF	1,9600629	PKLR	1,91570779	ACO1	1,71549872	REN	1,60834907	PTCRA	2,81424419
1026	TRO	1,43786086	MTIF2	1,58497903	CREB3L2	2,00399803	PTPRO	1,95010947	MMS19L	1,74955446	GRIN1	1,64247984	RPL8	2,92463589	1096	MCM5	1,4226403	FGFR3	1,55942607	BMP5	1,95920433	CFHR5	1,91567079	NSMAF	1,71545269	B4GALT1	1,60814154	VAMP7	2,81359605
1027	MTMR1	1,43763586	HPSE2	1,58486937	DARC	2,00256902	GOSR1	1,95010426	ATG4A	1,74928702	PTGER4	1,64119466	MTMR2	2,91914338	1097	ARHGAP1	1,42260045	EMX2	1,55925809	MYO1C	1,95910472	ERCC2	1,9156355	PRKRIR	1,71533003	ASAH1	1,60813033	DPYSL5	2,81192689
1028	ST8SIA2	1,43730019	OBFC2B	1,58468374	DNMT3L	2,00220312	SLC12A3	1,95006192	CD69	1,74851354	POLE2	1,64032148	CCL13	2,91837683	1098	STXBP4	1,42254555	COL13A1	1,55922008	GRIA1	1,95887297	VANGL2	1,91483361	AKR1C2	1,71514365	LIPC	1,60722551	ALG13	2,81115062
1029	CYP7A1	1,43719989	IL9	1,58428189	HES3	2,00104956	HOXA1	1,94962391	BMP5	1,74703851	WNT10B	1,63965073	HMGN1	2,91769539	1099	ENTPD6	1,42251144	ATP6V1B1	1,55921085	TNFRSF1B	1,9575847	F11	1,91426806	MPPED2	1,7150097	DAPK1	1,60705558	GHRL	2,81050355
1030	SLAIN1	1,43682152	IMMT	1,58395429	RAB5C	2,00092658	BST2	1,94917965	DCLRE1B	1,74648305	INS	1,63926758	TAGLN2	2,91397429	1100	HCK	1,42211174	MPG	1,55920629	NR2F2	1,95697072	HESX1	1,91415679	KDR	1,7148567	CDK5	1,60529006	YWHAQ	2,80380403
1031	KCNJ2	1,43679026	CRHBP	1,58388983	ATP6V0D1	2,0008287	XYLT2	1,94852107	PLD1	1,74644495	B3GNT2	1,6381493	FOXO4	2,91091472	1101	ZMYM2	1,42196655	CASP2	1,55884625	KIF5B	1,95680436	ELOVL6	1,9127219	NLN	1,71468046	PHC1	1,60493697	PON1	2,80271864
1032	PLD2	1,43636695	KDELR3	1,58386631	WNT9B	2,0008287	ADSSL1	1,94760344	NCOA2	1,74642922	MLH3	1,63794927	LRPPRC	2,91031647	1102	SCD5	1,42118776	CAPN2	1,55803671	ABCD1	1,95652139	SVIL	1,91226296	NCK2	1,7145919	LILRB3	1,60488216	FZD6	2,80267678
1033	EIF4G3	1,43629821	UBE1	1,58326981	TCF1	2,0005296	ADRBK2	1,94738547	RBL1	1,74494367	ADCY1	1,63589187	PROCR	2,90773793	1103	THY1	1,42078304	ALDH1B1	1,55757721	GADD45B	1,9565022	COL10A1	1,91212661	FOLH1	1,71433526	DCLRE1B	1,60447512	SMARCC2	2,80216116
1034	CD207	1,43600552	SEMA7A	1,58293524	IL2RB	2,00038757	G6PC2	1,94702225	TRAF3IP2	1,74480884	PSCD4	1,63541875	ACOT11	2,90632234	1104	BNIP1	1,42068827	NR4A2	1,55746213	MTHFD2	1,9554488	EIF1AY	1,91124863	ARPC5L	1,71431306	CYP11B1	1,60408237	TAL1	2,79974596
1035	MC5R	1,43580654	CD38	1,58207342	ENO1	1,99957465	POFUT1	1,94553031	SDHB	1,74448167	LGMN	1,63540373	GZMA	2,90533175	1105	DNAJC5	1,42067555	FUCA2	1,5571579	PRKAR2A	1,95543472	CDK2	1,91116948	CDK6	1,71243317	MAT2A	1,60397533	CAMK2D	2,79788109
1036	CD1A	1,43525365	DEFB4	1,58129601	WBSCR22	1,99906484	NPY1R	1,94532083	DBC1	1,74377517	TRPV6	1,63503971	CTSS	2,90364965	1106	NT5C1A	1,42029776	HCLS1	1,55655225	CHRNE	1,95413009	NRG2	1,91063595	UBE2I	1,71235544	TACR1	1,60353055	CYP51A1	2,79704372
1037	NEUROG1	1,43517784	PPARBP	1,58127622	DIO2	1,99794514	PPARGC1A	1,94530579	GAS6	1,74339001	NDUFB2	1,63486229	TPP1	2,90364965	1107	ACTN1	1,42004753	A4GALT	1,55631883	CYP4B1	1,95322374	NQO1	1,91059048	SLC22A18	1,71228271	MT2A	1,60327928	VIL2	2,79527595
1038	AK7	1,43499529	NCAM1	1,58098012	HNF4G	1,99745146	MYO1C	1,94496338	DPPA4	1,74295386	IL17RC	1,63469627	PSMB1	2,9019013	1108	ELK4	1,41941839	PPP5C	1,55623127	HRAS	1,9530112	GALNT5	1,91009813	ACACA	1,71203316	CD83	1,60275397	ADD1	2,79512
1039	PRKRA	1,43492597	FOXA2	1,58096556	ANAPC7	1,99710311	SNX4	1,94495801	COX5A	1,74283079	PAX1	1,63368142	MAP3K14	2,9015495	1109	WEE1	1,41916858	SH3GLB1	1,55571092	ALDH1B1	1,9529412	PPP2R2A	1,90994087	MAP3K7IP3	1,71187843	C9ORF47	1,60270491	IBSP	2,794076
1040	GDI1	1,43464353	DOT1L	1,58035902	TFAM	1,99684448	PTGES2	1,94475737	COX10	1,74153215	ABCC2	1,63278718	B3GALT5	2,89940442	1110	FH	1,41887251	PDE7A	1,55545885	NUP214	1,95287446	SMC4	1,9094176	B4GALT6	1,71145105	NAT5	1,60220026	CPSF6	2,79368584
1041	MMP13	1,43457138	TARS	1,58000276	NCAM1	1,99549874	ALPP	1,9442006	PHF21A	1,74104259	ANP32B	1,63199535	KRT8	2,89880168	1111	BFAR	1,41880609	MADD	1,55491477	FANCE	1,95142235	PAG1	1,90889696	FZD7	1,7107639	ADRBK2	1,60190333	DOLPP1	2,78939066
1042	TMEM166	1,43433196	BCL7A	1,57996624	PIWIL1	1,99476369	AURKA	1,9440864	GLI1	1,74083699	ACO2	1,63168336	CLTA	2,89658604	1112	ASL	1,41827005	GABARAPL2	1,55487373	MMP13	1,95084286	TACR2	1,90840816	MMP3	1,71033357	AP2B1	1,60057766	LARS2	2,7889871
1043	CDC42	1,43373287	GABRA5	1,57947383	NCL	1,99376816	TRAF6	1,94327021	CAST	1,74033147	PPP1R13L	1,63142939	CA1	2,89577697	1113	DVL2	1,41823638	NEDD4L	1,5545471	TRIP12	1,94978835	FH	1,90812682	NCL	1,71019035	SMAD4	1,60043069	SOCS2	2,78593702
1044	ATP6V0B	1,4335785	TANK	1,57947189	SLCO1C1	1,99332666	ACE	1,94312194	SRPR	1,74004832	CBX2	1,62989029	C13ORF15	2,89562845	1114	GBL	1,41782857	SOS1	1,55442091	GTF2H3	1,94884246	PELI2	1,90793658	GNPDA1	1,70981671	AACS	1,6001094	SEPHS1	2,78555751
1045	PAK6	1,43354567	CDA	1,57909337	MXI1	1,99301982	HIST3H3	1,94306217	MAP3K7IP1	1,73972699	MSH5	1,62908101	RB1	2,89549031	1115	B4GALT4	1,41759433	ITGB5	1,55439426	HSD17B6	1,94681466	DNAJC5	1,90752645	APOL2	1,7096749	CD22	1,5999948	AKAP9	2,78548089
1046	GSTA1	1,43332907	CAD	1,57878087	GALNAC4S-6S	1,9920661	ATP6V0E1	1,94267912	IFNA10	1,73952122	JUND	1,6290165	B4GALT7	2,89233067	1116	WAS	1,41756738	ATP1A1	1,55424364	OAS2	1,94678963	CDC37	1,90674966	DAPP1	1,70898414	MSX1	1,59986188	EIF4G1	2,78404353
1047	SCTR	1,43321578	MBTPS2	1,57701282	AKR1C1	1,9912089	MAF	1,94207329	SLC2A4	1,73949138	MAML3	1,62835661	SLC5A3	2,89041917	1117	CFHR5	1,41674022	NCKAP1	1,55414981	ZFX	1,94504252	COL6A1	1,90669827	GBL	1,7076248	RAD54B	1,59908008	NDUFA13	2,78371669
1048	FADD	1,43308893	GABPA	1,57671451	CYP2A7	1,99009491	C1GALT1C1	1,94185765	CPO	1,73910621	CYC1	1,6274808	ALDH1A3	2,88935063	1118	WASF2	1,41666766	CD160	1,55408533	GGA1	1,94489371	PPP3R2	1,90647177	IL10	1,70733702	COL4A6	1,59873642	MTA2	2,78119236
1049	PLA2G2D	1,4329041	COX15	1,57586731	ARPC3	1,98999302	NDUFA11	1,94184254	CDC25A	1,7388481	EPPK1	1,62737108	ANK2	2,88783428	1119	APOL2	1,41654524	HAT1	1,55398	KDR	1,94408267	SNCA	1,90606447	EME2	1,70654731	CD37	1,59827535	PGM1	2,78072412
1050	SESN1	1,4326595	ENPP7	1,57551144	ENTPD6	1,98989863	PACAP	1,94182047	CYP8B1	1,73860567	OXSM	1,62705489	HSP90B1	2,88587074	1120	GUCA1C	1,41633206	CDK3	1,5532959	SENP2	1,94213451	CADM3	1,90564671	FSHR	1,70651811	SCN2A	1,59712257	CNPY4	2,77779506

Table A4. Pooled-shRNA library screen on HEL cell line and MF-3: list of 2nd most depleted shRNAs for each experiment (ranking approach 1, RA1).

	NO ruxolitinib (setting 1)				Ruxolitinib (setting 2)				Ruxolitinib + CM (setting 3)				MF-3			
	Experiment 1		Experiment 2		Experiment 1		Experiment 2		Experiment 1		Experiment 2					
Rank	Gene	Fold change	Gene	Fold change	Gene	Fold change	Gene	Fold change	Gene	Fold change	Gene	Fold change	Gene	Fold change	Gene	Fold change
1121	HAP1	1,41581798	MUSK	1,55323536	IFNB1	1,94116127	S100A9	1,90562123	HCK	1,70609845	CYP2J2	1,59696989	TFDP1	2,77725034	SNX13	2,68311483
1122	MBL2	1,41578096	COQ2	1,55195654	CCL18	1,94103203	OPRL1	1,90560378	SEL1L	1,70594318	UXS1	1,59624134	EI24	2,77428462	DCTN1	2,68229722
1123	SLC25A1	1,41557942	HES3	1,55170492	PPAP2A	1,94031355	FANCE	1,9051797	AURKA	1,70559997	PPARGC1A	1,59620188	ACSL3	2,77394552	CYP2S1	2,68195681
1124	IDH2	1,41556387	PSME2	1,55160094	POLE3	1,93977415	HARS	1,90459422	HLA-DMB	1,70520429	HDAC11	1,59607771	ALPI	2,77165916	LRRK2	2,68164688
1125	BECN1	1,41493254	PRKCI	1,55119658	SULT1A1	1,93864795	CSNK1G1	1,90442387	DICER1	1,70444719	NKX2-2	1,59605998	PFDN2	2,77146338	CLDN23	1,39827128
1126	CYP7B1	1,41447548	APOBEC1	1,55035732	MAP3K7	1,93781806	ABCB8	1,90379309	HLA-DQA2	1,70444222	IL17F	1,59594825	PIGV	2,7690858	GFRA1	1,39799676
1127	GALNT5	1,41447111	PHKA2	1,55022727	PON3	1,93780741	PLA2G2E	1,90243864	ATG2A	1,70441874	RALBP1	1,59578262	PTPRU	2,76826152	PPAP2A	1,3976972
1128	NOX1	1,41351153	HS3ST3B1	1,55022371	B3GALT5	1,93768643	EGLN1	1,90181049	PRKAB2	1,7037442	MAP3K7IP3	1,59568497	DHCR24	2,76709878	TOP2A	1,39716773
1129	LPIN1	1,41327647	FCGRT	1,55002877	FGFR4	1,93683902	BTG3	1,90131887	SPN	1,70346295	DCC	1,59536754	HSP90AA1	2,76690964	KCNB1	1,39693938
1130	MAP2K4	1,4128721	FLOT1	1,54974035	SEPHS1	1,93661199	PAK6	1,90092811	ANGPT1	1,70294291	ALOX5AP	1,59514884	CELSR1	2,76598924	PXN	1,39672142
1131	HLCS	1,41227067	BLK	1,54952538	TAT	1,93553212	ADORA3	1,89993709	AGRP	1,70213255	SCP2	1,59508748	CD209	2,76569449	UCP2	1,39664461
1132	CR1	1,41186783	HMGCL	1,54917154	ENPP7	1,93539991	JAZF1	1,89974921	JAG1	1,70005076	CD200R1	1,59454479	UNG	2,76448524	GAS1	1,39661815
1133	HRH3	1,41180467	PLAT	1,54904386	DBC1	1,93505482	ACACB	1,89946812	HGFAC	1,69980813	CA5B	1,59431284	NDUFA1	2,76278426	LSM8	1,39658549
1134	TUBA1A	1,41177749	MLH1	1,54854869	PHKB	1,93488599	NFATC1	1,89932972	PON3	1,69911775	STX17	1,59401696	HS6ST3	2,76186369	CBLB	1,39654007
1135	VCAM1	1,41164957	ITGAV	1,54803903	COL10A1	1,93471834	MTMR1	1,8982523	HOXD13	1,69850932	TSLP	1,59365396	TNFRSF13B	2,75955748	ECGF1	1,39651014
1136	FSHR	1,41153982	KTN1	1,5478534	SMARCC1	1,93469619	AQP1	1,89767083	GABRA3	1,69825996	CDC34	1,59346009	SARS	2,75923528	ABCC2	1,39640259
1137	CCNA1	1,41153834	RORC	1,54727304	RHOA	1,93431334	CACNA2D2	1,8969251	MAPK13	1,69806227	C6	1,59342488	MTHFD2	2,756913	TRPV6	1,39607293
1138	LHB	1,41121157	ABCC8	1,54684618	DERA	1,93353505	ATIC	1,89605775	EPHB1	1,69783741	DNAJB11	1,59324076	ACSL6	2,75684928	IL1A	1,39597756
1139	PRDX4	1,41034815	OCIAD1	1,54605469	ENTPD7	1,93322591	GALNT10	1,89590121	CHRM5	1,69745487	HNF4G	1,59302059	GPX4	2,75616316	CCL5	1,39592898
1140	FUT5	1,41018047	EIF2B1	1,5460074	PKP4	1,93290385	ERN1	1,89483269	PC	1,6969164	CD207	1,59285298	XIST	2,75389833	CLTB	1,39576595
1141	SNCB	1,41016092	ATP6V1G3	1,54560147	DHRSX	1,9318364	GMPPA	1,89480696	BCKDHA	1,69688204	LIN7A	1,59241456	ALDH1A1	2,75383743	LEF1	1,39569143
1142	PHCA	1,41014517	AASDHPPT	1,54405594	NOD1	1,930759	PTK2	1,89350167	BDKRB2	1,69678337	AKR1C1	1,59234723	PIGM	2,7512577	IL9	1,39567521
1143	FBP1	1,40999275	RPS6KA5	1,54396334	GALNTL4	1,93063936	CDK7	1,89336994	ZIC1	1,69638431	BCL3	1,59230333	SLC25A4	2,75087514	THBS1	1,39561062
1144	AMPH	1,40973354	DDX4	1,54352746	XBP1	1,9304408	DHDDS	1,89267833	RNF4	1,69551874	EPHB1	1,59229518	VANGL2	2,75087514	CCL3	1,39519506
1145	HEXA	1,40953283	CSMD1	1,54345747	LPHN2	1,93038691	SLC18A1	1,89195258	NPR2	1,69462849	UCP3	1,59133553	RPN1	2,7508095	HHEX	1,39517526
1146	NR5A1	1,40944493	SMURF1	1,54318282	PIAS4	1,9300078	DARS	1,89125434	TARDBP	1,69418009	A1BG	1,59016421	ATG9B	2,75020878	HPN	1,39513282
1147	SRP19	1,40937284	NDUFA5	1,54310127	HPD	1,92941088	COL8A2	1,89117311	AACS	1,69203276	JAZF1	1,58985455	CCR5	2,74417997	OCRL	1,39403565
1148	XRCC2	1,40858964	AKR1A1	1,54309508	FZR1	1,92939601	PIGU	1,89086317	RABGAP1L	1,69198473	GART	1,58942193	MECR	2,74348595	BTC	1,39477526
1149	APAF1	1,40851125	ANGPT1	1,54287386	LTA	1,92930729	KCNC4	1,8854531	PIK3R5	1,69125014	ATP6V1G3	1,58804469	HAP1	2,74254668	RPS6KA1	1,39472605
1150	CXCL2	1,40846828	PPBP	1,54241255	ABCB1	1,92903233	APOBEC3B	1,88461653	NKD2	1,68990925	GRM3	1,58796791	WNT5B	2,74253756	UVRAG	1,39462825
1151	CSF2RA	1,40838944	IGFBP5	1,54240519	HELLS	1,92868696	ITSN1	1,88456117	PFKFB3	1,68951945	MALT1	1,58708386	TRPM4	2,74246956	RXRA	1,39427316
1152	MYH6	1,4075031	SRD5A2	1,54207721	CAPN11	1,92829226	CACNA1A	1,88393262	HMGCL	1,68919117	GALNT1	1,58638869	CREB3L3	2,74240927	PNPO	1,39407788
1153	ABCB6	1,40750259	DYSF	1,54191477	TAF2	1,9282435	NEU3	1,88393262	IKBKE	1,68911858	ADAM17	1,58595617	LTB	2,74217509	FGF6	1,39355762
1154	COL6A3	1,40734981	FUT4	1,54152701	DPYSL5	1,92653287	PREP	1,88314384	MAGI1	1,68907111	MYH6	1,58588008	PRPF40A	2,74187828	CBX2	1,39287542
1155	MAP3K7	1,4073496	ABCA4	1,54151671	PI4KB	1,92627249	LPHN3	1,88220941	FOXH1	1,68898304	ATP6V1F	1,58570192	SLC27A4	2,73898206	PTPRO	1,39244262
1156	CXCL6	1,40675829	HS6ST3	1,54090272	MAP4K1	1,92383094	TOP1	1,88214737	DCI	1,68882036	SCN3B	1,58514245	INHA	2,73728186	AIFM1	1,39233434
1157	SUMO1	1,40650144	HMGCS2	1,54037518	IL28B	1,92374909	SH3GLB2	1,88188362	ABCB1	1,68832822	CDKN2A	1,58469902	SYT2	2,73728186	CEBPA	1,39156723
1158	ABO	1,40627382	GRIA3	1,54022511	HOXC13	1,92360705	UBE2L3	1,88111702	UGT1A8	1,68832758	FCGR1A	1,58450271	MICA	2,73357134	PDE10A	1,39103158
1159	VNN3	1,40617555	ATP6V1C2	1,54007675	HSD17B4	1,92351566	NCOA1	1,88052081	NEUROD1	1,68796085	GLRX2	1,58405363	TRIM25	2,73039645	RASGRP1	1,39097987
1160	FANCG	1,40598784	GTF2F2	1,53991522	PRMT8	1,9229436	WDFY3	1,88039104	LARS2	1,68759838	DPPA3	1,58383392	WBSCR22	2,73027983	DRD1	1,39065091
1161	GNAQ	1,40576176	EGR1	1,53980522	CD5	1,92259311	DNAJA3	1,87996275	WDR61	1,68686751	IFI27	1,58365723	LRPAP1	2,72689038	ZFX	1,39033831
1162	ALDH3A2	1,40559403	AKAP3	1,53879411	MAOA	1,92179123	PTGER3	1,87669514	PI4KB	1,68644896	UBE2C	1,58325078	BMP3	2,72344425	KLF10	1,3903094
1163	MERTK	1,40548159	PIK3CA	1,53852938	TFAP2C	1,92169371	ZAP70	1,87657896	FLNC	1,68590769	GCKR	1,58259855	GBA	2,71963961	GPX5	1,39029889
1164	SMAD7	1,40509	ADIPOR2	1,53783367	GRIN2A	1,92146471	ITGAV	1,87584568	AHSG	1,68503858	FAT	1,58236677	CAB39	2,719142	RERE	1,39385432
1165	ALDH1L1	1,40499366	ARPC2	1,53782284	GH1	1,92081412	PLTP	1,87549484	PRPF40B	1,68467805	NFAT5	1,58236338	ADCY3	2,71885432	EPHB4	1,38956466
1166	MYBPC1	1,40498033	PPP1R13B	1,53779278	CYP11B1	1,92061077	ABCA3	1,87458604	RAD18	1,68419319	IL21R	1,58182435	BCL11B	2,717962	APH1B	1,3895474
1167	TXN	1,40486085	SLC12A1	1,53775512	RASGRP3	1,91967736	CRTC1	1,87420848	GNB1L	1,68405159	EXT1	1,58179378	INPP5B	2,71677009	TNKS1BP1	1,38925457
1168	ATP1B2	1,4046808	MLH3	1,53739989	ABLIM2	1,91953597	SLC13A5	1,87404949	FGF4	1,68390969	ACTR2	1,58167602	PYGM	2,71095882	CCL18	1,38905224
1169	AACS	1,40461264	ABCB6	1,53734118	FBP1	1,91887957	MX1	1,87404933	LDHAL6B	1,68275745	TPH2	1,58026727	FAF1	2,70994452	DDX50	1,38897665
1170	PDLIM4	1,40458559	MUS81	1,53590795	KLRC1	1,91863965	LIPC	1,87351697	HAL	1,68238964	LPL	1,58011487	IL9R	2,70716384	TAF2	1,38896533
1171	PARC	1,40451028	GNB3	1,53546086	MLH3	1,91765008	MMP14	1,87310084	IFNA8	1,68233107	POLK	1,57930677	CDCA8	2,70715535	STX4	1,38868946
1172	BST2	1,40394993	GATA1	1,53493439	MAML1	1,91759735	NEUROG3	1,87224477	MAT1A	1,68187966	TRAF1	1,57924035	TUBA1C	2,7069244	SHC1	1,38815441
1173	TLR10	1,40376345	ORC2L	1,5348845	XCR1	1,91627954	GAS1	1,87171727	HLA-F	1,68175832	PDHA1	1,57880852	GTF2B	2,70624708	CARD10	1,38729273
1174	CHRNA2	1,40354715	ADAM8	1,53485899	XRCC3	1,91501714	INPP5B	1,87121351	KCNC4	1,68162321	MBL2	1,57865744	ELK4	2,70445166	PTGES2	1,38723192
1175	IFNE1	1,40335504	POLR1B	1,53402359	PROM2	1,91472817	BST1	1,87051176	FZD9	1,68147327	MGAT3	1,57691283	RAD21	2,70442521	SPAM1	1,38723192
1176	MAP3K11	1,40310575	STX18	1,53383704	CD79B	1,91375557	TFR2	1,87020237	FGG	1,68040564	ITGB4BP	1,57685285	RPA4	2,70426324	NTAN1	1,38721693
1177	CSF1R	1,40252388	CSF1R	1,53381138	MTHFD1	1,91367035	TERF2IP	1,87015916	IGFBP3	1,67973977	EGLN1	1,57682902	CREB3	2,70382827	DVL1	1,38688731
1178	MTFMT	1,40159541	SMARCB1	1,5337879	GALNT7	1,91344688	MUC1	1,86854243	MADD	1,67846406	DDR1	1,57674536	APOA1	2,70342638	CYP2C18	1,38590195
1179	GPR18	1,40153991	GH1	1,53360556	SFN	1,91336015	VTN	1,86845976	CTNND1	1,67824509	NBN	1,5764751	LSS	2,69571661	COL11A2	1,38546187
1180	ADAM17	1,40146363	PLA2G2D	1,53223799	PLLP	1,91258662	ELOVL5	1,86728913	AKR1B10	1,67753621	MCHR1	1,57641758	CASP1	2,69363868	COL1A2	1,38515066
1181	PLCG2	1,40131371	JUN	1,53130329	CYP4F12	1,91221472	CD33	1,86633961	ARD1A	1,67750977	GGA1	1,57632793	DNAJA2	2,69239147	HBEGF	1,38500196
1182	MB	1,40125422	TOP2A	1,530466	FST	1,91069842	F11R	1,86600337	OLR1	1,67741264	CFHR5	1,57622869	ALCAM	2,69235932	SCN1A	1,38499902
1183	CA5A	1,40101871	ACAT2	1,53029721	GNPNAT1	1,91049802	RFC1	1,86593344	CD9	1,6772332	RASGRP1	1,57579889	ACADVL	2,68940855	MPST	1,38449642
1184	STX2	1,40055335	ACE	1,52999212	ELOVL5	1,91048041	ACVRL1	1,86591662	CYP4F12	1,67714925	SLC2A1	1,574448	AKT3	2,68740025	GBX2	1,38416312
1185	PRMT7	1,40051473	UGT2B28	1,52953675	KPNA6	1,91032617	HTR2A	1,8657177	SOCS5	1,67697542	CHST4	1,57432803	LOC402057	2,68675767	GRIN2B	1,38377609
1186	MTA3	1,40011091	TNKS2	1,52946948	IFNA5	1,90909737	KRT17	1,86398522	SLC6A12	1,6756178	SREBF1	1,57421196	DHRS1	2,6864748	CD3D	1,38367391
1187	DDIT4	1,39989144	UQCRC2	1,52904465	LARS2	1,90831424	FANCF	1,86397943	CEL	1,67556758	ALDH1L1	1,57408875	ADCY6	2,6864349	TKTL2	1,38356533
1188	CDA	1,39981512	SCD5	1,52888137	EIF4EBP1	1,9070814	TFRC	1,86325349	SMC6	1,67548453	LAMP1	1,57387413	FCER1G	2,685264	CDX2	1,38354921
1189	TUBG2	1,39964222	PELI3	1,52830506	ECE2	1,90487649	MLL	1,8631866	UBE2A	1,67489888	HLA-DOB	1,57253636	PDHX	2,68523862	MEPE	1,38342778
1190	FDXR	1,39951503	CIR	1,52828049	PECAM1	1,9039571	SLC27A4	1,86286985	UGCG	1,67448888	MCFD2	1,57229735	EIF4EBP1	2,68409409	EPB49	1,38313501

	NO ruxolitinib (setting 1)				Ruxolitinib (setting 2)				Ruxolitinib + CM (setting 3)				MF-3			
	Experiment 1		Experiment 2		Experiment 1		Experiment 2		Experiment 1		Experiment 2					
Rank	Gene	Fold change	Gene	Fold change	Gene	Fold change	Gene	Fold change	Gene	Fold change	Gene	Fold change	Gene	Fold change	Gene	Fold change
1191	INS	1,39940837	PER3	1,52810785	EEA1	1,9034297	LAMP1	1,86273529	ATG4D	1,67402878	BUB1	1,57223897	SNX13	2,68311483		
1192	LDHB	1,39920051	POLR2H	1,52806786	PRDX3	1,90334128	TUBA3C	1,86270865	NRG2	1,67301838	TARDBP	1,5721382	DCTN1	2,68229722		
1193	LY6E	1,39904664	CYP2S1	1,52789803	FUCA2	1,90183428	MSH5	1,8614945	PIGV	1,67279079	DARS	1,5719801	ABCD3	2,68195681		
1194	LRRK2	1,39864688	B4GALT1	1,52786903	SKIP	1,90163278	LCAT	1,86108218	PTGS2	1,67261942	DPPA2	1,57155606	FLAD1	2,67977325		
1195	CLDN23	1,39827128	PLIN	1,52785751	OAT	1,9012973	ESD	1,86106233	BCL2L11	1,67246034	GATA6	1,57105109	ITGB1	2,6794737		
1196	GFRA1	1,39799676	FZD1	1,5277967	B3GALT1	1,900655	CSNK1G3	1,8610127	MAP3K5	1,67182624	PDE4A	1,57103414	GPR77	2,67431499		
1197	PPAP2A	1,3976972	B4GALT5	1,52777969	IAPP	1,89977231	POLQ	1,86072124	CTSG	1,67159524	REM2	1,57038704	VAMP5	2,67361693		
1198	TOP2A	1,39716773	SERPINA6	1,52758389	PIK3R1	1,89940721	ARPC5	1,86021221	IGFBP2	1,67128414	NR2E1	1,56971679	PCNT	2,67342912		
1199	KCNB1	1,39693938	HES1	1,52752052	CCR8	1,89933125	POLM	1,86020595	ALDH1A3	1,67094131	ANKFY1	1,56961829	ALDH9A1	2,67340612		
1200	PXN	1,39672142	DNAJC5	1,52738428	ADCY7	1,89709944	OAT	1,85931784	ANAPC10	1,67021475	PAX8	1,56875502	UBE2A	2,67316544		
1201	UCP2	1,39664461	APBA1	1,52689928	TLR1	1,89661342	TNFRSF1A	1,85770715	MAG	1,67016875	MC4R	1,56864962	PLAU	2,67286263		
1202	GAS1	1,39661815	HYOU1	1,52645218	ATP5I	1,89607496	CIP29	1,85706332	NDUFV2	1,67014901	CARD9	1,56814477	PDE4A	2,67281047		
1203	LSM8	1,39658549	AKAP13	1,5262798	BCR	1,89590007	CLU	1,85683731	POLG	1,67007865	MYEF2	1,56760922	TLR8	2,67235474		
1204	CBLB	1,39654007	FRAP1	1,52515559	REXO2	1,8958629	ACAD8	1,85659159	TRAFD1	1,6692913	ARFIP2	1,56760477	CHGB	2,67196272		
1205	ECGF1	1,39651014	SPRED2	1,52462235	RRM2	1,89583365	TNFRSF1B	1,85658851	GSTM5	1,66855961	RELB	1,56731132	IFNA6	2,67059902		
1206	ABCC2	1,39640259	RTN4	1,52415636	AGA	1,89484961	MAP3K14	1,85591501	NR3C1	1,66851063	MAPK13	1,56681349	DTX1	2,66963171		
1207	TRPV6	1,39607293	GNAI3	1,52406962	GLI2	1,8931749	SSTR4	1,85486886	AMHR2	1,66846451	CSF1	1,56665187	RASAL1	2,66863383		
1208	IL1A	1,39597756	CD19	1,52373969	MAP3K10	1,89283207	NEDD4L	1,85478726	SHC3	1,66839562	TIAM1	1,56621535	FURIN	2,66824162		
1209	CCL5	1,39592898	TCF3	1,5236889	BCL2L11	1,89235129	C1QL2	1,85413953	PCK2	1,66799325	SPRED1	1,56616742	AGK	2,66814005		
1210	CLTB	1,39576595	APOA1	1,52348954	FLNC	1,89224826	IL5RA	1,8540681	UBE3A	1,66753354	NRP1	1,56581307	UBE2V1	2,66691381		
1211	LEF1	1,39569143	CYP46A1	1,52320398	SOX1	1,89079943	CCR8	1,85356266	GLI3	1,66732398	TNFAIP1	1,5657741	LRWD1	2,66511985		
1212	IL9	1,39567521	ST6GALNAC5	1,52311136	HDGF	1,89013688	CCNI	1,85343805	PARP1	1,66719267	EME1	1,56568161	HES7	2,66504939		
1213	THBS1	1,39561062	MYH8	1,5226859	TFCP2	1,88815087	CYP2J2	1,85312431	TGIF2	1,66672411	SOCS6	1,56537692	IGFBP7	2,66346417		
1214	CCL3	1,39519506	LIF	1,52259876	ATP1A1	1,88801217	IL2RG	1,85246984	ADAM17	1,66656627	CCND3	1,56519661	SULT1E1	2,66279639		
1215	HHEX	1,39517526	RAD54L	1,52223453	CNGA3	1,88783453	H19	1,8523719	HLA-DOA	1,66600091	STK11	1,56471925	IPMK	2,66162673		
1216	HPN	1,39513282	CDK6	1,5221372	CCNI	1,88708103	CLDN7	1,85232576	CCL7	1,66592172	NRF1	1,56466637	DDX18	2,65983041		
1217	OCRL	1,39403565	ACO1	1,52173478	IL12B	1,88639731	NRG3	1,8517948	CTSB	1,66506777	COL23A1	1,5639557	CCBP2	2,65811978		
1218	BTC	1,39477526	SRP54	1,52153615	TLR6	1,88623186	PIGV	1,85091498	SRP68	1,66447043	RBL1	1,5633234	SPIB	2,65434811		
1219	RPS6KA1	1,39472605	ATP6V0D2	1,5211118	AGXT2	1,88597393	UBE2D1	1,85038213	TXNRD1	1,66447043	BMP15	1,5629683	POLA2	2,65415917		
1220	UVRAG	1,39462825	IL18R1	1,52104681	COL11A2	1,88470579	IL11	1,85019862	KPNA6	1,66409794	JUN	1,56290129	SHFM1	2,65393071		
1221	RXRA	1,39427316	ADA	1,52060692	BIK	1,88465795	DRD1	1,85009995	AP2B1	1,66399432	GNB3	1,56279338	ALG11	2,65392646		
1222	PNPO	1,39407788	TIMP3	1,5203158	DHH	1,88461573	DPPA2	1,84908479	SHMT1	1,66097597	SPO11	1,56277961	IKBKAP	2,65297796		
1223	FGF6	1,39355762	C9ORF97	1,51952895	GAS6	1,88461573	GPC5	1,84885785	RASGRP3	1,66022869	ASMT	1,56258913	SERPINA1	2,65263706		
1224	CBX2	1,39287542	WEE1	1,51951187	MTMR6	1,88456027	SLC12A1	1,84879455	CKB	1,6594417	SFMBT2	1,56214475	TSG101	2,65125927		
1225	RBPJL	1,39244262	LSS	1,51949696	PTPRO	1,88383114	HLA-F	1,84873248	POSTN	1,65874119	GRIN3A	1,56176416	GTF2E1	2,64995936		
1226	AIFM1	1,39233434	SPRY1	1,51895259	ENPP1	1,88369451	SRXN1	1,8476633	C8B	1,65842435	CSF2	1,56169666	SNW1	2,64836803		
1227	CEBPA	1,39156723	SLC12A3	1,51866085	RAG1	1,8835316	CYC1	1,84610756	NFAT5	1,65841003	FAF1	1,56153614	TEK	2,64709742		
1228	PDE10A	1,39103158	CFB	1,51734418	SSR4	1,88331324	DPYSL5	1,84604861	PPM1D	1,65835682	ITPK1	1,56121273	NR2F2	2,64697		
1229	RASGRP1	1,39097987	NAT5	1,51666058	MST1	1,88320781	EBP	1,8452743	KTN1	1,65830272	CNTFR	1,56097103	GABRA2	2,64667544		
1230	DRD1	1,39065091	OGG1	1,51573487	RALB	1,88179121	RBBP7	1,8447497	SRP54	1,65812004	CD38	1,56047442	NFAT5	2,64432047		
1231	ZFX	1,39033831	ARPC1B	1,51558448	MCFD2	1,88163986	KIAA1394	1,84438012	TNK2	1,65772139	ITPR1	1,55996218	TOR1A	2,64363995		
1232	KLF10	1,3903094	MTMR1	1,51503807	SHH	1,88088412	POLR1A	1,84384111	ABCB7	1,65767506	CETN2	1,5593404	TICAM1	2,64291616		
1233	GPX5	1,39029889	AKAP6	1,51490871	TNFSF4	1,88022056	CLOCK	1,84357868	CPT2	1,65764403	RFC1	1,55922284	CPSF2	2,64015564		
1234	RERE	1,38985432	INHBB	1,51484949	CYP7B1	1,8780184	EPX	1,8420427	SORL1	1,65666317	HTR2A	1,55911945	ARPC5	2,64001415		
1235	EPHB4	1,38956466	AKAP7	1,51463767	TDP1	1,8786203	MBTPS2	1,84019843	HTR1E	1,65648355	NKRF	1,55885915	RXFP1	2,63991125		
1236	APH1B	1,3895474	IL17A	1,51345492	MC3R	1,87847936	FCGRT	1,84006406	MBL2	1,6563817	PACRG	1,55859522	CYP2D6	2,6382564		
1237	TNKS1BP1	1,38925457	CD58	1,51296949	DCTN1	1,87759484	GRM7	1,83992772	TGFBR2	1,65633691	BBC3	1,55827734	LTBP4	2,63771812		
1238	CCL18	1,38905224	SMPD1	1,51289657	ADORA2B	1,87755478	ZCCHC11	1,8398964	ANXA2	1,65569495	SYT1	1,55809484	GTF2A1L	2,63623804		
1239	DDX50	1,38897665	ATP5I	1,5124097	SMAD3	1,87580726	ATP5I	1,83876492	LRP5	1,6554818	TNFRSF1A	1,55703406	ESRRA	2,63621995		
1240	TAF2	1,38896533	MSTN	1,51180923	CAMK2G	1,87525216	MGAT3	1,83791184	FUT4	1,65508239	DPYD	1,5562888	APOBEC3G	2,63615097		
1241	STX4	1,38868946	GNPDA2	1,51145236	HPSE2	1,87512771	KREMEN1	1,83755787	CHGB	1,65479651	ATP1B1	1,55601435	IL12B	2,63587652		
1242	SHC1	1,38815441	PARG	1,51113346	CNTFR	1,87411443	CD5	1,83744045	GABARAP	1,65432231	MLH1	1,5557505	NGB	2,63581433		
1243	CARD10	1,38729273	FOSL1	1,51083112	C1RL	1,87206352	MAP3K8	1,83707472	NPAS2	1,65418746	CHEK1	1,55482983	DGAT2	2,63545169		
1244	PTGES2	1,38723192	ZBTB16	1,51076143	NES	1,87157246	A1BG	1,83564009	EHHADH	1,65324881	RPA2	1,5543452	HS6ST1	2,63525715		
1245	SPAM1	1,38723192	EBP	1,51062182	CDT1	1,87144987	SP1	1,83508742	ARHGDIB	1,65308057	KLF10	1,55419046	TREX1	2,63511974		
1246	NTAN1	1,38721693	PLCE1	1,51046483	DPYD	1,87139587	MPST	1,83473343	MAP4K2	1,65281303	BYSL	1,5539809	IKBKG	2,63388411		
1247	DVL1	1,38688731	RRM2B	1,51001588	NOS3	1,87075057	PFN1	1,83392723	IL22RA2	1,65279062	IRF1	1,55385166	KPNB1	2,63284547		
1248	CYP2C18	1,38590195	MYBPC2	1,51000732	SLCO1A2	1,87047054	CGN	1,83354502	MAP3K1	1,65235422	DDX47	1,55378983	ENPP6	2,62932673		
1249	COL11A2	1,38546187	PGA5	1,50950867	POLR2C	1,87026047	ASAH3L	1,83245268	MCPH1	1,65122639	STK36	1,55333514	BCL3	2,62929471		
1250	COL1A2	1,38515066	TRADD	1,50943966	HEXA	1,86996521	CDC27	1,83160109	PTGDS	1,64969521	PPT1	1,55329866	FYN	2,62870374		
1251	HBEGF	1,38500196	IRAK3	1,50886391	CHGB	1,86933466	ANXA6	1,8303324	RORC	1,64957386	CREM	1,55315876	AGXT2L1	2,62752821		
1252	SCN1A	1,38499902	TCF7L1	1,50877134	CCBP2	1,86918762	DHCR24	1,82876151	AKR1A1	1,64854207	EIF2AK4	1,55307432	NDUFB6	2,62635119		
1253	MPST	1,38449642	IRAK2	1,50865376	PLCE1	1,86912413	MYH8	1,82875151	TYR	1,64816255	GDF3	1,55305848	MARCO	2,62544506		
1254	GBX2	1,38416312	SPRY4	1,50753215

Table A4. Pooled-shRNA library screen on HEL cell line and MF-3: list of 2nd most depleted shRNAs for each experiment (ranking approach 1, RA1).

	NO ruxolitinib (setting 1)				Ruxolitinib (setting 2)				Ruxolitinib + CM (setting 3)				MF-3			NO ruxolitinib (setting 1)				Ruxolitinib (setting 2)				Ruxolitinib + CM (setting 3)				MF-3	
	Experiment 1		Experiment 2		Experiment 1		Experiment 2		Experiment 1		Experiment 2					Experiment 1		Experiment 2		Experiment 1		Experiment 2		Experiment 1		Experiment 2			
Rank	*Gene*	*Fold change*	*Gene*	*Fold change*	*Gene*	*Fold change*	*Gene*	*Fold change*	*Gene*	*Fold change*	*Gene*	*Fold change*	*Gene*	*Fold change*	*Rank*	*Gene*	*Fold change*	*Gene*	*Fold change*	*Gene*	*Fold change*	*Gene*	*Fold change*	*Gene*	*Fold change*	*Gene*	*Fold change*	*Gene*	*Fold change*
1261	LIFR	1,38312446	HOXD11	1,50694734	AP2M1	1,86427567	LRP5	1,82412585	CDC26	1,64526195	WWTR1	1,55002131	PPIC	2,61355338	1331	PYGM	1,36720982	ACYP1	1,48864635	GSTA3	1,83244659	FGF18	1,79326783	CDX2	1,6169112	PPBP	1,52454126	RBBP8	2,53577092
1262	IL23R	1,3830584	ALDH2	1,50644884	PCNA	1,8637434	STX2	1,82318212	MPG	1,64486662	ATG4D	1,55001613	FZD10	2,61271894	1332	WARS2	1,36709509	ATP6V0D1	1,48857156	PDLIM4	1,83240611	MAN2C1	1,79326165	STX4	1,6166399	NDST4	1,52431701	ABCG8	2,53446336
1263	ARPC3	1,38266177	TIMELESS	1,506426	ALG1	1,86337396	DLL3	1,82302675	STAT5A	1,64305288	EPB49	1,54981251	BMPR1A	2,60706327	1333	JUP	1,3669687	RCAN1	1,48829088	EZH1	1,83197881	PRKAB1	1,79291072	GPAA1	1,61614601	KPNA6	1,52403808	AGTR2	2,53169865
1264	SLC10A2	1,38245071	BCL9	1,50636384	SLC9A1	1,86314994	DLL4	1,82302519	HS3ST5	1,64290381	GRIN2C	1,54953353	ETV7	2,60581743	1334	PMS1	1,36617774	MSR1	1,48816408	FGF18	1,83165178	FUT9	1,79155762	ATP6V0E1	1,61563826	PTGES2	1,52351947	HLA-DOA	2,53119763
1265	EEA1	1,38173825	ACO2	1,50616554	FOXD3	1,86296193	VCAM1	1,82231468	CHST11	1,64264625	BCL2L11	1,54889114	ADM	2,60519326	1335	ATP1A4	1,36594226	ECE2	1,48749392	ITGB5	1,83044918	SMAD4	1,79134997	HOXD11	1,61561239	GPR35	1,52313158	FANCA	2,53088949
1266	CAMK1	1,38127183	REG1A	1,50606299	CPSF6	1,86259529	CCL3	1,82214399	HDC	1,6421615	NCL	1,54873331	CFHR1	2,60467957	1336	KTN1	1,3659381	PPAP2A	1,48663107	TRAF1	1,83024361	MAPK7	1,79116872	ACP2	1,61546684	GTF3C3	1,52295984	B3GAT3	2,53075544
1267	POLA2	1,38111134	TAF1	1,50568354	CPSF4	1,86204506	CCNB2	1,82189621	YWHAZ	1,64185683	NEK2	1,5482593	SNRPD2	2,60426937	1337	ACVR1	1,36579846	PTGER1	1,48594308	HEMK1	1,8301641	FZD3	1,79053697	ATP2B2	1,61542152	SNCB	1,52273735	COL11A1	2,53026464
1268	AASS	1,38073732	C1RL	1,50543955	GRB10	1,86146485	BCL11B	1,82163933	MYCBP	1,64107491	PRDX5	1,54823693	ACPP	2,60276778	1338	IDUA	1,36546645	CACNA1A	1,48549228	HSD11B2	1,82985131	FGFR4	1,79037031	SYNGR1	1,61531236	CLK1	1,52242328	RAB1A	2,53012335
1269	PDE5A	1,38072091	ABCD3	1,50509494	IGFBP6	1,86138242	MYEF2	1,8212118	CAT	1,64065306	KREMEN1	1,54794125	TCERG1	2,60117581	1339	MSLN	1,36467885	AURKB	1,48537914	G0S2	1,82980127	ORC1L	1,79008675	HOXA9	1,61476261	SOCS2	1,52225699	PSMA2	2,5259358
1270	CAPNS1	1,38066256	GGA1	1,50504875	SYT2	1,86103126	UQCRC1	1,82098367	ARF5	1,63978229	SARM1	1,54744492	ASMT	2,60049318	1340	PRKAA1	1,36458875	FLOT2	1,48497132	PDGFRB	1,82959338	NRAS	1,78708854	ADCY6	1,6134217	HOXA1	1,5221295	HPCAL1	2,52590229
1271	ADD1	1,38037312	GNG3	1,50494926	GOT2	1,86095542	ASRGL1	1,82035209	RDH14	1,63953354	TNFRSF13C	1,5474163	BDKRB1	2,60037184	1341	STEAP3	1,36403936	SPTLC2	1,48496232	ELA3B	1,82959293	TPK1	1,78708854	SERPINA5	1,61299718	MCM3	1,52184145	IL13	2,52574309
1272	CAMK2D	1,38029105	EXO1	1,5047121	MYH2	1,8596339	SMURF1	1,81969216	FMO1	1,63871993	LDHAL6A	1,54702932	IKZF1	2,59854746	1342	GLI2	1,36400642	PRIM2	1,48490768	UST	1,82920275	SH3BGRL	1,78627946	MEN1	1,61268658	NPY1R	1,52163245	ADCYAP1R1	2,52479432
1273	PGA5	1,38025613	GIPR	1,50464323	SHBG	1,85875152	XYLT1	1,81952374	PACAP	1,63849314	ALDH1B1	1,54683313	NR5A2	2,59303323	1343	PSMB5	1,36396896	THY1	1,4847869	BNIP2	1,82899917	ADAM8	1,78568726	P2RY1	1,61213631	MTMR6	1,52090708	WNT9A	2,52370661
1274	NPC1	1,38018493	TCP1	1,50425724	PRDX1	1,85863437	ARD1A	1,81788059	HRH4	1,63842051	AGXT	1,54656812	ST6GALNAC6	2,59117814	1344	MEF2C	1,36375787	TFPI	1,4847567	GPI	1,828662	MAPK9	1,78540735	MUSK	1,61179094	RALB	1,52022099	FCGR2A	2,51932915
1275	CST3	1,38005234	TICAM2	1,50422294	SPRY4	1,85744392	PER2	1,81779938	COL1A2	1,6382498	NGFR	1,54626824	PLA2G1B	2,5904708	1345	SMC4	1,36340507	DPM2	1,48460516	NCOA3	1,8278531	ITGA6	1,78448861	ST3GAL6	1,61131162	MAGI1	1,52008341	COQ6	2,51757387
1276	NR1H3	1,38000109	EPHB1	1,50421633	RPN2	1,85708495	SRC	1,81611915	CRHBP	1,63760834	CITED1	1,54607946	COL27A1	2,58823999	1346	HEY1	1,36334037	NFKBIL2	1,48450423	MAP1LC3A	1,82712275	MYF6	1,78438727	GRIN1	1,61122981	ALMS1	1,52006908	ESR2	2,51744974
1277	EIF4E2	1,37888363	PAK6	1,50398935	FLT4	1,85707829	EIF4E	1,8156809	MC2R	1,63751322	FZD4	1,54570742	BMP6	2,58777015	1347	AKR1B10	1,36329783	LGALS1	1,48432158	FABP2	1,82660617	UGT2B15	1,78436426	CALML6	1,60970501	AGPAT3	1,51916756	SHB	2,51728784
1278	NGB	1,37883338	IGFBP4	1,50385628	CRTAM	1,85704312	PPARG	1,81552426	PRKRA	1,63720917	HDAC1	1,545187	IFIH1	2,58777015	1348	CD79A	1,36320638	GYS1	1,4840146	EMX2	1,82550139	TNFRSF13C	1,78384467	EMX2	1,60963418	PLTP	1,51861014	SDS	2,51697304
1279	PHF1	1,37795894	ASNS	1,50378027	VDR	1,85681781	COL4A5	1,8153963	LEFTY2	1,63661882	CHRNA2	1,54425757	MC3R	2,58755845	1349	REPS1	1,36314935	CA4	1,48299641	PRC1	1,82519656	POLR3B	1,78379959	EIF4EBP1	1,60961845	LPHN1	1,51806075	EFNA3	2,5165638
1280	ATP6V0A2	1,37766089	MKI67	1,50347778	CTSG	1,85664417	ANP32A	1,81496792	REG1A	1,63647299	ATG9A	1,54405734	UBE2J1	2,58736737	1350	ACPP	1,36273145	AKR1C4	1,48293198	GABBR1	1,8251785	C1QBP	1,78324379	IDH1	1,60950933	DMC1	1,51771944	ENTPD8	2,51469451
1281	ROR2	1,37760159	C12ORF57	1,50322415	CYP46A1	1,85623068	ATP6V1A	1,81478297	GLB1	1,63574924	HESX1	1,54342328	MAFF	2,58621004	1351	RAB27A	1,36262889	CD81	1,48290346	GNAZ	1,8251272	JAG2	1,78288494	ITGB1BP3	1,60883498	GABRA3	1,51763208	NMUR2	2,51438446
1282	AGRN	1,37720531	UBE2C	1,5020494	FDFT1	1,85594865	HMBS	1,81472342	EIF4G3	1,63566464	CASP3	1,54311466	STRA6	2,58463934	1352	SPN	1,36262651	NPY1R	1,4825659	DDC	1,82496876	NEK2	1,78250395	PANK3	1,60833055	ACAT2	1,5173012	SH3GL3	2,51420586
1283	GAP43	1,37714075	ITGAL	1,50179068	CES2	1,85563152	DNAJA2	1,81343292	TRAF1	1,63557524	TLX3	1,54277397	GDF6	2,58413364	1353	SYN3	1,36247458	FZR1	1,4818356	PPP6C	1,82397446	GRIN3A	1,78213124	CALR	1,60780698	JAM2	1,5172207	AGPAT1	2,51146471
1284	SNCAIP	1,37684669	B3GNT6	1,50163148	TCP1	1,85529059	CHSY1	1,8124273	CDC20	1,63539138	BBS2	1,5425611	HOXA7	2,58076123	1354	POLQ	1,36240735	SESN3	1,48141847	ACACB	1,82377727	ANAPC5	1,78184047	RAB27A	1,60755115	PDE7B	1,51696328	SFRP4	2,51138099
1285	GADD45B	1,37665454	EGLN3	1,50156381	CXCL13	1,85400561	ACCN5	1,81238121	ADARB1	1,63465538	VPREB1	1,54245349	DRAM	2,58036277	1355	TSG101	1,36240396	ZAP70	1,48134734	PROC	1,82238175	RALA	1,78096849	BNIP3	1,60626546	AXIN2	1,51683677	MTA3	2,51097191
1286	PRKX	1,37663032	ADSSL1	1,50141119	GABARAP	1,85344189	GGA3	1,81197283	MST1R	1,63459893	LMX1B	1,54240352	SCNN1D	2,58022958	1356	SUCLA2	1,36226631	CYP1A2	1,48122466	MARS	1,82129561	C1RL	1,77936505	EGR3	1,60534261	NFYB	1,51628018	IFI27	2,50879778
1287	HLA-G	1,37660339	CADM3	1,50104406	CDK5R1	1,85312003	SDHA	1,81176644	CCR3	1,63433958	LAMP2	1,54219838	MALT1	2,57894638	1357	CFL1	1,36192092	SOCS5	1,4811445	PREP	1,82119213	LRDD	1,77849961	MAPK9	1,60499048	PPAP2C	1,51602243	HSD17B12	2,50713503
1288	NDUFS8	1,37632155	DPPA3	1,50104406	COL25A1	1,85311281	PELP1	1,81072954	TRRAP	1,6342163	MTHFD2	1,54200197	PENK	2,57868122	1358	CD40	1,36183293	UBE2H	1,48027569	FBXW7	1,82078889	PRDM2	1,7779186	RBKS	1,60458054	DRD1	1,51591507	FZD3	2,50058579
1289	C8B	1,37630383	CCNA2	1,50094467	SSTR4	1,85212896	PTPRF	1,80982606	FANCB	1,63418637	PANK3	1,54183434	STMN1	2,57820587	1359	KLRD1	1,36179581	RENBP	1,47986926	PAFAH2	1,82031159	SESN3	1,77754056	SSTR4	1,60430234	HAP1	1,51563284	GPR83	2,49636399
1290	H19	1,37587483	HOXD13	1,50090166	ATP6V1H	1,85147474	ADRA1A	1,80974833	PIR	1,63417067	AK1	1,54154022	AKR1C1	2,57795428	1360	ACTR2	1,36093719	AGXT	1,47929058	AKR1A1	1,81958603	CHRNA10	1,77703293	PAFAH2	1,60317272	ABL1	1,51511447	HTR1E	2,49556036
1291	GNG3	1,37585884	SRPR	1,50044949	MAML3	1,85138525	MAP2K6	1,80869341	FBP1	1,63400964	LPIN2	1,54100025	GOLGA5	2,57764219	1361	ADA	1,36074971	STAG2	1,47915115	METTL2B	1,8188601	SERPINA6	1,77670791	GTF2F1	1,60299985	SLAIN1	1,5150468	ADC	2,49527158
1292	TACR1	1,37567174	CD3G	1,49984675	GRB7	1,85102761	TFPI	1,80863707	ADORA2B	1,63386725	ADCY4	1,53989828	CSDA	2,5775998	1362	REL	1,36065942	WNT9A	1,47901703	FADS1	1,81882964	CHRM2	1,77641148	LGMN	1,60293767	CLTB	1,51381543	LHX2	2,49522693
1293	FUT9	1,37565073	IL7R	1,49947169	DGKZ	1,84947404	GOT1	1,80858958	CCNC	1,63341411	FCGRT	1,53924829	SQSTM1	2,57499962	1363	RPA4	1,36048956	PKLR	1,47901589	MAGI1	1,81855121	TLE1	1,77569258	GRID2	1,60198828	CLDN7	1,51366392	MARCKS	2,49472435
1294	CKS1B	1,37523349	TRO	1,4984595	DNAJC5	1,84943895	TLX3	1,80846364	GFPT1	1,63301378	PRKRIR	1,53915539	ALG10B	2,5739932	1364	NFS1	1,35985483	MAP1LC3A	1,47900919	NDUFV1	1,81785192	CXCL9	1,77534981	MNAT1	1,60190429	DAP	1,51287573	PKN1	2,49393135
1295	ETV5	1,37485318	CXCL13	1,49813216	SLC12A2	1,84921853	PLA2G5	1,80705942	FARSA	1,63291856	RPS6KA1	1,53742004	DAO	2,57093909	1365	TPP1	1,35957798	IFT172	1,47900722	MAP3K12	1,81781563	IFNA10	1,77406908	WDR1	1,60162851	CRTC1	1,51259709	AARS	2,49342339
1296	SPP1	1,37468826	SLC22A7	1,49756991	COMP	1,8490624	DEGS2	1,80657188	KCNN3	1,63291856	HSPA5	1,53707684	FOXH1	2,56980541	1366	TLR1	1,35950406	PTGES2	1,47873642	ACSL3	1,81691355	NRG1	1,77381457	SUZ12	1,60137698	PRIM2	1,51238651	CLDN23	2,49284273
1297	MPPED2	1,37456372	ICAM1	1,49707409	PDE4D	1,84837763	BTLA	1,80628639	UNC5CL	1,63235429	TNFRSF10A	1,53704067	GABPA	2,56958261	1367	HSD3B1	1,35934479	HMBS	1,47832702	ITGA5	1,81624474	CLK1	1,7733059	PF4	1,60090721	PER3	1,51209254	GSTA4	2,4926759
1298	BUB1	1,37449679	PSMB10	1,49700165	GUCY1B3	1,84808298	HSPD1	1,80536922	THRA	1,63234791	BPTF	1,5365192	PROM2	2,56727703	1368	BMP15	1,35932062	ONECUT1	1,47822183	MAP3K7IP3	1,81597232	GCAT	1,77274081	TGFBR1	1,60057922	B4GALT5	1,51192131	C1RL	2,49030516
1299	MPO	1,37444874	OLA1	1,49696622	ACP1	1,84773584	MYBPC1	1,80529045	SLC34A1	1,63212225	ACCN5	1,53648965	PSMB9	2,56601449	1369	LPIN3	1,35913859	IDUA	1,47816179	ERAF	1,81536106	ARHGEF4	1,77266967	EPHB4	1,60026009	COX6C	1,51077263	RANGAP1	2,48997692
1300	FOXA1	1,3744274	ADORA2B	1,49668612	TICAM2	1,84751879	DPF2	1,80528588	IFNB1	1,63121219	MOG	1,53600824	ZNF259	2,56495042	1370	FLNC	1,35893304	ATP6V1F	1,47810433	GK2	1,81424567	OLA1	1,77240242	GGA1	1,59998143	ANKHD1	1,51075663	CACNA1S	2,48932211
1301	AKAP3	1,37432577	FCGR3B	1,49660431	PRDX5	1,84685133	CADM1	1,80519937	GPT2	1,63095753	ARSB	1,53574915	RNF4	2,56420304	1371	NFYA	1,35891343	FGR	1,47785913	APOC3	1,81423162	UGDH	1,77147443	PPARA	1,59957947	CD5	1,51072031	MLH3	2,48784291
1302	GAD1	1,37383385	LIPC	1,49637273	LAMP2	1,84658534	GNB3	1,80512367	NPPA	1,63027038	HAND1	1,53558289	DEFA1	2,56264465	1372	FKBP5	1,35889995	RFX5	1,47759174	TLR7	1,8141458	IL2RB	1,77033168	GOT2	1,59942825	MYBPC2	1,51067771	FZD7	2,48594968
1303	CTSB	1,37328511	VSNL1	1,49624256	FLT1	1,84498061	TRAFD1	1,80445631	TBKBP1	1,62903482	KCNB1	1,53502077	HSD17B6	2,56250315	1373	ANKRD1	1,3584823	HCST	1,47756501	S100A8	1,8137658	PDK1	1,76986365	ACAT2	1,59941271	ARHGAP4	1,50989249	NDUFA8	2,48531623
1304	MGMT	1,37320808	SYP	1,49622278	RAB27A	1,84484067	CFHR3	1,80309265	MYL4	1,62849909	FOXN1	1,53401955	HLA-DRA	2,56086194	1374	PPAP2B	1,35802606	HSPD1	1,47743086	NR4A2	1,81360547	PRKY	1,76980896	CETN2	1,59865073	SMC4	1,50984113	SGK	2,48419043
1305	EDG1	1,37209263	BRD4	1,49619882	GOT1	1,84436074	ADAR	1,80294823	CD99	1,62738286	CSF1R	1,53383673	ATP6V0D2	2,55967558	1375	TNFAIP1	1,35739848	GSTA1	1,47737942	MAP2K6	1,81314866	UBE2E3	1,76963071	HLA-DPB1	1,59708484	COL6A1	1,5097835	BHMT2	2,48409585
1306	OXSM	1,37208167	GRB7	1,49614773	MGAT1	1,84407717	PLD1	1,80287654	IFNAR1	1,62694808	VIM	1,5329829	CRTAM	2,55877947	1376	PPARGC1A	1,35721598	GAB1	1,47724155	ADAM17	1,81294701	RECQL4	1,7694221	DLG7	1,59701253	HSD17B6	1,50977887	SLC30A4	2,48329445
1307	ATP6V0D1	1,37203552	MAPK7	1,49569885	RAD1	1,8439917	TLR4	1,80280453	CSGLCA-T	1,62652276	SOD1	1,53172683	GTF2H5	2,55489513	1377	RFX5	1,35707049	EIF2B2	1,47723858	DLX3	1,81251701	TNFAIP6	1,76884994	UNC13B	1,59690527	TREH	1,50975123	C3	2,48171229
1308	CLDN15	1,37159754	CDK2	1,494797	FZD8	1,84368042	PRPF19	1,80269264	TIMP4	1,62579179	GALNT5	1,53171195	KCNE1	2,55448744	1378	LMNB1	1,35688995	MPPED2	1,47596517	H19	1,81187263	PDE7A	1,76759366	IQGAP2	1,59669953	ABCB11	1,50912427	REPS1	2,48164405
1309	EDNRA	1,37146222	DKC1	1,49463902	SLC25A4	1,84278805	ABCB1	1,80227343	ITGB6	1,62572486	CPA3	1,53131208	STX16	2,554483	1379	EMX2	1,35669884	RXRA	1,47581494	AGER	1,81164761	RPE	1,76732085	LY6E	1,5961969	HES3	1,50906282	CKMT2	2,48063866
1310	PALB2	1,37125411	PPP2R2A	1,49441246	SERPINA4	1,84194469	LUM	1,80183338	VNN2	1,62570174	FOXO4	1,53083981	NOTCH3	2,55301746	1380	CRY2	1,35647642	CHGA	1,47473898	COQ2	1,81154484	SPRY4	1,76500548	LPO	1,59612742	CACNA1I	1,50854289	CYLD	2,48021952
1311	PIWIL1	1,37122051	IDI2	1,49423603	PROS1	1,84156406	L1CAM	1,80137352	PGK2	1,6253127	FOLH1	1,53073441	WNT9B	2,55217508	1381	IFNA8	1,3561545	CDK5R1	1,47442317	HAGH	1,81127056	ROR2	1,76490567	DARS	1,59601037	MMRN1	1,50839059	CDK10	2,47988665
1312	DHRS3	1,37097843	ARPC5	1,49384763	NEU3	1,84115499	NFS1	1,79928058	PRMT5	1,6251565	TNIP1	1,53046172	CARD6	2,55040609	1382	TP73	1,35599733	SAT1	1,47431298	AMY2A	1,81122712	FBLN1	1,76430727	FTH1	1,59597781	WBSCR22	1,50829562	LRRC15	2,47933738
1313	AKAP8	1,37096358	SQSTM1	1,49372416	MELK	1,8391922	MPI	1,79896148	ADCY9	1,62485746	TARS	1,53044559	BMP7	2,54904771	1383	HS3ST3B1	1,35591631	MC2R	1,47400587	FZD2	1,81016979	ARFGEF2	1,764062	PSEN2	1,59594351	GATM	1,50783398	GUCY1B3	2,47789783
1314	CCNA2	1,37045934	FTH1	1,49343392	ATP6V1F	1,83894444	BMP15	1,79890853	CSNK1G3	1,62440243	GCK	1,53029305	ITGB4BP	2,5488517	1384	RAD23B	1,35576687	FOXM1	1,47358978	BMP4	1,80960009	OCIAD1	1,76370793	CD82	1,59582979	PPP1CB	1,50760092	SLC10A1	2,47788303
1315	CS	1,37041924	MPST	1,49340672	XRCC1	1,83873739	GTF2I	1,79862741	RAF1	1,6242592	JUP	1,52989563	CKMT1A	2,5486015	1385	ATP1B1	1,35571829	MCFD2	1,47273549	EGR2	1,80924132	ABCA13	1,76350442	AOC3	1,5955563	PRPF40B	1,50736734	TNFSF18	2,47721256
1316	TNK2	1,37017786	DDEF2	1,49317583	KDELR2	1,83866056	GUCA1A	1,79824398	SCD	1,62332742	NRG1	1,52933565	HLA-B	2,54513638	1386	ITGB6	1,35569385	NOLA2	1,47269053	FLCN	1,80924057	CD22	1,7632793	LRRTM3	1,59540975	IL11	1,50732471	GTF2H4	2,4758842
1317	STX3	1,37017278	DBN1	1,49288086	COQ6	1,83746506	AKT3	1,79821832	UGT2A1	1,62237137	E2F3	1,52858045	DHH	2,54326866	1387	PGR	1,35554703	MAD2L2	1,47167497	PIAS1	1,80904156	EPHB4	1,76207096	PTH2R	1,59514849	PERP	1,50716893	CHRNA2	2,47557413
1318	B3GAT3	1,3698304	VCAM1	1,49286655	ATG4D	1,83732537	NPAS2	1,79794788	IL7R	1,62220741	ARD1A	1,52762492	SPRY2	2,5425345	1388	POLR3H	1,35547676	ADSS	1,47151146	ABCB9	1,80732076	GABRA5	1,76167521	SULT1E1	1,59494401	SSTR3	1,50649919	IMMT	2,47550877
1319	DPYSL5	1,36966004	CKB	1,49278932	PIGN	1,83687885	NDUFS7	1,79785507	AQP7	1,62134743	IGF2R	1,52756959	TGFB1	2,54160275	1389	ID4	1,35547292	LUM	1,47145609	ATP1A4	1,80642245	CCNB3	1,76158477	AGER	1,59493245	MMP14	1,50611604	ESR1	2,47204075
1320	NOTCH4	1,36939737	CARD9	1,49169325	SRPS4	1,83665138	CTH	1,79749845	ATG3	1,62117288	PIGA	1,5272445	MEOX2	2,54058819	1390	KIT	1,3554206	CDS2	1,47121863	HDAC2	1,80638757	CCNA2	1,76145985	IGFBP7	1,59492662	CFP	1,50605379	IL1R1	2,4711283
1321	SIGLEC1	1,36926251	GAS6	1,49164753	BCL7A	1,83607615	CAMK2G	1,7970996	IL17A	1,62094934	MAP1LC3B	1,5265742	SREBF1	2,54046946	1391	LDHAL6A	1,35541094	IRF1	1,47102598	AKT3	1,80618328	TCF3	1,76081878	CKMT1B	1,59457869	SMURF1	1,50575359	CCL17	2,4701801
1322	SMPD1	1,36906705	PKP4	1,49118752	SFRP2	1,83522321	SCN9A	1,79692656	PLA2G1B	1,62023149	OSBPL1A	1,52626012	MYL3	2,54025686	1392	ERCC5	1,3552366	CKMT1B	1,46996397	EPHB4	1,80618141	CTSL2	1,75941375	GIPR	1,59453867	FOSB	1,50538975	ACAD9	2,46972926
1323	PRF1	1,36898643	OAT	1,49101913	PTGFR	1,83518332	RAB5C	1,7967626	TNKS2	1,61969734	SOS2	1,52624377	ASS1	2,54016424	1393	MGAT3	1,35514993	PFKFB1	1,46943008	ERN1	1,80567255	MAP3K11	1,75854466	TLR10	1,59324585	UBE2D3	1,50518103	MAPRE2	2,46871232
1324	WNT5B	1,36894062	AMHR2	1,49078861	B3GAT2	1,83515539	GDF5	1,79675079	GDF3	1,61907684	SLC25A11	1,52594766	ATG9A	2,54006786	1394	GH1	1,35502105	GOT1	1,46942894	RAPSN	1,80511795	CA4	1,75804916	ST6GAL1	1,59303	WDR1	1,50505703	TBXAS1	2,46778046
1325	PTPN11	1,36878535	CAPRIN2	1,49062482	PLD2	1,83508947	NUMBL	1,79647652	BGN	1,61896964	UQCRC1	1,52593805	ATP5G3	2,5393062	1395	PPARA	1,35471696	CLK1	1,46937602	TGDS	1,80443085	ADA	1,7577504	NTF3	1,59274495	SCTR	1,50413792	CENTD2	2,46457825
1326	SF1	1,36875528	KPNA3	1,49052932	CHDH	1,83507422	RARB	1,79639559	GDNF	1,61896902	PRKAB1	1,52583087	XRCC1	2,53863024	1396	AGER	1,35468887	ADCYAP1R1	1,46933215	PIGB	1,80293174	C7	1,75760229	GATA6	1,59259465	SP1	1,50375733	IL11	2,46441632
1327	KCNJ4	1,368639	GNE	1,49021453	IRF2	1,83453569	WDR79	1,79623982	ST6GALNAC6	1,61866719	ENTPD7	1,52521885	KLRC1	2,53858012	1397	NEK1	1,35444654	NTRK1	1,46891468	GDNF	1,80268898	IL3RA	1,75697718	RPS6KA1	1,59225487	CCNT2	1,50346399	HMGCR	2,46432397
1328	CTSA	1,36788327	BCKDK	1,48982658	EBP	1,83399971	ACTN4	1,79537582	SMURF2	1,61826906	SLC38A1	1,52504413	NR2C2	2,5373277	1398	SCN11A	1,354222	LMAN1	1,46887984	HLA-DMA	1,8023232	RAB4A	1,75680376	HLA-C	1,59131709	CKB	1,50287298	KCNN4	2,46310822
1329	DKK3	1,36747463	HIP2	1,48946202	HOXA4	1,83373315	UGT2B28	1,7953113	NAT2	1,61743106	TAT	1,52493045	CITED1	2,53719314	1399	EIF4E	1,35351479	UGT2B4	1,46874251	DYSF	1,80206269	CKMT1B	1,75637515	GLUL	1,5911776	SEL1L	1,50270322	SSR4	2,46181946
1330	BIK	1,36730805	SQLE	1,48875923	VIP	1,83293172	ATG3	1,79474831	DFFB	1,61716824	TACR3	1,5246548	EFNA1	2,53672254	1400	ZFYVE16	1,35348125	AK5	1,46836816	BAG5	1,8020433	AKAP5	1,75469908	FANCE	1,59073882	CYP4B1	1,50254235	ITGB5	2,46155902

Table A4. Pooled-shRNA library screen on HEL cell line and MF-3: list of 2nd most depleted shRNAs for each experiment (ranking approach 1, RA1).

	NO ruxolitinib (setting 1)				Ruxolitinib (setting 2)				Ruxolitinib + CM (setting 3)				MF-3				NO ruxolitinib (setting 1)				Ruxolitinib (setting 2)				Ruxolitinib + CM (setting 3)				MF-3	
	Experiment 1		Experiment 2		Experiment 1		Experiment 2		Experiment 1		Experiment 2						Experiment 1		Experiment 2		Experiment 1		Experiment 2		Experiment 1		Experiment 2			
Rank	*Gene*	*Fold change*	*Gene*	*Fold change*	*Gene*	*Fold change*	*Gene*	*Fold change*	*Gene*	*Fold change*	*Gene*	*Fold change*	*Gene*	*Fold change*	*Rank*	*Gene*	*Fold change*	*Gene*	*Fold change*	*Gene*	*Fold change*	*Gene*	*Fold change*	*Gene*	*Fold change*	*Gene*	*Fold change*	*Gene*	*Fold change*
1401	SMARCC1	1,35340818	SLC13A5	1,46829895	EP300	1,80168332	DAPK3	1,75426366	DDX4	1,59041236	AKAP5	1,50238366	TKT	2,46146801	1471	IL3RA	1,34064456	RECQL	1,45053217	MAX	1,77120507	B3GAT3	1,72355029	AOC2	1,57020929	PRIM1	1,4847031	SOCS7	2,39228639
1402	PTPN22	1,35330729	LILRB3	1,46822842	CTTN	1,80130704	HLA-DMB	1,7535834	NAT5	1,59031017	SRY	1,50200964	MLYCD	2,46048414	1472	SST	1,34002101	MSH6	1,45018087	NFATC3	1,77056846	CSF3	1,72290855	SETD2	1,56975828	TRIO	1,48409277	SLC6A12	2,39202371
1403	PPP3CC	1,35305276	PHF21A	1,46760296	SLC22A7	1,80101991	TRAF1	1,7535834	MBTPS1	1,58996351	CSNK1A1L	1,50186576	ALG1	2,46055536	1473	IL9R	1,33970497	IL11	1,45016635	EIF4A2	1,77040898	BET1L	1,7222081	PLA2G12B	1,56957561	DAD1	1,48402659	BCL2L1	2,39093454
1404	FZD10	1,35284598	ITPKB	1,46663394	TLR2	1,80086924	FLOT1	1,75356642	PPP3CB	1,58957077	COL13A1	1,50184016	DLST	2,45916789	1474	RAB5C	1,33964605	NOS2A	1,44987762	PLA2G2E	1,77028867	ABL1	1,72131917	AGPAT3	1,56927287	C7	1,48383238	RANBP2	2,39083855
1405	FUT8	1,35260758	CCL3	1,46612187	AP3B1	1,80057472	NDUFV2	1,7533845	TEP1	1,58889895	TNFSF18	1,50171479	POLA	2,4578051	1475	JUNB	1,33951731	NDNL2	1,44931038	GLB1	1,77006174	MAD2L2	1,72081627	APPL1	1,56901029	PSEN2	1,48372611	ITGA9	2,39068331
1406	RBBP4	1,35252852	ATRX	1,46611017	LGMN	1,79976554	NR3C1	1,75337225	CTPS	1,5887566	GFAP	1,50158026	CASP8AP2	2,45722261	1476	TLR5	1,33940606	KCNH2	1,44909405	NLK	1,76970987	PNPLA3	1,7204868	CXCR6	1,56843474	SMO	1,48343388	KCNK3	2,39005551
1407	RCHY1	1,3522261	PRKRIR	1,4659739	PIGM	1,79975588	CDC34	1,75303108	APOC3	1,58862005	DDX19A	1,50156047	MAPK1	2,455728	1477	RORC	1,33935164	ZFX	1,4489317	INDO	1,76784207	TEAD2	1,72048358	PANK1	1,56843103	ACAD8	1,48323667	NRIP1	2,38997213
1408	KLRC2	1,35218358	C9ORF95	1,46595324	EIF2AK1	1,79952946	RETNLB	1,75283052	C8A	1,58858927	LARS	1,50141066	ALDH4A1	2,45454731	1478	CSNK2A2	1,33934681	GALNT17	1,44870337	ALOX15B	1,76771054	SLC6A11	1,72004558	BCKDK	1,56833982	SNAI1	1,4831333	NOTCH2	2,38954388
1409	PPP2R5B	1,35192059	CHRNB3	1,46563013	SEL1L	1,79931612	PTGS1	1,75275954	PRKACA	1,58798701	MUC1	1,50102086	CD3E	2,45330567	1479	RBBP7	1,3389924	TFR2	1,44821931	HYOU1	1,76764081	GLUL	1,71998977	CADM3	1,56820972	MTA1	1,48210517	SCN4A	2,38862071
1410	CHST4	1,35170248	NEUROD1	1,46435067	IL17RD	1,79878416	CES1	1,75146945	AMY2A	1,58790915	CSF3	1,50051114	TNFRSF17	2,45319197	1480	PAG1	1,33897664	PTGER3	1,44815097	HOXD13	1,76572103	PDCD4	1,7197311	RPIA	1,56792213	PPM1D	1,48189161	HSPA9	2,38830467
1411	CDC25A	1,35136191	CD151	1,46434542	FUT5	1,79828122	RAD23A	1,75137147	YES1	1,58775354	SNX13	1,50037143	SKIP	2,45306564	1481	ORC1L	1,3387612	DDX1	1,44741593	SPR	1,76409855	MAT1A	1,71941775	SLAMF1	1,56785926	ARFGAP3	1,48172315	TNFSF11	2,38764769
1412	HEXB	1,35122166	UCP2	1,46416045	CCNA2	1,79778426	NOTCH1	1,75069768	GSTA1	1,58714596	MYL4	1,49992401	MAP3K7	2,44989148	1482	HSF2	1,33847767	PXN	1,44722737	RING1	1,76400785	PDHA1	1,71910843	PGLS	1,56736218	STAT5B	1,48171038	LCP2	2,38629638
1413	NUMA1	1,35110274	CPB2	1,46396026	SIM1	1,79740307	CD55	1,75040953	PLA1A	1,58710371	RPS6KA3	1,49967326	ITM2B	2,44981834	1483	RARS	1,33793588	PRODH	1,44694319	CYP2C9	1,7635679	CYP26A1	1,71898936	GAB1	1,56731093	PMS1	1,4814467	MMP8	2,38457384
1414	ADCYAP1R1	1,35076611	RECQL5	1,46388461	F2RL1	1,79732721	COL23A1	1,74928778	IMPA1	1,58704415	PRKAG1	1,49887816	CHGA	2,44930166	1484	ADORA2A	1,33787854	EIF2AK2	1,44685201	LDB1	1,76307573	COPA	1,71814938	MMAB	1,56699052	EIF5A2	1,48134618	TTR	2,38430122
1415	GOLGA2	1,35026818	TNFRSF8	1,46379742	SP1	1,79720377	AGER	1,74904559	PPP5C	1,5870249	CBLB	1,49886407	LYCAT	2,44692542	1485	LDB1	1,3378331	GART	1,44656298	KRT19	1,76261173	KCNMB1	1,71743582	FOXP3	1,56628622	CIP29	1,48132981	TXNDC1	2,38014248
1416	APOBEC3F	1,34963089	CXCL6	1,46356331	GNPDA2	1,79715124	GTF2F2	1,74822949	DNAJB4	1,58702199	ZMAT3	1,49833671	C15ORF15	2,44687768	1486	PIGW	1,33770485	PRMT3	1,4465602	IL1B	1,7619789	ATP5L	1,71709897	CYP2B6	1,5662413	TNNT2	1,48131444	POLR2I	2,37939777
1417	TAF12	1,34934081	SETD2	1,46337386	PRMT5	1,79711066	PFKP	1,74814	PECAM1	1,58683027	MSLN	1,4979904	CLDN15	2,44616574	1487	ENPP1	1,33761822	UBE3A	1,4464849	CADM1	1,76143481	PPP3CC	1,71695479	PTPN6	1,56598813	PSMB8	1,48123104	EIF4EBP2	2,37924385
1418	MMP3	1,349232	WNT11	1,46300446	CFL1	1,79617035	C3	1,74777845	IL2RA	1,58614605	ACAT1	1,49773144	ARF1	2,44613271	1488	KCNH7	1,33740282	SULT1A4	1,4463029	CALM1	1,76020606	PKMYT1	1,71673532	PSMB5	1,565855	HCST	1,48121787	GCGR	2,37660014
1419	ILK	1,34905173	AKT3	1,46295015	CARM1	1,7960081	CDH5	1,74777814	MKI67	1,58525935	HOXD1	1,49757149	UVRAG	2,44474616	1489	NQO1	1,3370468	TUBG1	1,44628772	ANKRD1	1,75997685	TICAM2	1,71632741	UNC5B	1,56419702	CYP3A43	1,4811871	C9ORF97	2,37659647
1420	MUS81	1,34899922	CYP11B2	1,46285203	CELSR2	1,79586098	TNNT2	1,74757417	RAD17	1,58516791	COQ7	1,49746855	CD59	2,44411752	1490	FOXA2	1,33691469	RIPK2	1,44617577	GATM	1,75991328	PHF1	1,71590284	PTGDR	1,56419403	CSNK1G3	1,48055109	KCNE2	2,37600563
1421	PECAM1	1,34898818	CCR4	1,46262881	NOS2A	1,79514904	STAT6	1,74722098	TTR	1,58451243	TNKS	1,49742748	GRB2	2,44384615	1491	COL23A1	1,33686853	ANP32A	1,44514224	OXA1L	1,75984895	WEE1	1,71577545	TUBE1	1,56368227	TLR10	1,48019389	GALNTL4	2,37541269
1422	NOS2A	1,34895365	NXT1	1,46227201	FGF3	1,79499157	MYLK2	1,74674798	ERN1	1,58417086	ACTN1	1,4971291	DKFZP434E11	2,4395179	1492	IPMK	1,33659085	ATP5G3	1,444863	UBE2D3	1,75964437	BCAP29	1,71560325	FCN1	1,56361851	RPE	1,47974779	STX4	2,37511256
1423	DLX6	1,34889985	OXSM	1,46213179	FMOD	1,79477559	TAAR6	1,74615659	FMOD	1,5841458	ATP5A1	1,49704784	DDX23	2,43895456	1493	STX18	1,3364871	PLCB2	1,44467017	RGS5	1,75934807	ETV6	1,71558081	PDCD2	1,56350557	GSTA5	1,47908887	PORCN	2,37478121
1424	PGA4	1,34879203	KCNMB3	1,46143072	OTUB1	1,79420051	COX5A	1,74610249	PUM2	1,58400365	TGDS	1,49669898	HTR2C	2,43858954	1494	PRKCE	1,33645922	SKI	1,44390591	CBLB	1,75887026	GRB10	1,71535741	MYO1C	1,56345262	DTNBP1	1,47886856	ATOH1	2,37460649
1425	SOD2	1,34865067	GMPPB	1,46139566	PLTP	1,79342425	DDC	1,74506679	TLK1	1,58389917	SNX4	1,49665465	KDELR2	2,43770154	1495	CA6	1,33592889	CTSS	1,44388247	GTF2B	1,75884301	TBKBP1	1,71470438	IFNA14	1,56316756	APOBEC3F	1,47802426	ABCD2	2,37337279
1426	FS	1,34825747	NKD2	1,46138997	FZD7	1,79336829	TRPM4	1,74465798	PIK3C2G	1,58348087	HGD	1,49628947	GOS2	2,43705699	1496	PBEF1	1,33591126	VNN1	1,44385429	SIRT2	1,75858438	LAT2	1,71427867	CD38	1,56277939	WNT11	1,47752231	DGKI	2,3730869
1427	LPL	1,3479925	ITGA9	1,46116491	C1ORF103	1,79321861	SMO	1,74464979	STMN1	1,58331234	CPN1	1,49611211	NEURL	2,43632415	1497	SMAD3	1,3359049	CAT	1,44371789	OXTR	1,75841133	RAB27A	1,71395057	GANAB	1,56207039	NDUFA5	1,47703228	ARPC1B	2,37275461
1428	PFN2	1,34784918	ANAPC5	1,46108828	CUGBP2	1,7930828	GAB1	1,74443122	HSD3B1	1,5831538	BCL6	1,49539404	AMT	2,43612208	1498	SH2B2	1,33554951	PRPS2	1,44352251	FGF4	1,75759157	RBKS	1,71378304	AGPAT6	1,56105887	MYBPC3	1,477019	CHST7	2,37257103
1429	GCS1	1,34775175	WDFY3	1,46103314	EMR2	1,79265892	PARD3	1,74336969	LRRK2	1,58314392	AMY1B	1,49479183	DARC	2,43598501	1499	BTG2	1,33552344	CTSG	1,44306107	CPT1B	1,75737252	FLOT2	1,71372781	HOPX	1,56056541	PPP5C	1,47677792	TNFSF10	2,37202828
1430	SMAD4	1,34773849	PRKDC	1,46069377	ASS1	1,79207422	FBXW7	1,74310803	HLA-G	1,58269552	NR4A2	1,49460481	MAML1	2,43586404	1500	FUCA2	1,33549332	NBL1	1,44296675	DAXX	1,7572576	GALNT4	1,71358459	POLE2	1,55969159	PIGU	1,47657278	BECN1	2,37121111
1431	GFPT2	1,34737044	CHMP1B	1,46025887	RARS	1,79143586	LRMP	1,74126409	FOXO1	1,58200062	CELSR3	1,49416074	CES4	2,43559939	1501	HOXA4	1,33545182	PPP1R10	1,44255017	CDH5	1,75716907	PADI2	1,71343742	DBP	1,55913526	NPC1	1,47548802	B3GNT6	2,37106254
1432	HLA-DOB	1,34693697	KRT19	1,46012514	GPR109B	1,79135567	PRMT2	1,74123653	ITGAX	1,58129223	NT5C2	1,4939679	CD72	2,43524726	1502	CDC27	1,33485342	IRS4	1,44245493	APCS	1,75667927	PHF21A	1,71303121	CST3	1,55895714	STX5	1,47539682	PLAG1	2,37088072
1433	EEF1G	1,34681678	CHRNA2	1,46003562	SKP1A	1,79104317	ATG5	1,74049787	DDOST	1,58097401	HTR6	1,49373558	PECAM1	2,43495339	1503	DCLRE1B	1,33481259	LIN7A	1,44243907	IL5RA	1,75657315	BRS3	1,71295731	AKAP7	1,55859307	AZIN1	1,47538628	CADM3	2,37011961
1434	MYH8	1,34681247	COX6C	1,45954166	PAWR	1,79073085	CDK6	1,73977776	RASAL1	1,58074209	LRRTM3	1,49363563	A4GNT	2,43303686	1504	TRPC7	1,33465845	DYRK1A	1,44232316	SCARB1	1,75646802	PROCR	1,7120775	AKAP11	1,5585624	CIR	1,47474335	HGFAC	2,36887678
1435	RSAD2	1,34680691	ADAM17	1,45926479	FADD	1,78952254	SHBG	1,73912925	MMP13	1,5806099	CTSL1	1,49333346	IL17RD	2,43121317	1505	ABCA1	1,33460367	PECAM1	1,44206835	IL11	1,75582256	PPP1CA	1,71175924	CES7	1,55799727	KEAP1	1,47431152	TGFB2	2,3683193
1436	PROCR	1,34677472	CAMK2A	1,45916424	NDUFB2	1,7879984	KIF5B	1,73908447	PBEF1	1,58047258	SRPS4	1,49277182	CDC27	2,43052081	1506	MMS19L	1,33439616	LMX1B	1,44202116	HUS1	1,75562562	C1ORF103	1,71122386	BHMT2	1,55791526	MUTYH	1,47356286	POLE3	2,36702042
1437	SMARCC2	1,3464009	NR3C1	1,45896507	TDG	1,78687239	WDR61	1,73904056	PFDN2	1,58044508	DNMT3L	1,49271072	ADIPOR1	2,42978316	1507	MAPK11	1,33424501	IGFBP7	1,44197384	ZFP42	1,75473954	TLR10	1,71065108	LCT	1,55782418	CEACAM1	1,47307723	PDE5A	2,36600586
1438	DAO	1,34635862	AKAP11	1,45854011	DGAT2	1,7864563	EFNA2	1,73873188	LHCGR	1,57979544	CDC27	1,49257255	LTA	2,42977341	1508	BMP2	1,33411146	ETV5	1,44181071	STX2	1,7545882	SIRT6	1,71043413	PITPNB	1,55771083	DIABLO	1,47285753	CDK3	2,36592362
1439	MEN1	1,34635816	TXNRD1	1,45851276	PLCG1	1,78618962	AMPH	1,73849689	BPTF	1,57974474	APOB	1,49234894	MAPK8	2,42748146	1509	IRAK3	1,33339781	GSK3A	1,44168753	GFPT2	1,75457094	TRAF3IP1	1,70986047	NEK1	1,55734435	POLQ	1,4721092	P11	2,36555363
1440	ACSL3	1,34613737	MTA2	1,45849127	SMAD7	1,78586138	IL22	1,73841198	EIF2AK3	1,57961652	HTR1B	1,49220488	POLR2H	2,42670465	1510	SUOX	1,33313073	CDC7	1,44150968	C1R	1,75294391	CARD6	1,7095733	GOSR1	1,557172	HRB	1,47190396	F2R	2,36554143
1441	TNFSF8	1,34606447	IL2RA	1,45820245	C1QL3	1,78515071	CHRNA9	1,73825236	POLM	1,57940547	SUCLG1	1,49204763	CLU	2,42375662	1511	PIK3CG	1,33309643	MAP3K11	1,44143199	CCNB2	1,75237578	GDF2	1,70953791	ARHGAP1	1,55700428	ATP6V1H	1,47153771	GRB10	2,36512174
1442	APOD	1,34597041	GATM	1,45735956	PRKAR1A	1,78514502	SEMA7A	1,73739953	SOX2	1,57936722	NOS2A	1,49191628	UGT1A7	2,42296376	1512	ENTPD1	1,33287739	STAT5A	1,44143074	PPP2R2A	1,75222225	ACACA	1,70950258	MYH6	1,55677091	CTH	1,47150724	LRRTM3	2,36471204
1443	PDXK	1,3457291	CD3EAP	1,456642	CAPN1	1,78491983	BTG2	1,73727579	ATP5G3	1,57926911	AKR1C2	1,49153729	NEIL3	2,42143778	1513	ABCC4	1,33281861	CYP4F12	1,44124086	NEIL3	1,75220323	LPHN2	1,70931978	ADRA1B	1,55632287	C13ORF15	1,47108973	CPT1B	2,36413897
1444	TBKBP1	1,34561464	MAFA	1,45590035	ANXA2	1,78474289	IL13	1,735303	UQCRC1	1,57923651	MPPED2	1,49111854	ABCA4	2,41917566	1514	ATP6V1C1	1,33277659	MAML3	1,44116689	CAMK4	1,75214544	DYSF	1,70931862	SH3GLB1	1,55602041	GTF2H1	1,47096709	NOS1	2,36389073
1445	F2RL1	1,34508139	CHRM2	1,45545344	CASP3	1,78446823	LRRC41	1,73515605	RNF25	1,57829585	INPP5D	1,49072012	CSAR1	2,41793451	1515	IFI27	1,33272173	PIGP	1,44110855	MYL4	1,75069723	COL24A1	1,70918438	YWHAB	1,55591467	BMP6	1,47039921	EMR1	2,36294906
1446	MAP4K1	1,34506987	B3GALT6	1,45535077	RPS6KA1	1,78437098	HTR7	1,7350547	HELLS	1,57821891	EGLN3	1,49054058	EDA	2,41789824	1516	ADH1A	1,33262483	BECN1	1,44080152	GAD1	1,74972006	CSF2RA	1,70847385	ABCC6	1,55586319	PDK1	1,47000498	INHBB	2,36250354
1447	ANXA4	1,34501147	GNA13	1,45482984	AURKB	1,78426167	PIGT	1,73474056	SCAP	1,57818455	MC5R	1,49049827	AKAP6	2,41787517	1517	GPAA1	1,33259871	PDHA1	1,44004595	IRF9	1,74948077	STX5	1,70829779	SENP2	1,55527762	KCNN3	1,46998711	GPX5	2,36149478
1448	RAB5A	1,34497398	DLX3	1,45480674	KCNK1	1,78385823	SUFU	1,73460246	VCAN	1,57810331	CENTA1	1,48955114	COL16A1	2,41715659	1518	IFNA10	1,33251219	HEXA	1,43915229	SPRED2	1,74920011	CYBB	1,70829267	POFUT1	1,55511111	CUGBP2	1,46976579	MAPK13	2,36143887
1449	HPD	1,34497393	NPC1	1,45447762	B4GALT6	1,78283479	CAST	1,73423689	ITGA9	1,57797761	FABP5	1,48908641	IL1RAP	2,41466287	1519	ALDH1B1	1,3320243	C1R	1,43902065	ELK1	1,7487795	ACAA1	1,70740898	JAZF1	1,55502294	EHHADH	1,4696831	SSBP1	2,36085131
1450	MARS	1,34467212	AKAP5	1,45417226	FVT1	1,78270668	TACR1	1,7341053	PLTP	1,57747348	YWHAQ	1,4888292	SPR	2,41162668	1520	RARB	1,33175162	IL9R	1,438919	XPA	1,74858775	CYP1A1	1,70737368	MMP2	1,55497948	WDR61	1,46907369	EIF2AK3	2,35901562
1451	MYO1C	1,34448026	SDHA	1,45407246	CTNND1	1,78218603	GABBR1	1,73394603	SLC13A5	1,57744273	KRT8	1,48881151	UXT	2,4088984	1521	VLDLR	1,33169361	TNFSF4	1,43885594	IFNA8	1,74835403	ITGAX	1,70611098	INDO	1,5544462	PRMT2	1,46887405	C1QC	2,35751416
1452	BMPR2	1,34437933	MYBPC3	1,45400859	ATXN1	1,78196713	PFKFB4	1,73321488	ELK4	1,5773059	GATA4	1,488749	SHC1	2,40788369	1522	STX12	1,33158937	IL22RA1	1,43872428	FGF9	1,74766085	AKAP8	1,70578328	DAPK3	1,55408085	UGT2B4	1,46866109	FOSB	2,35654495
1453	UBE2E1	1,34405268	CYP2J2	1,45397936	NTSR1	1,7816332	EGR2	1,73303924	EEF1A2	1,57716021	COL21A1	1,48847762	NXT1	2,40645033	1523	DPPA4	1,33156694	PDE3A	1,43833792	GCNT1	1,74752887	B3GALT5	1,70576393	PLIN	1,55391331	HOXB4	1,46852911	WEE1	2,35606329
1454	APCS	1,34400722	CCNT2	1,45373293	TXNRD1	1,77976848	CDS2	1,73285024	GRIN2A	1,57701455	PARP1	1,48840993	GPT2	2,40568041	1524	WNT9A	1,33127477	STX5	1,43832536	PPARBP	1,74684673	ST6GALNAC3	1,70557303	SKIP	1,55388671	PRKRA	1,46820841	UBE2V2	2,35442832
1455	GPR161	1,34390261	MAP3K1	1,45368202	NOD2	1,77958055	KCNB1	1,73275679	AMDHD2	1,57692634	OAT	1,48819744	BCKDHB	2,40425227	1525	DICER1	1,33122258	GSTM3	1,43820383	HTRA2	1,74679222	STAT5A	1,70536509	CHRNA1	1,55377489	CISH	1,4679559	APC	2,35296629
1456	PTGDR	1,34376846	PROS1	1,45344012	RARB	1,77882496	TBK1	1,73248102	NKRF	1,57562635	HRH4	1,48746177	ACOX2	2,40381308	1526	TNIP1	1,33092234	IFNA2	1,43817987	MOBP	1,74658833	OPRM1	1,70532515	RRAD	1,55375871	GNAI1	1,46788167	PSMB8	2,35259851
1457	PRPS1	1,34364316	DLL4	1,45333977	NFAT5	1,77876238	CSGLCA-T	1,73140776	HMBS	1,57549529	NADK	1,48742081	ATP2B2	2,40009694	1527	DBT	1,3307759	KRAS	1,43809554	TCOF1	1,7458784	XRCC2	1,70488841	MALT1	1,55352491	AMDHD2	1,46762469	AIRE	2,34985231
1458	BET1	1,34339291	CP	1,4532485	TUB	1,77842535	TNFAIP3	1,73132238	GOLGA5	1,57486209	PFDN2	1,48709781	WBSCR17	2,39991157	1528	SAT1	1,3304662	RAMP1	1,43697186	C2	1,74515663	PDXK	1,70441421	ASNA1	1,55339603	FSTL1	1,4673939	MAP2K4	2,34872744
1459	ACCN5	1,34288705	NMNAT3	1,45290497	GLUL	1,77832731	BP75	1,73013435	BCL2	1,57477946	ZFX	1,48688983	ITGB1BP3	2,39905845	1529	F12	1,32964697	SLC23A1	1,43638918	PARK2	1,74495042	AZIN1	1,70403974	GPR171	1,55336581	ATP6V1A	1,4671453	ATP6V1F	2,34872209
1460	ST6GALNAC2	1,3428242	GSTP1	1,45288848	HLA-C	1,77748481	MCHR1	1,72951386	CNTF	1,57473785	SLC1A3	1,48670172	RIPK3	2,39762759	1530	CALML6	1,32945195	MSX1	1,43628588	CCL19	1,74408997	EEF1A2	1,70384511	GUCA1A	1,55259838	INHBB	1,467036	HSD3B2	2,34799145
1461	GDNF	1,34281604	CBLB	1,45288418	KLRD1	1,77733423	CD28	1,72919253	TFAP2C	1,57428444	RECK	1,48605919	HSPA1L	2,39691967	1531	CAP1	1,32922118	LEPR	1,43623555	CISH	1,7439171	IRF4	1,70362488	SFRS1ZIP1	1,55251955	PPP3R2	1,46694177	GIPR	2,34156019
1462	GDF2	1,34224347	COL24A1	1,45255746	CAMK2A	1,77597964	ALDH1L1	1,72846676	TNKS	1,57416226	TSG101	1,48586126	EXTL2	2,39669889	1532	GLRX	1,32918163	MCM6	1,43601471	NADSYN1	1,74359199	HPR	1,70360847	PPBP	1,55239214	IRF5	1,46680379	HRAS	2,34050118
1463	MBTPS1	1,34220848	RAP2B	1,45247795	JUNB	1,77594011	SULT1C4	1,72802614	CASP7	1,57411067	HEXA	1,48570518	ACCN1	2,39621752	1533	CDC20	1,32880494	ITCH	1,43600661	SMS	1,74243305	POLR1B	1,70359685	PRDX6	1,55147623	OPRK1	1,46671165	IL17RE	2,33935762
1464	TERT	1,34170738	CDC25A	1,45244915	PAK6	1,77591533	STRA6	1,72796018	CNP	1,57251019	BACE2	1,48560975	VIM	2,39551257	1534	LAMP2	1,32846946	PAX1	1,43553668	MMP10	1,74240485	CYP2C9	1,70335131	DRAM	1,55025111	CBS	1,46662714	LRP5	2,33884993
1465	PI4KB	1,34154093	CUGBP2	1,45242645	CTSL1	1,77336611	MEST	1,72692408	GNAS	1,57239525	TOP2B	1,48552717	SDHD	2,39431663	1535	SMC6	1,32844844	TDG	1,43523935	RPE	1,74224095	TNFSF4	1,70229803	COX5B	1,55002867	CCNB2	1,46642974	DPPA4	2,33774271
1466	PIGQ	1,34121025	ARPC3	1,45231111	RANBP9	1,77333139	EOMES	1,72665643	EGR2	1,57221565	GRIA2	1,48519351	ASNA1	2,39381517	1536	SP100	1,3284222	KATNAL1	1,43503541	CACNA1G	1,74205656	PLCG1	1,70221319	RTN4	1,54999506	BDKRB2	1,46617133	ALDH1B1	2,33752029
1467	AKAP1	1,34105099	PTPRO	1,45198858	KCNH2	1,77316683	HTR3E	1,72646926	DUSP6	1,57196649	HS6ST1	1,48516055	ERCC2	2,39381517	1537	DHODH	1,32827137	STAT5B	1,43494718	FCGR3B	1,74179111	CYP3A43	1,70012167	MYBPC2	1,54980268	THRB	1,46551884	KLF10	2,33748619
1468	ACSS2	1,34096339	NEU3	1,45195608	DCI	1,77313047	DNTT	1,72585015	ATP2A3	1,57187322	POLH	1,4851559	FCGR3B	2,39375994	1538	ITPKB	1,32785297	RAB5C	1,43481057	NEURL	1,74166609	SORBS1	1,69901751	STRAP	1,54979962	ATP5D	1,46500365	ID1	2,334702
1469	HK2	1,3408793	SERPINB9	1,45178236	LRRTM3	1,77246496	IGFBP3	1,72568768	SRD5A2	1,57147002	NDUFS8	1,48500819	ARF3	2,39333807	1539	MYBPC3	1,32777965	STK11	1,43477957	HEXB	1,74135005	CHRD	1,69877847	SCP2	1,54847775	TNFRSF8	1,46442919	ITGA2B	2,33455139
1470	FZR1	1,3406552	EME1	1,45082967	CCNE1	1,77133096	SYP	1,72540259	ABCA3	1,57030479	ITGB5	1,48473483	DLAT	2,39289597	1540	SFMBT2	1,32776372	NGFR	1,43473694	DGKH	1,74109844	GSTM4	1,69863147	LEFTY1	1,54813622	SLC6A1	1,46426483	BDH1	2,33407348

Table A4. Pooled-shRNA library screen on HEL cell line and MF-3: list of 2nd most depleted shRNAs for each experiment (ranking approach 1, RA1).

	NO ruxolitinib (setting 1)				Ruxolitinib (setting 2)				Ruxolitinib + CM (setting 3)				MF-3					NO ruxolitinib (setting 1)				Ruxolitinib (setting 2)				Ruxolitinib + CM (setting 3)				MF-3	
	Experiment 1		Experiment 2		Experiment 1		Experiment 2		Experiment 1		Experiment 2							Experiment 1		Experiment 2		Experiment 1		Experiment 2		Experiment 1		Experiment 2			
Rank	*Gene*	*Fold change*	*Gene*	*Fold change*	*Gene*	*Fold change*	*Gene*	*Fold change*	*Gene*	*Fold change*	*Gene*	*Fold change*	*Gene*	*Fold change*	*Rank*	*Gene*	*Fold change*	*Gene*	*Fold change*	*Gene*	*Fold change*	*Gene*	*Fold change*	*Gene*	*Fold change*	*Gene*	*Fold change*	*Gene*	*Fold change*	*Gene*	*Fold change*
1541	SULT1E1	1,32773492	RAB1B	1,43458847	SRXN1	1,74080189	CAMK2D	1,69723464	COL25A1	1,54752155	DOT1L	1,46398748	XRCC3	2,33219934	1611	ATP6V0A1	1,31562163	LALBA	1,42119585	GNPDA1	1,71496483	HSD17B6	1,66859056	LOC402057	1,52892388	ZFYVE9	1,4447246	CHRNA10	2,27221852
1542	GPR171	1,32756629	MAPK11	1,43377761	GABRG2	1,73981513	ABCC6	1,69653369	CADM1	1,54751909	BGN	1,46397062	LPIN2	2,33202596	1612	UGDH	1,31561991	ST8SIA2	1,42085023	CGN	1,71485282	EEF1D	1,66846692	FHL5	1,52850108	UST	1,44471365	DAPP1	2,2720543
1543	CLK3	1,32740575	RAD23A	1,43372888	EMR1	1,73947749	AVPR1B	1,69643176	FIGF	1,54750181	ACTN4	1,46345952	FUT9	2,33170839	1613	CDK3	1,31546155	ENTPD6	1,42071179	GPR18	1,7148146	PANK3	1,66844944	GCK	1,52801834	CLDN15	1,44457723	C7ORF16	2,27012717
1544	ATG4D	1,32731065	C1QC	1,4332628	CKMT1A	1,73912961	FMO3	1,69583185	DIDO1	1,54709664	PRKCE	1,46320983	KLK1	2,33151454	1614	IL13RA2	1,3152621	SIRT4	1,42041515	H2AFX	1,71474693	PSME3	1,66817479	ADAM8	1,52781148	SPRY4	1,44441916	ENTPD3	2,26977517
1545	NRG1	1,32697779	KCNK1	1,43301194	ABCC6	1,73902636	PSMB5	1,69557751	SHBG	1,54707624	STX12	1,46259287	IFIT1	2,32922183	1615	VCAN	1,31521926	UGT2B10	1,42024165	HSD17B2	1,71422053	MMP13	1,66779053	UGT8	1,52774377	BET1	1,44329742	RPS13	2,26956633
1546	CCNB3	1,32673959	CPO	1,43297439	ALDH1A2	1,73864557	MAP2K7	1,69476439	MSR1	1,54630157	FGF3	1,46258688	AP3M1	2,32845675	1616	IL12RB1	1,31517673	TSNAX	1,4197541	AMDHD1	1,71417166	CS	1,66759367	GTF2F2	1,52759997	PSCD1	1,44293329	SYP	2,26777424
1547	MTA1	1,3265086	ZCCHC11	1,43247988	NFATC4	1,73835461	LALBA	1,69445124	LIPF	1,5458668	CACNA1B	1,46241914	SCYL1	2,32686522	1617	DNAJC4	1,31510722	ITGB4BP	1,41869882	ANKRD6	1,71410505	IL17RC	1,66737358	RAB9A	1,52691822	NEUROG3	1,44281799	RPS3A	2,26753146
1548	GABARAPL2	1,3260774	COPA	1,4323439	CLTA	1,73809545	TCL1A	1,69432839	MB	1,54585923	CALB1	1,46216583	MELK	2,32654128	1618	IGF1	1,31508726	SPRY3	1,41857824	AASS	1,71377741	PGLS	1,66728284	COL4A3BP	1,52634186	BAG5	1,44280906	TRAF1	2,26743435
1549	COQ7	1,32599742	CBR1	1,43205385	CDK5	1,7379087	PLA1A	1,69371817	PLD2	1,54576959	DPM1	1,46203867	ADA	2,32571902	1619	STMN1	1,31506635	AIFM1	1,41815002	FCGRT	1,71377142	DLG7	1,66716947	GALC	1,52609911	ETV5	1,44263382	PPP3CB	2,26717949
1550	COL5A1	1,32587409	DNAJC3	1,43199524	PPP1CA	1,73717709	ATP2B3	1,69301314	TUBA3C	1,54565353	IL8RB	1,46203297	LTBP1	2,32521233	1620	SERPINA4	1,3149549	ENO1	1,41787347	MAP3K5	1,71321144	POLL	1,66715982	CAPNS2	1,52532182	NCSTN	1,44226837	BCR	2,26588504
1551	MMP9	1,3257979	DCI	1,43119111	PPBP	1,73715977	PRKCD	1,6921534	IL16	1,54561567	CSF2RA	1,4619613	RXRB	2,32464883	1621	CARD9	1,31461864	STXBP1	1,41785542	OPRM1	1,71264177	PIK3C2G	1,6665331	HTR3C	1,52511588	ICOS	1,44199283	ANXA4	2,26547533
1552	ADRB2	1,32576146	WT1	1,43101588	PI3	1,73685091	CYP11B2	1,69165952	CD22	1,54532502	LEP	1,46158595	GRM1	2,32284031	1622	RFXAP	1,31447881	IFNA8	1,41783161	CSF1R	1,7121093	NDUFV1	1,66630804	PPCS	1,52464571	STAT5A	1,44189096	MANBA	2,26473544
1553	XRCC1	1,32547138	NFYA	1,43093672	CTPS	1,73661372	H2AFY	1,69164903	ETV6	1,5449651	SCAP	1,46069656	BBS1	2,32095801	1623	ITPR3	1,31404953	CTBP2	1,41777646	STAMBPL1	1,71206699	HSP90B1	1,66600382	AKR1C1	1,52394672	MMP13	1,44110816	GHRHR	2,26469986
1554	CALR	1,32531577	MCL1	1,43075874	PIK3R4	1,73577762	DGKH	1,69132919	MTA1	1,5446814	PTPRJ	1,46059974	HBXIP	2,32017444	1624	ATP6V1C2	1,31403599	QPCT	1,4173278	AMPH	1,7119429	COL21A1	1,6656037	TNIP1	1,52348976	SEPHS1	1,44058599	UBQLN1	2,26426759
1555	MAPK8IP3	1,32487665	CUL1	1,43071019	RALA	1,73576246	ACSM1	1,69071093	EIF5	1,54429825	PCYT1A	1,46059527	MTTP	2,3194092	1625	CTSL1	1,31391017	GPX4	1,41717898	IFNA21	1,71188587	VKORC1	1,66549865	AK1	1,52297466	MEFV	1,44034415	CDK4	2,26271481
1556	EIF4A1	1,32485926	DNMT3B	1,43048371	PIGP	1,73559423	PPBP	1,6902423	GYPA	1,54428208	GABRA5	1,46038337	PDE1A	2,31521658	1626	FAM59A	1,3139101	CLDN7	1,41710284	CDS1	1,71182814	SLC23A1	1,6650204	PTPRN	1,52269424	PPIA4	1,43944454	DARS2	2,26182754
1557	CACNA1A	1,32481815	IFT57	1,43034936	MUS81	1,7355504	RASGRP3	1,68995924	MYB	1,54404364	PEU1	1,46034652	SRP72	2,31397413	1627	CYP2A13	1,31369058	SMARCE1	1,41653274	SRP72	1,71181908	ACP6	1,66478677	STX3	1,52212867	C1ORF103	1,43891234	POLR2L	2,26139528
1558	AGPAT3	1,32481295	SLC5A3	1,43027652	UGT2B4	1,73503263	MTA2	1,68820517	PHC1	1,54388936	IL12B	1,45993562	B4GALT1	2,31006844	1628	FRAT1	1,3135876	RHEB	1,41648856	CYP21A2	1,71173489	GNG3	1,66406551	ATP2A2	1,52149001	IRF6	1,43835959	NR1I2	2,26135668
1559	COL8A2	1,32468276	CREB3L2	1,4302117	ATRX	1,73416067	PDE6D	1,68736888	ITGB1	1,5438797	GTF2F2	1,45960162	CYP39A1	2,3085371	1629	SALL4	1,31343111	PADI2	1,41648413	COL4A5	1,71167064	ALDH5A1	1,66395539	GAP43	1,52033289	ST6GAL1	1,43792228	ACP6	2,26031001
1560	GNA11	1,32466525	ORM1	1,42980123	WDR1	1,73375411	GART	1,68703121	SMARCB1	1,5436264	HIST2H3C	1,45957866	MSH6	2,30766116	1630	TNFRSF8	1,31306234	GTF2B	1,41646189	CD160	1,71161321	ALDH3A2	1,6633767	KPNA3	1,52013485	NFKB1	1,43785715	EIF4E2	2,25982323
1561	ABCA13	1,32459997	EMR1	1,42974254	CSNK1E	1,73329467	PPARBP	1,68659091	ACVR1C	1,5435839	IL13RA1	1,45956703	IRX3	2,30710232	1631	CAT	1,31301685	YWHAB	1,41639629	PIGA	1,71145726	C3AR1	1,66289891	CASP2	1,51928984	PIK3C2B	1,437597	ATP2A2	2,25963798
1562	IL6	1,3242064	PFN1	1,42942784	HSD3B2	1,73247966	TARDBP	1,68642649	HSPA5	1,54283141	PIWIL3	1,45854972	LARS	2,30454666	1632	RRM2B	1,31298287	LTBR	1,41569319	DLG7	1,71127769	FGA	1,66283639	PRPS2	1,51919804	ZEB2	1,437597	HRH4	2,25841173
1563	UXS1	1,32408327	RAF1	1,42942175	UBE3A	1,73179733	VAMP5	1,68642649	P11	1,54207277	MAP3K7	1,45797648	CAPN3	2,30451269	1633	SESN3	1,31281928	CD3E	1,41512846	RXRA	1,71125328	GCK	1,66273711	CRY1	1,51916708	CTGF	1,43749863	SULT1B1	2,25712892
1564	PLLP	1,32399413	GLUL	1,42932959	MADD	1,73162753	ATP1B2	1,68639886	DMD	1,54179933	SLC22A18	1,45723706	NKX2-2	2,30443315	1634	PER1	1,31271054	DLG4	1,41498843	FBLN2	1,71083842	IL1R2	1,66216899	LDHC	1,5191099	PROX1	1,4374729	PRKAR1B	2,25694834
1565	GOLGA5	1,32398567	MAP4K2	1,42910589	MAL	1,73159788	FEZ1	1,68632382	CASP1	1,54175493	CSGLCA-T	1,45703455	CRHR1	2,30381414	1635	FGR	1,31262189	ATP6V0E1	1,41468829	PIGS	1,71041694	ARHGEF6	1,66173633	CPSF4	1,51863183	ST3GAL2	1,43746693	HCK	2,25551774
1566	GTF2I	1,32376105	TRIO	1,4288967	PCK1	1,73149383	IFNE1	1,68614242	AKR1C3	1,54173208	BMP4	1,45675627	C14ORF166	2,30316815	1636	BCR	1,31252462	AR	1,41456822	CD1E	1,7100031	GIPR	1,66109265	TNFRSF8	1,51824673	ENO3	1,43743226	PAFAH1B2	2,25186699
1567	CD160	1,32369488	AZI2	1,42826109	DNMT3B	1,73096032	TNFRSF11B	1,68589103	ATG4B	1,54164351	CPB2	1,45618441	PRODH	2,30219144	1637	HS6ST3	1,31247028	MFGE8	1,4139603	CPB2	1,70929431	NUMA1	1,66071846	DRD1	1,51752965	PIK3CB	1,43739715	RAD51	2,25183611
1568	ATG3	1,32365589	TLE1	1,4279954	PRKDC	1,73029645	TNKS	1,68525347	TFAM	1,54156842	ST6GALNAC6	1,45595365	GABBR1	2,30181228	1638	PTPRN	1,31213301	PGM3	1,41370667	IL13	1,70908505	ERBB2	1,6606046	DOCK9	1,51690113	BCL2	1,43677199	ENTPD4	2,25037358
1569	CNTF	1,32363211	FOLH1	1,42798383	PFKFB1	1,73010444	GFAP	1,68514402	CAPN7	1,54053377	HAT1	1,4559105	APOBEC3F	2,30110004	1639	RAB3B	1,31180226	KCNMA1	1,41355348	MGAT3	1,70859237	SLC18A3	1,66059467	LIG3	1,51653233	ERN1	1,4367325	HSPB2	2,25004066
1570	MUT	1,32360119	WASF2	1,42784605	NEUROD1	1,72967593	GRM4	1,68492205	RPRM	1,54037821	DNMT3B	1,45571157	CARS	2,29898577	1640	POLR2F	1,31173691	TAL1	1,4133099	SRC	1,70645702	GATA6	1,6604597	LILRB3	1,51624342	FASLG	1,4366572	IL6ST	2,24982797
1571	SOX17	1,32350477	RDH12	1,42745746	SUCLG1	1,72964775	GBE1	1,68466234	VSNL1	1,54032364	CTBP2	1,45569108	NOX1	2,29851044	1641	NAIP	1,31164485	NAPG	1,4131796	AVP	1,70641699	CASP7	1,66033767	CDK5	1,51617658	PGA3	1,4360977	POLE2	2,24963945
1572	GNAO1	1,32349464	OSBPL1A	1,4273818	CHMP1B	1,72956327	BHMT2	1,68352413	COMP	1,53970267	F13A1	1,45518021	PUM1	2,29656262	1642	ENO3	1,31126565	CST3	1,41250407	NME2	1,70641699	ASNS	1,6601567	DLL4	1,51572926	CAB39	1,43608857	APBB3	2,2495543
1573	MPI	1,32278851	FGF7	1,42717883	PLA2G12B	1,72933608	IFNA14	1,68262204	LEPR	1,53968114	GPX6	1,45496763	TOP2A	2,29588068	1643	ANAPC4	1,31124369	ADM	1,41203964	CAMK2D	1,70639216	GABRB1	1,66005823	BTG3	1,51571098	CLYBL	1,43580942	HLA-G	2,24784
1574	HRH4	1,32271922	PDE6A	1,42702159	ATP5B	1,72918229	MPO	1,68188212	LDHAL6A	1,53956934	LEF1	1,45461425	GSTZ1	2,29519178	1644	WNT11	1,31118298	MEIS1	1,41187238	BDKRB2	1,70614837	LDHAL6B	1,65997805	SDHC	1,51564926	GTF2B	1,43567137	CSNK1A1L	2,24737497
1575	IL12B	1,32258028	CTF1	1,42697839	EIF3H	1,72893149	RARA	1,68180459	ABCA4	1,53938507	VEGFA	1,45439718	PANK1	2,29462572	1645	ALG11	1,31090863	TLR5	1,41185656	IL4R	1,70489118	HSF2	1,65938156	AURKB	1,51561176	ATP5G3	1,43542072	PLA2G2D	2,24678273
1576	RET	1,32250038	TUBA8	1,426637	KLRK1	1,72891876	CD38	1,6816988	BCL6	1,5388066	QPCT	1,45368131	IDS	2,29274342	1646	AGPAT6	1,31088725	PROM2	1,41156119	PDGFB	1,70452149	MBP	1,65919114	FAS	1,51551489	CHEK2	1,43521437	MAD1L1	2,24655774
1577	CREM	1,32230597	S100B	1,42654086	NUP153	1,72873198	LCMT2	1,6816632	DLL3	1,53872843	TNKS2	1,45318436	FAM50A	2,2921974	1647	CXCL3	1,31071835	PIGU	1,41146992	ALAD	1,70293068	PFKL	1,65857091	PDE6D	1,51540061	CASP8AP2	1,43508433	GALNT2	2,2461523
1578	KERA	1,32228166	OXA1L	1,42645537	IL21R	1,72864007	B4GALT1	1,68123397	GRM3	1,53871532	SMCHD1	1,45311867	P2RY1	2,29138739	1648	GRM8	1,31070469	TUB	1,41131003	SPAM1	1,70254606	IL12B	1,65761397	DNAJC4	1,51503275	XRCC3	1,43487882	NT5E	2,24593564
1579	GSTP1	1,32214021	CXCL11	1,42642048	ANKFY1	1,72821513	MTHFD2	1,68109855	KCNMB4	1,53863649	CLDN11	1,45311272	CDC42	2,29130405	1649	SYT2	1,31061445	MYCBP	1,41103733	STUB1	1,70224863	CR1	1,65711087	WARS	1,51497413	SHC4	1,43475745	RECQL	2,24540273
1580	PDHX	1,32169971	ACP6	1,42636339	HMGCL	1,72817126	UGT2B11	1,68065518	IFI16	1,5380729	ANXA2	1,45304077	RPA2	2,2900552	1650	PIK3R3	1,31054591	TREX1	1,41095848	CARD9	1,70197729	AUH	1,65706454	CYGB	1,51490139	PRDX1	1,43474953	MAF	2,244848
1581	CYP27A1	1,32101802	SVIL	1,42604374	VCAM1	1,72791438	XRCC1	1,68025425	DNM1	1,53792923	CXCL2	1,45294504	MUT	2,28988963	1651	CPT1C	1,31051383	POLRMT	1,41095016	ORM1	1,70188976	PPP1R13B	1,65697564	HS3ST2	1,51415925	NR1H3	1,43445093	VARS2	2,24408718
1582	HRB	1,32085966	MOG	1,42573517	IRS1	1,72786849	ASGR2	1,68010907	WIF1	1,53727248	CAND1	1,4528458	LDHC	2,28859694	1652	CLDN17	1,3102227	LCAT	1,41082907	ID4	1,70109609	PMVK	1,65681246	PRDX5	1,51415508	SLCO1C1	1,43418601	FAU	2,24393694
1583	CLU	1,32059177	HSD3B1	1,42559582	TACR2	1,72772441	WDR1	1,67988065	HSD3B2	1,53692403	BLVRA	1,45148241	UGT2B28	2,28724711	1653	SMARCE1	1,31014927	RSAD2	1,41070679	SMARCE1	1,70109609	PLD3	1,65611935	GNAI3	1,51409709	HAGH	1,4339949	CYP2J2	2,24228213
1584	PLSCR4	1,32035955	CACNA2D2	1,42540507	PLA2G10	1,72727109	RAMP1	1,67987818	GREB1	1,53680483	ST3GAL5	1,45115923	RAD52	2,28723544	1654	STH	1,3098529	SEPHS1	1,41068121	POLR3G	1,70105249	SULT2A1	1,65597731	REL	1,51351219	NARS	1,43331262	IL8RB	2,24012361
1585	PTPRU	1,32011206	BRCA2	1,42533719	NRG3	1,72654456	HIST2H3C	1,67981622	TCF3	1,5358666	PLCG2	1,45114081	SUMO1	2,28665814	1655	SCAP	1,30955259	LRRTM3	1,41024568	XK	1,70064268	SRP54	1,65510641	LCN2	1,51337482	PPP1CA	1,43298757	DEDD2	2,23884445
1586	GPR64	1,32002362	GNAI1	1,42526039	F8A1	1,72644464	CUGBP2	1,67972561	VANGL2	1,53546613	AURKA	1,45096895	C8G	2,28614912	1656	IQGAP2	1,30933316	CENTD2	1,41010274	SLC1A1	1,70053966	ATP2A2	1,65466822	ITGAM	1,51327618	TERF2IP	1,43207134	ST8SIA5	2,23812801
1587	APEX2	1,31999521	BMP5	1,42521643	WIF1	1,72643253	PYGB	1,67946451	GZMA	1,53499815	BCKDK	1,4509625	GART	2,28614912	1657	IL16	1,30921749	NCOA3	1,40982699	PIK3C2B	1,7039037	MMP7	1,65420864	CTBP2	1,51319617	COL11A2	1,431941	PRPF19	2,23760101
1588	SSTR4	1,31967556	CTNNAL1	1,42490135	HTR2B	1,72642607	NCOA2	1,67921664	PPP6C	1,53487692	GOT1	1,45075521	EIF4E	2,28528802	1658	USP11	1,30919574	MTA1	1,40979455	KCNJ2	1,70016474	ENTPD6	1,65416187	MYT1	1,51309258	ADD1	1,4318934	CDC2	2,23670984
1589	NDUFV2	1,31961366	HEMK1	1,42464793	CD52	1,72622872	GNA11	1,67830846	VIM	1,53474883	MBTPS2	1,45053656	KRT18	2,28497524	1659	CHIA	1,30903054	EPHB4	1,40975579	APPBP2	1,70015024	ARPC3	1,65354003	ADC	1,5130341	RRAD	1,43153641	APOBEC1	2,2365994
1590	BGN	1,31936704	RBBP8	1,42455175	KLF10	1,72541057	HEXA	1,67752982	RCAN1	1,53467316	ICOSLG	1,44970035	PINK1	2,28352797	1660	CELSR1	1,30897588	MECR	1,40965614	EGR1	1,6993104	FGF12	1,65278842	NNT	1,51231706	TNF	1,43114763	RBPJL	2,23648587
1591	NOD2	1,31914562	NFAT5	1,42419556	PRKRA	1,72508729	ITPR1	1,67703594	LTA	1,53459884	COL10A1	1,44939934	NEU1	2,28339622	1661	MLH3	1,30892682	UBTF	1,40925335	C14ORF166	1,69902235	TUB	1,65272484	JUN	1,51181977	SIM1	1,43091354	VAMP2	2,23552316
1592	IDI2	1,31852698	NMI	1,42405823	B3GNT6	1,72506364	DGKQ	1,6767919	GSTZ1	1,53439628	SERPINB2	1,44914009	HIST1H2AA	2,28277455	1662	MDH2	1,3088802	DDX19A	1,40906861	GAB2	1,69883932	AASDHPPT	1,65265886	CRK	1,51171175	HMBS	1,43079775	TUBE1	2,23514654
1593	GADD45A	1,31827873	TNFRSF10A	1,42399092	NF1	1,72479418	AVP	1,67651081	CHRNB2	1,53399194	LRMP	1,44891872	NPR3	2,2819253	1663	DLST	1,30869753	SUZ12	1,40904583	SNX13	1,69852043	IL6	1,65255801	GDI1	1,51169434	EPHA2	1,43072771	BTC	2,23509223
1594	AZIN1	1,31821011	SUOX	1,4239176	CCR1	1,72320421	GSTA2	1,67568841	DTX2	1,53372532	KATNAL1	1,44846585	ANAPC2	2,28149501	1664	ZNF395	1,308309	CALML3	1,40818609	ERCC5	1,69850509	DKFZP434E11	1,65243949	MAML3	1,51154584	STXBP4	1,43042922	SERPINB9	2,23308399
1595	DDX19A	1,31816909	C1GALT1C1	1,42374182	ABCA8	1,7226037	RPS6KB2	1,67559401	TNIP2	1,53344796	TNFSF4	1,44832198	AGXT2	2,27967161	1665	ANGPT1	1,30809998	GPR83	1,40801177	PHC1	1,69845779	BGN	1,65079751	APOA4	1,51149075	PIGV	1,43029093	LY96	2,23284923
1596	TBXAS1	1,31813471	FGF18	1,42369393	TKTL2	1,72139123	GAD1	1,67505669	CTNNA3	1,53336652	TXN2	1,44819825	NAT5	2,27940723	1666	DPM1	1,3079465	C19ORF40	1,4076852	DYRK1B	1,6981849	AVPR2	1,65076985	KLF10	1,51148346	UBE2H	1,43029093	PDE4C	2,23223515
1597	DHDDS	1,31809708	FOXK1	1,42365096	RSAD2	1,72063343	CPT1C	1,67398636	AMT	1,53326886	OPRS1	1,44798005	IL15RA	2,27940066	1667	CHRNG	1,30792086	SOX4	1,40764026	SOX4	1,69795354	CHIA	1,65068794	RCHY1	1,51133438	ACSS1	1,4297338	ADH7	2,23126283
1598	PLA2G6	1,31801445	NT5C1B	1,42308449	GPX7	1,72036224	SIRT1	1,67387603	FEZ1	1,53301189	COQ2	1,44787979	MLXIPL	2,27915132	1668	F13B	1,30772863	BBS1	1,40738368	UGT2B11	1,69776935	AMY1A	1,65013503	SERPINE2	1,51132026	POLD1	1,42944208	MTHFD1	2,23120823
1599	RPRM	1,31791197	C9	1,42288052	SULT2A1	1,71887666	MSTN	1,67369051	HIST1H2AA	1,53300699	NEURL	1,44711808	SERPINA5	2,27697248	1669	PAX1	1,30767946	C4A	1,4071462	EPHA2	1,69769897	BCKDK	1,64902222	HGD	1,51122557	ETV6	1,42937242	GDF5	2,22995838
1600	MAPK7	1,3178718	HARS2	1,42283435	DVL1	1,71884475	TBXAS1	1,67241299	HS6ST3	1,53280242	ATP5I	1,44679496	KCNA5	2,27634151	1670	ENTPD7	1,30734054	CFD	1,40661626	DNM1	1,69738103	B4GALT3	1,64815595	IDH3A	1,51109416	STX2	1,42896655	CD1E	2,22924397
1601	CADM3	1,31773263	GPAM	1,42280318	DGAT1	1,71875093	MGAT1	1,67233743	UGT1A7	1,5326764	MMP2	1,44661498	TBKBP1	2,27490643	1671	IRAK4	1,30714929	CSF2	1,40645964	IFNE1	1,69703219	CYP4A22	1,64774203	HGSNAT	1,51065031	HTR4	1,42875161	GTF2H3	2,22901682
1602	PLA2G4D	1,31759858	SFRS12IP1	1,42266478	FSTL1	1,71867142	DGKZ	1,67230137	MSH6	1,53258139	FAM50A	1,44658625	PECR	2,27490299	1672	RAD17	1,30696839	DHODH	1,40499073	FABP1	1,6965615	NGB	1,64760608	IL5RA	1,50995164	ELOVL6	1,42828031	BTLA	2,22845249
1603	KREMEN1	1,31753825	PYGB	1,42262357	BLR1	1,71828469	CD72	1,67053032	DHH	1,53230938	TRAF3IP2	1,44626817	GABARAP	2,27413154	1673	ATP5J	1,30677209	CDK5RAP1	1,40493652	CCNA1	1,69620192	HOXA4	1,64696425	ATP6V1B1	1,50982687	CPSF4	1,42811314	FBL	2,22785019
1604	PLIN	1,31710653	LYN	1,42215995	ATP2A2	1,71772715	CTPS	1,6700483	SH3BGRL	1,53207632	HLA-C	1,44607005	CD19	2,27388798	1674	SLC1A1	1,30633474	EPX	1,40445621	NOTCH1	1,69591146	DNAJA4	1,6468417	CDH2	1,50933967	C1QB	1,42771757	OXA1L	2,22709377
1605	APOA5	1,31705437	NFKB2	1,42198705	PIGV	1,71659266	SIRT4	1,66976279	CA12	1,53185376	AGXT2	1,44602073	GSTP1	2,27376434	1675	GGT1	1,30609948	EXOC7	1,40412377	POLG	1,69591146	SLC15A1	1,6452461	SLC27A4	1,50928679	AKR1C3	1,42761925	AURKB	2,22642594
1606	PHKA2	1,31691036	AKAP8	1,42188833	RAB5A	1,71640281	LPL	1,66934358	SHC2	1,53147262	C1QA	1,44557732	ALB	2,27375844	1676	ODC1	1,30599098	DIDO1	1,40389044	ISG20	1,69527794	THY1	1,64464778	PMS1	1,50891887	RASGRF1	1,42731723	ITGA3	2,2263202
1607	KIF3A	1,3163053	AADAC	1,42185921	SPRY3	1,71624417	FRZB	1,6693061	NOS1	1,53108304	MAGEH1	1,4454792	PSMC2	2,27362341	1677	FGFR4	1,30596501	COQ7	1,40365428	PTPRF	1,69491494	GTF2E2	1,64422725	MGST1	1,50885851	VCL	1,42710045	ADH4	2,22368983
1608	YWHAB	1,31586552	GNAS	1,4216696	GABRA5	1,71591966	CAMKK1	1,66914961	RIPK2	1,53053328	SULT2B1	1,4453768	SPTAN1	2,27346393	1678	PIWIL3	1,30588088	CRP	1,40357877	CALB1	1,69444873	CARS2	1,64410981	CACNA1B	1,50819651	C8A	1,42707451	CALR	2,22134533
1609	SULT2B1	1,31569335	PRPF40B	1,42162342	UNC13B	1,71521702	ALG5	1,66912225	FTMT	1,52982342	CHRNA5	1,44526647	GSK3A	2,2727655	1679	NDST3	1,3057577	GSTM4	1,40353402	BPTF	1,69400146	CALB1	1,64403845	SYT2	1,50814702	PI4KB	1,42689761	CSNK1E	2,2181258
1610	ACP2	1,3156789	GALK1	1,42130702	PLP1	1,71506682	MEPE	1,66888517	MDH2	1,52950026	GNPDA2	1,44515073	PSEN1	2,2727655	1680	DDHD1	1,30558053	NAE1	1,40317664	KRT1	1,69231754	ATP6V1C1	1,6436972	FDXR	1,50791023	CDT1	1,42676962	ELOVL2	2,21679959

Table A4. Pooled-shRNA library screen on HEL cell line and MF-3: list of 2nd most depleted shRNAs for each experiment (ranking approach 1, RA1).

	NO ruxolitinib (setting 1)				Ruxolitinib (setting 2)				Ruxolitinib + CM (setting 3)				MF-3			NO ruxolitinib (setting 1)				Ruxolitinib (setting 2)				Ruxolitinib + CM (setting 3)				MF-3	
	Experiment 1		Experiment 2		Experiment 1		Experiment 2		Experiment 1		Experiment 2					Experiment 1		Experiment 2		Experiment 1		Experiment 2		Experiment 1		Experiment 2			
Rank	Gene	Fold change	Gene	Fold change	Gene	Fold change	Gene	Fold change	Gene	Fold change	Gene	Fold change	Gene	Fold change	Rank	Gene	Fold change	Gene	Fold change	Gene	Fold change	Gene	Fold change	Gene	Fold change	Gene	Fold change	Gene	Fold change
1681	NRAS	1,30555339	CCL13	1,40305344	DPM2	1,69224102	FOXD3	1,64319029	MTHFD2	1,50785534	NSDHL	1,42672746	EPAS1	2,21629605	1751	TUB	1,29152157	PIK3R2	1,38699661	UGT2A3	1,66466523	TIMP1	1,61436534	HSD11B2	1,48845643	CA2	1,41096667	MGAT2	2,16223746
1682	SOS2	1,30530642	LRP5	1,40289943	CDK2	1,69164809	HTRA2	1,64289172	DPM2	1,50620988	REPS1	1,42660157	BCL11A	2,21597203	1752	GMDS	1,29143444	IFNA10	1,38669313	CA14	1,66461596	GMNN	1,61406937	TRO	1,48803906	RECQL5	1,41057908	BBS2	2,16196999
1683	TRAF3	1,3052336	NKX2-2	1,40287679	TNFRSF1A	1,69053774	PRKRA	1,64288642	EIF4E2	1,50575667	C14ORF166	1,42588281	UROD	2,2155456	1753	ZFP36	1,29121611	PI4KB	1,38668891	TRAF3	1,66368559	EIF2AK2	1,61402899	VNN1	1,48795109	IFNA6	1,41027107	GRIK4	2,16092411
1684	DGAT1	1,30522461	JUND	1,40286838	MSX1	1,69028305	DKC1	1,64251704	GPI	1,50560668	CTSA	1,42583436	PRKCA	2,21465342	1754	COL7A1	1,29119113	NAIP	1,38619033	DKK3	1,66323726	KCNJ3	1,61355338	KIAA1394	1,48780793	ERN2	1,41008938	CHPF	2,15927142
1685	FGF4	1,30518286	LRP8	1,40279114	COL2A1	1,68992	PYCR1	1,64226741	CCNE1	1,50546964	IL16	1,42550151	DAPK3	2,21210979	1755	ADSSL1	1,29115333	GTF2H3	1,38594566	STEAP3	1,66177745	MLXIPL	1,61320841	GFPT2	1,48751187	ANGPTL4	1,41008337	RXRA	2,15771541
1686	SPTAN1	1,3044938	TGM2	1,40239454	CAT	1,68951929	RBPJL	1,6422172	FCGR2A	1,50535173	KLK6	1,42536175	NOTCH4	2,21140464	1756	CDK5RAP1	1,29111448	SKP1A	1,38594391	FLT3LG	1,66171064	ZIC1	1,61295373	PACRG	1,48720783	SNCAIP	1,40996478	ACAT1	2,15566306
1687	NME2	1,30426456	PDXK	1,40200163	SCN1B	1,68910456	TOP3A	1,64200372	POLH	1,50501612	FOSL1	1,42532164	SPAM1	2,21116879	1757	TRAF1	1,2905	PLA2G5	1,38586722	RNASEN	1,6614805	CYP2B6	1,61282377	PHF11	1,48719531	MB	1,40989491	CAV2	2,15533354
1688	ACADSB	1,304076	EIF4EBP1	1,40186902	CALML6	1,68885566	RGS16	1,64178793	SDHD	1,50490668	IL1RN	1,42490469	SLC16A3	2,21105375	1758	QARS	1,29031078	F5	1,38557536	MYLK	1,66090975	AGXT2L1	1,61237014	APH1B	1,48683871	ALCAM	1,40967893	TLX1	2,15468817
1689	ADCY9	1,30382461	ACSM1	1,40143271	ATP6V1B2	1,68867463	ATP6V1F	1,64152689	AMPH	1,50488948	BCR	1,42476093	AKR1A1	2,21043654	1759	WNT10B	1,29031078	KIF5B	1,38531111	ANXA4	1,66039448	CHRNA1	1,61211944	SLC25A11	1,48629617	AMPH	1,40949929	GPX2	2,15383585
1690	APBA2	1,30376744	DPPA4	1,40136698	GBE1	1,68847953	WWTR1	1,6414188	CPS1	1,50479729	PIWIL1	1,42457851	VAX2	2,20999323	1760	DKK2	1,29020093	ATG4C	1,38526306	CD79A	1,66022428	BIK	1,6115285	ATP6V1G2	1,48617277	ALOX15B	1,40941409	SDHB	2,15307601
1691	MAP3K3	1,30366876	CD48	1,40112024	NUMA1	1,68845792	CPSF1	1,64141365	CTH	1,50474224	CD47	1,42428758	RBPJ	2,20981683	1761	KCNA5	1,29014104	NOX1	1,38524432	CXCR3	1,66000858	TLR5	1,61143979	MTMR1	1,48614517	LRRK2	1,40941344	PRMT3	2,15190665
1692	HSD17B6	1,30363943	GRID2	1,40108726	MC4R	1,68803388	ZNF395	1,64136413	TEAD2	1,50420527	PDE6B	1,42414826	ACAT2	2,20936197	1762	LTA4H	1,29012538	LY9	1,3851851	PALB2	1,65997154	DNAJB11	1,61109244	CBR1	1,48517455	CDK5RAP1	1,40935601	BMPR2	2,1513782
1693	NR1I2	1,30296938	CYP27A1	1,40055768	NR4A1	1,68802895	CTGF	1,63991296	RPS6KB2	1,50363818	PDPK1	1,42403439	TNFAIP3	2,20839016	1763	CD8B	1,29001903	LDHAL6B	1,3851622	CDC26	1,65956989	FOSB	1,61099647	SH2D3C	1,48433895	NR5A1	1,40931776	STAG2	2,14986749
1694	IL18R1	1,30283323	PLA2G7	1,40054866	PINX1	1,68762822	CYP4B1	1,63905207	GGA3	1,50355668	BLK	1,42393943	GSTM4	2,20813824	1764	ALKBH3	1,28970208	ACVR2B	1,38492815	CLK1	1,65903921	PDE10A	1,61098247	ROR2	1,48431728	PSMD8	1,40917487	FANCG	2,14983632
1695	GDF5	1,30265967	ORC1L	1,40045052	IGFBP7	1,68750855	CDC6	1,63855348	MAT2A	1,50326305	C8B	1,42391701	HPR	2,20774552	1765	SRD5A1	1,28914393	GLB1	1,3848093	ATP1B2	1,65900115	MLH3	1,61008821	CKMT1A	1,48406701	BPNT1	1,40910118	INPP5D	2,14960683
1696	C19ORF40	1,30235324	APOB	1,40038075	MTTP	1,68722766	SRP68	1,63839299	TOP2B	1,50323332	IL7R	1,42370704	WNT2	2,20761131	1766	TXNRD1	1,28897592	MGST1	1,38476097	MYBPC1	1,65770178	RAG1	1,60951162	PRDX4	1,48375139	SERPINA1	1,40904928	SIRT1	2,14863992
1697	COQ2	1,30224475	CCR8	1,40037698	SLAIN1	1,68698312	NEUROG1	1,63793385	AGXT2L1	1,50284512	SFRP2	1,42351841	ATP5F1	2,20659561	1767	UQCRH	1,28896715	AMT	1,3842311	ARHGAP1	1,65757337	DCI	1,60947252	GPX5	1,48348001	NDUFA11	1,40877333	SLC22A7	2,14858938
1698	FOSL1	1,30183111	PFDN2	1,40035055	ATP5H	1,68678148	SIRT5	1,63787121	PGM1	1,50263735	PARK2	1,42347969	NSDHL	2,20544105	1768	POLR3K	1,28892617	NFS1	1,38384594	GNB3	1,65661966	ABCG5	1,60927163	ALG13	1,48329665	PDE4D	1,40875007	PDHA2	2,14850693
1699	C9ORF95	1,30165161	LRP6	1,40015468	SOCS5	1,68579942	PRF1	1,63786842	ACTG2	1,50202169	GFPT2	1,42300626	HOXA13	2,20531619	1769	MXI1	1,28886312	CYBB	1,38368021	ADAM8	1,65654249	PFDN2	1,60922218	HEXB	1,48301994	CPE	1,40824829	NUDC	2,14795884
1700	HOXA9	1,30161601	YES1	1,39927771	MAPK9	1,68546798	NEIL3	1,6366446	HSD17B6	1,50185266	USP9X	1,42289488	IL5	2,20372812	1770	ASH1L	1,28874898	CCNI	1,38367034	PRKCA	1,6561436	SLC6A13	1,60853203	CRKL	1,48278408	DHDDS	1,40824339	CAV1	2,14709737
1701	P2RY2	1,30161456	CREB3	1,39925461	HESX1	1,6850827	FOXA1	1,63643077	NQO1	1,50152988	RIPK2	1,42250142	RCAN1	2,20338736	1771	RNASE1	1,28870456	MUT	1,38350021	CAMKK2	1,65539137	INSIG2	1,60841815	CRHR1	1,48222333	CD276	1,4080441	KCNJ4	2,14600612
1702	LGALS1	1,30158084	AKR1C2	1,39918763	ZMYM2	1,6848666	ACYP1	1,63610941	HSP90AA1	1,50135005	NPY2R	1,42241265	SNCAIP	2,20338029	1772	ANXA2	1,28859648	FGF3	1,38346161	AASDHPPT	1,65514523	BCL9	1,60837054	TRPM4	1,482134	PFKFB1	1,4077494	SLC1A7	2,1459803
1703	PLD3	1,3008918	CFP	1,39888408	GLCE	1,68457466	ATP1A3	1,6356732	GPAM	1,50101423	CRTAM	1,42223549	ADARB1	2,20329849	1773	PTGFR	1,28852691	CYP1A1	1,38329076	SLC30A1	1,65497137	RAD18	1,60813938	SH3GLB2	1,48175497	PDE6A	1,40751022	SKI	2,14596867
1704	DKFZP434E11	1,30086355	THBD	1,39877486	PSCD1	1,68411936	FCGR2A	1,63424697	PFN2	1,50078859	NCOA2	1,42221856	COL22A1	2,20172905	1774	TFAP2A	1,28808626	RAB5A	1,38317352	SELP	1,65468573	PEMT	1,60765883	MAP3K14	1,48088427	KDR	1,40713956	ARHGEF2	2,14524735
1705	SLC1A2	1,30066496	KL	1,39856701	LRPPRC	1,68365977	GABARAPL2	1,63422367	CAPN2	1,50066325	PRKG2	1,42210449	ABCB1	2,20001008	1775	PAX6	1,28804465	CEBPA	1,38316953	PSMB5	1,65365784	NKX2-2	1,60757969	GATA4	1,4808585	CAPN10	1,40710082	GRAP2	2,14496749
1706	BNIP3	1,30001022	NEIL3	1,39849448	RFNG	1,68341177	AKR1A1	1,6339249	DCXR	1,50056436	DGAT1	1,42198821	OXTR	2,198959	1776	WDR61	1,28789875	ANXA6	1,3831225	PTGER3	1,65347858	KRAS	1,60738868	PLA2G2F	1,48075029	TRPM7	1,40692525	SCN7A	2,14481427
1707	TLR6	1,30001022	ATP6V1D	1,39821923	LUM	1,68283546	ATG4D	1,63366762	CLDN1	1,50044516	ST8SIA2	1,42183399	CDC25A	2,1972365	1777	C9ORF97	1,28788272	VCAN	1,38283699	DRD2	1,65337284	HLCS	1,60721651	CACNA1S	1,48034456	SYNE1	1,40640418	IDE	2,14478206
1708	PANK3	1,30000665	HTR7	1,39809609	DRAM	1,682775	CITED1	1,63352401	TNFRSF13C	1,49956852	CKMT2	1,42160746	TBL1XR1	2,19697863	1778	TFAP2C	1,28750312	TBL1X	1,38267912	TCF3	1,65311201	DRD3	1,60698587	PIGT	1,47950964	CYP11B2	1,40565893	GPR18	2,14324562
1709	FZD6	1,29964353	TTR	1,39785584	SHC1	1,68227533	SMARCE1	1,63320478	GALNT8	1,49932851	STAT6	1,42136298	ENG	2,19443948	1779	CCR1	1,28723737	CCL17	1,38263394	HOXA1	1,65276209	HBQ1	1,60671942	RXRG	1,47946837	ITGA1	1,40552392	RRAD	2,14319911
1710	YWHAZ	1,29960919	NCOA4	1,39785216	RAD23A	1,68217287	ALG14	1,63230695	IL18R1	1,4992432	SYNJ1	1,42105189	PPARA	2,19395468	1780	B4GALNT1	1,28709713	APCS	1,38251396	BCL3	1,65247744	ATG4A	1,60634461	APBB1	1,47936882	MAP3K11	1,40507577	ABCA7	2,14277759
1711	PTCH1	1,29957876	TIFA	1,39778501	NFS1	1,68185143	CPSF4	1,63175599	ACAA1	1,49924238	IL10	1,42041097	PDE4D	2,19384911	1781	ATP6V1D	1,28706203	C14ORF166	1,38177929	EGR4	1,65244231	AKAP11	1,60586212	EIF4E	1,47922244	ZBTB16	1,4049283	POLH	2,14172147
1712	DCC	1,29917939	SLC22A18	1,39772227	MPI	1,68172313	RSAD2	1,63167439	SCN1A	1,49918177	COL12A1	1,4202571	OGG1	2,1929417	1782	MAFG	1,28702853	CAP1	1,38145242	COL13A1	1,65207632	PIGN	1,60486534	PAK2	1,47898421	TOP3B	1,4044689	BID	2,14172116
1713	CDK2	1,29775988	ENG	1,39748314	NKRF	1,68072496	FBP1	1,63120168	HOXA4	1,49897457	SAA1	1,41993061	WRN	2,19237983	1783	LPHN2	1,28687591	SMPD2	1,3812228	ORC5L	1,65087403	CSF1R	1,604327	BAG1	1,47896514	MST1	1,40439519	MSH3	2,14171896
1714	ITGA3	1,29774126	GHSR	1,39742031	ANXA6	1,67999542	PLP1	1,63063245	GABARAPL1	1,49892887	MAGI3	1,41955111	UPA	2,19087633	1784	FMO2	1,28654814	ACHE	1,38053243	PTGES	1,65068931	FAM132A	1,60408817	NBL1	1,47868466	PRKX	1,40418096	SOX9	2,14171723
1715	VDR	1,2977292	SNAP25	1,39681075	MAFK	1,67837293	HGD	1,63037422	CLEC7A	1,49839558	GTF2I	1,41937179	TRIO	2,18990569	1785	NOX4	1,28644429	NOTCH2	1,38043003	CETN2	1,6504311	CLCA4	1,60393237	B3GAT3	1,47837054	TKTL2	1,4037007	LTF	2,14170028
1716	CKB	1,29772372	IL2RG	1,39645493	EME1	1,6781579	ESR1	1,6300628	CAMK2B	1,49827144	CARD6	1,41934517	UGT2B17	2,18973564	1786	SOCS1	1,28595974	HOXC13	1,38036081	ST6GALNAC5	1,65033513	SOD2	1,60364248	CSNK2B	1,47825302	NEK1	1,40357905	PIK3C2G	2,14055329
1717	UBE2E3	1,29772171	PDE10A	1,39635494	ACVR1B	1,67791245	HS3ST2	1,62987358	SLC6A13	1,4977192	SP100	1,41928587	MYCN	2,18937626	1787	KCNH2	1,28585265	GSS	1,38003351	CCR4	1,64994114	CPB2	1,60356451	CACNA1F	1,47823331	TNFRSF1B	1,40321889	PEBP1	2,13973939
1718	FAM50A	1,29771225	PFKM	1,39589783	DOK1	1,67684081	ICOSLG	1,62867928	DAPK2	1,49742208	MAFG	1,41913818	NDST4	2,18849106	1788	RTKN	1,28559456	HADHB	1,37998598	P4HB	1,64953839	MADD	1,60343473	ATP6V1H	1,47781517	TRAF3	1,40313554	RPL15	2,13752465
1719	ANP32A	1,29770843	MMP13	1,39536962	APOBEC1	1,67666375	EPHX1	1,62843187	HAP1	1,49741122	SMAD3	1,41864116	FXYD2	2,18847342	1789	CCNE2	1,2852081	KLF10	1,37986696	MBD1	1,64897312	ENPP7	1,60325667	DVL3	1,47771948	MUSK	1,40312393	NPR2	2,13687799
1720	CSNK1G1	1,29770736	ST3GAL5	1,39504523	COQ5	1,67638216	PAX1	1,62826575	IDH3B	1,49740505	TAF13	1,41863235	GADD45B	2,18771691	1790	CAB39	1,28514894	DDX20	1,37972152	HS6ST3	1,64715134	FABP3	1,60282208	ANP32B	1,47698283	FSCN2	1,40296856	DNAJB11	2,13648146
1721	SPRED1	1,29769997	CDC23	1,39503013	GHSR	1,67635054	TRAF3IP2	1,62780237	RENBP	1,4971787	XPA	1,41855302	CHRNA9	2,18687532	1791	NCOA2	1,28499387	TGIF1	1,37957208	NEUROG3	1,64713329	NDUFS4	1,6027674	MSTN	1,4768006	CASP4	1,4029544	CDR1	2,1353342
1722	SMS	1,29769822	C1QBP	1,39479811	GLI4	1,67578946	TMED10	1,62773085	RALB	1,49699089	RIPK1	1,41830164	TPH2	2,18569892	1792	SP1	1,2849903	CCDC6	1,37914051	SETD2	1,64703162	ADIPOR2	1,60275936	MT2A	1,47643526	STUB1	1,40281054	SULT1A2	2,13475392
1723	RAP1GAP	1,29694569	PEBP1	1,39446643	GALNS	1,67577132	RPS6KA3	1,62683986	KMO	1,49692935	CDC25A	1,41828945	PSAP	2,18469845	1793	WNT5A	1,28485658	MAP1LC3B	1,37903957	MEPE	1,64691746	EIF2AK1	1,60209729	SNAI1	1,47599385	ACO1	1,40260598	PLOD1	2,13355988
1724	TRPM7	1,29673791	SLC30A3	1,39439849	ESRRA	1,67536678	SMARCC1	1,6268332	PTK2	1,49680855	RFXANK	1,4182749	CD48	2,18279761	1794	ENPEP	1,28480332	GNPDA1	1,37894784	ADAM12	1,64682347	ADAM12	1,60133932	CYP26A1	1,47580375	PLCB2	1,40251314	STUB1	2,13332637
1725	EIF2B1	1,29645419	ACSS1	1,39416233	AGPS	1,67470409	HAP1	1,62658338	TIAM1	1,49650634	DGKQ	1,41805964	TNNT2	2,1827727	1795	AP2M1	1,28454256	TBXAS1	1,37863525	CHD8	1,64637554	HHIP	1,60132305	LTA4H	1,47565067	CYP3A4	1,40222608	AKAP13	2,13278288
1726	GNPDA2	1,296354	BUB1	1,39412725	NSDHL	1,67470155	TCF1	1,62631626	DCC	1,49639041	CELSR1	1,41719156	ICAM2	2,18169399	1796	REXO2	1,28438144	NPR1	1,37833437	PELI3	1,64582674	HERPUD1	1,60033981	SAT1	1,47519375	HOXA9	1,40221781	OCRL	2,13263129
1727	PGAM1	1,29595087	PF4	1,39393848	SDHC	1,67462319	PDPK1	1,62621625	COL1A1	1,49545381	ITGB3	1,41675632	P2RY5	2,18123724	1797	SLC12A2	1,2843336	CYP4F2	1,3782108	CDC42	1,64505421	NOD2	1,60013701	IL12RB2	1,4749842	PPARA	1,40201841	AXIN2	2,13228626
1728	SLC13A5	1,2957934	ERBB3	1,39357182	CSNK1G1	1,67397059	NFE2	1,62613118	PPP2R5C	1,49508407	CTPS	1,41589869	CNR2	2,1809533	1798	OBFC1	1,28411249	SUCLA2	1,37789819	CST3	1,64481737	IL11RA	1,60001543	FPR1	1,47477269	NFATC3	1,40199941	CSNK1G3	2,13190573
1729	PTPRH	1,29574484	PAX4	1,39334405	DNAJB9	1,67377882	TLR1	1,6257994	PEMT	1,49471765	ST6GALNAC3	1,41557726	ARNT	2,18026132	1799	CCL16	1,28404576	RECQL4	1,37779518	SELPLG	1,64441993	NNT	1,59921605	SLC2A3	1,47458004	GALNT7	1,40195695	LPIN1	2,13154689
1730	IARS	1,29523454	PLEC1	1,39315707	LARS	1,67314879	KCNH7	1,62577667	BFAR	1,49419513	AGTR1	1,41483736	PML	2,18018159	1800	COL9A1	1,28381367	C8B	1,37742565	RAB3A	1,64440965	HSPG2	1,59859687	BTG2	1,47444991	THBD	1,40177321	SULT2B1	2,13146468
1731	CNTN1	1,29460029	FRAT1	1,39313564	ABCD3	1,67311782	CALM1	1,62542608	CHD8	1,49416446	PLEC1	1,41482526	TCF3	2,17964006	1801	FLOT2	1,28361944	ITGA2B	1,37706019	MVP	1,64426798	KCNK3	1,5984495	ZBTB20	1,4742842	EBP	1,40148404	EIF2S1	2,13133107
1732	DUSP1	1,29434273	SFRP4	1,39277244	DVL2	1,67198058	KEAP1	1,62518988	HOXA1	1,49416446	CAMKK1	1,41470723	PIGX	2,1787657	1802	ARFGAP3	1,28323693	CRY2	1,37702698	FANCI	1,64361352	CAPRIN2	1,59830208	PRF1	1,47419077	LFNG	1,40142829	IFNK	2,12967058
1733	FKBP1A	1,29359815	XPA	1,3926981	SETDB1	1,67029154	CSK	1,624854	JAM2	1,49400582	WNT1	1,41469391	INPPL1	2,17788081	1803	NPY1R	1,28286284	HSD11B2	1,37681814	ANXA1	1,64309319	VNN2	1,59819853	LIF	1,47416193	VAV1	1,40136561	GTF2H1	2,12824899
1734	MEIS1	1,29355022	MAP3K3	1,39264258	SIGIRR	1,67004239	RAPSN	1,62381994	SLC22A7	1,49398199	GC	1,4141377	CPSF3	2,17614193	1804	PLA1A	1,28281222	PLA1A	1,3767894	NOV	1,64288345	IL2RA	1,59818628	SH3GL3	1,47412836	ATP2A2	1,40107658	PRDX1	2,12760609
1735	SEMA7A	1,29343346	XK	1,39249166	TUBE1	1,66967376	ALOXSAP	1,62374738	ANXA4	1,49395588	MFGE8	1,41393866	CPSF4	2,17594356	1805	CFHR1	1,28281014	FBXW2	1,37668069	C9	1,64245649	MTTP	1,59816169	RARS	1,47334816	IL1R2	1,40107366	IL17C	2,12751054
1736	ACO1	1,2933233	NCOR1	1,39208238	GAS1	1,66963237	TNIP2	1,62351824	CDK7	1,49376953	AKAP8	1,41381939	UBE2N	2,17591064	1806	FST	1,28271779	HMGA1	1,37667704	POLRMT	1,64239535	BRD4	1,59750714	MANBA	1,47307205	CYP26A1	1,40085394	EPB49	2,12665963
1737	MMP10	1,29330265	CRY1	1,39207567	COL16A1	1,66897436	ZMYND17	1,62186207	JAG2	1,49368794	MAX	1,41362263	DIDO1	2,17488534	1807	TAF13	1,28231574	SCN2B	1,37623699	EHHADH	1,64157334	QPRT	1,59735644	MCF2	1,47303437	GBE1	1,40059748	EDN1	2,12633334
1738	NR6A1	1,29325799	SDHD	1,39202739	EFNA1	1,66870827	CLTA	1,62159457	CPSF6	1,49274851	EPHA4	1,41316629	TFRC	2,17416189	1808	NDNL2	1,28206524	FMO2	1,37604566	LEFTY1	1,64117657	CAT	1,59718282	GATM	1,47282947	CCNE2	1,40043652	MTA1	2,12539556
1739	NDUFA4	1,29289091	NR1I3	1,39182092	GDF2	1,66794277	CHRND	1,62057801	JUND	1,49273949	WAS	1,41311514	TOLLIP	2,17309593	1809	STUB1	1,2819817	GNAO1	1,37594247	NODAL	1,64112184	IL12RB2	1,59672977	SERPINA10	1,47266617	RAB10	1,40037743	APOBEC3A	2,12535694
1740	GGA3	1,29278336	CARD6	1,39153668	INPP5E	1,66708341	PIWIL1	1,61995171	GGPS1	1,49270326	CDR1	1,41292962	B3GNT5	2,17235078	1810	EPHX1	1,28191674	PSMB5	1,3756283	CTNNAL1	1,64109569	BECN1	1,59609861	HHEX	1,4726318	IL22	1,40011359	STAT4	2,1251562
1741	PSCD4	1,29261756	SLC2A3	1,39042282	NR3C1	1,66689184	CAPN10	1,61993542	EME1	1,49235901	DKFZP434E11	1,41288746	FLNC	2,17140993	1811	GDF9	1,28161108	JAG2	1,375164	ST6GAL1	1,64106022	SCN11A	1,59549159	MELK	1,47237179	AP2M1	1,40005092	ATG16L2	2,12469687
1742	PTH2R	1,29231062	POLR1E	1,38949329	PIGH	1,66682569	RTKN	1,61943032	SEPHS1	1,49190144	AASS	1,41246776	YWHAH	2,16923153	1812	GAS6	1,28116047	CREB3L3	1,37481394	FGF7	1,64102159	DAP	1,59542395	KCNK3	1,47220981	PRKACG	1,40003922	SLCO1C1	2,12391933
1743	C1RL	1,29224733	HAP1	1,38873387	ILVBL	1,66680486	FGF20	1,61909754	SPO11	1,49115436	STAT1	1,41242508	BLVRB	2,16912676	1813	LRWD1	1,28112242	IRS1	1,37467435	GUCA1A	1,64067281	UQCRC2	1,59513381	CARTPT	1,47216788	MFNG	1,39985268	VANGL1	2,12347727
1744	XCR1	1,29214481	SOCS6	1,38863052	STX11	1,6662353	DDIT3	1,61896491	MAFG	1,49086812	HOXA11	1,41236504	HEL308	2,16893151	1814	FOXD3	1,28112037	MMRN1	1,37444087	CKMT1B	1,64040657	NADSYN1	1,59504209	SHC4	1,47188161	IL13	1,39852354	GABRG3	2,12326592
1745	GABRA4	1,29209692	ZNF395	1,38839095	GPX1	1,66601	FST	1,61753023	S100A8	1,49084529	VAMP7	1,41170359	NCL	2,16888765	1815	ATP6V1B1	1,28073077	MTHFS	1,37414888	TAGLN	1,64019611	AGPAT1	1,5946286	CHEK1	1,47165014	SKP2	1,39847367	SMARCA4	2,12308589
1746	YWHAG	1,29188374	VAX2	1,38830505	BDKRB1	1,6658196	PDE4B	1,61646878	SRXN1	1,49063288	CCDC6	1,41169456	RAB3A	2,16709774	1816	HES1	1,28073077	GRIK4	1,37366254	WIPI1	1,64003369	COX5B	1,59461077	MYC	1,47141774	RFX5	1,39824013	B4GALT3	2,12305204
1747	TNFSF13	1,29187134	CTSA	1,38825557	BP75	1,66528254	DDX4	1,61609549	SOCS6	1,4905063	DKK2	1,41131788	RPE	2,16689849	1817	CPT2	1,28071096	KLRA1	1,37366072	GSTA2	1,63994239	CYP19A1	1,59457174	FGB	1,4713299	GALNS	1,39820374	SOCS3	2,12187326
1748	POLR3G	1,29186553	SYT2	1,38780438	LAMP1	1,66496528	EMR2	1,61525222	TRIO	1,4903628	CTNND1	1,4110701	YY1	2,16408608	1818	UNC5B	1,28050256	IFNA14	1,37361391	WARS2	1,63980136	ATP6AP1	1,59437803	NDUFA11	1,47124741	CCL18	1,39807133	PPP3CC	2,12176323
1749	SHBG	1,29173156	SLC12A2	1,3876419	PTPN22	1,66481192	FKBP1A	1,61470609	PTCH2	1,49020798	KCNJ2	1,4110701	CYSLTR2	2,16353662	1819	MMP14	1,28043206	CDC6	1,37336175	PELP1	1,63964056	C1QA	1,59418076	IL2RG	1,4712393	LIF	1,39795788	EDNRB	2,1208841
1750	LIG3	1,2916075	APOA4	1,38706115	TUBA8	1,66478245	PIAS3	1,61436908	COL8A2	1,48976889	CD1A	1,41102411	SKP1A	2,16284998	1820	SULT2A1	1,28033842	AOC2	1,37328722	STX8	1,63954084	PDE1B	1,5939348	TLR5	1,47119375	SULT1E1	1,39788192	HSPA8	2,1202102

Table A4. Pooled-shRNA library screen on HEL cell line and MF-3: list of 2nd most depleted shRNAs for each experiment (ranking approach 1, RA1).

	NO ruxolitinib (setting 1)				Ruxolitinib (setting 2)				Ruxolitinib + CM (setting 3)				MF-3			
	Experiment 1		Experiment 2		Experiment 1		Experiment 2		Experiment 1		Experiment 2					
Rank	Gene	Fold change	Gene	Fold change	Gene	Fold change	Gene	Fold change	Gene	Fold change	Gene	Fold change	Gene	Fold change	Rank	Gene
1821	C1QL2	1,28033239	MYEF2	1,37309303	HBQ1	1,63937642	FYN	1,59354155	CCNG1	1,47081822	FH	1,39782002	ABCG1	2,11871941	1891	PRKDC
1822	SULT1C4	1,28031886	CDKN3	1,37301758	NR5A2	1,6390789	PSMF1	1,59348786	VKORC1	1,47076983	ST6GALNAC5	1,39773666	PDHA1	2,11733957	1892	S100A4
1823	ORC5L	1,28024698	XRCC5	1,37297906	C1QL2	1,63868533	CD9	1,59271846	EEA1	1,46904534	SLC6A3	1,3977059	PTCH1	2,11526217	1893	CCL28
1824	TREX2	1,27993595	SOS2	1,37296402	POLR1A	1,6385586	CPE	1,59239191	GPSN2	1,46872669	MAP3K12	1,39765638	OGDHL	2,11502493	1894	FAM132A
1825	STAT2	1,27990745	COL3A1	1,3728878	TOB2	1,63852032	EIF4A1	1,59190415	BTLA	1,46865183	DBN1	1,39758313	RDH5	2,11472337	1895	IL15
1826	GRAP2	1,27981421	XYLT1	1,37174033	CENTD3	1,63807766	CD79A	1,59155573	PSCD4	1,46850973	FOXK1	1,39711214	PPP2R2A	2,11455797	1896	OPRS1
1827	ACE2	1,27965217	CHUK	1,37137895	CALM3	1,63766709	MAML3	1,5911244	CACNA2D2	1,4684173	AP3B1	1,39706515	PNMT	2,11432224	1897	HSPB1
1828	NFATC3	1,27964637	CD37	1,37133817	BCAT2	1,63747388	SCN2A	1,59105837	DCLRE1A	1,46809166	KIAA1303	1,39682299	GRHPR	2,11423944	1898	TM2D1
1829	DIDO1	1,27963315	CPE	1,37111298	NEIL1	1,63728401	MR1	1,59032721	CCNG2	1,46808401	SKIP	1,39622564	TDGF1	2,11306702	1899	MAP2K2
1830	CXCL10	1,27963174	RDH14	1,37110144	PHKA2	1,63722585	RPA4	1,58954545	SARM1	1,46733723	CHDH	1,39606005	FTCD	2,11199548	1900	NRP1
1831	BDKRB1	1,27962289	NKD1	1,37097046	AADAC	1,63707914	CCR7	1,58860165	GNRHR	1,46702633	PANK2	1,39588685	SPI1	2,11167174	1901	CLDN10
1832	ACSL4	1,27962074	PAX6	1,37081305	EBI2	1,63701256	VCL	1,58826702	CAV1	1,46668235	CA5A	1,39587003	UTF1	2,11166351	1902	AADAC
1833	BCL6	1,27941748	CELSR2	1,37079303	HFE	1,63698612	IDH3G	1,58824236	PAX6	1,46638646	CMBL	1,39543298	RETNLB	2,11070303	1903	ST3GAL3
1834	BCL9	1,27900245	MAPK3	1,36992634	AGL	1,63694101	WASF2	1,58743327	C1RL	1,46604122	UBE2A	1,39472738	HMGB2	2,11035451	1904	DGKQ
1835	HADHB	1,27893017	EEF1G	1,36990438	SNCAIP	1,63692681	HRG	1,58714668	FBLN2	1,4656972	SLC30A3	1,39463732	TOB1	2,11010524	1905	GABRA5
1836	IFNB1	1,27883766	ATP1B1	1,3696592	CTSL2	1,63670299	NDUFS8	1,58706611	CARD10	1,46568265	TSC2	1,39462452	BRCA2	2,10919576	1906	MKKS
1837	TLR9	1,2788093	MYL4	1,36952264	GPT2	1,63608045	SMURF2	1,58698409	MGAT4B	1,46555208	BCAT1	1,39420409	KLF2	2,10870868	1907	THRB
1838	TFR2	1,2787746	DAXX	1,36938097	PGA4	1,63582712	SDHD	1,58689212	ACY1	1,46531437	IFIT3	1,39415015	FGF5	2,10861326	1908	LIPE
1839	LSS	1,2786841	RALBP1	1,36933529	APEX2	1,63560627	ATG2A	1,58665326	CSNK1G1	1,46510272	RAB27A	1,39396442	ABCC6	2,10857786	1909	NBN
1840	MITF	1,2784291	ENDOG	1,36906905	TNF	1,63525793	MAG	1,58610885	ATP5H	1,4648741	CDK2	1,39363649	SRP19	2,10691809	1910	SQSTM1
1841	ARSD	1,27834826	WNT2	1,36894246	UGT2B28	1,63522501	HLA-G	1,5860126	NKX6-1	1,46476781	DHH	1,39359293	GPX7	2,1067192	1911	MMAB
1842	CACNA1D	1,27833436	NGB	1,36881242	PLA2G4D	1,63518448	AGXT	1,585893	CFHR5	1,46470237	CYP7B1	1,39300317	MITF	2,10667842	1912	POLK
1843	PTH	1,27829099	GOLGA2	1,36859602	CYP4F2	1,63432219	LIN7A	1,58563461	SERPINA1	1,46460459	YWHAG	1,39234439	METTL2B	2,1055953	1913	ITGB5
1844	CSF2	1,27823645	CREBBP	1,36849798	GLRX2	1,63398886	PHF11	1,58473822	ALDH1L1	1,46437726	PURA	1,39143987	B3GAT2	2,10513868	1914	PTPN2
1845	LYCAT	1,27815706	POLR2I	1,36805086	PKN1	1,63398575	RXRG	1,5842939	DNAJC5	1,46404182	PADI2	1,39092714	DPEP1	2,10447646	1915	POLR2D
1846	FSCN2	1,27801361	NR3C2	1,36771956	CRLS1	1,6338996	ADCY1	1,58411267	ALG8	1,46402903	AKT3	1,39079799	PTPRJ	2,10200808	1916	TCOF1
1847	HGD	1,27795496	IL19	1,36766747	PIGU	1,63309634	ACVR1	1,58410059	KCNA7	1,46383904	MDC1	1,39078222	TNFSF4	2,10108681	1917	FOXC2
1848	IL17RE	1,27782205	STK36	1,3676145	GBL	1,6323361	PSME2	1,58397786	HLA-DOB	1,46379061	CACNA1G	1,39073644	NR0B2	2,09948904	1918	MAP2K1
1849	GSTM2	1,27764711	CALM1	1,36744647	PDE10A	1,63233053	OPRD1	1,5839002	KIT	1,46307695	SCN2B	1,39036465	ABCA6	2,0988712	1919	EME1
1850	ZBTB20	1,27761456	EIF2AK3	1,36734975	ABCA13	1,63200379	HEXB	1,58347711	FANCD2	1,46305968	EIF4E	1,39030398	SERPINA6	2,09864752	1920	GPX7
1851	ORC3L	1,27759529	PTH2R	1,36686509	SMURF1	1,63149015	ANK2	1,58315312	MAPK7	1,46280244	DDX20	1,39026103	FADD	2,09845934	1921	NLK
1852	RUNX3	1,27756995	EIF1	1,3663142	CRY1	1,63128191	FLT1	1,58306816	TLR3	1,46272371	SPRY2	1,39017407	NUDT4	2,09815444	1922	CHKB
1853	IRS4	1,27735567	CACNA1F	1,36626943	ST6GALNAC6	1,63104778	DHRS4	1,58230378	ADRA2B	1,4625109	TACR2	1,38922083	POLR1E	2,09749831	1923	MAD1L1
1854	HSPA1B	1,27714797	HSD17B6	1,36607534	REL	1,63101607	MTMR6	1,58215153	BCAT2	1,46185216	ADCY6	1,38884382	PC	2,09625358	1924	SPCS3
1855	NDST1	1,27678978	DVL3	1,36592309	ERBB2	1,63075911	ANKFY1	1,58184678	BAG5	1,46129308	PGA5	1,38853711	MRE11A	2,09546582	1925	RECQL
1856	DHRS4	1,27648685	GFRA1	1,36584461	SLC12A1	1,62998088	CDK5	1,5817038	AGXT2	1,4611066	NDUFA13	1,38851465	HK2	2,0949619	1926	PGDS
1857	PIK4CA	1,27642706	DCLRE1B	1,36577738	MCM6	1,62987267	PDGFRB	1,58145166	PTPRJ	1,46064303	TH	1,38848734	DBN1	2,09490235	1927	IFIT1
1858	ADCY1	1,276325	SLC30A1	1,36569498	HIG2	1,62942095	TPS3	1,58144315	CD83	1,46064174	SMARCC2	1,38826141	RUNX1	2,09459878	1928	ID2
1859	ATF1	1,27611878	TAPBP	1,36562152	CRP	1,62930148	F9	1,5812634	BP75	1,46036245	AKAP11	1,38820169	UGT1A5	2,09390206	1929	AVP
1860	S100B	1,27603586	CYGB	1,36489283	GNE	1,62928211	FMOD	1,58091537	KRT19	1,46020033	UPT1	1,38804487	AMY2A	2,09303018	1930	AGL
1861	QPCT	1,27593433	G6PC	1,36476959	FBLN1	1,62914062	SYN3	1,58085091	RPN1	1,46012993	PDE6D	1,38791352	APOA5	2,09205435	1931	IL5RA
1862	RAD1	1,27583492	P2RY1	1,36464748	NOTCH4	1,62863936	PRKAR2A	1,58064496	STXBP1	1,45981189	CYP1A2	1,38783658	IL25	2,09036494	1932	PLA2G2E
1863	GDF15	1,27575374	AIRE	1,36457196	CPSF2	1,62863221	SND1	1,58042988	PAN2	1,45908793	AK2	1,3876607	ADAM17	2,08996492	1933	LMX1B
1864	ACOT11	1,27571066	ADH5	1,3644319	MTAP	1,62843881	HSD17B2	1,5802029	PIGU	1,45884526	SLK	1,38692263	EZH1	2,0891896	1934	ACACA
1865	FGB	1,27553132	STAT6	1,36376505	FRAP1	1,62800402	BMP5	1,58010778	NAGLU	1,45881775	IRF2BP1	1,38643964	FAT	2,08783584	1935	AR
1866	ERBB2	1,2755201	SYNJ1	1,36350716	IGFBP5	1,62707826	ENO3	1,5799847	C22ORF28	1,45876466	GOPC	1,38621319	CTGF	2,08745353	1936	UBE2L6
1867	OSCAR	1,27532504	CD8B	1,36348233	MAP3K11	1,62597483	PPAP2C	1,57968698	OSCAR	1,45840957	SDHA	1,38587585	FN1	2,08599836	1937	PRKAA2
1868	FIGF	1,2750573	CYP26A1	1,36333569	AKR1C3	1,62570665	CTTN	1,57968451	ITPR3	1,45818766	RNASE1	1,38549002	GLI1	2,08597793	1938	ICAM2
1869	SELPLG	1,27480268	TERT	1,36313795	FZD1	1,62528898	CSNK1E	1,5794906	FAU	1,45808859	NLK	1,38544297	NCOA4	2,08582622	1939	SIRT6
1870	SPR	1,2747419	ANXA2	1,36303772	ACLY	1,62523133	HOXD13	1,57947437	CLEC5A	1,45776023	FCGR2A	1,38523359	ORC4L	2,08558555	1940	RAG2
1871	KALRN	1,27469573	IDS	1,3629552	WWTR1	1,62459195	SLC1A3	1,57937287	HBQ1	1,4576536	AIFM1	1,38503011	BCAP31	2,08477562	1941	EGR2
1872	POLR1B	1,27453984	SLC25A1	1,36248633	OLIG1	1,6231015	CNP	1,57906989	SCN10A	1,457565	MTTP	1,38472298	CHAT	2,08394734	1942	PLSCR1
1873	ITGA1	1,27438463	AGXT2L1	1,36232869	NKD2	1,62284322	KCNJ2	1,57883671	PPP1R13B	1,45745858	MYH2	1,38457946	PIK3CD	2,08342015	1943	ARPC1A
1874	NR4A3	1,27413003	UGP2	1,36227207	NTRK1	1,62275963	SOCS5	1,57840562	ITPR1	1,45728287	PRMT7	1,3840481	ACTN1	2,0831023	1944	C14ORF166
1875	DEFA1	1,27397786	ST3GAL2	1,36179811	PDE5A	1,62251818	MC2R	1,57609445	PLOD1	1,45709373	EPHX1	1,38402483	KARS	2,08292215	1945	DLL1
1876	GOPC	1,27383488	BMP2	1,36089303	TGFB2	1,62210727	PANK4	1,5759967	ALDH5A1	1,45700513	UBE2D1	1,3836357	CARD14	2,082756	1946	CYP8B1
1877	FZD7	1,27368601	GRM7	1,36080815	VISA	1,62207145	GNAS	1,57569886	XRCC4	1,45699674	ADH6	1,38357868	AASDH	2,0826186	1947	GNAZ
1878	RALB	1,27347493	CXCL9	1,3603891	S100A9	1,62163402	MME	1,5756454	MAFB	1,45689297	WDFY3	1,3832447	COL4A6	2,08183681	1948	COQ5
1879	THOP1	1,27334185	USP11	1,36009511	GSTM3	1,62160153	NBN	1,57557203	ADCYAP1R1	1,45620595	HBQ1	1,3830443	CTNNA2	2,07901548	1949	CPA3
1880	APPL1	1,27325328	PDE4D	1,35993591	MTIF2	1,62137304	RAB35	1,57521784	GTF2H1	1,45617996	CYP39A1	1,38283417	JUN	2,07650004	1950	B4GALT7
1881	SIRT7	1,27322168	IRF2BP1	1,35950913	AXIN2	1,62097622	CPSF6	1,57472248	TLN1	1,45589889	TCF7	1,38188839	GC	2,07573184	1951	CX3CL1
1882	GRM2	1,27303421	CKMT1A	1,35941937	ATG3	1,62094092	TGFB3	1,57458514	KRAS	1,4558765	B2M	1,38164032	CLTC	2,07543445	1952	STAMBPL1
1883	C4BPA	1,27261019	DLX6	1,35915834	MARCO	1,62087792	ROCK2	1,57450349	UQCRH	1,4554739	NANOG	1,38138144	APBB1	2,07525384	1953	ACP6
1884	FOS	1,27254486	FSTL1	1,3589502	PGF	1,62051774	SELPLG	1,57331541	SNX4	1,45541298	ENO1	1,38122245	DBC1	2,07445945	1954	PPP1CA
1885	VANGL2	1,27241154	FADD	1,35867771	ZMYND17	1,62044664	LIPE	1,57309187	SPP1	1,45537588	MAG	1,38110747	AKAP8	2,07397954	1955	VAX2
1886	SCN8A	1,27218945	LAT2	1,35866936	ARPC2	1,62044404	IFNB1	1,57271497	DPYSL2	1,45511574	HYAL1	1,38093161	UGT2B15	2,07369838	1956	DAZL
1887	TNNT1	1,2718507	BLVRB	1,35859003	NFE2	1,62040247	MYF5	1,57259873	RASA1	1,45507369	RAG2	1,38088724	EFNA5	2,07255847	1957	IFNA17
1888	RAB4A	1,27183725	TNFSF18	1,35859003	CSNK1A1L	1,62001896	TGFB3	1,5724886	AKAP5	1,45470208	ATP6V1C1	1,38008898	HPN	2,07226309	1958	NOV
1889	F8	1,27162706	VHL	1,35825051	CBS	1,61957461	MFGE8	1,57234547	EFNB2	1,45462082	RFNG	1,37988043	CTSL2	2,06867729	1959	B3GALT1
1890	FBXW7	1,27156158	RABGAP1L	1,35816455	ADARB1	1,61866012	LEPR	1,57227984	HIST2H3C	1,45414627	GSTM5	1,37976328	PLA2G4D	2,06798573	1960	DAPK3

	NO ruxolitinib (setting 1)				Ruxolitinib (setting 2)				Ruxolitinib + CM (setting 3)				MF-3			
	Experiment 1		Experiment 2		Experiment 1		Experiment 2		Experiment 1		Experiment 2					
Rank	Gene	Fold change	Gene	Fold change	Gene	Fold change	Gene	Fold change	Gene	Fold change	Gene	Fold change	Gene	Fold change	Rank	Gene
1891	PRKDC	1,27144198	ATG4D	1,357997	ATP1A3	1,61843985	BIRC5	1,57129842	CCND3	1,45337365	ACSL6	1,37968425	FGF12	2,06764648		
1892	S100A4	1,27139959	CACNA1S	1,35796194	PDCD2	1,61825551	TGM2	1,57082294	DKK3	1,45301937	BP75	1,37953099	HLA-DMA	2,06726397		
1893	CCL28	1,27135678	PRKAB1	1,3578649	NEK1	1,61781017	GAPDHS	1,57075162	GCKR	1,45286118	TAF1L	1,37919781	ALKBH2	2,06687313		
1894	FAM132A	1,27134296	CD40	1,35755027	KCNMB2	1,61740804	DDX47	1,57027596	IRS1	1,45259167	FGF8	1,37917964	RNASEL	2,06657608		
1895	IL15	1,27130245	APC	1,35753387	ADSSL1	1,61648099	ST8SIA2	1,56914611	GSTA3	1,45249641	NDRG2	1,37914101	ALOX15B	2,0646951		
1896	OPRS1	1,27111942	LMNB2	1,35749213	BST2	1,61573388	PPP1CB	1,56910178	WNT9B	1,45238737	TOP3A	1,37913401	PARP1	2,06370388		
1897	HSPB1	1,2709634	RAPSN	1,3574151	SH3GLB2	1,61571765	MYOG	1,56870492	SNX13	1,45228412	ARHGEF12	1,37909718	IFNA1	2,06142834		
1898	TM2D1	1,27091874	TAF1L	1,35725014	SYN3	1,6147189	DPPA4	1,56825667	COX15	1,45222733	IKBKAP	1,37884633	HDAC5	2,06108433		
1899	MAP2K2	1,27067989	DGKD	1,35710692	COL4A6	1,61445114	CD3G	1,56800319	BPNT1	1,45174342	GCS1	1,3784144	CASP6	2,05994744		
1900	NRP1	1,27044057	FGF6	1,35702124	ADRA1A	1,6123058	MTIF2	1,56770467	GNA11	1,45137061	PIK3R4	1,37806204	ITGA4	2,05855622		
1901	CLDN10	1,27039195	EFNA4	1,35697662	MEST	1,61189499	AKAP4	1,56743421	DKK4	1,45117939	PPP1R10	1,37805949	SCN2B	2,05789438		
1902	AADAC	1,27037967	IFI16	1,35620409	AZGP1	1,61152252	CHP	1,56703419	NDUFB7	1,45099216	IRAK2	1,3779447	NEUROD1	2,05708439		
1903	ST3GAL3	1,27024626	NFE2	1,35595832	NFKBIL2	1,61143526	PRKAG1	1,56696145	ANAPC11	1,45089837	PPS1L1	1,3778929	ADCYAP1	2,05695268		
1904	DGKQ	1,27023171	IGFBP2	1,3551886	XYLT1	1,61139718	ARG1	1,5669132	CCL2	1,45087292	WWP2	1,37761907	HOXD13	2,05693227		
1905	GABRA5	1,2701784	FOXH1	1,35518087	CLDN1	1,61126566	MAGI3	1,56673969	NEIL3	1,45077342	IAPP	1,37753345	CYP26A1	2,0567382		
1906	MKKS	1,27006638	DUSP6	1,35504482	LDHAL6B	1,61115857	ARNT	1,56590374	SLC23A1	1,45063059	PLA2G1B	1,37747898	IL2RB	2,0562504		
1907	THRB	1,26978826	ELA3B	1,3549837	NMNAT3	1,61111763	C6	1,5658005	PDHA2	1,45012359	ISG20	1,37732495	DSE	2,05413628		
1908	LIPE	1,26976757	GPR109B	1,35451438	DDX50	1,61111059	ATP6V0B	1,56525055	PRMT7	1,44987794	ATP6V1B2	1,377293	SAP18	2,05402069		
1909	NBN	1,26969044	EEA1	1,35421946	GLS2	1,61079978	LRRC15	1,56499428	GLCE	1,44945535	CASP8	1,37724864	HSF2	2,0538268		
1910	SQSTM1	1,26968837	SUCLG1	1,35419444	FAM50A	1,61057088	GOLGA2	1,56480357	CDO1	1,44940602	COL4A3	1,37719716	CPN1	2,05227531		
1911	MMAB	1,26964371	EDG4	1,35400254	GRID2	1,61019452	REM2	1,56477281	PDXP	1,44887454	HNF4A	1,37656376	HNF4A	2,05093998		
1912	POLK	1,26964111	EIF2B5	1,35390018	CD40	1,60997132	SLC10A2	1,56431949	PDE3A	1,44883273	UGT1A10	1,3765182	RRM1	2,05080756		
1913	ITGB5	1,26934365	DKFZP434E11	1,35347429	ABCA12	1,6099127	CCL18	1,56427889	PFKFB4	1,4485165	CYP4F12	1,3764474	ASGR2	2,05057202		
1914	PTPN2	1,26906346	CPA3	1,35332523	AKR1B1	1,60983882	HHEX	1,56393304	PPP3CC	1,44846218	VANGL2	1,37636232	RECK	2,05057202		
1915	POLR2D	1,26898302	FGF13	1,35251426	HSD3B1	1,60964144	CYP7B1	1,56344995	MADCAM1	1,44845691	VTN	1,37631128	CARD11	2,04961669		
1916	TCOF1	1,2685211	PPM1D	1,35238119	GRIK3	1,60957288	IGFBP7	1,56325222	SLCO1A2	1,44796556	RXFP1	1,37594156	CTLA4	2,04890483		
1917	FOXC2	1,26839996	KLRD1	1,35197393	POLR2K	1,60944293	CD48	1,56247897	PLA2G2E	1,44795726	SUMO2	1,37594156	CLDN14	2,04829213		
1918	MAP2K1	1,26838609	FGF12	1,35183047	ADRA1B	1,60933248	BBS1	1,56243908	BCL2A1	1,44771776	ASCC3	1,37558093	CHD8	2,04706623		
1919	EME1	1,26830303	UNC93B1	1,35167979	BFAR	1,60865984	FZD7	1,56091455	ADCY4	1,44758377	SOCS3	1,37547461	AGPAT4	2,04517703		
1920	GPX7	1,26830303	BCHE	1,35161961	SQSTM1	1,60809627	HTR3C	1,56065118	GALNT2	1,4472594	BAP1	1,37543613	MYLK	2,04395498		
1921	NLK	1,26828068	GDI1	1,35161301	GABARAPL1	1,60807578	PLA2G7	1,56051876	PDE5A	1,44689451	PMAIP1	1,37528111	KPNA6	2,04270535		
1922	CHKB	1,26821494	FAF1	1,3514659	MDH2	1,60793313	IL15RA	1,56022941	C1R	1,44674055	SUFU	1,37518391	P2RX7	2,04124167		
1923	MAD1L1	1,26800336	STX8	1,35102779	HDC	1,60774459	IL1RAP	1,55981938	SLC18A3	1,44643365	FBXW7	1,37507738	S100B	2,0395665		
1924	SPCS3	1,26745309	PTGS2	1,35095147	FUT6	1,60718285	EPOR	1,55917101	THY1	1,44623547	CYP27A1	1,37491118	FGF13	2,03954714		
1925	RECQL	1,26743884	HAND1	1,35082232	AQP7	1,60701022	ERCC5	1,5589145	FANCI	1,44560054	CTSD	1,37407995	PEU1	2,03809085		
1926	PGDS	1,26741897	KCNJ2	1,35033586	ABCB11	1,60668121	DKK2	1,55842544	SLC25A4	1,44534604	CREB3	1,37399352	MSH4	2,03685981		
1927	IFIT1	1,26739517	ZBTB32	1,35024767	MR1	1,60595484	FOXC2	1,55784589	NADK	1,44513494	TFAP2B	1,37358267	CETN2	2,03554597		
1928	ID2	1,26731723	ALKBH2	1,35018999	ALDH5A1	1,60498432	MAFG	1,55748237	MYH8	1,44509594	HBEGF	1,37320706	ADCY2	2,03525689		
1929	AVP	1,26725263	BGN	1,35012932	SLC25A1	1,60492598	SENP2	1,55726582	CACNA2D4	1,44493511	GRK5	1,37319064	INPP5E	2,03446711		
1930	AGL	1,26713634	OBFC1	1,35006651	AKAP8	1,60439077	EIF5	1,55639281	BUB3	1,44466165	TM2D1	1,3731689	UGT1A1	2,03391847		
1931	IL5RA	1,26696001	ARHGEF5	1,35004049	PENK	1,60407781	CRLS1	1,55619704	ILK	1,44421035	APBB1	1,37301123	PHKB	2,03278493		
1932	PLA2G2E	1,26669079	IQGAP2	1,34874482	KRAS	1,60399244	FAAH	1,55489403	PLCG1	1,44339321	MCL1	1,37285038	ORC1L	2,03206617		
1933	LMX1B	1,26645353	GABRA4	1,34866299	MT2A	1,60226122	GAL3ST1	1,55467193	ANXA6	1,44333208	DPF2	1,37271048	ZFP36	2,03119926		
1934	ACACA	1,26631814	APOBEC3B	1,34838196	TM2D1	1,60216008	GALNT8	1,55453129	ALDH6A1	1,44283537	ATM	1,37261942	SNCB	2,02788482		
1935	AR	1,26624125	AMDHD1	1,34816093	POLE	1,60178054	FDFT1	1,55401411	PSME3	1,44276909	GNA11	1,37241766	MAGEH1	2,02771267		
1936	UBE2L6	1,26623003	LMNB1	1,34785016	IL17RC	1,60170802	AMDHD2	1,55398424	MSH4	1,44276392	LMNB1	1,37234627	PPAT	2,02717513		
1937	PRKAA2	1,26616416	KNG1	1,34781793	CHP	1,60152755	ANGPT1	1,55264924	NADSYN1	1,4427302	CLDN10	1,37215311	GRM6	2,02659193		
1938	ICAM2	1,26605424	TRPM4	1,34758703	SH3BGRL	1,60146938	AHCY	1,55223647	TNFAIP1	1,44270954	AES	1,37129476	RFWD2	2,02612267		
1939	SIRT6	1,26595356	IL1RL1	1,3475313	PRKAG2	1,60117851	DKK3	1,55221201	HLA-E	1,44261807	CD2	1,37116389	F7	2,0260283		
1940	RAG2	1,2656819	MEFV	1,34739104	RAC2	1,60115909	RPRM	1,55166131	HEMK1	1,44243428	PIK3C2G	1,37113883	SEL1L	2,02579772		
1941	EGR2	1,26544861	RNASE1	1,34721611	EPB49	1,60099683	TFCP2	1,5512005	CHMP1B	1,44221087	ABCB7	1,37029428	RUNX3	2,02482255		
1942	PLSCR1	1,26544855	ERCC3	1,34710929	ADORA3	1,60084708	VPREB1	1,55084148	SLC30A3	1,44208749	CYP2A13	1,37024939	ABCA10	2,02414949		
1943	ARPC1A	1,26537988	PPP1CA	1,34680006	TYK2	1,60072457	NT5C	1,55067728	OLIG2	1,44184851	RASAL1	1,37013357	GCNT2	2,02279153		
1944	C14ORF166	1,26537174	HOXA9	1,34662267	TNFRSF17	1,60071927	STAT1	1,5503064	PAK6	1,44132141	MAD2L2	1,37001767	CLN3	2,02204504		
1945	DLL1	1,26531865	MELK	1,34631808	NSMAF	1,60005077	AGTR2	1,55015885	HRH3	1,44117477	SHOC2	1,36951632	RANBP9	2,02199336		
1946	CYP8B1	1,2653008	NR4A3	1,34622345	GOSR1	1,60002627	F12	1,54995827	XRCC5	1,44114192	ACAA2	1,3693557	TRIP12	2,02141166		
1947	GNAZ	1,26478526	HS3ST2	1,3461317	UBE2V1	1,59975985	SPCS1	1,54983304	AZIN1	1,43997281	C1R	1,368665	NLN	2,02105138		
1948	COQ5	1,2642516	HK1	1,34604549	BMPR1A	1,59973418	IL2	1,54975625	UGT2B28	1,43975241	PPP2R2A	1,36862864	PRIM2	2,0207882		
1949	CPA3	1,26423011	PLA2G6	1,34603546	HSD17B7	1,59962373	EIF5A2	1,54956369	CD276	1,43971814	XBP1	1,36778595	DGAT1	2,02018877		
1950	B4GALT7	1,26406237	MAT1A	1,34596599	GYPA	1,59829924	SLC38A1	1,54935422	PSEN1	1,43943341	CSF2RB	1,36755098	UCN	2,01999044		
1951	CX3CL1	1,26387656	XCR1	1,34588685	DPM1	1,59829857	EGR1	1,54903164	GGT1	1,43928061	HES7	1,36740223	SFN	2,01885978		
1952	STAMBPL1	1,26381115	CERK	1,34565155	HS3ST2	1,5980406	LMNB2	1,54898113	RAG1	1,43915256	ITGAV	1,36703508	AKAP11	2,01717319		
1953	ACP6	1,26376741	GTF2I	1,34534424	TPO	1,5978268	SKIP	1,54879372	GNG3	1,43914086	DLST	1,36689724	DUSP8	2,01617226		
1954	PPP1CA	1,26368491	MDH2	1,34530315	NCKAP1	1,59777011	CLC	1,54864203	TPO	1,43912674	DDOST	1,36655873	FUT1	2,01569719		
1955	VAX2	1,26354533	GLI1	1,3447607	GDF9	1,59708172	COPS5	1,54821332	FAM132A	1,43899526	VAX2	1,36599735	EPS15	2,01473152

Table A4. Pooled-shRNA library screen on HEL cell line and MF-3: list of 2nd most depleted shRNAs for each experiment (ranking approach 1, RA1).

	NO ruxolitinib (setting 1)				Ruxolitinib (setting 2)				Ruxolitinib + CM (setting 3)				MF-3					NO ruxolitinib (setting 1)				Ruxolitinib (setting 2)				Ruxolitinib + CM (setting 3)				MF-3	
	Experiment 1		Experiment 2		Experiment 1		Experiment 2		Experiment 1		Experiment 2							Experiment 1		Experiment 2		Experiment 1		Experiment 2		Experiment 1		Experiment 2			
Rank	Gene	Fold change	Gene	Fold change	Gene	Fold change	Gene	Fold change	Gene	Fold change	Gene	Fold change	Gene	Fold change	Rank	Gene	Fold change	Gene	Fold change	Gene	Fold change	Gene	Fold change	Gene	Fold change	Gene	Fold change	Gene	Fold change	Gene	Fold change
1961	GALNT9	1,26294736	RASGRP1	1,34322941	PKN2	1,59367409	UGT2A1	1,547454	CHIA	1,43657742	CALCA	1,36528192	SPN	2,01277728	2031	CPB2	1,25487861	LPIN1	1,33110361	SMAD5	1,56911263	PLCB2	1,52279209	FASLG	1,41857063	ABCB4	1,35189607	CSF2RB	1,97172906
1962	MDC1	1,26286135	GZMA	1,34320606	PGK2	1,59301833	PRDX4	1,54710062	TGM2	1,43582823	ERAF	1,36505472	DVL3	2,01239552	2032	ABCB11	1,25483164	ICOSLG	1,33108361	CACNA2D4	1,56832812	LGALS1	1,52247539	CHAT	1,41852597	GLS2	1,3518246	E2F4	1,97151682
1963	H2AFY	1,26284418	CR2	1,34306306	KRT8	1,59262423	PLD2	1,54632321	TXN	1,4356631	NEDD4L	1,36504932	PIGC	2,01239552	2033	CDKN3	1,25481219	AGPAT4	1,33107909	CHPF	1,5680352	PKN1	1,52196375	CDC25C	1,41781195	GLB1	1,35176884	GGA1	1,97025575
1964	GCK	1,26277951	ZBTB20	1,34302909	THY1	1,59257307	TOP2A	1,54602799	PRKAR1B	1,43541051	FGFR4	1,364934	APLP2	2,01195576	2034	SPI1	1,25469185	SH2B2	1,3309824	IGF1R	1,5677166	PTGFR	1,52174803	KCNE1	1,41769275	ACOX2	1,35161459	GFAP	1,97022519
1965	CYP1A1	1,26268878	AGMAT	1,34297963	IDI2	1,59254041	SUZ12	1,54517057	ARPC5	1,43535439	EZH1	1,3649201	NTRK2	2,01185988	2035	GTF2B	1,25459727	GMNN	1,33089927	AGTR2	1,5676468	HDAC1	1,52136228	CHUK	1,41762935	LPIN1	1,3511248	IMPDH1	1,96998389
1966	CYLD	1,26250602	CELSR3	1,34284848	SHC4	1,59249497	GLRX2	1,54506796	MTA2	1,43516434	CREBBP	1,36450017	AMPH	2,01170333	2036	ATP6V0D2	1,25455502	GALNT11	1,33071583	HTR1F	1,56755483	FGF7	1,52117503	CCR7	1,41736069	NFE2L2	1,3510643	RING1	1,96933396
1967	GABRA3	1,26246887	GALNT7	1,34270828	PHF11	1,59237034	TRIM21	1,54402327	ABCB10	1,43512261	FPR1	1,36440718	LMAN1	2,01162635	2037	ITPR1	1,25453075	RAG1	1,33044756	UAS	1,56724789	DMC1	1,52093444	CTBS	1,41734719	ABCB1	1,35088053	LRDD	1,96908684
1968	BACH1	1,26245448	PSCD1	1,34227777	TERF1	1,59164842	NR4A3	1,5430478	SH3KBP1	1,43493663	ADCY3	1,36417787	SMARCC1	2,01105939	2038	HHIP	1,25451904	CD2BP2	1,3297424	ACADM	1,56683162	INHBB	1,52054205	S100A9	1,41697459	ENTPD1	1,35080497	GALE	1,9689076
1969	GNAI3	1,26244759	CYP2C18	1,34216903	ATP6V0E1	1,59144614	DPP4	1,54269517	RAP2B	1,43487944	IFT172	1,36417701	PIK3C2A	2,00999397	2039	CYP27B1	1,2544182	PHCA	1,32935006	CDK5RAP1	1,56625098	DPYSL2	1,52019291	SERPINE1	1,41663737	CLDN20	1,35052581	CPT1A	1,96861058
1970	PDCD1	1,26234573	BET1	1,34207864	TMED10	1,59139064	WNT2	1,54160717	NP	1,43486122	DPP4	1,36399086	HMGCL	2,00974273	2040	PLEKHA8	1,25411719	PLCB3	1,32883415	ITGB4BP	1,56610593	LTB4R2	1,52018867	SPCS1	1,41653366	XRCC1	1,35013308	CST3	1,96838366
1971	P11	1,26207112	TRAF3	1,34147114	EME2	1,59128422	VNN1	1,5414177	NT5E	1,43479923	CPSF6	1,3638055	GPD2	2,00955666	2041	CRKL	1,25395515	PTPN11	1,32870943	SUZ12	1,56540379	EHHADH	1,52011131	ABCC1	1,41626087	ABCB9	1,3497703	IDH3G	1,96822103
1972	HOXD11	1,2614756	KDELR2	1,34107535	ADSL	1,59127225	SYK	1,54113439	PTGES2	1,43456547	CRYAB	1,36356008	NT5M	2,00870554	2042	UXT	1,25361756	APBA2	1,32844379	CPT1C	1,56516577	SORL1	1,51971765	CCL18	1,41586657	MTFMT	1,3495219	CYP19A1	1,96814567
1973	FOXP1	1,26142948	AK7	1,34085943	GSTO1	1,59022707	HPD	1,53908205	TYMS	1,43428197	PIGG	1,36355396	PSMB2	2,00777311	2043	GRK5	1,25359238	HLCS	1,32828841	HTR3E	1,56456796	GRIA3	1,51961048	DPYD	1,41580157	NOTCH1	1,34946725	DDX4	1,96785093
1974	MAF	1,26127499	IDH3B	1,34066884	PFN1	1,58990441	HELB	1,53835029	SF1	1,43383131	IRF8	1,36346023	KCNK1	2,00723208	2044	MTHFD2	1,25302399	SMS	1,3280761	FAAH	1,56409095	GDI2	1,51924337	REV3L	1,4156962	UGDH	1,3494143	NAE1	1,96704307
1975	RDH13	1,26100912	YY1	1,3404621	PRKRIR	1,58972749	TFAP2C	1,53760925	MVD	1,43347201	FABP1	1,36313552	DUSP10	2,00720135	2045	CD3EAP	1,25301084	RAB3S	1,32795539	CLC	1,56382336	GGH	1,51887474	CLDN23	1,41565852	SCN7A	1,34936311	MAP1LC3A	1,96620104
1976	SYNJ1	1,2609232	PSEN1	1,34042374	FOS	1,58950795	BGLAP	1,53756262	MCHR1	1,43344418	S100B	1,3629711	PAPSS1	2,00616218	2046	S100A12	1,25296516	BCKDHA	1,32789543	SERPINB9	1,56382332	DNMT3A	1,51871244	FLCN	1,41558361	ITCH	1,34878046	TLR5	1,96603799
1977	GRM4	1,26090321	KEAP1	1,34038055	ENTPD1	1,58731508	ACSL4	1,53686653	TP53BP1	1,43336229	CCL11	1,3629525	CEBPB	2,00525689	2047	UGT2B4	1,25294586	NDUFV1	1,32769939	CHRD	1,56350002	CDKN2D	1,51857214	UNG	1,41543095	SFRP4	1,34872006	G6PD	1,96513251
1978	LTA	1,26088107	GDF9	1,34033999	NCOA1	1,58692058	KRT19	1,5368433	PTH	1,43332587	FTMT	1,36286024	PF4	2,00485512	2048	EPOR	1,252904	VAV1	1,32767584	PRKCQ	1,56342409	IFNA6	1,51850775	PCK1	1,4151632	COL3A1	1,34861282	CLC	1,96377208
1979	STRA6	1,26074081	DAG1	1,34032489	GABARAPL2	1,58675272	CCNT2	1,53683407	SUFU	1,4333086	GSK3B	1,36284824	MLL	2,00430189	2049	SLC2A1	1,25277992	NRIP1	1,32765543	GYG1	1,56312921	BTK	1,51837853	HNF4G	1,41444011	MAPK14	1,34752373	NRG3	1,96184913
1980	RUNX2	1,26055849	IL23R	1,34015483	ACVRL1	1,58672806	DNMT3B	1,53666417	ALCAM	1,43312463	RAB3A	1,36264085	TLR6	2,00429006	2050	ALG13	1,25254227	KCNJ3	1,327533	IL17A	1,56310541	EDN1	1,51837436	IL23A	1,413902	CLDN16	1,34736377	CSF3R	1,96128155
1981	DGKA	1,26046999	HLA-DQB1	1,3400714	CEBPD	1,5861524	DRD4	1,53665899	GABPA	1,43310476	HSD17B3	1,36252436	KCNJ12	2,00311992	2051	AMY1C	1,25240137	EXT2	1,32721478	AARS	1,5629599	SLK	1,51800376	ELA1	1,41379964	CA8	1,34734924	GDF11	1,96122527
1982	ALDH1A3	1,26034097	MAPK8	1,33951834	AMHR2	1,58584621	PRKAA2	1,53615638	HAO1	1,43267364	OXA1L	1,36231826	SULT1C2	2,00288372	2052	IL17C	1,25226595	MVD	1,32707259	GLI1	1,56274314	ELA1	1,51786753	PPARGC1A	1,41358924	LTA4H	1,34709045	RPS3A	1,96082147
1983	TAL1	1,26016692	CARM1	1,33932109	CD3EAP	1,58541387	YWHAB	1,53588754	LFNG	1,43245554	HSD17B2	1,36217396	CD160	2,00199625	2053	UNC93B1	1,25217993	C4BPB	1,32706627	GALNT17	1,56233603	SH3GL3	1,51767034	CHRNB3	1,41281097	C4B	1,34665497	HSD17B3	1,9580779
1984	PGM3	1,26008612	SULT1C4	1,33931147	ALOXSAP	1,58489906	SLC25A11	1,53557503	MARS2	1,43186995	CCL1	1,36212526	GAL3ST1	2,00097251	2054	MICA	1,25213687	OPRL1	1,32636696	ACPT	1,56225471	C4BPA	1,51722664	AP2A1	1,41258369	FNTA	1,34643122	PAF1	1,95726591
1985	DDX54	1,2600256	ELAVL1	1,33888765	UPB1	1,58481437	DEDD	1,53549439	CYP7A1	1,43131397	FGF18	1,36211696	NKD2	2,00095029	2055	COL12A1	1,25193389	ALG9	1,32619421	HIP2	1,56205431	TRAF3	1,5172082	RB1	1,4124573	CDC20	1,34613068	SH3BGRL	1,95722555
1986	BTG1	1,25966804	BFAR	1,33876977	LRRK1	1,58391293	COL12A1	1,5354129	GTF2E2	1,43118223	FZD8	1,36171818	RFC1	2,00014476	2056	CD52	1,25189293	MAP2K7	1,32614915	PSCD4	1,56156017	GABRA3	1,516964	F11R	1,41209627	OXCT1	1,34603221	FTMT	1,95571274
1987	PIK3C2B	1,2596535	RFXAP	1,33860702	TH	1,58385201	P2RY6	1,53532695	COL22A1	1,4311075	IL18R1	1,36139786	CSAD	1,99924203	2057	DDIT3	1,25178305	HUS1	1,32470722	CYGB	1,56155347	MOBP	1,51670791	UCHL3	1,41196315	CLCF1	1,34600083	PLLP	1,95448344
1988	NFKBIL2	1,25963902	C6	1,33844869	TBK1	1,58250184	BAG5	1,53510669	SMARCC2	1,43039399	CD160	1,36118428	ABCC2	1,99906588	2058	NDUFB7	1,25171878	ARHGEF12	1,32445469	QPCT	1,56146683	INDO	1,51621675	APEX1	1,41116026	PHF21A	1,34578319	MUTYH	1,95406492
1989	ST3GAL6	1,25942579	EIF4A1	1,33826293	SLC12A3	1,58246279	PDE4D	1,53499732	TCF1	1,4302939	LRIG1	1,36104005	GPRC5A	1,99902471	2059	GSK3B	1,2515936	XIST	1,32440977	GCKR	1,56093097	GOPC	1,51616172	DDX19A	1,4111272	PPARBP	1,34559773	DDX51	1,95314864
1990	SMURF2	1,25935487	MPO	1,33822361	KREMEN1	1,58244692	GCA	1,53473042	SP100	1,43019504	SNX2	1,36068814	LAMP1	1,99899007	2060	FANCE	1,25117789	HSP90B1	1,32440751	SERPINA10	1,56086147	EPHB1	1,5160177	PPARBP	1,41032174	ANPEP	1,34539623	QARS	1,95305512
1991	RAB6A	1,25932964	BHMT2	1,33809254	BNIP3	1,58240962	PSMB10	1,53452114	KCNMB1	1,42996885	C1QC	1,36058739	MKKS	1,99881579	2061	DIXDC1	1,25108539	PRMT2	1,3241399	PDE4A	1,56042122	GOS2	1,51557221	MYBPC1	1,41010285	ADSS	1,34537322	CCL3L1	1,95150107
1992	PPP1CB	1,25918856	HRH1	1,33799031	C9ORF95	1,58157713	STX8	1,53452114	MLL	1,42995944	EMX2	1,35931944	CA4	1,99745797	2062	SERPINF2	1,25084272	IL24	1,32411433	PCK2	1,56000108	GABRG2	1,51528811	EEF1D	1,40997394	FN3K	1,34489861	CRY1	1,95090428
1993	COL15A1	1,25905677	MEST	1,33798878	BHMT2	1,58144588	INPP1	1,53423223	ATIC	1,42969612	PAK2	1,35916584	UCP1	1,99725799	2063	CD14	1,25066603	CDKN2A	1,32408426	ACTN3	1,55976223	APBB1	1,51497851	IL27RA	1,40975306	CENTD1	1,3447982	CFB	1,95082112
1994	CCR8	1,25875191	COPS5	1,33752701	SST	1,58124047	OBFC1	1,53400349	MGAT3	1,42934958	KCNH7	1,35881094	TICAM2	1,99713555	2064	PERP	1,2506062	RFK	1,32398715	ACMSD	1,55973089	MBD4	1,51493744	BBS2	1,40958154	ALDH6A1	1,34477039	FGR	1,95024535
1995	SERPINI1	1,25865863	FASLG	1,33745942	GTF2I	1,58076522	IFI16	1,53357186	KCNA4	1,42930325	GPR109B	1,35876914	COL21A1	1,99455143	2065	IL1R1	1,25059253	ETV7	1,32390957	EPHB1	1,55891901	MAP3K3	1,5141894	NME2	1,40907088	EIF5	1,34476931	RFX4	1,95024535
1996	MAP3K5	1,25865016	TBK1	1,33744955	GRAP2	1,58071116	AMY1C	1,53335368	NUP214	1,42892381	PIGO	1,35857837	LDB1	1,99326681	2066	LCMT2	1,25048219	POLL	1,32384798	P2RY12	1,55882806	C1QB	1,51280436	CTSL1	1,40905409	SUOX	1,34408972	STXBP1	1,94752936
1997	ICAM1	1,25846455	ATP1A4	1,33693209	SH3GLB1	1,58061113	NDUFA4	1,53242517	LPHN1	1,42808584	SCN8A	1,35761668	DUSP4	1,99323944	2067	PTGER4	1,25047759	DDR1	1,323616	CENTD2	1,5584367	ATP2A3	1,51232461	ICAM2	1,4087875	NR5A2	1,34389075	DIO2	1,94706807
1998	FOXM1	1,25838498	ADRB3	1,3368678	HSP90B1	1,57979064	MTA3	1,53190188	LTBP4	1,42796596	ANGPT2	1,35761574	AKR1D1	1,99315749	2068	FLT3	1,25041552	AOC3	1,32344559	ALG9	1,55817583	ST6GAL1	1,5120031	FOXA2	1,40871512	PLA2G6	1,3438613	STAT5B	1,94620806
1999	TLR7	1,25822841	LRRC41	1,33678203	FGF12	1,57901836	LPIN2	1,53180092	ENTPD1	1,42774148	PIK3C2A	1,35750867	HAO2	1,99200667	2069	NEFM	1,25026099	SOAT1	1,32309442	NAIP	1,55760402	BCAT2	1,51182445	CDH5	1,40830236	CRK	1,34380824	CSK	1,94551866
2000	EHHADH	1,25821334	NUDT12	1,33652447	GRHPR	1,57817947	CKB	1,53172793	NT5C	1,42772493	SST	1,35749866	GPR109B	1,99136315	2070	GAL	1,25007176	CD79B	1,3230268	KLK7	1,55746461	CASP3	1,51110419	PPP2R2A	1,40775368	SSTR4	1,34373007	UBE2D1	1,94539375
2001	SOCS5	1,2582113	KMO	1,33622018	IL1R1	1,57748882	PROS1	1,53152614	POLB	1,42768666	COX15	1,35732178	FAM59A	1,99120671	2071	HOPX	1,2495327	TGFB2	1,32276459	STAG2	1,5572599	ENTPD1	1,51104429	GPR37	1,40774168	PRKAG2	1,34357146	HOXD1	1,94526496
2002	RPE	1,25818323	FRZB	1,33618255	GNA11	1,57708717	VEGFA	1,53140401	FCGR3B	1,42724957	ZCCHC11	1,35610784	AASDHPPT	1,99111758	2072	KCNQ1	1,24947285	CETN2	1,32261239	INPP4B	1,55649777	LARS	1,51076154	TGFB1I1	1,40761195	SC5DL	1,34353424	BACE2	1,94502694
2003	KIAA1303	1,25805818	ARPC1A	1,33608771	ARFGAP1	1,57700184	DGKE	1,53041733	OSBPL1A	1,42703594	CACNA1A	1,35587033	PA2G4	1,99059371	2073	NADSYN1	1,24912924	KCNH7	1,32251173	CLCN7	1,55648103	GRM3	1,51058705	DNM2	1,40753848	MEF2A	1,34324267	AMDHD2	1,9447668
2004	HS3ST5	1,2580134	IFNGR1	1,33598229	TRAFD1	1,57698593	HARS2	1,5292585	CHRM4	1,42702426	HS6ST3	1,35587033	NDUFA12	1,99018876	2074	EIF4G1	1,24906521	GSTM5	1,32245416	KCNJ4	1,55644584	ACLY	1,51037917	IL9R	1,40730043	PRC1	1,34312824	ADRA2A	1,9445056
2005	ADORA2B	1,25799414	EFNA2	1,33595807	IL27RA	1,57675125	GRIA1	1,52923093	TEC	1,42662289	ALKBH3	1,35564409	FCGR2B	1,98953769	2075	CD1E	1,24905436	KIF3A	1,32228062	CTBS	1,55642565	AKAP1	1,50977926	CSAD	1,40729725	B4GALT7	1,34305704	E2F1	1,94424887
2006	OPRL1	1,25779908	ACACA	1,33587538	CDKN1B	1,57637722	FSTL1	1,52881844	CCL22	1,42638285	CUL1	1,35560768	TUB	1,9882845	2076	ST3GAL5	1,24905415	SCP2	1,32215388	ADRB3	1,5562571	MUT	1,50958393	LYN	1,40699271	PRKAA2	1,34297625	UBE2G2	1,94386646
2007	PDE4B	1,25767826	PGAM1	1,33536879	NT5C1B	1,57622901	C1R	1,52877365	PPIE	1,42625898	OPRL1	1,35553231	PMS1	1,98727263	2077	TPH1	1,2490501	ITGB7	1,32192468	CPE	1,55604126	JUNB	1,50954922	MCL1	1,40664974	HRK	1,34253719	GTF2A1	1,94299872
2008	UGT2B10	1,25767361	PDE6B	1,33534005	MTA3	1,57590906	CTNND1	1,52871734	MAFA	1,42547321	FOS	1,35521542	GTF3C3	1,98703889	2078	NKX6-1	1,24868221	IKBKE	1,3217875	ERCC3	1,55526486	MERTK	1,50913187	SMAD3	1,40656276	SHH	1,34219304	PTK2	1,94238397
2009	NR2E1	1,25756558	IDI1	1,33501142	SCN9A	1,57585262	MCM3	1,52846972	NPY2R	1,42528388	GRN	1,35500763	CBS	1,98653029	2079	CDT1	1,24839005	CDKN2D	1,32178149	COL12A1	1,55476689	GNAZ	1,50887054	PIGA	1,40620257	BRD4	1,34212153	UBE2D2	1,94138507
2010	IL22RA1	1,25724146	CLOCK	1,33479838	DNAJA3	1,57539651	AASDH	1,52820548	ANKFY1	1,42519647	DCK	1,35498955	EIF4B	1,98625476	2080	IL13	1,24831591	RPIA	1,32178149	T	1,55461493	S100A12	1,50799017	GRIA1	1,40618494	ENO2	1,34210881	HAO1	1,94132622
2011	IDH3B	1,25690099	WDR61	1,3347287	ABCB10	1,57517869	PTGDS	1,52796079	CYP7B1	1,42516739	COL9A1	1,35495416	MAP2	1,98612388	2081	ATP2B1	1,24820799	TFAM	1,32166578	LDLR	1,5542511	GIP	1,50736413	B3GNT4	1,40603864	STX8	1,34187934	TWIST1	1,94088065
2012	SP3	1,2567716	CACNA1H	1,33452217	OBFC2B	1,5750746	RING1	1,52778406	UCP2	1,42472368	C3	1,35481136	PSMA3	1,98451676	2082	ACTG2	1,24810005	SRY	1,32132025	IRS4	1,55421216	ICOS	1,50701906	PROCR	1,40589945	TEC	1,3418009	DTNBP1	1,94004628
2013	AKAP6	1,2566068	PDK1	1,33448346	ASNS	1,57425083	MTA1	1,5270533	CD81	1,42444056	GBX2	1,35481136	COL7A1	1,98405797	2083	GALNT8	1,2477888	NNT	1,32128939	CHST3	1,55322556	ASNA1	1,50691554	GNAT1	1,40580264	TFAM	1,34164784	PADI2	1,9396817
2014	RAD51C	1,25660004	RECK	1,33408528	LIG3	1,5741835	CAB39	1,5262868	DDIT3	1,42396979	HOXA10	1,35477514	SDHC	1,98278864	2084	C3	1,24769106	HELB	1,32128634	MAN1A1	1,55309615	F3	1,50635133	IL7	1,40578158	AHSG	1,34160562	PSMA4	1,93941461
2015	UBE2I	1,25656665	PARK7	1,33404304	CD8B	1,57382964	QPCT	1,52618566	F2R	1,4238264	CDA	1,35459376	BRCA1	1,98227968	2085	APBA3	1,24744996	MCF2	1,32121445	GNS	1,55247216	GDI1	1,50614691	HRB	1,40577396	FBP2	1,34159948	CD44	1,93933912
2016	WNT2	1,25651374	PSMD8	1,3336854	NDUFA4	1,57297308	XPA	1,52607453	CNTN1	1,42373536	SOX1	1,35457599	OPRL1	1,98087808	2086	CKMT1A	1,24729873	HCK	1,32096827	GPR64	1,55238884	TREM2	1,50613307	CD2BP2	1,40562216	NAPG	1,3415719	TFAM	1,93919663
2017	RECQL4	1,2565005	DVL2	1,33320676	PLIN	1,57274846	COL11A1	1,5256909	KATNB1	1,42332249	PEMT	1,3540121	IFNA16	1,98065356	2087	UGT8	1,24707839	FDPS	1,32082226	AIFM1	1,55224734	NAIP	1,50558359	DHRS7	1,40549551	DDC	1,3414995	SLPI	1,93862693
2018	GNE	1,25645013	MAGI3	1,33310855	NAGA	1,57255676	DMD	1,52530859	CD47	1,42309723	CNGB1	1,35391244	FRAT2	1,98063998	2088	HTR6	1,24654182	VSIG4	1,31999074	NR1I3	1,55209046	CHST2	1,5052536	SCARB1	1,40546173	NEU2	1,34139108	VEGFC	1,93819667
2019	PLTP	1,25624477	FDXR	1,33305477	ZBTB32	1,5725245	ATG4B	1,52521489	SHH	1,42254281	ARPC2	1,35377188	IL22RA1	1,98039151	2089	GPR68	1,24619886	FZD7	1,31944773	CDC20	1,55179149	CACNA1H	1,50488838	PIGG	1,40533031	CYP2C9	1,34117227	TFEB	1,93807593
2020	FTH1	1,25620449	LIPE	1,3326197	HCLS1	1,57224984	OXA1L	1,52514008	ATP5B	1,42203669	IL2	1,35360379	CCL7	1,98009061	2090	CD276	1,24616455	FABP4	1,31993753	SORL1	1,55156484	PLA2G4D	1,50482751	DUSP9	1,40525168	PSAP	1,34115272	FUCA1	1,9371508
2021	XRCC3	1,25609017	SPP1	1,332525	KCNC4	1,57213737	NCF4	1,52509996	PPAP2A	1,42179561	BIRC5	1,35323745	TNK2	1,97786454	2091	FRAT2	1,24612267	PRMT7	1,31983003	ETV7	1,5514211	CETP	1,50465967	ATP6V1A	1,40520941	GTF2E2	1,34090731	ALDH1A2	1,93687899
2022	ENPP7	1,25605517	GDF11	1,33250662	CAST	1,571453	COL5A3	1,52501935	COL5A2	1,4215653	DNAJA3	1,3530876	STAT1	1,97688514	2092	HAL	1,24581709	UBE2E2	1,31977055	ABCC1	1,55085767	ANKRD6	1,50460575	SPR	1,40517611	CSNK2B	1,34060104	IGFBP2	1,93562689
2023	SNX1	1,25595408	MBD1	1,33243031	CHEK2	1,57080023	CHKB	1,52479669	HDAC1	1,42105256	MYLK	1,35303539	TIRAP	1,97556392	2093	BRCA1	1,24571441	UBE2M	1,31967334	EEF1A2	1,55084386	NFATC3	1,50449125	MMP14	1,4051753	NTAN1	1,34054064	CACNA1B	1,93537644
2024	IGFBP7	1,25537739	LIPF	1,33241312	MBL2	1,57045496	WNT9B	1,52458108	FAM50A	1,42078146	ITPR3	1,35284198	PLCB3	1,97520046	2094	GTF2F2	1,2454917	GPR68	1,31959936	SDHD	1,55084386	PTPN22	1,5038357	LCMT2	1,40440192	CFLAR	1,34021007	CALCR	1,93485547
2025	POLD1	1,2553578	MEF2C	1,33211252	UBE2J1	1,57041042	HTR4	1,52447016	FOXD3	1,42067615	ACTG1	1,35279778	ACCN2	1,97487972	2095	CFHR3	1,2454358	BAI1	1,31945514	ARF1	1,55016698	AKT2	1,50345711	IL4	1,404399	HMGCL	1,34011694	CD80	1,93341898
2026	CLDN18	1,25531669	AMPH	1,33209472	IL7R	1,57035759	RAD21	1,5240334	LMAN1	1,42009092	FUT8	1,35264979	IL18R1	1,97474155	2096	SMCHD1	1,24530784	ALG3	1,31945465	MAP3K3	1,54991325	LHCGR	1,50308536	GTF2B	1,40435982	APC2	1,34006696	FBXW2	1,93293808
2027	PNPLA3	1,25525545	FUT6	1,33200526	REV1	1,56973684	CPS1	1,52372587	FOS	1,41951624	GFPT1	1,35262371	B3GNT4	1,97436885	2097	MC2R	1,24524682	ZFP36	1,3193584	PARC	1,54991325	ATP1B1	1,50297129	RXRA	1,40416317	MDH2	1,33998906	TYK2	1,93147612
2028	CEACAM1	1,25518203	APOBEC3F	1,33179999	BAI1	1,56937329	MBD1	1,5234905	CLEC10A	1,41903856	HLA-DPB1	1,35223346	NDRG2	1,97402703	2098	FMOD	1,2451924	DSP	1,31931149	CD33	1,5495891	SH2B2	1,502757	EED	1,40413684	POLR1D	1,3399608	CA9	1,93050286
2029	PFN1	1,25507183	FZD3	1,33143757	EXTL3	1,56931365	HES1	1,52345151	SCN9A	1,41888674	ACTN3	1,35210889	PDCD4	1,97340295	2099	TNFRSF13C	1,24513082	F12	1,31926563	UCP2	1,54958268	IFI44	1,50253164	NFATC2	1,40357146	MAFA	1,33992585	SULT1A1	1,92830564
2030	COL2A1	1,25493735	UXS1	1,33118632	GALNT5	1,56924142	ABCC8	1,52306868	DRD2	1,41885325	MAP2K4	1,35197845	PDE7A	1,97281416	2100	CES1	1,24501492	ACVR1C	1,31905463	NDUFB4	1,54946733	CEBPD	1,50248009	FGFR4	1,40349731	ABCB8	1,33944553	AANAT	1,92777818

Table A4. Pooled-shRNA library screen on HEL cell line and MF-3: list of 2nd most depleted shRNAs for each experiment (ranking approach 1, RA1).

	NO ruxolitinib (setting 1)				Ruxolitinib (setting 2)				Ruxolitinib + CM (setting 3)				MF-3				NO ruxolitinib (setting 1)				Ruxolitinib (setting 2)				Ruxolitinib + CM (setting 3)				MF-3	
	Experiment 1		Experiment 2		Experiment 1		Experiment 2		Experiment 1		Experiment 2						Experiment 1		Experiment 2		Experiment 1		Experiment 2		Experiment 1		Experiment 2			
Rank	*Gene*	*Fold change*	*Gene*	*Fold change*	*Gene*	*Fold change*	*Gene*	*Fold change*	*Gene*	*Fold change*	*Gene*	*Fold change*	*Gene*	*Fold change*	*Rank*	*Gene*	*Fold change*	*Gene*	*Fold change*	*Gene*	*Fold change*	*Gene*	*Fold change*	*Gene*	*Fold change*	*Gene*	*Fold change*	*Gene*	*Fold change*
2101	ADAMTS13	1,24488672	CDK5	1,31901141	MX1	1,54907395	MUS81	1,50231494	PPP3R2	1,40344725	BCL11B	1,33940227	DRD3	1,9274747	2171	GALNT1	1,23477972	PLTP	1,30867772	MAPK10	1,52923258	APOB	1,48131087	CD160	1,38693632	IL19	1,32716601	OLR1	1,89210841
2102	PYCR1	1,24473807	AANAT	1,31896599	HLA-DRB1	1,54877283	CREB3L2	1,50197394	C9ORF97	1,40308121	PEBP1	1,33935999	RAF1	1,9274501	2172	PTCH2	1,23476694	UGT2A1	1,30861696	PDE4B	1,52908542	GRIN2B	1,48118943	APOBEC4	1,38681829	FOXM1	1,32689084	LIMK1	1,89202605
2103	ORM1	1,24473448	KRT1	1,31887721	SPRED1	1,54849459	CALCRL	1,50171447	FCER2	1,40305404	CASP2	1,339344	STON1	1,92688355	2173	FGF2	1,23475681	SMCHD1	1,30855739	UAP1	1,52858009	TMEM166	1,48018157	CELSR1	1,38654461	CREB3L3	1,32642104	NTRK1	1,89152907
2104	DSE	1,2446321	SRC	1,31837529	GNRH1	1,54845443	FOXM1	1,5017092	CANX	1,40276755	GNB1L	1,33933723	HAL	1,9267464	2174	HIST2H3C	1,23455274	ABCB1	1,30836627	CLIC1	1,52817541	SLAIN1	1,48018106	MAGI3	1,38642515	FLOT2	1,32602906	AK3L1	1,89042458
2105	STRAP	1,24447157	IL2RB	1,31833162	IDH1	1,54836003	RAD1	1,50170843	PMVK	1,4026354	ALKBH2	1,33924108	HSD17B1	1,92597086	2175	NCR1	1,23453932	SEC22B	1,30835422	PRODH	1,5280698	BHLHB8	1,47998768	HK1	1,3863848	PREP	1,32535445	NME1	1,89030582
2106	GRB10	1,24422531	GPR37	1,31826214	GBGT1	1,54834911	SCN8A	1,50114914	GAPDHS	1,40250033	GDF2	1,33912771	SIPA1	1,92522326	2176	KLK10	1,23449418	CDT1	1,30808599	ACE	1,52774996	CHRNE	1,47915927	HSPB1	1,38636859	SERPINC1	1,32526442	NNT	1,88990661
2107	ITGB1BP3	1,24422426	LCN2	1,31824249	NT5M	1,54831509	DLL1	1,50061131	KCNJ3	1,40247824	KCNMB4	1,33906327	MKNK2	1,92445129	2177	PAWR	1,2337302	SLC10A1	1,30800647	CTNNA2	1,5273214	CR2	1,47897674	ADCY8	1,38560517	GGPS1	1,32508089	ADRB1	1,8899054
2108	GNA13	1,24369455	GRHPR	1,31814925	PRKD3	1,5478251	PTCH1	1,50025679	MARS	1,40244815	PTGFR	1,33897848	ATM	1,92430182	2178	BLVRB	1,23324174	HSD17B3	1,307895	GDF5	1,52670042	PGLYRP2	1,47869114	RRM2	1,38548469	MCRS1	1,32501225	TARS	1,88946907
2109	REPS2	1,24362866	HTR6	1,31808537	ZIC1	1,54762209	B3GNT4	1,49978247	H6PD	1,40229529	KMO	1,33894914	KCNC4	1,92373702	2179	ITPA	1,23293935	NR2F2	1,30787502	KHK	1,52579353	HUS1	1,47856176	CCL13	1,38530787	AMDHD1	1,32471297	FANCI	1,88919653
2110	APOBEC4	1,24356408	SH2D3C	1,31792368	NADK	1,54724196	FHL5	1,49960913	SEMA7A	1,40177412	S100A9	1,33893786	THRB	1,92347774	2180	IRS2	1,23280951	NRF1	1,30775451	PDE8A	1,52574086	MAPK3	1,47825699	BLM	1,38529464	COL2A1	1,3245854	CX3CR1	1,88853296
2111	IL10	1,24355523	BMP4	1,31783764	HSP90AA1	1,54723919	SPDEF	1,49898922	CDC27	1,40171788	AGER	1,33866847	SYNGR1	1,92323886	2181	CREB3	1,23265959	MAP3K10	1,30710505	STK11	1,52563557	DVL1	1,47824092	IL1RAP	1,38514439	SMS	1,32451978	PSMF1	1,88852769
2112	GGA1	1,24352025	ADRA1B	1,31783654	PFN2	1,54682009	TAF13	1,4989027	SLC27A1	1,40144784	EIF2B5	1,33863236	ANP32B	1,92190391	2182	ELK1	1,23232546	EOMES	1,30662107	BAAT	1,52525078	HIG2	1,47817829	PDK1	1,38405513	IDH3G	1,3244627	KDELR1	1,88819086
2113	SERPINB9	1,24350265	IL16	1,31781641	IL2RG	1,54562198	DNM2	1,49873324	PIF1	1,4005554	ASNS	1,33854737	RHOQ	1,92089813	2183	PLA2G1B	1,23224059	FLAD1	1,30595507	CR1	1,52508463	LIMK1	1,47813079	B3GNT6	1,38405	IFNGR1	1,32439711	ARD1A	1,88772854
2114	SETD2	1,24330301	COQ5	1,31732984	CAPN10	1,54561532	RHOA	1,49825832	CD1A	1,3994759	ATP6V0B	1,3384433	NR4A3	1,92084555	2184	GSTO2	1,23213023	PABPC1	1,30582546	CENTA1	1,524979	NSMAF	1,47789062	ATXN1	1,38397676	SMARCA4	1,32439711	PCAF	1,88696657
2115	SYNE1	1,24324772	MGAT4B	1,31705331	PSEN1	1,5453169	SUOX	1,49819926	FRZB	1,39946738	TFRC	1,33828142	GTF2F2	1,91792836	2185	IL12RB2	1,23211244	DNM2	1,30572828	CYP2C18	1,52489486	PIK3R2	1,47779643	IL10RB	1,38358906	TMED10	1,32408144	PSEN2	1,88653706
2116	EMP1	1,24314342	ABCA13	1,31702314	CDKN3	1,5449391	CX3CR1	1,49811001	PIK3R3	1,39941322	RAB5A	1,33812669	MDC1	1,91752362	2186	BCKDHA	1,23199377	B3GAT2	1,3056423	BLM	1,52486411	CASP4	1,47764314	THBD	1,38288346	TGFBR2	1,32398916	SND1	1,88616192
2117	ARRB2	1,24283399	PTH	1,31686302	CXCL9	1,54474603	GALNS	1,49797661	DLD	1,39940778	STON1	1,33807294	DBT	1,91709389	2187	PPFIA4	1,23185741	FECH	1,30561169	DEDD2	1,52484712	COQ5	1,47748675	COL6A1	1,38274159	HLA-DRB1	1,32395662	ITGA2	1,88495262
2118	TNKS	1,24280618	MYT1	1,31682194	MTFMT	1,54470301	DHH	1,49794845	DHX58	1,39894989	MTA2	1,33786526	MCL1	1,91478046	2188	SDC2	1,23157104	CAMK4	1,30534179	MAP3K8	1,52470998	NOV	1,47709421	CCNA1	1,3826387	CRKL	1,32390847	TFDP2	1,88491099
2119	ARNT2	1,24278604	MIOX	1,31670607	TFAP2B	1,54438581	DGKG	1,49771832	FZR1	1,39806179	BTG2	1,33784658	CUL3	1,91386011	2189	ATP6V1G3	1,23102089	TNF	1,30523197	HSF2	1,52447715	CLDN22	1,47674264	PNKP	1,38226872	PLA2G7	1,32389256	MAP2K6	1,8844327
2120	GNA15	1,24270799	TCIRG1	1,31652964	INHBA	1,54357664	ATP6V1D	1,49710369	PKN2	1,39768335	NFE2	1,33778239	CIDEB	1,91175012	2190	CUGBP2	1,23085094	PANK1	1,30491313	LCMT2	1,52371042	STXBP1	1,47645282	METTL2B	1,38218276	FGF12	1,32382244	PRDX3	1,88410123
2121	DNAJA3	1,24265095	ITGB2	1,31650495	FTMT	1,5435496	KDR	1,49665954	TIMP3	1,3976318	FGR	1,33759882	MAP3K7IP2	1,91048825	2191	ATP6V1H	1,23082323	APOBEC3G	1,30480697	AVPR2	1,5234599	IGFBP2	1,47600409	DHDDS	1,38212207	GDF11	1,32355787	FMO4	1,88402363
2122	IKZF1	1,24259716	MLL	1,31638215	DNAJC4	1,54331177	COL4A3BP	1,49557474	THBS1	1,39722151	XRCC4	1,33677808	ENO3	1,91048391	2192	DUSP6	1,2308027	CTNNA2	1,30479841	SYP	1,52345242	NKRF	1,47533114	ENPP7	1,38209486	TLR6	1,32338436	LIPC	1,88163727
2123	MSR1	1,24253806	BTG2	1,31616354	IL9	1,5431654	PMS1	1,49542741	NMUR2	1,39674031	FUCA1	1,33658602	HTR1A	1,91047592	2193	ACPT	1,2307486	TARDBP	1,30474261	QARS	1,52333999	MAP3K5	1,47518174	BTRC	1,381912	PKN1	1,32338008	CYB5R1	1,88139529
2124	KLC1	1,24245518	DEDD	1,31587581	MMP7	1,54310012	AGPAT4	1,49505282	IGF2	1,3959888	IL7	1,33654398	ST6GALNAC4	1,90980308	2194	F2R	1,23071476	PITX2	1,30431519	ELK4	1,52318076	RELA	1,47503367	ATP5L	1,38189207	MAP3K8	1,32336354	CDK1	1,88090696
2125	CACNA1F	1,24219129	STMN1	1,3156721	PAX4	1,54296798	PON1	1,4947322	AIRE	1,39591949	ECGF1	1,33636942	HRB	1,90953809	2195	C1QBP	1,23061986	PANK3	1,30429206	EPHB3	1,52234667	CD207	1,4750135	CRY2	1,38188304	METTL2B	1,32323403	GRN	1,88025789
2126	IRF2BP2	1,24206126	KLK6	1,31563099	ABO	1,54292441	HAL	1,49459233	SRY	1,39575727	TAF2	1,33622401	IL24	1,90929112	2196	BCHE	1,23052477	MMP10	1,30422152	POLR1E	1,5220902	ENTPD5	1,47415618	ABO	1,38186756	PTH	1,32320442	TSHR	1,87893203
2127	CFB	1,24201552	CD200R1	1,31561321	PPARGC1A	1,54272705	CHDH	1,49446362	GALNT10	1,39553828	DLX6	1,33618497	API5	1,90928283	2197	BMP4	1,23050057	TRAF1	1,30421337	NT5C	1,52198677	CNGB1	1,4741092	PDGFB	1,38169437	C19ORF40	1,32318422	NCK1	1,87876221
2128	DCLRE1A	1,24184884	TXN	1,31556688	DLD	1,54231683	CDC45L	1,4944207	EPOR	1,39540759	IARS	1,33576029	AGRP	1,90902853	2198	NTSR1	1,23031382	RRM2	1,30417483	POSTN	1,52102223	MARCKS	1,47409242	SCN1B	1,38149281	ADSSL1	1,32318395	TRAF3IP1	1,87753384
2129	IFIT2	1,24176903	BHLHB8	1,31546696	NUDT12	1,54228533	MAPK8	1,49405296	ACTN3	1,39517917	S100A12	1,33567765	CDX1	1,90861727	2199	NUP214	1,23027973	CD24	1,30393662	PXN	1,52051202	HTR1D	1,47373275	AKT1S1	1,38101224	CAPN9	1,32288974	ENTPD7	1,87707317
2130	SKP1A	1,2415716	PBEF1	1,31533357	PON1	1,54178656	CYP2A13	1,49327644	KITLG	1,39479825	AKAP7	1,33560861	BRS3	1,90811566	2200	LOC390243	1,22991774	CSF3	1,30376789	ROCK1	1,52041673	CTBS	1,47371733	HLA-DQB1	1,38067843	POLE4	1,32283183	PNKP	1,87673176
2131	MYLK2	1,24150819	UBE2A	1,31519717	CCL13	1,54064419	GGCX	1,49191026	ALS2	1,39461632	SUZ12	1,33553237	PPP1R13L	1,90758863	2201	CREB3L1	1,22990363	TOB2	1,3036645	TDGF1	1,52038554	ANXA2	1,47343029	BCAP29	1,38034153	PYCR1	1,32275433	CCL2	1,87615213
2132	IL12A	1,24093888	HSD17B7	1,31498408	NR3C2	1,54018987	GPX3	1,49189737	SLC1A3	1,39411952	EFNA1	1,33535015	IFRD1	1,90680461	2202	IL11RA	1,22985341	HADH	1,30350152	PER2	1,52031451	HRH4	1,47293454	POLA2	1,38015656	DNAJC3	1,32273143	IGF2R	1,87517731
2133	PRMT2	1,24044104	B4GALT6	1,31495532	PRPS2	1,53999372	MAL	1,49116613	ACCN1	1,39399083	CSTF3	1,33533025	SMUG1	1,90669466	2203	RIPK2	1,22981731	ADAMTS13	1,30327962	GRM3	1,52004143	CCL13	1,47260547	APBA1	1,38002805	ABO	1,32268379	BUB1B	1,87513597
2134	CRHBP	1,24027698	FBLN1	1,31466554	IGF2	1,53969864	GATM	1,49107254	LEP	1,39395631	IGFBP5	1,3353179	CS	1,9060575	2204	MARCO	1,22973419	PI3	1,30279685	TNK2	1,51984668	MAGI1	1,47255312	CALM1	1,37999399	PHCA	1,322546	SRD5A1	1,87512073
2135	EPHA4	1,24015179	NDUFA4	1,31463558	DISC1	1,53957428	TNFAIP1	1,49089976	GALNT5	1,39334412	PIGK	1,33524193	IFNA7	1,90564884	2205	CAND1	1,22950469	CNDP1	1,30259285	CHRM2	1,51963266	APPBP2	1,47199448	GNGT1	1,37958459	HUS1	1,32233407	ALDH5A1	1,87490517
2136	MBD4	1,24015179	CAMKK2	1,31459944	CBR3	1,53851306	MTAP	1,49079855	NCF4	1,3930509	ACACA	1,33467076	IL8RA	1,90557977	2206	CLC	1,22949752	ACP1	1,30250558	DPF2	1,51955068	AGMAT	1,47181987	AMPD3	1,37933925	DNM2	1,32232132	TRRAP	1,87427435
2137	APPL2	1,23968094	ACY3	1,31434679	ACP5	1,53849782	VWF	1,49074889	PPP2R2C	1,39280636	FDFT1	1,33457884	NDUFS8	1,90551409	2207	ATP5D	1,2293918	NOTCH4	1,30249869	SCYL1	1,51902935	SNAP29	1,47146445	CAPN9	1,37919818	ENTPD6	1,3220343	RELA	1,87384732
2138	SERPINB2	1,23960557	ANKRD6	1,31421627	WNT4	1,53849106	GALNT6	1,49074273	MYLK2	1,39271402	KIF5B	1,33392061	TMED10	1,90525943	2208	PRODH	1,2292764	FGF4	1,30248076	PPP1R10	1,5188444	SLC1A1	1,47131004	APBA2	1,37832122	BHLHB8	1,32191049	ANXA5	1,87339522
2139	ABCC1	1,23938095	DHCR7	1,31420879	ACP6	1,53834465	IL24	1,49061365	BLR1	1,39265201	MCM2	1,33352487	FANCB	1,90518376	2209	NDUFV1	1,22926824	IL1R2	1,3024418	PDHA2	1,51848903	MICA	1,47122537	OGG1	1,3782544	CLDN5	1,32178598	PRDX2	1,87283603
2140	ATP5G2	1,23931226	ATP5J	1,31416117	RXRG	1,53812902	RUNX2	1,49004505	UGT2B10	1,39252024	CERK	1,33337167	PDE1B	1,90471691	2210	POLR1D	1,22904954	CD72	1,3023458	GAMT	1,51846086	CD79B	1,47061523	SPRY2	1,37805295	ADORA2B	1,32140545	PDIA3	1,87158455
2141	MYOD1	1,2389734	SEL1L	1,31393629	CCR7	1,53806492	FABP5	1,48980352	SEC22B	1,39238059	A4GALT	1,33257492	PRKACB	1,90445397	2211	LRP6	1,2289486	PLA2G2E	1,3023458	BLVRB	1,51800417	CHRNA2	1,47000635	PRC1	1,37802805	CYP2U1	1,32139515	EPHB1	1,87126409
2142	FGF8	1,23897216	ITGA5	1,31328196	STAT6	1,53697402	AK1	1,48962616	IFNA5	1,39220648	SIRT6	1,3324887	UCP3	1,9034036	2212	AK1	1,22867053	GCAT	1,30209214	LYN	1,51749705	TCOF1	1,46986747	PLCB3	1,37800664	PIK3C3	1,32132702	MTMR1	1,87031589
2143	ST6GALNAC6	1,23884437	SP3	1,31286949	ACO1	1,53520263	MYBPC2	1,48956625	ADCY3	1,39211023	GLUD1	1,332001	SNX1	1,90333894	2213	PABPC1	1,22866705	ARFGEF2	1,30204554	PRKX	1,51691298	PAX6	1,4697966	TAF1L	1,37796161	APOC3	1,32127264	CELSR2	1,86963435
2144	CASP7	1,23842251	SALL4	1,31276549	TBX21	1,53519142	GNAI3	1,48899136	AMY1C	1,39197908	DVL2	1,33185837	GK2	1,90229628	2214	IL17RC	1,2286119	CALB1	1,30199702	IL17F	1,51654808	AKR1B1	1,46972524	UGT2B17	1,37795667	PER2	1,32122661	UBE1	1,8687781
2145	TPH2	1,23834786	SCN5A	1,31260887	A1BG	1,53513808	IGF2	1,48869305	GNS	1,39149944	SOD2	1,33177818	RAB11A	1,90218493	2215	BCL11A	1,22857542	LPIN2	1,30187864	F5	1,5163454	ATP6V0D1	1,4695901	PRPS1	1,37792582	SLC27A4	1,32120835	PHF1	1,86784099
2146	GABRA1	1,23826556	HTR1D	1,31256633	SLC30A3	1,53505259	PHCA	1,48825273	AZI2	1,39130824	ALG13	1,33165403	DNM1	1,90210801	2216	NMNAT3	1,22833948	TYMS	1,30153479	AP2A1	1,5149743	SLC1A2	1,46923557	TWIST1	1,37769166	DCLRE1A	1,32107969	PIK3AP1	1,86739661
2147	BHLHB3	1,23810554	SPDEF	1,31240654	FHIT	1,53486298	ACY3	1,48804869	KCNMB3	1,39094399	NFS1	1,3313963	AZGP1	1,90175353	2217	CHRM5	1,22817198	ATF1	1,30138472	UBE2H	1,51438056	IGF1R	1,46902938	SMURF1	1,3776464	GRHPR	1,32075545	MAD2L2	1,86695658
2148	AASDHPPT	1,23808827	HMGCS1	1,31240311	ICAM1	1,53482475	NRP1	1,48792955	BBS1	1,3905668	GPLD1	1,331355	OBFC2B	1,90107849	2218	TNNT2	1,22811425	HES6	1,30115018	PGLYRP2	1,51411313	PAFAH1B3	1,46887108	CYP39A1	1,37740774	CDH15	1,32073431	TNFRSF10B	1,86451486
2149	PDGFB	1,237336	DGKQ	1,31232866	INPP5B	1,53425599	ETV3	1,48762999	PARK7	1,3905668	PIK3R2	1,33131671	ATP5C1	1,90081852	2219	AHSG	1,22791027	B2M	1,30096747	AMD1	1,51410399	GLI3	1,46883073	PML	1,37734671	HERPUD1	1,32050104	PFKFB4	1,86339367
2150	HGFAC	1,23694144	TUBA3C	1,31230292	GSTM5	1,53419585	MPG	1,4872635	GRM4	1,39050047	TLR8	1,33118142	ELA3A	1,90076508	2220	LRMP	1,22790814	FCGR2A	1,30093117	DRD1	1,5139598	COL27A1	1,46851753	IDI2	1,37709867	IL8	1,32042117	TPK1	1,86306794
2151	DNM1	1,23677857	SLC2A1	1,3121742	MAPK12	1,53417477	SLC5A3	1,48714281	BAIAP2	1,39044182	MAP2K7	1,33068619	CTSK	1,9006124	2221	MMP7	1,2278333	PHKB	1,30078824	ARNT2	1,51387658	SERPINE2	1,46846453	RECQL5	1,37691749	GCNT2	1,3204138	ARMETL1	1,86218784
2152	ARPC4	1,23650758	PACRG	1,31212613	MANBA	1,53412576	ENPEP	1,48670429	MBP	1,39020594	FOXD3	1,33048191	DRD1	1,90008599	2222	LRP5	1,22781849	HLA-DPB1	1,30045323	ACTG1	1,51348015	TF	1,46838971	RARB	1,37690088	SLC18A3	1,32036752	RGS1	1,86182321
2153	APOA4	1,23644923	PKN1	1,31206306	DNAJC3	1,53352719	CAMP	1,48647088	GALNTL2	1,38993995	GRID2	1,33042447	CHRM2	1,89990679	2223	HDAC9	1,22772921	CNGA3	1,30036658	STX4	1,5133314	ANAPC4	1,46796155	CYP2C19	1,3768545	SLC32A1	1,32019099	ST6GALNAC3	1,86175174
2154	GATM	1,23641636	CSTF1	1,31197944	SP3	1,53292854	NEFM	1,48615819	FOXA3	1,38941424	GABRB1	1,33011146	CACNA1G	1,89947208	2224	UBE2V2	1,2276212	PDE5A	1,30031194	DAB1	1,51285693	PTPN11	1,46755419	AQP1	1,37606358	CPT1B	1,3196959	IL13RA2	1,86174803
2155	NCOA3	1,23640236	POLB	1,31184391	ICOSLG	1,53239326	ATP4A	1,48601051	TNFRSF19	1,38915112	HIST1H2AA	1,33010755	PPOX	1,8994168	2225	PFKM	1,22735764	PAWR	1,30003616	FMO3	1,51276455	ZFX	1,46639697	IL19	1,37567351	ALG2	1,31927881	NAGA	1,8605519
2156	RTN4	1,23631416	INHBA	1,31163153	LALBA	1,53139688	CDKN3	1,48587934	AICDA	1,38911499	DYRK1A	1,32994728	PAX6	1,89925592	2226	SARM1	1,22723491	VTN	1,29990991	DPAGT1	1,5125604	ILVBL	1,46608063	PPAT	1,37565481	KDELR1	1,31915888	POLR3K	1,86053045
2157	ANAPC10	1,23618949	EPHB2	1,31152908	RET	1,53127029	SHB	1,4858373	ANXA8	1,38868122	FMO4	1,32960043	RPL14	1,89871321	2227	ABCG8	1,2271465	MC5R	1,29963524	ACAA1	1,51250212	RFX5	1,46572198	VWF	1,37521199	METTL6	1,31910443	ENO2	1,85883072
2158	ARL4D	1,23582595	DDX51	1,31124922	MFGE8	1,53103447	AKR1C4	1,48567553	CCKBR	1,388406	CCBP2	1,32897825	OAT	1,89868274	2228	PPARG	1,22714242	PRPS1	1,29960305	CYP19A1	1,51249763	LEF1	1,46564801	SPTBN4	1,37494681	PGLS	1,31899299	TUBD1	1,85881403
2159	FAH	1,23576264	PLEKHA8	1,31108341	XRCC4	1,53101137	LIG1	1,48545062	PLCG2	1,38828131	KCNK1	1,32856366	AMOTL1	1,89767029	2229	LGMN	1,22694216	DARC	1,29949653	TAF1	1,51223608	FABP4	1,46555486	UGT1A1	1,37479354	PFKFB4	1,31897082	DNMBP	1,85873376
2160	CRLS1	1,23574276	TRAF2	1,31102099	BCL2L10	1,53060278	TAF12	1,48529558	DOT1L	1,38813166	GNAI3	1,32838366	SLC12A3	1,89757575	2230	APBA1	1,22644464	CPSF6	1,29932402	RRAD	1,51171747	MIMS19L	1,46555383	SLC15A1	1,37474175	FDPS	1,31893668	CHST11	1,85848908
2161	PRKG2	1,23570206	NCK1	1,31070377	GRIA2	1,53043518	CAMKK2	1,48473667	LARS	1,38786318	PYGL	1,32818041	GMNN	1,89752726	2231	AQP7	1,2262588	CA9	1,29918391	THOP1	1,51129594	DPPA3	1,4653054	RAB35	1,37459806	IFI44	1,31842667	STX8	1,85838332
2162	ABCB4	1,23569251	NFATC2	1,31045384	ACHE	1,53030465	AKR1C3	1,48451029	IFNA16	1,38777478	TSPAN7	1,32810136	IFNAR2	1,89703313	2232	GAPDHS	1,2261962	NT5C3	1,29900311	DAP	1,51101785	VNN3	1,4651175	CD4	1,37440705	MYC	1,31836386	TRAF3	1,85775347
2163	CR2	1,23562421	PPARA	1,31040892	ITGA2B	1,53026659	ATG7	1,48426613	STK36	1,38775938	GALNTL2	1,32807283	GSS	1,89679208	2233	KLRC1	1,22616893	SCN9A	1,29890092	MERTK	1,51098204	F2RL1	1,46505858	INPP5E	1,37394629	SPP1	1,31835899	KCNB1	1,85738553
2164	NOTCH2	1,23544613	VAMP5	1,31002203	BCAR1	1,53025054	IL8RA	1,48378752	SLC12A6	1,38767482	PUM2	1,32800306	YWHAZ	1,89678245	2234	NFE2	1,22596695	PITPNB	1,29862011	TLE1	1,51067505	MMP10	1,46505719	FGFR3	1,37388185	SCYL1	1,31816353	B4GALT6	1,85725409
2165	ARHGAP5	1,23534727	ATP5I	1,30997855	ERN2	1,52981797	GSK3B	1,48363542	TRAF3	1,38755293	YWHAB	1,32768342	CRP	1,89452337	2235	MTHFD1	1,22592862	EIF4E2	1,29828668	KLF2	1,51061799	GNPDA2	1,46500678	TACR1	1,37377487	NME2	1,31744678	ATP1A2	1,85705537
2166	STAT5B	1,23533684	HMOX1	1,30988986	NT5E	1,52981797	SPN	1,48311646	GORASP1	1,3874761	AK3L1	1,32751351	RFXANK	1,89430825	2236	CYP3A43	1,22582203	TEP1	1,29825261	KCNQ2	1,51031911	PIK3CB	1,46485351	CAMK2G	1,37338774	STAR	1,31670394	ARFIP2	1,85680567
2167	IL24	1,23526616	NOXO1	1,3098862	COL9A1	1,52977526	IL17RD	1,48291229	COL5A1	1,38732333	CHUK	1,32743202	WIF1	1,89368513	2237	CIITA	1,22559886	C8A	1,29808834	PTGES2	1,51015311	NGFR	1,46457635	PGF	1,37336731	ADH1B	1,31642586	WIPI1	1,85653471
2168	ALDH5A1	1,23527744	HNMT	1,30981108	REM2	1,52960232	ITGA2B	1,48246741	CSK	1,38719555	RGS4	1,32735561	WDFY3	1,89315405	2238	HCLS1	1,22559736	MMS19L	1,29781219	KLK6	1,50958514	APPL2	1,46419752	FAH	1,37335383	NUDT4	1,31629645	ABCA12	1,85637916
2169	ADCY6	1,23503231	CHP	1,30932073	MGAT2	1,5294378	KLK7	1,4822324	CARD11	1,38701005	CAMK1	1,32732151	PAFAH1B1	1,89280705	2239	SERPINA3	1,22559674	FOS	1,29767727	UGDH	1,50900221	GDF9	1,4641253	DNAJB9	1,37299578	HRG	1,31626574	CHP	1,85590164
2170	OPRD1	1,23485909	HLA-DOB	1,30913555	WEE1	1,52936208	SRPR	1,4819745	MAP3K9	1,38698679	AASDHPPT	1,32726384	ATP13A2	1,89272807	2240	STAT5A	1,22527922	ABLIM2	1,29753391	SPP1	1,50896758	DDR1	1,46398012	ENO3	1,3722983	CUL2	1,31624358	EBP	1,85552628

Table A4. Pooled-shRNA library screen on HEL cell line and MF-3: list of 2nd most depleted shRNAs for each experiment (ranking approach 1, RA1).

	NO ruxolitinib (setting 1)				Ruxolitinib (setting 2)				Ruxolitinib + CM (setting 3)				MF-3			NO ruxolitinib (setting 1)				Ruxolitinib (setting 2)				Ruxolitinib + CM (setting 3)				MF-3	
	Experiment 1		Experiment 2		Experiment 1		Experiment 2		Experiment 1		Experiment 2					Experiment 1		Experiment 2		Experiment 1		Experiment 2		Experiment 1		Experiment 2			
Rank	*Gene*	*Fold change*	*Gene*	*Fold change*	*Gene*	*Fold change*	*Gene*	*Fold change*	*Gene*	*Fold change*	*Gene*	*Fold change*	*Gene*	*Fold change*	*Rank*	*Gene*	*Fold change*	*Gene*	*Fold change*	*Gene*	*Fold change*	*Gene*	*Fold change*	*Gene*	*Fold change*	*Gene*	*Fold change*	*Gene*	*Fold change*
2241	SLC26A2	1,22526127	PDE6D	1,29731287	REG3A	1,50874306	MKI67	1,46382792	MSH5	1,37165689	HADH	1,31592757	GDF2	1,85543358	2311	ITGB2	1,21650757	TRIP12	1,28649417	CSK	1,48556983	CES7	1,444931	ESCO1	1,35694582	RDH12	1,3043978	GABRA5	1,82221385
2242	BBC3	1,22526091	MFNG	1,29716379	COL6A3	1,50841486	C12ORF57	1,46379538	PIAS1	1,37121517	SEC22B	1,3158789	HTR3C	1,8541654	2312	ACLY	1,21650004	ATXN1	1,28583223	ATP2B3	1,48556435	ERAF	1,4441056	UBB	1,35662355	PLEKHA8	1,30411196	TBX1	1,82197255
2243	CRHR1	1,22515562	GPC5	1,29709114	CSNK1G3	1,50834325	PANK1	1,46357968	HEXA	1,3711183	SLC27A1	1,3158789	PGF	1,8534729	2313	SCNN1B	1,21647014	KCNB1	1,28577516	CASP7	1,48523205	SHOC2	1,44387099	PFKFB1	1,35616855	GABRA6	1,30403066	PELI3	1,82169692
2244	HOXA1	1,22508272	IL13RA2	1,29706486	GTF2E2	1,50829348	NPR1	1,46345371	TP53INP1	1,37095711	ME1	1,31567182	POU5F1	1,85321536	2314	MAT1A	1,2160971	HAO1	1,28572788	AMY1A	1,485231	PMS2L3	1,44333419	CDC2L5	1,35581261	MAP4K5	1,303757	FES	1,82137166
2245	COX6C	1,22492406	CD276	1,29692048	HIST2H3C	1,50806768	REPS2	1,46337795	WBSCR22	1,37094027	ABCA10	1,31542908	BIK	1,85231617	2315	MST1	1,21600677	ENTPD1	1,28550377	LRRC15	1,48501596	DBN1	1,44279648	HOXC13	1,35503127	UQCRH	1,3037046	NRP1	1,82128448
2246	CEBPD	1,22451491	MAP3K7	1,29684502	TRIM25	1,50782539	QARS	1,46330584	GFAP	1,37080318	PEU3	1,31533972	HGF	1,85195772	2316	HSPA1A	1,21595266	OCRL	1,28545334	POLH	1,48441499	SSR4	1,44239947	RDH12	1,35495586	F5	1,30369271	GNG3	1,8207118
2247	IL1RL1	1,22395807	ABCB11	1,29664596	FASLG	1,50771565	ACP1	1,4631553	ZFP42	1,36989933	RTN4R	1,31525025	GNAL	1,85106092	2317	CCR7	1,21587228	COL18A1	1,28475484	PLEC1	1,48403498	GSTA3	1,44236312	SULT2B1	1,35490856	FOXL1	1,30368788	UBE2L3	1,82010919
2248	C8A	1,22388794	GABRB3	1,29658596	HLA-DOB	1,50736171	COL22A1	1,46286763	CA5A	1,36972693	CLEC5A	1,31509503	GGCX	1,85097634	2318	CDH15	1,21576276	CAPN9	1,28458426	GPX4	1,48369895	CRTAM	1,44235263	CXCL3	1,35479153	CPSF2	1,30342241	GATA4	1,8185346
2249	LY96	1,22371873	MAPK8IP3	1,29610953	WDR79	1,50709123	IL17D	1,46254827	TNF	1,3696932	HSP90AB1	1,31506123	CAV3	1,85063096	2319	PDHB	1,21512628	MCM5	1,28458121	LRWD1	1,48217764	UBE2H	1,44209388	ATG9A	1,35455024	DLD	1,30326363	TNFSF13	1,81838968
2250	GPRC5D	1,22370961	ATP2A3	1,29599966	CHRNA3	1,50697002	LYCAT	1,46222976	CREM	1,36963795	TRAF3IP1	1,31504628	GLRX	1,85041096	2320	MCHR1	1,2151243	GALNS	1,28439589	MAP1B	1,4821164	IKBKE	1,44186636	MAP3K10	1,35442701	IL2RG	1,30280382	PDE4B	1,81820963
2251	CYP11A1	1,22370766	GBX2	1,29583608	PEMT	1,50678084	STH	1,46187457	IFNGR2	1,36922246	TGFBI	1,3147603	F13A1	1,85040947	2321	NDUFS4	1,21497748	TRIP10	1,28387642	OCRL	1,48167785	GJA4	1,44180537	DDX52	1,35404547	BDH1	1,30244497	IL3	1,81810425
2252	CHRNA6	1,22364794	WWTR1	1,29580764	GNAS	1,5062251	TSPAN7	1,46183497	GPR39	1,3687512	DRD4	1,31466432	GCM1	1,85030332	2322	BHLHB8	1,21478393	DGAT2	1,28343613	PRKAR2B	1,48122317	YARS	1,44169804	AMY1B	1,35387808	POLL	1,30243329	HHIP	1,81525348
2253	TRIM21	1,22363105	PYCR1	1,29577239	IQGAP2	1,50542339	HOXD1	1,46183471	UBE2N	1,36867733	CTSK	1,31455158	EPHX2	1,85002395	2323	LIG4	1,21477715	NF1	1,28334707	HOXD11	1,48099519	ACO1	1,44131272	CD34	1,35369585	SDHD	1,30213623	CALML5	1,81470221
2254	COL4A3BP	1,22353902	MYH3	1,29568596	ORC4L	1,50389567	PLCB3	1,4616689	C9ORF95	1,36854721	GBP2	1,31443075	TSC1	1,84979847	2324	SMUG1	1,21470934	FAM132A	1,283275	PTPN12	1,48023664	FABP7	1,44125748	ACSS1	1,3533719	MVP	1,30208416	ERCC5	1,81456739
2255	CDC23	1,2235384	BPNT1	1,29560292	WDR61	1,50325322	ATG12	1,4615419	FUT9	1,36840438	MYO1C	1,31413696	POLG	1,84962428	2325	NRF1	1,21462117	GCA	1,28319029	IL1RN	1,48014946	POLK	1,44012619	PTEN	1,35333059	ERBB2	1,3017985	CHST2	1,81352823
2256	HDAC3	1,2235129	SOX2	1,29554517	DNMT3A	1,50323912	CISH	1,46031268	ATRX	1,36836533	PITX2	1,31412309	NAT2	1,8489671	2326	EGLN3	1,21460158	GPR171	1,28316231	AKAP3	1,48014725	GLCE	1,43944318	NANOG	1,35331406	CDKN1A	1,30166546	GLO1	1,81209653
2257	CHRM1	1,22347603	OLIG1	1,29532857	KCNE1	1,50272666	DGAT2	1,4602687	IGF1	1,36811322	LOC390243	1,31406114	ADCY7	1,84843151	2327	ANXA8	1,21459633	DCLRE1A	1,28304417	BNIP3L	1,48012777	MMP2	1,43918698	LMNA	1,35311936	CDKN3	1,30146074	BNIP3	1,81206205
2258	SSTR3	1,22323218	TNNT2	1,29462143	ARHGDIB	1,50268378	MBL2	1,46010281	SERPINB9	1,36792976	NFAM1	1,31388149	AZIN1	1,84799543	2328	GPRC5B	1,21459633	GSTZ1	1,283012	MAP3K4	1,47954223	TREH	1,43907409	VIP	1,35300858	EHD2	1,30134623	GSTA2	1,81199158
2259	HTR1F	1,22322111	LEF1	1,29455311	NEUROG1	1,5020373	ABCA8	1,45986128	PDE6C	1,36784044	PTPN6	1,31387942	ACTG2	1,84746453	2329	LIMK1	1,2145682	PGDS	1,28271788	FAT	1,47932938	SPIB	1,43862696	POLE3	1,35276023	MTR	1,30064784	RALGDS	1,81182631
2260	EIF5A2	1,22302897	HSD17B2	1,29408974	PYGB	1,50178243	FAM59A	1,45950105	SMPD2	1,36761069	TAF12	1,31375434	NFKBIL1	1,84744193	2330	PAH	1,21452019	LHPP	1,28258326	FASN	1,4789476	PC	1,43825429	BDH1	1,35252221	F8	1,30062777	EOMES	1,81099149
2261	ESR1	1,22297018	PAFAH1B3	1,29400659	NDST4	1,50153736	GNAQ	1,45946342	GPR161	1,36757333	CTSE	1,31362344	SLC12A6	1,84652367	2331	IL17RD	1,21444055	WASL	1,28249208	DAPK3	1,47893287	TRIP10	1,43815489	DUOX1	1,35231644	CFL2	1,30047505	ANXA1	1,81029584
2262	EFNA5	1,22294436	STXBP4	1,29393994	PLOD1	1,50048303	REV3L	1,45946187	KCNH7	1,36706965	TIMP4	1,31357118	ABCA13	1,84478687	2332	CD83	1,21426964	PRDX5	1,28247466	ITPR3	1,4787622	FZD8	1,43811113	MDM4	1,35214359	SP3	1,30043495	APEX2	1,81024461
2263	ACTG1	1,22282441	SFRP2	1,29374076	HLA-G	1,5000396	EPHB2	1,45903083	IRAK2	1,36625853	TNFSF14	1,31296591	CLDN18	1,84449279	2333	AARS	1,21426597	TNFRSF13C	1,28240711	BST1	1,47867255	NUP214	1,43775676	IFNA17	1,35193028	IL28RA	1,30042322	IL17RB	1,80972062
2264	RAD52	1,22276597	PSENEN	1,29367873	CD22	1,49990229	IARS	1,45861088	RARA	1,36616107	TYK2	1,3124909	SULT4A1	1,84372434	2334	TRADD	1,21413893	GRIA1	1,28236906	MAGI3	1,47806085	TOP3B	1,43704195	LY96	1,35191248	PLA2G2F	1,30013965	SLC32A1	1,80952457
2265	TDGF1	1,22233998	TIAM1	1,29361103	COL6A1	1,4997552	CNGA3	1,45854158	GNB1	1,36606757	TCF7L2	1,3121576	MC2R	1,8425338	2335	PSME1	1,21413537	LEFTY1	1,2821418	SCAP	1,47778828	DYRK1B	1,43685306	MGMT	1,35173755	FABP4	1,300056	MYBPC1	1,80947307
2266	CYP4A22	1,22231738	LDHAL6A	1,29356386	SLC2A3	1,49910964	NOTCH2	1,45827868	RELN	1,36600573	DHRS4	1,31214986	ESCO2	1,8420226	2336	ID1	1,21411338	ENTPD5	1,28212512	GRM7	1,47772267	PTCH2	1,43640999	HIPK2	1,35151256	SHC1	1,29955146	KCNIP3	1,80919316
2267	FGF12	1,22227961	ACSL3	1,29346956	SIRT6	1,49907622	GTF2H5	1,45816734	GSTO1	1,36564544	PRDX3	1,31176954	LCMT2	1,8418067	2337	T	1,21404517	HTR1F	1,28176829	GNG3	1,47738395	C22ORF28	1,43609979	PDCD4	1,35144793	SPAM1	1,29929442	NTAN1	1,80892359
2268	ERN2	1,22211403	BMP6	1,29346956	MSTN	1,49882324	PRKX	1,4580303	C19ORF40	1,36559571	TEAD2	1,31143956	HELB	1,84153889	2338	EIF2B4	1,21383765	HIST2H3C	1,28175735	ATG7	1,47710039	SCP2	1,43546383	TGIF1	1,35064897	BAI1	1,29921145	CD79B	1,80784005
2269	RAB3A	1,22199119	APOC1	1,29344996	TNFAIP6	1,49880571	ISG20	1,45740107	TCF4	1,36557624	PKP4	1,31134367	PRL	1,84146012	2339	FBL	1,21352082	AKR1B1	1,2815867	CHUK	1,47694311	AZI2	1,43540026	IL8RB	1,35034243	CHSY1	1,29890933	MDM4	1,80762642
2270	HSF1	1,22194919	TNFAIP1	1,29334987	RNASE1	1,49873859	KNG1	1,45740107	GABARAPL2	1,36539439	ATP6V1B1	1,31119842	MAP4K1	1,84140477	2340	FOLH1	1,21346354	EBI3	1,28099592	TRAF3IP1	1,47669372	ARHGEF5	1,43522073	PARG	1,34989417	WNT4	1,29877308	CCDC6	1,80711262
2271	CDC34	1,22194606	MGMT	1,29329104	B3GNT4	1,49871008	TANK	1,45692427	TPK1	1,365303	AGL	1,3111875	VEGFA	1,84062724	2341	AGMAT	1,21342071	CACNA2D3	1,28069971	MBP	1,47612006	ACY1	1,43509986	MMP7	1,34958646	SMARCE1	1,29877023	CYP2C9	1,80646765
2272	GSTA4	1,22191758	GRIA2	1,29305378	CDC7	1,49856434	ACVR2B	1,45644549	FOLR1	1,36498776	GLI1	1,3109975	AHSG	1,84056731	2342	SEPP1	1,21288066	SNAP23	1,28067679	DOCK9	1,47580109	FADS2	1,43490382	DOLPP1	1,34934385	FPGT	1,29872215	DIABLO	1,80580127
2273	CD97	1,22191327	RUNX3	1,29290363	SCD5	1,49848912	ASPA	1,45611625	CLC	1,36490804	CCNB3	1,31069414	SLC2A3	1,83944189	2343	ADRA1B	1,21281668	STON1	1,28063565	CD28P2	1,47544596	CHEK1	1,43445042	ADH1B	1,34905702	SLC2A3	1,29872072	GEN1	1,80553527
2274	NEIL2	1,22143964	GSTA2	1,29243718	GJD2	1,49785906	SNAP23	1,45574666	USP9X	1,36487138	GARS	1,30993053	KRAS	1,83802226	2344	MME	1,21238186	CTSK	1,28062306	COL5A1	1,47538775	TRIO	1,43437439	EFNA2	1,3485561	CYP3A7	1,29818082	FABP5	1,80495781
2275	CES7	1,22048983	CARD11	1,29232062	CFHR3	1,49764114	WNT3	1,45529448	IL13RA2	1,36430037	PIK3R5	1,30984968	IRF6	1,83743188	2345	AURKB	1,21207247	EIF5A2	1,2803342	PBEF1	1,47520415	EMR3	1,43421231	STAMBPL1	1,34837035	PTPRO	1,29795961	PMM1	1,80491447
2276	APP	1,22045085	ANAPC11	1,29231899	ARRB1	1,49709476	SULT1A4	1,45497138	EFNA3	1,36401822	CDH2	1,30957167	DGKE	1,83740254	2346	ZAP70	1,21200599	BGLAP	1,28011305	F10	1,47484008	TNF	1,43421224	FUT6	1,3480909	SORL1	1,29794901	EIF2S1	1,80258446
2277	PFKFB1	1,22044582	PDPK1	1,29228325	HTR1D	1,49656978	IL7	1,45478714	BAD	1,36394876	SCD5	1,30953423	PSCA	1,83731753	2347	CTTN	1,21199223	TREX2	1,27993347	CDKL2	1,4747244	PEG3	1,43399731	CACNA2D3	1,34785663	AKAP13	1,29764771	CXCL11	1,80255104
2278	SELL	1,22032028	CD68	1,29226152	IFNA17	1,49585714	ALOX5	1,45468912	CPB2	1,36380936	CPSF3	1,30948595	HBEGF	1,83624353	2348	PTTG1	1,21183539	CLDN19	1,27950721	CBR1	1,474638	SP3	1,43332502	FGA	1,34722807	ITGA9	1,29764771	MYH6	1,80233974
2279	TICAM2	1,22021544	PLG	1,29216419	NPR1	1,49585031	HDAC10	1,45461529	XAB2	1,36351915	APPBP2	1,3091007	PPAP2A	1,83620273	2349	FOXL1	1,21158572	MCAT	1,27939788	CYP2J2	1,47432764	STK11	1,43314074	EIF2B2	1,34713999	NOD1	1,29763506	KLK6	1,80155048
2280	PARP4	1,22003711	KDELR1	1,29200072	ENO3	1,4956387	APBA2	1,45384574	CRP	1,36327665	RPRM	1,3090519	RUVBL1	1,83614892	2350	NEDD4L	1,21158319	REL	1,27931974	FAS	1,47420683	NR2F2	1,43304608	GALNT17	1,3471275	MC2R	1,29759946	IL5RA	1,80143083
2281	LRIG1	1,21991952	PARP2	1,29188664	ORC1L	1,49554719	FLCN	1,45379515	GSN	1,36325225	PSME2	1,30892313	GALNT3	1,83598841	2351	BOK	1,21157626	FAH	1,27908437	PTGER2	1,47402398	NR5A2	1,43297561	PSENEN	1,34708072	CHGB	1,29742356	CPO	1,80062984
2282	PLA2G10	1,21982813	KLK7	1,29186404	IRAK1	1,49552589	GAA	1,4536715	MARCO	1,36284468	ENDOG	1,30883157	ARHGEF12	1,83565008	2352	COX5B	1,21157169	CTSL2	1,27843278	SLC6A4	1,47401221	ATP6V0D2	1,43296461	MAN1A1	1,34704278	UBE2M	1,29733855	SCN1B	1,80034611
2283	IGFBP5	1,21974998	QPRT	1,2914894	KCNN3	1,49537637	IGFBP6	1,45366691	FECH	1,36228164	NR3C1	1,3081308	GYPA	1,8352898	2353	GPRC5C	1,2114738	RHOA	1,27834154	EGLN3	1,47329093	TAF1L	1,43286296	SERPINA6	1,34677459	NEIL3	1,29698479	POR	1,7995226
2284	H6PD	1,21966361	C13ORF15	1,29123901	DMC1	1,49517789	WBSCR17	1,45355586	MAPK8	1,36218159	NPAS2	1,30779482	NPY2R	1,83481255	2354	GFAP	1,21117078	AP2A1	1,27830888	SLC16A3	1,47280982	CHAT	1,43271337	SPRY1	1,34677259	POLR2K	1,2968179	CAPNS1	1,79866429
2285	NFE2L2	1,21961685	S100A4	1,29110323	DHCR24	1,49457025	RTN4	1,45294643	KDELR3	1,3619553	ATP6V1D	1,30768695	FHL2	1,83465574	2355	ASNA1	1,21088648	BCR	1,27827531	ITGAX	1,4727988	FLT4	1,43173218	ALK	1,34674816	TBL1XR1	1,29648232	DTX2	1,79845023
2286	DGKZ	1,21912726	SHH	1,29107135	CAND1	1,49368638	DISC1	1,45284787	ATG10	1,36179542	GIT1	1,30767603	DHCR7	1,83390576	2356	SSTR5	1,21085483	HLA-DMB	1,27813708	PUM1	1,4724828	ATXN1	1,43150679	SCNN1D	1,34661153	CHRM2	1,29622863	AKT2	1,79645684
2287	KPNA3	1,21907022	AKT2	1,29078703	AKAP7	1,49361036	FOXA2	1,4526857	BHLHB9	1,36154327	CLCA1	1,30760718	DNM2	1,83336159	2357	LTBP4	1,21079927	DLAT	1,27766497	PLCB1	1,47172064	MAP1B	1,43128408	B3GALT1	1,34607849	FHIT	1,29615875	HADHB	1,79589718
2288	STAG2	1,21901697	RRAD	1,29078293	GANAB	1,49341195	MGAT4B	1,45237703	PPP1R10	1,36150669	RBBP7	1,30752065	MARS	1,83317939	2358	UCP1	1,21054136	TGIF2	1,27746954	THRB	1,47159371	POLRMT	1,43119506	TFCP2	1,34549336	SESN1	1,29581781	CLEC5A	1,7957246
2289	ARFGAP1	1,21898698	CA12	1,2906051	SLC38A1	1,4929446	PAPSS2	1,45191833	CDC2L6	1,36135394	ATP6V0A1	1,30751498	FSCN1	1,83152794	2359	GTF2A1	1,21047448	TNFRSF1B	1,2774223	CAP1	1,47144361	PRPS2	1,43102581	CHRM2	1,3454635	CCR2	1,29580965	MCM5	1,79555993
2290	GCKR	1,21888237	TAGLN	1,29046016	RARA	1,49288132	UGT2B4	1,45173733	SPRED2	1,36113231	BTK	1,30739769	MFNG	1,82969585	2360	REM2	1,21047127	ATP6V1G1	1,27730239	CLDN17	1,47136045	PROC	1,43077323	ZCCHC11	1,34539832	PRF1	1,29572256	MAG	1,79503034
2291	EDG4	1,21886836	AICDA	1,29035385	HMOX2	1,49266397	BAP1	1,45163611	BMP4	1,36110095	CSMD1	1,3072038	FN3K	1,82933741	2361	AKR1C4	1,21046584	PPP2CA	1,27707961	THBD	1,47123489	XK	1,43075029	GRB10	1,34534502	APBB3	1,29548621	GPR68	1,79489627
2292	DPPA2	1,21871773	TFAP2B	1,28964423	LIPA	1,49243981	GBX2	1,45155485	CELSR3	1,36098281	CHRNA9	1,3071803	LITAF	1,82933741	2362	PLAU	1,21022794	COL21A1	1,27689703	KLK1	1,4709204	CCND2	1,43073788	MAD2L2	1,34529555	DVL3	1,29527626	CYP2A6	1,79337708
2293	HMGCL	1,2186405	ATP6V1C1	1,28904914	POLQ	1,49164709	PSENEN	1,45129081	BCR	1,36095206	KITLG	1,30694496	TCEA3	1,82898714	2363	TRAF4	1,21019749	CHEK1	1,27665417	ABLIM1	1,47086642	STAR	1,43049438	GPRC5D	1,34508703	LCN2	1,29525453	HDAC10	1,79263421
2294	C1QL1	1,218112	GDI2	1,28895087	CLEC10A	1,49156627	GSTM3	1,45090501	KIF5B	1,36034722	CXCL11	1,30666594	FGB	1,8286095	2364	OTUB1	1,21009797	ARSB	1,2763509	NEFH	1,47085239	RASGRF1	1,43043205	GH1	1,34506368	PDE1B	1,29513043	MTHFR	1,79245171
2295	TWIST1	1,2180058	REV3L	1,28885002	PLAT	1,49131499	AKR1C2	1,45086466	PKN1	1,36024621	PC	1,30664521	PRKRIR	1,82794285	2365	FCER1G	1,20995584	FMOD	1,2761335	MAP1A	1,47056858	IBSP	1,42985022	TRPM2	1,344954	FAH	1,29504812	ATP5J2	1,79207228
2296	ADH5	1,21796631	ABO	1,28880553	SNAP29	1,49061636	NODAL	1,45084057	BST1	1,35997352	GOT2	1,30643716	UNC93B1	1,82779083	2366	HOXD13	1,20988668	HS6ST1	1,27593277	SLC25A11	1,47045152	LEFTY1	1,4298167	LIPE	1,34470022	GDI2	1,29492462	SMARCB1	1,79136974
2297	RAD51	1,21738361	CD36	1,28876969	DUT	1,49020746	UBE2V2	1,45069478	ATP1A3	1,35959689	MKNK2	1,3059257	HUS1	1,82694802	2367	ANAPC11	1,20962493	TPT3	1,27559332	BGN	1,4702637	RBBP4	1,42975051	ESD	1,34460892	ATG7	1,29491725	IL1A	1,79117991
2298	CAMKK2	1,2173312	GABRG3	1,28869759	SOD1	1,48999585	DBC1	1,45034844	CDK3	1,35956608	SCARB1	1,30574763	NEU3	1,82614727	2368	AXIN1	1,20962443	ARHGEF2	1,27555684	PPP2R2C	1,47019308	NEK1	1,42946939	PPP3R1	1,34388021	ACVR1	1,29467808	NDUFV1	1,79109012
2299	DIAPH2	1,21729512	AKR1C1	1,28857537	PMM1	1,48967462	RRM2	1,450185	AR	1,35955838	EIF2B4	1,30533667	PIGK	1,82502933	2369	GAA	1,20958347	FPGS	1,27544803	LIFR	1,46943507	MAD1L1	1,42917539	LPHN2	1,34367998	CDKN2D	1,29453413	CD6	1,79017943
2300	HEL308	1,21728322	PRKCE	1,28839977	RELN	1,48960239	BMP7	1,45010393	CD46	1,35875125	AGRN	1,30512266	RALB	1,82458639	2370	QPRT	1,20932425	CXCR3	1,27540182	ACSS2	1,4693253	CPO	1,4288677	CXCR4	1,34360029	ATP5J2	1,29409928	DNAJA4	1,78959366
2301	AIRE	1,21725343	COL5A3	1,28838873	KIT	1,48923527	GATA4	1,44912242	TPP1	1,35874033	P11	1,30497802	CD276	1,82406927	2371	EIF4G2	1,20879274	GOLGA5	1,27539305	ACSL1	1,46931495	RASGRP1	1,42883657	TRPM7	1,34307308	OXCT2	1,293334	CASP8	1,7895622
2302	HLA-DQB1	1,21719611	ENTPD3	1,28834702	MYT1	1,48892112	KCNJ4	1,44789012	UBE2E2	1,35866108	MCAT	1,30488566	GPLD1	1,82399417	2372	VTN	1,20866051	MAPK9	1,27533861	BCL9	1,46842431	CAPN1	1,42821924	MLH1	1,3427334	SLC33A1	1,29318953	LIG1	1,78913283
2303	CDC2L6	1,2171304	SHC1	1,28817417	CASP2	1,48823259	SFRP4	1,44733232	ARNT	1,35833331	FGF4	1,30482648	DCLRE1B	1,82372326	2373	DEGS1	1,20862561	CHRNA4	1,27531099	PURA	1,46840554	GFPT2	1,42817549	CHST4	1,3426443	KNG1	1,29314992	SIRT6	1,78813263
2304	POLB	1,21697142	TACR3	1,28815878	PANK3	1,48822883	PLG	1,44708617	CYP19A1	1,35826836	GOLGA5	1,30474367	UBE2B	1,82346495	2374	MAP3K2	1,20846679	DAPK3	1,27496486	TSPAN7	1,46815065	SDHC	1,42802416	NFS1	1,34251824	FANCL	1,29185122	ERBB2	1,78767733
2305	CACNA2D2	1,21691911	SPR	1,28812039	SLC6A13	1,48781004	KATNAL1	1,44671087	GSK3A	1,35822427	ATRX	1,30467734	TOP2B	1,82343765	2375	AHCY	1,20842771	CCND3	1,27476147	PADI2	1,46777362	PGR	1,4275322	GP5	1,34187384	GMPPB	1,29162983	ITPKB	1,78707518
2306	RAB1B	1,21675792	PROZ	1,28794746	ARG1	1,48762744	TLR3	1,4465097	GOPC	1,35800149	CAPN1	1,30463322	BLM	1,82325866	2376	COL6A1	1,20830946	PHF11	1,27474244	POLM	1,46741101	FUT5	1,42747823	UGT2A3	1,34175192	IL27	1,29137778	PTPRF	1,78521176
2307	C8G	1,2167407	TERF1	1,28784801	OPRS1	1,48757019	RAD54B	1,44650208	CR2	1,35767269	KHK	1,30461587	GAST	1,82303928	2377	KCNMB1	1,20814237	GAMT	1,2746368	LCAT	1,46728297	MCM10	1,42716752	MAGEH1	1,3416494	ITGAX	1,29131587	CYP3A5	1,78513299
2308	CACNA1H	1,21670941	C3AR1	1,2874754	COL21A1	1,48694734	GCDH	1,4464552	ERG	1,35742287	NAT6	1,30443696	CYP2A7	1,82261988	2378	FCGR2B	1,20806105	CEBPB	1,27459883	CFL2	1,46726943	A4GALT	1,42652235	PSMB8	1,34164807	P2RY5	1,29131417	SSTR1	1,78466375
2309	ALPL	1,21664919	KLRC1	1,28675316	FSCN3	1,48688987	C2	1,44627221	STX8	1,35735577	IFIH1	1,30440998	CDC14B	1,82236976	2379	GGH	1,20792294	CITED1	1,27448388	ACY1	1,46647149	FARSA	1,42621574	ORC1L	1,3412698	F11	1,29128837	GALNTL1	1,78438016
2310	DNAJB1	1,21658324	NES	1,2865901	ZEB2	1,48674872	TGM3	1,44547699	FUK	1,3572073	FMO1	1,30439843	DNAJC3	1,82227215	2380	UNC5CL	1,20790768	FAU	1,27445362	NDUFA8	1,46645423	IAPP	1,4259091	CYBB	1,34123548	SKI	1,29119641	FIGF	1,78434024

Table A4. Pooled-shRNA library screen on HEL cell line and MF-3: list of 2nd most depleted shRNAs for each experiment (ranking approach 1, RA1).

	NO ruxolitinib (setting 1)				Ruxolitinib (setting 2)				Ruxolitinib + CM (setting 3)				MF-3					NO ruxolitinib (setting 1)				Ruxolitinib (setting 2)				Ruxolitinib + CM (setting 3)				MF-3	
	Experiment 1		Experiment 2		Experiment 1		Experiment 2		Experiment 1		Experiment 2							Experiment 1		Experiment 2		Experiment 1		Experiment 2		Experiment 1		Experiment 2			
Rank	*Gene*	*Fold change*	*Gene*	*Fold change*	*Gene*	*Fold change*	*Gene*	*Fold change*	*Gene*	*Fold change*	*Gene*	*Fold change*	*Gene*	*Fold change*	*Rank*	*Gene*	*Fold change*	*Gene*	*Fold change*	*Gene*	*Fold change*	*Gene*	*Fold change*	*Gene*	*Fold change*	*Gene*	*Fold change*	*Gene*	*Fold change*	*Gene*	*Fold change*
2381	BLMH	1,20786097	ABCC6	1,27423381	GNAI3	1,46610279	EFNB2	1,42539695	KL	1,34089551	MAPRE2	1,29116626	MCM6	1,78245679	2451	FES	1,19999169	PPARGC1A	1,26356933	FOLH1	1,4445982	C9ORF95	1,40609383	MARCKS	1,32788733	POLE3	1,27826478	C1QL4	1,75181496
2382	FRZB	1,20778382	EMP1	1,27404277	IL6	1,46594182	DNAJC3	1,42531986	PROC	1,34088166	MGMT	1,29050706	PPBP	1,78205401	2452	CUL1	1,1997459	COMT	1,26342566	SFRP4	1,44421966	COL2A1	1,40587066	KALRN	1,32780989	NDST1	1,27786331	EDNRA	1,75181496
2383	FABP6	1,20771446	SLC12A6	1,27388544	SCN5A	1,46495065	EEF1G	1,4252367	PALB2	1,34085737	ABCA1	1,29029551	C7	1,78094203	2453	AGA	1,19973712	NEURL	1,26290092	ABL1	1,44396512	NSMCE2	1,40579969	STAR	1,32779244	DAZL	1,27769851	ACVR1	1,75060407
2384	CHRNA9	1,20764121	NDST4	1,27375386	HLA-E	1,46457087	SFMBT2	1,42514942	IL22RA1	1,34044142	HGS	1,29018572	CYP46A1	1,78035684	2454	ATP2A2	1,19958071	PPP3R2	1,26274912	BCL10	1,44395235	DEDD2	1,40523004	FOXM1	1,32774433	PLA2G12B	1,27745666	LRRK2	1,74990456
2385	ORC2L	1,20753192	DMGDH	1,27375114	RNF146	1,46401965	CXCL11	1,42498042	PTPN11	1,34040587	ACMSD	1,29002059	GANAB	1,77999433	2455	TFAM	1,19946859	IL3RA	1,26255169	NFATC2	1,4437022	GLUD1	1,40487181	EFNA1	1,32714703	SORBS1	1,27731087	PAN2	1,7495571
2386	GSTA3	1,20752161	FAM50A	1,27352801	GPSN2	1,46389387	AR	1,42468316	PDE3B	1,34035167	GSTA1	1,29002059	TUBA4A	1,77945348	2456	KCNK1	1,19943024	OPRS1	1,26229174	CD2AP	1,4435739	NSDHL	1,40452446	WBSCR17	1,32713154	IDI2	1,27707865	CYP7B1	1,74950963
2387	YY1	1,20747854	NR6A1	1,27348363	ARRB2	1,46291349	RCAN1	1,42441306	MAP3K7	1,34007516	DDEF2	1,28994828	CAMK1G	1,77856507	2457	GTF2H5	1,19936518	FUT9	1,26223252	PTGER4	1,44342709	MGST1	1,4039091	ABLIM2	1,32704209	CARD11	1,27707387	SORL1	1,74931021
2388	TMED10	1,20737301	EIF2B4	1,27341289	LYCAT	1,46269992	HSD3B1	1,42425146	LHX2	1,3400655	MARS2	1,28978216	RUVBL2	1,77845818	2458	TRAF3IP1	1,19935299	AMPD3	1,26206228	CLCA4	1,44319979	POLA2	1,40388455	CHRND	1,32703361	HBB	1,27688968	ALG5	1,74923157
2389	AKR1B1	1,20736856	GLP2R	1,27336158	GCAT	1,46264723	LHX8	1,42350713	CXCL12	1,34005165	HEY1	1,28949901	C2	1,77723196	2459	NKD1	1,1993226	FN3K	1,2618669	SERPINC1	1,44298099	TFAM	1,40378484	HERPUD1	1,32695093	DLL1	1,27649618	OGDH	1,7488374
2390	ATP6V1B2	1,20715147	MAP3K7IP3	1,27308813	TNIP2	1,46236905	CFD	1,42318192	MAP2K3	1,33974052	CCR6	1,28887636	TIFA	1,7763861	2460	DNMT1	1,19900243	CD1C	1,26182298	TEAD2	1,44272522	FMO2	1,40376023	UBE2D3	1,32652921	CSNK1A1	1,27646315	CLIC1	1,74857408
2391	BACE2	1,20714217	CLEC7A	1,27305094	RNF4	1,46228074	C9	1,42313471	NFKBIL2	1,33973924	GLP1R	1,28886378	B4GALNT1	1,7760174	2461	AGPAT1	1,19889345	GPX5	1,26173763	ARHGEF2	1,44258456	DGKD	1,40364175	IGFBP4	1,32645509	PIF1	1,27632227	TBX2	1,747703
2392	FOXO1	1,20711539	PRMT6	1,27302676	ACCN1	1,46202488	ANGPTL3	1,42210276	ADSS	1,33913767	EDA	1,28885781	IL22RA2	1,77555087	2462	HERPUD1	1,19875412	TFDP2	1,26163432	SREBF2	1,44257289	PENK	1,40296336	ATP2B3	1,32632277	GPR75	1,27601999	ANXA6	1,74701571
2393	PLAUR	1,2069393	BCL3	1,27286125	CHAT	1,46200583	DRAM	1,42194267	ABCB6	1,33912232	EPHB4	1,28866421	PHF11	1,77521135	2463	FGF18	1,19864279	STAT1	1,26154683	STX5	1,44233503	DHODH	1,40240329	APOB	1,32626704	UBE1	1,27598151	STXBP4	1,7466159
2394	BMPR1B	1,20675306	IDH1	1,27280026	TAF4	1,46061346	RAB6A	1,42187933	PRODH	1,33879851	DYRK1B	1,2885674	EPHA4	1,77513361	2464	NSDHL	1,19861456	ATP5G2	1,26076654	HARS2	1,44140366	PGDS	1,40178932	ELK3	1,32624401	APOBEC1	1,27592144	LDHAL6B	1,74640388
2395	PKP4	1,2066943	PIGM	1,27272279	BIRC3	1,46037989	DCLRE1B	1,42152027	CASP3	1,33866384	NFKBIB	1,28840762	SMPD2	1,77448786	2465	CPE	1,19816162	GYPA	1,26064728	UROD	1,4412107	VARS2	1,40156962	NDNL2	1,32620593	FANCE	1,27586121	CCR10	1,74568955
2396	NEURL	1,20662115	SERPINA4	1,27255588	TGFB3	1,46009892	ZBTB20	1,42129658	H2AFY2	1,33854057	ASGR2	1,28835513	NOS2A	1,77444876	2466	CTSS	1,1979989	MTA3	1,26034206	EIF2B1	1,43969234	IQGAP2	1,40151796	PIGS	1,32602445	BMP2	1,27559357	SCN9A	1,74563003
2397	ATP5J2	1,20656736	C1QB	1,27218855	NDUFS2	1,4598982	PITX2	1,42100706	KCNB1	1,3383325	HS3ST5	1,28823817	MAP1LC3B	1,7738846	2467	PTPN12	1,19757471	PTPRB	1,26015078	UBE2E2	1,43926781	CFTR	1,40139645	OXCT1	1,3260098	XK	1,27517353	XYLT2	1,74542195
2398	MAD2L2	1,20645163	GALNT6	1,27199307	PRDX6	1,45989277	CELSR1	1,42089558	ATM	1,33828385	PPP2R5B	1,28797472	LAMB1	1,77360007	2468	PYGO1	1,19733395	CYP7B1	1,26002587	PLA2G5	1,43827637	CDH15	1,40136055	ITGA5	1,32583783	PPAP2A	1,27474869	POLR3H	1,74531003
2399	CACNA1G	1,20626235	ELK1	1,27196556	TLN1	1,45970123	EDG4	1,42087427	PRKG2	1,33779003	S100A8	1,28757381	TRIM28	1,77291997	2469	IFT57	1,19732421	NR2E1	1,25984039	HTR4	1,43814472	BRCA1	1,40115825	FABP1	1,3258364	DGKE	1,27468055	EIF2B5	1,74448885
2400	CBR1	1,20621973	ANXA1	1,27190913	ARHGEF5	1,45927625	CSNK1D	1,42066023	DUSP8	1,33778454	SRC	1,28736279	MYC	1,7722962	2470	RPN2	1,19724507	EIF2AK4	1,25974892	TICAM1	1,43762895	HS3ST5	1,40106882	P4HB	1,32574289	PCSK2	1,27461705	IGFBP5	1,74432317
2401	LCAT	1,20595144	CCL28	1,27155229	NOG	1,45902144	IL17C	1,42057012	CCNA2	1,33733886	MAP4K1	1,28733629	ADCY4	1,77200152	2471	LY86	1,19723238	SESN1	1,25974569	GLI3	1,43733807	CHST3	1,4009611	CYP46A1	1,32572181	MMP9	1,27440117	PDE6G	1,74407816
2402	SEPHS1	1,20593179	GPR132	1,27141947	PPARG	1,45899684	IRF1	1,42049706	HTR3E	1,33716732	ESD	1,28703022	B3GALNT1	1,7719655	2472	ARF6	1,19675311	PAK2	1,25972153	SNAP23	1,43714952	FCGR3A	1,40080704	HNMT	1,325701	CCL5	1,27362099	KATNAL1	1,74381167
2403	ACCN1	1,20581492	HTR3B	1,27136793	PPAP2C	1,45810695	PICALM	1,42022041	GDF15	1,33705261	CYLD	1,28695634	SLC6A3	1,77046369	2473	DBH	1,19647473	SENP2	1,25945513	ATP13A2	1,43655826	HGS	1,40072675	UBE2D1	1,32548498	EMR1	1,27356203	KCNA4	1,74373488
2404	PDK2	1,20581452	KERA	1,27114637	ATP6AP1	1,45761247	IRAK1	1,4201833	OPRM1	1,33699884	TKTL1	1,28649304	IHH	1,77011654	2474	ACHE	1,19621693	TLR10	1,25942401	COX6C	1,43643104	ANXA1	1,4006769	EEF1G	1,3254684	MYOD1	1,27326521	NPPB	1,74321169
2405	LEP	1,20572326	HLA-E	1,27110166	PRKCE	1,45711618	PIGC	1,42014368	ZNF395	1,33686087	MPI	1,28612182	FGFR4	1,76984646	2475	PLP1	1,19618647	SCN11A	1,25900732	ATP1B1	1,43625429	RAB3A	1,39969432	FGL2	1,32503226	FANCF	1,27322868	PTTG1	1,74233779
2406	SIGIRR	1,20562551	APPBP2	1,27098545	IDH3A	1,4570975	PIK3CD	1,42005097	ST3GAL3	1,33669229	ACVR1B	1,28611233	CXCL3	1,76813285	2476	SLC38A1	1,19603732	TIMP4	1,25892721	GZMB	1,43617842	HYAL3	1,39912923	ACCN5	1,32456443	GAPDHS	1,27316614	BHLHB3	1,7423338
2407	EFNA3	1,20552266	PRKCA	1,2709395	BOK	1,45649559	PARG	1,41968942	RBPJL	1,33630422	SLC1A2	1,28596057	SPTLC2	1,76792075	2477	PTGS1	1,19580574	FGL2	1,25880647	POLR1D	1,43609161	TDP1	1,39858535	CDC23	1,32440757	ST3GAL4	1,27281072	KIF5B	1,74169709
2408	WBSCR17	1,20549795	CYP39A1	1,27086721	SERPINF2	1,45647715	BUB3	1,41914982	PFKL	1,33594257	CAPRIN2	1,28575342	FGF20	1,7668157	2478	SOD1	1,19563937	ROCK1	1,25854354	MMP3	1,43573895	GNB1	1,39854244	TH	1,3242765	PSEN1	1,2725954	POLD3	1,74142183
2409	HIG2	1,20548304	ERAP1	1,27085836	DKK1	1,4561646	CX3CL1	1,41908788	CDC34	1,3359375	DIAPH2	1,28575326	AP2B1	1,76641614	2479	B3GNT4	1,19554259	UBE2D2	1,25834181	GRIK4	1,43524451	CARM1	1,3984091	GHR	1,32411494	CASK	1,2723801	GNAQ	1,74111125
2410	CLIC1	1,20492996	TCF7L2	1,27057051	ASNA1	1,45527314	ADCY3	1,41907035	CREB3L3	1,33590142	KCNMB1	1,28550802	CR2	1,76624394	2480	APBB2	1,1954551	COL4A3BP	1,25813409	RPRM	1,4351931	HRK	1,39834399	PTGIR	1,32394483	RTN4	1,2723492	G3BP2	1,74072733
2411	GPAM	1,20487518	PTPRA	1,27055288	NPAS2	1,45517655	GEN1	1,41872531	EIF2B1	1,33576206	ATG4A	1,28513276	HIP1	1,76546968	2481	DDX47	1,19525938	ALDH6A1	1,25809888	EEF1G	1,43512142	PAX4	1,39809115	REPS2	1,32391629	HHIP	1,27222057	CDC7	1,73971598
2412	PIAS3	1,20487174	HRH4	1,27047641	GPR81	1,45512642	AGL	1,41866781	SNCA	1,33538396	GPR37	1,28505006	INSIG2	1,76534697	2482	ATRX	1,19508507	CXCR6	1,25779106	BMP15	1,43499411	KLRC3	1,39771867	DAP	1,32378767	TGFB3	1,27130188	DUOX1	1,73938771
2413	GLRX2	1,20486018	DRD4	1,27045196	BIRC5	1,45464561	MAP2K4	1,41861955	SNX2	1,33538072	ATP4A	1,28502139	MOG	1,76456802	2483	AP2A1	1,19477736	FZD2	1,25714296	GNMT	1,43440927	SALL1	1,39754076	PCSK2	1,32365136	ASPH	1,27113168	ARG2	1,73917823
2414	JAZF1	1,20420794	MAGI2	1,27037441	ATP5A1	1,45436398	ACTN1	1,41858385	AP2M1	1,33437999	ATP6V0D1	1,28496589	NCK2	1,76437826	2484	DPP4	1,19461024	MEPE	1,25713076	NR1H4	1,43421596	FZD4	1,39752434	SLC12A1	1,32365029	DTX2	1,27103783	FOXK1	1,7384424
2415	SHC3	1,20386009	DPYSL5	1,27021039	KPNA2	1,45434304	PRDX5	1,41858236	CA5B	1,33435914	IL22RA2	1,28472478	OSBPL3	1,76434657	2485	GOT1	1,19458388	TRIM14	1,25704248	CD82	1,43392836	SRD5A2	1,3972246	DLX6	1,32343275	PCGF2	1,27098204	CCK	1,73727477
2416	DAB2	1,20367911	COL4A2	1,27020912	GCNT2	1,45391259	SRY	1,41810019	CPT1B	1,33426879	CUL3	1,28429697	PDGFRB	1,76335139	2486	CA5B	1,19458243	ERBB2	1,25696918	ITGA1	1,4330133	FANCI	1,39701486	AMOTL1	1,32315639	SDHB	1,2707347	C19ORF40	1,73549306
2417	WWP2	1,20327056	DOK1	1,27009128	NSF	1,4539069	NR5A1	1,41797894	COL12A1	1,33380542	MBTPS1	1,2839178	DCN	1,76329081	2487	G6PC	1,19452922	SCLY	1,25669874	GALNTL2	1,43298017	GPR39	1,39695862	CDC42	1,32280824	SLC5A3	1,26971314	SMAD4	1,734465
2418	FYN	1,20325902	PPP2R5C	1,2698774	MYD88	1,45330113	UBE3A	1,41720317	CLCN7	1,33376167	CADM3	1,28380295	ABCA9	1,76307643	2488	ATG4A	1,19441919	FANCF	1,25657537	GMNN	1,43286057	AGRP	1,3963623	GAB2	1,32256991	ABCA8	1,26965281	LEFTY1	1,73404548
2419	ALDH2	1,20321102	CNPY3	1,26981394	GPRC5C	1,4532615	SFRP2	1,41628072	GRN	1,3337612	PTEN	1,28377676	ABP1	1,76296616	2489	F10	1,19422759	CPT1C	1,25612275	FAU	1,43266974	ACSS1	1,39626483	DAZL	1,32243606	CHRNE	1,26963845	HSPA1A	1,73384392
2420	GCGR	1,20301286	TRAF3IP1	1,2696557	GALNT6	1,45321599	CDC2L5	1,41590921	GRM1	1,33373228	KATNB1	1,28362789	GRM5	1,76282698	2490	PPCDC	1,19381411	TFAP2C	1,25583076	CLDN20	1,43261467	SHC3	1,39622932	ABL1	1,32203271	LRRC15	1,26941499	ACSS1	1,73365219
2421	AKR1C1	1,20296028	GUCA1C	1,26937625	NBL1	1,45317406	PLA2G2D	1,41553896	SRP9	1,3335623	RBBP8	1,28359244	SEC61A2	1,76268796	2491	DNAJA4	1,19377812	B4GALT2	1,25580921	VHL	1,43260388	MAP2K2	1,39607301	PAX1	1,32187969	TNFRSF11A	1,26903808	NMI	1,73307216
2422	IRF2BP1	1,20291863	PNMT	1,26906146	ALPP	1,45280578	LILRB3	1,4154836	NOD1	1,33353145	MCM10	1,28340794	PRKCE	1,76267502	2492	SEL1L	1,19370733	CRLS1	1,25578483	ABCB8	1,43258114	GLRX	1,39580775	DDX1	1,32166416	ATG4B	1,26885672	KCNMB4	1,73253556
2423	CCNI	1,20284405	GOPC	1,26892077	AGRN	1,45233366	H2AFX	1,41486468	CCR2	1,33349136	EOMES	1,2833494	FCER1A	1,76257791	2493	PROX1	1,19366694	IMPA2	1,25503946	GGH	1,43223447	F13B	1,39506201	NMI	1,32142956	DPPA4	1,26884322	CDK8	1,73236599
2424	NCF4	1,20281733	SCD	1,26881385	SYT1	1,45225906	MAML1	1,4142903	SCN11A	1,33341903	CFHR1	1,28323813	MVK	1,76221507	2494	SMURF1	1,19363643	HTR3C	1,25455042	IL17C	1,43194879	COL4A2	1,39463038	B4GALNT1	1,32113072	FABP6	1,26864938	CCNB3	1,73215501
2425	NODAL	1,20262355	IRF5	1,26860121	LDHAL6A	1,4521881	MYT1	1,41428968	NKIRAS1	1,33310632	AP2A1	1,28309935	NUMA1	1,76199302	2495	SOCS7	1,19308058	ABCA3	1,2545183	ACTN4	1,4315959	SHC4	1,39454324	NTSC1B	1,32107555	PTPN22	1,2685669	PRPS1	1,73150994
2426	CCR5	1,2024056	ISYNA1	1,26848684	THBS1	1,45194407	MFNG	1,41423455	GABRG2	1,33268449	HMOX2	1,28308613	NSMAF	1,76048271	2496	P4HB	1,19305222	GALNT8	1,25435725	MYCN	1,4313681	TCERG1	1,39453667	KIF3A	1,32077404	TGFA	1,26843119	SOS1	1,73145809
2427	EIF5	1,20233277	GCKR	1,26829244	REPS2	1,45070923	CD69	1,41342953	SCNN1B	1,33232699	CLCA4	1,28283533	RHEB	1,76044569	2497	EPN1	1,19303438	CA5B	1,25429774	NRF1	1,43134038	JAM2	1,39432225	LSS	1,32072723	TCF15	1,26805412	GSTK1	1,73138034
2428	CLDN7	1,2022552	TSPAN7	1,2680336	CCL3L1	1,4500225	CD46	1,41328274	NR0B1	1,33212675	CDC23	1,28262018	REL	1,76029547	2498	PTGS2	1,19303025	SPIB	1,25415563	DNAJB1	1,4311734	PAK2	1,39397933	KCNQ2	1,3204994	DRD2	1,26793552	TIMP3	1,73102582
2429	KCNQ5	1,20221155	CCNG2	1,26800437	CPS1	1,44964084	CD3E	1,41315159	SLC10A1	1,33204025	ANP32A	1,28257982	NT5C2	1,75951803	2499	GPR81	1,19302763	ASMT	1,25405899	BTG1	1,43108583	AKAP10	1,39391169	CCR1	1,32049698	AGMAT	1,26792861	HADHA	1,7297447
2430	ADRA2A	1,20204615	ARHGEF7	1,26757679	PPME1	1,44951769	SHC1	1,41296338	LY9	1,33171907	GANC	1,28194389	PRKCQ	1,75877167	2500	BDKRB2	1,19294704	F11R	1,25371037	OSBP	1,4304706	GYG1	1,39368248	PRPS1L1	1,32021591	ACTR3	1,26778133	YWHAG	1,72917783
2431	DAXX	1,20198502	IFIH1	1,26741032	TOP3B	1,44943243	PI3	1,4127467	ARHGEF4	1,33157608	BNIP1	1,28169467	NAIP	1,75871411	2501	HOXA10	1,19265736	B3GNT4	1,25330716	ZBTB16	1,43043983	IPMK	1,3929683	ITGB4BP	1,32002821	ASPA	1,26765007	CCL22	1,72906163
2432	RAB10	1,20197636	ALDH5A1	1,26733224	DRD4	1,44915739	CHRNG	1,41253478	ITGB5	1,33123004	AGTR2	1,28165246	PI3	1,75838239	2502	GSTO1	1,19261446	IL8RB	1,25321314	TREX2	1,43038091	CCK	1,39293105	IL23R	1,3196898	ITGB2	1,26739215	PREP	1,72895368
2433	GSTM4	1,20195576	RFX4	1,26720255	NDUFS8	1,44881263	CDC20	1,41219738	TAGLN	1,33077011	SPCS1	1,28153153	NEFH	1,75822949	2503	SEC61A2	1,19252053	ADRA1D	1,25313953	IL4	1,4300994	POSTN	1,39290588	TKTL2	1,31925179	GGCX	1,26724293	UCHL1	1,72762631
2434	MSH4	1,20192212	CGN	1,26697532	MCAT	1,44823879	PIGB	1,4114203	ELK1	1,33048022	PIAS3	1,28136126	BCL2L10	1,75793202	2504	ABLIM2	1,19233312	UBE2G2	1,25302644	MYEF2	1,43000615	CASP2	1,39272587	ALG10B	1,31919728	BBS1	1,26711658	PAK1	1,72735153
2435	B4GALT2	1,20185145	PSAP	1,26642346	FZD9	1,44812526	PTPN12	1,41095843	GMPPB	1,3300942	MYLK2	1,28129938	PARD3	1,75750968	2505	PDE2A	1,19231713	ATP6V1H	1,2527545	CA2	1,42984406	NR1H3	1,39261487	MYEF2	1,31905416	ZNF395	1,26708642	RNF2	1,72683463
2436	CTBS	1,20179719	FMO1	1,26625924	ADD1	1,44804701	DLD	1,41022368	PARP2	1,33006571	APOA2	1,28129578	CDC16	1,75724978	2506	PDXP	1,19229125	SERPINB2	1,25273922	IPMK	1,42958278	DPYD	1,3925642	BCL2L10	1,31904018	CD8B	1,26694682	GPR75	1,72676823
2437	YWHAH	1,20173138	SHC4	1,26612043	EPHA4	1,44801894	CPA3	1,41003089	CLTA	1,33006337	CAMK4	1,28109881	CD34	1,75676462	2507	WWTR1	1,19223076	NTHL1	1,25256115	SNAP25	1,42907121	FCER2	1,39235591	CACNA1I	1,31876988	APPL2	1,26690283	IFNGR1	1,72631424
2438	NR4A2	1,20155503	ME3	1,26583874	DHRS1	1,44795342	MYH6	1,40982332	DMC1	1,32964989	FOXO1	1,28095115	GLCE	1,75667609	2508	SIRT4	1,191972	TGDS	1,25246929	FCER1G	1,42847078	SULT1E1	1,39226828	PIGN	1,31876798	CALM3	1,26663223	PTCH2	1,725032
2439	PTGER3	1,20146676	MAP2K1	1,26568424	MAPK8	1,44755768	STX6	1,40981848	SOD2	1,32959929	AICDA	1,28064987	TAF10	1,75651636	2509	STS	1,19166378	SLK	1,25246099	FIGF	1,42764106	PPAT	1,39195813	DNMBP	1,31817597	IKBKE	1,26651691	IFT172	1,72451909
2440	ELOVL6	1,2014493	MAPRE2	1,26541589	PIGF	1,44751508	HNMT	1,40938988	TANK	1,32919166	FZD2	1,28053063	GABRA4	1,75507092	2510	LAP3	1,19137459	BUB3	1,25235527	FEZ1	1,42714722	GZMA	1,39130518	MYL3	1,318136	WT1	1,26626647	HLCS	1,72288944
2441	FAU	1,20131823	BCL11B	1,26532393	CA8	1,44744231	STUB1	1,40888456	RAG2	1,32919001	GRIA4	1,28036111	LYN	1,75502975	2511	CCL3L1	1,19135145	WNT5B	1,25234051	CITED2	1,42704937	TRAF5	1,39089102	DUSP4	1,31810861	HDAC5	1,26610621	DUSP1	1,72214472
2442	ATP5I	1,20131401	CD99	1,2652127	MMP14	1,44738746	CNPY3	1,40808155	NPR3	1,32909129	IKZF3	1,28025218	TBL1X	1,7546231	2512	NES	1,19119367	AXIN2	1,25231586	IL22RA2	1,4270054	MAPK8IP1	1,39062272	AGTR2	1,31646425	TANK	1,26543647	C1ORF142	1,72206527
2443	PRKAR1B	1,20123213	MCM3	1,26518056	GZMA	1,44715669	CTSD	1,40762091	GFRA1	1,32858861	BMP5	1,28017232	ABCA5	1,75457034	2513	ZIC1	1,19109971	VNN3	1,25221768	SYNJ1	1,42697009	SHH	1,39059119	RHEB	1,31615085	KCNJ3	1,26525544	NBL1	1,71899936
2444	OBFC2B	1,20121854	GPLD1	1,26511549	SC5DL	1,446779	ICAM5	1,40716604	TAP1	1,32857006	RAD18	1,27950685	PAX2	1,75448573	2514	HES3	1,19069664	GABRG2	1,2521543	CDIPT	1,42679768	DPPA5	1,38994921	AUH	1,31601414	SULT1C4	1,26484878	ADRA1A	1,71888522
2445	BAI1	1,20083003	RGS19	1,2647273	CACNA2D1	1,44656556	PIGS	1,40698816	CRYAB	1,32848578	ABCG5	1,27907962	TRPC7	1,75318633	2515	THBD	1,19061863	CALM3	1,25213067	BET1	1,42654889	FSCN2	1,38963899	LAMB1	1,31597351	UTF1	1,26484589	COL17A1	1,71885268
2446	PIGO	1,20081776	STRAP	1,26465368	PDE1B	1,44607919	PDE5A	1,40680095	GANC	1,32842465	TLR1	1,27901556	RAP1GAP	1,75313637	2516	CHST3	1,19052507	POLM	1,25165214	FUT7	1,42641334	FAF1	1,38944738	COQ3	1,31587082	DDX50	1,26462603	EBI2	1,7188474
2447	ANPEP	1,20080276	FUT7	1,26450614	TXN	1,44550294	FOXO1	1,40666936	COL24A1	1,32836345	MTHFS	1,27890032	GNRH1	1,75301462	2517	ALDH7A1	1,19003981	SPRED1	1,25153944	WT1	1,42633615	THTPA	1,38925165	ARSD	1,31583616	OSBPL5	1,26445019	THBD	1,71861654
2448	EGR3	1,20075328	GPRC5D	1,26423085	AVPR1B	1,44516462	ITPK1	1,40631402	BCHE	1,32831313	RENBP	1,27865256	F2RL2	1,75274843	2518	CIT	1,19002163	LRPPRC	1,25150303	TRAF3IP2	1,4262968	GRAP2	1,38924067	PKLR	1,31574552	FGF9	1,2643895	HOXA1	1,71841954
2449	EMR3	1,2006607	ISLR	1,26384305	IL18R1	1,44492121	PLCG2	1,40625039	PROS1	1,32814863	DBT	1,27836798	ATG4C	1,75236584	2519	HUS1	1,18990469	RHOQ	1,25128719	SOCS2	1,42618064	GARS	1,38913873	MEIS1	1,31541651	CCL19	1,26391707	FOSL2	1,71812531
2450	GPSN2	1,2002758	ERG	1,26375167	F11R	1,44468977	DUSP6	1,40619768	STAT5B	1,32792245	ERCC5	1,27829201	ACTN2	1,7522814	2520	CALM1	1,18987214	STX11	1,251203	CAPN2	1,42614839	PLAGL1	1,38881851	GABRA5	1,31519679	COL4A5	1,26384294	BAX	1,71790119

Table A4. Pooled-shRNA library screen on HEL cell line and MF-3: list of 2nd most depleted shRNAs for each experiment (ranking approach 1, RA1).

	NO ruxolitinib (setting 1)				Ruxolitinib (setting 2)				Ruxolitinib + CM (setting 3)				MF-3			NO ruxolitinib (setting 1)				Ruxolitinib (setting 2)				Ruxolitinib + CM (setting 3)				MF-3	
	Experiment 1		Experiment 2		Experiment 1		Experiment 2		Experiment 1		Experiment 2					Experiment 1		Experiment 2		Experiment 1		Experiment 2		Experiment 1		Experiment 2			
Rank	*Gene*	*Fold change*	*Gene*	*Fold change*	*Gene*	*Fold change*	*Gene*	*Fold change*	*Gene*	*Fold change*	*Gene*	*Fold change*	*Gene*	*Fold change*	*Rank*	*Gene*	*Fold change*	*Gene*	*Fold change*	*Gene*	*Fold change*	*Gene*	*Fold change*	*Gene*	*Fold change*	*Gene*	*Fold change*	*Gene*	*Fold change*
2521	RGS5	1,18976806	AKAP1	1,25116444	CASP8	1,42603434	TLK1	1,38833972	CYP2C9	1,31502585	COL7A1	1,26365887	CEBPA	1,71789083	2591	YAP1	1,18241092	ARHGEF6	1,24173653	NFYA	1,40811835	GNE	1,37105227	HPRT1	1,30151492	APBB2	1,2522167	B3GALT1	1,67846711
2522	BET1L	1,18970415	SELPLG	1,25116071	ESD	1,425904	MLH1	1,38811836	GAL	1,31492072	PAX5	1,26355953	RBL1	1,71788981	2592	IL17D	1,18232968	IL11RA	1,24163468	NFKBIL1	1,40784871	TRAF4	1,37025815	ATG9B	1,30128396	UGT2A3	1,25205354	MAGI1	1,6777373
2523	GNAI2	1,18962735	AMD1	1,25115725	CAMKK1	1,42468842	OAZ1	1,38810461	LRIG1	1,31475129	IDH3A	1,26339735	MEF2C	1,71719489	2593	EPHB1	1,18204661	DNAJA4	1,24163404	HLA-DOA	1,40777467	CITED2	1,37010804	MAPK11	1,30116161	PSENEN	1,25191006	PCGF2	1,67745988
2524	GOSR1	1,18947059	ACCN4	1,25035226	MAP2K2	1,42399064	PRKDC	1,38777603	CYP27A1	1,31467279	SEMA7A	1,2633285	AACS	1,71706842	2594	IFT172	1,18197837	ABCD1	1,24154248	CDC27	1,40699876	HFE	1,37005447	CCBP2	1,30085907	ACSL1	1,25180565	BMP10	1,67660417
2525	TRRAP	1,18935541	ARG1	1,25034531	P2RY1	1,42393137	ITGA1	1,38775641	ATP6V1B2	1,31461001	IL6R	1,26329428	PGLYRP2	1,71651258	2595	PSEN1	1,18167896	PHC1	1,24105599	APBB1	1,40663565	NR1I3	1,36971806	APPL2	1,30052971	ITSN1	1,25130759	BIRC5	1,67618815
2526	INPP5D	1,18923559	OXTR	1,25029134	BACE1	1,42376811	JAG1	1,38759778	SC5DL	1,3145436	CPSF1	1,26324993	ACOT12	1,71614934	2596	PCYT1A	1,18159653	FBXW7	1,24097493	CNPY4	1,40658347	SRP9	1,36966118	PLA2G7	1,3004119	HOXB6	1,25127437	ABCC5	1,67582428
2527	ACADVL	1,18922375	GHRL	1,25024084	FYN	1,42360041	FOS	1,387021	PTCH1	1,31404171	GAA	1,26323993	DDX56	1,71538682	2597	DDEF1	1,18153539	AMDHD2	1,24089787	UBE2L6	1,40648143	ANXA4	1,36939435	ACTG1	1,30023481	SERPING1	1,25118805	CDK2	1,67545333
2528	IRAK2	1,18916902	BTD	1,25008291	GAB1	1,42325048	CDT1	1,38686555	TGM1	1,31402043	CLDN19	1,26317323	MAPKAPK3	1,71435117	2598	SLC16A3	1,18134781	CAMK2B	1,24071944	DUSP6	1,40635327	ACADM	1,36894087	GALNS	1,30012011	CHRNA6	1,25086129	SLC9A3R1	1,67515508
2529	KCNQ2	1,18913248	RARS	1,24997774	EPPK1	1,42290915	MCF2	1,38678113	PIK3R4	1,31382421	CD2BP2	1,26305001	CPB2	1,71419142	2599	RRM2	1,18128974	EI24	1,24067874	HSPA5	1,4060234	ATG9B	1,36864689	CSF3R	1,29970596	LEPR	1,25084126	BIRC2	1,67470522
2530	MAN2B1	1,1890918	CALML6	1,24995493	RAG2	1,42285467	ITGB3	1,38659268	DERA	1,31371993	EDNRB	1,26303823	DUSP6	1,71413117	2600	SULT4A1	1,18127427	IL21	1,24067874	ECGF1	1,4056296	PRKCA	1,36841977	CEBPB	1,29938179	ADARB1	1,2508088	DCC	1,67464057
2531	HSPA5	1,18898588	HDAC11	1,2498362	TLR8	1,42279013	COL3A1	1,38654983	C13ORF15	1,31350416	PLIN	1,26283969	RET	1,71368008	2601	SOCS2	1,18122161	PIGQ	1,24009868	GNAI2	1,40507921	MIOX	1,36841157	DDX51	1,29889423	FGL2	1,25073913	MSR1	1,67461774
2532	PDIA3	1,18889239	GDF3	1,24976843	BAG3	1,42265973	NPEPPS	1,3863793	EHD2	1,31306077	NMNAT2	1,26282484	BCMO1	1,71354415	2602	APOC2	1,18114541	NDUFV2	1,24005855	WASL	1,40479859	TXN	1,36838923	EPHA4	1,29888063	YWHAH	1,25045976	RASGRP3	1,67384485
2533	PTGDS	1,18878711	RAPGEF1	1,24971492	UBE2V2	1,42257167	ITGB1BP3	1,38485663	ATP1B2	1,3129252	CRHR1	1,2624748	C4BPB	1,71260647	2603	HSD17B2	1,18108647	DPP4	1,24001393	MYOG	1,40476192	ACOX2	1,36757505	CAPN11	1,29862932	QARS	1,25032633	CACNA1A	1,6734697
2534	ABCG5	1,18875265	ABL1	1,24966815	UGT1A7	1,42255392	BCAR1	1,38456713	EDG4	1,3128801	HTR3B	1,26244401	PSAT1	1,7123495	2604	DDR1	1,1808485	LXN	1,23982695	P2RY5	1,40457333	BAK1	1,36735975	FGR	1,29826473	DDX54	1,25027239	CAST	1,67148594
2535	ATP2B3	1,18865129	GFPT1	1,24966815	ASRGL1	1,42226468	HOPX	1,38442339	POLR3K	1,31278602	FLAD1	1,26191028	EARS2	1,71219346	2605	SHC2	1,18080844	BTK	1,23975357	B4GALT7	1,40439707	FGF4	1,36728564	HAGH	1,29809132	GLUD2	1,24976082	CCNI	1,6710078
2536	MPG	1,18851931	HTRA2	1,24962867	ATP6V1G3	1,42182291	PLEC1	1,38374498	RAB1B	1,31274735	ZFP36	1,26182587	ACE2	1,71183676	2606	MCF2	1,18072229	FOXD3	1,23973752	CASK	1,40420396	METTL6	1,36678572	PADI2	1,29804112	ALG9	1,24959307	ATP5O	1,67086592
2537	HS2ST1	1,18845969	SH3KBP1	1,24952743	NP	1,42164532	SCD5	1,38364266	HDAC11	1,31274395	COL1A1	1,26178039	BCHE	1,71069589	2607	NDST2	1,18067544	ATP2A1	1,23939358	FDXR	1,40413317	ITPR3	1,36670573	GNAZ	1,29722405	PAWR	1,24934519	TAF2	1,67076777
2538	SRP72	1,18826284	HGFAC	1,24888571	SCN2B	1,42162129	B3GALT4	1,38353398	IRF9	1,31258071	IQGAP2	1,2617052	ATXN1	1,71037026	2608	POU2AF1	1,18063412	MAML1	1,23914507	SARM1	1,4038378	CCR6	1,36665612	TNFRSF1B	1,29680974	SLC25A1	1,24922954	SHMT1	1,66983243
2539	HIST1H2AA	1,18819326	TM2D1	1,24867729	KITLG	1,42158325	YWHAQ	1,38340176	NR1H4	1,31233695	MYB	1,26129995	CARS2	1,71035801	2609	PROM1	1,18038494	FCER1G	1,23906615	GDI2	1,40378984	DVL2	1,36629559	TLR1	1,29661058	PON3	1,24915591	EPO	1,66934457
2540	AP3B1	1,18801962	PROCR	1,24840315	ACTN1	1,4212943	PRDX3	1,38308247	IFI30	1,31206971	SAT1	1,26129291	RERE	1,70989793	2610	SCN4A	1,18029208	GABRA2	1,23896263	HRH4	1,40334715	GPAA1	1,36606591	TRAF4	1,29660606	NBL1	1,24895615	FABP6	1,66932845
2541	ZMAT3	1,18780365	SCNN1B	1,24830251	ATP6V0D2	1,42128282	TTR	1,38286341	CLCA4	1,31179995	PAG1	1,26126008	EGLN1	1,7089767	2611	UST	1,1802412	IBSP	1,23841225	AP2B1	1,40306385	AHSG	1,36593577	SMPD1	1,29620599	DMD	1,24841211	IFNE1	1,66823585
2542	PIK3CB	1,187746	NT5M	1,24810054	EBI3	1,42119161	RECK	1,38278041	ZFX	1,31146152	SETDB1	1,26118728	TRAF6	1,70823061	2612	ATP5B	1,18009035	IL12RB2	1,23827237	SIRT7	1,40255241	MARCO	1,3658919	IL17RD	1,29596736	MAN1A1	1,24837782	CTNNBIP1	1,668038
2543	HES6	1,1877386	ATP5O	1,24801379	MLYCD	1,42089827	TRPM7	1,3825032	LRPAP1	1,31143901	ACSM1	1,26080632	FASLG	1,70815863	2613	LILRB3	1,18004545	MOBP	1,23815539	CCL1	1,40232016	FUT6	1,36488996	COL7A1	1,29582809	STEAP3	1,24834377	MAP3K4	1,66749242
2544	SFRP2	1,18733653	OTUB1	1,24799462	RASAL1	1,42025005	CDC7	1,38199727	PPP1CB	1,311273	CACNA1S	1,26057273	SIRT4	1,70601103	2614	MYL2	1,17999741	CD22	1,23800338	HAP1	1,40203392	SULT1A2	1,3647535	NDUFB8	1,2956253	B3GALT5	1,24824613	ATN1	1,66669185
2545	ESD	1,18723436	IL13	1,24798873	PDE2A	1,41991708	TDG	1,38170528	DPF2	1,31115816	LMNB2	1,26056121	DKK4	1,70580931	2615	NOS3	1,17997111	HEXB	1,2378732	EMR3	1,40194632	BLM	1,36472039	UBE2E3	1,29561735	CYP3A5	1,24811001	HTRA2	1,6665575
2546	ARHGDIA	1,1871876	HOPX	1,24791332	MAG	1,41987068	NUDT12	1,38153284	GNE	1,31076193	ATP12A	1,26049325	MTHFS	1,70379915	2616	IFI30	1,17993208	PIAS3	1,23780883	OPRL1	1,40188331	CTBP2	1,36461183	KREMEN1	1,29557713	PLA1A	1,247686	CAD	1,66630651
2547	TCF3	1,18711042	HDAC4	1,24780862	PLA1A	1,41981716	GPX4	1,38124355	CD5	1,31062033	UBE3A	1,26036942	PRKCG	1,70334678	2617	SDHD	1,17980782	PLAU	1,23768489	OLA1	1,40095578	PLIN	1,36454748	POLG2	1,29535572	SPRED2	1,24736509	ARPC4	1,6661345
2548	HPGD	1,18701834	FADS1	1,24750978	HNMT	1,41887785	HLA-B	1,38114267	SERPINA4	1,31058617	IL2RA	1,26020479	CASP10	1,70251848	2618	NEUROG3	1,17971317	GABARAPL1	1,23756517	GALNT4	1,4008917	ALOX15B	1,36448178	ASPH	1,29524855	IL5RA	1,24707088	HMBS	1,66589863
2549	FANCI	1,18689295	EXT1	1,24735133	FZD10	1,41864373	GH1	1,38107121	TBK1	1,31029527	RDH14	1,26015305	FEN1	1,70125332	2619	PARP1	1,17971169	TOP2B	1,23731963	CAMK1G	1,40059702	UVRAG	1,36438806	SERPINB2	1,29524855	ENPEP	1,24677814	ARFGEF2	1,66587955
2550	MAP3K7IP1	1,18663752	SOD2	1,24731914	HLA-DQB1	1,41824574	PRMT6	1,38085448	GNRH1	1,31022572	PTPRF	1,259819	LRRK1		2620	PIAS4	1,17970769	BAK1	1,23725034	DAPP1	1,40053243	TLR7	1,36410054	BACH1	1,29523186	CTCF	1,24666239	MYBPC2	1,66565079
2551	PPP2R2A	1,18655745	SOX17	1,24720873	TRIM21	1,41802956	SEC22B	1,38045275	CDH1	1,31005163	GSTK1	1,25937415	ADRB2	1,69989041	2621	MGAT1	1,17970225	BRCA1	1,23716891	APOB	1,40026246	SOX4	1,36405897	CD79A	1,29498232	CHRNB1	1,24624577	ST8SIA1	1,66460122
2552	GP5	1,18645236	CSF2RB	1,24717798	SLC18A3	1,4177034	SSTR3	1,3799932	BCL3	1,30932109	ACVRL1	1,25921435	ROR2	1,69917166	2622	ACOX2	1,17953002	CPSF3	1,2368394	CYP11A1	1,39948425	MSH2	1,36397937	EDA	1,29473835	NAGS	1,24517957	GABRG1	1,66310485
2553	IL10RB	1,18621951	GCDH	1,24702587	CLDN11	1,41733259	SEL1L	1,37963535	CSF2RB	1,30888342	EIF2B2	1,25890186	SLC22A18	1,69910333	2623	HPR	1,17948057	BLR1	1,2365467	ATP2B2	1,39911323	MLYCD	1,36393121	BMPR1B	1,29472191	ERG	1,24514824	ATG2B	1,66238431
2554	CHEK2	1,18616137	MARCKS	1,24682193	ARHGEF12	1,41725328	PDIA3	1,37910925	PDE11A	1,3088579	CYP7A1	1,25888273	NLK	1,69839205	2624	MAP3K1	1,17934096	LYCAT	1,23647295	CIDEB	1,39881584	PARP1	1,363923	T	1,2943967	FTH1	1,24498714	UPK1B	1,66233158
2555	LDHAL6B	1,18615503	PIK3C3	1,24674441	PPP1CB	1,41715805	F8A1	1,37895026	FUCA1	1,30849686	ENPP7	1,25881909	XRCC5	1,69787867	2625	ELOVL5	1,1792808	GAB2	1,23569	CD19	1,39857393	EPHA2	1,36381214	IFNGR1	1,29432366	POLR3B	1,24475579	HIP2	1,66217954
2556	ABCD2	1,18599711	AGER	1,24661214	DHRS3	1,41703761	BCL2L2	1,37846177	CLDN17	1,30826104	IL12RB2	1,25873717	F9	1,69758017	2626	CYP4F12	1,17913173	AK3L1	1,2356532	PLD3	1,39854268	NKIRAS1	1,36350311	GPT	1,29373498	GABRG2	1,24444165	TAF13	1,66145526
2557	IL2RG	1,18570753	PRKAA2	1,24653431	ZAP70	1,41686146	SUPT6H	1,37826779	GSTP1	1,30796019	CITED2	1,25805752	AQP7	1,69740729	2627	ZEB2	1,17908872	HESX1	1,23554076	MAFG	1,39843479	DAB2	1,36317817	PLCB1	1,2933834	ACSS2	1,24404421	GNA11	1,66144751
2558	KIAA1394	1,18567803	WISP2	1,24624852	PARP2	1,41682914	SREBF1	1,37825772	PPIC	1,30785593	PLSCR4	1,25805317	MAFK	1,69723348	2628	CENTA1	1,1790866	RPN1	1,23538911	KCNA5	1,39780518	PRKRIR	1,36316339	NR1I2	1,29329438	B3GNT4	1,24375482	EPHB4	1,65992776
2559	PARG	1,18560273	NMUR2	1,24611766	FDPS	1,41656647	PROZ	1,37804216	NSDHL	1,30766316	NDNL2	1,25793113	HEXA	1,69608486	2629	GALK1	1,17905825	TRIM21	1,23518537	PTGS2	1,39769827	GRID2	1,3630336	IRF5	1,29327189	PSCD2	1,24330694	CTBS	1,65670135
2560	TFRC	1,18557438	EGR3	1,24563558	ALKBH2	1,41628478	AASS	1,37803742	NEK2	1,3076298	GPRC5D	1,25721323	TXLNA	1,6957185	2630	ADARB1	1,17897808	UFR	1,23512609	IL8	1,39730425	POLG2	1,36289811	COPA	1,29326242	HTRA2	1,24302123	CA2	1,65513352
2561	GLP1R	1,18524053	CKS1B	1,24561054	RPIA	1,41594595	GRM1	1,3779217	EPHX1	1,30754823	ADH1A	1,25713051	MIB1	1,69402545	2631	ARSB	1,17889406	EPN1	1,2351211	MEFV	1,39717982	VHL	1,36287758	FCGRT	1,29319789	TAF10	1,24296485	PALB2	1,6548974
2562	LMO1	1,18497243	OAZ1	1,24508307	FAM132A	1,41560069	CLDN20	1,37768087	RBBP8	1,30711561	MUS81	1,25700608	CCNC	1,69363578	2632	LHX2	1,17880265	T	1,23501199	NPC1	1,39683275	YES1	1,36280921	SMARCE1	1,29314192	CDK9	1,24285472	ANP32A	1,65463646
2563	FZD2	1,18484389	CLDN20	1,24490142	CD72	1,41541166	UGT2B10	1,37718091	HSPA8	1,30709475	SOX4	1,25688731	CHDH	1,6932276	2633	SLC1A3	1,17871474	PDE3B	1,23499171	PDGFRA	1,39653355	HCST	1,36273902	IDE	1,29309771	MSR1	1,24247435	LMNA	1,65418672
2564	HPSE	1,18474463	EDNRB	1,24483517	PRKCI	1,41506758	SIRT7	1,37669313	IDH2	1,30701089	ALG5	1,25686954	ADRBK2	1,69308634	2634	TRPM4	1,17870415	AZIN1	1,23495951	PFKFB4	1,39619315	PAWR	1,36244002	ACSM1	1,29303991	SULT1A2	1,24240267	PDE1C	1,65371262
2565	CHD8	1,18472033	NFATC1	1,24463381	THTPA	1,41491994	PKN2	1,37658555	ACVR2B	1,30681501	ATP1A4	1,25686945	MAPKAPK5	1,69293809	2635	MAML1	1,178648	RAP1GAP	1,2343613	SMUG1	1,39602223	GTF3C3	1,36239889	PCNT	1,2929027	PRMT6	1,24211883	MVP	1,65313923
2566	AP3M1	1,18457386	ETV6	1,24450179	GTF2F2	1,41456327	PTH2R	1,37618634	APOD	1,306772	SELPLG	1,25665584	FZD8	1,69244846	2636	H2AFX	1,17855924	CD180	1,23433293	SRD5A2	1,39576849	SCN1A	1,36171811	CXCL11	1,29268257	FCER2	1,24205708	SLC30A8	1,6529026
2567	OXA1L	1,18444561	TDP1	1,24445121	MADCAM1	1,41452655	GSTM5	1,37606113	PLA2G4C	1,30665591	CLDN17	1,25658837	IRAK1BP1	1,69161827	2637	CCDC6	1,17837621	NDRG2	1,23409319	SDC2	1,39519791	CNTFR	1,36118577	PRDX1	1,29258707	T	1,24205554	PRMT7	1,65289986
2568	RFX4	1,18433094	CD40LG	1,24444805	CACNA1S	1,41416282	SYNJ1	1,37595075	C4B	1,30644913	EED	1,25653077	JAK1	1,6905253	2638	BUB3	1,17795659	EGLN1	1,23408147	MSH6	1,39494817	TPO	1,361104	EN1	1,29238172	GAD2	1,24199908	CCL19	1,65276118
2569	SERPINE2	1,18428372	RANBP9	1,2443239	NAT5	1,41407669	MAPK13	1,37582585	TOB2	1,30634991	CDKL2	1,25614497	PPP2R5D	1,69052121	2639	BCAT2	1,17781589	SEC61A2	1,23394495	PPP1R3A	1,39494817	MTHFS	1,36106701	CHST12	1,29231883	CES7	1,24150805	TARDBP	1,65276118
2570	SPO11	1,18422186	EPHX2	1,24425492	TNFRSF11A	1,41326685	ATM	1,37554118	DTX3	1,30632312	CYP2B6	1,2558622	DARS	1,69024394	2640	ASAH3L	1,17752338	PDGFRB	1,2337738	CERK	1,39494363	CCL7	1,36096216	IL15RA	1,29207639	MBD1	1,24128491	GLI2	1,65203
2571	PDE4D	1,1839529	ARF3	1,24417288	PRDX4	1,4130033	ABCD3	1,37541925	MX1	1,30587036	AUH	1,25580567	CRK	1,69020231	2641	CTSD	1,17751794	RBPJ	1,23368502	PDIA3	1,39455319	MSH4	1,36085427	IKZF3	1,29207119	AGPAT4	1,24126172	MEF2A	1,65189944
2572	PTPRB	1,18382644	CAMK2G	1,24390791	STH	1,41267922	RPS6KA5	1,37535586	DDO	1,30571639	SESN3	1,25574714	CLTCL1	1,68980729	2642	POLR1A	1,17732636	SCN7A	1,23365319	GPR68	1,39443814	EMP1	1,36059987	PCNP	1,29205327	MMAB	1,2411151	HDAC3	1,6518911
2573	RGS19	1,18372876	DAO	1,24372303	BCL2L2	1,41258734	DCTN1	1,37527747	MAP2K7	1,30551664	PLG	1,25561394	PRKAB2	1,68965126	2643	ABCC3	1,17721116	AQP7	1,23339555	GAL	1,39395666	SLC25A1	1,3605689	CBX7	1,29202337	AMHR2	1,24110169	CPT2	1,65083896
2574	FBLN2	1,18356584	TLR1	1,24367751	BHLHB8	1,41216222	GRB7	1,37477181	APOBEC3B	1,30549366	MAPK8	1,2554304	IHX8	1,68849454	2644	ISG15	1,17704705	SCG2	1,23339196	DDX1	1,39359988	SRP72	1,36027603	TRIM25	1,29200891	MBD4	1,24094199	DLX6	1,65081189
2575	NDUFA1	1,1835496	CRYAB	1,24361239	DEDD	1,4120392	THRB	1,37444777	CD80	1,30547433	PECAM1	1,25539844	AQR	1,6882691	2645	NDUFA8	1,1768724	SOD1	1,23336384	WNT6	1,39352994	COL13A1	1,3598982	PIK3CA	1,29187259	MECP2	1,24089666	LRP6	1,65075379
2576	ALDH1A2	1,18352623	HLA-DRB1	1,24329167	RAD54B	1,41200121	CXCR3	1,37421323	NFATC4	1,30461343	DARC	1,25538223	ADAR	1,68775277	2646	RHOA	1,17643978	SYNE1	1,23319236	HHIP	1,39330931	IL7R	1,35979492	CBR3	1,29181814	ANGPTL2	1,24064562	GSTA1	1,65067159
2577	COL4A5	1,18346748	BMP7	1,24326247	FOXA1	1,41104148	TPH1	1,37417276	HHIP	1,30411994	CD3EAP	1,25518673	RECQL4	1,68727155	2647	NRG3	1,1762277	F2RL2	1,23263251	YWHAQ	1,39330652	REPS1	1,35919061	MEST	1,29139952	WDR79	1,24051588	SMAD1	1,65043178
2578	TNIP2	1,18346413	CHST3	1,24300693	BECN1	1,41097289	CDKN1B	1,37401084	RAD50	1,30403259	SHC2	1,25500856	ABCA2	1,68648896	2648	ADH4	1,17598645	TGFBR1	1,2322977	UCP1	1,39329725	FHIT	1,35870904	ACSS2	1,29109854	APOBEC4	1,2402488	CAND1	1,65031497
2579	ERG	1,18336441	MYC	1,24300693	UBTF	1,41092773	CRHBP	1,37386008	CISH	1,30360879	ANAPC11	1,25437393	CPA3	1,68550511	2649	ELAVL1	1,17597258	DTYMK	1,23218187	CITED1	1,39309047	RPIA	1,35844868	DDR1	1,29041498	ALDOB	1,24009627	FABP7	1,64943492
2580	EEF1D	1,18318286	NDUFS7	1,24283843	SLC15A1	1,41069535	P4HB	1,37356672	SERPINF2	1,30343475	CYP27B1	1,2536807	ABL2	1,68384745	2650	REG3A	1,17594261	RAB27A	1,23212287	ANP32A	1,3929172	CCND3	1,35839092	NDUFB4	1,2901694	CLTCL1	1,24002836	STS	1,64881633
2581	MYEF2	1,18312292	NR2C2	1,24261156	ITGB2	1,41067015	ATF5	1,37355232	NPC1	1,30330087	PRKAR2A	1,25350901	PDCD2	1,68331243	2651	POLE3	1,17588977	ABCG5	1,23197409	HMGCS2	1,3923921	HR	1,35839092	INS	1,29001472	MAP3K13	1,23989554	GLRX2	1,64833188
2582	HMOX1	1,18307272	BBC3	1,24260776	EDN1	1,41050531	ADFP	1,3725409	POU2AF1	1,30325024	TLR5	1,25349417	UNC13B	1,68294343	2652	LTB4R2	1,17559277	RELA	1,23193525	CLDN10	1,39236987	ACPP	1,35722122	STAT6	1,29000167	ARHGEF2	1,2397398	CD207	1,64812438
2583	CXCL9	1,18297848	CCNE1	1,2425799	SOS2	1,40996604	HOXA10	1,37243681	CAMK1	1,30276135	GPT	1,25342671	TOP1	1,68260449	2653	LARS2	1,17556802	TGFB3	1,23185871	IRF2BP1	1,39229738	LDB1	1,3568688	SCG2	1,28996472	MPG	1,23957659	MAOA	1,64728771
2584	C9ORF47	1,18290227	TGFB1	1,24234149	PROX1	1,40993747	ATP6V1H	1,37228232	ABCA12	1,30223953	PFN1	1,25341105	CCL1	1,68101635	2654	COL4A4	1,17549952	STAMBPL1	1,2317689	CHRNB1	1,39226944	INHBA	1,35671758	RERE	1,28988544	ABCA9	1,23927558	RAC3	1,64697739
2585	REV3L	1,18264033	DACT1	1,24232613	IFIT1	1,40925783	FMO4	1,37223792	SH2B2	1,30211529	NOS3	1,2531705	HEXB	1,68012129	2655	NUDT12	1,17545132	VNN2	1,23170618	HMOX1	1,39174972	STRAP	1,35636355	HOXA11	1,28984419	GRK4	1,23885646	ATP6V1E1	1,64688085
2586	ADIPOR2	1,18262325	CD9	1,24222274	PGLS	1,40925398	HLA-C	1,37201287	ABCD1	1,30209315	TPP1	1,25312443	SIRT2	1,67969336	2656	ACYP1	1,1753935	MYB	1,23160292	NPEPPS	1,39125028	CCNE2	1,3562470	TRAF5	1,28973802	CHST12	1,23863423	MAN2C1	1,64660754
2587	CDKN2D	1,18259915	LRP1	1,24218159	FHL5	1,40895223	ATP13A2	1,3719259	HES3	1,30206157	RAB7A	1,25293377	IL9	1,67947292	2657	VAMP2	1,17538071	XRCC3	1,23134346	COL3A1	1,39121517	BLMH	1,35608234	DSP	1,28955188	PBEF1	1,23842061	IL15	1,64612685
2588	MEF2A	1,18255979	ALDH4A1	1,24217565	CLK4	1,40892302	CFHR1	1,37172384	EREG	1,30170084	TRPC7	1,25263292	CUZD1	1,67904826	2658	ANKHD1	1,17529579	PPP1R3A	1,23111743	IL15RA	1,3901114	BNIP3	1,35597624	IL17C	1,28946036	CRLS1	1,23837444	BMI1	1,64600108
2589	DRD2	1,18255336	ATF3	1,24198631	ABCA4	1,40828227	XBP1	1,37112103	HOXA10	1,30158485	MGAT5	1,25236483	TP53BP1	1,67885383	2659	MAP1A	1,17520753	TUBB2C	1,23043935	C6	1,39002384	SULT1A1	1,35586689	YWHAG	1,28936602	PLD1	1,23836973	CD93	1,64583126
2590	TIMP4	1,18251083	APOD	1,24188973	CDC6	1,40825476	ID4	1,37110166	ATF2	1,30155214	CHRD	1,25236022	DCP1A	1,67879232	2660	CA12	1,17511919	BDNF	1,23027236	PC	1,39002305	IRF7	1,35580931	MECR	1,28814354	COASY	1,23833333	PPARG	1,64571036

Table A4. Pooled-shRNA library screen on HEL cell line and MF-3: list of 2nd most depleted shRNAs for each experiment (ranking approach 1, RA1).

	NO ruxolitinib (setting 1)				Ruxolitinib (setting 2)				Ruxolitinib + CM (setting 3)				MF-3				NO ruxolitinib (setting 1)				Ruxolitinib (setting 2)				Ruxolitinib + CM (setting 3)				MF-3	
	Experiment 1		Experiment 2		Experiment 1		Experiment 2		Experiment 1		Experiment 2						Experiment 1		Experiment 2		Experiment 1		Experiment 2		Experiment 1		Experiment 2			
Rank	Gene	Fold change	Gene	Fold change	Gene	Fold change	Gene	Fold change	Gene	Fold change	Gene	Fold change	Gene	Fold change	Rank	Gene	Fold change	Gene	Fold change	Gene	Fold change	Gene	Fold change	Gene	Fold change	Gene	Fold change	Gene	Fold change
2661	ENTPD3	1,17509807	POLK	1,22990491	KCNMB4	1,38977261	MAP3K4	1,355771	CFHR3	1,28812044	SLC23A1	1,23827134	NPC1	1,64561892	2731	AGXT2L1	1,16618035	CASP7	1,21843176	PROCR	1,37044024	ALDH3A1	1,34069214	CASP9	1,27324458	GSTO1	1,22711206	GUCA1C	1,61633715
2662	CERK	1,17489601	TRPV6	1,22971525	TAF1L	1,38970977	ITGB6	1,35508859	RASGRF1	1,28777186	ELAVL1	1,23806559	ACIN1	1,64502425	2732	NCKAP1	1,16602057	HDAC8	1,21836242	COQ3	1,37024418	PRDX6	1,34064304	ATF5	1,2731764	CGN	1,22710626	ATP6V1C2	1,61586136
2663	SMAD5	1,1746802	PTPRF	1,22889188	MFNG	1,38918218	ALG8	1,35486044	HADHA	1,2877248	ISYNA1	1,23805796	GFRA1	1,64492948	2733	CALB1	1,16598638	RAP1B	1,21831244	MAP2K3	1,36962153	SIM1	1,33988026	CALML3	1,27312075	ADFP	1,2270325	BMP1	1,61541089
2664	KIF5B	1,17466712	COL5A1	1,22867542	APOC1	1,38906521	NOD1	1,35478289	IFIT3	1,28734556	AKR1A1	1,23770684	APLN	1,64444743	2734	PKN2	1,16588077	THTPA	1,21819323	PSEN2	1,36937312	CASP10	1,33987099	CEBPD	1,27291626	NR4A3	1,22697641	CUL1	1,61525537
2665	TDP1	1,17463791	PRDX6	1,22853943	AKR1D1	1,38901236	CLEC7A	1,3547061	ARRB2	1,2869153	DLL4	1,23741537	BDH2	1,6443978	2735	TGM3	1,16575094	KCNJ12	1,21800326	SESN1	1,36899336	HTR6	1,33964391	PAH	1,27282883	CTTN	1,22662243	ENPP2	1,61512213
2666	CALML5	1,17461173	CCR6	1,22827953	PPP1R13B	1,38872183	AMHR2	1,35467097	ORM1	1,28686649	NFATC1	1,23740851	MGP	1,64382457	2736	A4GALT	1,16546029	ADH1C	1,21794094	ETV6	1,36873826	ECE2	1,33886823	ALPP	1,27171572	IL17RE	1,22638005	SMURF2	1,61504694
2667	NFATC1	1,17454294	POLD4	1,22814253	TAAR6	1,388712	EIF2B1	1,35426718	TRAF3IP1	1,28673966	ADC	1,23722575	TMEM166	1,6437537	2737	EMR1	1,16543182	AASS	1,21784635	SLC1A7	1,36824288	CETN2	1,33855841	NDUFS7	1,27160331	PLCB3	1,22629855	HMGB3	1,61487522
2668	DRD3	1,17436942	KALRN	1,22789827	WASF2	1,38817953	ACHE	1,3538861	AP3B1	1,2865163	PDHA2	1,23721923	HESX1	1,64314249	2738	GSN	1,1653813	FAT	1,21778693	UCP3	1,36792576	SALL4	1,33855494	WRN	1,27158805	GH1	1,22600981	ATG2A	1,61443407
2669	ALDOA	1,17435079	CCNB2	1,22787098	DHODH	1,38748233	CSRP1	1,3538786	RAB5A	1,28644365	SLAMF1	1,23673788	PAWR	1,64280232	2739	CYP3A7	1,16517876	ELK3	1,21721935	KEAP1	1,36777481	MYH3	1,33838873	S100A12	1,27146807	TCF4	1,22590847	AGT	1,61377897
2670	PICALM	1,17408284	NSMAF	1,22783882	CREBBP	1,38735291	WT1	1,35376147	WT1	1,28604281	PKN2	1,23660782	PGA5	1,64263045	2740	UGT2A1	1,16511043	BCAT2	1,21721753	ITGA9	1,36771761	PFKFB1	1,3383695	SRM	1,27146247	APLP2	1,22566133	SMCHD1	1,61364557
2671	PIK3C2A	1,17407087	MAFG	1,22763579	NBN	1,38725112	GYS1	1,35372837	CCNE2	1,28599976	AGPAT1	1,23636576	NPEPPS	1,64168287	2741	ENPP6	1,16508924	ACY1	1,21719679	NR4A3	1,36732768	TRIM28	1,33829053	MASP1	1,27144837	PALB2	1,22552674	WNT4	1,61304753
2672	HDC	1,17400644	DAP	1,22762946	QPRT	1,38720153	ITGB2	1,35362394	G6PC2	1,2856475	RAD17	1,23632591	AVPR1A	1,64118905	2742	NCL	1,16494213	TP53	1,21679592	TACR3	1,36694683	AURKB	1,33813163	GABRB3	1,27137764	UGT1A1	1,22547219	ITGB3	1,61280724
2673	ME2	1,17396555	DNTT	1,22748739	PRKCB1	1,38718327	IL17RB	1,35353156	FAF1	1,28520843	EPAS1	1,23622612	SDC2	1,64061448	2743	XK	1,16493061	ALG13	1,21663702	CES7	1,3666826	MAFB	1,33775252	CD2AP	1,27076079	SLC6A2	1,22543346	CBX4	1,61187567
2674	NADK	1,17394278	CHAT	1,22740869	UCHL1	1,38712827	NKD1	1,35346923	CFP	1,28517378	TPMT	1,23613705	PDE6H	1,63999438	2744	SERPINE1	1,16478016	RPS6KB2	1,21658248	NCOR1	1,36643967	RXFP1	1,33757922	FRAP1	1,27014377	IFI16	1,22533223	KIT	1,61154678
2675	KPNA2	1,17378289	CTNNBIP1	1,22738364	SORBS1	1,38696788	KHK	1,35324885	GCGR	1,28504652	CTSS	1,23606219	COMT	1,63977548	2745	CREBBP	1,16469389	NRG2	1,2165395	NMU	1,3659408	ICAM2	1,33753464	S100B	1,2700869	CDS2	1,22526793	REV1	1,61133614
2676	TIMELESS	1,17368327	SERPING1	1,22725484	PANK4	1,38664138	PON2	1,35323498	ORC5L	1,2844246	BECN1	1,23588836	MBP	1,63971849	2746	DGKD	1,16458298	AES	1,2163934	IL6ST	1,36582137	NOG	1,3374762	BMP15	1,26995023	ELA2B	1,22521623	HLX	1,6111147
2677	SLC5A3	1,17362708	INPP5D	1,22707347	FARSA	1,38605214	ZMAT3	1,35248138	TMEM166	1,28414193	SMC6	1,23565204	KCNMB3	1,63957801	2747	SRD5A2	1,16458254	ORC5L	1,21618307	GABRB1	1,36532642	OGFR	1,33733721	TMED10	1,26986783	SNAP23	1,22500004	SUFU	1,61102004
2678	PCYT1B	1,1735799	B4GALT7	1,22652724	ST3GAL4	1,38553204	POLR3H	1,35188689	PEBP1	1,28373459	UBE2E1	1,23565204	NOS1	1,6395443	2748	CES2	1,16436307	CYP19A1	1,21590672	CRYAB	1,36520031	TNFSF11	1,33634965	FUT7	1,26899823	C1RL	1,22456008	CREB5	1,61062909
2679	STX17	1,17354853	MEF2D	1,2264824	TARDBP	1,38520858	PRKD3	1,35142562	SLC12A2	1,28361039	PCK1	1,23551975	DDIT3	1,6385941	2749	RAB35	1,16404693	CLN3	1,21579621	CTPS2	1,36425296	PCK2	1,33555141	PDHA1	1,2686094	TNFRSF19	1,22447003	ITPR2	1,61020311
2680	FAF1	1,17305215	ANKFY1	1,22627857	FPGT	1,38468119	APEX1	1,35115937	GPR64	1,2834337	YWHAZ	1,23531931	KPNA2	1,63855767	2750	PMCH	1,16388212	MRE11A	1,21579534	HGD	1,36340471	NUP153	1,33546594	NEIL1	1,26816534	CLEC10A	1,22429782	COL15A1	1,61009724
2681	ABCC8	1,17298604	ENPP3	1,22627543	HSPA8	1,38458373	CDH2	1,35112858	ETV7	1,28338879	ORC4L	1,23522053	BFAR	1,638515	2751	FBLN1	1,16363599	UBE2V2	1,21578342	TOP2B	1,36294828	BFAR	1,33543639	CUL2	1,26707269	ADRA1A	1,22399315	PGD	1,60996685
2682	PRDX6	1,17282706	TREH	1,22598048	F13A1	1,38451243	EPAS1	1,35023563	CACNA2D1	1,28327933	SMAD7	1,23515734	PSMB6	1,63806704	2752	IBSP	1,16362608	CLTC	1,21569141	B3GAT1	1,3628662	PAH	1,33510894	C2	1,26675207	HYOU1	1,22389028	GPC5	1,60981889
2683	IGF2	1,17272997	SHC2	1,22588374	RFX5	1,38366072	CRAT	1,34981233	SEC61A2	1,28304434	GRIK4	1,23514345	STX12	1,63557892	2753	TUBB2A	1,16333649	VISA	1,21549458	NKIRAS1	1,36278606	IRAK1BP1	1,33505101	ERAF	1,26655046	PTH2R	1,22362754	REXO2	1,60975875
2684	RAP1B	1,17257284	MCM4	1,22562647	NDST1	1,38312743	B2M	1,34950241	AANAT	1,28301198	TLR3	1,23506164	SELP	1,63533793	2754	SERPINC1	1,16329045	BCL2L10	1,21514539	ACE2	1,36271628	PPM1D	1,33490351	RNASE1	1,26640386	IFNA17	1,22345224	CHN1	1,6092405
2685	PDHA2	1,17253073	CDKN1C	1,22543524	APOA4	1,38306379	FBXW11	1,34926912	MAPK10	1,28281618	HSF2	1,23506012	DDX19A	1,63507996	2755	PGF	1,16305523	PROC	1,21513936	PGR	1,36218913	AGPAT2	1,33488692	CBS	1,26584536	NLRP2	1,22344286	NF1	1,6072006
2686	SLC32A1	1,17247581	NDUFB5	1,22538214	GCH1	1,38281961	DERA	1,34915416	COL15A1	1,28250754	TNFRSF9	1,2347813	STAT6	1,63471455	2756	PDPK1	1,16288538	APOA2	1,21504652	FLOT2	1,36215456	UXS1	1,33481676	MIOX	1,26583405	SHISA5	1,22334149	GALNAC4S-6S	1,60695634
2687	APOC3	1,17226418	CSF3R	1,22536182	MAN2B2	1,38268075	SMC6	1,34915416	MAP3K12	1,2824619	CREB3L2	1,23452428	MEF2B	1,63456398	2757	SCN4B	1,16278316	FCER2	1,2150309	IKBKE	1,36203362	XCR1	1,33406309	TGFB2	1,26573899	FRAP1	1,22307592	DHRS4	1,60655831
2688	RPS6KA5	1,17217578	HNF4A	1,22509228	ACOT11	1,38168635	GPR34	1,34880707	NEURL	1,28232771	DIO2	1,23425688	ERN2	1,6344531	2758	IL2RB	1,16276378	CHST6	1,21480837	C5	1,36193524	RBP4	1,33391419	STMN2	1,2654045	EGR1	1,22301743	EEF1A2	1,60559927
2689	PPP2CA	1,17209183	CDX1	1,22490298	CHGA	1,38165518	ZBTB32	1,34850004	BDH2	1,28216497	PIK3R1	1,23422457	ATP4A	1,63347897	2759	AFP	1,16264244	IL1B	1,21429481	CYP4A11	1,36191567	PRKAR2B	1,33386407	CSRP1	1,26518419	ESCO2	1,22301276	COL9A2	1,6051116
2690	ITGAX	1,17192551	NUMB	1,2242991	GATA2	1,38122342	SEPHS1	1,34840763	HTR4	1,28212066	NCOR1	1,23387708	RELN	1,63337869	2760	NAPG	1,16244639	ADH4	1,21428333	PPP3CA	1,36155054	BCL3	1,33378725	SNX6	1,2650602	CHIA	1,22285556	LIFR	1,60453727
2691	UGP2	1,17155303	NR1H3	1,22427065	CYBB	1,38107148	GCNT1	1,34834973	CD36	1,28174767	ITGB7	1,23386727	UPE	1,63309164	2761	MAPK12	1,16244262	NT5C2	1,21340948	SPDEF	1,3613011	CHST4	1,33366285	BCMO1	1,26483352	PTPN12	1,22264109	HTR7	1,60312457
2692	GRIN3B	1,17153949	IFNAR1	1,22418326	CHST2	1,38099661	UPB1	1,34834157	ABCD2	1,28159585	GNAL	1,23377755	GAS1	1,63098655	2762	IL27	1,16241472	IL8RA	1,21281033	NEU1	1,36127909	NEURL	1,33357998	PIAS4	1,26475872	ITGA5	1,22232266	ATP6V1A	1,60296315
2693	IGFBP4	1,17132407	LDLR	1,22416457	SH3GL3	1,38090688	GABRG3	1,34820904	ABCC3	1,28147102	LMAN1	1,2337433	MAFA	1,63012167	2763	SRC	1,16232296	NDUFB2	1,21248016	KCNQ1	1,36088794	CD3EAP	1,33312941	LIFR	1,26460022	IFNAR1	1,22215985	NADK	1,60292159
2694	AMY2B	1,17123066	KCNK3	1,22404463	ATP5J2	1,38051509	KCNE2	1,34749281	TGFBI	1,28118484	IFNA16	1,2337418	FASN	1,62860152	2764	GALNS	1,16210013	PCYT1A	1,21229494	TPS3	1,3608738	PSMD14	1,33293873	PIAS3	1,26408936	HRH3	1,22214881	MAP4K5	1,6026328
2695	SNCA	1,1710012	TNFSF13B	1,22393823	CSGLCA-T	1,38043717	CCR5	1,34739344	KCNQ1	1,2811763	AMT	1,23368081	TRPC2	1,62800227	2765	SERPINA6	1,16201124	GUCY1B3	1,21222784	COL23A1	1,36043523	NPC1	1,33278066	SLC1A7	1,26386829	MDM2	1,22212914	NTHL1	1,60109777
2696	PRDM1	1,17099587	PIK3R5	1,22386695	DTX4	1,38033969	TBL1XR1	1,34736043	BAI1	1,28112113	AK7	1,23364572	FCN1	1,62778793	2766	MLH1	1,16167219	NTF3	1,21222103	DHX58	1,36019208	REG3A	1,33277811	OCRL	1,2636326	FUT9	1,22207366	PRKRA	1,60089325
2697	SORBS1	1,17094485	GNAQ	1,22372722	PYCR1	1,38002251	NADK	1,34704537	RGS19	1,28101518	ADRB3	1,23341951	HSPA5	1,62739835	2767	MAP4K5	1,16136477	MAPK8IP1	1,21197863	PHCA	1,36006895	GALNTL2	1,33273154	GRK1	1,26361165	CD1B	1,22178705	PTGES	1,60078763
2698	ARHGEF2	1,17089309	MST1R	1,22372722	PMCH	1,37989895	CYP2S1	1,34698814	CCNB2	1,28076662	RASGRP3	1,23318976	GJB1	1,62672979	2768	HTR4	1,16129398	ERN1	1,2113567	PICALM	1,36006895	MAN1B1	1,33253993	FBXW11	1,26350258	ABCA7	1,2217359	CYP1A2	1,60048905
2699	TAF1	1,1707571	LARS2	1,22360508	MAP1LC3B	1,37971659	MANBA	1,34659881	CEBPA	1,27986945	IRF3	1,2331575	AMH	1,62634682	2769	FSCN1	1,16123975	FDFT1	1,21135029	ACVR2B	1,35980687	CXCR6	1,33224939	WEE1	1,26342355	CD40LG	1,22169295	ADORA2A	1,60043072
2700	CHST2	1,17042798	ACCN1	1,22318758	BMP6	1,37960561	GBA3	1,34658151	DYRK1A	1,27975827	EGR4	1,23278427	SOX10	1,62600412	2770	CUZD1	1,16119969	MGAT2	1,21131569	DEGS1	1,35963194	SMUG1	1,33208098	CKMT2	1,26332357	DTX3	1,22159312	CALM2	1,59999163
2701	OGG1	1,17035286	KIT	1,22312519	PTGDS	1,37818167	CENTA1	1,34647677	BMP6	1,27966138	GNB1	1,23276659	KITLG	1,62590938	2771	ADC	1,16095049	FGF2	1,21128074	MSLN	1,35822942	LRWD1	1,33176619	IL3RA	1,26317875	SPI1	1,22158694	LPHN1	1,59948175
2702	CD5	1,17033658	ARHGEF4	1,22252912	PRPS1	1,37803152	STAT5B	1,3462633	HAT1	1,2793398	ATP2A3	1,23276093	PAK2	1,62574335	2772	NOG	1,160546	ID4	1,2112476	FAF1	1,35803787	MALT1	1,33143865	PRIM1	1,26278625	CHRNA3	1,22157305	SIX3	1,5993422
2703	NDUFA5	1,17023991	DAB2	1,22250986	IL10	1,37746555	ENTPD8	1,34585246	RALBP1	1,27850912	GJA4	1,23275077	SERPIND1	1,62554083	2773	GRM3	1,16045076	FLT4	1,2111367	SHC2	1,35756221	PTK6	1,33114921	TARS	1,26241644	SERPINA10	1,22128871	ALG8	1,59786814
2704	SCN7A	1,17022831	CYP2E1	1,22241237	CA3	1,37741755	CD2BP2	1,34577075	ARF1	1,27839452	NDUFB11	1,23263204	DDX54	1,6253296	2774	PROC	1,16040919	DDC	1,21093935	HK1	1,35722704	LIF	1,33108429	MET	1,26239954	LRPAP1	1,22099979	SLC10A2	1,59717774
2705	TRIO	1,1695946	ELOVL6	1,22199151	PTH	1,37740761	HSPA1A	1,34576379	SUMO2	1,27836603	GSTM3	1,23262321	B3GALT2	1,62525666	2775	DDX55	1,16040183	EMR3	1,21067843	CSTF3	1,35719354	TRADD	1,33069902	ITSN1	1,26227942	GORASP1	1,2208999	GSN	1,59694101
2706	PPARBP	1,16956041	CFLAR	1,22175855	VNN3	1,37739246	AGRN	1,34557745	GPR83	1,27784031	MSH6	1,23221408	ALDH2	1,6250214	2776	IFIH1	1,16025286	THBS1	1,21006647	HIPK2	1,35676177	ELAVL1	1,33061867	LAMP2	1,26227563	SPR	1,22053108	STX10	1,59619753
2707	COL10A1	1,16942669	RBPJL	1,22167983	CD55	1,37694387	SERPINC1	1,34553409	CA14	1,27783414	CD82	1,23204832	DCTD	1,62401168	2777	PDE6B	1,16014956	TH	1,21005184	PRMT6	1,35611499	ATP6V1C2	1,33057861	CD48	1,26223399	RGS19	1,22042067	ELA3B	1,59541033
2708	CCL2	1,16922449	ATP6V1B2	1,22167327	SHB	1,37674596	GOLGA5	1,34535383	PTGFR	1,27779494	DHCR24	1,23185351	RBBP4	1,62379789	2778	DPYD	1,15980079	ARF1	1,20974297	CYP3A43	1,35601508	TAF4	1,33045861	NLRP2	1,26222685	PIGL	1,22024215	DDR1	1,59508478
2709	GPT2	1,16865348	IRAK4	1,22140198	CCNB3	1,3764846	AMOTL1	1,34529226	SOCS3	1,27771344	CREB5	1,2314516	XK	1,62376466	2779	PIK3R2	1,15978089	MMP7	1,20972034	HCK	1,3551585	GLUD2	1,3303742	NUMBL	1,26196035	LARS2	1,2201219	ATP6V0A4	1,59463064
2710	TGFB2	1,1681609	ITGA2	1,22130626	CHRNB2	1,37624512	MIF	1,34489699	FUT8	1,27744846	NR1I2	1,23123507	BAP1	1,62352273	2780	C1R	1,15933253	B3GALT2	1,20935714	FOXL1	1,35486305	RDH14	1,33026448	CARD6	1,26184001	SOCS5	1,21980337	MAP3K7IP3	1,59386619
2711	SLC25A11	1,16802556	CAMKK1	1,22130133	CD1A	1,37550522	HMGCS2	1,34475746	RAB5C	1,27741978	ALDH3B1	1,23089202	MCC	1,62320406	2781	GAL3ST1	1,15932079	IKZF3	1,20902626	NAT6	1,354224	CMBL	1,32965074	KLK10	1,26135334	AQP7	1,21944893	PAX5	1,59386619
2712	SLC22A18	1,16779317	DHRS2	1,22126719	ACACA	1,37522525	CACNA1G	1,34471161	ACP6	1,27741375	B3GNT5	1,230676	SVIL	1,62265216	2782	CDC6	1,15907953	ACSL4	1,20893096	HOXD1	1,35415225	ATP5J2	1,32942858	CYP2A13	1,26097615	FGF10	1,219142	VNN1	1,59332658
2713	ITGA5	1,16774336	OXCT2	1,22067081	ATP12A	1,37495904	ACOT11	1,34463594	NFKB1	1,27740758	GRM7	1,23018533	BACE1	1,62182188	2783	DPM2	1,15889221	CX3CL1	1,20810559	FOSL2	1,35398186	ATF4	1,32909705	EGLN1	1,26075828	CKMT1B	1,21875372	PHC1	1,59331357
2714	GFPT1	1,16764599	CAPN3	1,22063253	MMP9	1,37470727	PDE1C	1,34455234	FLT1	1,27723782	HR	1,23015642	FSTL1	1,62148917	2784	ACMSD	1,15884271	IFITM1	1,20788037	LCP2	1,35332163	RHEB	1,32896703	ABCA13	1,2605656	TGFBR3	1,21845371	CCL15	1,59309857
2715	RBBP8	1,16759329	PPP3CC	1,22055014	PLAUR	1,37470297	PPAP2B	1,34432157	BCKDHB	1,27709381	DBC1	1,229918	RPS11	1,62147108	2785	CENTD1	1,15882765	COL25A1	1,2077927	TGM3	1,35294729	LHX2	1,32796502	MFGE8	1,26053692	AGK	1,2177567	FZD1	1,59281431
2716	ELA1	1,16757975	ADRBK2	1,22024264	CHRNA10	1,37464084	NAGLU	1,3442771	C1QB	1,27683449	WEE1	1,22971627	FHL5	1,62146295	2786	FN3K	1,15873287	EIF4EBP2	1,20754903	IFI35	1,35279353	PERP	1,32779354	QPRT	1,26038481	ORC1L	1,21761923	VAMP1	1,59209029
2717	CLDN16	1,16746107	DDIT4	1,22020593	TEK	1,37389681	CALML6	1,3439639	GLI4	1,27663768	FANCB	1,22966358	MAP1A	1,62096503	2787	DLX3	1,15872366	PDGFB	1,20747157	UGT8	1,35252687	NFYC	1,32749764	ABCA8	1,26034813	ST8SIA5	1,217487	ORC3L	1,59135413
2718	IL11	1,16724185	GYG1	1,22017799	HADHA	1,37364337	LY6E	1,34389146	APOC1	1,27647359	INHA	1,2296014	GSTO2	1,62076208	2788	MAPK3	1,15871906	PCK1	1,20741248	HLA-DRA	1,35229571	FTH1	1,32694199	TNFRSF17	1,26028461	CD63	1,21700841	ANPEP	1,59116689
2719	NPAS2	1,16723165	PTHR1	1,22012664	MYC	1,37334729	NFKB1	1,34362814	UTAF	1,2764677	ENPP6	1,22959393	LPHN3	1,62063752	2789	PLCG1	1,15871906	TYK2	1,20693783	BHLHB3	1,35204566	SMCHD1	1,32666566	RBPJ	1,25968302	OGG1	1,21666563	GTF2IRD1	1,59105068
2720	LMNB2	1,1671658	TRAF3IP2	1,22003079	UBE2E1	1,37331526	PTGER4	1,34355561	UCP1	1,27624268	THBS1	1,22946826	LDHA	1,61987746	2790	EXT2	1,15864645	GRM3	1,2068685	CLDN5	1,35174173	GANC	1,32657096	HTR1F	1,25965335	CD59	1,21646292	ITGB2	1,59101735
2721	HAND1	1,16709872	MX1	1,2196288	GPX5	1,3731696	LFNG	1,34332516	FOXO3	1,27547209	AKAP1	1,22944581	EZH2	1,61984939	2791	PRKCA	1,15864061	FNTB	1,20669115	SIX3	1,35109181	LIFR	1,32638197	LRWD1	1,25952618	HLA-DMA	1,21612442	STX18	1,59065747
2722	MAN1A1	1,16695397	FZD5	1,2195957	CYP2A13	1,371917	FOXL1	1,34326171	BCL10	1,2753888	HSPD1	1,22913367	CLDN5	1,61981145	2792	CD82	1,15861073	RAG2	1,2066423	IRS2	1,35096193	STX17	1,32611149	C1QC	1,25951251	UBE2V2	1,2160492	MTMR6	1,59039108
2723	DCTD	1,16688434	BMI1	1,21936918	DNAJA4	1,37190235	A2M	1,34314017	UBE2B	1,27491032	FOXP3	1,22903892	RARS	1,61945152	2793	SLC30A4	1,15850416	MAP3K14	1,20647288	WDFY3	1,3508353	ATP12A	1,32608242	MCM3	1,25935553	PDE1C	1,21558928	COX5A	1,59003084
2724	PPP3CB	1,16686957	RETNLB	1,21927139	SLC1A2	1,37182626	DAZAP2	1,34289847	CHST6	1,27451776	ATP2B3	1,22864791	POLE	1,61893107	2794	MTNR1B	1,15843288	GPT	1,2063652	PLG	1,35071016	CYLD	1,32607881	ATP5J	1,25870889	CD27	1,21536954	COX15	1,5899857
2725	ORC4L	1,16676658	CLDN15	1,21915376	FOXO3	1,37169504	PROM1	1,34289761	TREM2	1,27433621	BACE1	1,2283491	PDK2	1,61876313	2795	MANBA	1,15811566	AP3M1	1,20629548	FGF10	1,34993703	EPB49	1,32549452	LPIN2	1,2574464	POLR3K	1,2151885	CCR7	1,58967412
2726	PAPSS1	1,16661623	FCGR2B	1,21905268	AKAP5	1,37152917	ENDOG	1,34226821	FGF8	1,27433275	SDHC	1,22812434	IL19	1,61863921	2796	HTRA2	1,15810054	POLD1	1,20624075	F12	1,34879997	SERPINA4	1,32533204	CCL3L1	1,25717083	PIAS4	1,21513128	CALML3	1,58907513
2727	SCN1B	1,16661307	DEGS1	1,21903602	IHH	1,37135536	TGIF1	1,34209039	MR1	1,27400013	UGT2B17	1,22787637	IRF2BP1	1,61853098	2797	HRG	1,15787291	PLCG2	1,20593372	GAD2	1,34807318	ATP5A1	1,32517246	HDAC10	1,25712993	PNMT	1,21490723	GPT	1,58824699
2728	TCL1A	1,16659427	MBP	1,21880058	CDKN2D	1,37114689	SMARCA4	1,34191904	FHIT	1,2737638	LCAT	1,22786043	AKAP4	1,61789744	2798	CREB3L2	1,15776201	FAM59A	1,20589709	FANCB	1,34769729	ALAD	1,32515283	ALOXSAP	1,25709162	SH2B2	1,21477834	MYH2	1,58767157
2729	FGF13	1,16645098	PRPS1L1	1,2186912	RGS19	1,37109652	CACNA1S	1,34174871	GTF2I	1,27353488	CETP	1,22785068	NDUFS7	1,61788917	2799	PFKFB4	1,15767872	DHCR24	1,20582354	SULT1A4	1,34768146	UBE2C	1,32494446	DEDD2	1,25709162	ABLIM3	1,21466239	NEFM	1,58762099
2730	AKAP11	1,16628438	WBSCR17	1,21851921	GBX2	1,37098013	CBLB	1,34124652	NDUFS8	1,27350032	TRIP12	1,22768474	CYP2S1	1,61673006	2800	LDHA	1,1571306	NEIL1	1,20582354	B3GALT4	1,34763701	NQO2	1,32457171	TLR7	1,25674324	CCNE1	1,21439468	HOXD11	1,58723362

Table A4. Pooled-shRNA library screen on HEL cell line and MF-3: list of 2nd most depleted shRNAs for each experiment (ranking approach 1, RA1).

	NO ruxolitinib (setting 1)				Ruxolitinib (setting 2)				Ruxolitinib + CM (setting 3)				MF-3			NO ruxolitinib (setting 1)				Ruxolitinib (setting 2)				Ruxolitinib + CM (setting 3)				MF-3	
	Experiment 1		Experiment 2		Experiment 1		Experiment 2		Experiment 1		Experiment 2					Experiment 1		Experiment 2		Experiment 1		Experiment 2		Experiment 1		Experiment 2			
Rank	Gene	Fold change	Gene	Fold change	Gene	Fold change	Gene	Fold change	Gene	Fold change	Gene	Fold change	Gene	Fold change	Rank	Gene	Fold change	Gene	Fold change	Gene	Fold change	Gene	Fold change	Gene	Fold change	Gene	Fold change	Gene	Fold change
2801	INHBB	1,15708836	CSNK1A1L	1,20558738	KLRA1	1,34741509	PHC1	1,32438703	MICA	1,25636949	BTRC	1,21427054	KHK	1,58682398	2871	GNMT	1,14997404	FOXL1	1,19410371	KCNQ5	1,33019844	GALT	1,30532144	LTBP1	1,24128777	ACCN2	1,20410024	DEFB1	1,55827888
2802	GJB1	1,15690606	F10	1,20537564	SPRY2	1,34740509	STXBP4	1,32425251	SIGIRR	1,25628556	CCL16	1,21421898	PIK3R2	1,58664766	2872	SHC4	1,14973732	GRIK3	1,19396514	TCF4	1,3299364	ALKBH2	1,30514589	PRKCQ	1,24120839	ANGPTL3	1,20391977	LAT	1,55793468
2803	DCK	1,15690385	GRM1	1,20525845	ERAP1	1,3471615	MDC1	1,32418951	XRCC3	1,25539508	QPRT	1,21406958	CCNG2	1,58605597	2873	MAP3K10	1,14973502	LMNA	1,19390925	AGPAT1	1,32979406	GSK3A	1,30500564	PROZ	1,24072558	ITPKB	1,20379931	TRAFD1	1,55455739
2804	PPP5C	1,15647884	NUP153	1,20514824	CHST6	1,34714462	PNMT	1,32370473	SMARCD1	1,25536932	F2RL3	1,21403312	KCNJ11	1,58604079	2874	UBE2M	1,1496542	GNAI2	1,19329961	RORC	1,32956587	CRYAB	1,30485178	PAWR	1,24067938	C1GALT1	1,20371007	XCL1	1,55442129
2805	NAE1	1,15641518	ACAA1	1,20514521	SUMO3	1,3465857	NDUFA5	1,32321972	RAB1A	1,25528275	CBR1	1,21400805	ENPP7	1,58565356	2875	PHF21A	1,14963478	EME2	1,19318346	RAD51C	1,3292369	NAPG	1,30474953	FZD1	1,24040116	EDN3	1,20370064	HSPA2	1,55379871
2806	GALNT11	1,15640473	TOR1A	1,20509097	AZI2	1,34652641	PDE6C	1,32276715	BDKRB1	1,25512572	DPM2	1,21399878	STX6	1,58552184	2876	MINPP1	1,14958473	IFNG	1,19310891	PIK3R2	1,32895356	ABCA12	1,30464473	ATP5I	1,24036396	IDE	1,20350054	DPM2	1,55318296
2807	ADSS	1,15638339	FPR1	1,20487587	RAD50	1,34648245	GABRA4	1,3224857	DTX4	1,25448151	GPX2	1,21398597	PIK3R1	1,5854294	2877	WDFY3	1,14951288	AHR	1,1927622	OAZ1	1,32893881	RABGAP1L	1,30405379	CYLD	1,24021567	CDKL1	1,20340547	CACNA1C	1,5531364
2808	ATP4A	1,1563028	BTG3	1,20486212	SCN11A	1,34597441	THBS1	1,32246968	PCAF	1,25447229	NEFH	1,21396889	LRP8	1,58515217	2878	DIO2	1,14931435	FUT8	1,19274107	DMD	1,32888149	FCER1A	1,30380612	GNAO1	1,23982773	GPR39	1,20299756	ZBTB20	1,55292126
2809	HR	1,15615687	EPHX1	1,20447305	GPX3	1,3455843	C8G	1,32222888	HYAL2	1,25430431	PTPRN	1,21385203	EMR2	1,58447274	2879	IMPA1	1,14916105	SRXN1	1,19271858	CDH15	1,32880692	ARHGEF11	1,30345947	MTMR6	1,23933755	SH3BGRL	1,20289622	GJA3	1,55271081
2810	CARS2	1,15611232	NADSYN1	1,20444247	TBX2	1,34540379	PRPS1L1	1,32218436	LIPA	1,25395942	HRH1	1,21358863	AOC3	1,58417111	2880	ATG4B	1,14910526	OGDHL	1,19248558	POLK	1,32868094	TUBB4	1,30342333	ATG2B	1,2392435	GLUL	1,20275303	TNFRSF4	1,55229672
2811	CHP	1,15611232	CPT2	1,20408685	FKBP1A	1,34538725	CD2	1,32218405	PROX1	1,2535851	DGKI	1,21354468	HOXB4	1,58396519	2881	FUK	1,14891427	CYB5R3	1,19216686	LEF1	1,32861892	ZEB2	1,30341869	CAMKK2	1,23917912	ENTPD5	1,20264039	EPHB2	1,55226568
2812	APLP2	1,15609837	ADAM12	1,204058	C1S	1,34525494	TAF1	1,32207606	NEFL	1,25344777	SLC30A8	1,21341943	GUCY1A2	1,58388864	2882	AMPD1	1,1487608	SLCO1A2	1,19196426	CTNNB1	1,32820601	UGT2B17	1,30341818	TGM3	1,23895616	NDUFA4	1,20254353	MSTN	1,55171649
2813	LRDD	1,15607504	NOS1	1,20391475	CA5B	1,34516005	AIRE	1,32154354	CACNA1C	1,25320802	UCP2	1,21324358	ANGPTL2	1,58376996	2883	PTGER2	1,14875435	RAC3	1,19181085	SCN1A	1,32787794	RAB7A	1,30326925	AKR1C4	1,23895061	CBL	1,20253814	CYP2U1	1,55165951
2814	ALOX5	1,15600093	PRC1	1,20349877	TIRAP	1,34512155	TNFRSF17	1,32052965	PGM3	1,25304657	SPRY3	1,21317928	ALPL	1,58368277	2884	LCK	1,14865001	GALNT4	1,19166948	ELA2B	1,32773115	AXIN2	1,30274177	CDKN2D	1,2388375	PLA2G3	1,20241649	YWHAB	1,55091518
2815	C1GALT1	1,15592501	PCSK2	1,20347942	HDAC3	1,34510235	TGIF2	1,32041957	ALKBH3	1,25265496	SRF	1,21307969	DVL2	1,58357357	2885	TSC2	1,14858051	GNAZ	1,1916206	HSD11B1	1,32732058	ETV5	1,30257878	EPPK1	1,23855459	GSTM2	1,20210944	FUT2	1,54924798
2816	RFNG	1,15590239	ATG2A	1,20323985	SHISA5	1,34504903	GATA3	1,32011904	CHST2	1,25265496	GDF15	1,21234088	CCND3	1,5834577	2886	PYGB	1,14845699	CETP	1,19146666	GJA4	1,32726358	PARK2	1,30243456	ENTPD6	1,23831369	DHRS1	1,20198327	CDKL2	1,54903805
2817	NSUN2	1,15575571	GAD1	1,20280491	SUMO2	1,34471775	CLIC1	1,31990122	ATF4	1,2522425	UGT2A1	1,21130529	SSTR5	1,58307784	2887	CTNNB1	1,1483951	SLC23A2	1,19134291	MARCKS	1,32720466	APOA4	1,30232256	SLC16A3	1,23828908	SCN5A	1,20177472	SUMO3	1,54870295
2818	CYP2C19	1,15570878	UTF1	1,20270841	ITGB3	1,34369064	LYN	1,31941471	ENO1	1,25205056	CCR4	1,21103336	PTPRA	1,58303197	2888	PARK2	1,14827684	BHLHB3	1,19133157	C7	1,32698164	COASY	1,30224001	ALB	1,23825836	CTSL2	1,20177352	BAIAP2	1,54843717
2819	SLCO1A2	1,15563525	LRRC15	1,20267537	AKAP6	1,34364015	IFNA8	1,31928024	F12	1,25165989	TBX1	1,21094841	TNKS2	1,58283747	2889	CCL11	1,14822616	FARSB	1,19121773	TNNT2	1,32688869	IL17A	1,30221322	AADAC	1,23798127	CAP1	1,20158747	GNPNAT1	1,54822705
2820	HYI	1,15554402	ITGB6	1,2026685	TNKS2	1,34362268	GLS2	1,3192414	COMT	1,25146639	TICAM2	1,21091162	ATG3	1,58229108	2890	ID3	1,14802123	LCP2	1,19119163	NTSC2	1,32644066	CCL19	1,30178698	IL21R	1,23768247	NNT	1,20143598	PIAS3	1,54820501
2821	CRHR2	1,1552952	CD79A	1,20263503	LFNG	1,34322423	GFPT1	1,31901365	SCN2B	1,25119025	ABCC6	1,21076171	RBP4	1,58149462	2891	ANXA5	1,14793726	ACTN2	1,19106567	SYK	1,32642767	T	1,30148037	IL11RA	1,23721543	IFNAR2	1,20124553	TNIP2	1,54804558
2822	NDST4	1,1552858	CSGLCA-T	1,20230496	IL1R2	1,34320601	MS4A1	1,31879388	GPX3	1,25103587	TGIF1	1,21076171	AADAC	1,58037108	2892	HTR3C	1,1478869	SLC6A4	1,19092531	PIK3CG	1,32638059	HBXIP	1,30115728	SIRT4	1,23721242	FZD3	1,20103329	C4BPA	1,54797015
2823	PAX3	1,15519577	GDF2	1,20220025	CYP39A1	1,34259134	DCC	1,31868026	GLUD1	1,25097475	MAML1	1,21069984	SPRY3	1,57972785	2893	CD19	1,14775033	GPX6	1,19032274	PDE6H	1,32619761	ADARB1	1,30086889	AXIN2	1,23711435	PTGES	1,20096542	CUGBP1	1,54785066
2824	SORL1	1,15487089	PIK3R3	1,20213281	ADRBK2	1,3422963	CA3	1,31784075	MDM2	1,25088861	EFNA2	1,21066227	UGT1A8	1,57916969	2894	CALML3	1,14767001	PRDX3	1,19017389	CARS2	1,32619703	SNX2	1,30026377	CACNA1A	1,23661001	CDH5	1,20082141	GABRB3	1,54775936
2825	TRIP12	1,15482672	MMP14	1,20166587	F7	1,34218803	SLPI	1,3177474	OGFR	1,25074761	BHLHB9	1,2105447	EFNA4	1,57893801	2895	TRH	1,14735235	PRKAR2A	1,18996569	UGT1A9	1,32587415	DFFA	1,30020131	CYP4B1	1,23599599	CSRP3	1,20079308	CALM3	1,54742821
2826	HOXB6	1,15479468	PTGDS	1,20131205	TGM1	1,34207712	IL15	1,31773096	TDP1	1,25057208	SCN1B	1,21048799	ETFA	1,57873677	2896	NOS1AP	1,14719373	KCNN4	1,18943075	AK3L1	1,32565409	DBT	1,29990004	NAPG	1,23581102	SYN3	1,20008884	TNFSF8	1,54735309
2827	TUBB2C	1,15478287	AMPD1	1,20115566	PDE7A	1,34168389	APOA1	1,31686545	DEGS1	1,25039893	RANBP9	1,21040112	GALNT10	1,57849535	2897	GJA1	1,14713938	APEX1	1,18905053	RTKN	1,32561006	STAT2	1,29959306	LGALS1	1,23571345	PARC	1,20000968	KCNJ2	1,54574907
2828	EXTL2	1,15448326	EEF1A2	1,20092617	CNP	1,34156307	CHMP1B	1,31625397	ASMT	1,25004372	EEA1	1,21030098	PTPRN	1,57840279	2898	CAPN9	1,14662203	HAL	1,18901147	GOLGA5	1,3255592	PCAF	1,29937265	TAF4	1,23550343	TIMP1	1,19954771	CLCA2	1,54544537
2829	PIK3R5	1,15447467	MAP3K4	1,2008061	SPTAN1	1,34126354	GPR68	1,31568267	DPAGT1	1,24979051	CALML6	1,21026906	COL5A2	1,57780592	2899	FBXW2	1,14625733	IPMK	1,18898283	PCSK2	1,32544333	ENO1	1,29935562	FBP2	1,23546386	NDST2	1,19926861	POLR2G	1,54520145
2830	GSTZ1	1,1544259	INPPL1	1,20049576	DLL1	1,34083821	CAPN9	1,31557211	TICAM1	1,24959396	IGFBP4	1,21026753	KCNH7	1,57739365	2900	LCMT1	1,14625715	CCR10	1,18893514	HOXA10	1,32495655	REN	1,29895472	TAF13	1,23513829	TUBA3C	1,19907837	WNT8A	1,54490287
2831	ACY1	1,15439966	CPT1B	1,20022345	ST3GAL5	1,34063719	HSD11B2	1,31556392	TPH2	1,24942732	C9ORF95	1,21024208	IL6	1,57641332	2901	TRIP10	1,14625503	COL16A1	1,18890845	SLK	1,3246948	DMGDH	1,298562	PDLIM5	1,23477308	F7	1,19903126	WISP2	1,54452117
2832	HBQ1	1,15427052	ATP12A	1,20019902	HERPUD1	1,34060706	B3GALT2	1,31545335	REM2	1,24911349	MECR	1,20988274	TUBB3	1,576115	2902	NR2F2	1,1461583	SUFU	1,18890297	CXCL11	1,32466279	PDXP	1,29830611	DIAPH1	1,23474334	ADORA2A	1,19880499	UQCRC1	1,54445592
2833	PDE4A	1,15420234	DGKE	1,20014402	FABP4	1,34044241	MMP3	1,3153644	TNFSF13B	1,24885423	F3	1,20969665	TCF7L2	1,5759526	2903	NDUFB11	1,146117	CYP2A6	1,18867782	IDE	1,32435134	BACE2	1,2981155	CD274	1,23439768	CD1D	1,19868334	IDH3B	1,54433097
2834	MNAT1	1,15419154	MTMR6	1,19996329	C4BPB	1,34026453	MGAT4A	1,31521407	PDE7A	1,2477516	RALGDS	1,20942488	KCNQ2	1,57586107	2904	SCYL1	1,14611318	MAPK8IP2	1,18867094	LPL	1,32414724	SOCS2	1,29795941	LMX1B	1,2342266	PTGDR	1,19844135	EFNA2	1,54428206
2835	HSP90B1	1,15412323	BBS4	1,19980971	ELOVL6	1,34022214	MSX1	1,31419824	TSC1	1,24740802	HOXD11	1,20941066	AK5	1,57573917	2905	ATP1A3	1,14602272	CD47	1,18857629	CDK10	1,3239823	GMDS	1,29795437	HES1	1,23422019	ORC5L	1,19811495	KLK2	1,54404154
2836	ALOX15B	1,15408114	ESR1	1,19975153	PIP5K2B	1,3399963	GNAI1	1,31378524	DNAJB1	1,24717518	PTPN11	1,20940409	HIST2H3C	1,57556112	2906	GLI3	1,14594108	HFE	1,18856651	PRPS1L1	1,32379752	GNB1L	1,29771555	GDF6	1,23418095	KCNJ4	1,19793872	CACNA2D1	1,54363079
2837	IKBKE	1,15407065	IMPA1	1,19961447	CYP2E1	1,3397943	MDH2	1,3133667	ADCY7	1,24713733	EDN1	1,20930763	EIF2B2	1,5755226	2907	CPSF3	1,14590057	PMM1	1,18843175	IL24	1,32339956	PACRG	1,29733904	CDX1	1,23367548	GUCY1B3	1,19780124	ARNTL	1,54336024
2838	BCL2A1	1,15398715	C8G	1,19953684	EDA	1,3392786	CST3	1,31308883	A2M	1,24691552	FCER1G	1,20913323	FTO	1,57533418	2908	ANK2	1,14586028	LRWD1	1,18794336	SAA1	1,32336482	PIK3AP1	1,29691343	ATP5G1	1,23320661	MAP3K14	1,19764532	BMP8A	1,54300729
2839	MCM10	1,15392797	CHRM1	1,19941345	POFUT1	1,33830068	SLC16A3	1,31302371	WASF2	1,24683289	GALNT9	1,20899208	CHPT1	1,57469189	2909	GBA3	1,14570073	BCAP29	1,18777491	GATA4	1,32334225	SLC30A1	1,29666718	EGR4	1,23301214	MADD	1,19761609	BCAT1	1,54295154
2840	LPIN2	1,1536278	DGKZ	1,19931005	XIST	1,33697127	SMARCB1	1,3125366	FLT3LG	1,24651846	ECE2	1,20898254	TPP2	1,57414567	2910	PIWIL2	1,14567907	DCK	1,18771218	FCGR1A	1,32246916	CDKN1C	1,29657307	GSTM3	1,23300981	BUB3	1,19754028	KCNJ3	1,54264725
2841	DLL4	1,15320038	KLRC2	1,19916731	RELA	1,33679981	PIAS4	1,31212559	SUOX	1,2462954	ACVR2B	1,20876376	ANP32E	1,57348751	2911	SLC30A6	1,14565337	EREG	1,18765875	APOA1	1,32200581	CANX	1,29511314	PRKAB1	1,23272642	C1S	1,19746198	CD36	1,5408064
2842	MGAT2	1,15318684	FEZ1	1,19901517	TRPC7	1,33676522	UBE2E2	1,31186076	B3GALT6	1,24627067	DNAJB9	1,20863063	CARD10	1,57320385	2912	HMGB3	1,14561117	IL17RA	1,18760579	EGLN1	1,32152997	GRIN3B	1,29488591	COL4A2	1,23251837	VNN3	1,19711301	PDE10A	1,54067283
2843	ACTN2	1,1531274	CASP3	1,19888352	STAT1	1,33625472	AKAP9	1,3117825	KHK	1,24594373	BIRC2	1,2080391	NFYC	1,57195588	2913	STXBP1	1,14555596	PRKCB1	1,18753923	CDH2	1,32149849	GALNT9	1,29466332	ARSB	1,23249962	PMS2L3	1,1970263	PLA2G2F	1,54063116
2844	BCL7A	1,15272872	AP3B1	1,19885856	ASGR2	1,33607247	ABCG8	1,31131093	EPS15	1,24575567	ALPP	1,2079312	CD14	1,57100149	2914	PLA2G5	1,14545409	SCNN1D	1,18732758	INSIG2	1,32127775	APC2	1,29369534	REG3A	1,2324482	RAF1	1,19695759	IARS2	1,54041541
2845	DTX1	1,15229317	PPME1	1,19859395	GSTM2	1,33591667	VAX2	1,31120591	HSD17B10	1,24570489	RAD52	1,20781313	TH	1,57081059	2915	NOTCH3	1,14532303	DHH	1,18717984	GRM8	1,32072939	CXCL10	1,29368091	SLC30A8	1,23182527	STX3	1,19695173	ASCC3L1	1,53944684
2846	NCF2	1,15228407	CSK	1,19849934	FNTB	1,33571759	KLRC1	1,31120103	ITPK1	1,24543385	CD93	1,20756553	IRAK1	1,57044685	2916	DOLPP1	1,14527661	SNX1	1,18690767	PDE6D	1,32038663	SERPINA5	1,29330907	MAP1LC3A	1,2318133	DUSP8	1,19669407	ISL1	1,53913588
2847	FBXW11	1,1522052	HIG2	1,19845383	DBH	1,33488991	APOC3	1,31075871	EPRS	1,24533529	C9	1,20744136	IKBKB	1,57033681	2917	MAML3	1,14515272	NCF4	1,18690734	WRN	1,32024718	RPN1	1,29320095	CD1B	1,23174778	ALOX12	1,19665081	TBX21	1,53913588
2848	OLIG2	1,15212591	NEFL	1,19822676	KCNMA1	1,33469598	BMP6	1,3102364	CAMKK1	1,24517428	RUNX2	1,20724246	RAD51L1	1,56937193	2918	EMR2	1,14513151	INS	1,18667921	PARD3	1,31956699	PIGH	1,29215029	NDUFS4	1,23162817	RBP4	1,19647901	FGG	1,5387165
2849	PDE1B	1,15205628	CYP2C19	1,19808681	COL1A1	1,33408503	SOS2	1,30916173	SULT1C4	1,24483155	NFYA	1,20719435	HNF4G	1,56796748	2919	SLC1A7	1,14505369	PGLS	1,18667469	SUMO1	1,31950468	GLS	1,29177014	ABCG5	1,23157183	CBX5	1,19644538	ARHGAP1	1,53841734
2850	UGT2B28	1,15200484	CCK	1,19791418	TNFRSF19	1,33400441	ITGA3	1,30902702	TCL1A	1,24480712	HHEX	1,20713198	PDLIM4	1,56757051	2920	GLUL	1,14486585	GLI3	1,1866378	DVL3	1,31942992	GALK1	1,29170829	PDE1B	1,23140854	CACNA2D4	1,1964089	DDX50	1,53839037
2851	CD34	1,15199084	RET	1,19766587	INPP1	1,33398032	GRK4	1,30897067	GIP	1,24454827	MPO	1,20709608	ATF4	1,56753748	2921	AKAP5	1,14479642	CAB39	1,18626109	FMO4	1,31938321	CSRP3	1,29161478	PARD3	1,23132167	COL1A2	1,19638136	CHST4	1,53800244
2852	CSNK1E	1,15195079	TP53BP1	1,19738254	AMH	1,33374389	PDE6B	1,30894267	PTPN12	1,24448474	MCM4	1,20699307	SFRS12	1,56513359	2922	C12ORF57	1,14473096	GLS2	1,18605717	ITCH	1,31918189	FPR1	1,29139903	COL6A3	1,23121236	GUCY1A2	1,19614526	CTSE	1,53676174
2853	SUCLG1	1,1519018	POLG2	1,19695071	ARPC5	1,33345951	DCK	1,30872896	PGA5	1,24434144	CDC6	1,20690635	FOXP1	1,56470073	2923	UBE2D3	1,14470755	FSCN2	1,18599708	GABRA4	1,31863592	NUDT4	1,29130978	NFE2	1,23120484	FOXH1	1,19585931	POLL	1,53587594
2854	SLC23A2	1,15189465	HLA-C	1,19691844	MST1R	1,33338183	CD82	1,30805559	BACE2	1,2443408	TXLNA	1,20645953	LMO1	1,56431314	2924	ADAM10	1,14435553	GPSN2	1,18591516	AK1	1,31862957	BTRC	1,29117917	BCL11A	1,23112877	RAB1A	1,19575835	TDP1	1,53566608
2855	CDC14A	1,15181413	SMC6	1,19689098	HES1	1,3331423	APCS	1,30801848	PLA2G4A	1,24430917	RNASEN	1,20643432	IAPP	1,56416753	2925	GALE	1,14433793	GRB10	1,18582494	CD68	1,31855491	NFKBIL1	1,29098799	TFAP2A	1,23109813	GAMT	1,19564313	DDIT4	1,53507737
2856	CD2	1,15173168	PAFAH1B2	1,19673477	CCNE2	1,33313407	CLK4	1,30771012	VAMP2	1,24412816	ITPKA	1,20599558	ARPC2	1,56373262	2926	MAP3K9	1,14418478	ACP2	1,18582108	FGF2	1,31832692	TAGLN	1,29091103	FLOT1	1,23104911	MET	1,19558852	DNAJB4	1,53465774
2857	POSTN	1,15158499	MAFK	1,19644106	SERPINA6	1,3330746	IL19	1,30743518	LY86	1,24398595	HTR1E	1,20595966	ABCC3	1,56368878	2927	IRF5	1,14374453	PLA2G4C	1,18578551	LY86	1,31823554	DDIT4	1,29063334	CD40	1,23016418	CA6	1,1953322	STAT2	1,53401969
2858	AK3	1,1513209	PTPRN	1,1963444	LEPR	1,33237953	HLA-DMA	1,3074263	GAA	1,24397222	GGH	1,2058805	ZFP42	1,56262688	2928	KCNN3	1,14336482	BLM	1,18533035	ACY3	1,31801426	EGR3	1,29057052	SGK	1,23007431	TFPI	1,1952917	KNG1	1,53385905
2859	CYP1A2	1,15129754	SCAP	1,19632703	BIN1	1,33232001	BAI1	1,30741654	CLDN11	1,24366631	CLTA	1,20579693	PGA4	1,5624365	2929	DUOX1	1,14336396	PDE8B	1,18512925	AGXT2L1	1,31742701	BCL2L11	1,29034187	RTN4R	1,2298235	DNAJA4	1,19528572	CAMKK2	1,53253635
2860	GPI	1,15120002	ZEB2	1,19581188	GNAQ	1,33194428	ACTN2	1,3074115	NAGA	1,24349724	IJPE	1,20578887	CD4	1,56143354	2930	HOXD10	1,14327428	FZD4	1,18511295	CD9	1,31646502	CDCA8	1,29020835	HYI	1,22971807	ACP6	1,19510765	PPT2	1,53154018
2861	NARS	1,15109903	ACACB	1,19570745	RBP4	1,33185263	CNTF	1,30729238	GABRA4	1,24325959	CYP1A1	1,20572306	PTPN11	1,56129941	2931	MAGI3	1,14300542	ITPKA	1,18496166	IKZF1	1,31596595	PIGP	1,29009469	IRF2BP1	1,22963239	GZMA	1,19490306	PIGB	1,53139212
2862	TNF	1,15088315	JUP	1,19497783	CHRNG	1,33167321	FZD6	1,30704682	ATP6V1D	1,24322332	P2RY1	1,20553088	ANKRD1	1,56122874	2932	ATXN2	1,14271351	HDAC1	1,1846535	ST6GALNAC3	1,31589431	CCDC6	1,29007806	HELB	1,22933595	FUT4	1,19444019	ARHGAP6	1,53124475
2863	RAB23	1,15084893	GSK3B	1,19495221	GLUD2	1,33165698	AKAP7	1,30693867	CBX4	1,2430859	SMPD2	1,20544586	ADSSL1	1,56064209	2933	ARPC5	1,14257175	HDC	1,18438269	CDKN1C	1,31566342	GTF2A2	1,29003032	IRF8	1,22916222	TGM2	1,19440578	HIG2	1,53110055
2864	RBP4	1,15071975	MT2A	1,19482105	CER1	1,33161171	ATG10	1,30657167	PSMD8	1,24305231	DYSF	1,20523273	HS6ST2	1,56055421	2934	APEX1	1,14239145	DPF2	1,18412131	BMP1	1,3156328	NMUR2	1,28985742	ALDH18A1	1,22888096	NSMAF	1,1940838	IDH2	1,53098861
2865	GABRG2	1,15060481	GDNF	1,19481568	ADRA2A	1,33122456	CDS1	1,30649321	WNT2	1,24303788	GABRB2	1,20499336	ERAP1	1,56048157	2935	HLA-DPA1	1,14229416	INHA	1,18412131	HOPX	1,31557661	SOCS6	1,28984534	DIO1	1,22847193	MAP2K6	1,19349857	ANGPT1	1,53034567
2866	TGFBI	1,15046129	CHRNE	1,19467681	FOXM1	1,33119577	STAMBPL1	1,30618943	ALDH7A1	1,24258	LMNA	1,20489773	PRNP	1,55983252	2936	MAPK10	1,14219464	NDST2	1,18411114	LTBP4	1,31510455	PF4	1,28984373	PRMT2	1,22843564	GNA13	1,19344691	FLOT1	1,53023361
2867	RANBP9	1,15044968	MAFF	1,19467214	FBXW11	1,33109397	TEC	1,30614583	OAS2	1,24230435	ADM	1,20487729	FGF6	1,55970073	2937	SCN5A	1,1421738	DAZAP2	1,1840876	EDN3	1,31487041	CCL28	1,28889055	ACO2	1,2281975	WNT5B	1,19326845	FCGRT	1,52970997
2868	COL6A2	1,15044117	PMS1	1,19458224	MAPK1	1,33092092	MAP3K10	1,30599708	PDE4D	1,2420746	PTPRA	1,20476333	DGKA	1,55898956	2938	RING1	1,14213914	MYF6	1,18404796	DDOST	1,31406585	MCPH1	1,2886222	PPP1CA	1,22817362	GABRA2	1,1928909	NDNL2	1,52938453
2869	FABP4	1,15034842	INPP4B	1,19433412	KL	1,33047437	TCF4	1,30578032	UBE2V2	1,24198324	UGT2B10	1,2045235	DPPA5	1,5583898	2939	IDH3G	1,14208594	DISC1	1,18378905	CAMP	1,31395649	USP9X	1,28813724	CHST13	1,22807133	GABRG1	1,19282629	HFE	1,52847882
2870	TP53BP2	1,15025502	CRK	1,19431394	PTPRN	1,33034894	CD14	1,30568948	NFYA	1,2413131	PLA2G2D	1,20432852	ATP1A1	1,5583109	2940	CRY1	1,14195541	DHX58	1,18375386	CPA3	1,31362226	ALDH6A1	1,2878433	FNTB	1,22803989	NFATC2	1,19278542	WNT5A	1,52838592

Table A4. Pooled-shRNA library screen on HEL cell line and MF-3: list of 2nd most depleted shRNAs for each experiment (ranking approach 1, RA1).

	NO ruxolitinib (setting 1)				Ruxolitinib (setting 2)				Ruxolitinib + CM (setting 3)				MF-3			NO ruxolitinib (setting 1)				Ruxolitinib (setting 2)				Ruxolitinib + CM (setting 3)				MF-3	
	Experiment 1		Experiment 2		Experiment 1		Experiment 2		Experiment 1		Experiment 2					Experiment 1		Experiment 2		Experiment 1		Experiment 2		Experiment 1		Experiment 2			
Rank	*Gene*	*Fold change*	*Gene*	*Fold change*	*Gene*	*Fold change*	*Gene*	*Fold change*	*Gene*	*Fold change*	*Gene*	*Fold change*	*Gene*	*Fold change*	*Rank*	*Gene*	*Fold change*	*Gene*	*Fold change*	*Gene*	*Fold change*	*Gene*	*Fold change*	*Gene*	*Fold change*	*Gene*	*Fold change*	*Gene*	*Fold change*
2941	EOMES	1,14189486	PANK4	1,18368506	PCAF	1,31350476	ACP2	1,28774416	SUCLA2	1,22764238	CTBS	1,19271156	CAPN11	1,52814907	3011	AZGP1	1,13435533	DERA	1,17217254	SNX6	1,29329599	SETDB1	1,27338949	ISYNA1	1,21655285	CA4	1,18094128	GATM	1,50336803
2942	CYP2E1	1,14184102	CHRNB1	1,18361562	CCNG2	1,31327792	ECHS1	1,28762657	LIPT1	1,22761723	ATP6V0D2	1,19269231	IRAK2	1,5276574	3012	SIN3B	1,13426773	PSCD2	1,17193701	ETV5	1,29326344	FUT8	1,2733176	YWHAQ	1,21601068	PANK1	1,18065433	CNP	1,50306014
2943	MTHFS	1,14166476	ALB	1,18358595	EXTL2	1,31256664	MBTPS1	1,28710543	DAB2	1,22692591	IGFBP6	1,19267301	ARL4D	1,52704475	3013	CHRND	1,13418376	BAG1	1,17190896	ADCYAP1	1,29324893	FLT3	1,27330496	CRAT	1,21574931	CHP	1,18063386	TGFB3	1,50297054
2944	FCGR2A	1,14149295	ST3GAL6	1,18353475	GPR39	1,31251381	ADCY4	1,28699695	IAPP	1,2268926	PIP5K2B	1,19246409	F12	1,52692735	3014	EPO	1,13387074	HPN	1,17168704	FCN1	1,29323486	GPX5	1,27327221	NUMB	1,21552176	FRAT2	1,18042857	DEGS1	1,50205602
2945	ASMT	1,14148355	TNIP2	1,18352337	SMARCC2	1,31238365	FDPS	1,28684707	SYT1	1,22684564	DEGS1	1,19209954	CNTN1	1,52689638	3015	IFNA1	1,13347752	STAT4	1,17157289	PIK3R5	1,29224371	SUCLA2	1,27311487	FGF13	1,2152154	TNFRSF18	1,18017844	GALNT1	1,50163843
2946	VNN1	1,14136628	HTR1E	1,18315064	HYAL3	1,31210274	NCR1	1,28644023	ASAH3L	1,22658635	DIXDC1	1,19198133	TGDS	1,52662219	3016	FPGT	1,13340151	PAH	1,17155966	ACOX2	1,29206504	MELK	1,27277152	SNCAIP	1,2152154	FUT5	1,1798658	MPG	1,50075661
2947	CD55	1,14133404	HTR2A	1,18305583	ITPR1	1,3118506	MMRN1	1,2863647	AKT2	1,22648124	AKAP12	1,19176629	RASGRP1	1,52605081	3017	BRD4	1,13316429	CPN1	1,17148427	GALNT1	1,29183875	GNMT	1,27253329	RAB4A	1,215062	TXNRD2	1,17977314	A4GALT	1,50066189
2948	ACAD8	1,14125971	NEFM	1,18302481	RFWD2	1,31179966	MC4R	1,28607239	AKAP9	1,22583612	ATF2	1,19176522	C22ORF28	1,52591408	3018	NOS1	1,13314757	C1ORF142	1,17147691	PPIC	1,29177432	PTPRN	1,27250899	ATP5J2	1,21489249	TERF1	1,17975877	SRY	1,50001135
2949	KLRC4	1,14105514	UNG	1,18294704	GDF6	1,31167172	BCR	1,28553416	TSPAN7	1,22583454	DCXR	1,19168	CKM	1,52588751	3019	HLA-F	1,13308332	CD55	1,17124458	HK3	1,29126765	ACMSD	1,27242287	MMP9	1,21489004	PHF11	1,17956848	PSMD8	1,49973523
2950	DHRS1	1,14090067	IRS2	1,18291735	IL11RA	1,31100644	PIK3R1	1,28548948	FGF2	1,22548021	IRF2	1,19124731	C6	1,52531149	3020	PTPRJ	1,13277832	STUB1	1,17114945	CREM	1,29099589	RELN	1,27213445	ATP8A1	1,21479408	PTAFR	1,17940593	EEF2K	1,49928173
2951	OLIG1	1,14069267	HPD	1,18228101	MIOX	1,31094418	DCN	1,28537928	GADD45B	1,22541942	PRMT1	1,1911105	CRH	1,52507932	3021	RFXANK	1,13260568	CASP4	1,17112647	RAB1B	1,2908248	IFNGR1	1,27204611	GCAT	1,21477365	LRP6	1,17927761	ACTR3	1,49914047
2952	STAT1	1,14066442	ALK	1,18226656	IL2	1,31031331	IFIH1	1,28516899	F2RL2	1,22535343	SCN1A	1,19090235	SH3GL2	1,52378298	3022	F3	1,13254093	HOXA10	1,17105729	GJA1	1,2903313	CALML5	1,27202854	SOCS2	1,21447358	TP53BP1	1,17870028	CLCN2	1,49912581
2953	UCP3	1,14042696	SERPINA1	1,18203663	ALG8	1,31018087	UBE2B	1,284946	ARPC1B	1,22513217	PCYT1B	1,19083032	CD55	1,52317235	3023	ANKRD6	1,13239912	ABCA12	1,17103401	DICER1	1,29018039	PRMT1	1,27199689	ICAM1	1,2144717	NR1I3	1,17830195	CYP2A13	1,49826383
2954	G6PD	1,14019714	GALNT9	1,1819106	STXBP1	1,31009202	DEGS1	1,28484617	ABCB8	1,2248704	KCNJ12	1,19041456	ICOS	1,52313032	3024	EIF2S3	1,13238133	PTGDR	1,17101786	TRIP10	1,29016337	SLC10A1	1,2718005	LAMP1	1,2144692	IGFBP1	1,17817001	VIP	1,49810499
2955	CDIPT	1,13989745	CD1E	1,18187305	APLP2	1,30998048	GNS	1,28466385	IKZF2	1,22477804	GCAT	1,19041455	ANAPC7	1,52278275	3025	GLCE	1,13230995	STX6	1,1707109	PIK3C2G	1,29009761	PSAP	1,27152649	IRF3	1,21407624	ACADM	1,17777137	PPT1	1,49796313
2956	FOXK1	1,13989155	ECGF1	1,18184732	GAPDHS	1,30962227	OXSM	1,28440205	HARS2	1,22477268	RB1	1,18996409	MTHFD1L	1,52266372	3026	COMP	1,13222705	RASA1	1,17070687	INSR	1,28988051	PSCD1	1,27146376	RANBP9	1,21394482	NDUFA8	1,17751594	GALNT12	1,49775236
2957	MYT1	1,13973284	DMD	1,18169451	KERA	1,30795803	GDF3	1,28424117	TGFB3	1,22474521	SMARCB1	1,18987506	APOA2	1,52247178	3027	STK36	1,13220075	IGFBP6	1,17069364	IL12RB2	1,2898352	DBH	1,27133255	CASP8	1,21392161	MBP	1,17742967	CAPN9	1,49761989
2958	CTPS2	1,1397081	CCL18	1,18161177	PGA3	1,30791457	EPRS	1,28423287	IL13	1,22438829	PPME1	1,18985418	F10	1,52242759	3028	BMP3	1,13207845	KHK	1,17037737	LPIN1	1,28969238	PIK3R5	1,27130138	HTR3D	1,2137961	CTPS2	1,17740118	ADH1A	1,49682488
2959	ABCB1	1,13956557	IHH	1,18138236	MGST1	1,30763565	DHRS7	1,28373148	PON1	1,22366666	B4GALT6	1,18971302	MR1	1,52175996	3029	PIAS1	1,13178851	IARS	1,17036061	HLA-DMB	1,28940909	GDF6	1,27042264	PELI3	1,21377875	CIDEB	1,17739636	ROCK2	1,49656569
2960	WDR79	1,1395483	CD96	1,18137265	PTTG1	1,30733056	PARP4	1,28363047	CD2	1,2234928	PDE8A	1,18957014	TRH	1,52168465	3030	TNKS2	1,1316167	ENO3	1,17035171	NFATC1	1,28935345	ABCC1	1,27038829	PNPLA3	1,21370827	G6PC	1,17688497	TREX2	1,49649247
2961	TRAFD1	1,13941597	PNPLA3	1,18130901	CD46	1,30687588	MAGI2	1,28339849	PGDS	1,22340663	EMR3	1,18955666	MCFD2	1,52133981	3031	HOXA11	1,13156098	CDX2	1,17033424	SRY	1,28929759	CUL2	1,27013784	MPI	1,21327401	IRF2BP2	1,17677658	EEF1D	1,49614989
2962	FHIT	1,13941125	CHEK2	1,1809059	CD274	1,30669541	FAS	1,28338394	POLD1	1,22330645	RAB35	1,18948881	ETV6	1,52108601	3032	MYLK	1,13156098	HES7	1,17017506	SHOC2	1,28920949	PPCDC	1,27006427	PSME2	1,21296865	FOXC2	1,17675868	PIF1	1,49582491
2963	METTL6	1,1393673	DLST	1,18086891	F9	1,30653671	CD68	1,28312979	NKD1	1,22313051	TP53	1,18929926	APC2	1,52028383	3033	DARS	1,13084566	THRB	1,169818	COL9A2	1,28920947	NTRK2	1,26981523	IFNK	1,21285643	GRM1	1,17660813	HDAC4	1,49555685
2964	AICDA	1,13922379	TFRC	1,18043689	RAB10	1,3064721	POLR1D	1,28269349	FZD10	1,22292032	GCH1	1,18920001	GRIN3B	1,51957702	3034	PAXIP1	1,13069267	CD209	1,16976191	MPG	1,28917843	YWHAH	1,26981033	TF	1,21274274	CKM	1,17648182	NCOR1	1,49535475
2965	TGIF1	1,1392103	F13B	1,1804284	GTF2A2	1,30644793	TBX21	1,28264059	BCAP31	1,2228389	GNAQ	1,18919168	FARS2	1,51849096	3035	CHRNA4	1,13013346	MAGEH1	1,16975152	GNAO1	1,28907601	ALG3	1,26966854	PPP1R12B	1,21250217	IL15RA	1,17641385	RAD23B	1,4952527
2966	CHDH	1,13914714	PTAFR	1,18022627	NDUFA13	1,30625184	DLX6	1,28236752	TGFB1	1,2227396	BCAP29	1,18893189	MBTPS1	1,51845956	3036	GALNT14	1,12996878	MYL2	1,16963018	CLOCK	1,28899046	KLF10	1,26944132	NRG3	1,21221839	DAO	1,17632155	PROX1	1,49518421
2967	NPR1	1,13904622	BAD	1,18019335	KLC1	1,30609524	PTPN2	1,28205676	SULT1A2	1,22255215	ACPP	1,18881665	SHC2	1,51837737	3037	SUMO3	1,12996231	CITED2	1,16949454	IFT57	1,28883096	EXO1	1,26896031	ST6GALNAC3	1,21192199	MELK	1,17627823	ABCG5	1,4951285
2968	PIGN	1,13893821	SNAP29	1,18012395	TCF7L1	1,30607394	HEL308	1,28196634	BNIP3L	1,22249741	PPT2	1,18817041	GABRA6	1,51830202	3038	PTPRO	1,12969882	CTSE	1,16929645	TNFRSF8	1,28866373	BBC3	1,26881644	PICALM	1,21191007	ARHGAP1	1,17623123	NOXO1	1,4949509
2969	PIGV	1,13886592	FLCN	1,17944628	APBA1	1,30585101	CASR	1,28170304	IRAK1BP1	1,22249558	HLA-F	1,18816343	PRMT5	1,51811174	3039	ACVR1B	1,12964709	STS	1,16907867	VAX2	1,28832104	ORC5L	1,26841299	PPARD	1,21168721	ISLR	1,17603039	CAPN2	1,49491202
2970	CD46	1,13885096	GCK	1,17923374	FCGR2B	1,30574821	DPM1	1,28152772	HPGD	1,22226372	VAV3	1,18797026	IRF5	1,51763312	3040	SHOC2	1,12949904	LY75	1,1690326	COMT	1,28760985	CAPN2	1,26835256	DAZAP2	1,21148319	PARD3	1,17579711	TEAD2	1,49444056
2971	ADAM9	1,13884047	PIGS	1,17921251	LIPE	1,30568086	ECGF1	1,28113923	INHBC	1,22210859	APBA2	1,18787307	ITGAE	1,51721917	3041	FTCD	1,12946064	CCBP2	1,1687951	GMPPB	1,2870906	CTF1	1,26807189	HMGB2	1,21144366	TRPM4	1,17570712	WFS1	1,49358842
2972	FHL2	1,13883124	ICAM5	1,1791237	GALK1	1,3053664	C1ORF142	1,28092503	UGT1A10	1,22184754	GNG13	1,18746267	CIP29	1,51690511	3042	PCSK1	1,12928885	FCGR1A	1,16857983	CNR1	1,28682728	AQP7	1,26793166	UQCRC2	1,21138624	OAS2	1,17546842	RPS6	1,49358661
2973	MKNK1	1,13882928	DNAJB11	1,17905123	SIRT4	1,3051132	PHPT1	1,28067207	LIG1	1,22180382	FYN	1,18729656	CD46	1,516665	3043	YARS2	1,12922074	AOX1	1,16853664	ACSL4	1,28678246	NFKB2	1,26788052	HSPD1	1,21137496	B4GALT2	1,17532832	MST1	1,49308799
2974	B3GALT2	1,13882732	SOX4	1,17888237	CACNA1H	1,30377756	TXNRD2	1,28059354	EXTL2	1,22178448	CSF3R	1,18723296	MSH5	1,51493323	3044	PSME2	1,12915909	H2AFX	1,16848411	PLA2G2F	1,2862161	REV1	1,26775642	CDKN3	1,21131085	IL2RB	1,17464366	MAP3K8	1,49294702
2975	DHRSX	1,13877381	PTPN6	1,17873047	POLR3K	1,30359961	POLR2K	1,28022565	TREX1	1,22173714	IL21	1,18723101	HERPUD1	1,51483357	3045	RGS4	1,12907475	HSP90AA1	1,16825928	GORASP1	1,2861006	IFNA21	1,26774179	CHDH	1,21122229	MMP7	1,17430229	CERK	1,49218609
2976	CYP2U1	1,13862598	DPM1	1,17859805	ARHGEF7	1,30354589	CPT1B	1,28021554	GRHPR	1,22168529	ABCG8	1,18715274	PDCD1	1,51443517	3046	PKN1	1,12895904	PLA2G12B	1,16811293	DBT	1,28596508	LY86	1,2677211	ME2	1,21116624	ADCY8	1,17389358	NFATC3	1,49185901
2977	NMNAT1	1,13862028	CHKB	1,177496	PMAIP1	1,30343736	GCG	1,27999171	AMD1	1,22120849	NPEPPS	1,18707595	PPP1R1B	1,51436608	3047	TERF2IP	1,12892553	HIC1	1,16798998	PROZ	1,28558249	GC	1,26754297	FMO4	1,21109064	NODAL	1,17373912	CD247	1,49171042
2978	CFP	1,13860699	SORL1	1,17734114	MICA	1,30332149	BHLHB2	1,27993862	NBN	1,22109133	DPPA5	1,18704967	HDGF	1,51403495	3048	SH2D3C	1,12890073	TPH2	1,16739709	CA12	1,28546936	EPN1	1,26730213	CBLC	1,21061377	CSNK1G1	1,17335885	JAK2	1,49168315
2979	FGF20	1,13857242	TSC2	1,17704724	HPSE	1,30289793	SEC61A2	1,27976535	PIWIL2	1,22107586	DDX51	1,18696475	GLUD2	1,51398345	3049	IRF9	1,12881607	DYRK1B	1,16722692	GNB1	1,28505567	HIP1	1,26727928	PLD3	1,21059058	UBE2G2	1,17334374	HGD	1,4908386
2980	UBE2B	1,13847498	TMED10	1,17667951	NDUFS4	1,3028683	MAP2K1	1,27930165	TSHR	1,2210738	RXRG	1,18667575	CBX5	1,51347638	3050	TNFAIP3	1,12868209	PTPN2	1,16710818	IKZF2	1,28495367	SMPD1	1,26708273	RXFP1	1,21035511	TNFRSF13B	1,1733095	IFNA2	1,49079169
2981	RASGRP3	1,13817489	CHKA	1,17630047	PDCD4	1,30201941	TIMP4	1,27920701	CDH15	1,22087836	MYOG	1,18641541	PTPRC	1,5130177	3051	IFNGR1	1,12867261	SPCS3	1,16703454	NDUFS7	1,28487225	ARHGAP4	1,26701981	CCL11	1,20999377	SLC12A2	1,17309853	SLC6A13	1,49017617
2982	PPCS	1,13799713	HOXB4	1,17611492	GALNT8	1,3019138	PRPS1	1,27917135	CRTC1	1,22072358	DBH	1,18613748	MAT2B	1,51269624	3052	FGF3	1,12864536	KLKB1	1,166592	ST8SIA2	1,28432389	METTL2B	1,2670198	OSBPL5	1,20984303	CCL7	1,17306805	NDUFA10	1,48966634
2983	HSD17B12	1,13786844	TCF4	1,17599149	PLAU	1,30162064	APOC1	1,27897879	ARHGEF11	1,22065316	ADAM10	1,1861251	SETD2	1,5125133	3053	DUT	1,12862978	COPS3	1,16640578	DTYMK	1,28393842	PIF1	1,26657209	FUT3	1,20980115	CALCR	1,17305717	CD151	1,48936839
2984	B3GAT1	1,13785086	ECHS1	1,17597598	DLL4	1,30144713	CLEC10A	1,27846058	BBOX1	1,22023433	ABCB10	1,18604555	HTR2B	1,51250548	3054	MADD	1,12860122	PFKP	1,16640229	UNC93B1	1,28384468	MAGEH1	1,26636222	DEDD	1,20932335	FGA	1,17300987	BMP8B	1,48861787
2985	IRX3	1,13784666	CIDEB	1,17591338	MAP3K7IP1	1,30128862	PCSK2	1,27833109	ADH1C	1,22000963	GPR83	1,18541791	RPL10	1,51185703	3055	ST6GALNAC3	1,12852771	YARS	1,16631773	CFI	1,28325142	KIT	1,26577721	RAC3	1,20927003	AIRE	1,17267473	POLE4	1,48846377
2986	DHFR	1,13760654	HTR3D	1,17573184	PTCH2	1,30056795	COL16A1	1,27814156	CTNNAL1	1,2199803	KCNMB2	1,18539334	NDUFS1	1,51160718	3056	PTPRA	1,12851814	MAPK10	1,16630728	DDX54	1,28324095	HCLS1	1,26539327	IFI27	1,20917378	CKS1B	1,17255247	BTG2	1,48804735
2987	INPP1	1,13751673	RAB3A	1,17557746	CAPRIN2	1,29964493	IL1R1	1,27809106	RAB23	1,21995521	CEBPB	1,18531484	CREB3L1	1,51145953	3057	ADRA1A	1,12850489	CDC2L5	1,1661273	NCOA2	1,28299024	UBE2D2	1,26523052	DYRK1B	1,20907536	RARG	1,17233599	SEMA4A	1,48742279
2988	DMC1	1,13749495	F7	1,17544446	BACE2	1,29937545	ITGA5	1,27805338	GBA	1,21976319	F13B	1,18529263	CYBA	1,51139193	3058	B3GNT3	1,12850294	ALAD	1,16592818	SSTR3	1,28288184	SCN2B	1,26453462	GPX6	1,2087364	TRH	1,17222389	ALMS1	1,48722645
2989	P2RX7	1,13741979	KCNJ4	1,17539653	C13ORF15	1,29913773	PARP2	1,27803649	IL6R	1,21967153	ADA	1,1845227	STEAP3	1,51047332	3059	ACAT2	1,12826172	XBP1	1,16587975	PPP3CC	1,28230516	MVK	1,26447879	RGS4	1,20847544	SULT2A1	1,17186192	IRS1	1,4871506
2990	ITPKA	1,13718536	AGPAT2	1,17537979	DUSP14	1,29852912	GP1BA	1,27769929	EBP	1,219567	PGM3	1,18444305	CXCL10	1,5093244	3060	ENDOG	1,12824678	GLI2	1,16557047	AGT	1,28212269	ERBB4	1,26434603	ALG1	1,20839202	YAP1	1,17181557	CTH	1,48703156
2991	IL19	1,13696147	GPR39	1,17504889	COQ7	1,29836163	ACTR3	1,27759237	FZD5	1,21950373	VDR	1,18412763	PIGQ	1,5088893	3061	IDI1	1,12810434	ANPEP	1,16541103	MAPK13	1,28211913	AKTIP	1,26393399	UGP2	1,20823325	ASRGL1	1,17171442	CSF2	1,48629999
2992	BLR1	1,13684069	GPT2	1,17487273	HSD17B12	1,2983453	MST1R	1,27729012	CP	1,2195013	SLC10A1	1,18374946	GALNT4	1,50885554	3062	FZD4	1,12779342	SNX6	1,16529576	NTAN1	1,28101646	IL4	1,26393024	BST2	1,20816765	CNR2	1,17127579	SPRED1	1,48616596
2993	GCNT1	1,13675144	CRAT	1,17481206	CFLAR	1,29825256	IMPDH1	1,27702485	ARHGEF2	1,21942579	LCP2	1,18372974	SP100	1,50879911	3063	ASGR2	1,12775369	CBX2	1,16529378	GNB1L	1,28093606	GRN	1,26376561	FBXW7	1,20813199	SHC3	1,17105162	MYB	1,48604976
2994	SMARCB1	1,13660971	ATG5	1,17475392	IL8RA	1,29783753	ARL4D	1,27675778	MLXIPL	1,21911358	CD53	1,18371822	ADK	1,50868454	3064	ITSN1	1,12736849	BMP15	1,16528962	PSAP	1,28038667	CYP2E1	1,26364095	STAT2	1,208056	GAB1	1,17093894	SMAD7	1,48528926
2995	COL4A2	1,13626482	SLC25A11	1,17470463	PAH	1,29778908	EGR4	1,27669596	CLDN15	1,21879776	GHR	1,1831972	ENDOG	1,50839533	3065	HTR2A	1,12736799	GPR81	1,16484932	DAO	1,28011056	GALNT1	1,2631543	GABRA2	1,20792006	PAFAH1B2	1,17081296	IL11RA	1,48503576
2996	CDR1	1,13623494	IDE	1,17451823	MAD2L2	1,29761202	PURA	1,2766883	PDE6H	1,21872501	B3GALT6	1,18301569	GDI2	1,50833381	3066	CNGA3	1,12728259	PLD2	1,16482685	SMPD1	1,28004647	CHRNB1	1,26307128	GADD45A	1,20789917	RCAN1	1,17080662	IL17RA	1,4849725
2997	HMGB2	1,13618386	HLA-DOA	1,17409758	STAT5B	1,29751563	CAPN7	1,27653369	POLD4	1,21863511	PLAU	1,1828607	TPS3INP1	1,50820471	3067	CD40LG	1,12727494	CREB5	1,16475282	PTH2R	1,27884667	KCNMA1	1,26302888	FARSB	1,20778117	PPP3CA	1,17076319	SNRPA1	1,48448193
2998	STX8	1,13601467	TMEM166	1,17391124	CSF3R	1,29750606	ITPKA	1,27640805	MSX1	1,21860673	GDF9	1,18282888	ATXN2	1,50785124	3068	CD9	1,12723108	MMP2	1,16449541	FOXO1	1,27872079	SDS	1,26302239	GUCA1C	1,20774892	NCOA1	1,17043226	GRIN2C	1,48398784
2999	DNMT3A	1,13580405	APOE	1,17348574	ATP5L	1,29749635	BDKRB1	1,27612458	CETP	1,21850215	ATP8A1	1,18275676	NCF2	1,50741046	3069	ETV7	1,12718583	MPI	1,16385772	STRA6	1,27787202	TTF2	1,26279458	MVK	1,20770173	MAPK9	1,17040384	NUMB	1,48383252
3000	DACT1	1,13571472	B3GALT5	1,17342231	BTK	1,29748304	BTD	1,27594213	FDPS	1,21839867	CAT	1,1827542	IRS2	1,50667141	3070	PPME1	1,12706377	G6PC2	1,1636893	RGS16	1,27786329	SYNE1	1,26269883	DPYSL5	1,20751478	ATF1	1,1703706	GPR65	1,48363149
3001	TOP3B	1,13558089	ZIC1	1,17328602	HOXA9	1,2972915	HLA-E	1,27579177	ACAD9	1,2183926	DCLRE1C	1,18273177	IRF9	1,50636195	3071	ALDH3B2	1,12678323	GSTK1	1,16364039	CAMK1	1,27776617	FCGR2B	1,26268356	ARNTL	1,20751244	NES	1,17030612	NP	1,48306252
3002	KLRC3	1,13546979	ACLY	1,17312488	LRDD	1,29719042	MYC	1,27576916	IL1R2	1,21838697	IDH1	1,18268208	ADRB3	1,50608369	3072	ICAM5	1,12671424	S100A12	1,16362014	LRMP	1,27764362	CBR1	1,26248926	HTR2B	1,20731286	EMP1	1,17009987	LBP	1,48305803
3003	ECHS1	1,13522579	ACAN	1,17311974	CALML3	1,29660372	RAG2	1,27540366	IFNA7	1,21794112	CHST6	1,18234281	PLA2G10	1,50574051	3073	CPSF4	1,12661398	MAP2	1,16360176	ITGA2	1,27759772	GAMT	1,26238301	SST	1,20703656	HSD17B10	1,16974277	B3GNT2	1,48284278
3004	GRIA1	1,13518648	EFNA1	1,17308312	PROM1	1,29589964	LDHAL6A	1,27527278	AVPR1A	1,21754331	VIPR1	1,18221097	ASAH1	1,50530374	3074	DERA	1,12568888	MAP4K5	1,16355047	FCGR2A	1,27704364	CKS1B	1,26226363	TERT	1,20661775	STRAP	1,16926787	GOSR1	1,48280218
3005	NPEPPS	1,1351023	SLC1A1	1,17286717	GNG13	1,29560143	MAPK8IP3	1,2752562	PIK3AP1	1,21742708	MSH2	1,18193123	PRMT2	1,50518098	3075	CSNK1D	1,12564629	EMR2	1,16345759	ITGAM	1,27694199	SERPINB9	1,26210688	COL3A1	1,20659802	ARL4D	1,16924253	MADCAM1	1,48192096
3006	PHKG1	1,13509648	HIST1H2AA	1,17260088	ADC	1,29529593	IRF2BP1	1,27467945	GRB7	1,21742505	PTPN2	1,18166776	CLDN20	1,50468085	3076	PRPS1L1	1,12559784	CLDN14	1,16326121	TGFBI	1,27665532	DOCK9	1,26203534	SOS2	1,20602471	CAMK2B	1,1691231	MTAP	1,48164905
3007	TERF1	1,13509574	POLR3GL	1,17259737	BIRC2	1,29517633	FUT7	1,27460153	IFNA6	1,21728256	STAMBPL1	1,18140222	CAMK2B	1,50453275	3077	MARCKS	1,12534969	NCR1	1,1631671	SULT1A2	1,27592869	IRAK3	1,26202862	GALNT11	1,2059195	TBK1	1,16891538	PRDX6	1,48115586
3008	MGAT4B	1,13508167	PIK3R1	1,17251242	BCKDHA	1,29504015	BMP10	1,27430598	TFR2	1,21703954	LUM	1,18136032	CDKN1C	1,50437933	3078	PRKD3	1,12533535	PLA2G10	1,16301058	ABP1	1,27573849	ORC4L	1,26177861	APH1A	1,20583149	FARSB	1,16875139	REN	1,4804376
3009	TF	1,1349037	PAN2	1,17237208	DUSP8	1,2940578	INPP5D	1,27427707	COQ2	1,21686232	CD72	1,18112186	DRD4	1,50362244	3079	CREB5	1,12526292	FZD10	1,16298759	SEMA7A	1,27573347	PPP3R1	1,26174815	POLK	1,20546745	C5	1,16847912	BHLHB2	1,47958175
3010	MR1	1,13459131	CISH	1,17217426	HBEGF	1,29373561	GCLC	1,27368638	ARL4D	1,21670063	ATP6V1E1	1,18101518	NFKB2	1,50340719	3080	GLS	1,12518683	CRKL	1,16272955	CD36	1,27533687	ALG1	1,26174059	APPBP2	1,20537418	IL11RA	1,16817813	GBE1	1,47934322

Table A4. Pooled-shRNA library screen on HEL cell line and MF-3: list of 2nd most depleted shRNAs for each experiment (ranking approach 1, RA1).

	NO ruxolitinib (setting 1)				Ruxolitinib (setting 2)				Ruxolitinib + CM (setting 3)				MF-3			NO ruxolitinib (setting 1)				Ruxolitinib (setting 2)				Ruxolitinib + CM (setting 3)				MF-3	
	Experiment 1		Experiment 2		Experiment 1		Experiment 2		Experiment 1		Experiment 2					Experiment 1		Experiment 2		Experiment 1		Experiment 2		Experiment 1		Experiment 2			
Rank	*Gene*	*Fold change*	*Gene*	*Fold change*	*Gene*	*Fold change*	*Gene*	*Fold change*	*Gene*	*Fold change*	*Gene*	*Fold change*	*Gene*	*Fold change*	*Rank*	*Gene*	*Fold change*	*Gene*	*Fold change*	*Gene*	*Fold change*	*Gene*	*Fold change*	*Gene*	*Fold change*	*Gene*	*Fold change*	*Gene*	*Fold change*
3081	HFE	1,1250328	SPAM1	1,16272955	HMGA1	1,27507879	HMGA1	1,26159311	QARS	1,20524432	CHRNG	1,16814445	DICER1	1,47847682	3151	MAP1B	1,11813364	GANAB	1,15061474	OLIG2	1,25898212	ENPP6	1,24258954	AARS2	1,19169968	PON1	1,1552266	EXT1	1,45272068
3082	DEDD	1,12502503	LHX2	1,16271842	CFTR	1,27505371	SIGIRR	1,26114611	NEU2	1,20493213	CD46	1,16813707	CD22	1,47779249	3152	NKRF	1,11805838	KLK1	1,15026845	GGCX	1,258523	GAL	1,24241803	GPX4	1,19162742	RARA	1,15519584	SIGLEC1	1,45223376
3083	SCP2	1,12499793	APP	1,16255984	MAPK8IP2	1,27494651	SLC6A2	1,26098104	REN	1,20485156	APAF1	1,16801052	ACTA2	1,47676477	3153	DUSP9	1,11801019	BACE2	1,15015331	REPS1	1,25781991	ALPL	1,24240391	FBLN1	1,19156218	APRT	1,15519006	EBI3	1,45162642
3084	CYP1B1	1,12498621	PLD1	1,16246708	INPPL1	1,27486557	PRKCQ	1,26046964	ALKBH2	1,2046418	PHKA2	1,16755048	ITSN1	1,476619	3154	INPP4B	1,11789312	ANGPTL4	1,15007418	F11	1,25777788	FCER1G	1,2423351	KCNJ11	1,19137147	ETV3	1,15490077	TCF7L1	1,45128957
3085	BLM	1,1248921	PTTG1	1,16234795	CFHR1	1,27476606	ALDH2	1,26038354	ALG12	1,2046387	IL8RA	1,1675503	E2F2	1,47566455	3155	GRK1	1,11788007	PRKAG1	1,15003825	AHCY	1,25775775	PPYR1	1,24227355	PPYR1	1,19126794	AZI2	1,15483929	GRB14	1,45043601
3086	PML	1,12464751	NSDHL	1,16219754	TSC2	1,27450586	SPR	1,26017019	ETV3	1,2043328	HSD3B1	1,1670623	ITPKA	1,47565641	3156	CHAT	1,11751309	POLR1D	1,1499374	NANOG	1,25729345	PYGL	1,24220948	PYGL	1,19113941	ATP6V0A4	1,15473822	USP11	1,45007809
3087	JAM2	1,12440082	PIP5K2B	1,16192044	PSMD8	1,27408923	CUZD1	1,25955212	TRIP10	1,20405168	CYBB	1,16695245	CTSG	1,47524781	3157	PFDN2	1,11743806	SLC16A3	1,14972076	MLH1	1,25704723	PIK3C2A	1,24218961	EIF3H	1,19095694	ID3	1,15467824	IL22	1,44999068
3088	SLC15A1	1,12437183	ACVRL1	1,16179908	JUP	1,2740349	TWIST1	1,25949713	PANK4	1,20403268	IL6ST	1,16680585	C4B	1,47515142	3158	CSF2RB	1,11737292	BCKDHB	1,14971708	WBSCR17	1,25668753	HRH3	1,2421426	KLRC3	1,19037697	ARPC4	1,15460581	GAMT	1,44989488
3089	CCR6	1,12409383	TNK2	1,16153131	FN3K	1,27403076	PPP2R2C	1,25899908	IRAK4	1,20385467	IMPA1	1,1665679	CKB	1,47359354	3159	SRXN1	1,11717969	BCMO1	1,14960645	CD276	1,25657054	PTPN6	1,24202753	XPA	1,19036345	LTB4R2	1,15427439	FARSB	1,44954536
3090	GNAL	1,12402445	ARNT	1,16132374	SLPI	1,27385381	GCLM	1,25866697	HESX1	1,20364596	APOE	1,16566018	FOXA1	1,47241812	3160	DKK1	1,1171361	DRAM	1,1495271	IL17RA	1,25620961	F7	1,24192939	TRPC7	1,19015362	CD52	1,15424511	COL4A4	1,44913587
3091	CIDEB	1,12395591	ICAM2	1,16116654	CD2	1,27333635	CPN1	1,25841622	FGF10	1,20344694	ACLY	1,16544523	AGPAT6	1,47149433	3161	BIRC5	1,11712868	IFNGR2	1,14940564	HADH	1,25603298	FECH	1,24186321	ARFGAP1	1,19009976	PTCH1	1,15421071	PIGP	1,44837078
3092	GLUD2	1,12391818	ELA2B	1,16092234	PPP2CA	1,27287791	HIST1H2AA	1,25806815	ABCG2	1,20315579	GCGR	1,16540936	SERPING1	1,47137443	3162	EDNRB	1,11706754	GBE1	1,14936571	TLR5	1,25596837	MEF2C	1,24127656	HRH1	1,18994757	FGG	1,15392614	IL10RA	1,44812887
3093	ENO1	1,12387781	REG3A	1,16062252	PARP4	1,27272866	GALNT14	1,25784351	ENTPD8	1,20293793	DNAJA2	1,16510377	ATF5	1,47109014	3163	MELK	1,11699649	CSNK1D	1,14918666	ACAA2	1,25562525	ST3GAL3	1,24124055	NMNAT3	1,1897014	EFNA5	1,15384106	DAD1	1,44799645
3094	BHLHB2	1,12381654	RALGDS	1,16053516	CASP10	1,27270491	DNAJC4	1,25766993	TUBB2C	1,20268142	SULT1A1	1,16488369	PGK1	1,47094863	3164	BNIP3L	1,11654764	ATP5J2	1,14908745	ANK2	1,25522711	AARS	1,24018884	SLCO1C1	1,189536	NDUFS4	1,15372892	VSNL1	1,44736625
3095	FGL2	1,12376888	TAF12	1,16047001	HYAL1	1,27229514	ST6GALNAC4	1,25749091	APOC2	1,20266986	MAP2K3	1,16456946	TCF7	1,47084729	3165	CEBPB	1,11651558	GNB1	1,14903705	MGAT5	1,25491444	TAL1	1,23996206	EPX	1,18915546	FANCI	1,15372176	HCST	1,44723137
3096	VHL	1,12375349	WNT9B	1,16018645	MC5R	1,27202939	CCNE1	1,25703058	CREBBP	1,20254429	GGT1	1,16411322	PI4KB	1,4708099	3166	HMBS	1,11607146	CARS2	1,14867967	EREG	1,25423105	EXTL3	1,2397732	EMP1	1,18905889	PLA2G2E	1,15353619	IFNA14	1,44624997
3097	UGT1A9	1,12351509	GRM2	1,15993413	VCL	1,27148718	SH3KBP1	1,25698795	PNMT	1,20253143	FNTB	1,16321013	HRH2	1,47075233	3167	MCM3	1,11602121	KPNA2	1,1486524	ITGB6	1,25384889	VIL2	1,2393359	ACMSD	1,18902242	VSNL1	1,15348697	PRMT6	1,44588975
3098	NOXO1	1,12343714	PRKAG2	1,15969443	CSNK2A2	1,27090261	CALM3	1,25678556	F13B	1,20232976	ENPP3	1,16306366	ACVR1C	1,47069143	3168	CDC25C	1,11587371	CYP4B1	1,14862773	NFKB1	1,2534902	HPRT1	1,23859959	ALG2	1,18882493	MAFK	1,15340923	LIF	1,4455603
3099	PRDX3	1,12337676	POLR1A	1,15935129	LOC390243	1,27071147	IL18R1	1,25672836	CEP290	1,20228674	AMD1	1,16298862	QPCT	1,47062644	3169	CYP3A5	1,11568133	ALG14	1,14825237	COL1A2	1,25327386	ACADVL	1,2382536	BCAT1	1,18874796	APCS	1,15332281	CD2	1,44479912
3100	TBX1	1,12296113	CDIPT	1,15927774	ADCY8	1,27058857	SH2D3C	1,25663874	IRS2	1,20228606	CA3	1,16208606	ITGAL	1,47030045	3170	TAF4	1,1156235	ADH1A	1,14824381	PARG	1,25322409	S100B	1,23824773	VEGFA	1,18872248	CD55	1,1532041	TGFBR2	1,44476608
3101	CLOCK	1,12292585	NDUFS4	1,15927327	GDI1	1,27032142	FZD5	1,25640238	GTF2A1	1,20213925	PDK2	1,16198222	PANK3	1,47009786	3171	FGF10	1,11561473	SUMO1	1,14820755	SET	1,2532189	PTGS2	1,23805916	RTKN	1,1886927	SPTBN4	1,153106	MAP2K5	1,44392251
3102	TTR	1,12286307	YWHAG	1,15918587	NKIRAS2	1,26974616	BDH1	1,256165	MAN2B2	1,20208066	NPPB	1,16189651	AKR1C2	1,46997273	3172	EGLN1	1,11559491	RBP4	1,14813252	MTMR1	1,25300503	PANK2	1,23781585	PAPSS1	1,18865331	AMH	1,15282813	ATF7IP	1,44381286
3103	CHRNA3	1,12282875	LITAF	1,15887111	LMO1	1,26945879	ABCA2	1,25615026	ABCC2	1,20156867	CHKB	1,16188151	SLC1A3	1,46995809	3173	GNB1	1,11553617	AKAP9	1,14763948	ATG2A	1,25281125	GZMB	1,23778006	FTO	1,18838333	CD40	1,15281626	AVPR1B	1,44301699
3104	PDE6A	1,12277504	MSH2	1,15856789	SH2B2	1,26936741	B4GALT2	1,25563677	PLA2G4B	1,2013864	ZBTB20	1,16187375	IRF8	1,46990724	3174	TGFB3	1,11524471	F9	1,14754237	SOCS7	1,25272846	SPRY2	1,23737658	ARFGAP3	1,18831651	ABCA2	1,15271033	S100A6	1,44213766
3105	EGR4	1,12273274	MICA	1,15855175	TBL1XR1	1,26934267	CD24	1,2556337	EDN3	1,20087245	PDXP	1,16144995	TNFSF13B	1,46928919	3175	ARF1	1,11485715	PTGER4	1,14745275	PFKP	1,25265654	NCOA3	1,2373709	STX17	1,1882178	CUZD1	1,15241293	NDUFB5	1,44187989
3106	SCN10A	1,12268889	ACSL1	1,15837309	CHRNB3	1,26907822	MC5R	1,25458971	SH3GL2	1,20072567	COMT	1,16109344	COL4A3	1,46877775	3176	ATP5O	1,11451139	PPT2	1,14741836	DGKI	1,25243311	SERPINE1	1,23716596	GCLC	1,18810665	CAPN3	1,15239035	IL17D	1,44118372
3107	C4A	1,12260077	ATG4A	1,15809722	DHRS2	1,26904054	DIAPH2	1,25458362	ARHGEF7	1,20018033	IL9R	1,16100799	GAS2	1,46836595	3177	EXT1	1,11448438	CHRND	1,14732387	USP11	1,25205503	PLA2G2F	1,2369347	ATP2A1	1,1871338	GNAZ	1,15204418	EIF1	1,44113011
3108	ME1	1,1224963	BLNK	1,15789418	F13B	1,26894995	GLP2R	1,25439986	CSMD1	1,20011149	DPYS	1,16073856	ITPR3	1,46799515	3178	MBP	1,11445081	IFNA4	1,14724468	PPT1	1,25108094	ALG13	1,23649545	CRADD	1,18642301	KALRN	1,1519284	REV3L	1,44090767
3109	PIK3R1	1,12242257	LEFTY2	1,15785703	A4GALT	1,26878323	ISYNA1	1,25422902	NFATC3	1,19965129	CD68	1,16044303	MAML3	1,46774071	3179	CD58	1,11427523	CYP3A43	1,14697348	SEC61A2	1,25097981	CLCA1	1,23649545	CYP2D6	1,18621808	MMS19L	1,15174864	BAAT	1,44080401
3110	UGT1A10	1,12240525	SELE	1,15785703	ST3GAL2	1,26847294	HLA-DQB1	1,25416101	RAD54B	1,19961225	DIO1	1,16034464	GSK3B	1,46708381	3180	SREBF1	1,11427077	HADHA	1,14693593	ST3GAL3	1,25072023	ERCC1	1,23644355	ETS1	1,18594233	SLC26A2	1,15173609	PIAS1	1,44023058
3111	GABRB3	1,12230551	GJB1	1,15760456	F2RL2	1,26813571	C14ORF166	1,25389413	GTF2H5	1,19954097	CXCR4	1,1603241	PINX1	1,46698998	3181	SOAT1	1,11424918	GAPDHS	1,14689486	CFD	1,25070954	PDK2	1,23639163	HBEGF	1,18554472	PCAF	1,15165813	PARP4	1,44018873
3112	PHC1	1,12227878	SPRY2	1,15759237	YWHAH	1,26771524	ATRX	1,25381518	ADD1	1,19896363	DNAJA1	1,16003928	TCF4	1,46658944	3182	PIGP	1,11418732	SULT1E1	1,14688041	ITSN1	1,25024987	IL22RA1	1,23635879	REPS1	1,18541975	POLRMT	1,15121113	SERPINF2	1,43937048
3113	MX1	1,12225741	VWF	1,15753353	CD209	1,26761746	TSNAX	1,25380222	HPN	1,19890225	GRIN3B	1,16000457	MAN2B2	1,46658344	3183	MTA2	1,11403868	SLC1A7	1,14683705	F2R	1,2502133	CP	1,23630258	ISG15	1,18533752	CTF1	1,15064153	RECQL5	1,4391133
3114	IFITM1	1,12221255	IL17RE	1,15731579	IL22RA1	1,26723828	FES	1,25354495	CREB5	1,19876391	CALR	1,15993929	MDM2	1,4665647	3184	CD37	1,11396056	PLSCR1	1,14681026	SPN	1,25006794	PPCS	1,23619428	UXS1	1,18524557	ITPR2	1,15049236	PURA	1,43813234
3115	FGF7	1,12203951	PPP1CB	1,15729716	TREH	1,26721876	PDE2A	1,25347789	FN1	1,19821297	SRXN1	1,15989935	AGXT	1,46641932	3185	MCC	1,11392803	SDHC	1,14632312	ALG13	1,25002719	TH	1,23610667	GRIN2C	1,18503637	ACHE	1,15045592	ENPEP	1,43787785
3116	DTX4	1,12201474	SIRT2	1,15724617	YWHAB	1,26672447	SCN4B	1,25333891	COL9A2	1,19759018	BAIAP2	1,159784	SAA1	1,46603034	3186	MKNK2	1,11383455	PPAP2B	1,14617724	UBE2D2	1,2499266	ABCB9	1,23546526	SHISA5	1,18489879	ERBB4	1,1503434	GNAQ1	1,43681185
3117	MGST1	1,12199108	GNA11	1,15701183	PDE3B	1,26667031	GNA13	1,25322162	PCSK1	1,19747591	IL5	1,15970322	DCLRE1A	1,46579396	3187	HTR3E	1,11380931	SH3GL3	1,14590019	CRHBP	1,249863	GYPA	1,23514621	PDE1C	1,18488865	ALG1	1,15028315	ALDH7A1	1,43657416
3118	CHEK1	1,12187353	PPP2R5B	1,15645436	RDH14	1,26646736	HAND1	1,25302079	YWHAH	1,19702611	PDE4B	1,1595981	GCLC	1,46511656	3188	TCF4	1,11374906	GNAT1	1,14581717	YWHAZ	1,24971989	CLDN11	1,2343095	NFKBIL1	1,18471388	KLK10	1,15016384	ZNF395	1,43648805
3119	C2	1,12185545	PURA	1,15636481	SEPP1	1,26619703	PLSCR4	1,25186647	GJA1	1,19699385	ROCK1	1,15938403	EPHX1	1,46495076	3189	GANC	1,11366602	CHDH	1,14571234	CHST1	1,249605	TIAM1	1,23414574	SREBF1	1,18450142	EDG4	1,15016184	RAB6A	1,43646308
3120	LPO	1,12159362	TAF10	1,15625452	GCGR	1,26619047	SIRT2	1,25181936	AGPS	1,19695947	XIST	1,15936628	NT5C1B	1,46423687	3190	TRIM25	1,11364079	CACNA1G	1,14566252	CA6	1,24916085	ITM2B	1,23414448	OPRS1	1,18405394	VHL	1,14992398	LAMP2	1,43626159
3121	CD79B	1,12158701	CD1B	1,15619166	ATP5F1	1,26545981	PLA2G6	1,25071231	NR6A1	1,19671215	GJB1	1,159165	HSPA1B	1,46353965	3191	MAPKAPK3	1,11362048	TAF4	1,14562446	STS	1,24915589	PLA2G3	1,23414086	CYP1B1	1,183907	VCAN	1,14984236	ECE2	1,43617392
3122	TYMS	1,12156981	TPO	1,15566082	CD3E	1,2652312	RNF4	1,2505653	FARS2	1,19639256	GPR64	1,15912257	IRS4	1,46346787	3192	ALG3	1,1135837	SLC10A2	1,145601	LIPT1	1,24877813	DNMT1	1,23386558	ATG16L1	1,18379554	DACT1	1,1496271	MAPK10	1,43608504
3123	ETFA	1,12144576	DNAJA2	1,15534575	B4GALT3	1,26495377	ATG16L1	1,24996682	BLNK	1,19614076	IHH	1,15895699	IMPA1	1,46329136	3193	NTRK1	1,11352062	TRAF5	1,14531498	COASY	1,24845109	TAPBP	1,23328768	VHL	1,18363386	ACCN1	1,14931885	ZFYVE9	1,43591941
3124	C22ORF28	1,1212452	SLC15A1	1,15517804	SMARCD1	1,26442588	IFI35	1,24913233	NDUFA5	1,1959149	CDC2L6	1,15890121	PLCB1	1,46304587	3194	UBE2J1	1,11334616	METTL2B	1,14447769	MKKS	1,24832525	ADM	1,23316635	DAO	1,18354138	RDH11	1,14900457	PIGS	1,43573432
3125	VEGFA	1,12106173	HYAL3	1,15487233	HLA-DPB1	1,2638892	PTPN1	1,24912827	CARS2	1,19557179	MADCAM1	1,15884144	AKT1S1	1,46294634	3195	SOST	1,11334135	CTNND1	1,14410313	ACSS1	1,24717847	GNAO1	1,23284276	NOD2	1,18348998	THRA	1,1489719	LRP2	1,43551147
3126	EBI3	1,12098984	COL23A1	1,15474726	GGPS1	1,26348358	NRF1	1,24887996	GRIK3	1,19550584	CREB1	1,1586994	SIN3A	1,46284228	3196	GNB1L	1,11320854	PDE6H	1,14345004	TBXAS1	1,2471436	ORC2L	1,23283859	TRIM28	1,18311115	CX3CR1	1,14876737	GP1BA	1,43532899
3127	RAC3	1,12098892	CTPS	1,15426276	SCNN1B	1,26333667	LARS2	1,24871232	KLRC2	1,19535234	DUSP1	1,15849353	CAPN10	1,46135693	3197	ARHGEF1	1,11309523	S100A8	1,14336916	UPC	1,24707184	IRF2	1,23256674	UPB1	1,18303944	RPIA	1,14872271	CFHR3	1,4351562
3128	TDG	1,12098584	MDC1	1,15417957	CHRM5	1,26299341	NARS	1,24765103	PMAIP1	1,19530526	CAMK2A	1,15845738	CER1	1,46120319	3198	BCL11B	1,11307007	FGF20	1,14332295	GALNT10	1,24673873	ESRRA	1,2322812	GARS	1,18288462	AOC2	1,1486935	ICAM1	1,43494646
3129	CD47	1,12066585	PEG3	1,15383856	GPR161	1,26293464	SERPINA3	1,24743468	C1QBP	1,19526797	GYPA	1,15827358	ATP6V0A2	1,46099739	3199	CITED2	1,11301618	BACH1	1,14326159	APAF1	1,24668259	IDH1	1,2321507	GDI2	1,18287693	TBX21	1,14861443	C9ORF47	1,43492657
3130	ACVR2B	1,12058795	CTSD	1,15379498	NUMBL	1,26279508	LTBR	1,24740017	SLAIN1	1,19518771	CSK	1,15818517	PNLIP	1,46096223	3200	ARHGEF5	1,11301187	FN1	1,1425606	TXN2	1,24594129	GRWD1	1,23208535	EMR3	1,18275544	WNT9B	1,14836268	CD74	1,4346044
3131	CTBP2	1,12054422	C7	1,15360801	ASMT	1,26252479	ABLIM2	1,24739599	CAMK2D	1,19484887	AMY1A	1,15789612	EXO1	1,46090634	3201	PUM1	1,11293591	ATP2B3	1,14246697	DUOX1	1,24581034	COL9A2	1,23179122	TUBG2	1,18272921	GSS	1,14834004	GPRC5D	1,43339866
3132	BTK	1,12046963	SH3GL2	1,15351263	LMNB2	1,26250685	KPNA2	1,24734516	CACNA1D	1,19483132	NT5C	1,15784378	APRT	1,46015556	3202	ARPC5L	1,11281036	DGKG	1,14245055	SERPINA3	1,24579383	NTSC2	1,23174893	ASRGL1	1,18256813	ARNTL	1,1482265	RAB23	1,43258415
3133	CASP4	1,12037366	ACOT11	1,1534305	FRS2	1,26209342	FARSB	1,24713753	ZAP70	1,1948052	TNIP2	1,15782498	AMDHD1	1,45897055	3203	CDKN1C	1,11256986	ENPP6	1,14236667	DOLPP1	1,24571227	RARS	1,23162385	TNFSF13	1,18224631	TRIM25	1,14806515	MYL4	1,43251973
3134	MKI67	1,12014848	FOXO1	1,15320326	IL10RA	1,26191908	AK3	1,24691531	PTPN2	1,19459484	BMPR1B	1,15780886	ACVR2A	1,45853026	3204	DRD4	1,11253004	SLC1A2	1,14223183	SFRS12	1,24566061	C13ORF15	1,23131546	DIXDC1	1,18209197	NDUFB5	1,14796055	PCK2	1,43203898
3135	ACTN4	1,12012535	SMAD3	1,15305557	INHBC	1,26183017	IHH	1,24643267	SKIL	1,19449386	ADH7	1,15752092	CENTD1	1,45849986	3205	HYAL3	1,11246863	POLR3K	1,14219703	ATP6V1G2	1,24561498	KERA	1,23067242	ALDH3A1	1,18207945	CARM1	1,14760812	GALNT13	1,43157646
3136	ACIN1	1,12010944	SYT1	1,15291708	PDE6C	1,26148044	RAD50	1,24638713	GPR132	1,19427519	PSME3	1,1572927	TGFBI	1,45838001	3206	NDUFB8	1,11195375	SLCO1C1	1,14214782	GHRL	1,2454802	GHRL	1,23054652	GNAL	1,18207001	DOK1	1,14743018	COX10	1,43148322
3137	IFI16	1,12010921	LBP	1,15290886	MCF2	1,26107226	HMOX2	1,24620599	TOP2A	1,19410466	NOX4	1,15714366	INSR	1,45791248	3207	DDX51	1,11193591	MRPL19	1,14195771	ADH1A	1,24535234	MRE11A	1,23041143	CPSF3	1,1818706	APOA4	1,14724502	GRM7	1,43138747
3138	CCND2	1,11981619	GSTO1	1,15268621	POR	1,26085521	PGA4	1,24613057	CACYBP	1,19365448	IL17RD	1,15707267	IFIT3	1,45715493	3208	AKR1C2	1,1118119	OLAH	1,14177041	DPEP1	1,24534414	SMAD5	1,23033436	FKBP1A	1,18169643	TGFB2	1,14702266	FOXM1	1,43117354
3139	NPY2R	1,1198109	S100A9	1,15233031	CRAT	1,26082529	ARNTL	1,24603811	INPP4B	1,19356348	PDGFRB	1,15689979	SRPS4	1,45707323	3209	AGRP	1,11156277	SMUG1	1,14158305	IMPA1	1,24522834	TFAP2B	1,23029734	CSF2RA	1,18138449	GYS2	1,14698606	SMC6	1,43001038
3140	SLC6A2	1,11934619	KCNA5	1,15216387	PARP1	1,26082529	PGM3	1,2460252	MITF	1,19354467	AP3M1	1,15636618	SMN1	1,45601306	3210	PCSK2	1,11144642	SORBS1	1,14154263	TRPV6	1,24460106	HADH	1,23016665	MBD1	1,18136033	SHB	1,14683107	RAP2B	1,42994156
3141	FEN1	1,11934283	HSPA5	1,15207922	SNX2	1,26081471	CFP	1,2457224	ARF3	1,19352489	YES1	1,15628273	COL25A1	1,45591709	3211	CNPY3	1,1113088	F2RL3	1,14151397	CLDN15	1,24446208	ARHGEF7	1,2301305	APC	1,1805122	TTR	1,14668617	WWTR1	1,42993986
3142	COQ6	1,11933607	CD82	1,1520253	CTBP1	1,26069626	TM2D1	1,24565168	BAP1	1,19337491	BIN1	1,15619983	POLB	1,45578571	3212	B2M	1,11120093	REPS2	1,14074382	DCC	1,24393122	CHEK2	1,23011356	EPHB3	1,18039715	MYH3	1,14616047	PTH2R	1,42930941
3143	GRB7	1,11919138	PIGH	1,15192337	GPAM	1,25995724	EPO	1,24563832	NOTCH1	1,19309962	IRF4	1,15618129	CD38	1,45553037	3213	TUBB4	1,11100273	NR2F6	1,14034887	CD27	1,24385478	KATNB1	1,22999801	COL4A6	1,18028431	KCNQ1	1,14599959	RNF146	1,4285615
3144	CSNK1A1L	1,11916477	TLR7	1,15166855	FANCF	1,25985196	DAO	1,24562627	RAD51C	1,19284717	MEF2C	1,15607206	AGA	1,45500919	3214	BBS1	1,11063819	GPAA1	1,14034271	ATP5D	1,24334644	SCN10A	1,22988431	SELPLG	1,18026403	MYF6	1,14582151	SKIL	1,42770531
3145	SLC22A6	1,1189629	NEU2	1,15150966	NMNAT2	1,25982829	NANOS1	1,24560889	RDH5	1,19253536	CXCR3	1,1559706	BCKDHA	1,45457452	3215	CKMT1B	1,1103745	GZMB	1,1403223	UGP2	1,24265672	KCNQ5	1,22948157	PLAGL1	1,18015989	EFNA3	1,14574702	AREG	1,42696064
3146	PIK3CA	1,11888003	SHOC2	1,15147439	SMC6	1,25971374	GSTO1	1,24468095	KDELR1	1,19238089	FZD5	1,15594798	RUNX2	1,45422061	3216	GNAT1	1,11031113	FTMT	1,13988861	DAZAP2	1,24249024	PELI3	1,22917133	HS3ST1	1,1801269	DHX58	1,14571926	RDM1	1,42655883
3147	TGM2	1,11850716	STAT2	1,15139593	PMS1	1,25949385	SOAT1	1,24409085	CD72	1,19232462	SCN10A	1,15564937	TFCP2	1,45377663	3217	CHST12	1,11018312	LOC390243	1,13942118	KCNK3	1,24232376	PDGFRA	1,22847477	ATG4C	1,1800886	DISC1	1,14564586	FLT4	1,42646916
3148	UGT2A3	1,11823895	DCLRE1C	1,15130728	ANAPC5	1,25916806	CLDN18	1,2438504	DHFR	1,19215763	BCAT2	1,15552914	LCMT1	1,45317732	3218	HYAL4	1,11017043	NBN	1,13929842	UXT	1,24220538	TGFB1I1	1,22845227	IRF7	1,17991416	AMOTL1	1,14548212	ATP6V1H	1,42639036
3149	APOBEC3A	1,11821451	WWP2	1,15120933	ACVR1C	1,25909327	PLA2G10	1,2433431	PPP2CA	1,19192563	ABCC8	1,15523773	PSMA7	1,45306421	3219	WRN	1,11010404	SP100	1,13920848	CHRNA5	1,24151481	NR6A1	1,22842574	BTK	1,17988035	SULT4A1	1,14538919	CFL1	1,42507023
3150	IFIT3	1,11818604	RAD51L3	1,1506175	ZNF395	1,25901502	TSPO	1,24279561	TM2D1	1,19181241	PRKCI	1,15523773	PPP1R10	1,45302876	3220	POLM	1,10996818	TCOF1	1,13917867	GPRC5D	1,24137844	ARHGEF1	1,22675436	MAP2K6	1,17968205	NT5M	1,14528369	PIGF	1,42499487

Table A4. Pooled-shRNA library screen on HEL cell line and MF-3: list of 2nd most depleted shRNAs for each experiment (ranking approach 1, RA1).

	NO ruxolitinib (setting 1)				Ruxolitinib (setting 2)				Ruxolitinib + CM (setting 3)				MF-3				NO ruxolitinib (setting 1)				Ruxolitinib (setting 2)				Ruxolitinib + CM (setting 3)				MF-3	
	Experiment 1		Experiment 2		Experiment 1		Experiment 2		Experiment 1		Experiment 2						Experiment 1		Experiment 2		Experiment 1		Experiment 2		Experiment 1		Experiment 2			
Rank	*Gene*	*Fold change*	*Gene*	*Fold change*	*Gene*	*Fold change*	*Gene*	*Fold change*	*Gene*	*Fold change*	*Gene*	*Fold change*	*Gene*	*Fold change*	*Rank*	*Gene*	*Fold change*	*Gene*	*Fold change*	*Gene*	*Fold change*	*Gene*	*Fold change*	*Gene*	*Fold change*	*Gene*	*Fold change*	*Gene*	*Fold change*
3221	CYP4B1	1,10986312	CIITA	1,13885194	SPCS3	1,24130635	BCL2A1	1,22668744	MAP2K4	1,17954987	RAD50	1,14525123	ACVR1B	1,42497841	3291	SYK	1,10266297	GPX3	1,1297223	CBX3	1,22541389	RET	1,20993956	NFATC1	1,16660121	SLC6A13	1,13562146	MC5R	1,40000458
3222	DAB1	1,10978004	CD5	1,13878831	PPP3R2	1,24072925	AK5	1,22655879	HMGN1	1,1792131	PFN2	1,14514371	PCNP	1,42403252	3292	ADCY4	1,10251402	CREB3L1	1,12970634	TUBB2C	1,22531509	KCNA7	1,20987908	SLC6A2	1,16658802	PITPNB	1,13561585	PLEC1	1,39939216
3223	GSK3A	1,10974153	GAL	1,13873375	METTL6	1,24071339	ST6GALNAC2	1,22632373	FNTA	1,1787359	DHRS7	1,14500284	ATP6V0A1	1,42387913	3293	UNC13B	1,10249532	TCL1A	1,12954379	GPT	1,22529139	BDH2	1,20978472	HBB	1,16647115	MAFB	1,13554986	HDAC8	1,39895227
3224	COPS3	1,10941199	CRHR2	1,13871016	NANOS1	1,2406226	UQCRH	1,22625483	CFHR1	1,17866467	RBPJ	1,14485483	CSF2RA	1,42365555	3294	HDAC2	1,1024178	LPIN3	1,12948649	DLAT	1,22528036	ASPH	1,20933028	CA4	1,16626021	GPR68	1,13553592	SPRED2	1,3988312
3225	AMDHD1	1,10933554	IL5RA	1,13861939	BMPR1B	1,2405923	CA5B	1,22616449	HSP90B1	1,17849449	CACNA2D2	1,1445318	PDE8B	1,42345683	3295	PPYR1	1,10235721	SERPINA10	1,12929524	C3	1,22483859	GSS	1,2090198	HES2	1,16512271	DLG4	1,1353395	GRB7	1,39880481
3226	SOCS6	1,10923611	RDH11	1,13860345	LTBR	1,24055429	FKBP5	1,2260907	SVIL	1,17846113	F9	1,14445572	SOX17	1,42323287	3296	PSCD1	1,10223654	IKZF2	1,12926187	CYP17A1	1,22459628	KCNQ1	1,20895167	DES	1,16492094	CCL28	1,13502602	METTL6	1,39860117
3227	MAP3K7IP2	1,10921969	CD28	1,13798822	FOXH1	1,24004871	SHISA5	1,22606398	MAP3K3	1,17811462	PPP3CC	1,14436717	ALOX12	1,42304439	3297	ADCY5	1,10222398	COL1A1	1,12921747	GPX6	1,22452209	SLC30A3	1,20886443	POLR3H	1,16488132	GPR132	1,13471794	ADCY8	1,39822157
3228	SPIB	1,1089508	ARHGDIA	1,13749799	CREB3L3	1,24003487	ABCA4	1,22567331	TNFAIP6	1,17740724	HBXIP	1,14418774	RAB35	1,42297784	3298	FUT4	1,10213707	TBKBP1	1,12908657	NPR3	1,22412823	CD8B	1,20884257	CYP3A4	1,16472296	HDC	1,13470209	FTH1	1,39780831
3229	GABRG3	1,10887668	BAG5	1,13749403	CEP290	1,24003421	CDK5R1	1,22511613	GRIN3B	1,17735776	EPHB3	1,14412904	SMAD5	1,4227329	3299	GPR50	1,10203752	LTA	1,12906722	NKD1	1,22407265	TGFB1	1,20833413	TAF2	1,16417722	CARS2	1,13457156	PSCD2	1,39719798
3230	CPSF2	1,1088656	PPYR1	1,1374137	SLC33A1	1,2396186	BCHE	1,2249533	XIST	1,17728971	ARHGAP6	1,14349071	ACTN4	1,42215465	3300	CD81	1,10193255	EPOR	1,12896277	IL16	1,22401038	ERBB3	1,20782657	GDF2	1,16416955	GAST	1,1345039	AURKA	1,39708475
3231	CCR10	1,10884729	GALNT10	1,13720986	TUBB2A	1,23956755	HPSE	1,22479608	POLD3	1,17680534	SOCS7	1,14339489	IL12A	1,42153631	3301	UQCRC2	1,10187377	SULT1A1	1,12863	CDC45L	1,22344874	PUM2	1,20776347	STON1	1,16410339	MYL3	1,13434579	EIF4G3	1,39690157
3232	CTPS	1,10880259	BCL2L14	1,13710162	SUCLA2	1,2393703	SLC18A2	1,22469904	CDS2	1,17662433	RECQL	1,14321466	UGDH	1,42137675	3302	JAG2	1,10181506	APOBEC4	1,12855281	SLC26A2	1,2234385	ABCC3	1,20679111	CSTF3	1,16402742	HPX	1,13421256	MTR	1,39672251
3233	DBN1	1,10868778	MIF	1,13677821	HAO1	1,23907447	ARHGEF2	1,22444713	OAZ1	1,17662433	ACP2	1,14321248	ONECUT1	1,42106559	3303	GZMA	1,10168439	SERPINE2	1,12837382	CX3CR1	1,22327421	PDE3A	1,20644115	ITGB7	1,16391919	UBE2J1	1,13404212	CPS1	1,39664854
3234	HTR3B	1,10858001	SLC27A4	1,1364114	PPOX	1,23874562	NOS1	1,22419742	PIGB	1,17642274	IFITM1	1,14290969	CRTC1	1,42085432	3304	TGIF2	1,1016679	ACMSD	1,12804851	HLX	1,22304587	PRKACB	1,20637162	SPIB	1,16391919	TDP1	1,13372723	ETV5	1,3965007
3235	COL9A2	1,10855608	TNFAIP6	1,13605831	KALRN	1,23829087	DKK1	1,22399719	DCLRE1C	1,17607897	IRF7	1,14290969	TXN2	1,42081863	3305	CSF3R	1,10164743	NOV	1,12796143	PDE6B	1,22245788	IL28RA	1,20622419	ORC4L	1,16369945	PML	1,13352931	BNIP3L	1,39583999
3236	GALNT2	1,10854096	PLA2G3	1,13604146	PDXP	1,23812087	FN3K	1,22351117	UBE2M	1,17591744	CYP4A22	1,14280189	ASL	1,42059344	3306	LUM	1,10144041	UBE2E1	1,12721428	SP100	1,22240611	FZD2	1,20621202	KCNQ5	1,16343169	NOLA2	1,13351156	BLR1	1,39577041
3237	F11	1,10829091	HYAL1	1,13599048	NTHL1	1,23785608	ME2	1,22318642	DDIT4	1,17502703	HLA-DMB	1,14267345	SYNJ1	1,42012352	3307	MYH2	1,10141727	POLH	1,1271106	GTF2H5	1,22238179	OXCT2	1,20600296	ACLY	1,16296498	EFNA4	1,13350739	PRKACG	1,39570925
3238	PSENEN	1,10819586	MAPKAPK3	1,13594011	RECQL4	1,23756781	COL7A1	1,22309106	CARM1	1,17493105	FECH	1,14252445	HTATIP	1,41988461	3308	ARSA	1,10134516	CEACAM1	1,1268455	PPP2R5B	1,22206002	POLR3G	1,20578998	RFK	1,16264599	GPR34	1,13313227	GLS2	1,39529581
3239	GSTK1	1,10795422	PON2	1,13531815	CENTD1	1,23756122	INPP4B	1,22294428	DGKA	1,17475352	CCND1	1,14247347	SRF	1,41915386	3309	IL25	1,10120359	ZMYND17	1,126823	EOMES	1,22181892	WNT11	1,20575697	GPRC5C	1,1625864	MYT1	1,13298017	HAND1	1,39504108
3240	GATA4	1,10795193	PELI1	1,13515596	ATP6V0A1	1,23749731	SDC2	1,22277449	CAB39	1,17454615	BCHE	1,14235357	MAOB	1,41877777	3310	OAZ1	1,10092736	PGA4	1,12681592	GCK	1,22167958	TRPC7	1,2056191	LMO1	1,16230426	PHKB	1,13285416	TAT	1,39377586
3241	AGK	1,10780675	RNF25	1,13514329	EIF4A1	1,23743026	DKK4	1,22167173	GRIN2B	1,17454542	ST8SIA1	1,14201512	AK3	1,41725477	3311	AHR	1,10079481	EDN1	1,12677294	PSMB10	1,22157932	KLK1	1,20543824	TLR8	1,16204042	ICAM5	1,13245839	PER1	1,39351223
3242	ISG20	1,10759094	NFYC	1,13501431	A2M	1,23708398	KCNMB4	1,22165902	GLRX2	1,1745063	FZR1	1,14196682	PRPS2	1,41712314	3312	CARM1	1,10061121	SSR4	1,12663275	OSBPL5	1,22142982	RAP1B	1,20498061	CX3CL1	1,16191657	CCR1	1,13243347	GMPPA	1,3928561
3243	CMAS	1,10758827	PINK1	1,13470799	ALDH2	1,23688453	MMP8	1,22091347	UBE2G2	1,17435022	MAPK10	1,14195999	FZD2	1,41695708	3313	CA9	1,10060456	AKR1D1	1,1266081	DLG4	1,22135177	EBI3	1,20495726	CYP1A2	1,16166832	ABLIM2	1,13214048	SLC1A1	1,39224794
3244	OSBPL5	1,10756065	CHRM4	1,13448709	XDH	1,23585922	CACNA2D3	1,22058166	C3	1,17434373	GJA1	1,14190407	PON2	1,41659044	3314	JAK1	1,10055694	JAM2	1,12644443	KCNJ12	1,22112073	HMGB1	1,20486569	BAG3	1,16145589	NPR3	1,13207045	SERPINI1	1,39222481
3245	PDGFRB	1,10755762	BAG3	1,13441974	HDAC4	1,23573975	RORC	1,22045484	EOMES	1,17430169	ST6GALNAC2	1,14177661	TNIP3	1,41623674	3315	SLC30A1	1,10054337	CDS1	1,1262709	DDR1	1,22084808	SFRP1	1,20460099	KNG1	1,16127518	CXCL10	1,13166314	CSNK2B	1,39207976
3246	SPCS1	1,10749993	GAL3ST1	1,13435507	AGMAT	1,23513963	PRKCB1	1,22041095	BDNF	1,1738182	NR6A1	1,14177568	FAAH	1,41618913	3316	PDE1C	1,1005073	FUT5	1,12623039	CALR	1,22073172	SESN1	1,20439884	DHRS3	1,16110066	DAZAP2	1,13161518	PROM1	1,39204238
3247	GPR83	1,10744069	IRF8	1,13435159	PRKAR1B	1,23464293	HMGB2	1,22039591	IL28RA	1,17326114	ELA2	1,14165658	MTFMT	1,41535739	3317	ATF2	1,10044106	SKIP	1,12595752	LIG4	1,22066636	OAS2	1,20388862	OLA1	1,16093863	RNASEL	1,13129314	PLA2G7	1,39153668
3248	MOBP	1,10740429	ACCN5	1,13426543	FPR1	1,23457875	SMS	1,22026929	VNN3	1,17300031	MDM4	1,14161572	BTRC	1,41522393	3318	GC	1,10025989	RARA	1,12585257	SERPINE2	1,22065873	DUSP8	1,20384915	F8A1	1,16060026	APOC1	1,13127914	BACH1	1,39120826
3249	ABLIM1	1,10734097	GRN	1,13422751	PDE1C	1,2340821	VSNL1	1,2199102	ACSL4	1,17264888	COPA	1,14159284	AR	1,4146338	3319	UBE2V1	1,10010845	PLAGL1	1,12579147	PHKG1	1,2202242	TACR3	1,20364113	NCR1	1,16034749	UGT2B15	1,13109033	ALDH3A2	1,39033822
3250	CSTF1	1,10724813	LIPA	1,13418371	SMARCA4	1,23404932	LMNA	1,21983119	FOSB	1,17252985	NEUROG1	1,14145327	PLCB2	1,41454052	3320	SEC22B	1,10004993	HTR3E	1,12561718	HRH1	1,22006599	ITPKB	1,20341395	RAC2	1,16027004	FSCN1	1,13082798	ALDH3B1	1,38987812
3251	NEU2	1,10722166	TF	1,13404607	ENTPD8	1,23394184	RRAD	1,21970772	CASP8AP2	1,17246759	BAX	1,14144779	CREB1	1,4134377	3321	BMP8B	1,09993891	PSEN2	1,12557502	NOTCH2	1,22005326	TAP1	1,20333812	IFIT1	1,15990476	ABCD1	1,13041466	NCF4	1,38916681
3252	F9	1,10702066	MCPH1	1,13401826	ASAH3L	1,2330224	VCAN	1,21929856	TBXA2R	1,17244634	NR2F1	1,14132965	TRAF4	1,41296615	3322	EGR1	1,09988997	CYP2A13	1,12554364	SCN2A	1,21945942	MVP	1,20308498	PTK6	1,15987034	SMARCD1	1,13027638	ACTG1	1,38881785
3253	COL4A3	1,10698781	SFRS12	1,13399722	NDUFB7	1,23285484	IL10	1,21922297	SPCS3	1,1723992	CDIPT	1,14118207	MAP2K3	1,41260597	3323	ARNT	1,0998373	PFKFB4	1,12549019	VAV1	1,21925451	PPAP2A	1,20303686	VARS2	1,15982672	WBSCR17	1,13018134	B4GALT2	1,38849156
3254	HYAL1	1,10692441	CENTA1	1,13376226	NEFM	1,23283445	CREB1	1,21904552	C4BPB	1,17210534	SYK	1,14088591	GSTT1	1,41256777	3324	FUT7	1,0997235	SRF	1,12536607	BRCA1	1,21908176	OTUB1	1,20301882	ERBB2	1,15972782	HNMT	1,12965789	ADH1C	1,38822459
3255	PDK1	1,10679573	PRKG2	1,13375019	BUB3	1,23274591	P11	1,21875343	MERTK	1,17193671	CD96	1,14068893	ANKRD6	1,41204613	3325	FOLR1	1,09958968	ABCC3	1,12521463	MAPK8IP3	1,21873329	LPO	1,20280658	ANKHD1	1,15970707	SUCLA2	1,12957311	THBS2	1,38818831
3256	PKMYT1	1,10679444	AFP	1,13362763	CTCF	1,23255544	ABCA6	1,21797893	CITED2	1,17148833	CFH	1,14058818	SIM1	1,41192971	3326	PPOX	1,09949373	PNPO	1,12514247	POLG2	1,21872077	CYP1A2	1,20238271	PRKDC	1,15931334	UNC93B1	1,12956289	LOC390243	1,38712297
3257	TSPAN7	1,10678937	GAA	1,13355487	PPT2	1,23215025	BTG1	1,21777101	HSD17B3	1,17114437	GNPDA1	1,14058749	GBGT1	1,41180682	3327	SYT1	1,09925775	CAMK1G	1,12511854	CCKBR	1,218646	SERPINA1	1,20227305	ASNS	1,15922476	ACTG2	1,12886882	PRDM2	1,38675446
3258	INSR	1,10612492	PPCS	1,13352448	MYOD1	1,23212648	XIST	1,21734531	B4GALT2	1,17103445	VARS2	1,14043902	MYF5	1,41176735	3328	MRPL19	1,09909205	GLRX	1,12493378	GRIN3B	1,21852031	SST	1,20162588	GSTT1	1,1591902	PAH	1,12878619	ATRX	1,38648921
3259	CA3	1,1060978	ENO2	1,13350937	CYP2B6	1,23193525	GUCY1A3	1,21701305	BMI1	1,17103445	CRHBP	1,14018396	HARS2	1,41129303	3329	TRPC2	1,09907233	CD2	1,12489787	KCNB1	1,21841367	HSPB1	1,20138879	SIGLEC1	1,15897841	IL23R	1,12868981	C1QL3	1,38607328
3260	SOX6	1,1059989	MYF5	1,13316559	CACNA1D	1,23124052	SH3GL2	1,21697227	GJA4	1,17083462	GTF2E1	1,14011201	BMPR1B	1,41085607	3330	POLE	1,09890127	CLIC1	1,12444897	TBKBP1	1,21800428	UROD	1,20117827	CREB3L1	1,15893782	ESCO1	1,12858795	GAD2	1,38548176
3261	GRM7	1,10599747	PRKACG	1,13308335	PRDM1	1,23118054	GOSR2	1,21632298	CSNK1E	1,17048613	ARHGEF5	1,14004355	NKIRAS2	1,41051505	3331	MEFV	1,09885037	CHPT1	1,1243378	EPAS1	1,21794721	CBX5	1,2011253	INHA	1,1585395	IBSP	1,12832485	MTNR1A	1,38544219
3262	CTCF	1,10562911	LTBP4	1,13305657	POU2AF1	1,23097032	DLST	1,2160707	WNT11	1,17043335	PDCD1	1,13990599	RIPK1	1,41013481	3332	IDS	1,09869881	GDF6	1,12424141	CSNK1D	1,21771482	TNFSF10	1,2010006	FGF20	1,15775823	SIN3B	1,12809413	DHDDS	1,38534186
3263	DGKG	1,10555241	RNF2	1,1329901	HEL308	1,2309596	SEMA4A	1,21542371	SPRED1	1,17035154	LTBP4	1,13978291	ATP6V1E2	1,41006688	3333	DHRS2	1,09852633	HBXIP	1,12362815	DGKD	1,21733913	CYP2C18	1,20045129	ATP6V1C1	1,15768641	PFKP	1,12732146	DDEF1	1,38528322
3264	ATG9B	1,10553013	ACPP	1,13297677	ADCY6	1,23043144	KRT7	1,21479445	PRKAG2	1,17029544	SUMO1	1,13977197	BUB1	1,40993939	3334	OSBPL1A	1,09817975	GNB1L	1,1235467	HMGA1	1,21701268	RNF25	1,20028484	SLC30A6	1,1576666	FDXR	1,12728548	BBS4	1,38490829
3265	SQLE	1,10548452	PARD3	1,13291978	MCM4	1,23018817	ATN1	1,21470474	CDKL2	1,17025709	NPM2	1,13875576	GABARAPL2	1,40990077	3335	PPP3R2	1,09762218	CD63	1,1235081	MDC1	1,21683193	CREBBP	1,20026809	MAP4K1	1,15747237	S100A4	1,12721403	LHB	1,38474844
3266	ANXA1	1,105352	RXFP1	1,13291089	HIP1	1,23005266	HTR3D	1,21470421	ADRBK1	1,17025591	GNAO1	1,13870584	POLR3GL	1,40967215	3336	PTGIS	1,09747681	SCN3B	1,12348919	ENO2	1,21646945	MAFK	1,20011456	MIB1	1,15741581	NTF3	1,1269154	ARPC5L	1,38431044
3267	GUCY1A2	1,10534896	APOC2	1,13289514	PANK2	1,22999324	EME2	1,21419166	MEF2A	1,17023295	GSTA2	1,13857218	PRKAA1	1,40866895	3337	BAIAP2	1,09720668	SFMBT2	1,12327658	FAH	1,21600444	GPRC5C	1,19985529	PRMT6	1,15729846	STX10	1,12674636	CDKN3	1,38422478
3268	GYS1	1,10534885	BCAT1	1,13284967	HPGD	1,22995765	MAP3K2	1,21397054	SREBF2	1,16997159	COL8A2	1,13813738	PPP1CA	1,40864704	3338	ITPK1	1,09707603	UMK1	1,12323008	APC2	1,21594015	GPT2	1,19937835	KDELR2	1,15716558	GPC5	1,126423	SP3	1,3840204
3269	ALG14	1,1053054	ABCA5	1,13276444	ANGPTL3	1,22972868	ITGB5	1,21396969	MYD88	1,16992453	LDLR	1,13811543	CAMK2G	1,40810653	3339	LPHN3	1,09686798	CHST11	1,1232155	ST6GALNAC4	1,21582016	PRL	1,19912799	APLP2	1,15705635	PRKCG	1,12640903	HSD17B8	1,38325053
3270	PMAIP1	1,10511496	POLI	1,13272354	CFHR2	1,22957043	ANPEP	1,21380592	STX6	1,16969181	MGAT4A	1,13799225	DCXR	1,4080211	3340	GP6	1,09681722	P11	1,12313722	RAB24	1,21567299	PPP2CA	1,19908498	C7	1,15702081	GALNT4	1,12583925	ARSD	1,38300533
3271	BZW1	1,10500183	BTC	1,13233032	HSPA1A	1,22955916	REL	1,21344501	ITPR2	1,16967982	ZAP70	1,13781459	TACR1	1,40730642	3341	PTPN6	1,09653666	CTSB	1,1229229	ARSD	1,21545427	LDLR	1,19855736	GNG13	1,15678693	ITGA6	1,1256363	DAPK1	1,38294533
3272	TRAF5	1,10488264	EPHA2	1,13220527	MMS19L	1,22950461	GALNT7	1,21332384	FRS2	1,16931505	AK5	1,13770455	TOB2	1,40667744	3342	NEFL	1,09598194	FLT3LG	1,12267482	C12ORF57	1,215446	ALDOB	1,19823682	CHKB	1,15665834	NMNAT3	1,12562638	RABGAP1L	1,38252997
3273	IL7	1,10482879	NT5C	1,1321228	HRH3	1,22943017	DLG4	1,21325501	GNAI1	1,16926904	ATP6V1C2	1,13762827	PIR	1,40655084	3343	HSPA8	1,09571651	CYP3A7	1,12231381	ALMS1	1,21489773	ST3GAL5	1,1980664	TNC	1,1563465	AGPS	1,12557402	CRKL	1,38202224
3274	IKBKAP	1,10467154	LNPEP	1,13184747	EPHX2	1,22890031	APBB2	1,21281034	PIK3R2	1,169222	TPH1	1,13760353	TKTL2	1,40627483	3344	PAX8	1,09570453	ADRA1A	1,12195522	FGF13	1,21487084	PDLIM5	1,19799962	SRC	1,15617993	SQLE	1,12524839	PTH	1,38075272
3275	AKT1	1,10451536	EPB49	1,13150987	RECQL5	1,22885227	GPAM	1,21275927	DAB1	1,16907516	SERPINE1	1,1375494	HSPB1	1,40569447	3345	TOP3A	1,09568221	OSBP	1,12184755	FMO2	1,21478034	NDUFB11	1,19793574	PPOX	1,15604773	ACY3	1,12524257	F3	1,38067109
3276	PLA2G2F	1,10443396	CS	1,1314975	SCNN1A	1,22861169	CSAD	1,2127028	CLK1	1,16887766	DAPK3	1,13734362	WNT3	1,40448058	3346	ATP6V1F	1,09559035	DNAJB1	1,12178777	PTPRA	1,21467462	HBB	1,1974305	SRP72	1,1554573	C1QL1	1,12513199	ACHE	1,38033143
3277	PRKACG	1,10443097	GRIN3B	1,13141322	RBBP8	1,22859032	ALG2	1,21239706	IFNA21	1,16867644	MUT	1,13731062	CA7	1,40431408	3347	MIB1	1,09554015	VAMP2	1,12162153	FAM59A	1,21446566	BRCA2	1,19673388	HPCAL1	1,15538976	GNAT1	1,12508987	SUMO2	1,37940067
3278	TIAM1	1,10439558	TSHR	1,13134093	VWF	1,22813383	PIP5K2B	1,21189457	JUP	1,16819921	PHPT1	1,1371463	CSMD1	1,40430643	3348	ITGB3	1,09535581	ARHGAP1	1,12151505	FABP7	1,21433477	PIGG	1,19661125	FABP4	1,15529136	APOC2	1,12502142	BCL2L2	1,37855845
3279	TGDS	1,10424212	ARHGAP6	1,13129599	AGTR1	1,22764466	POLD3	1,21182212	GSS	1,16817788	IL22RA1	1,1370873	ABCA1	1,40417929	3349	SPDEF	1,09532173	CCL11	1,12145159	PIGL	1,21371223	IFITM1	1,1963567	BZW1	1,15521819	CALML3	1,12491149	H2AFY	1,37780448
3280	INPPL1	1,10423353	COL12A1	1,13114089	ATP5G2	1,22763146	CYSLTR1	1,21175996	MMP8	1,1679002	HTR1A	1,13673982	SREBF2	1,40387708	3350	FOXO3	1,09513143	ITPR1	1,12113312	MCPH1	1,21369182	MDM2	1,19635306	DGAT2	1,155174	HRH2	1,12475002	SLC38A1	1,37681452
3281	PURA	1,10421227	IFNE1	1,13108509	CREB3	1,22760969	ST3GAL2	1,21159194	PITX2	1,16776316	LDHAL6B	1,13659457	CHRD	1,40337782	3351	TARDBP	1,09502881	ATP5F1	1,12098903	GEN1	1,21367759	PRDM1	1,19630872	CYP2R1	1,15486083	HFE	1,12467596	ADIPOR2	1,37638946
3282	AMD1	1,10418801	HRH3	1,13104311	NDUFA12	1,22733313	ITGAM	1,2115271	COL4A5	1,16760432	EIF3H	1,13658832	KLK10	1,40300893	3352	GCM1	1,09489766	SNX2	1,12055602	AGK	1,21363305	CD1A	1,1958862	ORC2L	1,15476457	TCL1A	1,12427184	PTGER1	1,37569522
3283	CAV1	1,10356672	NMNAT1	1,13072364	SEC22B	1,22706802	MAN2B1	1,2114569	REV1	1,16730591	GANAB	1,13652309	COL3A1	1,4024425	3353	HTR1D	1,09481374	BBOX1	1,12042044	CYP3A7	1,2135644	GJD2	1,19568845	NFE2L2	1,15451107	ADCYAP1R1	1,12395493	IDUA	1,37548324
3284	DTX3	1,10337628	AMH	1,13067239	STX12	1,22665374	PLOD1	1,2109494	KCNJ9	1,16723721	EBI3	1,13647377	IDI1	1,40232514	3354	FABP3	1,09472924	TBX2	1,12034299	ZCCHC11	1,21344003	GPS	1,19555052	NDUFA8	1,15404297	DNMT1	1,1237361	COL8A2	1,37438105
3285	REN	1,1030901	CLK4	1,13050421	NQO2	1,22661516	CCL3L1	1,21087651	ACVR1B	1,16713005	DUOX1	1,1362217	ATP5G2	1,40205471	3355	GLA	1,09468368	MTAP	1,12032309	FOXC2	1,21251496	NLRP2	1,19543841	IL12A	1,15382132	STMN2	1,1235752	COL9A3	1,37352074
3286	HPCAL1	1,1030027	GNG13	1,1301916	RAB35	1,22652831	CRHR1	1,21086463	DNAJC3	1,16696239	MAOA	1,13614809	NDUFB2	1,40194191	3356	CLTCL1	1,09447982	ASCC3	1,12031904	G6PD	1,21239238	CCR10	1,1952927	CSRP3	1,15364721	CDC14A	1,12329753	CRHR2	1,37307181
3287	C6	1,10296494	AKR1C3	1,13009072	CLCF1	1,22635621	DAB1	1,21042606	GALT	1,16693461	KLKB1	1,13606173	DAAM1	1,40125926	3357	ACO2	1,09441106	FHIT	1,12023564	ADCY1	1,21216646	RNF2	1,1952897	IL8	1,15300065	GPR50	1,12321253	TBXA2R	1,37258154
3288	DNAJB11	1,1028128	IL15RA	1,12993695	CCL22	1,22632262	CACNA1C	1,2103668	MC4R	1,16688252	MYCN	1,13588979	CAP1	1,40097567	3358	CASP8	1,09405129	ACTN1	1,12023059	PRIM1	1,21159198	CD209	1,19442539	NLK	1,15289846	GPAA1	1,12300743	PAXIP1	1,37094905
3289	ALAS2	1,10277134	TLR3	1,12985558	AMY1B	1,22556838	CLDN14	1,21010649	SP3	1,16673662	REL	1,13588129	PARG	1,40035065	3359	POLG	1,09395428	UBE2L3	1,12006461	PPP1CC	1,21151443	GDF11	1,1942945	TPS3	1,15288588	TRIP10	1,122996	MCAT	1,37074668
3290	PARK7	1,10270515	GLCE	1,12980116	IRF1	1,22553811	RBBP8	1,21005399	MYH3	1,16667231	TEP1	1,1358594	PODXL	1,40003427	3360	DPPA3	1,09384262	CNR2	1,11991883	FGF1	1,21138563	SRF	1,19393436	ECGF1	1,15266584	YARS	1,12255307	RHOA	1,37073089

Table A4. Pooled-shRNA library screen on HEL cell line and MF-3: list of 2nd most depleted shRNAs for each experiment (ranking approach 1, RA1).

	NO ruxolitinib (setting 1)				Ruxolitinib (setting 2)				Ruxolitinib + CM (setting 3)				MF-3				NO ruxolitinib (setting 1)				Ruxolitinib (setting 2)				Ruxolitinib + CM (setting 3)				MF-3	
	Experiment 1		Experiment 2		Experiment 1		Experiment 2		Experiment 1		Experiment 2						Experiment 1		Experiment 2		Experiment 1		Experiment 2		Experiment 1		Experiment 2			
Rank	Gene	Fold change	Gene	Fold change	Gene	Fold change	Gene	Fold change	Gene	Fold change	Gene	Fold change	Gene	Fold change	Rank	Gene	Fold change	Gene	Fold change	Gene	Fold change	Gene	Fold change	Gene	Fold change	Gene	Fold change	Gene	Fold change
3361	PTPRF	1,09375698	DNMBP	1,11983001	PTPRB	1,21109058	CSF3R	1,19380469	PTGER3	1,15259433	EPRS	1,12249961	UGT1A9	1,3707188	3431	IL3	1,08554868	RAD50	1,11116287	B3GALT6	1,19573853	BLVRA	1,17869768	GBF1	1,14119265	PDCD4	1,11062301	LY6E	1,34265414
3362	GBGT1	1,09372865	COL8A2	1,11977961	DNAJA2	1,21106617	CLCN7	1,1936194	TUBB4	1,15252113	C4BPB	1,12235869	COL6A3	1,36992193	3432	TUBA4A	1,08536283	FHL5	1,11095355	ADCY2	1,19573593	NEU2	1,17867825	PRKCB1	1,14118198	TFAP2C	1,11062137	GNPDA2	1,34241569
3363	STX11	1,09368796	AMY1C	1,11967307	MUTYH	1,21068295	UBE2L6	1,1933601	MYL2	1,152327	NPM1	1,12234762	ACCN3	1,36932858	3433	PIK3CD	1,0853574	SLC30A8	1,11075525	C4BPA	1,19566075	OSBPL5	1,17867601	PPAP2B	1,14114255	PPYR1	1,11054505	RENBP	1,34241569
3364	EXTL3	1,09367849	CLC	1,11932383	PTPN11	1,21052221	MAPK1	1,19291394	AK3L1	1,15206359	CX3CL1	1,12231244	GRID2	1,36886628	3434	ABLIM3	1,08534059	MKKS	1,11065897	SLC5A3	1,19522301	LPHN1	1,17853476	DGKD	1,14051366	CSAD	1,11028277	CD274	1,34174856
3365	DARC	1,09360039	GRK1	1,11924843	ACADSB	1,21039859	PTHR1	1,19262079	AKT3	1,15198388	PIGC	1,12228951	ATP2A1	1,36874873	3435	MVD	1,08531689	NOD1	1,1102978	IRF3	1,19487123	TAF2	1,17848182	ISLR	1,14042822	DMGDH	1,11016906	MAGI2	1,34170763
3366	LARS	1,09352997	SND1	1,11917934	CSAD	1,21019968	AK3L1	1,19225275	HOXD1	1,15144978	SLPI	1,12214052	DLX3	1,36863069	3436	PPIE	1,08520139	CALR	1,11010825	BMP8B	1,19485294	G6PD	1,17844527	DUSP10	1,13992555	SCNN1B	1,10977225	EME2	1,3416594
3367	ADH7	1,09343863	HMOX2	1,11900869	CCND3	1,20997906	CENTD1	1,19200434	BIRC3	1,15113712	RRM2B	1,12212019	PER3	1,36853116	3437	PI3	1,0851225	MST1	1,1099456	TOP3A	1,1947287	YY1	1,17830173	GGH	1,13955554	ICAM1	1,10961889	TGFBR1	1,34165182
3368	LHPP	1,09336093	FPGT	1,11898695	ARFGEF2	1,20957988	RAB11A	1,19199326	AVPR1B	1,15089389	XRCC2	1,12154655	SCD5	1,36822189	3438	HLA-DOA	1,08509689	OAS2	1,10981668	SYNE1	1,19448735	RALGDS	1,17823619	TFAP2B	1,13945796	ILVBL	1,10958316	TBP	1,34082027
3369	SCARB1	1,09322174	NEK2	1,11889992	IL6R	1,20951579	LDHA	1,19198577	LNPEP	1,1507522	ARHGEF6	1,12152658	SOD1	1,36819055	3439	UBTF	1,08501983	CBX5	1,10972775	MTA2	1,19434602	NFKBIB	1,17822677	TNFRSF10B	1,13911167	FOXO3	1,10948288	F11	1,3408107
3370	CYP39A1	1,09313297	UBE2B	1,11878941	CABIN1	1,20929851	CHRNA5	1,19182894	POU2F2	1,15072181	BNIP3L	1,12097624	VARS	1,36773228	3440	PLEC1	1,08499606	CLDN1	1,10969035	TGM2	1,19402389	ALMS1	1,17818886	ARPC1A	1,13906536	GAL	1,10936969	RAB5A	1,33969663
3371	PIGG	1,09277211	A2M	1,11854318	UVRAG	1,20883995	DCLRE1C	1,1917763	POLE	1,15068951	MARCO	1,12067338	POLR3A	1,36760655	3441	CCNE1	1,08497253	HTR2B	1,10962663	PRMT2	1,19390239	PIK3CG	1,17808656	GALK1	1,1389891	H6PD	1,10924553	POLQ	1,33957327
3372	HK1	1,09274534	CCKAR	1,11838086	PSMB8	1,20873963	PCNP	1,19168242	KATNAL1	1,15062854	SOX17	1,12039881	CDK9	1,36756754	3442	MAP2K6	1,08482743	PTPRJ	1,10955474	DPP4	1,19380409	CCL22	1,17794163	ABCA7	1,13856563	PIGF	1,10916502	RAG1	1,33939036
3373	CYP2A6	1,09267952	IL2	1,11834073	LHX2	1,20841296	HBEGF	1,19145001	NTSR1	1,15057362	ATF4	1,12010621	MCM7	1,36750095	3443	ASNS	1,08476153	PDE4B	1,10923009	IFNA4	1,19333455	VAV1	1,17785754	ACVRL1	1,13804255	LPO	1,10914123	PITX2	1,3390599
3374	ACADL	1,09262322	GSTA3	1,11827992	KLK10	1,20807579	CACNA1D	1,19112655	PRKACG	1,1501891	PDGFRA	1,11983438	APEX1	1,36692552	3444	IL6ST	1,08466122	RARB	1,10914191	LXN	1,19286543	IL17RE	1,17782296	DHCR24	1,13748092	PNPLA3	1,10909143	MBL2	1,33893496
3375	C4B	1,09255719	B3GNT5	1,1182254	FABP5	1,20799136	TPI1	1,19099652	CD3E	1,15014079	ARPC1A	1,11982043	CPT1C	1,36681517	3445	NFATC4	1,08463289	NR1H4	1,10893585	JAG1	1,19202117	APC	1,17759998	HTR6	1,13743153	SPDEF	1,10907306	ETS2	1,33891966
3376	HMOX2	1,09232488	NRP1	1,1182052	IL13RA1	1,20751969	PTTG1	1,19075448	MEFV	1,14986592	CHRNB2	1,119815	SLC12A1	1,36667336	3446	APC	1,08441914	MS4A1	1,108932	STX3	1,1914935	POLR3K	1,17747403	TLX1	1,13708355	SSTR1	1,10870688	SYK	1,33780182
3377	CRH	1,09226048	KCNQ1	1,11800073	SERPINA5	1,20751707	KMO	1,19040868	ITGA1	1,14973215	CEBPD	1,11968501	PYCR1	1,36655046	3447	PREP	1,08437927	HOXD10	1,10890006	BCAP29	1,19138085	TRPC2	1,17650343	EPN1	1,13703136	ATG9B	1,10870529	KPNA3	1,33764061
3378	DOK1	1,09225911	TFCP2	1,1178832	GRK4	1,2072792	DOK1	1,19029033	HLA-A	1,14949295	ENTPD8	1,11950128	OXCT1	1,36504443	3448	IRF8	1,0843632	CDK9	1,10868401	MAPRE2	1,19132188	IL23R	1,17632674	KLK7	1,1370243	CD274	1,10848776	MYL9	1,33647384
3379	HS3ST1	1,09223738	NR5A1	1,11775638	IL27	1,20722307	SLC12A6	1,19006953	TFPI	1,14936959	NRCAM	1,11921748	GNG13	1,36478414	3449	PECR	1,08426449	TNFRSF13B	1,10861266	NEFL	1,19111767	IFNA4	1,17590327	PIGP	1,13677676	ESR1	1,10841465	CDKN2C	1,33644946
3380	ACSS1	1,09219103	GNGT1	1,1176464	FMO1	1,20714696	CREB5	1,18972698	B2M	1,14935391	OTUB1	1,1191196	FEZ1	1,36463914	3450	SUFU	1,08417151	MAG	1,10852873	NKX6-1	1,19105191	PINK1	1,17569892	MLC1	1,1366887	IRS2	1,10833241	CIT	1,33600401
3381	COL3A1	1,0921641	LPO	1,11742448	RCAN1	1,207135	IL6R	1,18954568	LTB4R2	1,14917281	DTX4	1,11905369	GALNT6	1,36452972	3451	BHMT	1,08411447	TGM1	1,10851265	IFNGR1	1,19076779	UBE2D3	1,17497636	JPH3	1,13581426	ARHGEF7	1,10831647	CXCL9	1,33566376
3382	CCL7	1,09198001	CDKN1B	1,11741587	IRF5	1,2069666	S100A8	1,18947257	CARD9	1,14910845	ARHGDIB	1,11895141	PRMT8	1,36235259	3452	LNPEP	1,08405202	ALG1	1,10835921	MYF6	1,19068096	IL1RL1	1,17468414	PARP4	1,13563108	TNFSF13B	1,10813147	FAM132A	1,33553999
3383	PEU1	1,09195342	DHRS3	1,11730641	S100B	1,20675737	GANAB	1,18937197	OLAH	1,14861794	EPN1	1,11892622	ACPT	1,36233481	3453	ROCK1	1,0839641	DDHD1	1,10802859	PRNP	1,19061133	HOXA9	1,17449061	KCNMA1	1,1356073	PDIA3	1,10809795	STK11	1,33546131
3384	FOXP3	1,09163738	IDH3A	1,11723119	B2M	1,20664525	ALCAM	1,18922266	VIPR1	1,14827754	CAMK2D	1,11881126	FGF4	1,36201198	3454	GABRG1	1,08387165	NPEPPS	1,10776804	SMAD1	1,19060798	ACIN1	1,17438777	NFKBIB	1,13554239	PRODH	1,10807624	CADM1	1,33536547
3385	PTPN1	1,09157533	HSP90AB1	1,1171287	EPO	1,20630664	MAPRE2	1,18912455	GBGT1	1,14808598	HTR1D	1,11871334	TSLP	1,3619842	3455	FZD3	1,08383412	ABCB10	1,10769185	RDH12	1,19056221	SLC6A3	1,17423046	KLK6	1,1355025	TGM3	1,10786771	ABCB11	1,33520012
3386	HRH1	1,09153712	ATP4A	1,11710276	EPOR	1,20596142	PTPRA	1,18834316	XRCC2	1,14777962	ALG3	1,11860559	RAD50	1,36024633	3456	APH1A	1,08367609	IL13RA1	1,10763974	GABRG3	1,19047682	TSC2	1,17415947	EGFR	1,13545024	TLX1	1,10784863	RPL4	1,33456617
3387	PNLIP	1,09146481	CD97	1,1170506	FGA	1,20537386	TIRAP	1,18830781	KCNMB2	1,14771293	COL9A2	1,11846302	DHFR	1,3595707	3457	SIRT2	1,08362472	DIAPH2	1,10760459	PKMYT1	1,19018353	PLA2G4C	1,17397485	SLPI	1,13535338	HLX	1,10783059	PLA2G12A	1,33416449
3388	STAT3	1,0913384	YWHAH	1,11677315	TMEM166	1,20529977	IL1RN	1,18822721	SNAP23	1,14770659	RHEB	1,11836443	NCOA2	1,35888759	3458	HPRT1	1,08342672	BZW1	1,10728551	ATP6V1C2	1,18939935	GRM8	1,1738544	UXT	1,13475894	ALDH5A1	1,1077261	AIFM1	1,33362909
3389	CFH	1,09125684	PANK2	1,11671986	PSENEN	1,20515287	LTF	1,18818576	AARS	1,14766704	PGR	1,11833399	NR5A1	1,358677	3459	AGPAT2	1,08330818	PICALM	1,10728512	ADM	1,18928308	B3GAT2	1,17348251	WASF1	1,1347176	EEF1A2	1,1074605	NEUROG1	1,33350807
3390	CCND3	1,09120313	PTGES	1,116712	RBPJ	1,20457393	CYP2D6	1,18798797	DCTD	1,14763829	NDUFV1	1,11822711	LXN	1,35789111	3460	HGS	1,08307232	GRK4	1,10698308	TRPM2	1,1889391	NFE2L2	1,17323436	PPT1	1,1345883	RRM2	1,10699736	PHF21A	1,33328857
3391	CSNK2B	1,09118843	ALG5	1,11655693	MAPK8IP1	1,20456644	CYCS	1,18792004	CD97	1,14737007	DFFA	1,11799562	NDST3	1,35751705	3461	PRC1	1,08304208	DIO2	1,10688097	MAP2K1	1,1888972	COX6C	1,17319514	PLA2G10	1,13448495	CMAS	1,10637134	CPSF1	1,33323618
3392	ATF3	1,09106976	KCNN3	1,11653102	TUBB3	1,20417441	SLCO1C1	1,18726433	TCIRG1	1,1473625	TNFSF13	1,11763952	CSTF2	1,35740701	3462	ACVR1C	1,08299003	PRKD3	1,10658861	TNFRSF4	1,18870797	DNAJB1	1,17318876	C1ORF103	1,13444633	HIPK2	1,10629064	CHST3	1,3328309
3393	DKC1	1,09087263	ITSN1	1,11639729	ABCG5	1,20408896	LAP3	1,18667968	WNT4	1,14729292	UBE2L6	1,11757108	CD1A	1,35685287	3463	GLUD1	1,08293088	PRMT8	1,10633249	EFNA5	1,18838568	HSD17B10	1,17312505	HYAL3	1,13438824	REXO2	1,10621888	HPSE2	1,33223534
3394	XRCC4	1,09076352	GALNT14	1,11638032	AICDA	1,20400234	BIRC2	1,18660616	DRD5	1,14696213	WNT3	1,11751602	CSNK2A2	1,3565274	3464	POMC	1,08292953	ABCA10	1,10616474	LY9	1,18799056	UNC13B	1,17260351	CCR8	1,13426912	UCP1	1,10607081	HTR1D	1,33202735
3395	EPPK1	1,09072574	NPY2R	1,11624595	TFRC	1,20389846	CASP9	1,18652262	RET	1,14680331	HSD17B8	1,11746608	ATP6V1G2	1,35639786	3465	CYP26A1	1,08274813	SLC26A2	1,10615394	ADORA1	1,18793287	PIGL	1,17245696	PINK1	1,13390158	SALL1	1,10607027	ITGA5	1,33162964
3396	DLAT	1,09042906	RPRM	1,1161495	UBE2C	1,20358259	SLC30A8	1,18635359	COL2A1	1,14671194	CES1	1,11733132	PRF1	1,35631942	3466	PPP1R13L	1,08259559	NPAS2	1,10586287	SLC23A2	1,18766117	FUCA1	1,17190244	CHST3	1,13352573	LIG4	1,10595792	COL2A1	1,33097029
3397	FN1	1,09001875	IL10	1,11607513	SLC32A1	1,20321169	EXOC7	1,18621651	PRDX3	1,14661281	SCN11A	1,11731934	TPO	1,35604537	3467	COL5A3	1,08215182	RAB1A	1,10581693	EI24	1,18728133	NDST1	1,17180729	SLC32A1	1,13348692	IL13RA2	1,10594189	PMP22	1,33089951
3398	PIP3-E	1,08989901	VPREB1	1,11605739	HGS	1,20286759	GBGT1	1,18605549	SLC33A1	1,14661281	BIRC3	1,11689044	GALC	1,35584596	3468	SCN3B	1,08197435	AUH	1,1056713	CFH	1,1871083	HMGN1	1,17150869	SLC23A2	1,13330879	ITGB6	1,10556758	CBLB	1,33075073
3399	MAG	1,08975224	CHST13	1,11565111	TNFAIP1	1,20268037	PSEN2	1,18594331	PLA2G2D	1,14633531	FXYD2	1,11653313	BDNF	1,35527627	3469	TXLNA	1,08191157	APOC3	1,10557138	PGAP1	1,18572936	P2RY5	1,17134629	IL6ST	1,13323945	RAD23A	1,10552031	CCL18	1,33046983
3400	AOX1	1,08963939	MAFB	1,1156312	LHX8	1,20207066	NEIL1	1,18536903	CTSL2	1,14606329	AKR1D1	1,11652452	SELPLG	1,35471295	3470	ACSM1	1,08159018	TOP3A	1,10538362	DLX6	1,18509024	CLTCL1	1,17097661	HTR1D	1,13320103	POR	1,10545487	SLC23A1	1,32954902
3401	GSTA2	1,08957765	GGT1	1,1155823	DIXDC1	1,20193817	BCL11A	1,1850212	NR5A2	1,14591274	SENP2	1,11613647	HYOU1	1,35460496	3471	SLC30A3	1,08153944	CDC45L	1,10530497	GOLGA2	1,18505414	GNGT1	1,17092604	LDLR	1,13314195	ENTPD3	1,10540392	PGR	1,32947693
3402	CABIN1	1,08944059	PGR	1,11555526	PAX8	1,20179755	WNT10B	1,1846479	CHGA	1,14584293	MYBPC1	1,11604395	GALNT7	1,35422378	3472	ITGA2B	1,08137386	CASP8AP2	1,10520543	APPL2	1,18431607	CSTF1	1,17071907	CX3CR1	1,13293568	EXOC7	1,10525761	TNFRSF19	1,32938712
3403	FAT	1,08940217	CD80	1,11553238	LDHA	1,20178962	DDEF2	1,18461191	SQLE	1,14569061	CASR	1,11601896	CD97	1,35292349	3473	CDC7	1,08122925	GTF2H5	1,10512513	GPR50	1,18410693	FAM50A	1,17045056	CD14	1,13264695	IL4	1,10492432	LY86	1,32925344
3404	DNAJC3	1,08916689	ME2	1,11536397	EPHX1	1,20153898	CERK	1,1840789	ABCG8	1,14562319	MSH4	1,11556522	NFATC4	1,35282187	3474	CYP19A1	1,08111795	CCL3L1	1,10466719	IFNGR2	1,1840246	UGT8	1,17022184	CHSY1	1,13248389	CLK4	1,10445818	UBE2E2	1,32869305
3405	DRD5	1,08876535	GP1BA	1,11527953	CD53	1,2015336	THOP1	1,18364771	E2F2	1,14554515	RAB6A	1,11539935	TGFA	1,35215889	3475	XPC	1,08109741	ACOX2	1,10440538	APOE	1,18395537	CHST6	1,17007715	CD24	1,13205764	TEK	1,10445268	TYMS	1,3284353
3406	TAGLN2	1,08873917	GABRA1	1,11504942	VARS2	1,20145752	TOR1A	1,18332704	ATP1A4	1,14521645	EGR3	1,11522213	NFE2	1,35202483	3476	MIF	1,08097223	ASRGL1	1,10429117	STX6	1,18352206	ADRA2A	1,16962201	PRKAR2A	1,13167594	TYMS	1,10444593	ABCB9	1,32763965
3407	ETV6	1,08858728	AMY1B	1,11498846	FARSB	1,20143183	PRKAG2	1,18307491	LXN	1,14513676	CCR7	1,11471375	ILVBL	1,35198974	3477	RAB9A	1,08093626	SDC2	1,10422333	PRKG2	1,18320759	GP6	1,16934525	CAMP	1,13164372	ATG10	1,10415425	ALDH1L1	1,3276049
3408	HAO2	1,08843344	G6PD	1,11491235	MBTPS2	1,2012046	STS	1,18292932	KLRC1	1,14502252	NOX1	1,11468154	DTX3L	1,35197837	3478	AMY1A	1,0809129	ID3	1,10421801	ISYNA1	1,18307645	NDUFB7	1,16928109	EIF2B4	1,1316342	SLC30A6	1,10388636	BZW1	1,32737319
3409	IAPP	1,08831678	NCOA1	1,11488761	POMC	1,20092728	RFNG	1,18249177	TNFRSF9	1,14502252	ATF3	1,11465336	GPI	1,3518334	3479	GABRB1	1,0804697	IRF7	1,10380165	NR5A1	1,18287761	ATP5G2	1,16890034	PEU1	1,1315035	SIRT4	1,10381158	DOK2	1,32721301
3410	ZBTB16	1,08828793	PTCRA	1,11478048	PEU1	1,2005921	NTAN1	1,18243034	ST3GAL5	1,14499608	BCL2L2	1,11455668	NOTCH1	1,35120201	3480	KPNA6	1,08036407	UG1	1,10366065	GUCA1C	1,18276058	GRIK4	1,16808263	PDE6B	1,1313543	GSTA3	1,10329467	DIO1	1,32703379
3411	COL4A1	1,08821073	DGKI	1,11475817	CDKN1A	1,20017558	PARC	1,18224168	IL9	1,1446832	HYAL3	1,11446044	ILK	1,35068319	3481	PGLYRP2	1,08026671	TNFSF14	1,10365883	CPSF3	1,18246862	PCYT1B	1,16779219	FBXW2	1,13114927	LIPA	1,10315337	DOK1	1,3265446
3412	RXRG	1,08816879	TGFBRAP1	1,11468509	PRL	1,2001731	ITPR2	1,18216808	ARPC4	1,14458696	CYP2C19	1,11434298	DMGDH	1,35056063	3482	KATNAL1	1,08007182	BIRC2	1,10346836	WFS1	1,18216061	LY9	1,16767045	STX2	1,1308743	CD80	1,10311238	CDH15	1,32590879
3413	KLK6	1,08798368	NR1H2	1,11458649	NDUFA5	1,19992756	DAZL	1,18181611	ACOX2	1,1445786	TXNDC1	1,11394294	ALG9	1,35037238	3483	RAB11A	1,08006521	CYP27B1	1,1034503	IRAK3	1,18214576	ARPC1A	1,16758539	RAPSN	1,13052549	HEXB	1,10298815	AMPD1	1,32506548
3414	ADORA1	1,08788571	ALDH3B1	1,11416239	HIC1	1,19991038	CA12	1,18169616	B3GNT5	1,14423621	PRKCA	1,11334677	FMN2	1,34937075	3484	EZH1	1,07972739	CSNK1A1	1,10340053	CHRNA1	1,18158211	PRMT8	1,16753104	FCGR1A	1,1305208	DNM1	1,10289376	ADRA2B	1,32462338
3415	CNPY4	1,0878774	PCK2	1,11412958	FPGS	1,19914134	ZFYVE9	1,18158683	SEPP1	1,14409189	NR1H4	1,11317646	PAX1	1,34892945	3485	UROD	1,07971996	BDKRB2	1,10333486	SCN4B	1,18125872	OSBPL1A	1,16750476	CFL2	1,13041461	PPP2CA	1,1026068	GNB1	1,32442989
3416	SET	1,08766108	GALNT1	1,11410934	CD48	1,19847581	CA2	1,18154061	GLP2R	1,14409057	GALNT6	1,11309296	IL7R	1,34874723	3486	OGFR	1,07962581	CHRNA3	1,10317819	RASGRF1	1,18068756	CTSB	1,16733405	WFS1	1,13040283	WNT7B	1,1025689	UGT2B10	1,32423353
3417	RFK	1,08753624	CREM	1,11410295	RNF216	1,19847298	APOBEC3F	1,1814744	HMOX1	1,14391169	RDH5	1,11302432	MYLK2	1,34867164	3487	ELA3B	1,07940537	PLCB1	1,10305527	CTNNBIP1	1,1803719	ALOX15	1,16655146	FSCN2	1,13002118	CSDA	1,10209322	KLKB1	1,3233426
3418	PLG	1,08727924	CYP2U1	1,11400268	TP53BP1	1,19843171	SNX13	1,18133975	DGKE	1,14334896	CCR3	1,11281031	CDKSRAP1	1,34811828	3488	DLG4	1,07916551	ST6GALNAC3	1,10294926	CXCL10	1,17996371	RARG	1,16647489	HDAC3	1,12994933	GPRC5B	1,1020877	MFGE8	1,3228053
3419	CTSE	1,08684821	RXRG	1,11372248	CPN1	1,19823964	DTX4	1,18083287	WNT3	1,14312794	ATP1A3	1,11279802	FANCD2	1,34784448	3489	ATG10	1,07903022	PIGW	1,10268486	FZD4	1,17984302	CALCR	1,16634054	CD27	1,1299481	SERPINF2	1,10195454	ARRB2	1,32179014
3420	SRY	1,08659017	MMP3	1,11363133	RECK	1,19807143	DNM1	1,18083168	SFRS12	1,14310904	BCAR1	1,11273874	TCF15	1,34783651	3490	MLYCD	1,07889885	ATP1A3	1,10246858	GOPC	1,17980504	PPP5C	1,16630778	AGL	1,12963814	IDUA	1,10180686	SLC13A5	1,32106661
3421	HLA-B	1,086533	KATNB1	1,11360845	MVD	1,19787711	CNDP1	1,18067356	CCNI	1,14310665	ORC3L	1,11205628	DNMT1	1,34693004	3491	PAK2	1,0788355	COL6A3	1,10245393	BAK1	1,17929898	LTBP1	1,16625867	MAP3K8	1,1292988	CD36	1,10170275	SERPINE1	1,32105808
3422	CD22	1,08633876	KCNE1	1,11344113	CUL2	1,19758589	BZW1	1,18057831	NAE1	1,14254971	POLA2	1,11184533	PYCARD	1,34605454	3492	S100A8	1,07881607	DNAJA1	1,10196865	BYSL	1,17900736	EIF4E2	1,16602483	ETV5	1,12928182	VAMP5	1,10143593	JAG2	1,32052929
3423	PHPT1	1,08629053	INHBC	1,11279853	FRZB	1,19747961	ANGPTL4	1,18049389	TERF1	1,14249522	PRPS1	1,11164925	ANXA3	1,3459642	3493	CSNK2A1	1,07872121	METTL6	1,10192005	EIF2B4	1,1789968	SAT1	1,16577383	PDCD1	1,12910872	ACACB	1,10101991	DES	1,32030246
3424	EDA	1,08617166	RDH5	1,11253503	TNFRSF10A	1,19740877	GADD45A	1,17995985	CD33	1,14233849	C4BPA	1,11160554	ACADS	1,344851	3494	UGT1A6	1,07870476	PREP	1,1017058	CLEC7A	1,17886131	CTSE	1,16570562	ALMS1	1,1287404	CSNK1E	1,10057195	SLC1A4	1,32027087
3425	TREM1	1,08607412	NTRK2	1,1123893	TRPM4	1,19682785	FAT	1,17995324	COQ7	1,14203142	PPARD	1,11130629	UCP2	1,34454553	3495	CCNB2	1,07868557	LPHN2	1,10164458	ARF3	1,1776609	RFX4	1,16568792	S100A4	1,12849997	PPAP2B	1,10055429	CCND2	1,31851711
3426	APOE	1,08606368	ACTN3	1,11226264	EIF1	1,19664298	SLC23A2	1,17980316	GNAQ	1,14200661	LTBP1	1,11109159	TACC3	1,34440193	3496	CAST	1,07833773	RAB6A	1,10161027	CDC25L	1,17721031	CFLAR	1,16529997	IREB2	1,12830525	INPP5B	1,10027313	SLC2A1	1,31776057
3427	COL22A1	1,08606117	PIGV	1,11202733	COX15	1,19652862	ERAP1	1,1796511	CUZD1	1,1419426	FOLR1	1,11106441	EHHADH	1,34425654	3497	RNF146	1,07824531	MAP2K2	1,10144955	MTHFS	1,17677365	CHKA	1,1652177	PIK3CG	1,12819449	BDH2	1,10014478	NSMCE2	1,3165517
3428	HMGA1	1,08595407	IRAK1BP1	1,11170211	ICOS	1,19626229	PGF	1,17958854	LYCAT	1,14172019	MINPP1	1,11100729	C8B	1,34403202	3498	ST3GAL2	1,07800903	GPRC5C	1,10118576	DHRS7	1,17676827	RBPJ	1,16503607	ADCYAP1	1,12800781	MAP3K3	1,0999844	EHD2	1,31652425
3429	RAD18	1,08575081	HK3	1,11151244	MAN2C1	1,19600699	AMD1	1,17940689	ENPP2	1,14163138	CYSLTR1	1,11100474	HOXA11	1,34345721	3499	PSMD8	1,07793335	AGRN	1,10117258	TARS	1,17674104	DTX2	1,16466399	ARHGEF1	1,12795546	DHCR7	1,09980777	HES1	1,31623514
3430	DGKI	1,08557191	CNP	1,11143539	ENPP6	1,19581035	SRD5A1	1,17914337	DDX50	1,14146675	CFTR	1,11069055	UGT2A1	1,34284176	3500	LMNA	1,07733432	GFAP	1,10108343	DCLRE1A	1,17660255	TNFRSF10A	1,16404636	ADFP	1,12781735	RPS6KA5	1,0995275	ATP6AP1	1,31585002

Table A4. Pooled-shRNA library screen on HEL cell line and MF-3: list of 2nd most depleted shRNAs for each experiment (ranking approach 1, RA1).

	NO ruxolitinib (setting 1)				Ruxolitinib (setting 2)				Ruxolitinib + CM (setting 3)				MF-3				NO ruxolitinib (setting 1)				Ruxolitinib (setting 2)				Ruxolitinib + CM (setting 3)				MF-3	
	Experiment 1		Experiment 2		Experiment 1		Experiment 2		Experiment 1		Experiment 2						Experiment 1		Experiment 2		Experiment 1		Experiment 2		Experiment 1		Experiment 2			
Rank	*Gene*	*Fold change*	*Gene*	*Fold change*	*Gene*	*Fold change*	*Gene*	*Fold change*	*Gene*	*Fold change*	*Gene*	*Fold change*	*Gene*	*Fold change*	*Rank*	*Gene*	*Fold change*	*Gene*	*Fold change*	*Gene*	*Fold change*	*Gene*	*Fold change*	*Gene*	*Fold change*	*Gene*	*Fold change*	*Gene*	*Fold change*
3501	TPO	1,07710526	F2RL1	1,10088375	CD180	1,17659064	MAPKAPK2	1,16397203	ACCN2	1,12730901	REG3A	1,09935618	HYI	1,3156449	3571	DAP	1,06985425	STX3	1,090744	REN	1,16053895	EEF2K	1,14792502	PCYT1B	1,11677026	HSPA1A	1,08743305	PSENEN	1,29018913
3502	CFHR2	1,07691236	GPR50	1,10069594	RAC3	1,17652749	IUP	1,16389896	ME1	1,12695968	LHCGR	1,09874591	CCNB1	1,31541334	3572	GSTT1	1,06913211	IFNA17	1,09070296	GPR75	1,16045614	UGT1A10	1,1475306	GYS1	1,11656567	CEBPA	1,08714683	PIWIL3	1,28953109
3503	MST1R	1,07687168	IFNA13	1,10049489	ALPL	1,17649769	TIFA	1,16388119	CAPRIN2	1,12695892	ADCY9	1,09872649	GABRA3	1,31508884	3573	NFATC2	1,06909679	NKIRAS1	1,09049636	PTEN	1,16038271	MAP4K5	1,14752225	MS4A1	1,11655051	IFNA4	1,08700663	NANOS1	1,28950718
3504	ABCA6	1,07662203	DES	1,10015814	ID3	1,1761402	CACYBP	1,16339029	DTX1	1,12665329	OSBP	1,09836988	ATP2B3	1,31479153	3574	ZBTB32	1,06892941	NOS3	1,0904715	RAB7A	1,16023656	DVL3	1,14735986	PIP5K2B	1,11650116	TCF1	1,08677711	AMPD3	1,28942192
3505	TBX21	1,07651358	ATF2	1,10013858	IL17RE	1,17583574	RANBP9	1,16339029	CD244	1,12641275	SH3KBP1	1,09810061	CAPRIN2	1,31461577	3575	ALG2	1,06877449	TUBA4A	1,09016678	BLNK	1,1601571	IL6ST	1,14700793	PTGES	1,11643352	POLR1C	1,08665442	CD58	1,28938494
3506	FANCF	1,07643659	HP1BP3	1,10012134	AKAP9	1,17581718	ATP1A2	1,16270431	COX6C	1,12631055	CLIC1	1,09808337	CDH1	1,31454329	3576	RELA	1,06866549	C1QL2	1,09012703	ANGPT2	1,16004109	CTCF	1,14698323	PPFIA4	1,11633325	POU2F2	1,08614891	SUCLG1	1,2890871
3507	CTLA4	1,07627325	LHX8	1,09975495	CCND1	1,17576176	FPGT	1,16265501	AKR1D1	1,12626014	LTB	1,09805609	NR2F1	1,31410452	3577	EIF2AK3	1,06859018	NFKBIL1	1,09006414	C1QB	1,15993709	MSH6	1,14650971	MAP3K4	1,11628815	MR1	1,08609518	HYAL3	1,28907471
3508	NKIRAS1	1,0762452	EXTL3	1,09962195	GMDS	1,1755545	BNIP3L	1,16263748	ECHS1	1,12600307	NAGLU	1,0977348	ATP2A3	1,3139651	3578	DOK2	1,06857128	FGF11	1,08974206	CMAS	1,15947944	IRS2	1,14647608	MCM4	1,11595143	SREBF2	1,08598513	GABRA1	1,28896127
3509	VANGL1	1,07615813	SST	1,09960717	NCR1	1,17548588	NAGS	1,16253731	ADORA2A	1,1254878	SEC61A2	1,09762134	RNF19A	1,31363097	3579	GRWD1	1,06848922	GFI1	1,089673	SESN3	1,15900588	TGFB2	1,14617882	ATP12A	1,11583144	HP1BP3	1,08587863	TRADD	1,28885715
3510	NF1	1,07613594	TLR8	1,09950102	HS6ST2	1,17520696	EXTL2	1,16253567	RELA	1,12536609	TRIB3	1,09752718	XPA	1,31271761	3580	FUT3	1,06820818	NCOA2	1,0895994	CCR6	1,15900401	KALRN	1,14592954	CMAS	1,11571832	PTGS2	1,08586775	MET	1,28847571
3511	BHMT2	1,07605591	FANCI	1,0994646	FUT3	1,17515324	DPM2	1,16252543	APBA3	1,12528935	GDF1	1,0970939	MYH3	1,31268715	3581	GYS2	1,06813678	NDEL1	1,08938468	UQCRH	1,15889988	NPR3	1,14564238	PDXK	1,11569474	CACNA2D3	1,08553264	CD79A	1,28847483
3512	FMO4	1,076023	IL4	1,09934091	COL19A1	1,1747363	ANXA8	1,16241733	GAD2	1,12524211	DUSP4	1,09693307	ID4	1,31265217	3582	UBE2D1	1,06811092	TRPC2	1,08913494	IL7	1,15878924	TLN1	1,14550119	PRL	1,1155818	AKR1B1	1,08551846	PPARGC1A	1,28814399
3513	SRP9	1,07595626	IFNA6	1,0986232	PPCDC	1,17471402	RAC2	1,1617678	GPR50	1,12523201	FMO3	1,09671983	ADCY9	1,31139818	3583	FNTB	1,06795369	DBC1	1,0890051	NOS1	1,15861615	MGAT5	1,14503509	SALL4	1,11552437	SIGIRR	1,08538333	FPR1	1,28779729
3514	UBE2N	1,07591175	EEF1B2	1,0985673	UROS	1,17470323	SLCO1A2	1,16172431	SLC5A3	1,12521885	SLC10A2	1,09631217	NDUFA5	1,31135728	3584	TFDP1	1,0678722	PCYT1B	1,0890051	CCR5	1,15840852	EED	1,14453057	RNASEL	1,11515233	LCMT2	1,08523563	CYP2C19	1,2877798
3515	CPT1B	1,0758057	CCKBR	1,09845899	MCC	1,17462772	SMAD3	1,16158557	STS	1,1244254	A2M	1,09627871	KIF3A	1,31093355	3585	GPRC5A	1,067815	RGS4	1,08897001	DNMBP	1,157794	S100A6	1,14417089	CLCF1	1,11506512	MSH3	1,08521656	S100A4	1,28704214
3516	CD27	1,07576478	CFH	1,09833754	PTAFR	1,17430139	AP3B1	1,16148898	AADAT	1,12440418	ETV7	1,09565349	PDE6A	1,31042223	3586	CDK9	1,06779688	RAC2	1,08894405	CAMK2B	1,1577647	HIP2	1,1440252	CDKN2B	1,11482573	CASP7	1,08487285	LSM8	1,28687126
3517	ADIPOQ	1,07567087	ADC	1,0982454	EIF2AK3	1,17408462	NDUFB5	1,16140358	PRKCZ	1,12429574	OCRL	1,09526893	CR1	1,31021304	3587	CETN2	1,06769571	TRIM28	1,08888871	LIN7A	1,15775029	DRD5	1,14401179	CYP2A6	1,11461872	CBX3	1,08466796	MEPE	1,28630591
3518	CDK5R1	1,0753715	ATP6V1E2	1,09798607	DES	1,17360905	NMNAT3	1,16076866	MAN2B1	1,12416399	TAPBP	1,09493847	ALK	1,31011936	3588	PRKCQ	1,06768123	ALKBH3	1,08883912	PIGC	1,15770688	CRKL	1,14401063	KIAA1303	1,11458933	GRB7	1,08459735	EDG4	1,28628871
3519	CD72	1,07529165	PDLIM5	1,09794807	PAFAH1B3	1,17340917	IL13RA2	1,16038923	GPX2	1,1240639	CDC45L	1,09492384	SRXN1	1,30958621	3589	C1ORF103	1,06767801	LAMP1	1,08870556	NTF3	1,1573563	CTNNB1	1,14394114	IL11	1,11413563	SOX6	1,08448654	GPHN	1,28563434
3520	GLP2R	1,07524509	FKBP1A	1,0978993	BTG3	1,1731613	DUSP10	1,1600683	HPSE	1,12403981	ID1	1,09492384	PLAUR	1,30842513	3590	PAX5	1,06765015	ADIPOQ	1,08859826	TNFSF13B	1,15696248	LIPF	1,14393078	FABP7	1,11387247	SERPINA5	1,08395337	ENPP3	1,28550138
3521	INHBA	1,07492783	C1S	1,09782655	ABCG8	1,17303558	PRKCI	1,15944687	ACSL5	1,12357401	TERT	1,09485882	VSIG4	1,30789176	3591	GLS2	1,06756911	SKIL	1,0884948	ATF2	1,15666098	CA13	1,1435181	DNAJA4	1,11381281	ISG15	1,08393216	DDOST	1,28506753
3522	CYB5R1	1,07490691	CR1	1,09779397	EXOC7	1,17265699	TUBD1	1,15901947	CPT1C	1,12355431	HYI	1,09467001	PPAP2B	1,30788599	3592	STX5	1,06755707	SIRT6	1,08820604	DEGS2	1,1564865	IREB2	1,14281998	NDST4	1,11380333	CHRNA4	1,08387843	LTA4H	1,2850521
3523	MBTPS2	1,07487645	DCN	1,09777972	CD47	1,17261454	CHST13	1,15885552	GBX2	1,12348622	DHRS2	1,09461872	ANGPTL6	1,30752608	3593	CYP2R1	1,06753116	ALPL	1,08820478	TGIF2	1,15648594	LIPA	1,14269937	MIF	1,11337981	MAPK3	1,08371352	COL19A1	1,28505077
3524	TPI1	1,07473763	ESD	1,09766276	LTBP1	1,17244768	HIPK2	1,158649	TNNT2	1,12323003	SMUG1	1,09458914	AGL	1,30721776	3594	FAAH	1,06714764	PUM2	1,08812912	PIGG	1,15617653	ITGA4	1,14251271	PDK2	1,11325797	TICAM1	1,0836766	ECHS1	1,28504865
3525	KCNJ3	1,07464294	HYI	1,09757391	MYH3	1,17231987	PCGF2	1,15848162	AKT1	1,12314826	PAXIP1	1,09451003	CLDN1	1,30697349	3595	CASR	1,06711078	HLA-B	1,08807257	ATP6V1E2	1,15616425	KLK10	1,14233803	ECSIT	1,11299165	ADORA1	1,08358025	WDR79	1,28482409
3526	GCH1	1,07423959	PTCH2	1,09733706	CFP	1,1720676	TPH2	1,15848162	GLS	1,12309315	BMP8B	1,09445433	POLRMT	1,30689471	3596	CREB1	1,06706715	PDE2A	1,08789386	HMGB3	1,15609691	CYP4A11	1,14221199	RGS5	1,11277911	UNG	1,0835033	HTR1B	1,28468534
3527	SH3GL3	1,07405014	SCN8A	1,09714681	IRF7	1,17202793	SCG2	1,15820692	YARS2	1,12301595	CD34	1,09392731	CCL28	1,30574332	3597	CLCA4	1,06696554	CRHR1	1,08780544	CASP8AP2	1,15596376	UBE2E1	1,14191529	TBP	1,11262472	ADCY7	1,08338496	GGA3	1,28455469
3528	PTGES	1,0738974	MAPK12	1,09714376	CHRNA6	1,17190301	SCN5A	1,15751277	ACYP1	1,12284185	PDE8B	1,09353451	KATNB1	1,30549388	3598	ARHGEF12	1,06693315	GRIN2B	1,08751619	KCNN4	1,1558596	GALE	1,14181344	TBX21	1,11259337	PRKACB	1,08334505	PPP1R13B	1,28444722
3529	AKTIP	1,07378343	KCNE2	1,09696067	PLA2G4C	1,1715572	CASP8	1,1574229	IL17RC	1,12252329	HLA-DQB1	1,09352892	SLC6A2	1,30544247	3599	TLK1	1,06681387	QARS	1,08690273	VAMP2	1,15542191	PLAU	1,14175399	CKM	1,11248417	CTBP1	1,08333609	BAK1	1,28418135
3530	PPAT	1,073609	DRD2	1,09688006	TTF2	1,1714919	HMOX1	1,15727606	GPR77	1,12251365	ABCG1	1,09349024	NFKBIL2	1,30503853	3600	FTMT	1,06673106	KCNMB1	1,08688348	ANGPT1	1,15505753	DNAJA1	1,14170773	HAO2	1,11175659	NDUFB7	1,08323872	PLA2G3	1,28340298
3531	ABL2	1,07351485	SSTR1	1,09687992	RAD52	1,17108431	BAIAP2	1,15707376	MAP4K5	1,12239824	CCR10	1,09287804	PRKAR2B	1,30502608	3601	SYP	1,06650094	ATP6V1G2	1,08674179	PDE8B	1,15491829	POLH	1,14146712	ACAN	1,11140112	NUDC	1,08295406	DDB2	1,28310847
3532	MYCN	1,07341169	PPAP2C	1,09673074	POLE4	1,17102267	GPR161	1,15705026	ENTPD5	1,12231861	IFNA14	1,09278601	NPY	1,30416509	3602	DBC1	1,06646029	MMP8	1,08673642	PCYT1B	1,15449857	CAMK1G	1,14123864	POLRMT	1,11115827	RORC	1,08294511	TGIF1	1,28295988
3533	PPP3R1	1,07340555	DUSP8	1,09673008	KIF3A	1,17086821	ROCK1	1,1569587	C14ORF166	1,12184936	DAB2	1,09264034	BBOX1	1,30388126	3603	ALOX12	1,06618274	ARNT2	1,08642107	NUDC	1,15439188	FGF2	1,14107177	FRAT2	1,11092003	AADAT	1,08259279	GABRB1	1,28227978
3534	RECQL5	1,07320172	NDUFB7	1,09666757	GALNT14	1,1704173	TERF1	1,15667035	CENTA1	1,12184936	KLRA1	1,09264034	LDHB	1,30323232	3604	C7	1,06592566	LPHN1	1,08571654	CUL1	1,15414963	GALNT11	1,14052355	PYCR1	1,11074393	TOB2	1,08254421	ZFX	1,28180593
3535	WT1	1,07310921	NODAL	1,09651337	GALNT11	1,17037993	PHKG1	1,15652337	DHCR7	1,12182172	NEUROD1	1,09253558	MAPK11	1,30280101	3605	ARF4	1,06591712	SAA1	1,08568889	SCNN1D	1,15370322	PXN	1,14035888	IARS	1,1106616	POMC	1,0824458	GCK	1,28041176
3536	UPB1	1,07286509	BMP3	1,09645436	GTF2A1	1,17014721	ESR2	1,15640668	HUS1	1,12158746	AGA	1,09246485	TCL1A	1,30251737	3606	LCT	1,06586501	SREBF2	1,08567098	C8A	1,15327278	DIXDC1	1,14009666	ABLIM3	1,11019306	KPNA2	1,08222819	CALCRL	1,28001754
3537	UHRF1	1,07284334	POLE3	1,09604913	LY75	1,17005717	CCR1	1,1561878	LRPPRC	1,12154659	PSMF1	1,09239507	RBM8A	1,30226243	3607	CSRP3	1,0658528	TSC1	1,08536997	BCKDHB	1,1531447	SCAP	1,13983863	SERPIND1	1,10994438	JUNB	1,08206114	CDC25	1,27967431
3538	TSC1	1,07277165	FABP7	1,09594846	VIL2	1,16976529	ADH6	1,15615433	CBLB	1,12146435	NCR1	1,09237695	TNIP1	1,30219851	3608	EEF1A2	1,06557792	CACNA1C	1,08528872	C1GALT1	1,15283663	CDX1	1,13971548	GNA15	1,10982147	FAS	1,0819003	ABLIM2	1,2791288
3539	SHISA5	1,0727342	NOG	1,0958695	YWHAG	1,1696231	MSH3	1,1555996	RAD1	1,12135781	CEP290	1,09187615	MGAT4A	1,30218468	3609	GALNT4	1,06523226	PPIC	1,08522999	ATP6V0B	1,15272848	GCH1	1,1397131	HSD17B12	1,10969127	SPIB	1,08182581	ST8SIA2	1,27900025
3540	RNF19A	1,07272615	AHSG	1,0955764	PNPO	1,16937546	DGKI	1,15536656	HS3ST3A1	1,12108311	PLA2G10	1,09183344	GALNS	1,30198937	3610	B3GALT5	1,06522802	SGK	1,08508928	MEF2C	1,15265111	CDC14A	1,13961981	FABP6	1,10958593	LXN	1,08166128	PRKD3	1,27871764
3541	ALDOB	1,07262499	HSPA1A	1,0955621	HSPB1	1,16930332	CLDN19	1,15499927	CDC45L	1,12107602	KLK7	1,09177941	AGPAT2	1,3013939	3611	APBB1	1,06521105	GNRHR	1,08491517	ALDH7A1	1,15255233	PPME1	1,13952941	MVP	1,1094941	FGF2	1,08147956	CLTB	1,2786265
3542	CTSK	1,07249881	AXIN1	1,09488258	PMVK	1,16910025	SOST	1,15457203	CDA	1,12104802	BMI1	1,09165174	EDN3	1,30119885	3612	PIGC	1,06512683	IL1RN	1,08479231	CYB5R3	1,1525166	AMY1B	1,13946461	CHRNA3	1,1091156	RFK	1,08136894	PNPLA3	1,27827111
3543	CHRNB1	1,07241346	FGA	1,0946763	DNM2	1,16907612	DARS2	1,15429231	C10ORF110	1,12085089	TBKBP1	1,09153886	IL17A	1,30108054	3613	ELK3	1,06508252	CNTF	1,084734	CACNA1F	1,15234049	CREB3	1,13912334	GJA3	1,10908563	FMO2	1,08135678	FBLN2	1,2779107
3544	FCER1A	1,07219929	MAN2B1	1,09465541	TAPBP	1,16894096	CRK	1,1540124	BBC3	1,12068111	CPT1C	1,09135268	TYR	1,30096117	3614	KRT19	1,06479648	ACTR3	1,08442844	DIAPH2	1,15218748	POLD1	1,13912334	APLN	1,10901684	BDKRB1	1,0812094	MMP2	1,27783908
3545	ASPA	1,07218438	CLCA4	1,09450071	GDF1	1,16884879	CNR2	1,15372226	FOXC2	1,12065378	OLAH	1,09100999	S100A8	1,30095634	3615	LRRTM3	1,06469526	HOXD1	1,08405833	B4GALT2	1,15188358	WWP2	1,13887747	SLC9A3R1	1,10895795	RARB	1,0811715	P2RY6	1,27775993
3546	GCLC	1,0720653	KCNQ2	1,09393111	PERP	1,16869253	IKBKAP	1,153529	CCL4	1,12061775	IL1B	1,09079238	COSLG	1,30047777	3616	POLR3GL	1,06469389	PTGFR	1,08343572	GATA3	1,15181842	KCNQ2	1,13820852	CES2	1,10862222	PDLIM5	1,0809806	PSMD2	1,27772357
3547	COL17A1	1,07204171	PDE4A	1,09377424	ARPC5L	1,16804624	CYP3A7	1,15348478	NDUFB2	1,1203134	GPX4	1,09021692	PABPC1	1,30019984	3617	SIPA1	1,06453679	CDH2	1,08342566	LSS	1,15159654	POLB	1,13790843	STX12	1,10858719	CHST13	1,08083057	PGLS	1,2761555
3548	KLK1	1,07202805	CAPN7	1,09372623	SSTR5	1,16732159	KCNIP3	1,15343925	AK5	1,12011982	ATP13A2	1,09019067	ALPPL2	1,29971885	3618	TFDP2	1,06432834	FYN	1,08322497	IFNA16	1,15156066	AP2A1	1,13789735	C3AR1	1,10818207	CCL3	1,08067078	NMU	1,27632431
3549	AUH	1,07195419	PECR	1,09369174	LHCGR	1,16718452	HLA-DRA	1,15272307	PDPK1	1,1200308	RAB11A	1,09010447	ACY3	1,29953949	3619	FAS	1,06429341	CTBP1	1,08321639	KRT7	1,1514523	SOD1	1,13776218	GRK5	1,10801109	ARSE	1,08045578	DDO	1,27601391
3550	HOXC13	1,07190208	ITPA	1,09337761	LIG1	1,1669052	DDX51	1,15269614	STH	1,11995837	RFWD2	1,09004067	APOBEC3B	1,29885753	3620	CSK	1,06428129	ITPR3	1,08308825	ACAN	1,15145013	DUSP1	1,13749815	DPM1	1,10747056	MCF2	1,08022038	TAP2	1,27572484
3551	MS4A1	1,07183251	IFI27	1,09326266	ACP2	1,16684949	POLG	1,15265204	DLG4	1,11973126	GLA	1,09001093	COQ3	1,29810426	3621	ATG7	1,0642472	SLAIN1	1,08304837	CHST12	1,15134143	KLRK1	1,13716395	HCST	1,1074657	GCM1	1,07973853	DTX4	1,27570095
3552	RAD50	1,07179912	UGT2B17	1,09315416	ENTPD4	1,16663468	APH1A	1,15230237	PTGIS	1,11972436	WASF1	1,08957706	TM2D1	1,29792338	3622	DYRK1B	1,06423662	CMAS	1,08295841	ESR2	1,15125535	NDRG2	1,13704925	MUTYH	1,10727946	NR2C2	1,07967692	PPCDC	1,2751413
3553	TLR8	1,07171813	HSF2	1,09281478	CCR3	1,16531442	CYB5R3	1,15209972	NAGS	1,11959938	KCNH2	1,08949872	PRLR	1,29778179	3623	BP75	1,0642075	POLR3G	1,08290798	ADAM10	1,15103638	RAB1A	1,13673388	PLG	1,10721696	HLCS	1,07943779	C8A	1,2750284
3554	NPR3	1,07160189	ATP2B1	1,09270387	COL22A1	1,16506528	CSNK2A1	1,15158533	PLA2G6	1,11948199	SNAP29	1,08905446	FLCN	1,29708778	3624	ARHGEF6	1,06370994	MSI1	1,08288735	HSPA1B	1,15102182	PPP1R3A	1,13667657	PAX8	1,10720157	STH	1,07910541	SMARCE1	1,27477692
3555	DAZAP2	1,07156396	HBQ1	1,09230591	BCL11A	1,164873	BACH1	1,1514895	ACCN4	1,11934394	ERCC1	1,08866662	SRM	1,29673192	3625	HSD3B7	1,06360177	PSMB8	1,08282507	MYL2	1,150934	FNTB	1,13655555	CBX5	1,10717094	TLR7	1,07904808	GATA3	1,27422453
3556	RALA	1,07154491	POLR3B	1,09209828	BGLAP	1,16465706	IFNGR2	1,15137674	CLDN5	1,11934094	HTR3D	1,08850035	GNB3	1,29670484	3626	BMP8A	1,06351716	COL4A4	1,08273658	HPRT1	1,1508897	CLDN10	1,13634561	DBN1	1,10688571	HPSE2	1,07886888	TLK1	1,27409905
3557	ITPR2	1,07118199	HSPB1	1,09193737	ASAH1	1,16452436	ABLIM3	1,15137131	ADCY2	1,11928903	GABRE	1,08842946	NQO1	1,29649149	3627	CD1B	1,06345285	ARPC5L	1,08269107	CYP1A2	1,15062772	GPR83	1,1362421	CTNNB1	1,10686338	CFB	1,07871089	NDUFS4	1,2740179
3558	EIF4A2	1,07087638	EGFR	1,09182721	MAP3K1	1,16431389	NPPB	1,15124353	OTUB1	1,11911965	GCLC	1,08833349	OSCAR	1,2962901	3628	RAB7A	1,06345152	GBF1	1,08259425	ARPC4	1,15061601	B3GAT1	1,13610349	PFN1	1,10682176	SIRT2	1,07867421	QPRT	1,2735416
3559	CPSF1	1,0708277	TAF2	1,09173863	GP5	1,16425712	ADRB2	1,15113603	WNT10B	1,11911592	GBGT1	1,08830387	EDG1	1,29383563	3629	USP9X	1,0630054	TRPM2	1,08236703	ALDH3B1	1,15021178	ABCG2	1,13503043	TNFRSF11A	1,1066539	FPGS	1,07849027	PLA2G4B	1,27336619
3560	PACRG	1,07081127	FGF10	1,09158513	CTSD	1,16363563	MKKS	1,15107457	ATP1A2	1,11859527	CHGA	1,08825095	PTGES2	1,2934147	3630	ATP6V1G1	1,06286208	FABP6	1,08233381	EDG4	1,15004425	ACTG2	1,13493127	HP1BP3	1,10651714	CYP1B1	1,07844335	FGF7	1,27301957
3561	FGG	1,07057453	SHC3	1,09152309	CAPN3	1,16341353	POLE3	1,15091675	MYF5	1,11841976	ADSL	1,08816765	RAPSN	1,29227924	3631	VKORC1	1,06283754	CDH15	1,08225734	IKZF3	1,14978834	CYP2C19	1,13461991	FCGR3A	1,10640635	PARP2	1,07805944	POLR2C	1,27171546
3562	HBXIP	1,07046187	AKAP10	1,09148165	EMP1	1,16329391	ALOX12	1,15073327	GRWD1	1,11814463	JPH3	1,08815782	POLR1C	1,29199996	3632	PMM1	1,06278624	CYP2C8	1,08218887	LCN2	1,14937065	HP1BP3	1,13435714	TNIP3	1,10637144	TP53BP2	1,0778522	ADAMTS13	1,27158489
3563	PDE8A	1,07044945	BRS3	1,09148097	ABCC3	1,16296624	NANOG	1,15013976	MKNK1	1,118114	ASS1	1,08809424	RGS19	1,29170577	3633	NEU1	1,06274938	MAP3K9	1,08186233	ALOX15	1,1493405	ACAT2	1,1341432	COL5A3	1,10634363	HSP90B1	1,07780364	CCNA2	1,2714841
3564	BBS2	1,07044691	DNM1	1,09142573	SUFU	1,16235362	GUCY1A2	1,15003011	STAT4	1,11779421	IFIT1	1,08809242	CALML6	1,29154974	3634	PRL	1,06261096	NAT6	1,08164671	NAPG	1,14909705	OGG1	1,13381679	APAF1	1,10624332	TDGF1	1,07761672	AFP	1,27126784
3565	MAPK13	1,07042573	MALT1	1,0913794	ARHGEF6	1,16233145	RDH12	1,14976065	FZD8	1,11774915	ALK	1,08804538	SNRPN	1,29152031	3635	TFAP2B	1,06226032	WFS1	1,08155825	ADRB2	1,14906544	TRPM2	1,13371522	DOK1	1,10615188	PMCH	1,07753297	CYP24A1	1,27045281
3566	ICOS	1,0702776	SCNN1A	1,09115027	RETNLB	1,1620368	CCNA1	1,14957824	APBB2	1,11744212	DDX55	1,08791189	BP75	1,29144883	3636	DES	1,06209076	NUDC	1,08117396	IRP1	1,14875445	CFL2	1,13370092	DKK1	1,10606581	ADAM9	1,07722217	VWF	1,26982675
3567	PTK2B	1,06997466	CHST14	1,09110565	CNDP1	1,16165777	CD244	1,14946401	C6	1,11738935	NAE1	1,08775037	FANCF	1,29139838	3637	PIGB	1,06166866	KCNQ5	1,08090159	ALKBH3	1,14865621	CPEB1	1,1333846	SELE	1,10591633	AK3	1,07720968	ATP6V1C1	1,26943593
3568	HELB	1,06991435	CYP2D6	1,09109081	OXCT2	1,16143621	RAP1GAP	1,1490046	HDAC5	1,11704188	GALNTL1	1,08773197	EPPK1	1,290979	3638	SGK	1,06162861	CFTR	1,08067094	NDUFB5	1,14824071	GSTT1	1,13316708	CYP2J2	1,10579263	ARG1	1,07689497	DEDD	1,26860939
3569	ARAF	1,06986427	PAX3	1,09097501	BDH2	1,16090525	GLI4	1,14896029	CSDA	1,11695887	UGT2B11	1,08762077	GPAA1	1,29066353	3639	BAD	1,06116336	BNIP3L	1,08058967	DFFA	1,14786668	PSMD8	1,13311519	EXTL1	1,10573265	IMPA2	1,07679179	WISP1	1,26750823
3570	SCG2	1,06985515	EDA	1,09080981	MKNK2	1,16057915	IFNA16	1,14814834	BAG4	1,11683536	HPRT1	1,08759445	GGH	1,29021205	3640	SLC33A1	1,06107147	CSNK1G1	1,08057849	POLR3B	1,14756665	CFH	1,13304588	PIGW	1,10559452	FBXW11	1,07651143	MAPKAPK2	1,26709403

Table A4. Pooled-shRNA library screen on HEL cell line and MF-3: list of 2nd most depleted shRNAs for each experiment (ranking approach 1, RA1).

	NO ruxolitinib (setting 1)				Ruxolitinib (setting 2)				Ruxolitinib + CM (setting 3)				MF-3				NO ruxolitinib (setting 1)				Ruxolitinib (setting 2)				Ruxolitinib + CM (setting 3)				MF-3	
	Experiment 1		Experiment 2		Experiment 1		Experiment 2		Experiment 1		Experiment 2						Experiment 1		Experiment 2		Experiment 1		Experiment 2		Experiment 1		Experiment 2			
Rank	*Gene*	*Fold change*	*Gene*	*Fold change*	*Gene*	*Fold change*	*Gene*	*Fold change*	*Gene*	*Fold change*	*Gene*	*Fold change*	*Gene*	*Fold change*	*Rank*	*Gene*	*Fold change*	*Gene*	*Fold change*	*Gene*	*Fold change*	*Gene*	*Fold change*	*Gene*	*Fold change*	*Gene*	*Fold change*	*Gene*	*Fold change*	*Gene*	*Fold change*
3641	CAPRIN2	1,06106227	FANCA	1,08055338	C4B	1,14708872	CDK9	1,13287831	RBP4	1,1051095	OAZ1	1,07641284	ANAPC5	1,26702086	3711	GIT1	1,0511618	ST3GAL4	1,07072111	FLT3	1,13155845	UXT	1,12151917	SLC18A1	1,09360104	ALDH3A2	1,06448952	ALOX12B	1,23837539
3642	ABCA9	1,06084085	RAB4A	1,08054117	BCL2A1	1,14694789	SPTBN4	1,13285933	INPP1	1,10451966	CA9	1,07637022	EPHA2	1,26686632	3712	CHRNA5	1,05097325	GPX2	1,07052628	ALOX12	1,13104036	CDKN1A	1,12086229	UBE2E1	1,09351713	GNA15	1,06444297	POLR1B	1,2382865
3643	ABCC6	1,06083256	ZFYVE16	1,08039299	GRK5	1,14687138	IKZF2	1,13267019	GRM2	1,10445932	CCL2	1,07600472	SMO	1,26661344	3713	IFI44	1,05096384	SMARCC2	1,07029545	NTRK2	1,13097307	MYCN	1,12039246	NDUFB11	1,09350538	POU2AF1	1,06427003	PRKX	1,23704148
3644	CHRM4	1,06074454	GABRG1	1,08038839	VPREB1	1,14679096	NFKBIL2	1,1325352	DOK2	1,10440318	PDHB	1,0759746	PEG3	1,2662604	3714	TUBB3	1,05064342	CCR2	1,07018238	BDH1	1,1309698	MAN1A1	1,12014746	ALG14	1,09307204	FANCA	1,064232	SCP2	1,23697829
3645	PMP22	1,06039146	PIP3-E	1,08029273	POLA2	1,14662142	RECQL5	1,13252049	HIG2	1,1037528	TCEA3	1,0758731	CYP4F2	1,2660967	3715	FSCN3	1,05039614	GNMT	1,07002863	YARS2	1,13069878	NFYA	1,12006965	WWTR1	1,09303205	CACNA1D	1,06380342	CDS3	1,23656902
3646	GYPA	1,06036555	PPP3R1	1,08021384	RAD51L3	1,14656368	C1QL1	1,13251443	MYCN	1,10367441	NMU	1,07569523	CIITA	1,26595693	3716	ADRA2B	1,05023239	ADORA1	1,06993022	MAP3K13	1,13068534	XRCC3	1,11967872	OTC	1,09270751	GEN1	1,06372035	GNA15	1,23582717
3647	NR1H4	1,06018157	PIWIL1	1,08016529	PECR	1,1463772	PPP1R13L	1,13244119	TLR6	1,10366467	COL11A1	1,07562021	PIGT	1,26579544	3717	CTBP1	1,05005588	GDF15	1,06972596	ABCC4	1,13066379	TLR2	1,11946989	PAXIP1	1,09266374	GPX3	1,06368392	GALNT11	1,23562483
3648	FRS2	1,05993971	SOX1	1,08007917	ADCY3	1,1461923	F2RL2	1,13186435	CHPF	1,10351016	TIMP3	1,07547768	GABRE	1,26555314	3718	ST6GAL1	1,05003921	COL4A6	1,06952207	MC2R	1,13009214	NME1	1,11898134	LALBA	1,09246942	GBA3	1,06356681	INDO	1,23476846
3649	DHRS7	1,05972065	ERCC5	1,07985359	KRT18	1,14618486	BDNF	1,13179853	PGA3	1,10324366	AGXT2L1	1,07545596	DKK3	1,26552567	3719	KLK7	1,05002096	SLC6A13	1,06946954	PIAS3	1,13002004	HIST17B12	1,11889772	B3GALNT1	1,09241001	MAP2	1,06352915	SIN3B	1,23460736
3650	MAPK8	1,05944742	NOD2	1,07983961	GABRB3	1,14566052	MYBPC3	1,13177136	NEFH	1,10322106	CD79A	1,0751727	RPA3	1,2654966	3720	HS6ST2	1,04991578	POU2AF1	1,06933403	TGIF1	1,12999492	IL2S	1,11870803	TUBA8	1,0918894	EIF4EBP1	1,06340494	CCNK	1,23429939
3651	ITGAV	1,05933673	CFI	1,07964987	DHCR7	1,14533596	ATP5G3	1,13151477	B3GNT7	1,10268955	HSPA8	1,0751727	CDC25C	1,26546841	3721	GBE1	1,04985299	PARC	1,06930143	GRN	1,12995195	LNPEP	1,11857496	NTSM	1,09166172	PTCRA	1,06338234	ACAN	1,23423381
3652	ALDH18A1	1,05915585	BAIAP2	1,07961565	RAD51L1	1,14507886	SCNN1A	1,13150548	FZD3	1,10243775	APLP1	1,07514765	PCNA	1,26505833	3722	CCR4	1,04976953	PGD	1,06917727	TIMP4	1,12987955	AES	1,11819813	ROCK1	1,09143589	CCL13	1,06336811	BTG3	1,234093
3653	TPMT	1,05887057	SETDB1	1,07954954	BBC3	1,14506737	GTF2E1	1,13115874	CPA3	1,10241958	GRIN2D	1,07506718	APOC1	1,26406819	3723	IL21R	1,04953035	NPM1	1,0689325	HIST1H2AA	1,12954647	C4BPB	1,11799582	DHRS4	1,0914094	DIAPH1	1,0629969	COQ2	1,23405453
3654	SLC27A4	1,05870312	EFNA5	1,0795452	XRCC2	1,14472911	CDR1	1,13106255	TKTL1	1,10240694	HMGB2	1,07498111	CMAS	1,2637635	3724	ACVRL1	1,04952696	OPRK1	1,06890667	ATG4B	1,1294952	ELK1	1,11796102	LMNB2	1,09131383	RAPGEF1	1,0628975	WNT7A	1,23403019
3655	MT2A	1,05865144	NDST1	1,07948911	EN1	1,14455105	NSUN2	1,13057041	AK3	1,10237645	ATG5	1,07493656	ELAVL1	1,2633621	3725	ADRB1	1,04932119	MTTP	1,06863871	ST6GALNAC2	1,12938707	BMP2	1,11793607	CD93	1,0912623	TTF2	1,06283199	EGR3	1,23363398
3656	TCIRG1	1,05846752	NEFH	1,07945813	IFI44	1,14452752	GPR50	1,13053432	TDGF1	1,10236646	POLE	1,07476825	ATP6V0B	1,2631653	3726	CD48	1,04928609	MAP3K13	1,06848679	PPP3R1	1,12923294	PDE6H	1,11774844	CNGA3	1,09045085	HDAC6	1,06255129	APBA2	1,23336962
3657	SFRS12	1,05841079	STX16	1,07919052	HDAC8	1,14428475	BTC	1,13033023	MME	1,10232329	BLM	1,07467053	ACO1	1,26308253	3727	GPR39	1,04915195	PC	1,06842459	TIAM1	1,12922025	FBXW2	1,11756769	FLOT2	1,09043974	ATP6V1G2	1,06252965	CCR6	1,23313794
3658	CSDA	1,05810894	CCR5	1,07905343	HMGB2	1,14422913	SNCAIP	1,13029852	ADIPOR1	1,10217954	PTGDS	1,07437842	ERG	1,26290381	3728	MSH3	1,04908119	CMBL	1,06826421	SKI	1,12902349	CHST12	1,11751188	GRIK4	1,0904067	B3GALT2	1,06246469	DIAPH2	1,23297809
3659	DGKB	1,05801839	IGF2	1,07904492	ITGB7	1,14394442	CYR61	1,13025288	SCD5	1,10195814	OLIG1	1,0742796	ATG4A	1,26249923	3729	CHGA	1,04895474	CACYBP	1,06823313	PAPSS2	1,1289977	IDUA	1,11712138	PRMT1	1,09031258	RPN1	1,06227738	LMX1B	1,23294514
3660	HIPK2	1,05781738	ALG2	1,07898228	SGK	1,14390243	CLDN1	1,13007168	USP11	1,10184743	LCT	1,07421775	TSC2	1,2613114	3730	FABP1	1,04884308	ITGA1	1,06805834	GAST	1,12867602	TYMS	1,117119	HOXB4	1,0902959	KLK1	1,06221879	GNAT1	1,23294483
3661	MBD1	1,05747201	HSPA1B	1,07883495	CLU	1,14328898	DHRSX	1,12990328	TAF10	1,10130087	PTPRU	1,07414236	IMPA2	1,26082759	3731	GALT	1,04879385	CD33	1,06789384	PCSK1	1,12857235	ASH1L	1,11686413	SDHA	1,08981811	TFAP2A	1,0621434	ZDHHC8	1,23271401
3662	COL16A1	1,05745203	TGM3	1,07830468	DUSP9	1,14321525	PGAP1	1,12962867	GCLM	1,10124792	HTR1F	1,07365994	SLC23A2	1,26035508	3732	BGLAP	1,04863231	REPS1	1,0678648	KATNAL1	1,12830144	COQ6	1,1162005	NCOA4	1,08975227	TAP2	1,06197468	IL8	1,23231559
3663	B3GALNT1	1,05743708	STX12	1,07824942	CREB3L1	1,14318826	PDE8A	1,12948715	MGP	1,10118788	ELK1	1,07338496	OLA1	1,26027218	3733	PIGH	1,04843369	CA14	1,06786267	PNMT	1,12823161	GAS2	1,11584105	S100A6	1,08929374	NDUFA1	1,06175039	IL10RB	1,23221318
3664	PPIC	1,05739982	ACSS2	1,07805287	TGFA	1,14318544	FEN1	1,12948202	COPS3	1,10112905	SEPP1	1,07337679	CHST12	1,25952202	3734	PROZ	1,04841588	DHRS4	1,06770911	SSTR2	1,12695802	IL13RA1	1,11567483	UBE2D2	1,08883601	H2AFY2	1,06129092	HTR3E	1,23193425
3665	LHX8	1,05739651	GTF2A1	1,07797454	ANGPTL2	1,14281065	ABCC4	1,12942852	DAG1	1,10112724	GCDH	1,07333264	DKC1	1,25928945	3735	IFI35	1,04825367	ARFGAP1	1,0675556	ALDH3B2	1,12689134	TNC	1,11534535	ST6GALNAC4	1,08860095	CDKN1B	1,06118405	CHRNB1	1,23183515
3666	NOTCH1	1,05733186	SLC1A4	1,07795693	PFDN2	1,14223523	HOXD11	1,12919536	GSTA4	1,10088889	MAP3K9	1,07298309	PIP3-E	1,25900984	3736	PRKACB	1,04819782	TRH	1,06753439	RPA4	1,12588912	FGF5	1,11518367	CYP17A1	1,08858211	POLD3	1,06088529	ESCO1	1,23149157
3667	IRS1	1,05697641	KLRK1	1,07789134	ADCY9	1,14174885	CREM	1,12911785	CLOCK	1,10072308	BZW1	1,07294593	ATP5I	1,25873461	3737	XRCC5	1,04815476	ARPC4	1,06747694	BRCA2	1,12509116	ALAS2	1,11513973	EIF4EBP2	1,08858211	GP1BA	1,06065168	SOCS1	1,2313101
3668	CMA1	1,05683322	SNCAIP	1,07782491	C19ORF40	1,14171792	DCLRE1A	1,12904053	PYGB	1,10061871	IKZF1	1,07266735	LIPF	1,258497	3738	ADFP	1,04802937	CKM	1,06745088	PPP1R13L	1,12508195	ENPP3	1,11500198	MAP2K2	1,08857974	BTC	1,06047173	ALOX15	1,23115239
3669	PRKAR2A	1,05683322	ITPR2	1,0776857	SFMBT2	1,14101152	FGR	1,12875428	MCC	1,10046175	PRDX6	1,0722867	AP2A1	1,25833083	3739	ENTPD5	1,04802167	RFNG	1,06730993	ECHS1	1,12323345	UBE2J1	1,1146012	TACR3	1,08842052	ADRA2A	1,06035693	BHLHB9	1,23095306
3670	PRPS2	1,05679069	CDKL2	1,0776175	TSHR	1,14098397	NR1H4	1,12840037	ADH1A	1,10024455	FZD6	1,07198734	UBE2I	1,25783478	3740	TGFB1	1,04799727	PRKACB	1,06697658	DCN	1,12309712	MINPP1	1,11442323	TAP2	1,08833631	STMN1	1,06027039	EREG	1,23083558
3671	NR2F1	1,05663544	CHRNA1	1,07758689	ANAPC11	1,14036241	AP3M1	1,12803973	MAP1A	1,10022364	HDAC3	1,07187442	ETV3	1,25748984	3741	TREH	1,04798399	TGFB1I1	1,06673474	TRIM28	1,12302515	COL1A1	1,11399757	P2RY5	1,08827092	DDHD1	1,05999778	RAB24	1,23060394
3672	TIMP3	1,05656877	RAD1	1,07749383	BLMH	1,14000029	CAP1	1,12788517	CASK	1,10018532	GABARAPL2	1,07165004	NMNAT1	1,25693925	3742	SMARCD1	1,0478683	CA8	1,06659958	GPR34	1,12295806	ADCY6	1,11394444	ATP6V1E2	1,08780956	SMURF2	1,05960976	FST	1,23034823
3673	IFNA4	1,05630319	PGF	1,07749239	EED	1,13958415	TSHR	1,12781705	SFRP4	1,10013506	PEG3	1,0712147	CSGLCA-T	1,2562744	3743	B3GALT4	1,04782267	KIAA1303	1,06657397	E2F1	1,12281256	PTAFR	1,11354188	GRM8	1,08755923	CYB5R1	1,05960878	CACNA1I	1,23028953
3674	TRAF3IP2	1,05629802	SOCS1	1,07748341	PEBP1	1,1394594	HK1	1,12779382	EGR1	1,10004067	MNAT1	1,07104764	TNKS	1,25622234	3744	PC	1,04762614	F11	1,0649975	DAG1	1,122215	SERPINF2	1,11342661	FGF18	1,08751449	CRHR2	1,05933146	GAP43	1,22996028
3675	CAPN7	1,05557595	CSNK2B	1,07713702	GABRA2	1,13934751	FMO1	1,12750825	FMO2	1,09978788	MAP2K1	1,07064355	EIF2B4	1,25578221	3745	IKBKB	1,04760832	FEN1	1,066447	UQCRC1	1,12211668	FZD10	1,11306703	GRIA3	1,08745813	PINX1	1,05915984	SOX4	1,22960118
3676	VARS2	1,05549138	SRP72	1,07678699	IRAK1BP1	1,13928097	RGS5	1,1274368	COL21A1	1,09947014	ASNA1	1,07055239	B3GALT4	1,25572949	3746	RNASEL	1,04751034	GPI	1,06628408	KLKB1	1,12204094	NFAM1	1,11300228	C4BPA	1,08729014	COQ5	1,05871346	PAX8	1,22937354
3677	AES	1,0554229	CD46	1,07664483	CD69	1,1392712	GALNT13	1,12739539	CMBL	1,09941748	UGP2	1,07024398	IRAK3	1,25565286	3747	GFI1	1,04740064	DIAPH1	1,06601862	P11	1,12138332	ARHGDIB	1,1129129	CERK	1,08720756	FGF1	1,05853331	AKAP3	1,22911838
3678	IVD	1,05526536	CD93	1,07654888	ATP6V0A4	1,1391343	STX11	1,12720795	DACT1	1,09913207	UROD	1,06996833	PRKCZ	1,25515664	3748	PAK1	1,04731917	PLD3	1,06597812	IRAK4	1,12117192	TAGLN2	1,11263269	LCMT1	1,0871842	DGKD	1,05800579	ASPA	1,22899471
3679	KITLG	1,05522865	XRCC4	1,07613501	UBE2B	1,1388901	IDE	1,12713557	ANXA1	1,09895335	CYP46A1	1,06968282	FBXW11	1,25430265	3749	ATOH1	1,04720277	MYCN	1,06585384	CSRP1	1,12101427	CYP27B1	1,11243524	CHRNA5	1,08699498	CA13	1,05773631	KIAA1303	1,22827046
3680	POLD3	1,05516042	CTNNA3	1,07611417	GNAT1	1,13879775	WASF1	1,12652119	GPR68	1,09842263	HK1	1,06941284	IRF3	1,25379488	3750	CXCR3	1,04710778	ALG8	1,06531509	CHRNA9	1,12055015	HDAC11	1,11241876	OPRL1	1,08636519	THTPA	1,05771714	PAH	1,22824111
3681	TNFRSF13B	1,05512788	IKZF1	1,07603778	DLST	1,13866186	CPSF2	1,12647986	MAP1LC3B	1,09833121	MIOX	1,06926539	RPS6KA3	1,25376293	3751	WNT3	1,04704355	FZD9	1,06489958	PML	1,12046495	IRF3	1,1118823	GTF3C3	1,08631184	GNS	1,05758502	ODC1	1,22792108
3682	PPP1R10	1,05489249	SIPA1	1,07602126	RECQL	1,13771216	CSTF3	1,12634617	NR1H2	1,09825478	PLA2G2A	1,06892394	TLR3	1,25359315	3752	EPHA2	1,04703479	ABCC1	1,06484864	PLCD1	1,12039582	CABIN1	1,11183259	CTBP1	1,08625802	SMAD1	1,05755879	ABCB7	1,22757651
3683	LITAF	1,05487646	EZH1	1,07579758	RPS6KA5	1,1377106	CD200R1	1,12625533	FGF7	1,098218	GSTO2	1,0689139	EPRS	1,25322442	3753	GREB1	1,0469632	UBQLN1	1,06440217	TBL1X	1,12027966	AHR	1,11179309	ATP6V0A4	1,08625025	ATN1	1,05747846	KLRC3	1,22660737
3684	KCNJ12	1,0547836	MYL3	1,07543832	TF	1,13737517	CA8	1,12608989	MYLK	1,0980767	MEIS1	1,06882328	BCL10	1,25321722	3754	FARSA	1,04677999	LDHB	1,06416925	ALDOA	1,12023811	DAG1	1,11171563	HMGB1	1,08625025	SRP72	1,05741854	PIK3CG	1,22562504
3685	ATP13A2	1,05459126	MAP2K6	1,07532859	SCP2	1,13718977	ATP6V1G1	1,12605284	NFYB	1,09765425	SLC22A6	1,06877469	GNB1L	1,25200523	3755	BAK1	1,04660564	CBR3	1,0640868	GALK2	1,11973821	GDF15	1,11161722	MLYCD	1,08577222	IFNG	1,05731305	DGKQ	1,22545969
3686	PLA2G3	1,05422864	EPAS1	1,07512923	CD28	1,13713547	DNMBP	1,12583591	THOP1	1,09763561	TUBA8	1,06858444	NDUFB8	1,25144731	3756	THTPA	1,04641467	P4HB	1,0639655	ETFA	1,11968268	MAP3K12	1,11109267	RNF19A	1,08577081	SERPINE2	1,05718341	UGT1A10	1,22517077
3687	FURIN	1,05403705	LY86	1,0750767	PITX2	1,1370597	ARSD	1,12575968	CPT1A	1,0975265	SOX9	1,06841549	CDX2	1,24917154	3757	CX3CR1	1,0464116	APH1A	1,06390098	HADHB	1,11959682	RAB1B	1,11095596	DSE	1,08512501	DIDO1	1,05715963	APOBEC2	1,22495647
3688	RAB1A	1,05398844	SOST	1,07496622	PAX5	1,13664732	ADCY8	1,12536163	ERAP1	1,09750103	STS	1,06831249	CISH	1,24844645	3758	IKZF2	1,04635031	FRS2	1,06384008	RAB6A	1,11916549	POLE	1,11066856	F11	1,08510737	PRDX4	1,05700987	NR2E1	1,22417532
3689	KLRK1	1,0537522	ALDH18A1	1,07490995	HDAC6	1,13658457	HLA-DPB1	1,12532248	CA9	1,09685952	BHMT	1,06818675	CA5B	1,24772515	3759	PITX2	1,04633096	FCN1	1,06376796	ACTR2	1,11886043	CIITA	1,11056578	KCNK1	1,08482468	C1QL2	1,0569881	PTPN2	1,22411905
3690	UBE2D2	1,05365255	ANGPTL6	1,07474144	MTNR1A	1,13621043	PPARD	1,12531081	B4GALT3	1,09630319	DUSP10	1,06793825	MUC1	1,24692399	3760	TRPM2	1,04621669	SLC1A3	1,0635475	CD97	1,11784747	FAH	1,10977379	LIMK1	1,08464255	PMM1	1,05691214	ENO1	1,22333875
3691	MYF6	1,05359075	ST8SIA1	1,07445555	ZBTB7A	1,13619052	CSNK2A2	1,12516239	CTSK	1,09598676	HLA-DPA1	1,06779186	TSNAX	1,24644419	3761	NR2C2	1,04611726	DTX4	1,06353403	PANK1	1,11771069	NES	1,10976476	XDH	1,08451415	GALNT11	1,05636067	CPEB1	1,22330131
3692	GHR	1,05355394	LDHA	1,07441694	CDK5R2	1,13605715	CYP46A1	1,12454249	MYL9	1,0959462	AR	1,06776469	SLC25A11	1,24550751	3762	AKT2	1,04604584	CDCA8	1,06345225	GP1BA	1,11732264	IKBKB	1,10963456	MKNK2	1,08436704	ARF1	1,0562452	MCF2	1,22322191
3693	MGP	1,05316552	GATA4	1,07424748	HRK	1,13587217	CDKN2B	1,12439355	NFKB2	1,09583825	DSE	1,06763465	MTNR1B	1,24458416	3763	EIF4EBP2	1,04596652	ABCA6	1,06337164	GRIN2D	1,11673298	IL27	1,10907955	HCLS1	1,0837797	NOS1	1,05619028	MAN1A1	1,22322048
3694	NAT6	1,05309791	UBE2L6	1,07422911	CYP27A1	1,13586201	ABCD1	1,12422544	IL2	1,0956512	EIF4A2	1,0676288	SFRS12IP1	1,24453274	3764	HSD17B3	1,04593307	POLE	1,06334443	UGT1A10	1,116208	IL16	1,10903231	NDST2	1,08354287	NSF	1,05615497	GRIN1	1,22291269
3695	SAA1	1,05301927	ST3GAL3	1,07409366	LMX1B	1,13565663	MAP1LC3B	1,12411994	TGDS	1,09524861	PRKAR1B	1,06739627	UBE2M	1,24436666	3765	AFMID	1,04564786	DGKA	1,06325121	RFXAP	1,11597305	SARM1	1,1084096	KLRK1	1,08342356	COL4A4	1,05600092	ARFGAP1	1,22268278
3696	ASAH1	1,05281444	ATP6V0B	1,07402404	ATP6V1D	1,13557646	CALML3	1,12398287	UCP3	1,0951786	GABRD	1,06723028	NEUROG3	1,24424685	3766	RFWD2	1,04560882	ACVR1B	1,06311449	DGKE	1,11584814	CD96	1,10786253	ADAM12	1,08325905	CHRM5	1,0559435	MEF2D	1,22268149
3697	AXIN2	1,05272589	LAP3	1,07400437	SULT1C2	1,13438421	NR2F1	1,12388909	DPYS	1,09498419	MAGI2	1,06719015	NDUFS2	1,24309411	3767	ABCD3	1,04555897	MLC1	1,06307852	ATP2A1	1,11565454	DHXS8	1,10776661	LMNB1	1,08313833	GRM2	1,05558302	DNAJA3	1,22187155
3698	NME1	1,05267693	DIXDC1	1,07378436	UGT2B17	1,13433908	UGT2A3	1,1233201	ICOSLG	1,09492394	HIP2	1,06705114	RANBP1	1,24256325	3768	DNAJA1	1,0454085	CPSF4	1,06300404	FUT4	1,11536698	CDIPT	1,10752975	POMC	1,08221877	EN1	1,05538796	GBF1	1,22157411
3699	GANAB	1,05263219	CCND1	1,07367493	TANK	1,13409691	INHA	1,12306501	MSH3	1,09477661	CHST11	1,06686329	CYP11B2	1,24220465	3769	HCCS	1,04540189	PMAIP1	1,06295051	ABCA6	1,11511209	TUBG2	1,10746888	RFX4	1,08210794	NDST3	1,05523912	SENP2	1,22129843
3700	TBP	1,05258895	ATG12	1,07301755	SOX17	1,13396534	HOXD10	1,12304832	BGLAP	1,09469106	PDE6C	1,06678215	TUBG1	1,24195072	3770	RPA2	1,04538599	ADH7	1,06290874	MAFB	1,11504662	POLD4	1,10722414	SSR4	1,08195278	TNFSF9	1,05522641	KCNQ1	1,22083252
3701	HADH	1,05257065	BYSL	1,07275228	PIGQ	1,13394723	MYOD1	1,12296691	IL10RA	1,09455564	PINK1	1,06633722	HOXB6	1,24178536	3771	MAPT	1,04536824	ALOX5AP	1,06273213	AMY1C	1,11486751	SIX3	1,10719522	MINPP1	1,081357	ABCA13	1,05507558	AXIN1	1,22003979
3702	BCL2L14	1,05255453	GANC	1,07266624	DCK	1,13389858	POLR1C	1,12253384	NOS3	1,09450083	GTF2H5	1,06630985	CSE1L	1,24165959	3772	LRRC15	1,04485824	VIL2	1,0627118	NAGS	1,11481085	FDXR	1,10710044	EBI3	1,08063677	CYR61	1,05487569	GCLM	1,21990392
3703	LRP1	1,05241491	CYP1B1	1,07260762	EGR3	1,13381527	ABL2	1,12243622	CRHR2	1,09405553	ADHFE1	1,06604896	BLNK	1,24153226	3773	ABL1	1,04451603	SCARB1	1,06224714	DDO	1,11476565	CAPN3	1,10709072	ACTN2	1,0805608	CDO1	1,05477968	CCL4	1,21983309
3704	PLA2G12B	1,05226151	PIGL	1,07256926	BMP10	1,13381374	MEF2A	1,12231294	HSP90AB1	1,09403175	TLR2	1,06569408	CCL5	1,24123149	3774	OTC	1,04445202	SMARCD1	1,06220848	UHRF1	1,11465898	HSD17B7	1,10693358	GATA2	1,0804177	TMEM166	1,05450516	AGRN	1,21974025
3705	ESRRA	1,05220109	PSME3	1,0723929	ARPC1A	1,13328562	NUMB	1,12207516	CHEK2	1,09400835	SCG2	1,06552479	ABAT	1,24119828	3775	AGPAT4	1,04434261	APC2	1,06209696	DCLRE1C	1,11439836	DNAJB9	1,1068855	SSTR2	1,08035532	ALDH2	1,05411651	GRM3	1,21937945
3706	GDF1	1,05219514	OPRD1	1,0719183	MS4A1	1,13321934	PTPRJ	1,1218314	LBP	1,0939099	STX16	1,06536721	NDUFB4	1,24097803	3776	GABARAPL1	1,04421587	TXN2	1,06206554	PHKA1	1,11415214	PLA2G4A	1,10687615	HADHB	1,0801048	HLA-E	1,05407066	NFKBIB	1,21934529
3707	ALDH6A1	1,05210758	DNMT3A	1,0715267	STAT4	1,13310596	FGF1	1,12166711	CSNK1A1	1,09385371	ASAH3L	1,06497719	POLS	1,24085208	3777	ACTR3	1,04419534	OSBPL5	1,06195962	ARNTL	1,1139462	PIGF	1,1063865	PTK2B	1,07985684	JAK1	1,05331484	ALAD	1,21912507
3708	GADD45G	1,05156789	ENTPD4	1,07146176	KATNB1	1,13296367	CHAD	1,12162825	TCF15	1,09373533	ALG8	1,06492282	UBE2E1	1,24078323	3778	GLI4	1,04407901	SLC18A1	1,0617987	NUMB	1,11365183	MUSK	1,10588736	SNIP1	1,07971347	BAAT	1,05330022	IARS	1,2189262
3709	SERPING1	1,05134697	MAL	1,07125154	DPYS	1,13289305	CHUK	1,12157707	DUSP14	1,09365109	ALDH3B2	1,0648564	CD1C	1,23997643	3779	TIRAP	1,04379312	PDHA2	1,06174984	IFNG	1,11361493	TYK2	1,10541623	ITGA6	1,07968115	CDS1	1,05319438	MBD4	1,21888152
3710	NTRK2	1,05124193	CSAD	1,07078151	IFNA1	1,13273654	APAF1	1,12155177	GLUD2	1,09360455	PROZ	1,06453147	DLG7	1,23940776	3780	GRID2	1,04369166	TXNRD2	1,06143999	ZBTB20	1,11360414	TUBE1	1,10510091	PDIA3	1,07938744	SFRS12	1,05312622	PRB1	1,21876581

Table A4. Pooled-shRNA library screen on HEL cell line and MF-3: list of 2nd most depleted shRNAs for each experiment (ranking approach 1, RA1).

	NO ruxolitinib (setting 1)				Ruxolitinib (setting 2)				Ruxolitinib + CM (setting 3)				MF-3				NO ruxolitinib (setting 1)				Ruxolitinib (setting 2)				Ruxolitinib + CM (setting 3)				MF-3	
	Experiment 1		Experiment 2		Experiment 1		Experiment 2		Experiment 1		Experiment 2						Experiment 1		Experiment 2		Experiment 1		Experiment 2		Experiment 1		Experiment 2			
Rank	Gene	Fold change	Gene	Fold change	Gene	Fold change	Gene	Fold change	Gene	Fold change	Gene	Fold change	Gene	Fold change	Rank	Gene	Fold change	Gene	Fold change	Gene	Fold change	Gene	Fold change	Gene	Fold change	Gene	Fold change	Gene	Fold change
3781	BTRC	1,04358161	DRD3	1,06129844	DMGDH	1,11352024	SUMO3	1,10499595	SCN7A	1,07908838	HSD17B12	1,05308243	NEIL2	1,21797555	3851	DAG1	1,03538645	MAPK14	1,04827771	ELAVL1	1,09406974	DUSP14	1,09104447	MAML1	1,06675368	POLR3H	1,04029162	TUBA8	1,197214
3782	BDH2	1,04340438	SLPI	1,06117281	GPR37	1,11300665	NDUFA1	1,10498862	DPP4	1,07895019	DAPP1	1,05282057	MAT1A	1,21756168	3852	CA14	1,03534835	EPRS	1,04792423	PIGW	1,09394949	CCL11	1,09089177	EMR1	1,06635947	UVRAG	1,04015296	NDUFV2	1,19631314
3783	IL17A	1,04322153	ERBB4	1,06064965	HNF4A	1,11297268	EIF3H	1,10491947	BMP8A	1,07875241	BRCA1	1,05274841	MCM3	1,21745325	3853	HNMT	1,0351274	TNFRSF9	1,04767276	HBB	1,09381433	ERCC4	1,09074033	MAPKAPK3	1,06628861	AVP	1,04007062	LAT2	1,19606553
3784	HTR3D	1,0432137	GAD2	1,06048103	NSUN2	1,11266284	AKR1B10	1,10487168	PINX1	1,07839692	DDX1	1,05222058	FZR1	1,21734785	3854	MAFF	1,03501499	CD34	1,04684391	SH3GL2	1,09350933	ASMT	1,09069393	NEU1	1,0658498	WFS1	1,03993226	IL12RB1	1,19530547
3785	ATP8A1	1,04311979	HSD3B7	1,06035553	APBA3	1,11128313	CTNNA2	1,10482953	CLN3	1,07827707	CBLC	1,05206939	MPI	1,21722204	3855	TP53	1,03490841	SFRP1	1,04635966	HLCS	1,09345941	NMI	1,09066258	PLA2G4D	1,06583473	TRAF5	1,03991269	KLRC4	1,19505223
3786	CP	1,04299851	COQ3	1,06035218	PPARD	1,11116114	BCL7A	1,10445839	NR2E1	1,0782144	GLI4	1,05206326	PPP2R5C	1,21664643	3856	MTTP	1,03481147	TNKS	1,04634403	ARFGAP3	1,0933928	PDE8B	1,09034518	TBL1X	1,06574273	GPR81	1,03966572	SNAP29	1,19489552
3787	PSME3	1,04290843	DDX55	1,0603452	PRMT1	1,11082736	LCP2	1,1040481	SDC2	1,07813043	CFHR2	1,05205888	EIF3H	1,21657135	3857	PLA2G12A	1,03409925	MVP	1,04604046	CCL5	1,09331528	CD53	1,09021026	NPR1	1,06551634	CCKBR	1,03963614	SNAP25	1,19355694
3788	FANCC	1,04272721	PPAT	1,06028544	CX3CL1	1,11041649	CPT1A	1,10398316	CCR10	1,07798516	CHRNA1	1,052043	INS	1,21616009	3858	ADSL	1,03407093	CYP11A1	1,04597369	PIP3-E	1,09260169	GSTP1	1,08994892	CA3	1,06551339	ITGA4	1,03929931	BHLHB8	1,19349286
3789	INSIG2	1,04263899	BMP1	1,06023752	CACNA1A	1,11013337	GPX2	1,10396479	TCOF1	1,0777054	ABCA3	1,05198649	FVT1	1,2158054	3859	SDS	1,03400696	ELA1	1,04592136	SELE	1,09248672	INPPL1	1,08976788	CHRNB1	1,06538815	P4HB	1,03926133	PSCD1	1,19280196
3790	PRKRIR	1,04259546	RELN	1,06019209	HBXIP	1,1101086	TLX1	1,10392447	ENTPD4	1,07769977	GAS2	1,0519762	BAG3	1,21507464	3860	HIP1	1,03390501	POMC	1,04586171	MRPL19	1,09240119	HSPA8	1,0897425	TP73	1,06514497	SYP	1,03875572	MUSK	1,1923526
3791	ABCB10	1,04217542	UGT8	1,05990397	AGRP	1,10876446	HADHA	1,10376829	KLRA1	1,07752904	POLB	1,05196872	FSCN3	1,21491792	3861	MYST4	1,03373763	TLX3	1,04572237	CCL28	1,09192233	PRDX1	1,08950993	DARS2	1,06510594	FRS2	1,03862346	BBC3	1,19227046
3792	PINX1	1,04211902	CDKL1	1,05987547	IKBKAP	1,10863577	TSC1	1,10371045	B3GAT1	1,07718907	RELN	1,05196334	WNT7B	1,21448093	3862	CHMP1B	1,0335321	TAP2	1,04569467	XPC	1,0915245	NKX6-1	1,08946359	CNR2	1,06465051	DTX1	1,03852657	ATP1B1	1,19158849
3793	CD3E	1,0420328	HYAL4	1,05958037	CYP3A4	1,10843553	ASAH1	1,10358287	COL11A1	1,07693611	CCNI	1,05194973	GPRC5B	1,21437487	3863	TNFSF13B	1,03348748	DFFA	1,04557984	STX10	1,09101137	PSMB8	1,08899299	RDH11	1,06454736	GATA3	1,03846964	CYP11A1	1,19125242
3794	BAAT	1,0419572	CASP8	1,05937277	CCL7	1,10810258	ADIPOQ	1,10355471	EDNRB	1,07690174	IRAK3	1,05192329	MMS19L	1,21419963	3864	SPRY3	1,033331	NAGS	1,04554568	CYP3A5	1,09093476	GPSN2	1,08877471	CREB1	1,06452704	DUSP6	1,0383004	GLA	1,19100874
3795	ERCC1	1,04189066	HS3ST5	1,05897278	RHEB	1,10775295	SNX1	1,10340313	SETDB1	1,07661727	CABIN1	1,05091871	STRAP	1,21408953	3865	ERAP1	1,03327052	FGF8	1,04538073	RAB23	1,09089792	TLR8	1,08825571	CSNK1D	1,06447562	GCLM	1,03823343	CES7	1,19072769
3796	RDM1	1,04183922	NOX4	1,05889994	DBN1	1,10635875	RTN4R	1,10301976	ID4	1,07660413	SLC16A3	1,05058159	GOLGA2	1,21353021	3866	GAS2	1,03317427	FOXO3	1,04528719	HMGCS1	1,09057435	PINX1	1,0881689	ACHE	1,06416102	ELK3	1,03805462	CASP9	1,19061584
3797	G3BP2	1,04181331	HS2ST1	1,05882969	PIF1	1,10631858	CYP24A1	1,10287894	MAOB	1,07659347	HBA2	1,0505104	SPO11	1,21206737	3867	ATP2B2	1,03314705	PRKCZ	1,04522592	TYMS	1,09056788	TRH	1,08813899	APOBEC3G	1,06368627	HLA-DOA	1,03792385	FCGR3A	1,18987923
3798	WNT9B	1,04181331	PAPSS1	1,05872896	STAT2	1,10631858	ENO2	1,10240194	CD86	1,07649226	ADRA1D	1,05031754	ISYNA1	1,2115612	3868	CKMT2	1,03307994	CLCA1	1,04488359	FTCD	1,09052766	ABCB11	1,08811846	EPHX2	1,06328	TCIRG1	1,03784237	CYP4B1	1,18971796
3799	APC2	1,04172829	SCN1B	1,05862411	BMP3	1,10612196	MAPKAPK3	1,1022278	NPTX1	1,0761678	MAP3K10	1,05002095	GPR34	1,21155489	3869	ABCD1	1,03293229	VARS2	1,04461438	DDX51	1,09002925	CPSF3	1,08800094	AGRN	1,06324496	ARNT2	1,03784049	OSBPL1A	1,18968241
3800	PHF11	1,04170995	ID1	1,05851614	CACYBP	1,10601043	CTBP1	1,10199245	FABP5	1,07610039	AKT2	1,04998234	APOD	1,21144798	3870	ADAM8	1,03292232	PDHB	1,04461097	NDEL1	1,0899965	EEA1	1,08781805	F2RL1	1,06291944	RAP1B	1,03771876	SUCLG2	1,18947622
3801	P2RY6	1,04134865	TLK1	1,05848198	MYBPC2	1,10558989	TXN2	1,10112973	PEG3	1,07592658	DNMBP	1,04993337	RARA	1,21141754	3871	KCNMB2	1,03270791	MAOB	1,04456315	HS3ST1	1,08979376	NUDC	1,08773713	BHLHB8	1,06213549	GRWD1	1,0369784	TAPBP	1,1892676
3802	SPRED2	1,04131494	SMURF2	1,05845873	DACT1	1,10554332	SOX10	1,10111875	NEUROG1	1,07497576	WNT2	1,049728	CARM1	1,21024045	3872	DCXR	1,03269237	ASPA	1,0443627	AKR1B10	1,0894544	TNFRSF11A	1,08684916	MAPK12	1,06202344	INHBA	1,03679758	HSPG2	1,18916123
3803	TOP2B	1,04128741	REV1	1,05821234	RAP1GAP	1,10543468	CYP2C8	1,10110669	ATN1	1,07481006	GMNN	1,04947336	BAI1	1,21012986	3873	CALM3	1,03264219	GALNTL1	1,04412723	CDR1	1,08938456	BAG3	1,0862978	LIG4	1,06181275	RECQL4	1,03668103	GNMT	1,18894751
3804	SDHC	1,0411435	RAB7A	1,05782223	APH1A	1,10518363	TUBB2C	1,10089786	GALNT14	1,07467782	GNA12	1,04913756	CSF1	1,20974213	3874	PINK1	1,03257658	IL8	1,0440551	ATF4	1,08897063	GRIN2A	1,08621007	NDUFA1	1,06157277	PDE11A	1,03665483	TPH1	1,18881527
3805	MSH5	1,04072854	GLI4	1,05772178	C8G	1,1049821	IMPA1	1,10084514	CASP10	1,0746457	VKORC1	1,04878339	TIMP4	1,20968996	3875	GCNT2	1,03239815	MAN1B1	1,0440345	ITGAE	1,08878179	NTHL1	1,08601035	HOXD10	1,06152205	COL4A1	1,03661203	EME1	1,18850587
3806	ADRBK2	1,04061488	MKNK1	1,05759041	NAGLU	1,10489181	ACVR1C	1,10029181	TNFRSF4	1,07453804	GTF2A2	1,04866681	WNT1	1,20943332	3876	DDX1	1,03229926	DUSP9	1,04381921	LITAF	1,08842971	ITGA2	1,08583409	GABRA1	1,06132312	FSHB	1,03653012	CLYBL	1,1879375
3807	TNFSF18	1,04051213	KRT7	1,05740509	CTSK	1,10459826	IRF5	1,10010553	DNAJA2	1,07426635	FLT3LG	1,04858199	CAPN1	1,20936203	3877	CA4	1,03225039	DCXR	1,0437653	TSC1	1,08837843	ANGPTL2	1,08566257	SSTR5	1,06121243	CLCN7	1,03626624	ACADM	1,18730819
3808	APOC1	1,04040276	ORC3L	1,05724895	TCF7L2	1,10450652	EGF	1,09973824	GLRX	1,07405771	INPPL1	1,04841008	PCYT1B	1,20907716	3878	ADRA1D	1,03224467	CLTCL1	1,04343074	CREB1	1,08832429	CCR2	1,08533615	ALG3	1,06120178	NFYC	1,03610406	CD52	1,18724051
3809	GMNN	1,04035657	NDUFB11	1,05714742	ST3GAL6	1,10425417	BMP4	1,09940519	ST6GALNAC5	1,07397927	PGLYRP2	1,04835264	HK3	1,20904404	3879	ATF5	1,03220745	ANKHD1	1,04313246	GRM2	1,08815664	ADCY9	1,08533492	ERBB4	1,06078083	MERTK	1,03606305	APH1B	1,1864333
3810	MYL3	1,04019669	GLRX2	1,05710696	ENPP2	1,10421376	EIF2B5	1,09851293	ADCY5	1,07388212	IL1RL1	1,04802836	ATP6V1G1	1,20890418	3880	ALG8	1,03212652	IRX3	1,04312362	CLCA1	1,08797171	FN1	1,0849501	DGAT1	1,06077537	B4GALT3	1,03575054	RNASE1	1,18639859
3811	ALCAM	1,03987167	TUBD1	1,05667118	DAZL	1,10416588	KLRA1	1,09823931	RFWD2	1,07382527	LIMK1	1,04787153	NFKBIE	1,20857423	3881	TH	1,03212441	PLA2G4B	1,04291376	CHST13	1,08795034	INSR	1,08466071	EXT1	1,0604763	PIGH	1,03524374	GNA12	1,18630647
3812	IL17RB	1,0397876	DHRS7	1,05533033	YAP1	1,10412486	BLNK	1,09814872	QPCT	1,07382024	PIGS	1,04775279	SHBG	1,20857423	3882	DUSP4	1,03206741	CDKN1A	1,0424784	P2RY6	1,08788408	MAPK12	1,08427132	ANP32A	1,06021414	UGT1A8	1,03523149	CACYBP	1,18564366
3813	DPPA5	1,03951937	OGFR	1,05514042	TPH2	1,10387489	KIAA1303	1,09802548	GLO1	1,07379923	CD99	1,04755087	CHRNA5	1,20846867	3883	CACNA1E	1,03201851	HAGH	1,04241294	B3GALT2	1,08766914	TNFRSF8	1,08389293	FANCA	1,05998459	PTX3	1,03500228	IFNA8	1,18532625
3814	UBE2A	1,03951529	UBE2N	1,05512756	MTR	1,10263331	KLK6	1,09799254	STX11	1,07379833	ARF3	1,04747502	MECP2	1,20835463	3884	CASP9	1,03197492	PIGG	1,04238584	FURIN	1,08710913	NOS2A	1,08384449	CA6	1,05977473	LY86	1,03482508	CAT	1,18517577
3815	SLC6A4	1,03934114	BNIP2	1,05512357	CHIA	1,10242355	SSTR2	1,09773456	C4A	1,07375374	PYGB	1,04722863	OPRK1	1,20759058	3885	GTF2E1	1,03194098	SLC32A1	1,04238029	TGFB1I1	1,08702474	ADCY5	1,08362929	SRF	1,05892832	PPP1R1B	1,0347537	FZD9	1,1846853
3816	MGAT4A	1,03928564	DKK1	1,0549865	BTD	1,10235301	MEFV	1,09765908	RAD52	1,07367079	PIK3CA	1,04704545	NEU4	1,20731341	3886	SFRP4	1,03193787	SH3BGRL	1,04196607	HSD17B10	1,08659266	YARS2	1,08321186	DIAPH2	1,05882734	KCNQ2	1,0346468	ALDOA	1,18450412
3817	FANCA	1,03926755	COL7A1	1,05491866	ITPA	1,10199042	GPR37	1,09722543	E2F3	1,07343092	IREB2	1,04676645	USP9X	1,20639898	3887	FPR1	1,03178442	EXTL2	1,04188116	APOD	1,08655785	PPIE	1,08316601	COPS5	1,05874845	GHRL	1,03446191	CRLS1	1,18376814
3818	LALBA	1,03923724	GAST	1,05482216	SCLY	1,10146705	MITF	1,09716233	HFE	1,0733928	TP73	1,04666918	NDUFB7	1,20632109	3888	GHRHR	1,031728	TKTL1	1,0418339	TBXA2R	1,08646388	HTR1A	1,0827614	GCH1	1,05871983	LYN	1,03431571	RFC5	1,18368051
3819	NPPB	1,03892403	SALL1	1,05479872	FANCA	1,10145574	CLN3	1,09705258	PDE2A	1,07315304	IRAK1	1,04665451	DGKG	1,20614556	3889	FLT3LG	1,03155791	GC	1,04127571	FOXP3	1,08584507	LTA	1,08242569	SIRT6	1,05849745	AMY1C	1,03418331	CLCN7	1,18365944
3820	E2F2	1,03873757	TOP3B	1,05452722	AFP	1,1008847	OXTR	1,09669551	HSPA1B	1,07271113	SDC2	1,0464403	GNRHR	1,20592435	3890	IL10RA	1,03152913	ATP2B2	1,04089895	LTF	1,08565443	CYP1B1	1,08234708	CFB	1,05832969	LAP3	1,03396317	CRHBP	1,18269529
3821	CXCR4	1,03870818	ADSL	1,0541647	CDX1	1,10075414	UBE2N	1,09646388	BET1L	1,07269028	SDS	1,04628898	CD24	1,20552904	3891	IL4	1,03148522	DTX2	1,04084018	HSPG2	1,0856011	GDF1	1,08213375	CYP3A43	1,05805577	ARHGEF1	1,03355453	DUSP9	1,18222239
3822	NDRG2	1,03870423	IL17RD	1,05414777	SLAMF1	1,1006743	ATP8A1	1,09646169	CSTF2	1,0723554	DHFR	1,04600138	PLA1A	1,20542545	3892	CFL2	1,03128454	ANK2	1,04078626	DKK2	1,08550943	TRIM25	1,08200223	SERPINB5	1,05793412	SLC1A1	1,03344709	CYP3A4	1,18215107
3823	NOD1	1,03825838	ALDH3A2	1,05407068	AMOTL1	1,10035031	MNAT1	1,09634757	IL5	1,07232021	ATP5O	1,04588875	ADORA2B	1,20507016	3893	CD53	1,03072314	POU2F2	1,04059497	MAN1B1	1,08481126	SP100	1,08091377	RGS1	1,05790981	ABCC1	1,03344572	TXNRD2	1,18204722
3824	IL1B	1,03810591	CACNA1D	1,05405973	SALL4	1,09985568	EDNRB	1,09604258	PIWIL1	1,07210211	RING1	1,04576177	TRPM7	1,20496794	3894	ADIPOR1	1,03071535	RAB24	1,04046478	MNAT1	1,08449277	GPT	1,07992313	PYCARD	1,05767751	NRG2	1,03335896	FUT5	1,18169611
3825	BRS3	1,03806143	NANOS1	1,05402117	DTX2	1,09984933	OLIG2	1,09560475	MAPT	1,0717305	ABCC4	1,04550085	CARTPT	1,20494612	3895	MAFB	1,03067938	IFI30	1,04037717	CD96	1,08430059	IL8	1,07972016	MRE11A	1,05749121	ALG12	1,03333138	ANAPC4	1,18169413
3826	ANGPTL4	1,03802955	CCL22	1,05399873	ERCC1	1,0997764	PML	1,09551958	HRK	1,07170388	NTRK2	1,04506462	P2RY2	1,20493844	3896	BHLHB9	1,0299774	RUNX2	1,04029928	OGG1	1,0840818	CES2	1,07960562	NR5A1	1,05739183	MAPK12	1,0332144	APPL1	1,18146622
3827	CNTFR	1,03798549	IL25	1,05346034	TTR	1,09944544	CLDN16	1,09544411	WNT6	1,07168699	HSD17B7	1,0449738	EFNB2	1,20488474	3897	PSAP	1,02974949	MSH4	1,04020191	ENDOG	1,08401659	PRODH	1,07947652	EIF4A2	1,05738223	IL9	1,03304551	CFI	1,18137114
3828	NDEL1	1,03767793	TIRAP	1,05281127	HIBCH	1,09932059	EI24	1,0950935	DPPA5	1,07113461	CHST14	1,04485875	POLG2	1,20471023	3898	ANXA6	1,02959302	ARAF	1,03983356	GTF3C3	1,0839051	DTX1	1,07914356	COL4A4	1,05735212	ABCA5	1,03279742	IL2RG	1,18121025
3829	PDE8B	1,03741339	PDE6C	1,05261642	IL3	1,09929493	THPO	1,09447059	APCS	1,07105765	SRM	1,04484871	APH1A	1,20425713	3899	CD28	1,02949617	FANCC	1,03975708	GNAI1	1,08369427	DOT1L	1,07875008	CD28	1,05717338	HS2ST1	1,03277426	CD8A	1,1808994
3830	HOXB4	1,03724998	MITF	1,05257628	DDX55	1,09899092	AMPD3	1,09434655	REXO2	1,07099253	RNF25	1,04429127	CNDP1	1,20370114	3900	KDELR1	1,02940614	IRF2	1,03973217	AP3M1	1,08367676	HTR1F	1,07801398	TAGLN2	1,05712127	LSS	1,0325113	SCARB1	1,18068948
3831	CAMP	1,03717808	TRIM25	1,052571	CIITA	1,09898679	AKR1D1	1,09432523	HDAC2	1,07094489	RAP1GAP	1,04426211	GDF1	1,20324335	3901	CD6	1,02907393	HIF1A	1,0397146	DPPA4	1,08330146	CUL1	1,07727764	HSD17B8	1,05650211	CSNK1G2	1,03234425	INHBC	1,18068157
3832	ATP1A2	1,03714736	CD7	1,0525312	ATG9B	1,09891819	COL1A2	1,09431418	ARHGAP6	1,07090563	PRKCB1	1,04413559	HTR1F	1,20274568	3902	H2AFY2	1,02903825	CDC25B	1,03965157	PGM3	1,08306586	ANKHD1	1,07709171	MDC1	1,05645152	HPCAL1	1,03233337	GH1	1,18058871
3833	CRYAB	1,03713299	MR1	1,05233957	GHR	1,09870189	HEY1	1,09414235	RSAD2	1,07033982	MAP3K7IP1	1,04389305	WARS	1,20268618	3903	CD7	1,02899266	GGH	1,03950682	PMS2L3	1,08275299	S100A4	1,07708778	CYBA	1,05643241	USH1C	1,03221093	TNFAIP6	1,18026119
3834	DOT1L	1,03703955	DOCK9	1,05221458	FGFR2	1,09852961	UTF1	1,093865	AMH	1,07030504	GLI3	1,04382839	XRCC6	1,20232957	3904	NANOG	1,0286397	IAPP	1,03931042	BTC	1,08272492	PDHB	1,07648764	BYSL	1,05636095	B3GNT7	1,03217768	CD3D	1,17972838
3835	PAN2	1,03702384	S100A6	1,05196601	TAP1	1,09817331	AZGP1	1,09335591	ADH4	1,07016999	NOG	1,04374131	INPP4B	1,20207201	3905	TLN1	1,02861646	MAP1A	1,03920215	CLDN14	1,08245597	CCR3	1,07535336	SOD1	1,05629549	RAD1	1,03198773	CACNA2D4	1,1794902
3836	PTHR1	1,03695396	CFHR1	1,05169933	S100A4	1,09807074	NCF2	1,09321279	ASIP	1,06990693	ANP32E	1,04364642	GGPS1	1,20195659	3906	NANOS1	1,02847609	FLT1	1,03901104	SLC30A6	1,08240374	FGF10	1,07474082	PIGF	1,05621552	TREM1	1,03182196	ARHGEF1	1,17943571
3837	GIP	1,03676465	GLUD1	1,05144457	VEGFC	1,09704284	F10	1,09293312	SOX4	1,06969033	HCCS	1,04330017	LY9	1,2018945	3907	ARHGEF7	1,02800457	CLDN17	1,03894035	AGPAT4	1,08228163	APLP2	1,07463396	BRD4	1,05611867	ESRRA	1,03181045	BCAT2	1,17924421
3838	CD69	1,03627656	FZD6	1,05054693	CYBA	1,09672547	GRM2	1,09272368	GRK4	1,06908601	DEDD2	1,04316897	RELB	1,20161099	3908	SLC34A1	1,02798348	UGT1A10	1,03885568	FGR	1,08223654	KCNJ12	1,07444688	ABCA5	1,0560684	CCND2	1,03179649	SLC30A1	1,17911518
3839	GRN	1,0362468	ADRB1	1,05039817	ADAMTS13	1,09650967	DDX55	1,09259478	ATP5D	1,0687644	ELK4	1,04315644	FBP2	1,20158367	3909	HSD17B10	1,02788548	SARM1	1,03881732	EEF2K	1,0820315	LRRK1	1,07432225	DISC1	1,05590301	UBE2N	1,03149062	BAG1	1,17859834
3840	PADI2	1,03618232	GJD2	1,05032599	H6PD	1,09639149	CEP290	1,09242814	TBXAS1	1,06872175	IMPDH2	1,04271155	MCRS1	1,2013114	3910	CD80	1,02772693	GP6	1,03864388	NOX1	1,08156422	ARF3	1,07421652	TRAF2	1,05523984	CLC	1,03140759	ARHGDIB	1,17852082
3841	HOXA13	1,03598621	RAB23	1,05010413	ERCC4	1,09621159	SERPINI1	1,09209812	ATP13A2	1,06867844	TFDP2	1,04252995	ORM1	1,20127137	3911	GALNTL2	1,02757189	AGTR1	1,03861748	POLR1B	1,08135292	CASP8AP2	1,07406449	DDX55	1,05522509	UGT2B28	1,03131994	GABARAPL1	1,178502
3842	ACVR2A	1,03593761	FBXW11	1,05008326	SMURF2	1,09608552	MYL3	1,09208103	GSTA2	1,06856064	HTR3E	1,04244723	BET1L	1,20056278	3912	PFKL	1,02753686	SRD5A1	1,03834552	ADH1C	1,08123603	UCP1	1,07399407	SESN3	1,05486865	CAPN7	1,03130085	CALM1	1,17839765
3843	KCNIP3	1,0359068	LMO1	1,04963982	IL21	1,09603986	GNA15	1,0920515	IFNA4	1,06823445	HSPB1	1,04236679	C12ORF57	1,20046649	3913	RETNLB	1,02739189	FRAT2	1,03822979	OXCT1	1,08118953	COMT	1,07285756	AMY1A	1,05477383	BRS3	1,03120692	TERF2IP	1,17824107
3844	CADM1	1,03586744	RPA4	1,04961912	PYGL	1,09582723	CEBPA	1,09204467	ICAM5	1,06806195	APEX2	1,04172708	PAPPA	1,19996497	3914	S100A6	1,02710786	TP53BP2	1,03800389	EGFR	1,08068266	EZH2	1,07275751	SEMA3A	1,05475594	CYP2C8	1,03099176	ACAA2	1,17823341
3845	PPAP2C	1,035852	SMARCA4	1,04960709	TAP2	1,09566525	PPP3CB	1,0914159	IMPDH2	1,06805208	IFNA1	1,04124134	ELOVL5	1,1998903	3915	GHRL	1,02695857	BMP8B	1,03728331	GDF3	1,08068243	NKIRAS2	1,07209596	BAK1	1,05453723	PLAT	1,03090211	ATG12	1,17793547
3846	UROS	1,03555417	CLCF1	1,049398	APC	1,09554921	LEFTY2	1,09129573	IFT57	1,06799462	CD86	1,04070802	SELE	1,19983633	3916	MECP2	1,02686868	MYOG	1,03719109	CDKN2C	1,08062701	HDAC4	1,07203973	IKBKAP	1,0544646	ANXA3	1,03083343	ATP8A1	1,17760958
3847	PLCB1	1,03553712	LCMT2	1,04900626	IDH3B	1,09542238	KPNA3	1,09122697	CYP4A22	1,06778891	GTF2A1	1,0406629	MAPK3	1,19935862	3917	TXN2	1,02679002	CCNA1	1,03709226	FCGR3A	1,08014229	TRO	1,07184286	ILVBL	1,05441651	DRAM	1,03066494	HSD17B7	1,17760958
3848	CD244	1,03551949	HSD17B10	1,04890468	HSP90AB1	1,09447905	GABRG1	1,09119546	CSTF1	1,06761896	ABCG2	1,04063359	NMNAT2	1,1989649	3918	CNDP1	1,02678299	PRKAR1B	1,03665888	NFYC	1,08005294	ARF1	1,07149392	TUBB2A	1,05425147	GRAP2	1,03049528	NT5C	1,17757536
3849	LRRC41	1,03547653	SCSDL	1,04839108	AUH	1,09446826	SUMO1	1,09116891	MOBP	1,06754897	UBE2L3	1,04040265	FARSA	1,19874172	3919	HTATIP	1,02676361	GCS1	1,03647677	PAN2	1,07995148	SDHB	1,07113062	RFNG	1,05424339	KLC1	1,03015943	AKTIP	1,17717264
3850	GRHPR	1,03543158	SERPINA3	1,04835527	ALDOB	1,0943548	EPHB3	1,09107411	IFNE1	1,06722218	NFKBIL1	1,04030045	PER2	1,19727358	3920	RAD23A	1,02672365	DAZL	1,03643272	MMP2	1,07930213	CTNNBIP1	1,0711121	SRD5A1	1,05384111	SRD5A1	1,03006823	NDST2	1,17696781

Table A4. Pooled-shRNA library screen on HEL cell line and MF-3: list of 2nd most depleted shRNAs for each experiment (ranking approach 1, RA1).

	NO ruxolitinib (setting 1)				Ruxolitinib (setting 2)				Ruxolitinib + CM (setting 3)				MF-3			NO ruxolitinib (setting 1)				Ruxolitinib (setting 2)				Ruxolitinib + CM (setting 3)				MF-3	
	Experiment 1		Experiment 2		Experiment 1		Experiment 2		Experiment 1		Experiment 2					Experiment 1		Experiment 2		Experiment 1		Experiment 2		Experiment 1		Experiment 2			
Rank	*Gene*	*Fold change*	*Gene*	*Fold change*	*Gene*	*Fold change*	*Gene*	*Fold change*	*Gene*	*Fold change*	*Gene*	*Fold change*	*Gene*	*Fold change*	*Rank*	*Gene*	*Fold change*	*Gene*	*Fold change*	*Gene*	*Fold change*	*Gene*	*Fold change*	*Gene*	*Fold change*	*Gene*	*Fold change*	*Gene*	*Fold change*
3921	PHKA1	1,02669494	AKTIP	1,03629872	TRAF4	1,07925648	IGFBP1	1,07097978	SUMO1	1,05384111	EZH2	1,02988146	AUH	1,17661426	3991	ATP2A1	1,01905832	P2RY6	1,02532036	KLK2	1,06135028	ACCN1	1,05668148	DHRS1	1,04103293	PIGN	1,01889331	PSMD6	1,15402071
3922	LY75	1,02668916	KCNMB4	1,03627655	ALAS2	1,07867215	GNA12	1,07092626	ELOVL6	1,05382161	PTHR1	1,02980918	GSTA3	1,17648191	3992	SLC18A2	1,01902948	IFNA16	1,0253046	MDH1	1,06131006	LCT	1,05621872	MAD1L1	1,04076288	CDK5R2	1,01881639	GPRC5C	1,15401796
3923	ATP6V1G2	1,02648643	CHST12	1,03619304	APOC2	1,07861525	DRD2	1,07042363	ANGPT2	1,05358048	AVPR2	1,02927145	F2RL1	1,17616026	3993	BMP1	1,0188324	HDAC10	1,02529059	RAF1	1,06083674	EEF1B2	1,05604464	AASDHPPT	1,04006943	UGT1A5	1,01870652	FSHB	1,15382203
3924	PA2G4	1,02637868	BAG4	1,03612762	ATP5O	1,07775956	HDAC2	1,07012377	FANCF	1,05352613	FKBP1A	1,02897617	HOXA10	1,17607625	3994	MSH2	1,01881206	RERE	1,02513411	IFIT3	1,06081599	ADAMTS13	1,0552392	GHRHR	1,03985745	PIR	1,01802062	APPL2	1,15152876
3925	WNT4	1,02619184	DAB1	1,03604442	GCA	1,07758326	DHRS3	1,06945908	SOX17	1,05339005	OLIG2	1,02884162	HEY1	1,17560162	3995	DDC	1,01863581	HPGD	1,02507751	RAP1B	1,0606634	EFNA5	1,05496745	ZFYVE16	1,03970429	CD180	1,01801189	C4A	1,15056691
3926	CALCA	1,0260746	ATG9B	1,03576972	MRE11A	1,07743324	ACVR1B	1,06914711	PI3	1,05338294	MCPH1	1,02879529	CDKN2A	1,17487711	3996	CTSL2	1,01837614	CA3	1,02501676	PAXIP1	1,06050042	MECR	1,05475333	GLA	1,03964001	GRB10	1,01765647	ME3	1,15044098
3927	FLJ21865	1,02581748	TFDP1	1,03535945	SIRPA	1,07707946	EDN3	1,06910643	PPT2	1,05327578	SLC1A7	1,02862224	AKR1B10	1,17486996	3997	ME3	1,01812082	CASP9	1,02479916	APEX1	1,06038858	FCGR1A	1,05473833	ARHGEF6	1,03940915	C3AR1	1,01748753	ABCG2	1,15043541
3928	CDK5	1,02564247	COL2A1	1,03530939	ERBB4	1,0770059	COL19A1	1,06874894	NR0B2	1,05288769	ETS2	1,02826882	FRAP1	1,17456426	3998	STX6	1,01801461	IVD	1,02458863	PLEKHA8	1,05988965	RFXAP	1,05469546	COASY	1,03933149	CD1E	1,01742414	DHRS2	1,15016783
3929	DHH	1,02558423	NPPB	1,03529158	ABCA10	1,07687295	PDE11A	1,06842247	EPHA2	1,05279549	FLCN	1,02823381	PRKAR1A	1,17373258	3999	FRAP1	1,01792218	IFIT1	1,02454216	TLX1	1,0597385	FPGS	1,05464999	ME3	1,03912308	APBA3	1,01715469	POLR3G	1,14993815
3930	CDC25B	1,02556901	ERCC1	1,03482257	KMO	1,07641644	CD1B	1,06835782	UTF1	1,05278325	CBR3	1,02812672	CYP8B1	1,17370017	4000	CCKBR	1,01791996	BHLHB9	1,024539	GJB1	1,05963823	ETV7	1,05454637	CALCR	1,03912066	ECSIT	1,01698351	C1S	1,14978684
3931	COL11A1	1,02551538	COL15A1	1,03476252	SCN3B	1,07613957	MUTYH	1,06790776	SSTR1	1,05218477	UAP1	1,02787438	SET	1,17350849	4001	SNIP1	1,0178554	CD6	1,02450414	TFAP2A	1,05939894	SQLE	1,05441347	RIPK1	1,03898209	RPN2	1,01650732	ACSS2	1,14952733
3932	CLCF1	1,02510589	HPRT1	1,03467654	CHRM4	1,07604733	GRM6	1,06784455	ASGR2	1,05169339	FABP3	1,02742961	C1QL2	1,17321406	4002	SLPI	1,01757142	MSH3	1,02447797	P2RX7	1,05938278	GABRA1	1,05413516	ZEB2	1,03868212	MAL	1,01648691	TUBB2A	1,14900915
3933	GCA	1,02509444	AGPAT1	1,03458861	CD14	1,07554015	TNFSF18	1,06783221	CTSS	1,05168883	LTBR	1,02740663	JAZF1	1,17302074	4003	IHH	1,01740662	ETFA	1,02436486	NDUFB8	1,05935117	GNAT1	1,05411172	SEMA4A	1,03867112	GDI1	1,01639795	PLA2G2A	1,1488708
3934	UGT2B11	1,02470778	CHST2	1,03432349	CHKA	1,07500374	PNLIP	1,0674594	OPRK1	1,05130235	APOBEC3G	1,02728812	XYLT1	1,17279856	4004	PAFAH1B2	1,01732807	EDN3	1,02393719	APOBEC2	1,05846482	FRAP1	1,0540938	CDK5R1	1,03865574	PUM1	1,01633047	COL4A1	1,14847186
3935	GPR34	1,02453107	MAP2K3	1,03419536	CHEK1	1,07490366	SMARCD1	1,06741743	CHAD	1,0511527	EPX	1,0272811	PIWIL2	1,1722758	4005	COL1A1	1,01724721	PDCD1	1,02378548	UGT2A1	1,05833265	DUOX1	1,05395788	HS2ST1	1,03852841	PTK2B	1,01629485	OLIG1	1,14836428
3936	GSTM3	1,02442135	PDE4C	1,03414038	GBA	1,07460553	UBE2V1	1,06721916	GNA12	1,05109144	HPGD	1,02726639	GABRG2	1,17158848	4006	IFNG	1,01716358	PARP4	1,02373871	ALDH4A1	1,05757449	FANCB	1,05393843	ALAS2	1,03849675	LRWD1	1,01623393	ATF3	1,14789123
3937	GP1BA	1,02436031	PIGB	1,03408939	ADH6	1,07459431	APOBEC2	1,0668315	SYP	1,05066382	MCM6	1,02686194	GRASP	1,1709248	4007	MTR	1,01656781	MYD88	1,02371992	SIRT1	1,05724412	UNC93B1	1,05383829	GALNT4	1,03825555	PDE2A	1,01611327	BMP15	1,14759303
3938	TNFAIP6	1,02427249	HMGB2	1,03354392	CKB	1,0745665	DCXR	1,06674265	NDUFA12	1,05053099	ADORA3	1,02677529	AOC2	1,17035545	4008	CNP	1,01644516	CA13	1,02366412	GPRC5B	1,05708661	ALDH1A1	1,05352472	GC	1,03803419	RNF2	1,01610751	ABLIM1	1,1475201
3939	BTD	1,0239844	EIF4A2	1,03353852	SIN3B	1,07356599	ALDH3B2	1,06569581	CDK8	1,05045055	SULT1C2	1,02667082	H2AFX	1,17021629	4009	FOXH1	1,01632083	CHRM5	1,02362265	TFDP1	1,05706382	FOXK1	1,05334892	INPP5D	1,03768878	MAPKAPK3	1,01582768	PSMD11	1,14731723
3940	CBR3	1,02396543	WASF1	1,03349643	CSTF1	1,07353195	TNFRSF4	1,06565726	POLE4	1,05037098	ATP1B2	1,02666782	PKM2	1,16959511	4010	ITGB7	1,01617199	MDM2	1,02349124	HTR3D	1,05668408	CCR4	1,05285636	HRH2	1,03766935	PIP3-E	1,01528082	EHMT1	1,14552928
3941	PROS1	1,02394279	RAD54B	1,03322447	ALG11	1,07311934	DPEP1	1,06563047	OSBP	1,05011918	CYP2C18	1,02659982	FRS2	1,16909519	4011	NPM1	1,01598942	GPRC5A	1,02340752	PINK1	1,05665611	ADH1A	1,05272988	ITM2B	1,03674112	CYP19A1	1,01485408	PHCA	1,14508087
3942	NFYC	1,02377145	MAP1B	1,03315678	MAP3K9	1,07301287	LRPAP1	1,06553379	MAS1	1,05002629	KLRC3	1,02653567	PAK6	1,16903126	4012	EEF1B2	1,01571302	AGK	1,02339258	COL15A1	1,05660467	NEFL	1,05220695	CALM3	1,03642374	GSTT1	1,01478631	ST3GAL2	1,14473509
3943	GDF6	1,02377134	GJA4	1,03290413	POLD1	1,07287293	NDUFA8	1,06542319	NCOR2	1,04966779	GUSB	1,02633594	IREB2	1,16840922	4013	CALCR	1,01561801	VAV3	1,02332183	CPT1A	1,05651933	ANAPC11	1,05210746	SLC25A1	1,03618528	BCL7A	1,01477918	VAV1	1,14446745
3944	GRIN2C	1,02371751	NLRP2	1,03258318	MAP2K4	1,07280262	UNC5CL	1,06534464	ATP4A	1,04962716	VNN2	1,02618039	LALBA	1,168364	4014	SULT1A1	1,0155655	SPI1	1,02321112	SOST	1,05647598	CD86	1,05138729	CPE	1,03614152	PPCDC	1,0144214	RDH11	1,14433584
3945	PDE6C	1,02359293	CUZD1	1,03237291	BCL2L14	1,07268053	GUCA1B	1,06510455	CALML5	1,04942007	MMP3	1,02609159	SESN3	1,16818641	4015	TSNAX	1,01516427	IFNA21	1,02294423	POLI	1,05574828	ATP6V1E1	1,05129014	TBL1XR1	1,03592997	ALDH18A1	1,0144131	FDXR	1,1443114
3946	AZI2	1,02348022	MAP3K12	1,03224176	KLRC3	1,0725031	OLIG1	1,06444365	A4GNT	1,04928662	PPIC	1,02606007	IRF2	1,16779169	4016	FCGR3B	1,01498922	TBX1	1,02291974	BBS4	1,05526994	CTSK	1,05127605	AKAP4	1,03565053	AGT	1,0143787	CFLAR	1,14426752
3947	C5	1,02340631	PAPSS2	1,0321862	ATP8A1	1,07194748	SCN1B	1,06443083	OXCT2	1,04888467	SYNJ2	1,02599039	RALBP1	1,16755568	4017	CYP17A1	1,01468192	DOLPP1	1,02281712	ATP5J	1,05502021	CD180	1,05120853	RUNX2	1,03553543	NCF4	1,01434565	POU2AF1	1,14421596
3948	AGTR1	1,02338014	BCL10	1,03218175	TRAF5	1,07148577	HMGCS1	1,06441068	ITPA	1,04865479	PTGIR	1,02578728	IL1RL1	1,16739593	4018	ETS1	1,01456615	FGFR2	1,02230844	ITPK1	1,05493623	ADRA1B	1,05092534	CDKN1B	1,03544023	GALK1	1,014179	AQP1	1,14418412
3949	LBP	1,02336349	SULT1A2	1,03206032	RARG	1,07130456	ARNT2	1,06431617	SMO	1,04849498	GALT	1,02541619	MCM2	1,16705202	4019	VAV1	1,0145269	CCR7	1,02198498	ADH4	1,05456936	NEUROD1	1,0508938	MEF2C	1,03534898	TREX2	1,01393647	TRIM14	1,14397618
3950	SCN3A	1,02324893	TBXA2R	1,0319889	CCKAR	1,07115694	FGFR2	1,06423326	TPI1	1,0484469	ATP6V1E2	1,02474876	TOP3B	1,1668445	4020	XYLT1	1,01426366	CD244	1,0218522	ACCN4	1,05455573	LTA4H	1,05082168	CD59	1,03514805	ATP5F1	1,01391427	PDE6D	1,14392113
3951	PDLIM5	1,02324495	SLC6A3	1,03193317	CRADD	1,07107759	MT2A	1,06418348	ABCD3	1,04843159	TUBB3	1,0247272	CD82	1,1668205	4021	SCN2B	1,01423058	PCGF2	1,02154819	SREBF1	1,05431024	AFMID	1,05076585	MAPK1	1,03479994	MTRR	1,01371588	L1CAM	1,14299802
3952	PTAFR	1,02315309	UBE2D1	1,03188895	CD93	1,0703247	IL10RA	1,06392047	ALDOB	1,04789537	IGFBP3	1,02469867	MAN1B1	1,16615407	4022	TYK2	1,01420647	PCNT	1,02145176	CD1C	1,05425992	PGD	1,05074931	HDAC6	1,03464207	SLCO1A2	1,01355878	GOT2	1,14293684
3953	RNF2	1,02312652	GBGT1	1,03178848	SOAT1	1,07027672	SCNN1B	1,06318992	E2F1	1,04747596	IFT57	1,02458329	CDC25B	1,16543904	4023	PGA3	1,0141041	GIP	1,02137113	SULT1C4	1,05421694	BHLHB9	1,05070579	GEN1	1,03460713	ANXA5	1,01354559	TXN	1,14288713
3954	CLDN11	1,02312437	ADFP	1,03102536	ADH5	1,06999063	NEFH	1,06242333	PRKACB	1,04728063	PRL	1,02412266	ADRA1B	1,16531537	4024	IL2RA	1,0137352	PAXIP1	1,02107403	CREB5	1,05401106	PEBP1	1,05050976	PDHB	1,03434098	HADHA	1,01331558	HLA-DMB	1,1428035
3955	BCL10	1,02297748	ANGPTL3	1,03101798	ARL4D	1,06978868	ELK3	1,06208051	PREP	1,04716378	CACNA1F	1,02369077	MAPK8IP2	1,16491356	4025	P2RY1	1,01350975	SLC34A1	1,02088146	SULT4A1	1,0539156	RNF19A	1,05031565	MAN1B1	1,03398326	MSI1	1,01322371	GJA1	1,14271081
3956	BAG3	1,02295963	MAP4K1	1,03067973	BDNF	1,06968998	NDUFA12	1,06206761	SIN3B	1,04687093	GOSR2	1,02301243	CHRNG	1,16462634	4026	DFFA	1,0132936	PPT1	1,02085344	MTNR1B	1,05344278	HLX	1,05017522	GNB3	1,03383248	MARCKS	1,01298552	LAP3	1,14263269
3957	PLA2G4A	1,02263717	ABCA8	1,03066506	ACIN1	1,06968807	DPYS	1,06201269	BTC	1,04667353	PIK3CG	1,02296081	BCL6	1,16455353	4027	SVIL	1,01315352	ADCY6	1,02065676	IDUA	1,05279049	TNIP3	1,04997401	CCDC6	1,03379995	LPHN2	1,01270414	TNC	1,14223923
3958	CKM	1,02255796	SCN1A	1,03008756	ALG14	1,06947699	GORASP1	1,06200378	IL25	1,04652668	B3GALT4	1,02295995	AVEN	1,16436293	4028	RECK	1,01315076	MASP1	1,02030332	IL1RL1	1,05261555	P2RY1	1,04942656	PDE4C	1,03377748	TUBB2A	1,01234347	IL27	1,1422317
3959	FCER2	1,02248348	GUCY1A2	1,02997954	GLP2R	1,0692034	AGPAT3	1,06161873	RAD51L3	1,04629135	DCN	1,02291752	EP300	1,16433125	4029	CCNG2	1,01314314	ENTPD8	1,02014207	IFITM1	1,05182088	YWHAZ	1,0493653	MAPKAPK2	1,03369083	WNT6	1,01233619	RAD54L	1,14164423
3960	FANCB	1,02246192	CLDN10	1,02976283	CNR2	1,06894344	MAPK10	1,06150191	GHRL	1,04628041	NSUN2	1,02270091	BUB3	1,16391553	4030	GALNTL1	1,01309874	COL27A1	1,01996021	TIFA	1,05164697	HYI	1,0493401	CTSD	1,03328273	HDAC8	1,01228217	GUCY1A3	1,14148994
3961	CD209	1,02233824	POLE4	1,02949766	CLDN19	1,06875663	ARSE	1,06147846	IBSP	1,04613695	NEIL2	1,02251937	PDE7B	1,16377432	4031	PKM2	1,01302237	NFE2L2	1,01970439	GRWD1	1,05153839	HEMK1	1,04918947	SNX1	1,03309205	DUSP9	1,01209291	SUZ12	1,1409422
3962	CDCA8	1,02232963	PPP1R1B	1,02949246	DNAJB11	1,06833604	EGFR	1,06127826	CYP3A5	1,04602295	PTK6	1,02247192	VISA	1,16352612	4032	PDE6D	1,01294723	YAP1	1,01948357	RNF25	1,05149449	PDCD1	1,04916734	SOX6	1,03303531	NEIL1	1,01206828	CANT1	1,14083049
3963	NTSM	1,02223522	MCRS1	1,02916116	C1ORF142	1,06829502	SRM	1,06124011	ADORA1	1,04589456	TRPM2	1,02242728	COL10A1	1,16340011	4033	FCGRT	1,01291436	F3	1,01947285	COL7A1	1,05145414	ID3	1,04914238	FCER1A	1,03298629	RAC3	1,01158626	ABCA3	1,14039136
3964	PON2	1,02221161	TBL1XR1	1,02912316	COL4A4	1,06813342	H6PD	1,06115879	MCM5	1,04556212	SKIL	1,02221171	PPP6C	1,16312174	4034	ACAA2	1,01276275	DUSP4	1,01941284	TP73	1,05134164	ATP2B2	1,04867308	FKBP5	1,03296993	UNC13B	1,01143852	ANGPT2	1,13994003
3965	NQO2	1,02205488	HTR1A	1,02908159	ALDH6A1	1,06781866	EMR1	1,06094176	AKAP10	1,04543775	ME3	1,02215426	LPO	1,16293611	4035	EZH2	1,01269404	PPCDC	1,01921256	CADM3	1,05111068	LTBP4	1,04837424	CDKN2C	1,03287331	UBE2V1	1,01122617	DAPK2	1,13965403
3966	SHH	1,02185636	GLP1R	1,02897953	DOT1L	1,06739207	MAP4K1	1,06035464	SOAT1	1,04532877	TBL1X	1,0218412	CLOCK	1,16281494	4036	CD3G	1,01249807	GUCY1A3	1,0191652	FES	1,05070103	LRP1	1,04830598	LHPP	1,03277766	ACVR2A	1,01116223	SYNJ2	1,13899479
3967	JPH3	1,02184907	CHIA	1,02809799	TYR	1,06684622	SLC33A1	1,06017656	UNC93B1	1,04512112	CDK5R1	1,02154754	FKBP5	1,1619827	4037	POU5F1	1,01235678	LRPAP1	1,01908465	AK3	1,05068191	CYP3A5	1,04810672	ELA3B	1,03233517	SEMA3A	1,01094387	IQGAP2	1,13790134
3968	KEAP1	1,02152524	DLL1	1,02808563	SLC9A3R1	1,06681425	RNF216	1,05985598	LIN7A	1,0450538	GPX5	1,02154298	KCNH2	1,1618527	4038	NT5C2	1,01223893	CNGB1	1,0189545	SKP2	1,05049939	APLN	1,04741926	CEACAM1	1,03188404	DOCK9	1,01054603	NPAS2	1,13755646
3969	NFKBIL1	1,02133208	IL17C	1,02799047	TRPC2	1,0667925	MGAT2	1,0597624	RAP1B	1,04503334	CTSB	1,02149749	NEK2	1,16177737	4039	NLRP2	1,01187138	ARHGEF1	1,0188502	ELOVL2	1,05040258	LBP	1,04721868	VPREB1	1,03186218	LRDD	1,01039273	SLC6A4	1,1375309
3970	IDH3A	1,02114746	GALNTL2	1,02793824	FGB	1,06662845	NEIL2	1,05967467	HR	1,04498	ALDH7A1	1,02135848	KRT7	1,16167193	4040	SPTBN4	1,01174637	POLR3H	1,01875155	UGT1A5	1,04971985	ADCYAP1	1,04716777	ID3	1,03171947	FLT3	1,01018515	MPPED2	1,13728857
3971	CHKA	1,02091864	MINPP1	1,02783039	ME3	1,06639108	TXLNA	1,05966035	SMUG1	1,04446195	CREB3L1	1,02135423	CLEC7A	1,16071451	4041	ITGB4BP	1,01148922	PIGO	1,01866838	HSD3B7	1,04944904	TP53BP1	1,04711639	DGKB	1,03170096	OBFC2B	1,01004342	ABCC1	1,13715978
3972	DMD	1,02091834	IL7	1,02771639	EIF5	1,06628601	HLA-DOA	1,05949128	BRAF	1,04435145	DVL1	1,02134241	PITPNB	1,16031515	4042	CAPN10	1,01143875	GRM6	1,01856552	AANAT	1,04868471	DTYMK	1,04683758	TRIM21	1,03163418	PROM1	1,01001325	GANC	1,13581587
3973	C3AR1	1,02076963	CAMK1	1,02762067	BCAP31	1,06615321	HSP90AB1	1,05939172	EZH2	1,04429831	DCT	1,02126602	SOX6	1,15980638	4043	EIF3H	1,01125059	SKP2	1,01852076	UBE2L3	1,04864374	IVD	1,04683608	IL2RB	1,03160894	APOBEC3B	1,00988546	DYSF	1,13538233
3974	CHST13	1,02075577	ALDOB	1,02754583	GANC	1,06598957	MKNK1	1,05936251	NSF	1,0438876	UBTF	1,02113317	PDE8A	1,15980275	4044	MTNR1A	1,0111584	ABCB4	1,0184643	GRK1	1,0484489	ZDHHC8	1,046828	CDKN2A	1,03145652	GABARAPL1	1,00980999	KRT1	1,13521396
3975	CLDN14	1,02073462	NEU1	1,02749345	LPHN1	1,06514892	FCGR3B	1,05934532	BMP10	1,04373386	FOSL2	1,0210051	FAH	1,15979581	4045	EXO1	1,01098243	ALOX5	1,01836908	HTR1E	1,04838054	POLI	1,04681224	PLAU	1,03134828	GBA	1,00956717	THOP1	1,13516861
3976	WASL	1,02055703	FUCA1	1,0273677	GLP1R	1,06512975	FUT3	1,05924584	BIN1	1,04363598	PCSK1	1,02099914	IFNA21	1,15956839	4046	BMP5	1,01083901	CCND2	1,01832521	ST8SIA1	1,04835907	ARF4	1,04677528	IMPA2	1,03127606	JAG1	1,00953112	CARD9	1,13505751
3977	GSTM5	1,02042133	NR0B1	1,02722965	FOXK1	1,06483796	PHKA1	1,05920092	KCNJ4	1,04356658	PAN2	1,02050641	SFRP1	1,15935873	4047	RTN4R	1,01078012	CD59	1,01814677	ADCY5	1,04828707	RHOQ	1,04670935	NANOS1	1,03119115	AMPD3	1,00947257	PTX3	1,13464419
3978	LHCGR	1,02040453	ESCO1	1,02712717	RAD18	1,06476702	MYD88	1,05888438	VAV1	1,04324522	PDE3B	1,02031432	OAZ1	1,15921088	4048	SOX4	1,01061556	CSDA	1,01807328	RTN4	1,04826351	PCSK1	1,04664793	ZMAT3	1,03054362	IRX3	1,00914354	GBL	1,13445649
3979	ACAN	1,02038118	BRAF	1,02671864	GNAL	1,06469288	ACPT	1,05871048	CNDP1	1,0431223	AKAP9	1,02010079	GP6	1,1585615	4049	AKAP9	1,01028777	SHISA5	1,01796754	ARAF	1,04816713	ACTN3	1,04647016	CYB5R1	1,03053241	COL19A1	1,00912123	MYST4	1,13396292
3980	ALPPL2	1,02032719	APAF1	1,02669531	DNAJA1	1,06449088	CAMK2B	1,05867937	GP6	1,04308525	PCNT	1,01987686	HLA-DPA1	1,15825733	4050	EFNA1	1,01024588	UGDH	1,01759353	ELA1	1,04714062	GJB1	1,04644003	ELOVL5	1,03048825	AMY2B	1,00886608	PARK2	1,13395161
3981	GNGT1	1,02026867	ITGB3	1,02649259	MSI1	1,06377435	SCN3B	1,05851064	DCN	1,04288239	AFP	1,01978787	PSMD7	1,15760742	4051	CUL2	1,00956173	UVRAG	1,01750456	MSH2	1,04666375	CLDN5	1,04642106	ERCC1	1,03013987	ELOVL2	1,00878626	ACADL	1,13342728
3982	BCL3	1,02007159	MEF2A	1,02644193	LNPEP	1,06376502	CDKL1	1,05833185	IL17RA	1,04287319	MVK	1,01951578	CLCA1	1,15706494	4052	ELA2B	1,00948515	NCF2	1,01721361	DGKG	1,04609174	HSPA5	1,04607575	LAP3	1,02997724	DEFB1	1,0084625	AKT1	1,13311497
3983	MCPH1	1,01979478	E2F2	1,02634962	USP9X	1,06374274	PTEN	1,05807127	ACY3	1,04281832	DES	1,01942422	CYR61	1,15626019	4053	UBE2G1	1,00947323	SMAD1	1,01717362	TAGLN2	1,045982	FTO	1,04573037	ITGB4	1,02921362	CACNA1H	1,00834834	ADAM10	1,13306251
3984	CETP	1,01977164	NANOG	1,02631343	PTHR1	1,06352373	RAB10	1,05803541	TYK2	1,04252301	CD44	1,01938682	SEPT2	1,15621235	4054	IFNK	1,00941906	BCAP31	1,01715108	NMNAT1	1,04582092	FGF6	1,04544814	HIC1	1,02893089	MGP	1,0083455	GPR35	1,13258534
3985	DRAM	1,01973009	CD1A	1,02560331	GHRH	1,0632801	CCBP2	1,05796111	WNT5A	1,04222135	APBA1	1,01920856	DLX1	1,1561918	4055	CDKN1B	1,00922204	NME1	1,01714782	NFKB2	1,04555654	CPT2	1,04503217	DMGDH	1,02877944	CAMK1G	1,00816473	THRA	1,13229526
3986	CDX1	1,01959319	GUSB	1,02548587	JAM2	1,0632753	PPOX	1,05780404	SALL1	1,0419063	BET1L	1,01918108	COPS3	1,15564984	4056	TTF2	1,00882559	GBA	1,01713504	CDS2	1,04513767	APOC2	1,04495526	UBTF	1,02861343	STAT4	1,00813711	CCL20	1,13216406
3987	SLC9A3R1	1,01930732	AKT1S1	1,02547223	BMPR2	1,06284571	APOBEC4	1,0577687	KLK1	1,04171787	F12	1,01917708	NDEL1	1,15514555	4057	HSD17B7	1,00878942	ASGR2	1,01695733	FEN1	1,04508681	PDE3B	1,04464703	CHRNA6	1,02841493	MTMR1	1,00811376	SCN8A	1,13191588
3988	ST3GAL4	1,0191756	ANGPT2	1,02541876	CHKB	1,06268732	THRA	1,0574908	PTPN1	1,04151572	IPMK	1,01908906	SLAMF1	1,1545693	4058	NAGLU	1,0087133	ABCG2	1,01653862	SLC6A3	1,0448452	IRX3	1,04444749	PAX5	1,02829911	UGT1A6	1,00795087	HRG	1,13157304
3989	TIFA	1,01912086	GLUD2	1,0253394	ALG5	1,06242342	HADHB	1,05736157	HLA-DRA	1,04146117	PGAP1	1,01907794	PHB2	1,15450955	4059	ANP32E	1,00852307	DBT	1,01647398	HSD17B8	1,04430928	HTATIP	1,0441653	PRNP	1,028205	ST6GALNAC4	1,00731856	SERPINB5	1,13149962
3990	IFNAR1	1,0190595	WNT6	1,02533569	DDEF2	1,06222246	TGM1	1,0571086	AKR1B1	1,04134657	SIGLEC1	1,01893846	ABCB10	1,15419592	4060	CFTR	1,0084925	TNFSF11	1,01640778	RAB9A	1,04423386	EREG	1,04396507	PANK2	1,02791392	YARS2	1,00719585	IFNA5	1,13140698

Table A4. Pooled-shRNA library screen on HEL cell line and MF-3: list of 2nd most depleted shRNAs for each experiment (ranking approach 1, RA1).

	NO ruxolitinib (setting 1)				Ruxolitinib (setting 2)				Ruxolitinib + CM (setting 3)				MF-3				NO ruxolitinib (setting 1)				Ruxolitinib (setting 2)				Ruxolitinib + CM (setting 3)				MF-3			
	Experiment 1		Experiment 2		Experiment 1		Experiment 2		Experiment 1		Experiment 2						Experiment 1		Experiment 2		Experiment 1		Experiment 2		Experiment 1		Experiment 2					
Rank	*Gene*	*Fold change*	*Gene*	*Fold change*	*Gene*	*Fold change*	*Gene*	*Fold change*	*Gene*	*Fold change*	*Gene*	*Fold change*	*Gene*	*Fold change*	*Rank*	*Gene*	*Fold change*	*Gene*	*Fold change*	*Gene*	*Fold change*	*Gene*	*Fold change*	*Gene*	*Fold change*	*Gene*	*Fold change*	*Gene*	*Fold change*	*Gene*	*Fold change*
4061	CCL4	1,0083169	GBA3	1,01629141	CYB5R1	1,04400154	CFI	1,04289365	GPR81	1,0276904	FKBP5	1,00703997	GOPC	1,13053037	4131	HDAC5	1,00027139	FOLR1	1,00385377	CCL2	1,02528518	GTF2A1	1,02754169	UROD	1,01324783	CD8A	0,9942807	PTAFR	1,10552965
4062	C1ORF142	1,00828711	HBEGF	1,01605659	GALNT9	1,04362759	SLAMF1	1,04284947	STUB1	1,02738802	EPHX2	1,006741	DNAJC4	1,13027951	4132	CSNK1A1	1,00009983	TBP	1,00370048	HS3ST5	1,02525283	CDC25C	1,02751876	FZD6	1,01273681	FUT1	0,99391231	FOXO1	1,10446455
4063	BAG5	1,0079188	UPB1	1,0155389	MAPT	1,04358235	CCKBR	1,04284235	SOD3	1,02737614	IFNA8	1,00617108	CFP	1,13021095	4133	MYH3	1,00008845	EBI2	1,00341905	S100A6	1,02504754	YAP1	1,02749315	HOXA7	1,01263137	HSPA2	0,99390503	HSP90AB1	1,1043081
4064	TNFSF10	1,00785299	UBE2J1	1,01502052	PON2	1,04302422	HOXA7	1,04263284	PHCA	1,02728098	ERCC4	1,00585536	FGFR2	1,12989095	4134	GSTM1	0,99995976	HEY1	1,00330349	RPN1	1,0248128	NPY2R	1,0271732	BOK	1,01256887	S100A6	0,99381119	POLR2A	1,10408129
4065	POLL	1,00769237	VEGFC	1,0148751	RTN4R	1,04271476	CDC25B	1,04237913	RAB11A	1,02711544	NME1	1,00569406	S100A9	1,12957719	4135	LIPT1	0,99958476	GYS2	1,0030671	NPM2	1,02472383	ATP6V1B1	1,02702958	F2RL3	1,01241112	POLI	0,99341735	APOA4	1,10405026
4066	DDO	1,00732553	FSCN1	1,01462265	APBB3	1,04246978	GPR132	1,04233442	PAPPA	1,02706638	PRPS2	1,00548011	GHR	1,1288509	4136	CDH2	0,99951507	SIRPA	1,00288964	GABRA1	1,02465867	F13A1	1,02688254	ABLIM1	1,01219773	CD48	0,99336001	GRIN2D	1,10401722
4067	WNT6	1,00728229	RNASEL	1,01440087	RAB11A	1,04242421	MSI1	1,04202508	RGS16	1,02702522	FZD7	1,00494809	CDK7	1,12759163	4137	MVK	0,99943793	RFWD2	1,00288169	CASP9	1,02440361	CDK5R2	1,02650063	CHP	1,01216011	FBXW2	0,99332569	ADORA1	1,10348187
4068	SMAD1	1,00721153	TAF13	1,01415073	LTB4R2	1,04189162	IRF2BP2	1,04193494	CLDN14	1,02674169	BCAP31	1,00474889	DFFA	1,12642777	4138	DEDD2	0,99926025	ATN1	1,00283825	GADD45A	1,02406049	GRIA2	1,02633015	RAB10	1,01204718	GALNT2	0,99328371	ATF1	1,10296776
4069	FZD8	1,00708641	GPRC5B	1,013973	C3AR1	1,04163429	ELA2B	1,04141483	ARF6	1,02664442	C9ORF97	1,00454367	CD226	1,12591508	4139	GNG13	0,99890482	SIM1	1,00279595	RUNX3	1,02373762	CDS2	1,0261871	ATOH1	1,0118312	CCL3L1	0,99310181	FGFR3	1,10257764
4070	ATG5	1,00692493	DOK2	1,01325335	TNFSF11	1,04153039	TCF7L2	1,04125938	PTAFR	1,0265244	FCN1	1,00434101	SAT1	1,12590908	4140	PGD	0,99876735	CBX3	1,00261797	POLB	1,02354922	TUBA8	1,02589963	C1GALT1	1,0110811	TXN	0,99309332	PDXP	1,10249875
4071	TLR3	1,00689074	EIF5	1,01315083	MVK	1,04058207	GPR77	1,04121652	IL1RL1	1,02644458	NOS1AP	1,00431361	DOCK9	1,125803	4141	TXNDC1	0,99867776	IL5	1,00248157	OGFR	1,02346457	EIF1	1,02522896	VAV3	1,01036227	HSPA1B	0,99260786	CTSL1	1,10224066
4072	DHCR24	1,00679172	FMO4	1,01270593	COL5A3	1,040342	KCNMB2	1,04119396	GRIN2D	1,02643633	KCNMA1	1,00421321	EXTL1	1,12513215	4142	EREG	0,99834039	PTEN	1,00230153	EIF4E2	1,02341742	NR2C2	1,02449735	EPO	1,01026473	PIGW	0,99224408	UNC5B	1,10191614
4073	PARD3	1,00677619	HSPA8	1,01239253	AGPAT3	1,04021912	SSTR5	1,04117965	F9	1,02624833	ZFYVE16	1,00380417	HDAC6	1,12474637	4143	PON1	0,99831148	LTB4R2	1,00225149	ABCC5	1,02337544	MYL9	1,02447669	SLC38A1	1,01010622	COL18A1	0,99200383	NT5C3	1,1017762
4074	BDNF	1,00669617	LTB	1,01218178	KCNE2	1,03990217	PIK3CA	1,04058742	RDM1	1,02546663	INSIG2	1,0035054	ALOX5AP	1,12447695	4144	ATP12A	0,99818631	CA2	1,0021298	CD200R1	1,02331796	CLDN23	1,02434391	KCNJ12	1,0098283	ADIPOQ	0,99181186	RDH12	1,10174137
4075	TUBD1	1,00663472	ALDH7A1	1,01216601	ARHGEF11	1,03963101	NMU	1,04028534	ITPKA	1,02542311	MICA	1,00347484	ARAF	1,12436621	4145	COL27A1	0,99815492	UCHL3	1,00176502	PHPT1	1,02257405	PTGIR	1,02429804	IDH3G	1,0097033	GSTP1	0,99133172	DLL3	1,10158201
4076	MAP1LC3B	1,00658965	SERPINA5	1,01202907	FOLR1	1,0393769	APOBEC3G	1,04016713	ITPKB	1,02495475	APOA1	1,00337205	CD47	1,12429	4146	PUM2	0,99806763	SCN3A	1,00173392	ATF1	1,02229131	CLCA2	1,02424407	MGAT4A	1,00959434	UCHL1	0,99129739	CFHR4	1,10139618
4077	GBP2	1,00625454	CYP3A5	1,01198541	DDX4	1,03903401	IDH3A	1,0399508	FAM59A	1,02461944	FUT7	1,00334242	PMCH	1,1240408	4147	PELI3	0,99777194	KITLG	1,00144898	WNT2	1,02222925	DTX3	1,02421812	GRB14	1,00886775	SCNN1A	0,99107227	VDR	1,1013162
4078	ASS1	1,0062335	GRM8	1,01183357	INPP5D	1,03857889	TNFRSF13B	1,03958238	TBX1	1,02455567	CD24	1,0032785	RALA	1,12345139	4148	DNMBP	0,99765854	CA6	1,00129408	AES	1,02197416	PITPNB	1,02389017	GOLGA2	1,00846904	F8A1	0,99045547	CDC6	1,10126302
4079	MRE11A	1,0062335	RGS5	1,01166735	RIPK1	1,03840677	NMNAT1	1,03932159	GDF9	1,02454158	VEGFC	1,00316623	PRKAB1	1,1231659	4149	SH3GL2	0,99753131	APBB2	1,00123255	CDC14A	1,02195117	WISP2	1,02246735	CTF1	1,00829041	ACY1	0,98966678	COL6A2	1,10123184
4080	PDE11A	1,00570811	ADRA2B	1,01160786	OLAH	1,03836613	FUT1	1,03928409	PIK3R1	1,0244355	MYL2	1,00312528	ADH5	1,12310458	4150	SLC18A3	0,99748226	GTF2E1	1,00113546	OTX2	1,02187755	UCP3	1,02245052	ALAD	1,00827006	IFITM3	0,98893756	CXCR6	1,10113763
4081	ZMYND17	1,00527456	ANXA5	1,01141002	ADIPOR2	1,03813913	MAP2K3	1,03922591	DDHD1	1,02427707	ADAM12	1,00306594	FLT3LG	1,12256638	4151	DCN	0,99744786	WNT10B	1,00093296	PDK2	1,02177514	F5	1,0223027	CDK9	1,00793014	PRKCZ	0,98892771	GALNT8	1,10094501
4082	CD200R1	1,00521291	FXYD2	1,0113137	ALPPL2	1,03718859	IL1B	1,03916196	VANGL1	1,02419865	ABCA4	1,00285856	FABP1	1,12252391	4152	PCK1	0,99737072	PLOD1	1,0008525	RFX4	1,02159356	ATF2	1,02222691	CD63	1,00788154	HLA-A	0,98883354	PYGB	1,10053157
4083	LIF	1,00509851	CD27	1,01100215	SRF	1,03704737	SMAD1	1,03904477	SMAD1	1,02405665	NCK2	1,00281847	GUCA1A	1,12146758	4153	TXNRD2	0,99725154	DPAGT1	1,00084316	MAP2	1,02123959	TNFRSF10D	1,02219074	JAK1	1,00758456	ATG16L1	0,98792325	DPAGT1	1,10045218
4084	SPRY2	1,00462196	FKBP5	1,01099983	MTA1	1,03698265	PMAIP1	1,03883232	ALDH4A1	1,02373921	LRP1	1,00273667	TRIB3	1,12131873	4154	CDKN1A	0,99717611	RTN4R	1,00070952	TNFSF10	1,02114508	TRIP12	1,02210306	PPP3CA	1,00671268	CLDN18	0,98786524	NEU2	1,10022267
4085	PIN1	1,00454598	GRAP2	1,01067176	EXT1	1,03692598	DUSP9	1,0384724	IFNAR2	1,02363481	PHKA1	1,00211681	PHKG1	1,1204732	4155	CACNA2D4	0,99707661	FSCN3	1,00066494	RAB4A	1,02087877	PECR	1,02204968	ALDH3A2	1,00665948	HLA-DRA	0,98785683	UBB	1,10010935
4086	GRASP	1,00450584	NSUN2	1,01055927	IL18	1,03689101	ADCY2	1,03838907	MCAT	1,02347593	TGM1	1,00210204	CCNB2	1,12040759	4156	CAMKK1	0,99681639	LTBP1	1,00048971	ITPKA	1,02059883	ARPC4	1,02179249	B3GALT5	1,00660234	P2RX7	0,98784545	GADD45G	1,10006203
4087	DNAJA2	1,00440258	GSTA4	1,01040722	CRHR1	1,03655207	SIN3B	1,03828411	P2RY6	1,02340028	GATA2	1,00160573	SERPINC1	1,12005493	4157	TAP2	0,99677574	TGFA	1,00044979	CNGB1	1,02045066	DPAGT1	1,02169279	ADM	1,00659863	APOBEC3A	0,9878117	DAP	1,10000788
4088	COL25A1	1,00433942	ITGB1BP3	1,01038094	ASIP	1,03605588	GHR	1,03796456	ARNT2	1,02306995	HPSE	1,00116855	EXT2	1,11991325	4158	GTF3C3	0,99677499	SCN4B	1,00021829	MAPKAPK2	1,02036617	GABRB3	1,02160326	NRG1	1,00652711	RASA1	0,98747772	FLJ21865	1,09835101
4089	GTF2A2	1,00421034	PDXP	1,01036723	ATF3	1,03524674	VANGL1	1,03790183	PAX4	1,02305721	SIRPA	1,0011622	PTGER3	1,11988939	4159	LDLR	0,99671672	PINX1	1,00000175	FECH	1,01974617	ACP5	1,02147395	KLC1	1,00610574	CSTF2	0,98719055	GMPPB	1,09773626
4090	IGFBP1	1,0039137	SCN10A	1,01023005	GSTZ1	1,03514835	TGFA	1,03762182	HSD17B7	1,0224789	PIGP	1,00104169	DPM1	1,11922145	4160	A4GNT	0,99644769	PGLYRP2	0,99977515	SCD	1,01953722	CHPT1	1,02145453	EBI2	1,00578412	TAF4	0,98666889	GRIA3	1,09772198
4091	HTR2B	1,00390984	DSE	1,00993728	OPRK1	1,03511178	ANXA5	1,0370992	GJD2	1,02247406	SLC12A6	1,00101321	CAMK1	1,11905216	4161	CHRNE	0,99641396	PDE8A	0,99950489	CDCA8	1,01949456	SKP2	1,0209062	NMU	1,00574025	BACH1	0,98656102	ERCC1	1,09707526
4092	APLN	1,00378355	BMP10	1,00993079	LAP3	1,03417507	MYLK	1,03690433	ANXA5	1,02240075	NKX6-1	1,00096311	BIRC3	1,11842348	4162	PRMT1	0,99617669	P2RX7	0,99949314	WWP2	1,01927797	MAP3K7IP1	1,02043369	RAD23A	1,00561375	RPS6KB2	0,9865391	GHSR	1,09654087
4093	DLX1	1,00372979	WNT4	1,00987674	HOXD10	1,03406582	TNFSF13B	1,03660831	NRP1	1,02174623	PTTG1	1,00084286	GRIA2	1,11838411	4163	FGF1	0,99617021	EGF	0,99920537	CTSE	1,0192187	BMP3	1,01975373	CA8	1,00551984	TOR1A	0,98645118	AMY1B	1,09576552
4094	RDH5	1,0037221	AMPD2	1,00965458	LIMK1	1,03386675	STMN2	1,03658475	MMRN1	1,02157601	BCL2L14	1,00072264	CA13	1,11835446	4164	ATF4	0,99613271	NDUFA8	0,99880227	NLRP2	1,01895561	NT5M	1,01914171	AMDHD1	1,00551667	KLRC4	0,98644721	CCL11	1,094648
4095	STAT4	1,0037067	HIPK2	1,00948337	IL5	1,03375902	CHRM5	1,03650956	PPP1R3A	1,02057219	AKR1B10	1,00063532	AGPAT3	1,11819361	4165	F2RL2	0,99594335	TNC	0,99868561	GNA12	1,01891313	GRIN2D	1,01912275	INSR	1,00544282	LHX8	0,98642687	FOLH1	1,09429921
4096	BCKDHB	1,00336991	PRMT1	1,00944326	CAPN9	1,03372607	CTLA4	1,03642388	KCNH2	1,02050048	IKBKB	1,00052892	PAPOLA	1,11764987	4166	SYNJ2	0,99553277	BHMT	0,99823082	RALGDS	1,01834598	LDHB	1,01908089	MGAT2	1,00497766	CDC25C	0,9863828	FBP1	1,09386504
4097	CACNA2D1	1,0031496	TYR	1,00942069	CRH	1,03367811	ALG9	1,03625246	PAFAH1B3	1,02007298	VANGL1	1,00042466	DCLRE1C	1,11714709	4167	CENTD2	0,99546125	INDO	0,9982225	SERPINE1	1,01818318	DIO1	1,0188723	CHST1	1,00486298	NKIRAS2	0,98611467	REPS2	1,09371949
4098	RDH11	1,00314858	PLCD1	1,0090526	BACH1	1,03356458	OGDHL	1,03621971	ARHGDIA	1,01984373	SLC34A1	1,00017231	CASP12	1,11689877	4168	UGT2B17	0,99544746	PROX1	0,99814651	CD244	1,01802253	COL4A4	1,01875678	CDS1	1,00446501	GLCE	0,98611116	EPS8	1,09365245
4099	NMNAT2	1,00314495	CREB1	1,00899594	WNT11	1,03295042	RALBP1	1,03568127	YAP1	1,01946695	OTX2	1,0000657	HIC1	1,11655798	4169	CBX3	0,99533235	IL6ST	0,99813287	MSH4	1,0177453	CKM	1,01864779	THBS2	1,00441693	CLDN1	0,98610993	EGR1	1,09363473
4100	SND1	1,00310716	CPT1A	1,00882812	ID1	1,03285523	CUL3	1,03567277	GP9	1,01934309	C8G	0,99953242	HBQ1	1,11648971	4170	PDE3A	0,99508388	FANCL	0,99811039	BRS3	1,01765799	GTF2H2	1,01861617	LDHA	1,00419209	TGFB1I1	0,98610881	CAPNS2	1,0932652
4101	AP2B1	1,00307697	WNT5A	1,00872343	SNIP1	1,03192757	IRAK4	1,03535326	C8G	1,01837365	FN1	0,99938741	IL16	1,11621093	4171	NAGS	0,99503935	BDH2	0,99769677	CANX	1,01759011	PNPO	1,0181153	RFXAP	1,00356267	GUCY1A3	0,98530456	ERCC4	1,09298022
4102	KATNB1	1,00297662	CPEB1	1,00855536	HPX	1,0318735	ECSIT	1,035336	PLA2G5	1,01808513	EGF	0,99887617	ECGF1	1,11587033	4172	TLR2	0,99479357	ADH6	0,99766803	CACNA2D3	1,01744896	WIPI2	1,0181141	GHRH	1,00291235	GFI1	0,98506627	CANX	1,09287481
4103	DUSP8	1,00270191	DUOX1	1,00846022	MDM4	1,03185012	MAP2	1,0351862	EI24	1,01772866	INSR	0,99879146	CYCS	1,11542353	4173	ESR2	0,99475607	APOBEC3A	0,99739167	CRKL	1,01733377	CD99	1,01800666	KLKB1	1,00289796	LBP	0,98491537	CLDN22	1,09274341
4104	EGFR	1,00265746	HLX	1,00845184	APOBEC3A	1,03176558	NDST2	1,03498386	DNMT3A	1,01761149	PON2	0,99876725	RAB7A	1,11536409	4174	GATA2	0,99471579	SIRT1	0,99732994	FGG	1,01711482	GREB1	1,01792393	SKP2	1,00245679	BAG1	0,98487488	CD33	1,09236989
4105	DOCK9	1,00251249	NADK	1,00844739	APOBEC4	1,03158818	SCLY	1,03481112	FAAH	1,01729331	FRZB	0,99870684	NTF3	1,11488605	4175	LAMP1	0,99462236	STAT3	0,99697921	GALNT12	1,01698708	PIGW	1,01731567	NES	1,00191295	CNPY4	0,98486032	TRPV1	1,09236989
4106	HLA-DRA	1,00251249	CES7	1,00843719	SHC3	1,03141827	PEU1	1,03468862	IFI44	1,01675783	PGDS	0,99846705	CDKN2D	1,11451764	4176	CACYBP	0,99423419	PDK2	0,99696638	UGT1A5	1,0169315	TNFSF10	1,00161456	RBPJL	0,9847612	PSME1	1,09126368
4107	KHK	1,00238219	FAAH	1,0084298	APOBEC3G	1,03106622	DIAPH1	1,03415516	ORC3L	1,01641902	SH3GL3	0,99838333	GPR161	1,1143706	4177	GATA3	0,99418812	NTAN1	0,99675273	COL8A2	1,01634365	CREB3L1	1,01687221	ADH6	1,00143895	CD1C	0,98435624	MAGI3	1,09119737
4108	ACP5	1,0022912	ADCYAP1	1,00809456	ESCO1	1,03105055	NOTCH3	1,0338758	IVD	1,01631403	SGK	0,99832952	MAP3K13	1,11426261	4178	CD36	0,99402289	POSTN	0,99654585	EPRS	1,01510049	OTC	1,01681258	BHLHB2	1,00116871	CYP4F3	0,98416915	RTKN	1,090973
4109	GALNT17	1,00222494	PML	1,00739756	AKT1	1,03084396	B3GNT7	1,03370678	SMAD6	1,01603481	BMP8A	0,99832214	SOD2	1,11308043	4179	GRIK3	0,9939501	ZBTB7A	0,99635121	KDELR1	1,01485645	PTK2B	1,01680681	CHPT1	1,00107859	LY75	0,98415538	EXOC7	1,09074481
4110	ISYNA1	1,00210831	PAK3	1,00703922	CLN3	1,03070783	BIN1	1,03331716	NAT6	1,01592884	MANBA	0,99821901	HLA-DRB1	1,11290465	4180	HES7	0,99380791	BAX	0,99549671	RNASEL	1,01422479	SMAD2	1,01655256	TREH	1,00042891	POLD4	0,98378722	CSTF2T	1,09037496
4111	MAP2	1,00167653	ASPH	1,00681576	CSNK1A1	1,03070222	CIDEB	1,03327232	UVRAG	1,01576535	KLRC2	0,9980786	MAPK7	1,11251741	4181	NUDC	0,99351061	HCCS	0,99548205	PDE3A	1,01416341	CACNA2D4	1,01628326	UGT1A6	1,00032712	RAB24	0,98358612	HMOX2	1,09013171
4112	HDAC8	1,0015434	PAX5	1,00662659	FGF8	1,03024921	SEPP1	1,03314674	DPEP1	1,01560653	SRPR	0,99789144	F11R	1,11209081	4182	UBE2G2	0,99345205	CASR	0,99543338	PDPK1	1,01400513	ENTPD4	1,01531104	SLC11A1	1,00021871	PLA2G4C	0,98354567	STX3	1,08948504
4113	ITGA4	1,00145392	PRDX1	1,00660338	NOX4	1,02993713	GABARAPL1	1,03202894	CD55	1,0153686	FGF13	0,99751557	MMP7	1,11198961	4183	TP53INP1	0,99338288	FUT3	0,99498401	SFRP1	1,01387718	STX12	1,01496732	SIRT2	1,00018436	GIP	0,98348276	TCOF1	1,08932078
4114	CHST14	1,00143603	CENTD1	1,00652487	EPHB2	1,02988941	GNAI2	1,03172373	GSTM2	1,01531159	MME	0,99684158	CLCA4	1,11134764	4184	OSBP	0,99333226	COL4A1	0,99483603	NR0B1	1,01386074	IL5	1,014894	SERPINA3	0,99993917	GJD2	0,98323414	ST6GALNAC5	1,08930316
4115	IFNA6	1,00138694	CHRNA6	1,00626933	AMPD1	1,02949515	SLC26A2	1,03142066	LOC390243	1,0152117	RFXAP	0,99666281	MBD1	1,11112887	4185	TIMP1	0,99330887	MMP9	0,9947972	B3GNT3	1,01378651	DEFB1	1,01440783	CHKA	0,99992098	AKT1S1	0,98305069	THBS1	1,08897083
4116	PIK3C3	1,00133497	TLX1	1,00619546	IREB2	1,02944908	TBL1X	1,0313178	IRF4	1,01517056	CDC25B	0,99660087	INHBA	1,11109696	4186	OXCT2	0,99305364	DPPA5	0,99457982	AHR	1,01373582	MAP3K9	1,01422952	SOCS1	0,9997586	EBI2	0,98297615	NR4A1	1,08868148
4117	RAG1	1,00131225	CPSF1	1,00596373	MARS2	1,02925855	ACCN4	1,03120386	DRD4	1,01508392	RAD51L1	0,99650791	HMGA1	1,11079405	4187	ENTPD8	0,99302325	NOS1AP	0,9944843	GSTK1	1,01360609	A4GNT	1,01409918	TRH	0,99924085	HYAL4	0,98273647	PDPK1	1,08814105
4118	MFNG	1,00117898	SOCS2	1,00573727	NR2F6	1,02866402	CCL4	1,03087186	ERCC4	1,0149231	CACYBP	0,99632371	MSI1	1,11049244	4188	BRAF	0,9929899	AK3	0,99425504	BMP2	1,01351968	TKTL1	1,01395233	THTPA	0,99905659	KCNA5	0,98262268	TRIP10	1,08747334
4119	GPT	1,00111065	GALT	1,00554705	CD24	1,02837158	DHCR7	1,03062574	GABRG3	1,01492261	KL	0,99621417	ST3GAL1	1,11027383	4189	CPEB1	0,99293322	SOX9	0,99406305	CYP2R1	1,01343957	ALDH7A1	1,01345718	NOTCH3	0,99900915	FCGR2B	0,98234304	PTEN	1,08698982
4120	PDE1A	1,00108878	COQ6	1,00526252	NEU4	1,02812222	CD19	1,03038736	NDST1	1,01445343	CYP11A1	0,99617636	DBH	1,10993081	4190	APBB3	0,99281105	NFAM1	0,99355664	CKS1B	1,01266112	GPRC5B	1,01327632	LRRK1	0,99876049	CDKN2B	0,98221022	ALG2	1,08695754
4121	SRM	1,00105387	EZH2	1,0052545	PTGIR	1,02808497	ADCY7	1,02974695	ATG12	1,0142641	BAG3	0,99576148	TKTL1	1,10976177	4191	CSTF2	0,99279279	THRA	0,99355008	CHRNA4	1,01250133	FNTA	1,0125437	ACADSB	0,99871865	OGFR	0,98209898	F8	1,08664319
4122	ADAR	1,00101787	PAX8	1,00516869	ATN1	1,02778735	ORC3L	1,02962067	AMY2B	1,01414285	ARPC5L	0,99568708	NCOA1	1,10948328	4192	CHRNB2	0,992648	GNA15	0,9932273	CD37	1,01236838	AGPP	1,01247675	STAT3	0,99843309	IL17C	0,98182235	CYP27A1	1,08614584
4123	HEMK1	1,00088173	BTG1	1,0049789	CKM	1,02747678	ACTG1	1,02954465	DFFA	1,01369971	KRT18	0,99562117	CDC14A	1,10933157	4193	C1QL3	0,99258107	FOXP3	0,99309816	GAS2	1,0122664	TAF10	1,01224429	HTR3A	0,99839933	CDC26	0,98171448	SCTR	1,08445217
4124	OAS1	1,00075284	COL1A2	1,00492387	CASR	1,02744749	ARFGAP3	1,02901621	DUSP1	1,01361406	E2F1	0,99552637	PLA2G2E	1,10891408	4194	ECSIT	0,99255582	GNS	0,99301631	CD1D	1,01188199	BLR1	1,01214207	FAT	0,99838835	AGRP	0,98132678	PKN2	1,08417792
4125	FARSB	1,00061947	FZD8	1,00477201	TRIB3	1,02720057	PIR	1,02892754	KCNIP3	1,01360919	EHMT2	0,99544215	MGAT3	1,10864138	4195	CMBL	0,99243398	RGS1	0,99295989	ACTR3	1,01186423	CBX3	1,01127194	KLF2	0,99717809	PAPSS1	0,98119272	CDC45L	1,08344977
4126	PTCRA	1,00061526	ANXA8	1,00476824	DGKA	1,02704422	AADAC	1,0288529	ABCC5	1,01351807	CRH	0,99519633	PRKCD	1,10804785	4196	SLC6A3	0,99217305	MLYCD	0,99275985	CCR2	1,01148928	WNT5A	1,01115488	ATP6V1E1	0,99646314	TPI1	0,98117997	NAGLU	1,08308306
4127	AKR1C3	1,00046549	TIMP1	1,00474773	INHA	1,02626763	NDST3	1,02877044	SIRT5	1,0134734	ANXA1	0,99506651	ATP2B1	1,10760033	4197	PPP3CA	0,9921286	ITGAX	0,99267367	CUL3	1,01113278	FGF8	1,01108307	CD96	0,99618798	ALG6	0,98109942	STX17	1,08217254
4128	AMPD3	1,00044385	TLN1	1,00417975	PNLIP	1,02612538	MRPL19	1,02875278	XPC	1,01339743	INHBC	0,99499236	MPST	1,10708201	4198	DCLRE1C	0,99212657	URMP	0,99262811	GCDH	1,01112696	PAPPA	1,01054257	GBE1	0,99615271	NDEL1	0,98093948	CYP3A43	1,08207789
4129	EPHB3	1,00040117	UCP3	1,00415496	ACAT2	1,02609966	LIG4	1,02864385	ASCC3	1,01331799	FCER1A	0,99494436	ROCK1	1,10680418	4199	TNFRSF9	0,9920995	TNFSF10	0,99216267	IFNA6	1,01083257	GJA3	1,01045275	SCN3A	0,99605659	VIL2	0,98087663	CFL2	1,08204241
4130	TNFRSF17	1,00038285	AGPS	1,00397395	AMPD3	1,02546045	PGA3	1,02772478	C1S	1,01330597	COL5A1	0,99458629	GUCA1B	1,10667306	4200	SNAP23	0,99199827	GJA1	0,99208141	EZH2	1,01055659	MET	1,01016906	EXOC7	0,9958131	PIGB	0,98072604	HOXA9	1,08123398

Table A4. Pooled-shRNA library screen on HEL cell line and MF-3: list of 2nd most depleted shRNAs for each experiment (ranking approach 1, RA1).

	NO ruxolitinib (setting 1)				Ruxolitinib (setting 2)				Ruxolitinib + CM (setting 3)				MF-3				NO ruxolitinib (setting 1)				Ruxolitinib (setting 2)				Ruxolitinib + CM (setting 3)				MF-3	
	Experiment 1		Experiment 2		Experiment 1		Experiment 2		Experiment 1		Experiment 2						Experiment 1		Experiment 2		Experiment 1		Experiment 2		Experiment 1		Experiment 2			
Rank	*Gene*	*Fold change*	*Gene*	*Fold change*	*Gene*	*Fold change*	*Gene*	*Fold change*	*Gene*	*Fold change*	*Gene*	*Fold change*	*Gene*	*Fold change*	*Rank*	*Gene*	*Fold change*	*Gene*	*Fold change*	*Gene*	*Fold change*	*Gene*	*Fold change*	*Gene*	*Fold change*	*Gene*	*Fold change*	*Gene*	*Fold change*
4201	RXFP1	0,99162844	CYP2B6	0,99179708	TCEA3	1,00769361	B4GALT7	1,01012723	SHOC2	0,99579674	MASP1	0,98059129	ANKHD1	1,08110741	4271	BCAP31	0,9830952	IL21R	0,97871478	SCN10A	0,98369266	HPCAL1	0,99544311	TOP3A	0,98276316	AZGP1	0,96625791	MGMT	1,05420095
4202	STX10	0,99138938	GOT2	0,99146894	ZDHHC8	1,00749368	GRB14	1,01009887	PDE8B	0,99570511	NR1H2	0,9805701	EEF2	1,08070194	4272	SNX13	0,98255523	IKBKAP	0,97824466	UCHL3	0,98359453	IFNA13	0,99525996	AES	0,98275564	MYST4	0,96581899	COL5A3	1,05414247
4203	SKIP	0,99134007	ACADM	0,99143101	GRM6	1,00694517	PUM1	1,00999615	GJB1	0,99565507	AXIN1	0,98049832	HSPA12A	1,08068032	4273	DDX52	0,98227253	KCNJ11	0,97812018	IL13RA2	0,98348405	ATF7IP	0,99520482	BBS4	0,98264584	FGF6	0,96542185	APOBEC4	1,05392666
4204	GPR75	0,9913121	GTF3C3	0,99127732	ETV3	1,00690838	TUBB2A	1,00993245	PAK3	0,99535735	TRAF2	0,98017933	AMY1A	1,08036295	4274	PPARD	0,98213063	SLC18A3	0,97766384	ALDH9A1	0,98226605	FLJ21865	0,99513508	CNPY4	0,98261772	GPAM	0,9653154	IL3RA	1,05222783
4205	LTBP1	0,9911588	HAO2	0,99119403	HTR3A	1,00640545	PPP1CC	1,00977251	BRCA2	0,995022	UBQLN1	0,98014367	CBR3	1,08024039	4275	PPT2	0,98209016	SLC9A3R1	0,9775888	SCN3A	0,98198245	ATF1	0,99502268	ATP6V0A1	0,98239818	LCMT1	0,96474863	IGF1R	1,0515335
4206	HLA-A	0,9910974	COL11A2	0,99080601	CD86	1,00633311	PPIA4	1,00939624	NMNAT2	0,99461038	PCK2	0,98009837	CACNA1E	1,08017761	4276	OLR1	0,98113253	EEF2K	0,97744597	ANKHD1	0,98187353	ATP6V1G2	0,99489676	CCL5	0,98219304	GALNT13	0,96455364	B3GAT1	1,05150454
4207	LTF	0,99108913	NEU4	0,9906617	CD59	1,00610052	INHBC	1,00923673	PDE4A	0,99454745	WISP2	0,98004073	COL23A1	1,07977842	4277	CDS2	0,98077265	ATP5D	0,97733404	PRKCH	0,98173556	GPR64	0,99468979	ALOX12B	0,98186747	EPOR	0,96441678	CYB5R3	1,05133127
4208	HS3ST3A1	0,99097006	OTX2	0,98983164	SND1	1,00604876	CHRNB3	1,00923422	LTBR	0,99428382	BLNK	0,97976427	HOXC13	1,07965181	4278	HDAC10	0,98072965	UXT	0,97725961	ABCA2	0,98167911	TNFRSF10B	0,99453699	MTIF2	0,98162083	MAPK1	0,96436794	CXCL6	1,05116536
4209	ATG4C	0,99068585	SMAD2	0,9897421	UNC5CL	1,00577794	GALNT12	1,00887983	PTTG1	0,99416223	CRAT	0,97944633	CXCL13	1,07961427	4279	CRAT	0,98053866	AKR1B10	0,97708801	ARHGDIA	0,98159507	P2RY2	0,99432475	SERPING1	0,98108717	PRNP	0,96434398	AADAT	1,05084325
4210	DVL3	0,99021607	BCAR1	0,98964533	JAK3	1,00574831	NCOR1	1,00841572	ITGA2	0,99412116	ACADVL	0,97941906	SHISA5	1,07944808	4280	TRPV1	0,98052545	GTF2H2	0,97681908	ALDH3A1	0,9815366	SLC1A7	0,9941746	GMNN	0,98101843	ALDH3A1	0,96428136	GRIN2A	1,05010555
4211	GALNT12	0,99007625	THOP1	0,98962217	SOCS1	1,00548132	RDH11	1,00839237	ST8SIA1	0,99381954	MLXIPL	0,97934703	HS3ST5	1,07943981	4281	TSHR	0,98049446	ABCA7	0,97680622	IGFBP4	0,98125051	GPRC5D	0,99378224	SPDEF	0,98099766	LHPP	0,96409481	GBX2	1,04998257
4212	RASA1	0,98985938	JPH3	0,98918469	TAF10	1,00544029	CYP2A6	1,00817181	MAP3K13	0,99357649	C4A	0,9789207	CYP4F12	1,07925789	4282	EPHX2	0,98046534	IL12A	0,97665875	MYL3	0,98124778	CNR1	0,99367392	PDE4B	0,98083352	ALAS2	0,96398335	ANXA8	1,04960196
4213	NR0B1	0,9898314	SSTR5	0,98913118	DCXR	1,00499547	CCL2	1,00817085	IL13RA1	0,99347426	CTNNA2	0,97884884	RAB5C	1,07923891	4283	CD93	0,97982228	COL9A2	0,97623314	FKBP5	0,98115961	AP2B1	0,99356317	GMDS	0,98043521	CD9	0,96377569	SCN2A	1,04899974
4214	STMN2	0,98980766	MGAT4A	0,98886684	HBA2	1,00373742	DOLPP1	1,00813862	ATG5	0,99328699	RAB4A	0,97882327	NPY1R	1,07923668	4284	RELN	0,97968246	IRF9	0,97607266	GUCY1A2	0,98104602	NAT6	0,99354279	PIK3C2B	0,98027637	BMP1	0,96320987	ACP5	1,0487673
4215	ACSL5	0,98976965	SLC30A6	0,98869271	CD34	1,0036805	BAAT	1,00776506	ABCA6	0,99293163	SLC9A3R1	0,97872709	CD2AP	1,07872452	4285	IREB2	0,97959743	HEL308	0,97605306	PDK1	0,9808633	HRH1	0,99314334	NSUN2	0,98020265	LIPF	0,96314738	IFITM3	1,04874302
4216	CLCN7	0,98957312	GORASP1	0,98863763	ALDH18A1	1,00361588	GALNTL1	1,00776473	SNAP29	0,99278384	STX6	0,97866576	CDKN2B	1,07867901	4286	TNFSF14	0,97958039	UQCRH	0,97594896	DTX3	0,98019877	STX16	0,99256222	INPPL1	0,97998256	GADD45G	0,96301861	CYSLTR1	1,04841541
4217	F7	0,98940077	CNR1	0,98840125	LMNA	1,00329352	POU2AF1	1,00736014	RXRB	0,99264964	GRM4	0,97862935	GALK2	1,07808335	4287	ALDH9A1	0,97939318	CPSF2	0,97579151	TGFBR1	0,97980778	MEIS1	0,99252903	TRADD	0,97940398	ARFGEF2	0,96297707	PIGL	1,04840434
4218	BIRC2	0,98937515	ARHGAP4	0,98784411	HMBS	1,00308879	GGT1	1,00718131	NOS1AP	0,99261632	EIF4A1	0,97844509	HSF1	1,07784547	4288	MAN1B1	0,97900331	RGS16	0,97551224	GP9	0,97977623	CDKL2	0,9918136	AHR	0,97929764	BCL11A	0,96275272	CENTD3	1,04839444
4219	GDF11	0,98916515	SIN3B	0,98776348	MAPK14	1,00219944	MYH2	1,00716553	MAPK3	0,99252789	NKD1	0,97839541	SLC22A6	1,07783893	4289	CYSLTR1	0,97900106	C2	0,97546341	MYST4	0,97975286	CD4	0,99152512	MFNG	0,9792675	TIRAP	0,9624978	RFK	1,04792119
4220	CDC45L	0,98915545	NFATC4	0,98765585	EIF4EBP2	1,00217938	FOXH1	1,00677428	LAT	0,99181403	IL3RA	0,97834647	PLD2	1,07725027	4290	ATP6V1E1	0,97887052	IRF2BP2	0,97528956	TFDP2	0,97963277	EDA	0,99148357	CDK10	0,97921573	HLA-B	0,96219376	IL21	1,04788094
4221	HSD11B1	0,98882205	SERPINE1	0,98763445	UBQLN1	1,00203555	KCNA5	1,00614508	ATP5G2	0,99169099	EI24	0,97808954	SHOC2	1,07675496	4291	EEF2K	0,97866369	DHRS1	0,9751641	FBP2	0,9795387	GABRD	0,99141881	FURIN	0,97915163	DGAT2	0,96212436	CDIPT	1,04722743
4222	KRAS	0,98849746	FOXC2	0,98751742	LCMT1	1,001968	HES2	1,00582854	GPR75	0,99154747	FAAH	0,97808893	ACO2	1,07671955	4292	ITGAM	0,97854332	GTF2A2	0,97498398	SLC12A6	0,97916734	BMP1	0,99139297	CXCL10	0,97906522	CYP2S1	0,9617551	WASF3	1,04698026
4223	COL19A1	0,98847101	PCNP	0,98738167	VANGL1	1,00193908	CSNK1A1L	1,00531794	GUCY1A3	0,99154432	HIF1A	0,97792489	LGALS1	1,07595904	4293	ERCC2	0,97836994	ISG20	0,97486734	ABCB4	0,97911878	ENTPD3	0,99126881	FST	0,9789665	PLA2G4A	0,96172351	TGFB1I1	1,0469779
4224	ASCC3	0,98837565	HDAC2	0,98717612	BHMT	1,00164779	PAK3	1,00514023	ITGB3	0,99122014	F2RL1	0,97791987	ARHGAP5	1,07546649	4294	GDI2	0,97831912	MAP2K4	0,97908277	ADRA2B	0,99097528	NTHL1	0,97884293	EIF1	0,96140153	CDC40	1,04643913		
4225	KCNJ9	0,98834442	ADCY7	0,98698571	UGT1A1	1,0013053	ERG	1,00478762	CYR61	0,99120079	NMNAT1	0,97785405	CACNA2D3	1,07544745	4295	TAP1	0,97776132	ASH1L	0,97470952	ICAM5	0,9789257	KCNN4	0,990096	STAT1	0,97857458	SNX6	0,96109051	FECH	1,04633527		
4226	LIPF	0,98810606	UCP1	0,98686296	FHL2	1,00041005	CLCF1	1,00411926	PTPRA	0,99113623	CDC2L5	0,97773556	TERT	1,07532311	4296	GJA4	0,97765843	NKIRAS2	0,97465814	PAK3	0,9788829	CA14	0,98943023	COL23A1	0,97834817	KCNA7	0,96108659	GNE	1,0463057		
4227	ISLR	0,9879419	APBB3	0,98666267	GABRG1	1,00019157	TREX2	1,00407869	APBB3	0,99093716	CSRP1	0,97769923	RAD51L3	1,07480764	4297	CSAD	0,97764362	AGRP	0,97437139	UBE2J2	0,97887833	LITAF	0,98934245	HLA-DMA	0,97822501	OTC	0,96066697	APBA3	1,04569858		
4228	ERBB3	0,98777666	ACIN1	0,9866481	GGT1	1,00004048	PAFAH1B2	1,00397478	MAL	0,99077072	FGF7	0,97734207	PGAM1	1,07435518	4298	SLAMF1	0,97756723	CX3CR1	0,97437138	SYNJ2	0,97831004	PDE4C	0,98931588	GPRC5A	0,97744902	ELA1	0,96002724	TXNRD1	1,04562101		
4229	CNGB1	0,98738117	ABLIM1	0,98640055	DPPA5	0,99977846	GHRH	1,00389216	STX10	0,99057879	AANAT	0,9772423	MASP1	1,0739629	4299	PRKD1	0,97723287	CACNA2D4	0,97396454	POLL	0,9779672	RGS19	0,9892032	B3GALT4	0,97736459	AADAC	0,95953198	UBE2F	1,04469041		
4230	TOB2	0,98719948	PRKCQ	0,98637977	ATP1A2	0,99970714	PDE4A	1,00366656	DTYMK	0,99054935	ATP2B2	0,97714264	UXS1	1,07386627	4300	AGPS	0,97717956	ADCY9	0,97387538	TXLNA	0,97756431	BAD	0,98876355	GYG1	0,97731758	KLRK1	0,95930659	DUT	1,04454104		
4231	CASP3	0,98716457	HLA-DRA	0,98617445	PRKCG	0,999679	ALDH9A1	1,00349802	TRPV6	0,99003181	COPS5	0,97710653	ZBTB16	1,07358952	4301	KCNMB3	0,97709686	GALK2	0,97384589	UBE2M	0,97741222	MAPT	0,98864801	SULT4A1	0,97706132	HADHB	0,9592897	IRF1	1,04430782		
4232	CYSLTR2	0,98716248	FAS	0,98599384	FNTA	0,9994717	TNFRSF9	1,0034004	IL3	0,9899687	SSTR5	0,97707004	DSP	1,07185969	4302	SMAD2	0,97680031	REN	0,97345043	C4A	0,97692878	CSNK1G2	0,98861168	TOR1A	0,9770141	BAG4	0,95919331	FLT1	1,04415654		
4233	CD2AP	0,98701242	GABRD	0,9856472	APP	0,99907314	HK3	1,00321631	IGFBP6	0,98996676	GPRC5C	0,97675958	HIPK2	1,07129351	4303	XDH	0,97679457	HMGB1	0,97337705	TEP1	0,97687785	PPIC	0,9884566	GTF2H2	0,97684735	RNF146	0,95912481	TAF12	1,04392052		
4234	LEFTY2	0,9868919	PON1	0,98561129	SIPA1	0,99867047	SKI	1,00315259	JUNB	0,98984518	DPEP1	0,97629135	UAP1	1,07124178	4304	F13A1	0,97674079	DUSP10	0,97330509	GRIN2B	0,97643093	TPP1	0,98817815	COL6A2	0,97676296	RAB23	0,95905393	AP2M1	1,04359374		
4235	IRF3	0,98667554	MAPKAPK2	0,98559718	ADIPOQ	0,99827141	SOCS7	1,00314986	PGLYRP2	0,98973454	DCP1A	0,97556979	MAP3K12	1,07051962	4305	PAPPA	0,97665016	RAC1	0,97322088	ADH7	0,97612233	HTR2B	0,98801247	ASS1	0,97631846	HOXA7	0,95903097	CFD	1,04330578		
4236	HAGH	0,98659557	SUMO3	0,98544716	DDEF1	0,99821704	CD1E	1,003109	LCP2	0,98972692	RDM1	0,97533372	SALL1	1,07009816	4306	TYR	0,97632973	BDKRB1	0,97286206	CDC25B	0,97598434	B3GALT6	0,98779832	GRIA4	0,97620405	GRIA1	0,95877958	HES2	1,04327159		
4237	SETDB1	0,98656547	RTKN	0,98539179	STX16	0,99814067	ZBTB7A	1,00262916	LPIN3	0,9896929	PTGER3	0,97530828	GRM4	1,06972798	4307	RAD51L1	0,97599619	HOXA7	0,97278845	SOX9	0,97569364	COL25A1	0,98764112	IFNG	0,97614316	CD3E	0,95876262	NPTX1	1,04317102		
4238	PIF1	0,98635565	FUK	0,98494506	IVD	0,99804753	IL17RA	1,0022008	GCNT2	0,98923899	GOLGA2	0,97529181	UGT1A4	1,06959691	4308	YES1	0,97587933	AKT1	0,9727585	UHPP	0,97546985	ADH7	0,98751687	SMCHD1	0,97605172	ALOX5	0,95839129	ALDH3B2	1,04311377		
4239	INHA	0,98629768	POU5F1	0,98459768	PTPN6	0,99800578	TAP2	1,00212766	RETNLB	0,98902962	NR2F6	0,97503309	NOD2	1,06814857	4309	RHEB	0,97579937	GUCA1B	0,97234254	DARS2	0,97543399	MAOB	0,98751592	MYH2	0,97604992	CACNA2D1	0,95826823	CALB1	1,04228143		
4240	ST8SIA1	0,98629602	OAS1	0,98448518	PCNT	0,99724679	HES7	1,00210891	POLR3GL	0,98900426	SLC11A1	0,97475864	OAS2	1,0678776	4310	PRKAG2	0,97575384	PIGN	0,97214222	CD3G	0,97534438	CHRNA4	0,98743222	MAGI2	0,9757482	BCMO1	0,95799294	MCPH1	1,04227527		
4241	SLC30A8	0,98616934	NQO2	0,98446738	GSTT1	0,99703102	CMAS	1,00136317	APOA1	0,98872719	NDUFA12	0,97463568	TBK1	1,06778469	4311	BCAP29	0,97558905	BTRC	0,97202306	TNFRSF13B	0,97515926	CYP2U1	0,98740197	HYAL1	0,97554486	SH2D3C	0,95786616	CDS1	1,04226188		
4242	HMGCS1	0,98616416	NFKB1	0,98443598	ARNT	0,99690928	UAP1	1,00117729	SUMO3	0,98870425	ECHS1	0,97435958	CBX7	1,06726722	4312	GRIK4	0,9754766	RAB10	0,97188837	WNT5A	0,97495531	KLK2	0,98710524	PODXL	0,975099	EREG	0,95775686	PFKP	1,04196956		
4243	OGDHL	0,98606923	BMPR1B	0,98438741	POU5F1	0,99645339	DAPP1	1,00103612	HDAC8	0,98817801	MAN1B1	0,9742618	SF1	1,06726722	4313	RCAN1	0,97522948	MAN2B2	0,97139793	SEPT2	0,97442421	GRIA4	0,98641226	CLIC1	0,97458205	CYP2A6	0,9572988	TERF1	1,0414021		
4244	MARS2	0,98605071	ANP32E	0,98429575	SH2D3C	0,99589042	PRC1	1,00102003	CALCRL	0,98817672	LRP2	0,97415388	GYS1	1,06714797	4314	MTMR2	0,97516947	ATP5G1	0,97101378	CEBPA	0,97432515	DHRS1	0,98618631	DDB2	0,97387224	CHAT	0,9569506	DLL1	1,0411914		
4245	HIC1	0,98593683	JAK3	0,98428643	HYI	0,99551859	DGKA	1,00061481	PON2	0,98716982	CPO	0,97361033	RAPGEF1	1,06674854	4315	AKAP10	0,97498247	IFNA1	0,97058657	IARS	0,97428178	SCD	0,98522426	CYP11A1	0,9738273	COQ6	0,95654787	ALDH18A1	1,04054294		
4246	DIO1	0,98585455	SOX10	0,98422773	CSDA	0,99549786	TXNDC1	1,00016593	NDUFA4	0,9870761	GBP1	0,97348141	LIG3	1,06663426	4316	NDUFA12	0,97481199	SYK	0,97025934	CBL	0,97412092	AKT1S1	0,9848461	DNAJB11	0,97357815	NPTX1	0,95608178	CDA	1,04022631		
4247	MYL9	0,98562302	TNFSF13	0,98399347	BCMO1	0,99533466	PRKCZ	1,00010371	COQ6	0,98669698	PIWIL2	0,97340928	NRG2	1,06593662	4317	CYP2S1	0,97473423	HS3ST1	0,97010842	SERPINB5	0,97404676	DHFR	0,98458058	CSNK1G2	0,97354572	PAK1	0,95593924	GNAI2	1,04001678		
4248	ABCA4	0,98560664	UGT2A3	0,98390687	PPCS	0,99525248	HS6ST2	0,99993112	UHRF1	0,98668756	PDXK	0,97287553	PRPF40B	1,06551536	4318	CLDN20	0,97465338	ALDH9A1	0,9701031	CLTCL1	0,97383916	ELA2A	0,98405665	PAK1	0,97342689	ADK	0,95584939	CCKAR	1,03972543		
4249	DEFB1	0,98540938	HBB	0,98377668	TBX1	0,99525232	AMPD2	0,99967812	IHH	0,98628834	PAK3	0,97282753	MEIS1	1,06498556	4319	TGM1	0,97439684	ATP6V1E1	0,96986148	NRCAM	0,97336154	DCTD	0,98374163	GSK3B	0,97342008	NCF2	0,95568522	CSNK1G2	1,03966611		
4250	LTBR	0,98533485	MAPT	0,98365713	CYP2S1	0,99508281	IMPDH2	0,99964364	ACTR3	0,98621905	ARHGDIA	0,97274535	FLT3	1,064617	4320	C4BPB	0,97433863	ALDOA	0,9694928	A4GNT	0,97335493	GAST	0,98348699	DEFB1	0,97320001	ACPT	0,95557601	LIN7A	1,03842222		
4251	CCND1	0,9852457	DVL1	0,98296106	PTK2B	0,99451153	FOLR1	0,99947636	ADORA3	0,98604145	FBLN1	0,9724317	BMP2	1,06370994	4321	MAGI2	0,97414847	EIF3H	0,9694423	MECP2	0,97272837	ATP6V0A4	0,98344698	GTF2E1	0,97275704	SERPINA3	0,95532053	FUK	1,03813925		
4252	PDCD4	0,98523629	CYLD	0,98292049	MAPK11	0,99400324	SREBF2	0,99895887	CASR	0,98586394	ST3GAL6	0,97206513	RPL11	1,06349921	4322	APOBEC3B	0,97412736	COASY	0,96926462	GALT	0,97261195	PPT1	0,98297581	NPY	0,97267891	PLAUR	0,95497019	WIPI2	1,03811035		
4253	HTR1A	0,98509903	TLR2	0,98290377	EDG1	0,99330902	CHST14	0,99867848	F10	0,98577045	SOAT1	0,97174635	BPNT1	1,06320711	4323	SULT1A2	0,97411236	ALDH3A1	0,96911827	UBE2G2	0,97223373	MMP9	0,98205727	NDUFV1	0,97224223	PA2G4	0,95445404	POLR1A	1,03784377		
4254	MLC1	0,98474457	MDM4	0,98276404	SRD5A1	0,99279025	BMPR1B	0,9986652	PUM1	0,98569445	SOX10	0,9714159	OGFR	1,06250251	4324	OLAH	0,97400065	FES	0,96864925	RPS6KB2	0,97213739	BCAT1	0,98149536	HSD3B7	0,97210502	SERPINB9	0,95409965	HTR3A	1,03764057		
4255	IMPDH2	0,98467828	EN1	0,98260891	HMGN1	0,99253152	COL18A1	0,9986652	P2RX7	0,98565421	NTHL1	0,97134824	PKP4	1,06218903	4325	ARHGDIB	0,97369312	CLCN7	0,96858314	TLK1	0,97195457	CACNA1F	0,98124357	C1QL2	0,97203899	MCM5	0,95395405	STAMBPL1	1,03738261		
4256	RALBP1	0,98464536	DLD	0,98210759	RALBP1	0,99222918	PA2G4	0,99858137	TXNDC1	0,98545105	GUCA1B	0,97123278	NSUN2	1,06171198	4326	CA2	0,97365236	EHHADH	0,96827887	STX17	0,97194675	AXIN1	0,98050804	NME1	0,97161502	GP9	0,95370831	TRPV6	1,03733224		
4257	MYOG	0,9846286	CYB5R1	0,98210271	CPT2	0,99184904	TP53BP2	0,99835342	NEFM	0,98504428	ACSL5	0,9710395	NEIL1	1,06170075	4327	RPN1	0,97354476	TICAM1	0,96820918	HPCAL1	0,97173854	ABLIM1	0,98011072	SOX10	0,97150503	CALCRL	0,95359524	PIGH	1,03649489		
4258	SLC27A1	0,98461425	PPOX	0,98187317	SLC22A6	0,99070423	PLCB1	0,99814645	LTF	0,98497999	UBE2B	0,97079206	B4GALT5	1,0613384	4328	GALNT7	0,97320518	PODXL	0,96818999	DAPK2	0,97108433	ATP2A1	0,97997141	ABP1	0,97098687	AVPR1A	0,95351773	MAPK14	1,03638382		
4259	ALOX5AP	0,9845977	KCNMB2	0,98170001	CTF1	0,9896376	NFATC4	0,99808336	NCOA1	0,98473563	JAK3	0,97076629	PPFIA4	1,0604395	4329	ERBB4	0,97297264	GSTO2	0,96761199	GOSR2	0,97092201	ACAA2	0,97982265	PIGL	0,97094832	GPRC5A	0,95333778	CHEK1	1,03548705		
4260	BIN1	0,98451543	EPPK1	0,98092981	EBF1	0,98886224	EIF4EBP2	0,99787154	AFMID	0,98453097	RAD51L3	0,97023831	PFN2	1,060014	4330	HBA2	0,972625	SEMA4A	0,96749094	ITPKB	0,97085239	BNIP2	0,97965247	B3GALT2	0,97091414	DEDD	0,95330052	STX11	1,03530583		
4261	TP53BP1	0,98448488	CACNA2D1	0,98077569	ZMAT3	0,98847966	ENPP2	0,99727059	CD200R1	0,98435627	DGKG	0,96991578	COL12A1	1,05837298	4331	PCNT	0,97252033	JAG1	0,96724511	CCND2	0,97085152	APBB3	0,97946864	RAB6A	0,9708161	SIX3	0,95327699	SOX1	1,03526849		
4262	CCK	0,98438233	GEN1	0,9804865	ESR1	0,98752377	HTR3B	0,99719429	TNFSF9	0,98370133	GUCA1C	0,96965881	GGT1	1,05794447	4332	FUCA1	0,97250305	JAK1	0,96680329	HTR6	0,97015748	OSBP	0,97929097	APOBEC3C	0,97047806	LAT	0,95306245	TIMP1	1,0346448		
4263	ABCA12	0,98411302	MET	0,9803153	BCL6	0,98705327	PLSCR1	0,99675745	ALOX12	0,98358398	WWP1	0,96957322	CLK4	1,0579441	4333	RHOQ	0,97247525	YWHAZ	0,96628542	MASP1	0,97006464	DACT1	0,979236	ADAM10	0,97040989	ATP1A2	0,95262796	MOBP	1,03439534		
4264	SLC10A1	0,98381422	CCR1	0,98024416	MAPK3	0,98681329	ME3	0,99643092	JAK3	0,98358261	GNRH1	0,96897672	HSD17B10	1,05794142	4334	PANK1	0,97246121	AADAT	0,96618725	PTPRJ	0,96982758	C4B	0,97907315	SULT1A1	0,96940473	POLR1B	0,95244103	ZMYND17	1,03327601		
4265	MTHFR	0,98355422	NDUFB8	0,98006351	MEF2A	0,98586272	GUCA1C	0,9963594	IFI35	0,98350003	NDUFS7	0,96830176	SRP9	1,05709072	4335	MSI1	0,97245277	HR	0,96604525	DIAPH1	0,96955197	SULT4A1	0,97873538	BCL2L14	0,96935168	UQCRC2	0,95212807	NR4A2	1,03244254		
4266	CD274	0,98339038	PSMB9	0,97978699	CD7	0,98569375	PLCD1	0,9963163	E2F4	0,98345291	MLYCD	0,9682557	ID2	1,05678137	4336	CTNNA3	0,97239024	ATG7	0,96601543	HTR3B	0,96909682	MADCAM1	0,97852776	PRKD3	0,96907362	B4GALT4	0,95195277	BET1	1,03217521		
4267	UBE2J2	0,9832168	ABCC5	0,97964099	HR	0,98560786	GPR81	0,99614342	TFRC	0,98340595	CD69	0,9681315	PAPSS2	1,05509974	4337	POLH	0,97232112	CDK10	0,96592257	PPYR1	0,9688605	OPRK1	0,97852623	NEIL2	0,9686833	BTG1	0,95193141	ATG10	1,03209293		
4268	PAFAH1B3	0,98317241	HES2	0,97928218	HSPA2	0,98531473	HS2ST1	0,9960159	PDGFRA	0,98302015	LYCAT	0,96759373	GRM2	1,0547577	4338	TBL1X	0,97225203	INPP1	0,96588058	SEMA4A	0,96879296	CACNA2D1	0,97843323	MAPK8IP1	0,96813137	UGT1A9	0,95163508	CEBPD	1,03146221		
4269	LPHN1	0,98315767	MTR	0,97926239	ADIPOR1	0,98497565	HPN	0,9959213	FYN	0,98287464	GALNT12	0,96634797	ST3GAL5	1,05475631	4339	ARHGAP6	0,97200299	GATA2	0,96566464	HRH2	0,9686824	CALCA	0,97838284	LAMC1	0,967859	LPA	0,95157676	ALDH6A1	1,03135781		
4270	SEMA4A	0,98311754	SLC18A2	0,9791026	ENPP3	0,98469363	HSPA1B	0,99557214	MAPRE2	0,98282347	CD3G	0,96632956	HPSE	1,05468565	4340	RASGRF1	0,97194823	UPT1	0,96518828	ITM2B	0,96818576	CD27	0,97806092	DDC	0,96768543	GMDS	0,95133254	TNFRSF8	1,03133698		

Table A4. Pooled-shRNA library screen on HEL cell line and MF-3: list of 2nd most depleted shRNAs for each experiment (ranking approach 1, RA1).

	NO ruxolitinib (setting 1)				Ruxolitinib (setting 2)				Ruxolitinib + CM (setting 3)				MF-3				NO ruxolitinib (setting 1)				Ruxolitinib (setting 2)				Ruxolitinib + CM (setting 3)				MF-3	
	Experiment 1		Experiment 2		Experiment 1		Experiment 2		Experiment 1		Experiment 2						Experiment 1		Experiment 2		Experiment 1		Experiment 2		Experiment 1		Experiment 2			
Rank	*Gene*	*Fold change*	*Gene*	*Fold change*	*Gene*	*Fold change*	*Gene*	*Fold change*	*Gene*	*Fold change*	*Gene*	*Fold change*	*Gene*	*Fold change*	*Rank*	*Gene*	*Fold change*	*Gene*	*Fold change*	*Gene*	*Fold change*	*Gene*	*Fold change*	*Gene*	*Fold change*	*Gene*	*Fold change*	*Gene*	*Fold change*
4341	BAX	0,9719301	NPM2	0,96514288	E2F4	0,9681799	PAX8	0,97786875	CYSLTR1	0,96653999	COL6A2	0,95086843	ABCD1	1,03042501	4411	UAP1	0,95965429	CBX4	0,9538089	TNKS	0,94801561	ORM1	0,95810846	CD7	0,95494268	CRADD	0,93976572	CA6	1,00324359
4342	OAS2	0,97184269	IGFBP1	0,9650531	HDAC5	0,96805551	HSD11B1	0,9770586	ARHGEF5	0,96632434	ITGAE	0,95084036	ERBB3	1,03039139	4412	ARF3	0,95957077	NPY	0,95371514	CD63	0,9476255	SOX6	0,95779991	PDGFA	0,95492248	WNT5A	0,9393167	ATP5A1	1,00304112
4343	INHBC	0,97141702	ALOX15	0,9649657	NME1	0,96793117	CSNK1A1	0,97642074	SFMBT2	0,96625524	PDE3A	0,95040408	RBBP7	1,03019181	4413	MMP2	0,95937582	SYNJ2	0,95361664	GJA3	0,94762109	CEACAM1	0,95777883	POLR1D	0,95473038	NEU1	0,93928356	FUT7	1,00288225
4344	HMGB1	0,97101641	C3	0,96489043	PCNP	0,96776741	IKZF1	0,97601723	EPS8	0,96620023	CYP24A1	0,95040026	ENPP1	1,03005983	4414	EDN3	0,95933055	CDKN2C	0,95359653	COL4A1	0,94746384	GPI	0,95726579	ACACB	0,9547223	CANX	0,93920504	IFNA13	1,00282691
4345	IRF7	0,97096876	SLC30A4	0,96473454	ABCG2	0,96758825	PAN2	0,97567432	SLC1A4	0,96616901	MTNR1A	0,95032025	PLSCR4	1,02972301	4415	ATP6V0A4	0,95918398	F8A1	0,95358524	KCNJ11	0,94727669	CEBPB	0,95704782	CYCS	0,95451946	TP53INP1	0,93904567	NOX4	1,00211955
4346	UGT1A3	0,97094335	PROM1	0,96430327	LEFTY2	0,9670073	GSTO2	0,97557038	PNLIP	0,96602396	UNC5CL	0,94998488	GATA2	1,02904904	4416	NEUROD1	0,95908733	CDC14A	0,95345354	PODXL	0,94694402	SEPT2	0,95683596	CLU	0,95370527	COL15A1	0,93884219	HAGH	1,00054365
4347	GJA3	0,97064631	RDM1	0,96377833	MAPKAPK3	0,96696069	CD1C	0,97545735	PLCB2	0,96574184	TFCP2	0,94986461	LILRB3	1,02891472	4417	SFRP1	0,95893216	HSPA2	0,95331032	ATP5G3	0,94642221	GSN	0,95656612	SCN4B	0,95349608	ARFGAP1	0,93875262	NPM1	1,00023846
4348	POLR1C	0,9704592	CFL2	0,9636702	WNT5B	0,96627231	UGT1A9	0,97539484	ALDOA	0,96547545	P2RY2	0,94979473	CHRND	1,0287652	4418	ERCC4	0,95867418	SEMA3A	0,95309409	ADCY4	0,94602246	VAMP2	0,95636464	PGR	0,9532378	TSHR	0,93839882	TRPM2	0,99990736
4349	IFNA16	0,9698963	TTF2	0,96361997	ANGPTL4	0,96612123	ATG4C	0,97514272	ALDH3B1	0,96508886	CNPY3	0,94978612	CA5A	1,02854908	4419	MAPK8IP1	0,95860488	STX10	0,95296687	SOX10	0,94493715	SLC6A4	0,95616124	CABIN1	0,95305344	IL10RA	0,93811727	F8A1	0,99974844
4350	KLRA1	0,96981415	DMC1	0,96343975	MDM2	0,96607035	CRH	0,97507107	LTB	0,96499486	C2	0,94952861	IFI35	1,02801435	4420	PANK4	0,95844667	CHRNB2	0,95269814	GIT1	0,94479043	MASP1	0,95592358	FSCN3	0,95256693	RETNLB	0,9378721	VKORC1	0,99942627
4351	KRT18	0,96973613	MAPK1	0,96303064	PIGO	0,96583234	FSCN3	0,97481554	ANP32E	0,96437263	HAO1	0,94935029	IL1B	1,02799683	4421	ITGA2	0,95814063	TUBB3	0,95222785	FSHB	0,94421682	HPGD	0,95566459	PIGH	0,9524929	CCNG2	0,93779261	FGF1	0,99919171
4352	CPN1	0,96965511	CALCA	0,96302812	CYP1B1	0,96578263	PRNP	0,97369172	ARAF	0,96421999	ACAN	0,94931107	SNX6	1,02795828	4422	MYBPC2	0,95807956	ACP5	0,95200664	GRASP	0,94373136	KCNN3	0,95552927	CPSF1	0,95227842	P2RY6	0,93777828	PPAP2C	0,99914647
4353	CD1C	0,96945895	LRDD	0,96245515	CALCA	0,96576696	GNG13	0,97314029	PSCD1	0,96401739	ATP2A1	0,94831399	EN1	1,02734908	4423	REV1	0,95806438	PIK3CG	0,95176853	DNMT1	0,9437111	GABRB2	0,95538084	NFAM1	0,95214246	FSCN3	0,93764712	TNFRSF18	0,9989963
4354	GUCA1B	0,96941556	CFHR2	0,9624188	NR0B2	0,96540212	GABRA2	0,97304412	CNR1	0,96393999	ADIPOR1	0,94806245	ERN1	1,02586056	4424	ATG16L1	0,95757543	PGK1	0,95175198	TGFBR3	0,94361663	AGK	0,955258	COL13A1	0,95132223	LNPEP	0,93763936	COPS5	0,99851768
4355	WFS1	0,96904689	ADRBK1	0,96231589	PLD1	0,96524325	KCNJ9	0,97286893	HEL308	0,96386948	PPCS	0,94755654	CTTN	1,02534514	4425	DPYS	0,95740011	GALNT2	0,95159937	DEFB1	0,94348671	GPX7	0,9551187	COQ5	0,95127549	F11R	0,93763002	TNFRSF10A	0,99800961
4356	MAPK1	0,96892523	GNA12	0,96230923	TRIO	0,96443618	POLE4	0,97264855	BAX	0,96384162	GLP2R	0,94749248	CD3G	1,02524666	4426	FUT1	0,95717837	GHRHR	0,95158197	ATOH1	0,94313177	FXYD2	0,95508832	RAB24	0,95120226	CCK	0,93710885	ASRGL1	0,99785403
4357	NRCAM	0,96874253	HLA-DMA	0,96167953	BLVRA	0,96403733	ALG12	0,97259425	PPME1	0,96354855	CYP4A11	0,94744706	PRKCB1	1,02466002	4427	BMI1	0,95707091	CTTN	0,95126899	TCL1A	0,94290162	IFITM3	0,95480809	DCT	0,951074	GALNT14	0,93699342	GCAT	0,99746176
4358	AKR1D1	0,9685634	NDUFB4	0,96147223	ACVR2A	0,96401195	NAT5	0,97236219	B3GNT3	0,96333547	GNE	0,94707565	WAS	1,02447563	4428	AVPR1A	0,95690524	GATA3	0,9511994	AMDHD2	0,94270942	TLR6	0,95457212	GBP2	0,95103299	PNPO	0,93696127	XCR1	0,99725861
4359	ZDHHC8	0,96853553	AK1	0,96130577	GALE	0,96363191	RDH13	0,97233499	AHCY	0,96312922	TRPV1	0,94702738	ERCC3	1,02389606	4429	IDE	0,95656299	GRIN2C	0,95111364	LPA	0,94214977	KLC1	0,95408071	FANCL	0,95078103	SUMO3	0,9369441	CDC20	0,99696044
4360	CD63	0,96852336	TRAF4	0,96129982	ACSL5	0,96324376	JUND	0,97122191	PPP1R1B	0,96312921	TBP	0,94702001	MLH1	1,02369398	4430	TCF7L2	0,95641831	PMS2	0,95077866	RDH13	0,94185916	IKZF3	0,95400151	TGFA	0,95071197	LAMC1	0,93692903	REG3A	0,99656669
4361	POLRMT	0,96841266	BIRC3	0,96112868	CNTF	0,96298273	ADSL	0,97068726	CTTN	0,9630211	CXCL6	0,94660919	FMO2	1,02290465	4431	PDGFRA	0,95613429	DARS2	0,95051661	GABRB2	0,94179205	CHST1	0,9534074	CCND1	0,95061369	RGS16	0,93688093	PARC	0,99474302
4362	BYSL	0,96811557	GABRB1	0,96074471	PPP1R1B	0,96289899	CYP4F3	0,97003548	BLVRA	0,96295394	IGF2	0,94658471	GBP2	1,02259172	4432	PCNP	0,95603011	APLN	0,95049353	FTO	0,94090957	ABCA9	0,95331932	FN3K	0,95015216	EFNB2	0,93687213	DNAJA1	0,99462648
4363	CRK	0,96787024	UBE2J2	0,96056668	ACADVL	0,96265908	RAB9A	0,96986748	ALDH9A1	0,96290479	ALDH4A1	0,94648703	SH2D3C	1,02220943	4433	IFNA13	0,95598916	HSD17B8	0,95002416	TLR3	0,9401196	NDUFB8	0,95294364	LPA	0,95011902	PLSCR1	0,93564563	GP9	0,99398944
4364	CLDN5	0,96775802	ALPPL2	0,96051426	PEG3	0,96235913	APOBEC3A	0,96941398	B4GALT4	0,96284072	BMPR2	0,94644632	ARHGEF4	1,02180799	4434	HIP2	0,95586225	CUL3	0,9498607	POLR3A	0,93980528	SOX17	0,95286005	TBX2	0,94944549	FTCD	0,93556702	APBB2	0,9933217
4365	APOBEC3C	0,96725346	NPR3	0,96003987	BAG1	0,96219994	BHMT	0,96909815	RHOQ	0,96252623	MYL9	0,94641302	GZMB	1,02140209	4435	FGFR1	0,95580944	DBH	0,9497303	MT3	0,9397805	CLDN17	0,95256376	CD6	0,94916841	CIITA	0,93521275	MSH2	0,99299333
4366	SULT1C2	0,96716373	STMN2	0,95942938	RUNX2	0,96183323	CYBA	0,96827016	EIF1	0,96252417	UBE2E2	0,9463361	SUCLA2	1,02070189	4436	NR2F6	0,9554641	NMNAT2	0,94970127	AKAP10	0,9396764	GSTK1	0,95253872	CAMK1G	0,9488161	PDE4C	0,93489724	HTR3D	0,99056763
4367	IL6R	0,96710717	DDB2	0,95933474	FXYD2	0,96181844	RERE	0,9679885	TSPO	0,96245108	DUSP14	0,94622461	NOS1AP	1,02023184	4437	ARPC1B	0,95532612	CLDN16	0,94961108	NFKBIB	0,93940273	WASF3	0,95206387	MAPK8IP2	0,94857108	CMA1	0,93485472	EPN1	0,98953865
4368	ARFGEF2	0,9670078	SULT4A1	0,95909326	VAV2	0,96124225	CHRM4	0,96719782	ATF3	0,96242631	LRRK1	0,94608989	AGMAT	1,02015006	4438	BCL2L2	0,95529638	DPYS	0,94933011	CCL4	0,9390341	CTSS	0,95203955	UCHL1	0,94806011	MT3	0,93428546	GALNT14	0,98939757
4369	LCP2	0,96692744	IFRD1	0,95894733	CTSB	0,96121099	EFNA1	0,96718713	CAPN3	0,96233691	RPA4	0,94593847	PDLIM5	1,019905	4439	DPAGT1	0,95510338	HMGN1	0,94927508	SLC6A2	0,93864268	LPA	0,95172397	USH1C	0,94774871	GLG1	0,93380863	GABRD	0,98893133
4370	LIG1	0,9666123	GGCX	0,95891586	GRIA4	0,96079148	ABCA10	0,9671565	FGF1	0,96206001	ID4	0,94564482	KMO	1,01975084	4440	CCKAR	0,95484682	ITPK1	0,94920702	BAD	0,93825112	EPHX2	0,95160263	F13A1	0,94743579	GPR161	0,93377503	TSPO	0,98891395
4371	DUSP10	0,96651474	KLF2	0,95891586	SLC10A1	0,96035684	FLT3LG	0,9669041	ADHFE1	0,96205876	CD14	0,94550258	PTGIS	1,01965106	4441	TEP1	0,95478898	TCF15	0,94910261	ME2	0,9380219	ARHGDIA	0,95039164	TP53BP2	0,94729292	TNFSF10	0,93358941	ITPR1	0,98884968
4372	SLK	0,96645769	CDC25C	0,95886349	GDF15	0,96029214	MAPK11	0,96678383	FSHB	0,96201535	MYD88	0,94543264	CD9	1,01767615	4442	ABCA8	0,95459356	P2RY5	0,94910173	BHLHB2	0,93727847	LCN2	0,95018203	POR	0,94710344	IFNA21	0,93357322	PDE3A	0,98870381
4373	GALNT6	0,9662561	FURIN	0,95882183	ST8SIA5	0,96022662	OLAH	0,96664977	HS6ST2	0,96142476	GABRB3	0,94530433	GALNTL2	1,01677743	4443	AMY1B	0,95444469	MNAT1	0,9490009	LILRB3	0,93654978	AGPS	0,94986871	CAV2	0,94681371	EBF1	0,9334094	SH3GLB2	0,98861651
4374	CYB5R3	0,96608021	CYP4F3	0,95877513	ECSIT	0,96008463	ST8SIA1	0,96658528	PLAUR	0,96119907	ACADSB	0,94529594	BTD	1,01675748	4444	VAV3	0,9542207	GABRB2	0,94894681	ROCK2	0,93649189	ITGB7	0,94952727	CD1E	0,94640019	SERPINB5	0,93269851	CSTF1	0,98850789
4375	IL27RA	0,96567959	LIG4	0,95863704	GPR77	0,95982919	JPH3	0,96627577	P2RY2	0,96118216	SET	0,9451909	IL4	1,01640633	4445	PLOD1	0,95366438	TRAFD1	0,94850416	ALDH1A1	0,93622314	ZNF259	0,94951842	LRDD	0,94634644	TNFAIP6	0,93263881	BRAF	0,98840728
4376	PER2	0,96564661	HPSE	0,95861708	IFNAR1	0,95957209	SCN4A	0,96544468	NPEPPS	0,96103199	TAAR6	0,94478407	CD180	1,01637582	4446	RB1	0,95362195	GPX7	0,94843619	TRAF2	0,9360539	COPS3	0,94873489	NPM2	0,94629627	ADCYAP1	0,93232093	HCCS	0,98822086
4377	CALCRL	0,96546594	ABCA9	0,95861299	THPO	0,95945084	GPRC5A	0,9647826	MEPE	0,96101503	PIN1	0,94470051	PIK3C3	1,01602938	4447	SOX10	0,95361844	PRL	0,94828549	CHAD	0,93589373	CYP3A4	0,94822151	RAC1	0,94617387	MITF	0,93218733	PTGS2	0,98814398
4378	MMP8	0,96543901	RAB11A	0,95853777	BCAT1	0,95925196	ATOH1	0,964759	CLTCL1	0,96062293	POU5F1	0,94457718	TNFSF9	1,01562041	4448	PRKCG	0,95332845	IFITM3	0,94781072	NCOA4	0,93552597	GOT2	0,94778343	IRX3	0,94585827	PPP1R3A	0,93198987	CTNNAL1	0,98740688
4379	ATG2B	0,96510533	CRADD	0,95839454	MAOB	0,95919653	MTHFR	0,96475793	SMARCA4	0,96050115	STAT2	0,94456146	RORC	1,0153084	4449	SH3KBP1	0,95331639	GDF1	0,94778433	RFK	0,9355152	CD1D	0,94769804	ATF1	0,94508141	GYS1	0,9319616	ATP5H	0,98692417
4380	HDAC4	0,96501268	UGT1A4	0,95836004	NPPB	0,95835914	UGT1A3	0,96411056	MAP1B	0,96037311	WASF3	0,94451635	CYP4A22	1,01499486	4450	MDH1	0,95321021	HMGB3	0,94731298	APOA2	0,93523925	HMGB3	0,94736799	STX16	0,94467835	CRY1	0,93186957	PLA2G5	0,98674747
4381	PGLS	0,96481234	C5	0,95828	SH3KBP1	0,95726981	BCAP31	0,96391007	POLR3G	0,96026595	EEF2K	0,94439973	GLUL	1,01491255	4451	ABCG2	0,95308281	COL22A1	0,94696995	IGFBP1	0,9349142	MIB1	0,94736613	WIPI2	0,94466107	MAPK8IP1	0,93175864	CMA1	0,98571218
4382	POLE4	0,96460595	TPI1	0,95789403	ITGA4	0,95702596	PDGFB	0,96390478	NPM1	0,95995055	EGFR	0,94438093	DHRSX	1,01433212	4452	CD33	0,95307948	GADD45A	0,94689135	BRD4	0,93484188	FCN1	0,94727082	LY75	0,94423953	MAPKAPK2	0,93166781	PUM2	0,98470235
4383	GALK2	0,96437546	ST6GALNAC2	0,95758598	GYS1	0,95601212	AFP	0,96373823	BTG1	0,95985066	DERA	0,94433975	CHRM1	1,01410207	4453	NMU	0,95302151	PPP3CB	0,94675692	ANP32E	0,93397292	FSCN1	0,94685797	AGTR1	0,94404825	ZIC1	0,93137528	IFNA4	0,98403544
4384	CER1	0,96419993	BHLHB2	0,95755641	LAT	0,95598505	STX10	0,96362159	ID1	0,95976711	APOD	0,94413273	CRAT	1,01400646	4454	FECH	0,95274749	VCL	0,94661753	ACTN2	0,93391936	VAV3	0,94674157	ENPP3	0,94365062	PLD2	0,93133768	EGF	0,98402904
4385	CYR61	0,96394151	AARS2	0,95751466	GUCA1B	0,95499398	NOS3	0,96339383	CCR4	0,95976092	BCL2L10	0,94397945	PLA2G6	1,01350736	4455	MAP3K13	0,95211706	SULT1C2	0,9465897	RAB1A	0,93340647	CCNB1	0,9460377	FOXL1	0,94351799	NOD2	0,93126771	FADS1	0,98391653
4386	IRAK1	0,96390559	CD69	0,95730444	RDH5	0,95485943	MKNK2	0,96306551	RAB7A	0,95963989	CNP	0,94388718	NTSR1	1,01285963	4456	DDEF2	0,95197124	COL17A1	0,9461424	RDH11	0,93336058	BAG1	0,94585047	APOE	0,94305541	AVEN	0,93066715	VTN	0,98373653
4387	HSPA2	0,96379123	GCM1	0,95709246	CEACAM1	0,95456858	APOBEC3C	0,9628283	CNGB1	0,95842609	HPN	0,94381871	DHODH	1,01273201	4457	XAB2	0,9518474	RAD52	0,94507239	WASF1	0,93329897	STMN1	0,94579855	IDS	0,9429213	ATF5	0,929898	PIAS4	0,98312873
4388	CAMK1G	0,96365326	CUL2	0,95696551	FRAT2	0,95434012	MAN2B2	0,96280527	CD3EAP	0,95842498	FHL2	0,94372836	FOXN1	1,01198745	4458	RAD51L3	0,95156956	ISG15	0,94490828	AXIN1	0,93307584	HAO1	0,94536921	CUL1	0,94264893	PNLIP	0,92979725	EGR2	0,98217098
4389	DKK4	0,96347642	UROD	0,95678792	FLAD1	0,9540483	ATP6V1B2	0,96274279	SOX1	0,95841911	FGFR2	0,94362655	PIK3R3	1,0119843	4459	ADM	0,95135843	CD86	0,94483537	MAP4K5	0,93307321	GRIN2C	0,94452766	PER2	0,94193212	PHF1	0,92977704	CLEC10A	0,98191118
4390	FCGR1A	0,96311535	ALCAM	0,95652081	GTF2E1	0,95388646	HIC1	0,9625113	IFNA13	0,95839614	HMGA1	0,94292879	OSBPL5	1,01112085	4460	PPT1	0,95128916	DKK4	0,94466822	MCM3	0,93300523	CBL	0,94433223	ACVR1	0,94184482	PYCARD	0,92968464	GALK1	0,98113241
4391	MUTYH	0,96303221	ECSIT	0,95645961	HMGB1	0,95386244	PTPRU	0,96247829	SCLY	0,95823358	HIG2	0,94287507	PROZ	1,01110728	4461	PYCARD	0,95122114	PRKCG	0,94428497	HP1BP3	0,93290248	TBX2	0,94432257	HMOX2	0,94180542	RAB9A	0,92920174	DAB1	0,98071913
4392	FANCL	0,96284738	TRIB3	0,95640772	GABRE	0,95361214	SGK	0,96228884	MTHFR	0,95820499	ABCC3	0,94283779	SCN5A	1,01076212	4462	RALGDS	0,95119122	MTNR1A	0,94428146	COL17A1	0,93245469	BAG4	0,94407448	PPCDC	0,94092933	ARAF	0,92893386	COPA	0,98024655
4393	NFKBIB	0,96280083	NDUFA12	0,95621083	PITPNB	0,95361173	NTF3	0,96226449	ADH7	0,95819352	SLC1A6	0,94267412	OSBP	1,01046473	4463	HDAC6	0,95108586	GRASP	0,94400281	KCNJ9	0,93131449	GSTM1	0,94077934	GSTM1	0,92881341	ARHGEF6	0,97891324		
4394	GRIN2D	0,96262329	PIGC	0,9560761	CYP24A1	0,95350878	CD63	0,96211092	GDF11	0,95795612	STX11	0,94254962	STX2	1,01005492	4464	CPT1A	0,95102357	EPS8	0,94379945	POU2F2	0,93079049	HSD3B7	0,94397778	TOP3B	0,94077738	CNR1	0,92858053	CDC26	0,97821245
4395	EDN1	0,96248248	HERPUD1	0,95596654	RHOQ	0,95343076	HYAL1	0,96199898	GALNT1	0,95752107	SSTR2	0,94241785	ETS1	1,00976029	4465	CYBA	0,95087202	ARF4	0,94344669	GSTO2	0,93065776	CSTF2	0,94325101	GAS2	0,94025399	CLEC7A	0,92854447	GPR64	0,97820719
4396	ALG9	0,96234572	MAD1L1	0,95592731	TXNDC1	0,95317084	ADRBK1	0,96178179	RALGDS	0,9574613	CPT1A	0,94228567	PTGER4	1,00865141	4466	MAT2B	0,95076944	CAMP	0,94335512	TRH	0,93057616	ALDH18A1	0,94289648	SYK	0,94023281	SFRP1	0,92839962	WNT6	0,97767551
4397	NFAM1	0,96230667	TFAP2A	0,95591293	MECR	0,95303463	CTNNA3	0,96143542	ABCB4	0,95734959	NCOA4	0,94218615	IL18	1,0082212	4467	SALL1	0,95069137	STH	0,94304878	SDS	0,93014378	FOXO3	0,94245482	ACVR2A	0,9401459	HEL308	0,92834751	SERPINA3	0,97728081		
4398	CDK5R2	0,96230246	EBF1	0,95548182	TGFB1	0,95303416	C4A	0,9613055	RNF2	0,95723542	PGF	0,94206867	CHEK2	1,00766889	4468	THRA	0,95067334	CCNE2	0,94303975	HOXB4	0,93009322	GSTA4	0,94243698	DNMT1	0,93962146	WIPI2	0,92834371	NCR1	0,97718756		
4399	GYG1	0,96226981	ADRB2	0,95534783	PDE1A	0,95299895	ETS2	0,9606317	NODAL	0,9572138	SLC30A4	0,94167334	ACTN3	1,00720659	4469	CUL3	0,95043475	EHMT2	0,94302524	MEIS1	0,93008344	BMP8B	0,94240791	MEF2B	0,93960906	PRKCH	0,92825235	PARP2	0,97685009		
4400	APLP1	0,96223873	KRT18	0,95525786	B3GALNT1	0,95257699	ADIPOR1	0,96057961	HNF4A	0,95710456	GAB2	0,94156129	CAPN7	1,00715933	4470	CACNA2D3	0,95023128	OTC	0,94285447	XAB2	0,92992969	AGT	0,94238453	GCDH	0,93952874	PROC	0,92793438	SCNN1B	0,97663566		
4401	CTNNA2	0,96182802	PSAT1	0,95505164	GLO1	0,95257214	ATP5F1	0,96056735	GABRB2	0,95682496	BCL10	0,94140346	ABCB8	1,00710087	4471	B3GNT7	0,94958279	RNF19A	0,94254851	MIB1	0,92967861	ANGPT2	0,94234019	NR1I3	0,9390891	MTHFR	0,92779754	BGLAP	0,97658613		
4402	UTF1	0,9612542	BCL2A1	0,95500907	SOX6	0,95187496	CD80	0,96029047	TREX2	0,95679982	CPT2	0,9412638	HSD3B7	1,00670994	4472	PIK3C2G	0,9493639	CYP17A1	0,94226754	ARPC1B	0,92931287	NOX4	0,94226754	ARPC3	0,9386214	WRN	0,92764336	GCDH	0,97606024		
4403	HLA-DMA	0,960959	FLJ21865	0,95489659	IKBKB	0,95151714	NR2F6	0,96003155	ANGPTL3	0,95674746	NFATC4	0,94117997	UGCG	1,00647038	4473	MCM4	0,94923848	NEUROG3	0,94228872	GC	0,928979	MAP3K1	0,94133749	GUCA1B	0,93859953	AHR	0,92757015	OLAH	0,97473446		
4404	RGS16	0,96093905	SPTBN4	0,95481114	CDKN2A	0,95126214	CD34	0,95989587	NEUROG3	0,95673018	CCL4	0,9409013	LPA	1,00631812	4474	MAP2K3	0,94916205	C4BPA	0,942284	AKTIP	0,92891274	GJA1	0,93964311	STK11	0,93859213	UGT8	0,92730099	TNKS1BP1	0,97446078		
4405	TCF15	0,96091438	PDE1C	0,95480779	GUSB	0,95064326	ANP32E	0,95984798	NTAN1	0,95659656	B3GNT3	0,94088382	PARK7	1,00607221	4475	LFNG	0,94891425	FANCB	0,94215343	ADK	0,92834369	PTGES	0,93918533	PLA2G2A	0,93820742	FLT1	0,92696438	LCT	0,97416567		
4406	AADAT	0,96080015	LGMN	0,95471966	LPIN3	0,95048668	RXRB	0,95982982	NOS2A	0,95647428	BBOX1	0,94072032	CMBL	1,00592186	4476	PMS2L3	0,94882567	IL6R	0,94211576	LAMC1	0,92775376	KIF3A	0,93906911	PAFAH1B2	0,93770554	INPP4B	0,92660229	HPRT1	0,97414954		
4407	KCNMA1	0,95994237	CTCF	0,95461884	TBP	0,95033446	TP53INP1	0,95979104	AXIN1	0,95639995	UBE2D2	0,94044868	TLR2	1,00443231	4477	TRIB3	0,94871995	ATP1A2	0,94203154	SULT1E1	0,92706958	GATA2	0,93892595	GSTK1	0,93749056	PHKG1	0,92622531	TAAR6	0,97414134		
4408	IL1RN	0,9598313	ACADSB	0,95458722	CA13	0,94958026	IRF8	0,95927536	DBT	0,9562402	FTO	0,94018485	TGM2	1,00417264	4478	CHRNB3	0,94853561	CALML5	0,94164344	RXRB	0,92690636	MAPK8IP2	0,93886462	IL21	0,93725365	THOP1	0,92593989	BAD	0,97352022		
4409	SMO	0,95981297	UNC5CL	0,95440279	CYP2A6	0,9494155	ATP6V1E2	0,95899792	SMAD2	0,95545732	KCNQ5	0,93997435	TFAP2A	1,00384913	4479	IFNA21	0,94818144	NRCAM	0,94160477	VIPR1	0,92659865	PTX3	0,93860765	IPMK	0,93725023	HSPG2	0,92522888	NDUFA4	0,97340669		
4410	GNRHR	0,959744	H2AFY2	0,95400365	PAX3	0,94891348	MAPK14	0,9581202	PLSCR1	0,95512831	HTR2B	0,93980488	PPP5C	1,0032697	4480	NEIL1	0,94815331	EHD2	0,94124519	PYCARD	0,92606016	NRCAM	0,93853097	ADIPOQ	0,9370941	GRM8	0,92484244	MB	0,97280632		

Table A4. Pooled-shRNA library screen on HEL cell line and MF-3: list of 2nd most depleted shRNAs for each experiment (ranking approach 1, RA1).

	NO ruxolitinib (setting 1)				Ruxolitinib (setting 2)				Ruxolitinib + CM (setting 3)				MF-3				NO ruxolitinib (setting 1)				Ruxolitinib (setting 2)				Ruxolitinib + CM (setting 3)				MF-3	
	Experiment 1		Experiment 2		Experiment 1		Experiment 2		Experiment 1		Experiment 2						Experiment 1		Experiment 2		Experiment 1		Experiment 2		Experiment 1		Experiment 2			
Rank	*Gene*	*Fold change*	*Gene*	*Fold change*	*Gene*	*Fold change*	*Gene*	*Fold change*	*Gene*	*Fold change*	*Gene*	*Fold change*	*Gene*	*Fold change*	*Rank*	*Gene*	*Fold change*	*Gene*	*Fold change*	*Gene*	*Fold change*	*Gene*	*Fold change*	*Gene*	*Fold change*	*Gene*	*Fold change*	*Gene*	*Fold change*
4481	GCG	0,94808483	UGT2B15	0,94094804	DDB2	0,92559981	CHN1	0,93805685	ACSL1	0,93656271	PARP4	0,92479981	ARHGAP4	0,97248133	4551	SKP2	0,93564197	ATP8A1	0,92348536	ABCA9	0,90630879	IL21	0,91897552	PMM1	0,9189935	BCKDHA	0,9091741	PIP5K2B	0,94328739
4482	MAFK	0,94794571	CANX	0,94094317	BHLHB9	0,9241856	PAX3	0,93789227	ACPT	0,93644849	PLCD1	0,92473896	BNIP2	0,97193154	4552	GLI1	0,93485626	C4B	0,92328553	ABCG1	0,90593106	KCNK1	0,91850757	FLT3	0,91878874	RAC2	0,90914149	CCL3	0,94328582
4483	CA8	0,94793041	ACAD9	0,94077116	UBE2N	0,92410829	GPR65	0,93771239	ASPA	0,93613878	LEFTY2	0,92456748	ITGB4	0,9717518	4553	GAD2	0,93470353	HS3ST3A1	0,92317841	ALG2	0,90591151	C1QL3	0,91766588	CD8A	0,91876282	HK3	0,90884424	STX1A	0,94328582
4484	VCL	0,94727851	PAPPA	0,94074041	CBX5	0,92350644	FABP6	0,93770292	GCG	0,9355159	PSMB5	0,92377269	CBL	0,97127328	4554	CNR1	0,93469199	MT3	0,92315218	SLC18A2	0,90576642	SLC30A4	0,91758641	PGAP1	0,91806647	IFNE1	0,90855784	COL6A1	0,94296361
4485	BBOX1	0,94724984	TAGLN2	0,93960557	LRPAP1	0,92346573	COL17A1	0,93759558	IKBKB	0,93546258	STAT3	0,92350935	ABCC4	0,97102614	4555	ITM2B	0,9345782	ADCY5	0,92307496	NOTCH3	0,90511987	ACSL1	0,91741447	GOSR2	0,91754225	HSD3B7	0,90851614	CEL	0,94213292
4486	ATP5G1	0,94706076	CALCRL	0,93949304	ATP6V1B1	0,92307902	CACNA1I	0,93682353	APRT	0,9353197	BLVRB	0,92344772	XRCC4	0,97065316	4556	PANK2	0,93427736	PMP22	0,92294543	NPY	0,9050764	DHRS2	0,91689248	GABRB1	0,91743337	BRCA2	0,90851238	CEP290	0,94189176
4487	PCK2	0,94698505	ATP13A2	0,93899743	HPR	0,9223204	ATP2B1	0,93629446	IL17RB	0,9350209	GRK1	0,92286437	HDAC11	0,97006072	4557	JAK3	0,93416431	NR1I2	0,92275243	BAIAP2	0,90464745	IDS	0,91662864	ACAA2	0,91678594	NR0B2	0,90802063	ELK3	0,94136018
4488	RAC2	0,94693747	BMPR2	0,93896056	ATF7IP	0,92195846	AMY2B	0,93628315	EHMT2	0,93493279	PAX3	0,92255092	CYBB	0,96961468	4558	FDPS	0,93414096	GLA	0,92246057	ABCA5	0,90439968	EXT2	0,9164999	CPN1	0,9166489	GYG1	0,90729113	TNFRSF10D	0,9405596
4489	PRLR	0,94627382	AFMID	0,93894709	CDKL1	0,92187162	GTF2H4	0,93623146	A4GALT	0,93451435	DOK2	0,92252883	SPCS1	0,96953144	4559	ZNF259	0,93388093	ERN2	0,92235526	IL17RB	0,90435917	MAP1A	0,91638879	NCOR1	0,91598647	PRKD3	0,90704439	ADAM8	0,93886363
4490	SNAP25	0,94623941	AMY2B	0,9388426	ELA2A	0,92076216	ALDOA	0,93609631	IL18	0,93428941	CHPT1	0,9220859	EEF1B2	0,9693834	4560	MAOB	0,93358161	ITGA4	0,92218	HDAC9	0,90337489	RNASEL	0,91626456	TTF2	0,91582642	TRAFD1	0,90694639	C1QBP	0,93787749
4491	RNF25	0,94617125	PRF1	0,93883587	CYP11B2	0,92062101	RECQL	0,9357555	GABRG1	0,93406554	MAFF	0,92193583	CCR4	0,96902253	4561	ANKFY1	0,93345343	HLA-DPA1	0,92165348	NR1H2	0,90309186	GRIK3	0,91607519	UGT1A5	0,91536367	IRAK4	0,90665584	AFMID	0,93752535
4492	AARS2	0,94609779	GPR77	0,93856055	TUBB4	0,92053885	CRY2	0,9353653	TREM1	0,93336241	CLN3	0,92192121	LGMN	0,96891883	4562	PRNP	0,93333635	MANBA	0,92159568	AVPR1A	0,90294483	B4GALT4	0,91568217	FUT1	0,91517785	HMGCS1	0,90658088	GNAS	0,93697315
4493	SCN2A	0,9460156	ASAH1	0,93833462	EIF2B5	0,92008629	CRHR2	0,93515791	HTR1A	0,93317811	SLC30A1	0,921825	PFKFB1	0,96872268	4563	MAN2B2	0,93333041	FGF5	0,92154365	ATG2B	0,90269473	AADAT	0,91562333	POLR1B	0,91455057	NEFL	0,90606991	MAPT	0,93601457
4494	CACNA1I	0,94560858	TREM1	0,93805794	ATP2A3	0,91983775	CD93	0,93448584	CSNK2A1	0,93296876	SMAD6	0,92145123	PIGN	0,96850611	4564	TAPBP	0,93309194	POR	0,92124613	MAGI2	0,90244553	NOS1AP	0,91473505	CIITA	0,91438979	COL5A3	0,9056741	ARF5	0,93554045
4495	SLC1A6	0,94557069	TNFRSF4	0,93797906	SIGLEC1	0,91963046	NPTX1	0,93437546	WASL	0,93283145	MST1R	0,92132271	UBE2H	0,9682258	4565	PARP2	0,93284113	IMPDH2	0,92108646	KCNIP3	0,90232841	HDAC9	0,91457015	NRF1	0,91389367	FUT6	0,9053867	EIF1AX	0,93550247
4496	CYBB	0,94555597	PARK2	0,93790289	TNFSF13	0,91947597	TGFBI	0,9343314	IFITM3	0,93203699	LTF	0,92092499	PXN	0,9680979	4566	GRM1	0,93222474	GRIA4	0,92100147	PSMB9	0,90231576	FURIN	0,91447517	NQO2	0,91383862	EIF2B1	0,90530203	HRH3	0,93490584
4497	DTX2	0,94534323	ITM2B	0,93757609	FN1	0,91921989	GBP2	0,93338827	APC2	0,9316357	AFMID	0,92039748	SETDB1	0,96809396	4567	RAPGEF1	0,93215027	LAMC1	0,92067911	SQLE	0,90188248	CHRNA6	0,9127918	INHBA	0,91314786	GABRA4	0,905251	TAGLN	0,9348263
4498	IRAK1BP1	0,94519858	ROCK2	0,93689802	SOD3	0,91915301	RAD51L3	0,93327136	IL1RN	0,9315344	ADRA2B	0,92005355	C10ORF110	0,96763406	4568	CANX	0,93196615	IRF3	0,92060363	CYP4F3	0,90146865	IL18	0,9125134	SULT1A4	0,91275521	ACCN4	0,90505118	BDKRB2	0,93399227
4499	DMGDH	0,94512141	SMO	0,93660444	TAF12	0,91894607	FBP2	0,93313745	MAP2	0,93141947	FEN1	0,92000717	HSD11B1	0,96762653	4569	ATP6V1E2	0,93185724	MADCAM1	0,92059112	TNIP3	0,90017937	POMC	0,91178454	BIRC2	0,9127295	UROS	0,9050434	GTF2I	0,93190884
4500	SCLY	0,94506477	ALDH3B2	0,93647559	LMNB1	0,91873007	MARS2	0,9330677	CUL3	0,93136123	GALNT10	0,91975789	KLRA1	0,9672047	4570	ELA3A	0,93166933	EFNA3	0,92044557	GCLC	0,89967464	ST3GAL4	0,91146623	G6PD	0,91271361	BCL2A1	0,90401269	HS3ST1	0,93159807
4501	CLN3	0,94497802	AVPR1A	0,93635849	CCK	0,91857441	SIGLEC1	0,93295888	IL17RE	0,93127777	MAN2B1	0,91972773	NUP214	0,96537354	4571	EPAS1	0,93165392	CYP2R1	0,92039809	GHRHR	0,89944489	CCKAR	0,91145028	ABCG1	0,91261115	KRT7	0,90395189	CSF3	0,9314099
4502	WASF3	0,94496492	BIN1	0,93599118	HS2ST1	0,91803596	ADH1C	0,93289824	GABRD	0,93121176	APOBEC2	0,91970563	RRM2	0,96510871	4572	PNMT	0,93161627	PDGFRA	0,92009097	PIWIL2	0,89929856	RDM1	0,91118252	FCER1G	0,9125073	ARF4	0,90372834	TF	0,92991318
4503	BMP10	0,94475267	C1QL1	0,93594046	TOR1A	0,91788429	GFI1	0,93284144	SPI1	0,93106915	ADH1C	0,91960968	BLMH	0,96486618	4573	ZFYVE9	0,93143968	BDH1	0,92002372	ANXA5	0,89794108	HRH2	0,91106958	GLP1R	0,9123744	SEMA4A	0,90360556	EGFR	0,92954049
4504	HTR1E	0,94457132	COL6A2	0,93591098	LPO	0,91742705	RFWD2	0,93179303	MAFK	0,93091265	CPEB1	0,91948575	PERP	0,96477004	4574	GGCX	0,93136467	ADIPOR1	0,92002003	IRX3	0,89791724	SLC34A1	0,91057726	KCNA5	0,91186384	F2RL2	0,90353564	NKIRAS1	0,92875319
4505	GEN1	0,94456642	ELA3A	0,93559614	GLA	0,91686781	DDHD1	0,93155405	ARFGEF2	0,93089943	KIT	0,91913239	FCGR1A	0,96439848	4575	PLA2G2A	0,93093799	KLRC3	0,91957081	PNPLA3	0,89740425	ADORA2A	0,91045457	PXN	0,91116394	FANCC	0,90347301	UBE2C	0,92775173
4506	ACSL1	0,94450187	SRM	0,93526181	CA9	0,91666689	BIRC3	0,93133839	SFRP1	0,93084244	PANK4	0,91879485	NUMBL	0,96402364	4576	TCEA3	0,92866079	MAP3K7IP1	0,91951235	BRAF	0,89687049	HCCS	0,91014924	ELA2B	0,91072112	GPR77	0,90330253	GNAZ	0,9264683
4507	PRKCZ	0,94437945	KLC1	0,93488363	ALCAM	0,9165354	CRY1	0,93111996	MYST4	0,93074718	OGDHL	0,91841036	ALDOB	0,96167037	4577	ACADM	0,92800151	CHN1	0,91929266	HLA-B	0,89676848	B3GALNT1	0,9100895	WWP2	0,91059021	SLC1A4	0,90326625	COASY	0,92543043
4508	SLC25A4	0,943987	DTX3	0,93471987	BZW1	0,916214	SET	0,93080294	OBFC2B	0,93060654	WASL	0,91836788	ADRBK1	0,96100184	4578	ST6GALNAC4	0,92773273	ALG6	0,91895834	ELA3A	0,89672775	RNF146	0,91004313	VCL	0,91051709	GTF2H2	0,90322052	GDF9	0,92463556
4509	BAG4	0,94382773	GALNT12	0,93466738	ACVR1	0,91588311	CCL5	0,93071664	KCNE2	0,93048747	DLAT	0,91813297	PDGFRA	0,96031093	4579	NR0B2	0,92770751	FNTA	0,9188816	GUCY1A3	0,89558401	ELOVL2	0,90974339	TIRAP	0,91028136	NPR1	0,90270132	HSD3B1	0,92424275
4510	LCN2	0,9437291	ST6GAL1	0,93460478	HOXA7	0,91574876	FANCL	0,93062032	BHMT	0,93010113	MKNK1	0,91773577	FOXO3	0,95983407	4580	WIPI2	0,92763131	UHRF1	0,91867672	NR1I2	0,89553796	MTMR2	0,90927924	AP3M1	0,9101035	ACP5	0,90208842	PPIE	0,92336554
4511	CHST6	0,94370825	CSNK2A1	0,93436743	FANCM	0,91566431	PSMB9	0,93049704	SERPINI1	0,92835802	NUP153	0,91753866	SERPINA4	0,9598079	4581	ATP5L	0,92736177	CSRP1	0,91669899	CNPY3	0,89482255	CFHR2	0,90894896	C5	0,91001637	TNFRSF17	0,90206454	OBFC1	0,92220514
4512	LAMB1	0,94347928	GP5	0,93403712	TSNAX	0,91534904	ACAN	0,93042973	G6PC	0,9283146	GHRH	0,91744902	GNS	0,95979276	4582	KMO	0,92735488	CALCR	0,91667048	GNGT1	0,89444467	CYP17A1	0,90849544	CALCA	0,90977011	LMO1	0,90204773	PLIN	0,92186212
4513	CCNB1	0,94346511	HTR3A	0,93400026	PDHB	0,91534458	ASIP	0,93029982	ABCA10	0,92786991	ADRB1	0,91722079	PKLR	0,95968783	4583	USH1C	0,92728873	PTK6	0,91664846	TCF15	0,89427446	LCMT1	0,90824819	POLI	0,90943322	XYLT1	0,90133376	HPGD	0,9204593
4514	IL13RA1	0,94303336	CD1D	0,93383893	COL11A1	0,91528365	COL4A1	0,93025659	CA2	0,92777536	HDAC2	0,91658683	DDHD1	0,95936746	4584	NDUFA13	0,927005	GPR64	0,91657182	MINPP1	0,89376032	ADH4	0,90774522	PFKP	0,90907245	HSPA1L	0,90109653	APOBEC3C	0,92012577
4515	ADH6	0,9430302	SDS	0,93376797	PDCD1	0,91484068	ETS1	0,9295465	CTNNA2	0,92760144	TSPO	0,91635742	CD1D	0,95821172	4585	ACAD9	0,92699451	GRASP	0,91650176	OGDHL	0,89366239	CYP2R1	0,90701498	IKBKG	0,90903634	CD7	0,9010616	PLA2G4C	0,91993119
4516	OPRK1	0,94297756	PLSCR4	0,93335973	HES2	0,91438658	UCHL3	0,92893626	CACNA1E	0,927503	GSTA4	0,91598666	CBLC	0,95718461	4586	UGT1A8	0,9269003	SEPT2	0,91640562	RAP2B	0,89354274	ALDH4A1	0,90679199	POU5F1	0,9090146	ITGAM	0,9010027	PMS2L3	0,91932304
4517	WASF1	0,94277326	ORC4L	0,93306071	GABRD	0,91394842	FOSL2	0,92878141	DLL1	0,92717197	AKT1	0,9159633	MGAT4B	0,95546971	4587	ALDH4A1	0,92678683	ARNTL	0,91598296	ADRA1D	0,89336534	NFATC2	0,90676349	TIFA	0,90898363	SCN3A	0,90084082	HP1BP3	0,91928187
4518	TRAF2	0,94265053	AMOTL1	0,93297471	CD80	0,91393772	SAA1	0,92875674	SCN3B	0,92704772	KLRC1	0,91594494	HS2ST1	0,95498689	4588	TBXA2R	0,92675475	MGAT5	0,91546758	MMP8	0,89265551	ARSA	0,9062808	RPA4	0,90878007	FCGR3A	0,90062652	GPR50	0,91918234
4519	MAPRE2	0,94247658	CDK5R2	0,93255436	CALCR	0,91393076	IFNA1	0,92875159	GDF1	0,92692451	CYP2D6	0,91585996	CES1	0,95478481	4589	GRM6	0,92668823	LHCGR	0,91525953	TP53INP1	0,89233203	ASCC3	0,90561479	CENTD2	0,90780866	TNIP3	0,89998873	ARSB	0,91898107
4520	NTHL1	0,9424426	SERPINB5	0,93249738	SLC18A1	0,91321807	RAPGEF1	0,92869074	IRF2BP2	0,92643997	PPAT	0,91562814	TGM1	0,95446115	4590	APOBEC2	0,92660799	ESR2	0,91511817	B3GNT5	0,89216501	KLRC2	0,9054904	ZFYVE9	0,90649802	IFNA13	0,89978405	NOS3	0,91866283
4521	DLD	0,94222861	APOBEC2	0,93181367	ABCA7	0,91314067	TICAM1	0,92845602	COL18A1	0,92643129	C1ORF142	0,91553091	PIWIL1	0,95427225	4591	CYP2C8	0,92647856	HSD17B12	0,91510967	CARTPT	0,89214726	COQ3	0,90520351	DDEF1	0,90555253	HIC1	0,89962453	SSTR4	0,91866267
4522	NNT	0,94148846	DAPP1	0,93152629	APOBEC3C	0,91311475	MAP3K13	0,92822811	CLDN19	0,92636486	IFRD1	0,91542805	DDC	0,95381052	4592	ACTN3	0,92636876	XPC	0,9150496	CRK	0,89208247	ABP1	0,90514517	HTATIP	0,90450901	MAP1B	0,89948151	DPYS	0,91815954
4523	ALG6	0,94130184	PIGF	0,93148091	CCR10	0,91276089	PIGQ	0,9279911	CTLA4	0,92633844	ACOT11	0,9153064	DNAJC5	0,95360829	4593	ENPP2	0,92561535	LAMB1	0,91502044	TPI1	0,89126216	MYL2	0,90503285	COL19A1	0,90399178	FES	0,89942039	MYOG	0,91711404
4524	MAP3K4	0,94052708	GHR	0,93144267	ENTPD3	0,91187703	CD97	0,92762733	PLEC1	0,92556814	CDX1	0,91494263	ADORA3	0,95341989	4594	ERN1	0,925158	PGAP1	0,9149452	POLR1C	0,89098297	UBE2J2	0,90500757	TXN2	0,90367413	GHRHR	0,89936898	HHEX	0,91709017
4525	RAD54B	0,9403633	GOSR2	0,93128539	ANPEP	0,91180103	ATP5O	0,92719994	FGF5	0,92525433	PAPPA	0,91490508	IGFBP6	0,95292848	4595	HIF1A	0,92513779	ADCY2	0,91473611	SERPIND1	0,89081378	ATP5D	0,90405035	FEN1	0,90359504	MS4A1	0,89936701	CHRNB2	0,91452726
4526	MYB	0,94015704	FOSB	0,93109024	GPX2	0,9117808	RAB24	0,92701044	ETFA	0,92484088	COL17A1	0,91489318	ABCC8	0,95283774	4596	IL1R2	0,92497134	TPP1	0,91455961	PLA2G2A	0,89056	SLC32A1	0,90380611	CDC25B	0,90350735	E2F4	0,89928345	SCN1A	0,91436088
4527	BCL2L10	0,94012264	CYSLTR1	0,93063929	ALOX5	0,91173884	TUBB3	0,92685595	ZBTB32	0,92428119	HMGN1	0,91471492	CCL16	0,95263026	4597	PRB1	0,92464073	OLIG2	0,91445637	CTSS	0,89036614	ALG6	0,90327974	CLDN20	0,90348234	ZDHHC8	0,89860035	CHKB	0,91316647
4528	HK3	0,94007247	PLA2G2F	0,93053888	EPN1	0,91163551	MCM4	0,92659248	FES	0,92413554	RERE	0,91464632	MPL	0,95234826	4598	PTK6	0,92452499	FCER1A	0,91406962	EDNRB	0,88983706	GLP1R	0,90313588	FSCN1	0,90292242	C1QL3	0,89815066	HGSNAT	0,91248461
4529	GPR37	0,93999584	IFI35	0,93038659	CRY2	0,91163519	BCKDHB	0,92623506	ST6GALNAC2	0,92382825	CHRM4	0,91448305	UQCRH	0,95220232	4599	LRPAP1	0,92444813	NR5A2	0,91381427	LTA4H	0,88981926	MDH1	0,90224407	ATP5F1	0,90281017	TSC1	0,89725119	GDI1	0,91176471
4530	DARS2	0,93998303	GRWD1	0,92959975	AHSG	0,91110105	NEU4	0,92471942	HADH	0,92360479	MGAT2	0,91438422	PSMD14	0,95191592	4600	PIGF	0,92407401	PA2G4	0,9137908	SLC30A4	0,88925222	TNFSF9	0,90185373	BMP2	0,9025406	VAV2	0,89717476	USH1C	0,91108245
4531	GHRH	0,93962456	HRH2	0,92947667	ITGB4	0,91084271	GCNT2	0,92454363	FGFR2	0,92324855	THPO	0,91372576	IFITM1	0,95155167	4601	BBS4	0,92401655	CLDN11	0,91348888	TNFRSF9	0,88862245	ACVR2A	0,90160259	SLC6A4	0,90197329	KCNN4	0,89704989	DLD	0,91077068
4532	FUT6	0,93937626	GMDS	0,92890443	DDHD1	0,91058333	PAPSS1	0,9243828	EXO1	0,92322524	DHRS3	0,9136774	STK36	0,95120152	4602	FXYD2	0,92395641	BLMH	0,91330552	MGAT4A	0,88861696	HBA2	0,90116308	ESR2	0,90173723	NQO2	0,8970478	POFUT1	0,91017174
4533	ADRBK1	0,9393735	POLD3	0,92888163	ANXA3	0,91051563	CER1	0,92436177	DGKG	0,9229866	ETS1	0,91352294	DNMT3A	0,95055121	4603	SIM1	0,92385384	SOX6	0,91281228	AIRE	0,88817085	HDAC8	0,90024719	CD53	0,90078392	APP	0,89678914	FGF11	0,91011297
4534	GRIA4	0,93926686	ALOX12B	0,92873204	PDGFA	0,91049783	FHL2	0,92420339	PTCRA	0,92287424	MAPT	0,91344032	ME2	0,95036114	4604	GCLM	0,9235901	MYOD1	0,91257511	ARSE	0,88792097	UROS	0,89990583	PMP22	0,90071865	GRM6	0,89673518	EMR3	0,9097594
4535	MGAT5	0,93924108	TNFRSF17	0,92872225	NOS1AP	0,9103482	ADHFE1	0,92404068	ZMYND17	0,92285076	SLC23A2	0,91269961	ANAPC10	0,94989291	4605	NPM2	0,92338122	DIO1	0,91248403	HTATIP	0,88772306	FANCA	0,89953411	NDUFB5	0,9001708	CTLA4	0,89660578	CITED2	0,90946353
4536	GNA12	0,93889265	CHRNA9	0,92860801	LIPF	0,90898253	TGFBRAP1	0,92374657	POLR3A	0,92278827	COL6A3	0,91269614	SPTBN4	0,94935964	4606	P2RY5	0,92317419	GCLC	0,91230639	UGT1A4	0,88758363	TBX1	0,89944597	ALOX5	0,90009301	ABCA6	0,8965686	TNFRSF11A	0,90897685
4537	FPGS	0,93882242	CHST1	0,92850039	PLA2G7	0,90895777	UNG	0,923475	CCR6	0,92255007	UGT1A3	0,91255892	MC4R	0,94933628	4607	GOT2	0,92316107	GADD45G	0,91211898	E2F2	0,88757773	COL6A2	0,89895843	ZDHHC8	0,89978691	EXTL3	0,89650411	FNTA	0,90889689
4538	ALOX12B	0,93864836	BET1L	0,92842445	GALNTL1	0,90888811	B3GNT3	0,92320088	EXTL3	0,92224527	TAGLN2	0,91190281	STX5	0,94872283	4608	AMH	0,92315662	MIB1	0,91210729	RASA1	0,88732563	PCNT	0,89844773	BMP1	0,89977569	DOLPP1	0,89648318	IRF2BP2	0,9087424
4539	KLK2	0,93835373	NDUFA13	0,92841394	ITGB1BP3	0,90868409	UCHL1	0,92308824	APOBEC2	0,92203488	RAC1	0,91153514	SLC27A1	0,94846138	4609	PLCB3	0,92312817	DNMT1	0,9120627	HCCS	0,88729209	OLR1	0,8984385	TNFRSF13B	0,89918568	UCHL3	0,89641443	FUCA2	0,9061071
4540	FTO	0,93832069	NR0B2	0,92840878	ELK3	0,90858762	ABCA5	0,92302716	ATP5O	0,92176622	HDAC10	0,91150399	ACVR2B	0,94794479	4610	SMARCA4	0,92286137	PRNP	0,91204002	PTPN2	0,8870834	EBI2	0,89781503	CTPS2	0,89915329	NUMB	0,89589831	CLDN7	0,9057273
4541	PLCD1	0,93820192	AGT	0,92830362	PIN1	0,90840736	GSTZ1	0,92274702	ATP6V1G1	0,92168075	ALAD	0,91141353	F5	0,94761844	4611	CD86	0,92283914	IL17RB	0,91193348	KIAA1303	0,88675515	NSF	0,89704835	ENO2	0,89902987	GP6	0,89586634	NCKAP1	0,90542555
4542	PIP5K2B	0,9379512	GSTT1	0,92748186	MSH3	0,90797343	UBE2G2	0,92271983	GFI1	0,92131549	GRB14	0,91095624	AKAP10	0,94757971	4612	PRKCH	0,92278586	MUTYH	0,91191944	PDE11A	0,88670792	NR0B2	0,89690985	KLK2	0,89891081	NR0B1	0,89585293	HIST3H3	0,90537543
4543	HNF4A	0,93791269	PPP3CA	0,9273268	GTF2H4	0,90792311	ITGAE	0,92236594	SOX9	0,9210915	HTR3A	0,91082471	APOE	0,94728923	4613	PEBP1	0,92246795	KLK10	0,91179179	CYLD	0,88657226	SOX1	0,89615245	EDG1	0,89764383	TAP1	0,8958273	DMC1	0,9053056
4544	ANAPC5	0,93784793	PAK1	0,92718752	HDAC10	0,9079193	BRAF	0,92147811	HMGA1	0,92102396	FURIN	0,91078262	GLG1	0,94708823	4614	NT5C	0,9223261	ALOX12	0,91133617	CYP27B1	0,88646409	FGF11	0,89597988	IKZF1	0,8975465	TXNRD1	0,89578351	B3GNT7	0,90391779
4545	SUZ12	0,9371271	B3GNT3	0,92672428	PPP3CB	0,90712541	KDELR1	0,92132995	ELAVL1	0,92087098	IL12A	0,91058326	IGF2	0,9464554	4615	COASY	0,92202699	UGT1A5	0,91073693	CCNB1	0,88636608	CCND1	0,89543746	POLL	0,89683422	APH1A	0,89566824	C1QB	0,90364835
4546	POLG2	0,93674597	KCNA7	0,92560747	MTRR	0,90705751	DES	0,92120771	SLC30A4	0,92050442	EXT2	0,91045134	LFNG	0,9463748	4616	GUSB	0,9217882	RNF216	0,91066876	DSE	0,88623293	TRPV1	0,89540004	FGF11	0,89660117	CD2AP	0,89440451	BCAP29	0,90331101
4547	AMOTL1	0,93654063	MTMR2	0,92549537	ATG16L2	0,90700379	APOE	0,92117945	SLC18A2	0,91995548	ESR2	0,91009114	WNK1	0,94585313	4617	GBA	0,92143445	ADRA2A	0,90997581	PPAT	0,88594171	NDEL1	0,89486789	GCM1	0,89653835	CRY2	0,89410622	CBX2	0,90298926
4548	CCL22	0,93633605	CD8A	0,92489302	SEMA3A	0,90695353	GBA	0,91930131	TCEA3	0,91990983	GCG	0,90987009	CHRNA4	0,94578909	4618	MDM4	0,92136065	MDH1	0,90976061	PGK1	0,88585243	ASS1	0,89454669	PAX3	0,89647498	KPNA3	0,89352991	SUPT6H	0,90277919
4549	CSGLCA-T	0,93613749	CYR61	0,92391045	UQCRC2	0,9066488	LMO1	0,91922936	HYAL4	0,91990141	CD6	0,9098473	ECSIT	0,94570591	4619	CAV2	0,92122405	ALMS1	0,90971697	NPTX1	0,88562014	LAMB1	0,89430515	SND1	0,89632979	CTNNA3	0,8934976	MEST	0,90239144
4550	VWF	0,93599503	NPTX1	0,92364574	RBPJL	0,90639935	GLO1	0,91904811	ESR1	0,91937576	HMOX1	0,9093439	TLN1	0,94451102	4620	NDUFB5	0,92119674	FANCD2	0,90915299	WNT10B	0,88559142	ST3GAL6	0,89383953	KLRC4	0,89631322	NFKB2	0,89349502	DEFB4	0,90189676

Table A4. Pooled-shRNA library screen on HEL cell line and MF-3: list of 2nd most depleted shRNAs for each experiment (ranking approach 1, RA1).

	NO ruxolitinib (setting 1)				Ruxolitinib (setting 2)				Ruxolitinib + CM (setting 3)				MF-3				NO ruxolitinib (setting 1)				Ruxolitinib (setting 2)				Ruxolitinib + CM (setting 3)				MF-3	
	Experiment 1		Experiment 2		Experiment 1		Experiment 2		Experiment 1		Experiment 2						Experiment 1		Experiment 2		Experiment 1		Experiment 2		Experiment 1		Experiment 2					
Rank	*Gene*	*Fold change*	*Gene*	*Fold change*	*Gene*	*Fold change*	*Gene*	*Fold change*	*Gene*	*Fold change*	*Gene*	*Fold change*	*Gene*	*Fold change*	*Rank*	*Gene*	*Fold change*	*Gene*	*Fold change*	*Gene*	*Fold change*	*Gene*	*Fold change*	*Gene*	*Fold change*	*Gene*	*Fold change*	*Gene*	*Fold change*	*Gene*	*Fold change*
4621	VPREB1	0,92114334	PMS2L3	0,90881582	LTB	0,88558412	DDB2	0,89364952	MTNR1A	0,89596111	G6PD	0,89342061	CLK1	0,90126355	4691	IL28RA	0,90434572	GTF2H4	0,88263565	GSS	0,85614742	ATF3	0,87073176	TNFSF14	0,87861356	ALG11	0,87377525	ELA2A	0,8545155
4622	GPR132	0,92074812	NDST3	0,90847932	APLN	0,88531529	MT3	0,89349527	BMPR2	0,89588726	ITM2B	0,89326929	RPS6KB2	0,90052449	4692	CSRP1	0,90426491	PGA3	0,88247784	GALNT13	0,85572371	EN1	0,8705163	PECR	0,87859746	LAMB1	0,8734547	MS4A1	0,85426997
4623	CAMK2B	0,92068533	SLC11A1	0,90812475	APOBEC3B	0,88498978	USH1C	0,89346924	GZMB	0,89586211	MAP3K1	0,89323662	ATP1B2	0,90004263	4693	HES2	0,90421769	GALNT13	0,88241864	SNX1	0,85565669	RB1	0,87039603	NPPB	0,87798154	CNTF	0,87318945	TNNT1	0,85401185
4624	IFRD1	0,92063959	MVK	0,9078653	WISP2	0,88444808	SOD3	0,89341345	IGFBP1	0,89533824	OXTR	0,89293714	HMOX1	0,89995076	4694	FGF5	0,90320605	GSN	0,88222636	AKT1S1	0,85544477	TEP1	0,87028279	RNF146	0,87744251	TNC	0,87317114	HDAC2	0,85301989
4625	GNS	0,92057911	WASF3	0,90760901	UGT2B15	0,88386987	KCNJ11	0,8933749	MST1	0,89513859	IL25	0,8925428	NUDT1	0,89958013	4695	CYP24A1	0,90255965	PYGL	0,88204143	JAK1	0,85485104	MYB	0,8696207	TUBA4A	0,87738588	FLJ21865	0,87312076	IFNA10	0,85270155
4626	PSMB9	0,92044671	CYP3A4	0,90740575	TUBD1	0,88374043	KLF2	0,89334782	ADRB1	0,8950971	KCNIP3	0,89169233	PMS2	0,89870349	4696	KCNJ11	0,90245333	ALG12	0,88143376	UGT1A3	0,85419984	TCEA3	0,86900136	PSMB10	0,87725822	GADD45A	0,8722151	HOPX	0,85246003
4627	ABCA5	0,91987815	PNLIP	0,90704775	CYR61	0,88357269	WNT6	0,893086	ASAH1	0,8946139	ELA3A	0,891591	TTF2	0,89842816	4697	ADHFE1	0,90229629	ELOVL2	0,88099537	MAFF	0,85328013	EHMT2	0,86893346	APLP1	0,87709843	KLK2	0,87199051	PRKD1	0,85243982
4628	SEPT2	0,91956996	DCT	0,90683543	CETP	0,88334431	MTRR	0,8928161	XYLT1	0,89437076	DNAJB1	0,89128668	NCOA3	0,89828456	4698	AKT1S1	0,90228028	SREBF1	0,88074108	DCT	0,8526054	ADRB1	0,86867467	GALNT13	0,876317	DRD5	0,8719464	PDK1	0,85189968
4629	VEGFC	0,91936973	IFNAR2	0,90635916	IFI30	0,88258998	MGP	0,89269156	MTR	0,89435663	MKKS	0,89090292	IFNGR2	0,89813477	4699	MASP1	0,90223441	ADAM10	0,88069158	RNF19A	0,85117042	SOCS1	0,86845933	CYP2C18	0,87618467	FADS1	0,87170369	SIRT7	0,8508147
4630	GAMT	0,91920163	MYL9	0,90587016	NR2C2	0,88253578	STAT4	0,89245575	ELA3A	0,8941036	FGF20	0,89034725	C1GALT1C1	0,89753025	4700	ROCK2	0,90185882	SLC6A2	0,88034498	CD8A	0,8509285	PIP3-E	0,8683367	SLC26A2	0,87618089	DAPK2	0,87163292	CYP4F3	0,85075754
4631	APOA2	0,91891076	ACPT	0,90509754	CPEB1	0,88236741	UGP2	0,89242567	ARSE	0,89383985	TRAF4	0,89001183	F2RL3	0,89721595	4701	GABRA2	0,9013333	FARSA	0,88023896	CTNNA3	0,85084935	IFRD1	0,8682611	HLA-B	0,87561632	NKIRAS1	0,87136681	SEMA7A	0,85043612
4632	TICAM1	0,91869016	PFKL	0,90509754	KLRC2	0,88225935	STAG2	0,89222429	ITGAE	0,89372502	SNIP1	0,88986616	DVL1	0,89711197	4702	FANCD2	0,90126028	ELA2	0,88023386	GDF11	0,84964604	RAC3	0,86797519	HLCS	0,87526141	BBS4	0,87132464	MAP3K2	0,85019124
4633	EI24	0,9180205	COL19A1	0,90504629	CD6	0,88191165	TEK	0,89204849	GPRC5B	0,8936419	IRAK1BP1	0,88960869	DOCK1	0,89703561	4703	CBX7	0,90050347	PHKA1	0,88008864	DLX1	0,84941946	ATG16L2	0,8674789	TFDP1	0,87463927	GTF2H4	0,87120706	POMC	0,85010385
4634	ABCG1	0,91741273	EPO	0,90500142	TP53BP2	0,88160138	ABCG1	0,89168111	NDST3	0,89345838	TUBB4	0,88924203	ACP2	0,89701473	4704	EED	0,90047271	NKX6-1	0,87962463	NFAM1	0,84910819	ATP5J	0,86684332	TNFSF11	0,87405099	KCNE2	0,87102312	XDH	0,84975698
4635	GABRE	0,91693419	FHL2	0,90473144	TKTL1	0,88147277	CDK10	0,89080532	TEK	0,89333064	XPC	0,88892004	GOSR2	0,89532609	4705	NUMB	0,89874976	ADH1B	0,87953431	DHFR	0,84894484	C1GALT1	0,86657269	NTRK2	0,87383474	GABRA1	0,87091982	ELA2B	0,84964244
4636	CYP4A11	0,9164199	UBE2V1	0,90424852	GALNT2	0,88050759	PDHA2	0,89020036	UGT2B11	0,89287095	CAV2	0,88889859	FCER2	0,89285618	4706	CYCS	0,8987097	PTK2B	0,87942666	IFNAR2	0,84849809	PTCRA	0,86656837	HMGCS1	0,87328049	ENPP2	0,87090394	PLG	0,84955071
4637	TKTL1	0,9161049	ACADVL	0,90407981	FUCA1	0,88046412	ARAF	0,89000956	CIDEB	0,89273082	ASH1L	0,88866794	C1GALT1	0,89086596	4707	PTGIR	0,89857586	EXTL1	0,87934174	LBP	0,84796237	ACADSB	0,86555299	GTF2A2	0,8730108	BHLHB2	0,87029333	PRKCH	0,8494416
4638	RNF216	0,91590709	FANCM	0,90401971	PLA2G4B	0,87883796	EBF1	0,8897718	MAP3K2	0,89225723	ITPA	0,88855481	SMPD1	0,88752161	4708	ALMS1	0,898476	DUSP1	0,87926281	TNFRSF10D	0,84771173	RAB23	0,86546727	IFITM1	0,87237136	RNF19A	0,87019656	PSMC6	0,84889204
4639	MDM2	0,91549429	PUM1	0,90363069	ANXA8	0,87805228	PRKCG	0,8889798	GABRE	0,89221457	SOCS1	0,88843305	CASP2	0,88670201	4709	NPY	0,89835739	UGT1A1	0,8791861	RDM1	0,84762141	TRIB3	0,86512255	COL17A1	0,87232736	RDH13	0,87018603	EIF4A1	0,84844692
4640	PRMT8	0,91549402	CCL2	0,90359584	DHRS4	0,87784094	SLC1A4	0,88880421	ST3GAL4	0,89213567	PSMB10	0,88818993	SPRY1	0,88656244	4710	CD96	0,89775071	CYCS	0,87898424	GRIN2C	0,84725129	CENTD2	0,86501389	CCL16	0,87223562	PSMB9	0,87010667	HLA-E	0,84516067
4641	KLF2	0,91518753	ARFGAP3	0,90342343	ATN1	0,87729044	XAB2	0,88834141	SCN5A	0,8920913	PPOX	0,88812523	NAGS	0,88558365	4711	TGFA	0,897723	CYP4A11	0,87857082	WWP1	0,84681736	GYS2	0,86448873	PMS2L3	0,8719669	NDUFB4	0,86965612	TLR1	0,84511188
4642	C1S	0,91489581	IMPDH1	0,90304788	NRP1	0,87715659	WNT4	0,88823396	MSI1	0,89154068	HDAC9	0,8880202	PLSCR1	0,8849759	4712	CARTPT	0,89744736	RXRB	0,87826447	ATG4C	0,84651693	CDKN2C	0,86431287	DVL1	0,87195579	HIBCH	0,86958129	TLR10	0,84495726
4643	GTF2H4	0,91481316	VIPR1	0,90277364	TNFSF18	0,87696175	DIO2	0,88754018	CD209	0,89090954	ITGB1BP3	0,88712834	DHRS3	0,88376472	4713	TSPO	0,89711455	GRB14	0,87813487	PTK6	0,84545255	OTX2	0,8637214	NFYC	0,87177895	SNX1	0,86790711	MEN1	0,84485387
4644	SOX9	0,91454781	GCG	0,90272235	SCN4A	0,87690275	ARFGAP1	0,887302	SCYL1	0,89084483	ICAM2	0,88653748	ABCA8	0,88328609	4714	SIRT1	0,89696963	PDE1A	0,87803712	GP6	0,84538916	PRKAR1B	0,86320068	GALE	0,87113228	KLF2	0,86640162	NFATC1	0,8447132
4645	NCOA4	0,91447038	CD53	0,90263361	SPI1	0,87669478	POLR3A	0,88686258	OLIG1	0,89079331	BAD	0,88578978	P4HB	0,88184728	4715	PODXL	0,89657281	FTCD	0,8778662	PAPSS1	0,84536362	NPY	0,86267392	NDUFA13	0,87095105	PICALM	0,86621708	TDG	0,84311352
4646	GPX4	0,91441771	P2RY2	0,90209958	FANCL	0,8765418	CD274	0,88594352	ANPEP	0,89030547	A4GNT	0,88559799	COMP	0,88071746	4716	LEPR	0,89654209	PTPRU	0,87782946	CDKN2B	0,84536216	XPC	0,8622632	SIRPA	0,87045752	ABCC5	0,86602321	MKNK1	0,84309958
4647	MT3	0,91437603	FGF1	0,90135807	NEU2	0,87607832	EIF4A2	0,88530789	BLMH	0,88967632	DPAGT1	0,88553518	SMAD6	0,88038001	4717	HSPA1L	0,89643821	APLP2	0,87752001	EHMT2	0,84517516	PYCARD	0,86192062	TAF12	0,87026245	CACNA1E	0,86573788	RARG	0,84130329
4648	NEFH	0,91413979	PIR	0,90079655	BET1L	0,87607069	NR0B1	0,88521359	GAST	0,88956492	CNDP1	0,885492	CHIA	0,88012326	4718	LEFTY1	0,89615842	ACVR1	0,87744642	UNG	0,84472305	BBS4	0,8610154	POLR3B	0,86976073	PARG	0,86571287	MAP3K11	0,84106014
4649	SIX3	0,91400521	CLEC10A	0,90070017	EXT2	0,87602128	MCC	0,88476789	MTRR	0,88941445	SLC6A4	0,88539621	SCN10A	0,87956782	4719	CYP2D6	0,89607144	UBE2F	0,87741349	CYSLTR1	0,84465611	HS3ST1	0,86094066	PRLR	0,86961978	PODXL	0,8646107	CD99	0,84081043
4650	HRH2	0,91371833	UGT1A6	0,90055251	CHST14	0,87596516	HS3ST3A1	0,88433514	CMA1	0,88929884	IL17RB	0,88527869	PPP2R2C	0,8789666	4720	FOSB	0,89598818	ITGAE	0,87697007	HSPA1L	0,84390518	PIWIL2	0,86042583	EIF2B5	0,86897552	DAB1	0,86456353	EHMT2	0,84044346
4651	ETV3	0,91366392	ABP1	0,90034176	HYAL4	0,87479261	ALG11	0,88404632	RAD51L1	0,88912015	BOK	0,88516367	ASIP	0,87796542	4721	CFI	0,89548595	ACAA2	0,87688009	PLA2G12A	0,84356574	JAK3	0,8599117	ELA2A	0,86825405	TNFRSF10B	0,8638275	FPGS	0,83994202
4652	ALDH3A1	0,91333061	SOCS7	0,90022755	KLRC4	0,8745302	CKMT2	0,88378581	ALDH1A1	0,88888579	BDNF	0,88497997	PRPS1L1	0,87777636	4722	PAPSS2	0,89535303	PTX3	0,87686822	CRHR2	0,84355351	LRP2	0,85947886	CTCF	0,86770402	INPP1	0,8637165	FOSL1	0,83970113
4653	MAPKAPK2	0,91272106	CLDN23	0,90010486	GIP	0,87402542	UGT1A8	0,88316177	EPAS1	0,88870686	ABP1	0,88477485	TAP1	0,87753427	4723	CDK10	0,89521874	CKMT2	0,87654562	GTF2H2	0,84353319	IGFBP4	0,8592962	MAT2B	0,86675883	PDGFA	0,8632612	ABLIM3	0,83938948
4654	TGFB1I1	0,91262363	CBX7	0,90001704	PLSCR4	0,87119448	ITGB4	0,88307404	CHST14	0,88832066	CDKN1C	0,88437762	CAMK2A	0,87700666	4724	ARHGAP4	0,89511732	LAT	0,87647276	CLDN16	0,84078245	PLA2G4B	0,85903856	CLCA1	0,86666605	TGFB1	0,86185567	CNPY3	0,83912665
4655	CDKN2B	0,91258237	CYBA	0,89967524	MBTPS1	0,87073754	FRS2	0,88306587	AGT	0,88823445	CHMP1B	0,88437762	PTHR1	0,87680382	4725	MAPK14	0,89481752	CTLA4	0,87611785	TNC	0,84065649	FSHB	0,85894154	APOBEC3A	0,86653978	LIG1	0,86053814	RRM2B	0,83678903
4656	WISP2	0,91227297	RIPK1	0,89925404	MKNK1	0,87063442	PRKG2	0,88306305	AFP	0,88810563	SIRT1	0,88403112	CASP3	0,87673929	4726	CEP290	0,89469532	SIRT7	0,87552232	BAG4	0,84054096	GPX1	0,85871728	PGD	0,86627445	MAS1	0,86042405	ALLC	0,83622076
4657	MTRR	0,9122479	ATOH1	0,89908987	IFITM3	0,87023977	RIPK1	0,8823109	ZNF259	0,88798334	CCL22	0,88342715	CSNK2A1	0,87554392	4727	ST8SIA5	0,89458445	ACY1	0,875244	FGF5	0,84016014	JAK1	0,85799118	VIL2	0,86599402	ATOH1	0,8597377	NNMT	0,83550963
4658	PRKY	0,91219643	PIF1	0,89881719	TCIRG1	0,87021383	KRT18	0,88215383	FPGS	0,88795746	CSNK1D	0,88331729	HAT1	0,87512665	4728	NCOA1	0,89451139	ZDHHC8	0,87442513	CHPT1	0,83966449	GALK2	0,85703277	LRP2	0,86582765	E2F2	0,8595915	MSX1	0,83549017
4659	YWHAQ	0,91187806	IL10RA	0,89862035	FCER2	0,86972158	FOXP3	0,88174663	TSNAX	0,88752948	TYR	0,88296421	AOX1	0,87509892	4729	OXTR	0,89389883	PPARD	0,8742813	PFKL	0,83961942	ELA2	0,85691947	F3	0,86571721	UGT1A4	0,85932495	CCND1	0,8346487
4660	EIF2B5	0,91166174	CBLC	0,89829366	IBSP	0,86971853	STAT3	0,88169337	SYNJ2	0,88752395	LITAF	0,88267941	SNX2	0,87396921	4730	SRF	0,89374268	EED	0,87425998	APLP1	0,83955136	GSTM2	0,85655629	ADK	0,86542555	NPY	0,85913938	CENTA1	0,83396333
4661	ELA2A	0,91154281	ALAS2	0,89636378	PIK3CA	0,86965008	ARHGAP6	0,88096409	ASH1L	0,88750955	CHRND	0,88203369	SCN4B	0,87291297	4731	PTEN	0,89315942	CTPS2	0,8742492	ADORA2A	0,83866716	GHRHR	0,85519004	BMP8B	0,86504686	ARF6	0,85892586	FZD5	0,83286058
4662	TNFRSF10B	0,91114991	CXCL10	0,89548667	VNN2	0,86881201	GUSB	0,8809103	GAMT	0,88694388	MOBP	0,88156918	ANXA2	0,8728907	4732	DHCR7	0,89307475	CNPY4	0,87412449	GLG1	0,83786717	ERN2	0,85480633	C1QL1	0,86442392	NANOS1	0,85799472	CLDN16	0,83205072
4663	STK11	0,91107611	FGG	0,89514827	CAPN7	0,86799786	MVD	0,88085963	MAPK14	0,8864138	APOBEC3C	0,8813286	XBP1	0,87278551	4733	DDB2	0,89276982	AP2B1	0,87379225	AADAT	0,83680316	AMPD1	0,85461679	ATP2B1	0,86384503	HDAC4	0,85791825	MYOD1	0,83126179
4664	CD180	0,91012661	ASIP	0,8939409	SERPINA1	0,86685478	TGFBR1	0,88050655	DBH	0,88637866	CER1	0,88122089	IMPDH2	0,87230909	4734	ATG16L2	0,89237674	PDE11A	0,87373227	SERPINI1	0,83673602	IFNAR2	0,85438057	BRCA1	0,86375365	G3BP2	0,85786732	PPCS	0,83066936
4665	ABCA2	0,90915182	RB1	0,89392415	ASH1L	0,86678736	RAD51L1	0,87900666	COL4A1	0,88615852	SCLY	0,88117719	SRP68	0,87177806	4735	KCNE2	0,89217631	GPR34	0,87348162	GNRHR	0,83537821	APOA2	0,85351588	TPMT	0,86349123	NOTCH3	0,85767541	HADH	0,83064215
4666	APOBEC3G	0,9089205	PRLR	0,89314659	CDC25C	0,86597131	IMPA2	0,87843365	CDK5R2	0,8859368	HOXA13	0,8806577	SLAIN1	0,87022785	4736	ALG12	0,89191328	TRPV1	0,8734274	GSTM1	0,83486844	CHST11	0,85328718	GUCY1A2	0,86281787	IL17RA	0,85766749	DKK1	0,83056575
4667	VIL2	0,90890719	ATXN2	0,89287407	CD99	0,86591225	CSDA	0,87783539	KRT18	0,88550778	SH3GL2	0,88055262	HNMT	0,8697281	4737	EHMT2	0,89163458	BCL2L2	0,87309473	NR2E1	0,8344896	CD47	0,85297659	AMPD1	0,86255949	KCNJ9	0,85736151	RAD1	0,83000456
4668	XIST	0,90888483	ATP6V0A1	0,89282495	GBF1	0,86543555	TCIRG1	0,87754498	PHKG1	0,88529271	SERPINI1	0,88053256	ACYP2	0,86965392	4738	TNC	0,89137456	CSTF2	0,87289966	IMPA2	0,8338926	PPP3CA	0,85288733	AZGP1	0,8622584	DDB2	0,85712323	SERPINE2	0,82951277
4669	HSD17B8	0,90849583	GALE	0,8926947	AMPD2	0,86537102	CTPS2	0,87751989	GALNTL1	0,88503298	SCNN1D	0,88014342	TEC	0,86867634	4739	THBS2	0,89099288	FUT1	0,87235977	NPM1	0,83333922	EMX2	0,85273321	FLJ21865	0,86174292	GLO1	0,85661912	UGT8	0,8291503
4670	ADK	0,90826639	B3GALT4	0,89081194	PTCRA	0,8652981	PPP1R1B	0,87694978	IL27	0,88469719	CDCA8	0,88006594	LHPP	0,8684136	4740	LRP2	0,89093228	HPCAL1	0,87232224	H2AFY2	0,83308664	ATG2B	0,8527239	KCNN4	0,86162338	CASP10	0,85659274	CD86	0,82912235
4671	IFITM3	0,90823783	PCSK1	0,89078563	NDST3	0,86524679	LAT	0,8767355	SDS	0,88449711	CALML5	0,87986957	ESD	0,86807044	4741	UBE2E2	0,89055262	GJA3	0,87214266	WNT3	0,83210285	NDUFB4	0,8526901	SOCS7	0,86098451	ALDH1A1	0,85640873	ATIC	0,82860381
4672	CYP4F3	0,90818299	HDAC5	0,89064328	CSNK1G2	0,86517712	SFRS12	0,87643776	PLSCR4	0,88412647	MAOB	0,87983115	MMP9	0,86776464	4742	MAS1	0,890168	DCTD	0,87171046	SCN7A	0,83209548	TUBA4A	0,85176085	VEGFC	0,86053472	PSAT1	0,85559051	SLC25A1	0,82843536
4673	CBX4	0,90800401	CD44	0,89026961	COL18A1	0,86510794	ABCC5	0,8763988	CDCA8	0,88369596	SLC15A1	0,87972865	HMGCS1	0,8669318	4743	BLNK	0,88934794	TNFSF9	0,87170525	SSTR1	0,83167022	ZFYVE16	0,85130122	ADRA2A	0,86050615	GJA3	0,85481929	NDUFB11	0,82825088
4674	BDH1	0,90798938	POLR1C	0,89025282	HPN	0,86500235	GBF1	0,87639658	LRRC15	0,88330736	TSNAX	0,87957243	NUP153	0,86609178	4744	ENO2	0,88923546	ATG2B	0,87167802	VAV3	0,83010438	SCN3A	0,85031781	SIRT1	0,8604294	NEU4	0,85405515	SLC30A3	0,82779399
4675	AMDHD2	0,90745298	ENPP2	0,88999324	PRF1	0,8635505	TBP	0,87611007	RNF216	0,88183995	MAD1L1	0,87947646	TGFBR3	0,86578004	4745	ALDH1A1	0,88905457	MTRR	0,87160983	CYP2C19	0,8300814	GLA	0,84992964	ACADVL	0,86010269	DCTD	0,85374303	RAB9A	0,82769015
4676	IL21	0,9070196	GIT1	0,88926955	BTRC	0,86283049	IFNAR1	0,87605608	HSD11B1	0,88173276	ST3GAL3	0,87915484	GUSB	0,8643243	4746	SERPIND1	0,8886245	HBA2	0,87057132	DCP1A	0,8298688	SERPINB5	0,84927403	BAAT	0,85999538	TF	0,8536045	CNTF	0,82753179
4677	SNAP29	0,90646108	CCL4	0,88925926	ARF4	0,86209335	POR	0,87453571	PIGO	0,88170174	COQ3	0,87915041	NFKBIA	0,86333744	4747	UGT1A5	0,88852351	AGPAT3	0,87053861	G3BP2	0,82925639	SYT1	0,84910394	NRCAM	0,85934772	ZBTB7A	0,8521433	DTYMK	0,82723638
4678	ALG5	0,90642131	GRIN2D	0,88886102	STAT3	0,86200201	WWP1	0,87404859	ACOT11	0,88101576	CCKAR	0,87888244	AGPS	0,86333101	4748	EXOC7	0,88845312	BCL11A	0,87052935	SLC11A1	0,82888024	HDAC5	0,84902035	IFRD1	0,85911125	COPS3	0,85206549	PRKCI	0,82629201
4679	ALG1	0,90624681	TNFRSF10B	0,88782803	RAPGEF1	0,86197299	ADH1B	0,87392018	EEF2K	0,88085115	PMP22	0,87827616	REG1A	0,86008776	4749	EBI2	0,88753744	LTF	0,87044702	GFI1	0,82871305	GADD45G	0,84846204	CHRNA4	0,85910042	CLDN14	0,85188375	TRIM21	0,82557094
4680	SDHB	0,90624403	YARS2	0,88716495	ISG15	0,86172747	CRADD	0,87385673	ACP5	0,88063805	KCNJ11	0,87797145	COL1A1	0,85822389	4750	CBL	0,88751059	CFHR4	0,87005249	CUZD1	0,8283345	BCL10	0,84753316	TRIB3	0,85896834	PCNP	0,85100981	STMN2	0,82492597
4681	CFHR4	0,9057783	EPHB3	0,88689264	HAND1	0,86053367	DDEF1	0,87371183	UAP1	0,880304	EPS8	0,87785502	RIPK2	0,85798036	4751	NPTX1	0,88743681	UAP1	0,86994451	PDE4C	0,82687865	STX3	0,84660711	PRB1	0,85871483	VWF	0,85040127	GIP	0,82479629
4682	UGT1A1	0,90566638	ADORA2A	0,8868908	RB1	0,85907729	CYP11A1	0,87366014	WNT5B	0,88014681	ADCY5	0,87687557	MIF	0,85761628	4752	SMAD6	0,88621139	HS6ST2	0,86956259	MAN2B1	0,82626166	POLR3GL	0,8459757	PARK2	0,85807352	TNFSF11	0,85031732	ADHFE1	0,82346719
4683	KCNA7	0,90562276	UGT2B11	0,88649792	JUND	0,85845107	GABRE	0,87364061	PRMT8	0,88006657	NUDT12	0,87643957	ERAF	0,85714098	4753	ITGAE	0,88612128	IFNK	0,86935182	PRKY	0,8262157	TFDP2	0,84596049	PDE8A	0,85805759	DDX52	0,85027466	ABO	0,82239544
4684	ATP5G3	0,90553903	HDAC6	0,88605481	PA2G4	0,85835067	MCRS1	0,87349714	MGAT5	0,87974002	FUT3	0,87637297	NEFL	0,85691006	4754	CAPN3	0,88456944	CACNA1E	0,86856897	ADRBK1	0,82591904	CYB5R1	0,84467442	EBF1	0,85792166	PROS1	0,84944623	SERPINA10	0,82232775
4685	NDUFB4	0,90546242	HIBCH	0,88599122	HS3ST3A1	0,85832872	TYR	0,87338345	SIPA1	0,8796368	SULT1A4	0,87629188	HES6	0,85607721	4755	EPS8	0,88450558	NAGLU	0,86828406	MTMR2	0,82589812	C1S	0,84402309	GTF2H4	0,85760996	MRPL19	0,84881091	PDGFA	0,82157586
4686	POLI	0,90505435	SLC1A6	0,8857922	NMUR2	0,8579241	PLAUR	0,87306722	FZD2	0,87963261	CSTF1	0,87600313	GJA4	0,85557468	4756	MYC	0,88424528	HDAC9	0,86811028	ATF5	0,82578565	KLRC4	0,84401704	TFDP2	0,85698919	COL22A1	0,84863705	LIG4	0,82153449
4687	ASIP	0,90501627	IKBKB	0,88475515	PTX3	0,85719816	DOK2	0,87300607	C1ORF142	0,87920188	RELA	0,8759657	CLDN11	0,85547975	4757	HAO1	0,88410996	SEPP1	0,86767128	EPS8	0,82547552	UBE2F	0,84230257	NCF2	0,85666904	EDG1	0,84820733	SLC6A1	0,82083006
4688	CLEC10A	0,90480628	ERCC4	0,88451588	MLC1	0,85707377	ADAM10	0,87291243	NMNAT1	0,87901154	ALPL	0,87547398	RAB10	0,8552707	4758	RRAD	0,88391892	HLA-A	0,86750642	B3GNT7	0,82530355	KLKB1	0,84117827	BRS3	0,85666606	IL3	0,84793662	NANOG	0,82077523
4689	PDE4C	0,90464107	B4GALT4	0,88442098	MYB	0,85691114	HSPA2	0,87253467	TCF7L2	0,87872264	FUK	0,87538684	CD5	0,85520058	4759	THPO	0,88386953	DDO	0,86630727	ARSA	0,82526718	CXCR4	0,84035362	MTNR1B	0,85628673	PDGFB	0,84776103	ADFP	0,82059454
4690	LTB	0,90459302	MYST4	0,88324148	TSPO	0,85675894	AVEN	0,87107157	UROS	0,87870054	RFX4	0,87493851	PRKAG1	0,85491806	4760	EPS15	0,88259582	ATG16L1	0,86455032	PGD	0,82520027	E2F1	0,8397777	MT3	0,85590292	ACIN1	0,84744369	NUDT12	0,81909874

Table A4. Pooled-shRNA library screen on HEL cell line and MF-3: list of 2nd most depleted shRNAs for each experiment (ranking approach 1, RA1).

	NO ruxolitinib (setting 1)				Ruxolitinib (setting 2)				Ruxolitinib + CM (setting 3)				MF-3				NO ruxolitinib (setting 1)				Ruxolitinib (setting 2)				Ruxolitinib + CM (setting 3)				MF-3	
	Experiment 1		Experiment 2		Experiment 1		Experiment 2		Experiment 1		Experiment 2						Experiment 1		Experiment 2		Experiment 1		Experiment 2		Experiment 1		Experiment 2			
Rank	*Gene*	*Fold change*	*Gene*	*Fold change*	*Gene*	*Fold change*	*Gene*	*Fold change*	*Gene*	*Fold change*	*Gene*	*Fold change*	*Gene*	*Fold change*	*Rank*	*Gene*	*Fold change*	*Gene*	*Fold change*	*Gene*	*Fold change*	*Gene*	*Fold change*	*Gene*	*Fold change*	*Gene*	*Fold change*	*Gene*	*Fold change*
4761	ITGB4	0,88250346	PYCARD	0,86454984	DUSP10	0,82445333	PPT2	0,83965743	FHL2	0,85525929	PTPN1	0,84697464	PLD1	0,81795666	4831	CHPT1	0,86294428	WIPI2	0,8392623	GREB1	0,79116963	AKT1	0,80698327	UBE2J2	0,82390487	ENTPD4	0,82332775	BLVRA	0,76583915
4762	LPA	0,8824668	GBP2	0,86431589	PSAT1	0,82296614	ADRA1D	0,83959373	WWP1	0,85487704	CDC7	0,84693481	TRAF2	0,81771159	4832	BIRC3	0,86282702	AARS	0,83921766	TPP1	0,79094093	BMPR2	0,80689171	ST8SIA5	0,82205074	FARSA	0,82257074	SC4MOL	0,76583378
4763	CRADD	0,88224398	B3GAT1	0,86412073	SLC1A4	0,82270604	NR1H2	0,83951204	UBE2J1	0,85416573	OLR1	0,84665129	TACR2	0,81747063	4833	KCNN4	0,86264287	INSR	0,83889248	PLSCR1	0,79071229	VIPR1	0,80648608	CYP24A1	0,82181067	SIPA1	0,82128967	CD40	0,76392713
4764	IL17RA	0,88184491	DUSP14	0,86398395	GNA15	0,82230684	FADS1	0,83932631	PLCD1	0,85355863	PAFAH1B3	0,84650741	WT1	0,81736715	4834	RGS1	0,8625196	HOXA13	0,83776359	HOXA13	0,78996992	LXN	0,80635272	TSC2	0,82146119	BMP10	0,82103397	SLC11A1	0,76248598
4765	CD1D	0,88136096	SCN4A	0,86396708	HTR1A	0,82227793	ACTR2	0,83932481	TAPBP	0,85237941	POLR3A	0,84632103	CHMP1B	0,81687614	4835	CLDN1	0,86208484	BAAT	0,83776288	RGS1	0,78938203	LY75	0,80597599	PLA2G3	0,82121734	BLMH	0,82067399	ARF6	0,76215364
4766	SKI	0,88132833	CYSLTR2	0,8629942	SLC34A1	0,82226773	TFDP1	0,83843355	UGT1A9	0,85236511	HOPX	0,84612451	GAPDHS	0,8168748	4836	FANCM	0,86181081	PPP1R13L	0,83760662	MCM5	0,78881375	ESCO1	0,80447972	FCGR2B	0,82045314	CD244	0,82009615	LPHN2	0,76207697
4767	PDE3B	0,88118506	CASP10	0,86281458	CALCRL	0,82173911	SLC27A1	0,83777829	NR4A3	0,85221652	IFI35	0,84552592	CD200R1	0,81595965	4837	MCRS1	0,86132497	TP53INP1	0,83681557	ARHGAP6	0,78689798	FANCD2	0,80327491	OTX2	0,81865638	BTD	0,8197425	STAT3	0,76205067
4768	SULT1A4	0,88012765	ACVR2A	0,86270226	MUT	0,82131657	PMCH	0,83751738	EFNA5	0,8518714	BMP3	0,84543263	SLK	0,81562685	4838	ESCO1	0,86090749	GLG1	0,83655806	NNT	0,78580524	PODXL	0,80318207	MECP2	0,81838203	CYP17A1	0,81827391	DPYD	0,76008017
4769	ETS2	0,87972501	STX17	0,86257251	CYP2C8	0,82119627	PIN1	0,83706558	CLCA2	0,85151218	MAPK11	0,84509631	PAK3	0,81543752	4839	DAPP1	0,86067338	WNT3	0,83599064	FTH1	0,78535703	IKBKG	0,80192218	SULT1C2	0,81794177	APLN	0,81822701	BCAR1	0,75882996
4770	AK3L1	0,8796761	TPMT	0,86076584	TRPV1	0,82108161	NEU1	0,83662465	F7	0,85061476	HS3ST1	0,84493206	IL10	0,81430495	4840	ADH1C	0,86021267	NMU	0,83589437	CLDN23	0,78419707	RGS1	0,80099583	CER1	0,81683967	HOXD10	0,81816477	DIAPH1	0,75879581
4771	IMPA2	0,87954491	ABL2	0,86030929	CBX4	0,82093736	ABCA7	0,83662404	CRH	0,84870888	COX5B	0,84448616	NR1H2	0,81404655	4841	UBQLN1	0,85949369	RNF146	0,8352314	PCGF2	0,78328897	SCN7A	0,80047265	SCN4A	0,81674405	PXN	0,81705854	GHRH	0,75838807
4772	SCNN1D	0,87890164	CARTPT	0,85986192	LAMB1	0,81977319	ETFA	0,83649714	PRKCG	0,84783427	CBX4	0,84434395	TP53BP2	0,81082498	4842	STX16	0,85944129	MTHFR	0,83520638	DUSP4	0,78302382	PRKD1	0,80010527	ELA2	0,8166228	SMAD2	0,81686893	ATP5D	0,75838717
4773	SLC18A1	0,87838326	ADK	0,8590715	LCT	0,8193669	SLC9A3R1	0,83554141	CCK	0,84746221	LPIN3	0,84429606	SP1	0,81066253	4843	DPEP1	0,85866803	TSPO	0,83498004	SLC30A8	0,78252544	ABCB4	0,80005459	FOXK1	0,81640352	CD97	0,8156916	GREB1	0,75815186
4774	GOSR2	0,87797345	SLAMF1	0,85892502	GBP2	0,81921694	TFAP2A	0,83497593	CYB5R3	0,84604702	FGF5	0,84389798	FBXW7	0,80974889	4844	UGT2B15	0,8578344	ASS1	0,83443753	SRM	0,78102549	BCL2L14	0,79966212	SLC6A3	0,81533764	ATG16L2	0,81484295	CYC1	0,75807665
4775	E2F1	0,87766316	ABCG1	0,85857061	EHD2	0,81853212	ATP6V0A1	0,83490955	FANCC	0,84560122	GREB1	0,84367527	NEK1	0,8097322	4845	SERPINA5	0,85764309	GCGR	0,8343697	HLA-DPA1	0,7808843	PDGFA	0,79924696	HDAC4	0,81488924	DDO	0,81378818	EIF2AK1	0,75551753
4776	VAV2	0,87748786	PLA2G12A	0,85823821	FSCN1	0,81848977	PAX5	0,83440349	CACNA1G	0,84442351	LDHA	0,84347666	CEACAM1	0,80778227	4846	GALNT13	0,85741725	DEFB1	0,8342221	CSTF2	0,78087964	NPM2	0,79828334	CD44	0,81486344	NMUR2	0,81355952	HOXA4	0,75415669
4777	CNR2	0,87694428	SNIP1	0,85771884	AMY2B	0,81818532	FANCC	0,83435222	UBQLN1	0,84374761	HES2	0,84334592	THPO	0,8074473	4847	CASP10	0,85734908	CDKN2B	0,83413867	UTF1	0,78066167	ADK	0,79809271	SLC1A6	0,81323048	GRIN2B	0,81325762	ALDOC	0,75319722
4778	CASK	0,87692397	AZGP1	0,85763	DTX1	0,81796491	RDH5	0,83336089	ZBTB7A	0,84374166	CP	0,84296072	ADIPOQ	0,80577695	4848	EBF1	0,85690616	ACSL5	0,83395011	DGKB	0,77971013	BMI1	0,79728377	BMP3	0,81302445	POLR3GL	0,81297722	SFRP2	0,75229284
4779	IFNAR2	0,87658577	CSNK1G2	0,85757565	SMAD2	0,81718063	GCGR	0,83188102	ALDH3B2	0,84359867	ADRA1B	0,8428235	ABCB6	0,80528064	4849	MYD88	0,85689591	LRRK1	0,83306897	FABP3	0,77938758	LTB	0,79669327	AVEN	0,81217476	NDUFB6	0,81279777	GATA6	0,75225016
4780	NFKB1	0,87651437	SLC27A1	0,85702622	MET	0,81702273	RASA1	0,83131547	PIGC	0,84308162	ASIP	0,84277277	PLP1	0,80527424	4850	ATP5F1	0,8567679	CXCR4	0,83291713	PAK1	0,77901021	BCL2L10	0,79545852	CFHR2	0,81203996	PDE1A	0,81242283	CD3EAP	0,75187587
4781	ANGPTL3	0,87610558	LCMT1	0,85625713	CCL11	0,81656951	HSD17B8	0,83108864	PRKCI	0,84254211	SOST	0,84250428	FUT3	0,80318034	4851	CBX5	0,85667897	CMA1	0,83281718	ENTPD5	0,77825113	IFNG	0,7954359	MAFF	0,81197741	IKBKG	0,81208511	MINPP1	0,75143311
4782	WWP1	0,8758836	DGKB	0,85624012	ATP6V1E1	0,81305464	DCT	0,83105346	APOA2	0,84219663	ANK2	0,84169834	PLCD1	0,8023563	4852	GLG1	0,85659714	ALDH1A1	0,83249574	CHN1	0,77801726	ARF6	0,79268024	CPEB1	0,81171855	ETFA	0,81118699	PDE6B	0,75060483
4783	CYP2B6	0,87552328	CEP290	0,85590528	ADHFE1	0,81294313	AVPR1A	0,83058458	RDH13	0,84196716	DLX1	0,84116801	PSME3	0,80219723	4853	CBLC	0,85603155	MGP	0,83207708	CMA1	0,77756602	BOK	0,79117079	NOX4	0,81154454	VAMP2	0,80972391	ACSL5	0,74883653
4784	NEU4	0,87522989	H6PD	0,85561536	ICAM2	0,81194262	GRK1	0,83022439	SIRT7	0,84163894	CCNB1	0,84083351	DHX58	0,80136844	4854	NKIRAS2	0,85568219	CER1	0,83133835	DOK2	0,77739001	HIBCH	0,79072231	PRKY	0,81145596	CHAD	0,80920109	TLR4	0,74840209
4785	DIAPH1	0,87456399	GLO1	0,85561352	MITF	0,81177715	AMH	0,83008465	MSH2	0,84060991	PRMT8	0,84073104	POLI	0,8000386	4855	VIPR1	0,85512975	DPEP1	0,83131864	NDUFB11	0,77728616	PSAT1	0,78855263	ANK2	0,8111326	FANCD2	0,8086774	UBE2D3	0,74808141
4786	GBF1	0,87452563	IL3	0,85556683	MTHFR	0,81160881	UGT1A6	0,82925594	ABCC4	0,84060546	B3GALNT1	0,84017934	APCS	0,79903286	4856	CD44	0,85496156	PRKY	0,83038793	PAFAH1B2	0,77674327	SEMA3A	0,78849676	CYP4F3	0,81102144	RGS1	0,80730651	CTNND1	0,74757263
4787	GLO1	0,87383827	ZNF259	0,85533216	GIPR	0,81000416	TNFSF14	0,82889367	CDIPT	0,84038464	CHRNB3	0,84004433	COL5A1	0,79888346	4857	RIPK1	0,85399719	FBP2	0,82998433	HLA-A	0,776398	MYST4	0,78778497	CDKN1A	0,81014953	IFNK	0,80538883	CHRNB3	0,74648282
4788	TGFBRAP1	0,87335739	APOBEC3C	0,85483195	ME1	0,80871802	GP9	0,82879753	HLA-DPA1	0,83998239	UHRF1	0,83986935	ADAM12	0,7985216	4858	OTX2	0,85395765	GCH1	0,82979004	HIF1A	0,77618727	IL12A	0,78757985	PTHR1	0,80950435	ROCK2	0,80456854	CNGA3	0,74633298
4789	PTX3	0,87332538	XDH	0,85375642	SLC1A3	0,80866634	ACAD9	0,82866507	NOG	0,83980472	POLR3G	0,83965376	RASGRF1	0,79773705	4859	GTF2H2	0,85370399	ARSE	0,82881629	NCF2	0,77591346	SIRPA	0,78734906	CD180	0,80835559	CD19	0,80353989	NCSTN	0,74620902
4790	SEMA3A	0,87331953	ZFYVE9	0,85351791	CACNA1I	0,8083044	SCNN1D	0,82863229	TLX3	0,83870872	CASP9	0,83907798	PIGU	0,79762505	4860	EN1	0,8536844	CRH	0,82810449	SALL1	0,77584971	AARS2	0,78690083	ALPPL2	0,80822762	MIB1	0,80327235	FGFR1	0,74357516
4791	TAAR6	0,87323479	DLX1	0,85325253	ERG	0,80777374	SSTR1	0,82735762	ATXN2	0,83843245	PPP2R2C	0,83850883	RDH13	0,79554941	4861	DAPK2	0,85207574	TRPC7	0,82779559	TNFRSF10B	0,77517353	ANXA3	0,78653514	HCCS	0,80694013	CA12	0,80304593	SQLE	0,74274773
4792	E2F3	0,8730696	GP9	0,85288409	DRD5	0,80700696	B3GNT5	0,82609072	FXYD2	0,83833289	CDKN2C	0,83838168	DEGS2	0,79433839	4862	IL2	0,85169901	SMAD6	0,82746788	GCLM	0,77488996	CFHR4	0,78617315	ABCA2	0,80655145	GZMB	0,8028099	APLP1	0,73951771
4793	CLCA1	0,87301587	CYP24A1	0,8527268	CALML5	0,80646353	UBQLN1	0,82492322	DNAJA3	0,83770303	DGKB	0,83824939	CKS1B	0,79320556	4863	IMPDH1	0,85086574	TNFRSF10D	0,82739252	CHST11	0,77301633	TREM1	0,78520285	GPR34	0,80654853	IFI30	0,80184386	CTNNB1	0,73897009
4794	ADCY7	0,87290959	USH1C	0,85225959	ADFP	0,8063274	EHD2	0,82366938	CD3G	0,83759227	MTMR2	0,83715116	CABIN1	0,7917219	4864	FNTA	0,84951494	A4GNT	0,82737511	NR2F1	0,77181754	CD7	0,78493802	MTMR2	0,80635581	PRDM1	0,80135436	APOC2	0,73846896
4795	CD59	0,8727969	ARSD	0,85191248	ATP2B1	0,80614295	E2F4	0,82310741	GATA3	0,83748075	GNGT1	0,83637239	AKAP7	0,7915648	4865	CHST11	0,84887267	E2F4	0,82633645	IL28RA	0,77088581	MDM4	0,78333109	SEPT2	0,80593496	HMGB1	0,80119002	KCNJ9	0,73569967
4796	EIF1	0,87241325	SERPINI1	0,85186162	TNFSF9	0,80514242	DSE	0,82291948	TRPV1	0,837348	ATG2B	0,83617263	ISG20	0,79080339	4866	KRT7	0,84805092	LRP2	0,82596057	ZNF259	0,77069076	ALOX12B	0,78275865	UBE2L3	0,80311677	ADCY2	0,80064779	IFNG	0,73445332
4797	SOD3	0,8722461	HSD11B1	0,85162373	GPR65	0,80467554	PAK1	0,82265474	SLC22A6	0,83725579	MAPK8IP2	0,83474614	LHCGR	0,79046158	4867	NTF3	0,84767431	MARS2	0,82590514	GCM1	0,7699996	P2RX7	0,78251418	CCNB1	0,7997354	CYCS	0,80018967	TGFBRAP1	0,73271644
4798	UBE2H	0,87223655	SET	0,85114383	FUK	0,80434934	H2AFY2	0,82221606	HMGB3	0,83690176	ABLIM1	0,83452796	CYP3A7	0,78867095	4868	POLR3B	0,84763974	NR2F1	0,82561124	UGT1A8	0,76907783	ISG15	0,78213423	CYP2U1	0,7995093	ANXA8	0,7992889	CYP7A1	0,7297012
4799	ANGPTL2	0,87202284	SLC33A1	0,85090747	CD4	0,8041908	CBLC	0,82150577	ANGPTL4	0,83597587	IDS	0,83428658	RNF25	0,78665939	4869	HBB	0,84763792	ETS2	0,82443688	ABL2	0,76903751	UGT1A1	0,78191862	FANCM	0,79798107	PPP3CB	0,79918709	MXI1	0,72962776
4800	GP9	0,87199895	ARHGDIB	0,85016201	TPMT	0,80407094	SULT1C2	0,82107458	IFNA1	0,83587613	ATG2A	0,83424396	H2AFY2	0,78570677	4870	FGFR2	0,8472712	MKNK2	0,8236252	GSK3B	0,76786932	PGK1	0,78018324	GRASP	0,79404722	CD4	0,79879685	DLG4	0,72748875
4801	TNIP3	0,87169986	LCT	0,84933946	TXNRD2	0,80352217	CNPY4	0,82079072	DIO2	0,83550696	DARS2	0,83406118	WDR1	0,78410014	4871	PGK1	0,84647745	KLK2	0,82210082	MCRS1	0,76707291	PAXIP1	0,77951519	CACNA1H	0,79389769	CD209	0,7981996	PIK4CA	0,72556164
4802	ELOVL2	0,87153249	SSTR2	0,84915481	RAC1	0,80266532	TNFSF13	0,81974213	ENPP6	0,83526352	DDEF1	0,83397314	PANK4	0,7838308	4872	SLC1A4	0,84608124	ABCA2	0,82164572	KPNA3	0,76561183	PRB1	0,77901755	UBE2V1	0,79362686	ATP2B1	0,79817194	CYGB	0,72273725
4803	FSHB	0,87095703	ABCG8	0,84841523	COPS3	0,8024739	DLX1	0,81966324	GPC5	0,83526006	AMPD2	0,83370962	PAFAH1B3	0,78365396	4873	MET	0,84556193	GREB1	0,82096913	GADD45G	0,76468319	DGKB	0,77810843	HLX	0,79355485	PFKL	0,79780402	MAPK12	0,72181052
4804	IL5	0,8706956	NEIL2	0,84783463	MAS1	0,80178537	NPM1	0,81964454	FTCD	0,83524592	CYP2R1	0,83346591	ARSA	0,78346514	4874	HIBCH	0,84500296	UGT1A3	0,82048757	TGFBRAP1	0,76282171	PRKAR1A	0,77759329	TXNRD2	0,79338617	ITGB4	0,79773642	CTNNA1	0,71994349
4805	CLDN19	0,87050749	PHPT1	0,84765779	B4GALT4	0,80156519	TCF15	0,8195805	BTD	0,83484349	ALOX15	0,83313552	CASP7	0,78294271	4875	LRRK1	0,84451037	FGFR1	0,81921602	CFHR4	0,76211288	EFNA3	0,77740218	NUDC	0,79290259	CBX7	0,7974768	IKBKE	0,71516876
4806	GZMB	0,86955465	E2F1	0,84744652	CP	0,80109083	SERPIND1	0,81910181	ABCA9	0,83472974	PLCB1	0,83300311	TIMELESS	0,78287607	4876	IRF2	0,8433585	TUBB4	0,81882764	JPH3	0,76062217	NDUFA13	0,77664549	CYP3A7	0,79118943	CA14	0,79715336	GSR	0,71447894
4807	CDC2L5	0,86950309	KCNJ9	0,84725612	GRB14	0,80030257	CHRNB2	0,81834819	HMGCS2	0,83393553	IVD	0,83277596	GPX6	0,78235649	4877	HP1BP3	0,8430954	THPO	0,81640252	ACAD9	0,75890501	ALDH3B1	0,77583531	HOXA13	0,79068392	CFI	0,79644237	PPYR1	0,71142471
4808	SERPINB5	0,86941794	ETS1	0,84654879	MAGEH1	0,79962171	FGFR1	0,81786651	BCAR1	0,83370985	TGFBRAP1	0,83267057	CTCF	0,78234039	4878	A2M	0,8423289	RDH13	0,81555372	ELA2	0,75884619	SIPA1	0,77427936	GSTO2	0,7905337	B3GAT1	0,7956597	PAFAH2	0,71114224
4809	DCT	0,86917225	NDUFB6	0,84630587	GSN	0,79959257	WFS1	0,81775499	RAPGEF1	0,83369453	FGF11	0,83253744	BPTF	0,78231453	4879	RAC1	0,84079487	ADHFE1	0,81403881	CYSLTR2	0,75773667	NCOA4	0,77412487	CA13	0,79047866	TNFRSF11B	0,79495666	SLC12A2	0,71102383
4810	ACCN4	0,8686323	GSTM2	0,84595277	UBE2F	0,79933364	BYSL	0,81688138	POLR1C	0,83352138	ATP5G2	0,83178878	XAB2	0,78214447	4880	GRB14	0,84031912	DRD5	0,81353936	SLC27A1	0,75725607	MAS1	0,77386166	PSAT1	0,79015958	ATXN2	0,79495532	HEMK1	0,70993909
4811	POR	0,8684635	GAS2	0,84569501	CDK9	0,79897059	EIF2B4	0,8167819	PA2G4	0,83243567	GAL3ST1	0,83172771	RAMP1	0,78149421	4881	EHD2	0,83785281	HSPA1L	0,81160265	CLCA2	0,75669184	HYAL4	0,7731046	GNMT	0,78948939	NFKBIL2	0,79335585	SORBS1	0,70774515
4812	PYGL	0,86838941	ARF6	0,84515202	P2RY2	0,79875836	MTNR1B	0,8162126	ADRB2	0,83186309	MAP1A	0,83043645	KCNN3	0,78140911	4882	PEG3	0,83772206	UGT1A8	0,81074522	WASF3	0,75655131	ATXN2	0,77248706	CYP2C8	0,78945711	SIRT7	0,7925405	LPL	0,70745606
4813	HADHA	0,86819953	UROS	0,84477217	AVEN	0,79855118	SNIP1	0,81597153	MKKS	0,83184298	DKK1	0,82855714	LRMP	0,77948206	4883	LAT	0,83744758	UGT1A9	0,81062027	IFRD1	0,75621222	APLP1	0,77176546	TUBD1	0,7893351	ALDH9A1	0,79246428	DDX55	0,70715235
4814	NMUR2	0,86807641	FOSL2	0,8441536	SPTBN4	0,79749653	KRT8	0,81580154	MYF6	0,83131775	PRLR	0,82847237	ADSS	0,77747465	4884	IKBKG	0,83712917	NOTCH3	0,8104244	GPR132	0,75578453	ELA3A	0,77120248	NDEL1	0,78893076	XAB2	0,79196311	MAP2K7	0,70642624
4815	RARG	0,86791151	PTGIR	0,84399834	FUT1	0,79743189	CD8A	0,81526306	INSIG2	0,83060549	GDF6	0,82837027	ANAPC11	0,77703003	4885	PDGFA	0,83646096	FLT3	0,80992136	UGT1A6	0,75491086	SLC11A1	0,7678447	ARF4	0,78806938	HAO2	0,79041208	ELA2	0,70637136
4816	ATN1	0,8673231	SERPIND1	0,84389486	BMP8A	0,79742945	HTR3A	0,81513914	ALG11	0,83039471	PAPSS2	0,82735072	ASPH	0,77696587	4886	FBP2	0,83638114	CLDN5	0,80938504	ALOX12B	0,75489912	MTR	0,76669124	GPX7	0,78709024	ADRBK1	0,78967683	HIBCH	0,7035453
4817	ZBTB7A	0,86699146	SIGLEC1	0,8433927	FANCD2	0,79689581	FRAT2	0,81505728	PTX3	0,8301054	UBE2J2	0,8272435	CD40LG	0,77540127	4887	MAPK8IP2	0,83417024	DDEF1	0,8089853	GPRC5A	0,75482458	MTNR1A	0,76635514	PIGQ	0,78668185	MAP3K4	0,78967444	SHC4	0,70342839
4818	SOX1	0,86692499	TAAR6	0,84335412	IMPDH1	0,79683095	HDAC6	0,81503542	ALG6	0,82998225	GPX1	0,8267739	EEF1G	0,77525834	4888	SLC12A6	0,83356163	B3GNT7	0,80724137	SLC1A6	0,75481751	HAO2	0,76613197	WASF3	0,78645164	DDIT3	0,78856424	SEPP1	0,69932867
4819	PITPNB	0,86650583	TNIP3	0,84314583	IRF2BP2	0,79543686	MLC1	0,8149106	PNPO	0,82972953	IMPDH1	0,82676851	GRIP1	0,77497369	4889	ELA2	0,83182447	TUBB2A	0,80646251	IL25	0,75474737	SPI1	0,76514991	TNFRSF10D	0,78490999	FANCM	0,78833285	SOD3	0,69871273
4820	ENTPD4	0,86608555	CD274	0,8428217	SLC22A18	0,79461307	NR1I2	0,81460164	LHX8	0,82954551	ELA2A	0,82655406	CXCR4	0,77405414	4890	POLR3A	0,83170866	ATG16L2	0,80617313	FGFR1	0,75446754	GCM1	0,7650091	ARSA	0,78461873	AARS2	0,78711851	PRKY	0,69456724
4821	HOXA7	0,86569708	LPA	0,84258176	ETS1	0,7944993	ACSL5	0,81378814	SYNE1	0,828966	GNMT	0,82653869	HTR2A	0,77386659	4891	GABRB2	0,83019027	GHRH	0,80617005	CD1B	0,7537852	DAPK2	0,76299009	CCKAR	0,7844048	CHN1	0,78669271	GPR81	0,69420698
4822	CD99	0,86509303	ATF5	0,84245675	LRP2	0,79368816	HTR1E	0,81278584	PCGF2	0,82896256	PIGQ	0,82639051	MAPK8IP1	0,77228329	4892	CD4	0,8292948	DTX1	0,80604446	CYP2D6	0,75358984	LPIN3	0,76296005	GUSB	0,7841722	MDH1	0,78647873	CD1B	0,69391989
4823	IFNGR2	0,86500118	PLAUR	0,8416529	MGP	0,79352385	CARTPT	0,81272743	TAAR6	0,82883394	ARSA	0,82587695	TP53	0,76973823	4893	FOSL2	0,8290402	IREB2	0,80551449	EXTL1	0,75276435	EPS8	0,76200783	GSTM1	0,78039885	SCN4A	0,78631708	MMRN1	0,69342946
4824	AMPD2	0,86459376	RARG	0,84162658	ITPR2	0,79352296	BAX	0,81197037	ITGA4	0,82869085	F10	0,8256336	EDG7	0,76963869	4894	ALDH3B1	0,82794336	ANGPTL2	0,80335887	IMPDH2	0,75257264	UGT1A4	0,76168051	PDE1A	0,78024522	CYB5R3	0,78621366	TLR9	0,69023776
4825	GUCY1A3	0,86450753	F13A1	0,84151228	ADRB1	0,79331678	SMAD6	0,81104439	GAL3ST1	0,82801613	ACAD9	0,82466308	PIK3R5	0,76962082	4895	CHRNA1	0,82757545	TAP1	0,80255914	AARS2	0,75199944	FUK	0,76124346	SET	0,77948477	EPO	0,78533893	RNF216	0,68895856
4826	PSAT1	0,86429856	TXNDC1	0,84114007	ETS2	0,79299782	CD59	0,80969299	ATG16L2	0,82627183	ADH4	0,82447105	CTPS	0,76923912	4896	TRIM28	0,82742512	RAD51L1	0,80244568	GLS	0,75153143	GAD2	0,76113337	BCL2L2	0,77742107	CARTPT	0,78524288	ATF2	0,68831699
4827	GJD2	0,86428854	ABCC4	0,84092271	ADRA2B	0,79241038	HSPA1L	0,80889343	ROCK2	0,82492185	EXTL1	0,82416618	CCR1	0,7681084	4897	CHST1	0,82733602	RAB9A	0,80241656	FCER1A	0,75062964	C5	0,76112994	CENTD1	0,77731036	PGD	0,78516448	LUM	0,68805964
4828	ASRGL1	0,86393169	PRDM1	0,84053442	TNFSF14	0,79224806	NMNAT2	0,80871778	CHN1	0,82443669	PRKY	0,82360255	DNAJB9	0,76779731	4898	NDUFB6	0,82727457	PMCH	0,800846	TUBA4A	0,75034625	SLC22A18	0,76075722	THPO	0,77729761	RHOQ	0,78511656	CHRNE	0,68772822
4829	ARNTL	0,86356213	PRKD1	0,84032812	POLR3GL	0,79220796	COL15A1	0,80858273	HDAC9	0,82442605	DGKA	0,82353997	PPP1CB	0,76745557	4899	TNFSF11	0,82603209	PPP2R2C	0,79852288	USH1C	0,74981932	PRKCH	0,76025703	PRKCH	0,7660985	PRB1	0,78474707	JUNB	0,68680693
4830	TNFRSF4	0,86328564	VANGL1	0,84006816	DDX52	0,79177859	VEGFC	0,80796956	TGFBRAP1	0,82439178	ATF7IP	0,82352556	DAZAP2	0,76602903	4900	ALAD	0,82574883	LTA4H	0,79848608	PLA2G4A	0,74971323	ADORA1	0,75913223	MDH1	0,77586737	SEPT2	0,78472792	CYP2R1	0,68225971

Table A4. Pooled-shRNA library screen on HEL cell line and MF-3: list of 2nd most depleted shRNAs for each experiment (ranking approach 1, RA1).

	NO ruxolitinib (setting 1)				Ruxolitinib (setting 2)				Ruxolitinib + CM (setting 3)				MF-3					NO ruxolitinib (setting 1)				Ruxolitinib (setting 2)				Ruxolitinib + CM (setting 3)				MF-3	
	Experiment 1		Experiment 2		Experiment 1		Experiment 2		Experiment 1		Experiment 2							Experiment 1		Experiment 2		Experiment 1		Experiment 2		Experiment 1		Experiment 2			
Rank	*Gene*	*Fold change*	*Gene*	*Fold change*	*Gene*	*Fold change*	*Gene*	*Fold change*	*Gene*	*Fold change*	*Gene*	*Fold change*	*Gene*	*Fold change*	*Rank*	*Gene*	*Fold change*	*Gene*	*Fold change*	*Gene*	*Fold change*	*Gene*	*Fold change*	*Gene*	*Fold change*	*Gene*	*Fold change*	*Gene*	*Fold change*	*Gene*	*Fold change*
4901	RXRB	0,82537111	AVEN	0,79763335	SERPING1	0,74956444	EXTL1	0,75832526	ANGPTL2	0,77399841	CHST1	0,78458991	OCIAD1	0,68126612	4971	CHAD	0,7299443	DCP1A	0,69065006	CAV2	0,5648041	APRT	0,6115524	HIBCH	0,64541095	GP5	0,64758944	CYP2B6	0,45944839
4902	CYP3A4	0,82447394	ME1	0,7971152	CKMT2	0,74903466	TPMT	0,75725671	HSPA2	0,77386584	SND1	0,78222438	CD63	0,68126277	4972	PPP2R2C	0,71415078	C1GALT1	0,66798945	ZFYVE16	0,53191258	CBX4	0,6059222	CCR5	0,64534845	IFNGR2	0,64495029	JAK3	0,44988486
4903	HLX	0,82445383	OLR1	0,79654823	DIO1	0,7468956	HLA-DPA1	0,75660422	RAP1GAP	0,77177191	GPR65	0,78129521	SCNN1A	0,6801699	4973	SERPINA1	0,69712078	CHAD	0,65907473	STMN2	0,5315334	BMP8A	0,60342885	NKIRAS2	0,64489692	AARS	0,63395326	GSTM3	0,43810353
4904	SIRPA	0,82433062	BOK	0,79602142	AFMID	0,7467279	ALPPL2	0,75655687	UBE2L6	0,77021842	GPI	0,78037787	GABRB2	0,67875789	4974	AVEN	0,66956825	E2F3	0,6376206	IKBKG	0,47577142	CYSLTR2	0,56771495	GPR65	0,60859692	PAX6	0,58078536	UHRF1	0,43626977
4905	CA13	0,82285225	GNRH1	0,79545243	PAPPA	0,74645023	BBOX1	0,75648039	CYSLTR2	0,76862463	RNF216	0,77775335	PRKAA2	0,67665523																
4906	UGT1A4	0,82253558	IKBKG	0,79349843	SCG2	0,74595132	FTCD	0,75571119	GALNT12	0,76846635	SOD3	0,77739358	MNAT1	0,67385033																
4907	LAMC1	0,82246769	DHFR	0,7925933	CYP2U1	0,74545115	BCMO1	0,75521727	PHPT1	0,76819256	HS6ST2	0,77625286	RAC1	0,672022																
4908	UNG	0,82240105	SLC22A6	0,79215686	FANCC	0,74464093	IFI30	0,74895249	WISP2	0,76808014	UPB1	0,77601004	GPR39	0,66972194																
4909	HTR3A	0,82229013	CBL	0,79149167	WIPI2	0,74412854	PMP22	0,74771851	GRM6	0,76789565	TUBD1	0,7754099	RPS6KB1	0,66834464																
4910	RAB24	0,82160591	IL28RA	0,79060934	CTLA4	0,74408804	GALNT2	0,74649861	PIN1	0,7657537	GRASP	0,77493513	GLP1R	0,66621611																
4911	UBE2F	0,81849876	APLP1	0,79033047	CBLC	0,74164334	CAMK1	0,7458236	RARG	0,76526903	ALOX12B	0,7747734	CHRM4	0,66595182																
4912	CASP8AP2	0,81752143	ARSA	0,7900216	AKT2	0,74146153	AGTR1	0,74514762	UGT1A3	0,76257574	PGK1	0,77362253	LMNB1	0,66461837																
4913	PGAP1	0,81719021	HTATIP	0,78655758	ALG6	0,73713658	MAFF	0,74379905	AMPD2	0,76155495	HMGB3	0,77315675	CYP1A1	0,66231261																
4914	ADCYAP1	0,81656975	TCEA3	0,78620509	PRKCZ	0,73614967	E2F3	0,74206365	PGK1	0,75964285	MAN2B2	0,77308564	ZFYVE16	0,66213046																
4915	APRT	0,81622144	ST8SIA5	0,78555868	CBX7	0,73461154	VAV2	0,74153016	GIT1	0,75935322	SLC18A2	0,77243676	CHAD	0,66136628																
4916	DCP1A	0,81560575	CCL5	0,78467874	MYL9	0,73452532	ST8SIA5	0,74036755	OAS1	0,75810999	PPP3R1	0,7714746	HMGB1	0,65774658																
4917	IKZF3	0,81552684	COL11A1	0,78444836	SMAD6	0,73247304	SLC22A6	0,73994769	SOST	0,75793591	GALE	0,77145808	CUGBP2	0,65747043																
4918	GPR77	0,8153282	CLCA2	0,78404564	CACNA1E	0,73118502	MAT2B	0,73900148	NDUFB6	0,75695727	CFHR4	0,7713756	GP5	0,6562851																
4919	PPP1R1B	0,81492546	CSNK2A2	0,78367805	CXCR4	0,72900188	TP73	0,73885614	GALK2	0,75613117	XDH	0,76729877	CXCL2	0,65476391																
4920	GCDH	0,81490037	PIN1	0,7832951	PTPRU	0,72802287	G3BP2	0,7369235	ADRBK2	0,7544881	BCKDHB	0,76545047	SLC1A2	0,65300688																
4921	TNFSF9	0,81336002	PHKG1	0,78290717	NEIL2	0,72496727	MCM5	0,73570874	CLDN16	0,7543174	CENTD2	0,76519945	ALG6	0,6522685																
4922	BCMO1	0,81318387	MAS1	0,78232231	OLR1	0,72382059	GPR75	0,73567796	CDKL1	0,75420702	HSD11B1	0,76497065	HOXD10	0,65155398																
4923	ARSE	0,81185965	ETV3	0,78120134	APBB2	0,72255948	LAMC1	0,73459831	AKTIP	0,75339789	PMS2	0,76372874	APOC3	0,64966165																
4924	CLCA2	0,81125528	ABLIM3	0,78071717	IFNK	0,72197891	IL3	0,73413734	FGFR1	0,75334203	ALPPL2	0,76199262	SEMA3A	0,64895202																
4925	TNFRSF10D	0,81068063	IL18	0,77925809	POLD3	0,72113157	ME1	0,73063575	CTGF	0,75104698	OAS1	0,76033393	HTR3B	0,64772819																
4926	B3GNT5	0,81008466	GNAL	0,77771377	FGF11	0,71925293	HIF1A	0,72965834	ALG9	0,7493874	TUBA4A	0,76000595	ABCB4	0,64713675																
4927	ATF7IP	0,80811665	TGFBR3	0,77536311	CSNK2A1	0,71582984	TBXA2R	0,72856834	ACADM	0,74909866	RGS5	0,7576893	ADCY5	0,64657773																
4928	ADCY2	0,80701675	UCHL1	0,77522448	PMS2	0,71409804	RAC1	0,72669124	IL1B	0,74784712	TNFRSF10D	0,75748177	NMNAT3	0,64125405																
4929	GPX2	0,80602603	GCLM	0,77506914	COL6A2	0,71331266	HOXB4	0,72470271	C1QL3	0,74561922	HTATIP	0,75702155	GSTM2	0,63988972																
4930	GNRH1	0,8057662	KLRC4	0,77297088	IDS	0,71301875	DUSP4	0,72423586	HBXIP	0,74432083	ZNF259	0,75554976	POLR2J	0,63855502																
4931	IGFBP6	0,80424617	FSHB	0,77245257	CEBPB	0,71189696	HOXA13	0,72380928	DLX1	0,74419757	ARSD	0,75505088	UGT2B11	0,63780381																
4932	JUND	0,803746	MCC	0,77231713	APRT	0,71117698	HLA-A	0,72357956	OXTR	0,74376846	TGFBR1	0,75377323	SARM1	0,63098715																
4933	SLC11A1	0,80279566	C1QL3	0,77229202	GAL3ST1	0,71054359	SKIL	0,72007312	CD1C	0,74364021	AMPD1	0,74779428	DAB2	0,6271249																
4934	SSTR1	0,80213184	ITGAM	0,77003096	MAT2B	0,70822265	PDE1A	0,71986809	HSPA1L	0,74206298	EXTL2	0,74720143	MAPK8IP3	0,6267211																
4935	IL22RA2	0,80134929	ALG11	0,76918547	FABP6	0,70769746	CD6	0,71967977	NOTCH2	0,73926189	RAB1B	0,7437031	FUT4	0,62395677																
4936	MADCAM1	0,80098845	SOD3	0,76918394	BBOX1	0,70709172	CD44	0,71892442	PHKA1	0,73736337	TFDP1	0,74191032	PPP3CA	0,62201333																
4937	ALOX15	0,80013148	SIX3	0,76902731	RERE	0,70504162	SERPING1	0,71684287	ERN2	0,73628814	TBXA2R	0,73953013	SFMBT2	0,62025507																
4938	GPR65	0,79959181	CACNA1I	0,76596555	ARHGEF1	0,70433687	PRLR	0,71551662	HIF1A	0,73475863	MAT2B	0,73823149	CDK6	0,62020938																
4939	F8A1	0,79894777	EDG1	0,76247447	GSTA4	0,70289198	CBX7	0,71500147	CD1D	0,7343652	TRPC2	0,73579727	DRD5	0,6198718																
4940	PIGL	0,79673818	PIWIL2	0,7621012	ATG5	0,69728623	POU5F1	0,71333256	ACIN1	0,73146895	IL18	0,73512183	LRP1	0,61009947																
4941	TGFBR3	0,79650684	BMP8A	0,76148234	PRB1	0,69666043	EDG1	0,7120363	CBL	0,72924679	POLG2	0,73432153	JUND	0,60942871																
4942	CD8A	0,79635933	NFKBIB	0,76099644	ARF6	0,69503718	EXT1	0,71129104	ADSL	0,72426317	UXT	0,7308559	TFAP2B	0,60768302																
4943	MAGEH1	0,79522022	MTNR1B	0,75931426	CMBL	0,68964488	POU2F2	0,70993041	NR2F6	0,7225982	CCR5	0,7294166	HSPE1	0,60757174																
4944	ANXA3	0,79240715	MAT2B	0,7589087	FLJ21865	0,68815983	GIT1	0,70365855	MCRS1	0,72201602	AKTIP	0,72721599	SMAD2	0,60633863																
4945	CHN1	0,79040949	XAB2	0,75790095	OAS1	0,6824987	FANCM	0,69962653	TRPC2	0,72159657	TNFRSF4	0,72637325	SLC26A2	0,60556511																
4946	ABP1	0,79004702	ATF7IP	0,75764627	PIR	0,68024711	PMS2	0,69842832	NEU4	0,71955822	CLDN23	0,72307387	UGP2	0,60521932																
4947	PLA2G4C	0,78817978	DAPK2	0,75313063	ADH1B	0,67794081	SLC1A6	0,69819579	CNPY3	0,71911486	CSNK2A2	0,72208597	ME1	0,60384091																
4948	BCAT1	0,78646414	POLR3A	0,75296968	FZD6	0,67562916	ID1	0,69776872	GLG1	0,71736753	GNRHR	0,7219639	ORC2L	0,59891351																
4949	SKIL	0,78467225	ANXA3	0,75236332	HAO2	0,67338586	CMA1	0,69694577	ETS2	0,71685525	HS3ST3A1	0,72194967	MLC1	0,59530017																
4950	CSNK1G2	0,78335629	PDGFA	0,75211075	ALG12	0,67300234	OAS1	0,69328534	UBE2F	0,71622163	GALK2	0,72006588	SOAT1	0,5944331																
4951	AGT	0,78033042	GPX1	0,7517471	SKIL	0,67270783	DDX52	0,69247832	PLA2G12A	0,71461129	MLC1	0,71812773	FZD4	0,59142954																
4952	TFCP2	0,77946747	CCNB1	0,75006286	CYCS	0,67083803	SYNJ2	0,69139978	ELOVL2	0,7132717	CYSLTR2	0,71664881	EIF5	0,5905614																
4953	ABCC5	0,77896651	DDX52	0,7476444	PDLIM5	0,67012283	SOX9	0,6847715	NR2F1	0,70972205	UBE2F	0,71520607	PDXK	0,58921083																
4954	E2F4	0,77826509	APRT	0,74621301	IL12A	0,66623321	DCP1A	0,68100286	ATF7IP	0,69955534	CAPN2	0,71361049	ACLY	0,58888513																
4955	NR1H2	0,7721671	B3GALNT1	0,74375772	CD44	0,66021167	IFNK	0,6792699	PPP1R13L	0,69801694	NDUFB8	0,70988294	BST2	0,58857791																
4956	FGF11	0,76954598	VAV2	0,7437239	ZFYVE9	0,65539845	CAV2	0,67775433	PTPRU	0,69729025	CLCA2	0,69962498	NOG	0,5883495																
4957	IL18	0,76834285	GPR65	0,74345426	GCG	0,65029014	XDH	0,67228475	SIX3	0,69277895	PLA2G4B	0,69954519	DFFB	0,5851261																
4958	FCN1	0,7681089	GPR75	0,74336103	PAX6	0,64533937	PLA2G12A	0,67019662	CFI	0,6915658	AKAP10	0,69774276	MAP1B	0,58416844																
4959	TGFBR1	0,76633206	KCNIP3	0,74064794	DCTD	0,64474964	CACNA1E	0,66759965	VAV2	0,68862444	ABL2	0,69619912	CAMP	0,58003071																
4960	PCGF2	0,76600144	CAV2	0,73728565	ATG16L1	0,64456122	GSTM1	0,66676717	CBX3	0,68844204	MMP8	0,6925793	DACT1	0,57997419																
4961	PLA2G4B	0,76540443	GABRE	0,73578655	BAX	0,63750537	UHRF1	0,66322449	UGT1A4	0,68838486	SERPIND1	0,68981921	PTGFR	0,57632046																
4962	CDKL1	0,76390737	CD4	0,73272376	PMP22	0,63611379	PLA2G2A	0,66108371	CFHR4	0,68833016	MRE11A	0,68537764	CDC23	0,567475																
4963	UCHL1	0,75795875	GSTM1	0,73270648	PRLR	0,63572863	GNRHR	0,6536807	G3BP2	0,68524762	MCC	0,68423767	MAX	0,56738992																
4964	EXTL1	0,75170454	PLA2G2A	0,72858005	TREM1	0,62878039	ITPA	0,6523705	ALOX15	0,68253243	PLA2G12A	0,68380544	HR	0,56644882																
4965	CDKL2	0,74971388	PRKCH	0,72816014	SMO	0,61864809	NDUFB6	0,65185703	ANXA3	0,67741767	AASDH	0,67640266	SCG2	0,56073509																
4966	PAK3	0,74951382	ITGB4	0,72146405	ASCC3	0,61834588	PRKY	0,64748829	APP	0,67679994	CSNK2A1	0,6745312	CDC2L6	0,559972																
4967	RARA	0,74819008	WWP1	0,72143701	POLD4	0,61496803	GLG1	0,64382475	DCP1A	0,67326442	CDK10	0,67418285	GTF2H2	0,55811821																
4968	PMS2	0,74527522	PRB1	0,72138415	THRA	0,59879313	GNRH1	0,63904004	SAA1	0,66950765	MTNR1B	0,67127259	A1BG	0,52311866																
4969	TEK	0,74138928	ELA2A	0,71096261	NDUFB6	0,57924179	SLC30A6	0,62871841	GPX1	0,65703757	GSN	0,66442619	ASH1L	0,48371452																
4970	GPX1	0,7339629	G3BP2	0,70360412	E2F3	0,57309604	FGG	0,62251282	CSNK2A2	0,65131449	FGFR1	0,66119583	B3GALT6	0,47134677																

Table A5. List of 143 genes for which there were ≥ 2 shRNAs having FC ≥ 3 or resulting among the top 2% depleted in BOTH replicates in one or more experimental conditions (alphabetical order).

GENE name	*Criteria satisfied by both replicates of each condition*					
	Baseline	***Ruxo***	***Ruxo+HS5***	***Baseline***	***Ruxo***	***Ruxo+HS5***
	N of shRNAs with at least 3FC	N of shRNAs with at least 3FC	N of shRNAs with at least 3FC	N of shRNAs in the top 2%	N of shRNAs in the top 2%	N of shRNAs in the top 2%
ABCB5	0	1	2	0	0	2
ACCN3	0	2	1	0	0	1
ACOX3	0	2	1	0	1	0
ACTA2	1	2	1	1	1	1
ALG10B	0	2	1	2	0	1
ANAPC2	0	2	2	1	2	2
AQR	1	2	2	1	2	1
ASCC3L1	1	3	3	2	2	2
ATP5C1	0	2	0	0	0	0
BCL2L1	1	1	2	3	0	1
C15ORF15	0	2	0	0	0	0
CAPN5	0	2	3	1	1	0
CAV3	0	2	1	1	0	0
CCL20	0	2	1	0	1	1
CD247	0	1	2	0	0	1
CD3D	0	2	1	0	0	1
CDC2	1	3	0	1	0	0
CDC2L1	0	3	2	1	2	0
CDC40	0	2	2	0	1	0
CEL	0	2	0	0	0	0
CIRBP	0	2	1	1	0	1
CLDN2	0	2	0	0	1	0
CLEC5A	0	2	0	0	0	0
CSE1L	3	4	1	3	2	0
CYP51A1	1	2	2	1	0	1
DDX23	0	2	1	0	0	0
DDX41	0	3	2	1	2	1
DEFB4	0	2	0	0	0	0
DNAJB2	0	2	2	1	1	1
EDNRA	0	2	0	0	0	0
EEF2	2	2	3	2	0	2

GENE name	*Criteria satisfied by both replicates of each condition*					
	Baseline	***Ruxo***	***Ruxo+HS5***	***Baseline***	***Ruxo***	***Ruxo+HS5***
	N of shRNAs with at least 3FC	N of shRNAs with at least 3FC	N of shRNAs with at least 3FC	N of shRNAs in the top 2%	N of shRNAs in the top 2%	N of shRNAs in the top 2%
EFNB1	0	2	1	0	0	0
EFTUD2	1	2	3	1	1	1
EIF1AX	0	2	1	0	0	1
EIF2S2	1	3	3	2	2	1
ENG	0	2	0	0	0	0
FLI1	1	4	1	1	1	1
GALNT3	0	2	0	0	0	0
GBP1	0	2	1	0	0	0
GNB2L1	0	2	1	2	1	0
GPD2	0	2	0	0	0	0
GPHN	0	2	0	0	0	0
GRB2	0	1	2	1	0	0
GRIN1	0	2	0	0	0	0
GRM5	0	2	0	0	0	0
GSR	0	1	2	0	0	2
GTF2A1L	0	2	0	0	0	0
GTF2F1	0	1	0	2	0	0
HNRPK	0	2	2	1	0	0
HSPA9	1	2	1	2	2	1
HSPE1	0	5	1	1	0	0
HTR1B	0	2	1	0	1	1
IARS2	0	2	0	0	0	0
ID2	0	2	0	0	0	0
IGF2R	0	2	1	0	0	0
IL12RB1	0	2	1	0	1	1
IL23A	0	2	0	0	0	0
INPP4A	0	2	1	0	1	1
ITK	0	1	2	0	0	0
JAK2	1	3	2	2	1	1
KPNB1	0	2	2	1	1	2
MAPKAPK5	0	2	0	1	1	0
MPL	0	3	3	0	0	1
NDE1	0	2	0	1	0	0
NDUFA10	0	2	1	1	0	0

GENE name	*Criteria satisfied by both replicates of each condition*					
	Baseline	***Ruxo***	***Ruxo+HS5***	***Baseline***	***Ruxo***	***Ruxo+HS5***
	N of shRNAs with at least 3FC	N of shRNAs with at least 3FC	N of shRNAs with at least 3FC	N of shRNAs in the top 2%	N of shRNAs in the top 2%	N of shRNAs in the top 2%
NEDD8	1	2	2	2	1	2
NLN	0	2	0	0	1	0
NUDT1	0	2	1	0	0	0
OGDH	0	2	2	1	0	0
PAX2	0	2	0	1	1	0
PDHX	1	2	2	1	1	1
PGAM1	0	2	0	0	0	0
PHB2	0	4	3	2	3	2
POLR2A	0	1	1	2	0	0
POLR2D	0	2	1	0	0	1
POLR2F	0	2	2	0	1	1
POLR2J	0	1	2	0	1	0
PORCN	0	2	0	0	0	0
PRDX2	0	2	2	0	0	2
PRKAB2	0	2	1	0	1	0
PRPF40A	1	3	3	2	2	2
PSCA	0	3	1	0	0	1
PSMA2	4	5	5	4	5	5
PSMA3	2	3	4	4	3	3
PSMA4	1	3	2	1	1	2
PSMA7	1	2	1	1	0	1
PSMB1	0	2	2	0	0	1
PSMB2	2	5	4	4	3	4
PSMB4	0	3	2	1	2	2
PSMB7	0	4	4	0	3	3
PSMC1	0	4	4	0	3	0
PSMC2	0	2	1	0	0	1
PSMC3	0	1	2	0	0	1
PSMC6	0	3	2	0	1	1
PSMD1	3	4	2	3	3	2
PSMD11	1	4	3	1	2	2
PSMD13	0	2	1	0	1	0
PSMD2	1	3	2	1	1	1
PSMD3	1	2	2	1	1	1

GENE name	*Criteria satisfied by both replicates of each condition*					
	Baseline	***Ruxo***	***Ruxo+HS5***	***Baseline***	***Ruxo***	***Ruxo+HS5***
	N of shRNAs with at least 3FC	N of shRNAs with at least 3FC	N of shRNAs with at least 3FC	N of shRNAs in the top 2%	N of shRNAs in the top 2%	N of shRNAs in the top 2%
PSMD6	0	4	4	2	3	2
RAN	2	6	5	5	4	4
RANBP1	0	3	1	1	1	0
RANBP2	0	2	0	0	1	0
RBM8A	0	2	2	1	1	1
RIPK3	0	3	1	0	1	0
RPA1	0	2	2	1	1	1
RPL10	0	3	4	1	1	0
RPL11	1	4	5	2	0	3
RPL12	0	3	2	3	1	2
RPL13	0	1	2	1	0	0
RPL14	0	3	2	1	3	0
RPL15	0	2	1	0	1	0
RPL4	1	4	1	1	1	1
RPL6	1	3	1	1	1	1
RPL8	0	2	1	0	1	1
RPS11	0	3	1	1	1	1
RPS13	1	4	3	3	4	2
RPS3A	1	2	2	2	1	1
RPS6	0	2	1	1	2	1
RPSA	0	3	1	0	1	1
RRM1	3	4	4	3	4	2
RTF1	2	2	3	3	2	3
RUVBL1	0	2	2	0	0	1
RUVBL2	0	5	3	0	1	3
SAP18	0	1	2	0	0	0
SARS	1	2	2	1	1	0
SHFM1	0	2	1	1	1	1
SHMT1	0	2	0	0	0	0
SHMT2	0	2	0	0	0	0
SIN3A	0	1	2	0	0	2
SNRPA1	0	2	2	0	0	1
SNRPD2	0	4	2	2	3	2
SNRPN	1	3	3	2	3	3

GENE name	*Criteria satisfied by both replicates of each condition*					
	Baseline	***Ruxo***	***Ruxo+HS5***	***Baseline***	***Ruxo***	***Ruxo+HS5***
	N of shRNAs with at least 3FC	N of shRNAs with at least 3FC	N of shRNAs with at least 3FC	N of shRNAs in the top 2%	N of shRNAs in the top 2%	N of shRNAs in the top 2%
SNW1	1	2	2	2	2	2
SOS1	0	2	1	0	0	0
STX19	0	2	0	1	0	0
STX1A	1	2	1	1	0	1
SULT1B1	0	2	2	1	2	0
TUBA1C	0	2	2	1	2	2
VAMP1	0	2	1	0	0	0
WNT3A	0	2	0	0	0	0
WNT8A	0	2	1	0	1	1
XRCC6	0	2	0	0	0	0

Table A6. Top essential genes for viability or proliferation of HEL cells under various conditions – ranking approach 3 (RA3).

	condition true for both replicates of each condition								
	Baseline	***Ruxo***	***Ruxo +HS-5***	***Baseline***	***Ruxo***	***Ruxo +HS-5***			
GENE name	N of shRNAs with at least 3FC	N of shRNAs with at least 3FC	N of shRNAs with at least 3FC	N of shRNAs in the top 2%	N of shRNAs in the top 2%	N of shRNAs in the top 2%	N of settings with ≥2 shRNA with 3FC	N of settings with ≥2 shRNA in the top 2%	**Gene with highest score sum**
RAN	2	6	5	5	4	4	3	3	6
PSMA2	4	5	5	4	5	5	3	3	6
PSMB2	2	5	4	4	3	4	3	3	6
PSMA3	2	3	4	4	3	3	3	3	6
PSMD1	3	4	2	3	3	2	3	3	6
RRM1	3	4	4	3	4	2	3	3	6
RTF1	2	2	3	3	2	3	3	3	6
PHB2	0	4	3	2	3	2	2	3	5
PSMD6	0	4	4	2	3	2	2	3	5
RPS13	1	4	3	3	4	2	2	3	5
SNRPD2	0	4	2	2	3	2	2	3	5
ASCC3L1	1	3	3	2	2	2	2	3	5
EEF2	2	2	3	2	0	2	3	2	5
PRPF40A	1	3	3	2	2	2	2	3	5
SNRPN	1	3	3	2	3	3	2	3	5
SNW1	1	2	2	2	2	2	2	3	5
RPL11	1	4	5	2	0	3	2	2	4
EIF2S2	1	3	3	2	2	1	2	2	4
RPL12	0	3	2	3	1	2	2	2	4
NEDD8	1	2	2	2	1	2	2	2	4
JAK2	1	3	2	2	1	1	2	1	3
RPS3A	1	2	2	2	1	1	2	1	3

Table A7. Differentially expressed genes in CD34+ MF cells treated with ruxolitinib.
This table lists the genes from the most downregulated to the most upregulated ones having a $\log_2$ fold change >1 in absolute value and an adjusted P-value <0.05.

Gene	$\log_2$ Fold Change	Standard Error ($\log_2$ fold change)	P-value	Adjusted P-value
H19	-6.745	1.296	1.93E-07	2.07E-05
PAK3	-5.975	1.449	3.71E-05	1.41E-03
IL7R	-4.402	0.82	7.82E-08	9.53E-06
STC2	-3.812	0.907	2.63E-05	1.08E-03
LRRC77P	-3.316	0.575	7.99E-09	1.42E-06
ADM2	-3.261	0.561	6.06E-09	1.14E-06
GLI2	-3.123	0.631	7.32E-07	6.35E-05
IL17RB	-3.071	0.433	1.25E-12	6.40E-10
KCNJ15	-3.07	0.87	4.15E-04	9.21E-03
CHAC1	-2.971	0.688	1.57E-05	7.21E-04
CBS	-2.891	0.413	2.52E-12	1.16E-09
FHAD1	-2.801	0.835	7.96E-04	1.47E-02
IGFBP5	-2.794	0.534	1.68E-07	1.86E-05
CCL24	-2.577	0.639	5.52E-05	1.96E-03
TNFRSF18	-2.569	0.241	1.81E-26	7.90E-23
SLAMF1	-2.568	0.424	1.42E-09	3.31E-07
HSPA7	-2.49	0.812	2.18E-03	3.14E-02
ERFE	-2.49	0.348	8.31E-13	5.37E-10
SERPINA1	-2.477	0.562	1.05E-05	5.25E-04
IL19	-2.415	0.573	2.47E-05	1.03E-03
CCL2	-2.4	0.362	3.36E-11	1.22E-08
ZNF804B	-2.389	0.707	7.29E-04	1.39E-02
LINC01948	-2.317	0.477	1.21E-06	9.39E-05
AL138916.1	-2.304	0.8	3.99E-03	4.76E-02
EGR1	-2.292	0.543	2.46E-05	1.03E-03
AC109466.1	-2.231	0.522	1.93E-05	8.50E-04
RUBCNL	-2.186	0.603	2.86E-04	6.96E-03
CCDC3	-2.155	0.559	1.17E-04	3.50E-03
ELFN1	-2.144	0.488	1.10E-05	5.45E-04
FPR1	-2.118	0.432	9.55E-07	7.85E-05
IL2RA	-2.086	0.458	5.17E-06	3.00E-04
PSAT1	-2.051	0.246	7.23E-17	1.05E-13
DHH	-1.981	0.686	3.88E-03	4.66E-02
GGT5	-1.964	0.424	3.57E-06	2.22E-04
FAM47E-STBD1	-1.931	0.288	1.87E-11	7.10E-09
HP	-1.93	0.655	3.23E-03	4.12E-02
LINC00032	-1.926	0.552	4.82E-04	1.02E-02

CHDH	-1.883	0.475	7.32E-05	2.45E-03
ENPP2	-1.863	0.495	1.69E-04	4.66E-03
PPFIA4	-1.851	0.376	8.47E-07	7.16E-05
CCDC170	-1.842	0.356	2.34E-07	2.37E-05
GLP1R	-1.836	0.604	2.37E-03	3.33E-02
IGFBP4	-1.818	0.626	3.68E-03	4.48E-02
IER3	-1.809	0.333	5.79E-08	7.48E-06
SIGLEC12	-1.808	0.422	1.82E-05	8.18E-04
CD80	-1.796	0.418	1.77E-05	8.00E-04
FPR2	-1.786	0.37	1.40E-06	1.05E-04
CD163	-1.783	0.591	2.54E-03	3.49E-02
IL2RB	-1.774	0.567	1.77E-03	2.68E-02
SOCS3	-1.738	0.423	3.93E-05	1.48E-03
TGFBI	-1.725	0.413	2.98E-05	1.18E-03
SLC9A2	-1.711	0.479	3.58E-04	8.24E-03
HORMAD2	-1.695	0.44	1.17E-04	3.51E-03
OSM	-1.692	0.457	2.11E-04	5.54E-03
AF127936.1	-1.69	0.512	9.69E-04	1.71E-02
MT-RNR1	-1.688	0.216	5.48E-15	4.78E-12
LOXL1	-1.665	0.187	4.91E-19	1.43E-15
SERTM2	-1.663	0.526	1.57E-03	2.46E-02
LINC02204	-1.646	0.393	2.82E-05	1.14E-03
CFH	-1.645	0.3	4.30E-08	5.73E-06
AL109837.3	-1.641	0.297	3.17E-08	4.50E-06
AL031293.1	-1.625	0.364	8.31E-06	4.41E-04
ULBP1	-1.623	0.487	8.61E-04	1.56E-02
PIM1	-1.616	0.381	2.25E-05	9.67E-04
AC015911.11	-1.612	0.497	1.18E-03	1.99E-02
RNVU1-31	-1.609	0.393	4.18E-05	1.55E-03
BATF3	-1.604	0.32	5.20E-07	4.72E-05
CACNA2D1	-1.596	0.394	5.21E-05	1.86E-03
MMP9	-1.583	0.273	6.64E-09	1.22E-06
ADGRG3	-1.582	0.427	2.08E-04	5.47E-03
IL18RAP	-1.578	0.377	2.78E-05	1.13E-03
ST6GALNAC3	-1.569	0.394	6.95E-05	2.35E-03
MT-ATP8	-1.553	0.217	8.88E-13	5.53E-10
BCYRN1	-1.534	0.529	3.70E-03	4.50E-02
TNFRSF8	-1.532	0.378	5.01E-05	1.81E-03
GSG1L	-1.529	0.396	1.14E-04	3.44E-03
CLEC7A	-1.527	0.482	1.53E-03	2.42E-02
CD22	-1.516	0.422	3.27E-04	7.75E-03
MUC1	-1.485	0.266	2.25E-08	3.42E-06

SOCS1	-1.477	0.353	2.85E-05	1.15E-03
SCN2A	-1.47	0.373	8.18E-05	2.67E-03
TREM1	-1.469	0.472	1.87E-03	2.80E-02
LIF	-1.461	0.419	4.96E-04	1.04E-02
AZIN2	-1.456	0.27	6.85E-08	8.66E-06
MT-TF	-1.454	0.326	8.43E-06	4.44E-04
ENPP6	-1.453	0.437	8.75E-04	1.58E-02
NDUFA4L2	-1.448	0.421	5.74E-04	1.16E-02
LTB	-1.447	0.356	4.83E-05	1.75E-03
ADAMTS14	-1.412	0.383	2.30E-04	5.89E-03
AL034397.2	-1.411	0.333	2.26E-05	9.67E-04
ALDH1L2	-1.394	0.264	1.30E-07	1.51E-05
RPL41P1	-1.392	0.412	7.29E-04	1.39E-02
MT-ND3	-1.385	0.226	9.37E-10	2.24E-07
SYN1	-1.375	0.476	3.85E-03	4.63E-02
AC005324.3	-1.365	0.351	1.01E-04	3.16E-03
SLAMF8	-1.359	0.286	2.04E-06	1.41E-04
MT-TL1	-1.288	0.269	1.73E-06	1.24E-04
TNFRSF4	-1.277	0.327	9.56E-05	3.04E-03
TMEM273	-1.276	0.346	2.26E-04	5.84E-03
AC011246.1	-1.26	0.177	1.05E-12	5.73E-10
STAT4	-1.259	0.157	8.87E-16	1.03E-12
TM4SF1	-1.257	0.336	1.82E-04	4.96E-03
GDF15	-1.249	0.3	3.15E-05	1.24E-03
AL591506.1	-1.245	0.419	2.97E-03	3.89E-02
CHRM3-AS2	-1.244	0.321	1.04E-04	3.22E-03
SPP1	-1.243	0.218	1.22E-08	2.02E-06
MTATP6P1	-1.226	0.181	1.42E-11	5.62E-09
MT-ND4L	-1.225	0.186	5.13E-11	1.69E-08
LINC01091	-1.213	0.267	5.44E-06	3.09E-04
ID1	-1.203	0.364	9.52E-04	1.69E-02
FCRLB	-1.201	0.252	1.85E-06	1.31E-04
AL109615.3	-1.187	0.332	3.53E-04	8.16E-03
MT-ND2	-1.175	0.178	3.91E-11	1.39E-08
MT-ATP6	-1.171	0.17	5.34E-12	2.22E-09
CIB3	-1.17	0.397	3.17E-03	4.08E-02
CD69	-1.154	0.383	2.55E-03	3.49E-02
RN7SL471P	-1.153	0.204	1.50E-08	2.40E-06
ICAM1	-1.151	0.377	2.24E-03	3.20E-02
MT-ND4	-1.151	0.166	4.12E-12	1.75E-09
MT-ND5	-1.123	0.162	3.80E-12	1.66E-09
ENOX1	-1.118	0.33	7.09E-04	1.36E-02

CISH	-1.117	0.148	3.64E-14	2.76E-11
F5	-1.108	0.38	3.54E-03	4.37E-02
DHRS9	-1.108	0.173	1.48E-10	4.08E-08
MT-ND6	-1.108	0.213	1.86E-07	2.02E-05
TRDC	-1.086	0.353	2.11E-03	3.06E-02
PPM1E	-1.066	0.349	2.27E-03	3.23E-02
MB21D2	-1.065	0.254	2.81E-05	1.14E-03
DDN	-1.057	0.319	9.30E-04	1.66E-02
AC084082.1	-1.054	0.311	7.02E-04	1.35E-02
ASIC1	-1.048	0.265	7.62E-05	2.52E-03
RNY1	-1.046	0.181	7.24E-09	1.30E-06
BATF2	-1.039	0.296	4.59E-04	9.86E-03
RAB20	-1.038	0.176	3.94E-09	8.08E-07
GPR84	-1.034	0.353	3.35E-03	4.22E-02
CTSL	-1.03	0.214	1.53E-06	1.11E-04
MT-TM	-1.023	0.229	8.23E-06	4.39E-04
AC234582.1	-1.019	0.225	5.87E-06	3.30E-04
HRH2	-1.011	0.345	3.41E-03	4.27E-02
ARG2	-1	0.293	6.48E-04	1.27E-02
AP002992.1	1.012	0.305	9.20E-04	1.65E-02
FLT3	1.015	0.316	1.33E-03	2.17E-02
KANK4	1.018	0.302	7.48E-04	1.41E-02
AC092979.2	1.041	0.33	1.60E-03	2.48E-02
MIR3142HG	1.059	0.16	4.06E-11	1.42E-08
AL138963.4	1.059	0.245	1.49E-05	6.93E-04
MMP28	1.064	0.179	2.64E-09	5.89E-07
TRIM73	1.075	0.243	1.00E-05	5.07E-04
COL9A2	1.082	0.168	1.21E-10	3.45E-08
TOB1-AS1	1.082	0.344	1.65E-03	2.53E-02
LGI4	1.088	0.299	2.72E-04	6.70E-03
AC083870.1	1.094	0.373	3.37E-03	4.24E-02
TMPRSS9	1.095	0.243	6.37E-06	3.53E-04
AP000695.2	1.104	0.275	5.97E-05	2.07E-03
LINC00920	1.106	0.384	4.01E-03	4.77E-02
CRHBP	1.16	0.237	9.87E-07	7.94E-05
AP002907.1	1.165	0.388	2.67E-03	3.61E-02
USP30-AS1	1.177	0.353	8.66E-04	1.57E-02
AC234782.4	1.243	0.266	2.89E-06	1.87E-04
PDZD7	1.249	0.394	1.50E-03	2.37E-02
NTN5	1.254	0.372	7.47E-04	1.41E-02
FSIP2-AS1	1.261	0.368	6.03E-04	1.21E-02
LTK	1.293	0.265	1.06E-06	8.40E-05

TNK2-AS1	1.297	0.405	1.37E-03	2.23E-02
CASC15	1.303	0.219	2.53E-09	5.73E-07
AF165147.1	1.324	0.366	2.99E-04	7.22E-03
LINC02082	1.342	0.443	2.47E-03	3.42E-02
RHBDF1	1.353	0.465	3.59E-03	4.40E-02
GAL3ST4	1.36	0.209	7.79E-11	2.41E-08
AC020656.2	1.373	0.457	2.64E-03	3.58E-02
LINC02718	1.383	0.322	1.73E-05	7.86E-04
AC009560.4	1.432	0.487	3.27E-03	4.16E-02
MEGF10	1.457	0.492	3.03E-03	3.96E-02
LINC02147	1.461	0.495	3.13E-03	4.05E-02
TAS1R3	1.462	0.37	7.72E-05	2.54E-03
ECEL1P1	1.485	0.46	1.24E-03	2.06E-02
LINC02801	1.539	0.276	2.35E-08	3.50E-06
CCDC187	1.573	0.362	1.38E-05	6.54E-04
WSCD2	1.612	0.546	3.16E-03	4.07E-02
SDK2	1.665	0.56	2.95E-03	3.87E-02
AL136181.1	1.82	0.534	6.63E-04	1.30E-02
AC010745.5	1.924	0.608	1.55E-03	2.43E-02
CNTNAP2	2.1	0.262	9.90E-16	1.08E-12
ADCY2	3.22	0.833	1.10E-04	3.38E-03
MIR3648-2	3.665	1.255	3.48E-03	4.33E-02
PRLR	3.71	1.087	6.39E-04	1.26E-02

Table A8. Downregulated signalling pathways by ruxolitinib in CD34+ MF cells.
Listed are all gene sets having a nominal P-value <0.05.

Gene set name (GS)	SIZE	ES	NES	NOM p-val	FDR q-val	FWER p-val	RANK AT MAX	LEADING EDGE
KEGG_OXIDATIVE_PHOSPHORYLATION	101	-0.773	-2.386	0	0	0	2506	tags=51%, list=14%, signal=60%
KEGG_SYSTEMIC_LUPUS_ERYTHEMATOSUS	96	-0.744	-2.298	0	0	0	2538	tags=53%, list=15%, signal=62%
KEGG_PARKINSONS_DISEASE	105	-0.711	-2.215	0	0	0	1926	tags=43%, list=11%, signal=48%
KEGG_HUNTINGTONS_DISEASE	147	-0.666	-2.16	0	0	0	2501	tags=38%, list=14%, signal=44%
KEGG_CYTOKINE_CYTOKINE_RECEPTOR_INTERACTION	140	-0.656	-2.129	0	0	0	1169	tags=18%, list=7%, signal=19%
KEGG_SPLICEOSOME	119	-0.666	-2.091	0	0	0	2935	tags=51%, list=17%, signal=61%
KEGG_PROTEASOME	40	-0.766	-2.013	0	0.00015	0.001	2886	tags=73%, list=17%, signal=87%
KEGG_AMINOACYL_TRNA_BIOSYNTHESIS	39	-0.756	-2.005	0	0.00013	0.001	2225	tags=49%, list=13%, signal=56%
KEGG_ALZHEIMERS_DISEASE	131	-0.619	-1.979	0	0.00061	0.005	2501	tags=34%, list=14%, signal=39%
KEGG_DNA_REPLICATION	31	-0.775	-1.979	0	0.00055	0.005	2688	tags=71%, list=15%, signal=84%
KEGG_CARDIAC_MUSCLE_CONTRACTION	48	-0.714	-1.953	0	0.00109	0.01	2475	tags=44%, list=14%, signal=51%
KEGG_GLYCINE_SERINE_AND_THREONINE_METABOLISM	25	-0.793	-1.926	0	0.00184	0.019	799	tags=28%, list=5%, signal=29%
BIOCARTA_TH1TH2_PATHWAY	17	-0.845	-1.919	0	0.00203	0.023	193	tags=12%, list=1%, signal=12%
KEGG_MISMATCH_REPAIR	22	-0.783	-1.896	0	0.00278	0.033	2688	tags=73%, list=15%, signal=86%
KEGG_JAK_STAT_SIGNALING_PATHWAY	94	-0.608	-1.858	0	0.00559	0.072	1277	tags=17%, list=7%, signal=18%
KEGG_CITRATE_CYCLE_TCA_CYCLE	27	-0.719	-1.831	0	0.00793	0.104	1360	tags=26%, list=8%, signal=28%
KEGG_SELENOAMINO_ACID_METABOLISM	22	-0.763	-1.82	0.00358	0.00859	0.119	2152	tags=36%, list=12%, signal=41%
KEGG_FRUCTOSE_AND_MANNOSE_METABOLISM	28	-0.717	-1.811	0	0.00973	0.142	3254	tags=57%, list=19%, signal=70%
KEGG_AMINO_SUGAR_AND_NUCLEOTIDE_SUGAR_METABOLISM	39	-0.693	-1.809	0.00175	0.00951	0.147	3525	tags=46%, list=20%, signal=58%
KEGG_PYRIMIDINE_METABOLISM	86	-0.597	-1.806	0	0.00965	0.156	3415	tags=47%, list=20%, signal=58%
KEGG_PPAR_SIGNALING_PATHWAY	40	-0.671	-1.806	0	0.00925	0.157	2224	tags=35%, list=13%, signal=40%
KEGG_CYSTEINE_AND_METHIONINE_METABOLISM	24	-0.74	-1.768	0.00173	0.01519	0.256	1904	tags=33%, list=11%, signal=37%
KEGG_PYRUVATE_METABOLISM	33	-0.67	-1.757	0	0.01719	0.3	1068	tags=27%, list=6%, signal=29%
KEGG_RNA_POLYMERASE	28	-0.694	-1.746	0.00349	0.01904	0.339	1443	tags=36%, list=8%, signal=39%
KEGG_GLYCOLYSIS_GLUCONEOGENESIS	38	-0.652	-1.742	0.00333	0.01889	0.35	980	tags=29%, list=6%, signal=31%
KEGG_GLUTATHIONE_METABOLISM	39	-0.65	-1.713	0.00348	0.02724	0.489	1708	tags=28%, list=10%, signal=31%
KEGG_TRYPTOPHAN_METABOLISM	31	-0.677	-1.688	0.00175	0.03671	0.601	3560	tags=32%, list=20%, signal=40%
KEGG_GALACTOSE_METABOLISM	22	-0.701	-1.672	0.00517	0.04256	0.657	3435	tags=50%, list=20%, signal=62%
BIOCARTA_G2_PATHWAY	24	-0.678	-1.665	0.01541	0.04512	0.698	3528	tags=50%, list=20%, signal=63%
KEGG_HOMOLOGOUS_RECOMBINATION	26	-0.669	-1.66	0.00694	0.04609	0.715	3149	tags=62%, list=18%, signal=75%
KEGG_NUCLEOTIDE_EXCISION_REPAIR	41	-0.617	-1.645	0.00664	0.05254	0.775	2724	tags=46%, list=16%, signal=55%

KEGG_BIOSYNTHESIS_OF_UNSATURATED_FATTY_ACIDS	21	-0.678	-1.642	0.0123	0.05283	0.791	3473	tags=48%, list=20%, signal=59%
BIOCARTA_NKT_PATHWAY	18	-0.708	-1.59	0.0239	0.08493	0.915	2	tags=6%, list=0%, signal=6%
KEGG_ONE_CARBON_POOL_BY_FOLATE	15	-0.725	-1.573	0.0239	0.09671	0.947	857	tags=33%, list=5%, signal=35%
KEGG_ARGININE_AND_PROLINE_METABOLISM	40	-0.586	-1.555	0.01868	0.11145	0.974	2056	tags=35%, list=12%, signal=40%
KEGG_DRUG_METABOLISM_OTHER_ENZYMES	21	-0.657	-1.538	0.04203	0.12427	0.981	3657	tags=43%, list=21%, signal=54%
KEGG_BLADDER_CANCER	39	-0.577	-1.531	0.01498	0.12943	0.988	3528	tags=38%, list=20%, signal=48%
KEGG_HEMATOPOIETIC_CELL_LINEAGE	55	-0.538	-1.522	0.01557	0.13438	0.991	456	tags=9%, list=3%, signal=9%
BIOCARTA_VEGF_PATHWAY	25	-0.633	-1.51	0.02574	0.14453	0.993	3085	tags=40%, list=18%, signal=49%
KEGG_COMPLEMENT_AND_COAGULATION_CASCADES	35	-0.568	-1.494	0.04085	0.15907	0.996	1104	tags=14%, list=6%, signal=15%
KEGG_BASAL_TRANSCRIPTION_FACTORS	28	-0.592	-1.489	0.03846	0.16166	0.996	1915	tags=21%, list=11%, signal=24%
KEGG_FC_GAMMA_R_MEDIATED_PHAGOCYTOSIS	84	-0.497	-1.488	0.01463	0.15863	0.996	2927	tags=23%, list=17%, signal=27%
KEGG_RNA_DEGRADATION	55	-0.527	-1.484	0.02254	0.1588	0.996	3572	tags=45%, list=20%, signal=57%
KEGG_CELL_CYCLE	117	-0.464	-1.479	0.0121	0.16189	0.997	3589	tags=43%, list=21%, signal=53%
KEGG_PURINE_METABOLISM	129	-0.466	-1.468	0.0104	0.17087	0.997	2747	tags=34%, list=16%, signal=40%
KEGG_N_GLYCAN_BIOSYNTHESIS	46	-0.529	-1.467	0.03959	0.16828	0.997	2589	tags=35%, list=15%, signal=41%

Table legend: SIZE = Number of genes in the gene set; ES = Enrichment score; NES = Normalized enrichment score; NOM p-val = Nominal p value; FDR q-val = False discovery rate; FWER p-val = Familywise-error rate; RANK AT MAX = The position in the ranked list at which the maximum enrichment score occurred; LEADING EDGE = Three statistics used to define the leading edge subset.

Table A9. Upregulated signalling pathways by ruxolitinib in CD34$^+$ MF cells.
Listed are all gene sets having a nominal P-value <0.05.

Gene set name (GS)	SIZE	ES	NES	NOM p-val	FDR q-val	FWER p-val	RANK AT MAX	LEADING EDGE
BIOCARTA_RELA_PATHWAY	15	0.737	1.702	0.00634	0.82135	0.601	436	tags=20%, list=3%, signal=20%
BIOCARTA_CHREBP_PATHWAY	15	0.66	1.548	0.04444	1	0.956	99	tags=13%, list=1%, signal=13%
BIOCARTA_PTEN_PATHWAY	16	0.659	1.535	0.04555	1	0.967	762	tags=25%, list=4%, signal=26%
BIOCARTA_CALCINEURIN_PATHWAY	17	0.651	1.533	0.04357	0.76237	0.968	1394	tags=18%, list=8%, signal=19%
BIOCARTA_VIP_PATHWAY	20	0.615	1.495	0.04695	0.7912	0.988	1647	tags=25%, list=9%, signal=28%
KEGG_VASCULAR_SMOOTH_MUSCLE_CONTRACTION	83	0.45	1.46	0.02653	0.82171	0.996	1539	tags=11%, list=9%, signal=12%
KEGG_RIBOSOME	80	0.459	1.447	0.03448	0.76626	0.997	3764	tags=48%, list=22%, signal=60%

Table legend: SIZE = Number of genes in the gene set; ES = Enrichment score; NES = Normalized enrichment score; NOM p-val = Nominal p value; FDR q-val = False discovery rate; FWER p-val = Familywise-error rate; RANK AT MAX = The position in the ranked list at which the maximum enrichment score occurred; LEADING EDGE = Three statistics used to define the leading edge subset.

Table A10. Negatively-enriched proteasome genes by ruxolitinib in CD34^{+} MF cells – GSEA details.

Gene	RANK IN GENE LIST	RANK METRIC SCORE	RUNNING ES	CORE ENRICHMENT
PSMC6	5019	0.381532222	-0.28191516	No
PSMD6	5425	0.332337558	-0.29943475	No
PSMA1	8766	0.01768841	-0.4911372	No
PSMA8	9817	-0.057690978	-0.55049896	No
PSME1	11293	-0.188765332	-0.6320202	No
PSMB10	11855	-0.257106006	-0.6598124	No
PSMC1	12414	-0.339740753	-0.6859992	No
PSMC2	13657	-0.580594301	-0.74733114	No
PSMA7	13716	-0.594460189	-0.7403571	No
POMP	13839	-0.628320098	-0.7364751	No
PSMD2	14016	-0.672260344	-0.73493546	No
PSMD11	14550	-0.847235262	-0.75088483	Yes
PSMC5	14581	-0.855801523	-0.73776925	Yes
PSMD7	14668	-0.893167496	-0.72722507	Yes
PSMF1	14841	-0.972161591	-0.720255	Yes
PSMA4	14885	-0.992333472	-0.7055192	Yes
PSMB4	14937	-1.012193918	-0.69089895	Yes
PSMB7	14939	-1.013000846	-0.6733903	Yes
PSME4	15072	-1.082569838	-0.6622062	Yes
PSMC4	15240	-1.160654664	-0.65168005	Yes
PSMA3	15347	-1.214071274	-0.63672096	Yes
PSMD12	15577	-1.351025462	-0.6264579	Yes
PSMB9	15610	-1.374755859	-0.6044583	Yes
PSMA5	15615	-1.376064777	-0.58082634	Yes
PSMD13	15704	-1.437568426	-0.56095684	Yes
PSMB6	15824	-1.512847304	-0.54156405	Yes
PSMD1	16001	-1.655567765	-0.5229732	Yes
PSMB8	16045	-1.686217904	-0.49620497	Yes
PSMD4	16167	-1.815277457	-0.47168282	Yes
PSME2	16238	-1.901265979	-0.44273767	Yes
PSME3	16279	-1.949509382	-0.41123134	Yes
PSMC3	16315	-1.984025002	-0.37883905	Yes
PSMD8	16422	-2.111506224	-0.34831774	Yes
PSMB1	16545	-2.321042538	-0.31508276	Yes
PSMD3	16785	-2.839381933	-0.27958548	Yes
PSMB2	16824	-2.9554286	-0.23052083	Yes
PSMD14	16893	-3.190919876	-0.17909722	Yes
SEM1	17019	-3.654277325	-0.12291548	Yes
PSMB5	17088	-4.0128479	-0.05723907	Yes
PSMB3	17150	-4.444596767	0.01632658	Yes

Table A11. Genes of potential relevance in MPN whose expression is regulated by CFZ in MF-4 and MF-24.

Gene	Protein	Effect of CFZ on its expression in MF-4	Effect of CFZ on its expression in MF-24	Evidence	Reason for potential relevance in MPN
ZFP36	also known as tristetrapolin (TTP), member of the tristetraprolin family of RNA-binding proteins	downregulated	upregulated	along with the other two members of this family (ZBP36L1 and ZBP36L2) it has a key role in the post-transcriptional regulation of the gene expression, with anti-inflammatory and tumour suppressor functions (1)	ZFP36L1 is downregulated in MF (2), while ZFP36 has been found upregulated in some ET patients (3) and in MF stem and progenitors cells where *JAK2*^{V617F} was accompanied by additional mutations in epigenetic modifiers and spliceosome machinery components (4)
CREBBP	CREB binding protein	downregulated	upregulated	a transcriptional co-activator known to repress the malignant transformation of haematopoietic cells (5)	loss of function promotes leukaemogenesis and has been reported in MDS (6), ALL (7), AML (8) and lymphoma (9)
RELB	RelB	upregulated	downregulated	key subunit of the non-canonical NF-κB pathway and forms an heterodimer with p100 (codified by NFKB2; this is upregulated by CFZ in MF-24)	This is particularly relevant as it could suggest a combined downregulation of both canonical (as shown in the Western Blot experiment in MF-19) and non-canonical pathway by CFZ. This would be partially in contrast with one study demonstrating that both 19S and 20S subunits of the 26S proteasome have a transcription repressing activity of the genes involved in the NF-κB non-canonical pathway (10), an effect that is abrogated by PIs. However, it has been shown that the effect of PIs on the NF-κB pathway regulation is cell-specific (11, 12). In regard to the impact of CFZ on the non-canonical pathway in MF cells, it would be important to investigate through Western Blot the effect of the CFZ on nuclear translocation of p52
IRAK-1	interleukin-1 receptor-associated kinase 1	no change	downregulated	serine-threonine kinase that mediates the signalling from toll-like receptors (TLR) and IL-1 receptor	IL-1 signalling has a crucial role in fibrotic process (13-15). Furthermore, it has been recently shown that a defective negative regulation of TLR signalling is a characteristic of monocytes of MF patients and it is responsible for the TNF-α excess seen in MF (16) and that a polymorphisms of mir-146a (an inhibitor of IRAK-1) causing its reduced expression is an independent marker of early progression to MF in PV and ET patients and increased JAK/STAT3 signalling (17). Of note, pacritinib is a JAK2/FLT3/IRAK-1 inhibitor and its effect on IRAK1 has been postulated to explain the higher spectrum of cytokine reduction compared to ruxolitinib therapy observed in MF patients (18)
FADD and TRADD	- Fas Associated Via Death Domain - TNFRSF1A Associated Via Death Domain	- no change - upregulated	- downregulated - downregulated	part of a membrane-bound complex activating NF-κB pathway downstream the TNF receptor 1 (TNFR1, canonical pathway)	among the marked inflammatory cytokine hyperactivation observed in MF, the TNF receptor signalling is one of the most important players and can drive clonal expansion (19)
- *NFKBIA* - *TNFAIP3* - *NKKBIE*	- *IκBa* - *A20* - *IκBe*	- upregulated - upregulated - downregulated	- upregulated - upregulated - downregulated	among the most important NF-κB inhibitors. A20 is an emerging candidate for targeted therapy in some inflammatory/autoimmune conditions and lymphomas where its decreased function is a key pathogenetic event (20). Of note, NKKBIE, which codifies for another NF-κB inhibitor, IκBe, is downregulated by CFZ. This could be related to the fact that the expression of this 3 protein seem to be tuned in different ways (21)	Upregulation of NF-κB inhibitors induced by CFZ could be relevant in MF, where hyperactivation of NF-κB pathway is a key pathogenetic determinant

Table A12. Genes downregulated by ruxolitinib, upregulated by CFZ and strongly upregulated by the treatment combination in MF-24 CD34+ cells.

Gene	Protein	Function	Reference
TLR4, TLR8, TLR6, TLR9, TLR7, TLR3	Toll-like receptors	Signalling through toll-like receptors culminates in the activation of NF-κB pathway.	(22)
NOS2	Nitric Oxide Synthase 2	An enzyme involved in the oxidative stress pathway, which synthetises nitric oxide, a molecule with both tumour-protecting or stimulating effects, based on its concentration.	(23)
IER3	Immediate early response 3	Involved in cellular stress response, inflammation and tumorigenesis.	(24)
ILR1 and IL1A	IL-1 receptor	Mediates the IL-1 induced activation of NF-κB pathway.	(25)
IRAK2	Interleukin-1 Receptor Associated Kinase 2	A critical mediator of ER stress and of UPR pro-apoptotic pathway.	(26)
IL12A	p35 subunit of IL-12	A cytokine with important immunoregulatory roles in host defence and immune homeostasis.	(27)
TBK1	Tank-binding kinase 1	A serine/threonine kinase that is a noncanonical IκB kinase family member, targeting the transcription factors IRF3 and IRF7 in the type I interferon response. It activates NF-κB pathway.	(28)
TNFRSF11A, TNFSF15, TNFRSF1A	TNF superfamily 15 and TNF receptor superfamily 11A (RANK) and 1A (TNFR1)	Involved in the activation of NF-κB pathway; TNFSF15 is also suppressor of angiogenesis and activator of some immune system functions.	(29-31)
CARD10	Caspase recruitment domain 10	It mediates the activation of NF-κB pathway.	(32)
EDARADD	Edar-associated death domain	Adaptor protein involved in activation of NF-κB pathway.	(33)
NKIRAS2	NF-κB inhibitor-interacting RAS-like protein 2	Acts as a potent negative regulator of NF-κB activity by preventing the degradation of the NF-κB inhibitor β.	(34)
ZNF675	zinc finger protein 675 (TRAF6-inhibitory zinc finger protein)	Inhibits NF-κB pathway.	(35)
CSF3	G-CSF (granulocyte colony-stimulating factor)	Crucial stimulator of the myeloid proliferation and is a NF-κB target gene.	(36)

Appendix References

1. Saini Y, Chen J, Patial S. The Tristetraprolin Family of RNA-Binding Proteins in Cancer: Progress and Future Prospects. Cancers (Basel). 2020;12(6).
2. Martinez-Calle N, Pascual M, Ordonez R, Eneriz ESJ, Kulis M, Miranda E, et al. Epigenomic profiling of myelofibrosis reveals widespread DNA methylation changes in enhancer elements and ZFP36L1 as a potential tumor suppressor gene that is epigenetically regulated. Haematologica. 2019;104(8):1572-9.
3. Puigdecanet E, Espinet B, Lozano JJ, Sumoy L, Bellosillo B, Arenillas L, et al. Gene expression profiling distinguishes JAK2V617F-negative from JAK2V617F-positive patients in essential thrombocythemia. Leukemia. 2008;22(7):1368-76.
4. Rodriguez-Meira A, Buck G, Clark SA, Povinelli BJ, Alcolea V, Louka E, et al. Unravelling Intratumoral Heterogeneity through High-Sensitivity Single-Cell Mutational Analysis and Parallel RNA Sequencing. Molecular cell. 2019;73(6):1292-305 e8.
5. Kung AL, Rebel VI, Bronson RT, Ch'ng LE, Sieff CA, Livingston DM, et al. Gene dose-dependent control of hematopoiesis and hematologic tumor suppression by CBP. Genes Dev. 2000;14(3):272-7.
6. Papaemmanuil E, Gerstung M, Malcovati L, Tauro S, Gundem G, Van Loo P, et al. Clinical and biological implications of driver mutations in myelodysplastic syndromes. Blood. 2013;122(22):3616-27; quiz 99.
7. Mullighan CG, Zhang J, Kasper LH, Lerach S, Payne-Turner D, Phillips LA, et al. CREBBP mutations in relapsed acute lymphoblastic leukaemia. Nature. 2011;471(7337):235-9.
8. Li Y, Lv X, Ge X, Yuan D, Ding M, Zhen C, et al. Mutational spectrum and associations with clinical features in patients with acute myeloid leukaemia based on nextgeneration sequencing. Mol Med Rep. 2019;19(5):4147-58.
9. Pasqualucci L, Dominguez-Sola D, Chiarenza A, Fabbri G, Grunn A, Trifonov V, et al. Inactivating mutations of acetyltransferase genes in B-cell lymphoma. Nature. 2011;471(7337):189-95.
10. Cullen SJ, Ponnappan S, Ponnappan U. Proteasome inhibition up-regulates inflammatory gene transcription induced by an atypical pathway of NF-kappaB activation. Biochem Pharmacol. 2010;79(5):706-14.
11. Hideshima T, Ikeda H, Chauhan D, Okawa Y, Raje N, Podar K, et al. Bortezomib induces canonical nuclear factor-kappaB activation in multiple myeloma cells. Blood. 2009;114(5):1046-52.
12. Meiners S, Ludwig A, Stangl V, Stangl K. Proteasome inhibitors: poisons and remedies. Med Res Rev. 2008;28(2):309-27.
13. Gieling RG, Wallace K, Han YP. Interleukin-1 participates in the progression from liver injury to fibrosis. Am J Physiol Gastrointest Liver Physiol. 2009;296(6):G1324-31.
14. Vesey DA, Cheung C, Cuttle L, Endre Z, Gobe G, Johnson DW. Interleukin-1beta stimulates human renal fibroblast proliferation and matrix protein production by means of a transforming growth factor-beta-dependent mechanism. J Lab Clin Med. 2002;140(5):342-50.
15. Zou Y, Cai Y, Lu D, Zhou Y, Yao Q, Zhang S. MicroRNA-146a-5p attenuates liver fibrosis by suppressing profibrogenic effects of TGFbeta1 and lipopolysaccharide. Cell Signal. 2017;39:1-8.
16. Lai HY, Brooks SA, Craver BM, Morse SJ, Nguyen TK, Haghighi N, et al. Defective negative regulation of Toll-like receptor signaling leads to excessive TNF-alpha in myeloproliferative neoplasm. Blood Adv. 2019;3(2):122-31.
17. Ferrer-Marin F AA, Bellosillo B, Zamora L, Kerguelen Fuentes A, Vélez P, Luño E, Juan Hernandez Boluda J, Ayala R, Fiallo D, García-Gutiérrez J, Arrizabalaga B, Gómez-

Casares M, Boque C, Garcia-Hernandez C, Hernández-Rivas J, Besses C, Vicente V, Alvarez-Larrán A, Teruel-Montoya R, González-Conejero R, Martínez C. rs2431697, a Polymorphism of Mir-146a, Is a Precozing Marker of Progression to Secondary Myelofibrosis: New Epigenetic Regulation of Jak/Stat3 Signaling. Blood. 2018;32 (Supplement 1): 3072.
18. Fisher DAC, Miner CA, Engle EK, Hu H, Collins TB, Zhou A, et al. Cytokine production in myelofibrosis exhibits differential responsiveness to JAK-STAT, MAP kinase, and NFkappaB signaling. Leukemia. 2019;33(8):1978-95.
19. Heaton WL, Senina AV, Pomicter AD, Salama ME, Clair PM, Yan D, et al. Autocrine Tnf signaling favors malignant cells in myelofibrosis in a Tnfr2-dependent fashion. Leukemia. 2018;32(11):2399-411.
20. Taibbi A, Furlan A, Sandonato L, Bova V, Galia M, Marin D, et al. Imaging findings of liver resection using a bipolar radiofrequency electrosurgical device--initial observations. European journal of radiology. 2012;81(4):663-70.
21. Kholodenko BN, Hancock JF, Kolch W. Signalling ballet in space and time. Nat Rev Mol Cell Biol. 2010;11(6):414-26.
22. Kawai T, Akira S. Signaling to NF-kappaB by Toll-like receptors. Trends Mol Med. 2007;13(11):460-9.
23. Vivarelli S, Falzone L, Basile MS, Candido S, Libra M. Nitric Oxide in Hematological Cancers: Partner or Rival? Antioxid Redox Signal. 2021;34(5):383-401.
24. Arlt A, Schafer H. Role of the immediate early response 3 (IER3) gene in cellular stress response, inflammation and tumorigenesis. Eur J Cell Biol. 2011;90(6-7):545-52.
25. Jurida L, Soelch J, Bartkuhn M, Handschick K, Muller H, Newel D, et al. The Activation of IL-1-Induced Enhancers Depends on TAK1 Kinase Activity and NF-kappaB p65. Cell Rep. 2015;10(5):726-39.
26. Benosman S, Ravanan P, Correa RG, Hou YC, Yu M, Gulen MF, et al. Interleukin-1 receptor-associated kinase-2 (IRAK2) is a critical mediator of endoplasmic reticulum (ER) stress signaling. PLoS One. 2013;8(5):e64256.
27. Ma X, Yan W, Zheng H, Du Q, Zhang L, Ban Y, et al. Regulation of IL-10 and IL-12 production and function in macrophages and dendritic cells. F1000Res. 2015;4.
28. Liu S, Marneth AE, Alexe G, Walker SR, Gandler HI, Ye DQ, et al. The kinases IKBKE and TBK1 regulate MYC-dependent survival pathways through YB-1 in AML and are targets for therapy. Blood Adv. 2018;2(23):3428-42.
29. Liu T, Zhang L, Joo D, Sun SC. NF-kappaB signaling in inflammation. Signal Transduct Target Ther. 2017;2.
30. Wajant H, Scheurich P. TNFR1-induced activation of the classical NF-kappaB pathway. FEBS J. 2011;278(6):862-76.
31. Zhang Z, Li LY. TNFSF15 Modulates Neovascularization and Inflammation. Cancer Microenviron. 2012;5(3):237-47.
32. Jiang C, Lin X. Regulation of NF-kappaB by the CARD proteins. Immunol Rev. 2012;246(1):141-53.
33. Morlon A, Munnich A, Smahi A. TAB2, TRAF6 and TAK1 are involved in NF-kappaB activation induced by the TNF-receptor, Edar and its adaptator Edaradd. Hum Mol Genet. 2005;14(23):3751-7.
34. Tago K, Funakoshi-Tago M, Sakinawa M, Mizuno N, Itoh H. KappaB-Ras is a nuclear-cytoplasmic small GTPase that inhibits NF-kappaB activation through the suppression of transcriptional activation of p65/RelA. J Biol Chem. 2010;285(40):30622-33.
35. Shin JN, Kim I, Lee JS, Koh GY, Lee ZH, Kim HH. A novel zinc finger protein that inhibits osteoclastogenesis and the function of tumor necrosis factor receptor-associated factor 6. J Biol Chem. 2002;277(10):8346-53.

36. Mussbacher M, Salzmann M, Brostjan C, Hoesel B, Schoergenhofer C, Datler H, et al. Cell Type-Specific Roles of NF-kappaB Linking Inflammation and Thrombosis. Front Immunol. 2019;10:85.